AGRICULTURAL RESEARCH INSTITUTE

PUSA

PROCEEDINGS

OF THE

ROYAL SOCIETY OF LONDON

SERIES A

CONTAINING PAPERS OF A MATHEMATICAL AND PHYSICAL CHARACTER.

VOL. CXII.

LONDON.

PRINTED FOR THE ROYAL SOCIETY AND SOLD BY
HARRISON AND SONS, LTD, ST MARTIN'S LANE,
PRINTERS IN ORDINARY TO HIS MAJESTY.

OCTOBER, 1926.

LONDON

HARRISON AND SONS, LTD., PRINTERS IN ORDINARY TO HIS MAJESTY,

ST MARTIN'S LANE

CONTENTS.

SERIES A. VOL CXII.

No A 760—August 3, 1926

No A 701.—September 1, 1926

PROCEEDINGS OF

THE ROYAL SOCIETY.

SECTION A —MATHEMATICAL AND PHYSICAL SCIENCES

Researches on the Mode of Distribution of the Constants of Samples taken at random from a Bivariate Normal Population.

By KARL PEARSON, F R S

(Received April 26, 1926)

(1) The theory of samples, whatever their size, has been largely developed of recent years This development may be said to have followed two independent lines. In the first of these there is no limitation to the nature of the frequency in the sampled population , that population has been supposed to be known by its momental coefficients, and the aim has been to determine the momental coefficients of the population of samples, and to find the successive momental coefficients of these momental coefficients themselves Thus we now know completely the first four momental coefficients of the distribution of means, and of standard deviations of samples of any size large or small taken from a finite population with any law of distribution These give us some general idea of how these means and standard deviations are likely to occur in practice But the expressions are very lengthy, and in the case of the third and fourth moments investigators have been reduced to approximations, or to supposing the population sampled "infinite," *i.e.*, to supposing an individual just drawn to be returned to the sampled population before the next drawing. Some recent researches, experimental and theoretical, seem to indicate that if the sample be not more than about one-fiftieth of the sampled population, it is, *for practical* purposes, indifferent whether we consider the population sampled finite or "infinite"

The second form of investigation is to obtain, if possible, not the momental constants, but the actual frequency distributions of the various characters which describe the distributions of samples Thus the distributions of the

means of samples from populations following certain types of frequency curves can now be written down in algebraical form. But thus far this method of inquiry has not been very fruitful, except in the case when the sampled population is supposed to follow a normal law and is considered infinite. In this case the distributions of the means, standard deviations, and the correlation coefficients have now been very completely studied. There are, however, other characters of samples, what we may term "compound characters," that contribute essentially to our knowledge of sampling, and of which it is possible to obtain the theoretical distributions Illustrations of this will be given in the present memoir It must be remembered, of course, that they only apply to samples from a *normal* population, but these samples may be as small or as large as we please, and the results may possibly tend to throw light on the corresponding distributions for samples in the case of non-normal sampled populations

(2) I suppose the sampled population bivariate, with variates x and y measured from the means m_1, m_2, the standard deviations σ_1, σ_2, and the correlation ρ. If the size of the population be N, the distribution will be given by the surface

$$z = \frac{N}{2\pi\sigma_1\sigma_2\sqrt{1-\rho^2}} e^{-\frac{1}{2}\frac{1}{1-\rho^2}\left(\frac{x^2}{\sigma_1^2} - \frac{2\rho xy}{\sigma_1\sigma_2} + \frac{y^2}{\sigma_2^2}\right)}. \qquad (1)$$

Let the size of the samples be M, the means, standard deviations and correlation coefficient of any individual sample be given by $\bar{x}$, $\bar{y}$, Σ_1, Σ_2 and r. Then it is known that the frequency surface for the distribution of these five variables is given by

$$z = z_0 e^{-\frac{M}{2}\left(\frac{(\bar{x}-m_1)^2}{\sigma_1^2} - \frac{2\rho(\bar{x}-m_1)(\bar{y}-m_2)}{\sigma_1\sigma_2} + \frac{(\bar{y}-m_2)^2}{\sigma_2^2}\right)\frac{1}{1-\rho^2}}$$
$$\times e^{-\frac{M}{2}\frac{1}{1-\rho^2}\left(\frac{\Sigma_1^2}{\sigma_1^2} - \frac{2r\Sigma_1\Sigma_2}{\sigma_1\sigma_2} + \frac{\Sigma_2^2}{\sigma_2^2}\right)} \Sigma_1^{M-2}\Sigma_2^{M-2}(1-r^2)^{\frac{M-4}{2}}$$
$$[d\bar{x}\, d\bar{y}\, d\Sigma_1\, d\Sigma_2\, dr]. \qquad (11)$$

It follows accordingly that if any "compound character" involves more than r, Σ_1 and Σ_2, *i.e.*, involves either $\bar{x}$ or $\bar{y}$ or both, we must use the complete five-variate surface to ascertain its distribution. We will illustrate the process in various cases

(3) *The Distribution of* $\Sigma_1\sqrt{1-r^2}$ *in Samples.*—If the population be normal' $\Sigma_1\sqrt{1-r^2}$ represents the standard deviation of any array about the mean of that array, and its "probable error" is a matter of considerable importance. In the case of any single array, the total number in the array varies from sample to

sample, and we are here concerned not with the value of the standard deviation as found from the single array, but as determined from Σ_1 and r of the whole sample. I write $\lambda = \Sigma_1\sqrt{1-r^2}$, and we need consider only the r, Σ_1, Σ_2 factor in (ii), for $\bar{x}$ and $\bar{y}$ are independent variates and can be supposed integrated out. To simplify the expressions we will put

$$s_1 = \sigma_1\sqrt{1-\rho^2}/\sqrt{\mathrm{M}} \quad \text{and} \quad s_2 = \sigma_2\sqrt{1-\rho^2}/\sqrt{\mathrm{M}}, \tag{iii}$$

and further throughout indicate the independent variables by placing their differentials in square brackets after the equation to the surface. As to the constant z_0 we can throw any additional factors into it which do not involve the independent variables themselves. It will thus change with each transformation of variables and with each integration; we shall indicate such changes by merely adding a dash to the letter z_0. The final value of z_0 is to be found by a simple integration of the remaining constant or compound character, and will be expressible in terms of the total number of samples and the constants of the distribution. This process is much simpler than substituting for z_0 its value *ab initio*, and following it through all the variate changes and integrations. Finally we may note that if we retain two of the original variates, two compound characters, or one original variate and one compound character, we get the corresponding correlation surfaces, from which the regression curves may be deduced. These are frequently of considerable interest, but become at times, both as to surface and regression curve, of considerable complexity.

In our present case, we start with

$$z = z_0' e^{-\frac{\mathrm{M}}{2(1-\rho^2)}\left(\frac{\Sigma_1^2}{\sigma_1^2} - \frac{2\rho r\Sigma_1\Sigma_2}{\sigma_1\sigma_2} + \frac{\Sigma_2^2}{\sigma_2^2}\right)} \Sigma_1^{\mathrm{M}-2}\Sigma_2^{\mathrm{M}-2}(1-r^2)^{\frac{\mathrm{M}-4}{2}}[d\Sigma_1\, d\Sigma_2\, dr],$$

and transform the variables to λ, Σ_2 and r, thus reaching

$$z = z_0' e^{-\frac{1}{2}\frac{\lambda^2}{s_1^2(1-r^2)}} e^{-\frac{1}{2}\frac{\Sigma_2^2}{s_2^2}} e^{\frac{r\rho\lambda\Sigma_2}{\sqrt{1-r^2}\,s_1 s_2}} \frac{\lambda^{\mathrm{M}-3}}{(1-r^2)^{1/2}}\Sigma_2^{\mathrm{M}-2}[d\lambda\, d\Sigma_2\, dr]$$

I now write $v = \frac{1}{2}\frac{\Sigma_2^2}{s_2^2}$, and transform the variables to λ, v and r, expanding the third exponential.

We have:

$$z = z_0'' e^{-\frac{1}{2}\frac{\lambda^2}{s_1^2(1-r^2)}} \frac{\lambda^{\mathrm{M}-3}}{(1-r^2)^{3/2}} e^{-v} \sum_{t=0}^{\infty} \frac{v^{\frac{\mathrm{M}-3}{2}+t}}{t!}\frac{(r\rho)^t(2s_2^2)^{\frac{t}{2}}\lambda^t}{s_1^t s_2^t(1-r^2)^{\frac{t}{2}}}[dv\, dr\, d\lambda],$$

and after integrating with regard to v from 0 to ∞:

$$z = z_0'' \frac{e^{-\frac{1}{2}\frac{\lambda^2}{s_1^2(1-r^2)}}}{(1-r^2)^{3/2}} \sum_{t=0}^{\infty} \frac{\lambda^{\mathrm{M}-2+t}\,2^{\frac{t}{2}}(r\rho)^t\,\Gamma\left(\frac{1}{2}(\mathrm{M}-1+t)\right)}{t!\; s_1^t(1-r^2)^{\frac{t}{2}}}[dv\, d\lambda].$$

We must now integrate this from $r = -1$ to $+1$. Let us put $r = \sin\theta$, and the general term in r being:

$$\frac{r^t \quad e^{-\frac{1}{2}\frac{\lambda^2}{s_1^2(1-r^2)}}}{(1-r^2)^{\frac{1}{2}}(1-r^2)^{3/2}},$$

we have for its integral:

$$e^{-\frac{1}{2}\frac{\lambda^2}{s_1^2}}\int_{-\frac{1}{2}\pi}^{+\frac{1}{2}\pi}\tan^t\theta\, e^{-\frac{1}{2}\frac{\lambda^2}{s_1^2}\tan^2\theta}\, d\tan\theta,$$

which vanishes when t is odd. When $t = 2\tau$, if $\gamma = s_1/\lambda$ and $u = \tan\theta$, we have the value

$$e^{-\frac{1}{2}\frac{\lambda^2}{s_1^2}}\int_{-\infty}^{+\infty} e^{-\frac{1}{2}\frac{u^2}{\gamma^2}}\, u^{2\tau}\, du,$$

which is equal to

$$e^{-\frac{1}{2}\frac{\lambda^2}{s_1^2}}\sqrt{2\pi}\gamma\,(2\tau-1)(2\tau-3)\ldots 1\,.\,\gamma^{2\tau}.$$

Hence

$$z = z_0'''\, e^{-\frac{1}{2}\frac{\lambda^2}{s_1^2}}\sum_{\tau=0}^{\infty}\frac{\lambda^{M-2+2\tau}\,2^\tau\rho^{2\tau}\,(2\tau-1)(2\tau-3)\ldots 1}{(2\tau)!\,s_1^{2\tau}}\,\Gamma\left(\tfrac{1}{2}(M-1)+\tau\right)\left(\frac{s_1}{\lambda}\right)^{2\tau+1}$$

$$= z_0^{IV}\, e^{-\frac{1}{2}\frac{\lambda^2}{s_1^2}}\lambda^{M-3}\sum_{\tau=0}^{\infty}\frac{(2\tau-1)(2\tau-3)\ldots 1\,(2\rho^2)^\tau}{(2\tau)!}\,\Gamma\left(\tfrac{1}{2}(M-1)+\tau\right)[d\lambda]$$

As the series in τ is independent of λ, it can be again thrown into the z_0^{IV}, and we have finally for the distribution of λ, the curve

$$z = z_0^{V}\, e^{-\frac{1}{2}\frac{M\lambda^2}{\sigma_1^2(1-\rho^2)}}\lambda^{M-3}. \qquad \text{(iv)}$$

Now the distribution curve for the standard deviation Σ of samples of size M taken from a normal population of standard deviation σ is well-known to be:

$$z = z_0^{VI}\, e^{-\frac{1}{2}\frac{M\Sigma^2}{\sigma^2}}\Sigma^{M-2}.$$

Hence the distribution of λ is not the same as that of samples taken from a population of standard deviation $\sigma_1\sqrt{1-\rho^2}$, the power term is $M-3$ and not $M-2$.

(iv) Provides the following points as to the distribution of λ—

(*a*) When M is of the order of 50, for all practical purposes the distribution of λ may be treated as a normal curve, mean value $= \sigma_1\sqrt{1-\rho^2}$ and standard deviation $= \dfrac{\sigma_1\sqrt{1-\rho^2}}{\sqrt{M}}$.

(*b*) The modal value of $\lambda = \lambda_{mo.} = \sqrt{\frac{M-3}{M}}\sigma_1\sqrt{1-\rho^2}$.

(*c*) The mean value of $\lambda = \lambda_{ms.} = \sqrt{\frac{2}{M}}\frac{\Gamma\left(\frac{M-1}{2}\right)}{\Gamma\left(\frac{M-2}{2}\right)}\sigma_1\sqrt{1-\rho^2}$.

(*d*) The standard deviation σ_λ of λ is given by

$$\sigma_\lambda^2 + \lambda_{ms}^2 = \frac{\sigma_1^2(1-\rho^2)}{M}(M-2),$$

and can thus be found for any given value of M.

(*e*) The frequency for any desired range of λ can be found from the *Tables of the Incomplete* Γ-*Functions, H M Stationery Office*

(4) *The Distribution of the Regression Coefficients* R_2.—The value of R_2 for the second variate on the first is: $R_2 = r\Sigma_2/\Sigma_1$. We shall accordingly again need only the second part of our five-variate surface (11) and shall transform the variates Σ_1, Σ_2 and r to Σ_1, Σ_2 and R_2. We have

$$z = z_0' e^{-\frac{1}{2(1-\rho^2)}\left(\frac{\Sigma_1^2}{\sigma_1^2} - \frac{2\rho R_2}{\sigma_1\sigma_2}\Sigma_1^2 + \frac{R_2^2\Sigma_1^2}{\sigma_2^2}\right)}\Sigma_1^{M-1}\Sigma_2^{M-1}\left(1 - \frac{R_2^2\Sigma_1^2}{\Sigma_2^2}\right)^{\frac{M-4}{2}}[d\Sigma_1\, d\Sigma_2\, dR_2]$$

Now $r = R_2\Sigma_1/\Sigma_2$ is always less than unity, and therefore whether M be even or odd the expansion of the binomial $\left(1 - \frac{R_2^2\Sigma_1^2}{\Sigma_2^2}\right)^{\frac{M-4}{2}}$ is legitimate. If M be even, there will be a finite number of terms, if M be odd, the series will still converge and gamma functions, such as $\Gamma(M/2 - s)$ where s is a positive integer, will still have a real value reducible by means of the relation

$$\Gamma(-m) = \Gamma(1-m)/(-m)$$

ultimately to $\Gamma(\frac{1}{2})$. We can accordingly write our binomial expansion:

$$\left(1 - \frac{R_2^2\Sigma_1^2}{\Sigma_2^2}\right)^{\frac{M-4}{2}} = \sum_t (-1)^t \frac{R_2^{2t}\Sigma_1^{2t}}{\Sigma_2^{2t}} \frac{\Gamma\left(\frac{M-2}{2}\right)}{\Gamma\left(\frac{M-2}{2} - t\right)t!}$$

and proceed without regard to whether M is even or odd We will first integrate with regard to Σ_2, writing:

$$v = \frac{1}{\sigma_2^2}\frac{\Sigma_2^2}{\sigma_2^2}.$$

We have

$$z = z_0'' e^{-v} S_t\left(v^{M-2-t} e^{-\frac{1}{2}\frac{\Sigma_1^2}{s_1^2}\left(1-\frac{2\rho s_1}{s_2}R_2\right)} \frac{(-1)^t R_2^{2t}\Sigma_1^{M-1+2t}}{(2s_2^2)^t \Gamma(M/2-1-t)t!}\right)[dv\, d\Sigma_1\, dR_2].$$

But

$$\int_0^\infty e^{-v} v^{\frac{1}{2}M-2-t} dv = \Gamma(\tfrac{1}{2}M-1-t)$$

Hence we get the surface for Σ_1 and R_2

$$z = z_0'' \sum_{t=0}^{\infty} \frac{(-1)^t R_2^{2t}\Sigma_1^{M-1+2t}}{(2s_2^2)^t t!} e^{-\frac{1}{2}\frac{\Sigma_1^2}{s_1^2}\left(1-\frac{2\rho s_1}{s_2}R_2\right)}[d\Sigma_1\, dR_2]. \qquad (v)$$

But the sum term in (v) is the negative exponential, or $e^{-\frac{1}{2}\frac{R_2^2\Sigma_1^2}{s_2^2}}$

$$z = z_0'' e^{-\frac{1}{2}\frac{\Sigma_1^2}{s_1^2}\left(1-\frac{2\rho s_2}{s_1}R_2+s_1^2\frac{R_2^2}{s_2^2}\right)}\Sigma_1^{M-1}[d\Sigma_1\, dR_2]. \qquad (vi)$$

This is the correlation surface of Σ_1 and R_2, *i.e.*, the correlation surface for a standard deviation of one variate and the regression coefficient of the second variate on this variate. It is clear that for a given value of Σ_1 the distribution of R_2 is a normal curve with mean and mode $= \rho s_2/s_1 = \rho\sigma_2/\sigma_1$, *i.e.*, the regression coefficient in the sampled population The regression line is therefore a horizontal straight line, but the standard deviation of the arrays of R_2 for a given Σ_1 is $s_2/\Sigma_1 = \dfrac{\sigma_2\sqrt{1-\rho^2}}{\Sigma_1\sqrt{M}}$, *i.e.*, the scedastic curve is a rectangular hyperbola This is a good illustration of how "correlation" can exist, when the regression line is horizontal, but the shapes of the array curves vary.

If we consider the regression of Σ_1 on R_2 we find for the modal value ${}_{R_2}\bar{\Sigma}_1$ of Σ_1 for a given R_2

$${}_{R_2}\bar{\Sigma}_1 = \sqrt{\frac{M-1}{M}}\frac{\sigma_1\sqrt{1-\rho^2}}{\left(1-2\rho\frac{\sigma_1}{\sigma_2}R_2+\frac{\sigma_1^2}{\sigma_2^2}R_2^2\right)^{\frac{1}{2}}} \qquad (vii)$$

a quartic curve, while for the mean ${}_{R_2}\bar{\Sigma}_1$ we find

$${}_{R_2}\bar{\Sigma}_1 = \sqrt{\frac{2}{M}}\frac{\Gamma(\frac{1}{2}(M+1))}{\Gamma(\frac{1}{2}M)}\frac{\sigma_1\sqrt{1-\rho^2}}{\left(1-2\rho\frac{\sigma_1}{\sigma_2}R_2+\frac{\sigma_1^2}{\sigma_2^2}R_2^2\right)^{\frac{1}{2}}}. \qquad (viii)$$

or a parallel quartic curve. These are further illustrations of how, even for $M \to \infty$, *i.e.*, for large samples, the regression need not become linear. Here, again, the standard deviation of the array of Σ_1 for a given R_2 is very far from constant, *i.e.*, the system is heteroscedastic.

We can now integrate the expression (vi) for Σ_1 and find at once

$$z = z_0''' \frac{1}{\left(1 - \frac{2\rho s_1}{s_2} R_2 + s_1^2 \frac{R_2^2}{s_2^2}\right)^{\frac{1}{2}M}}$$

$$= \frac{z_0^{\text{IV}}}{\left(\frac{\sigma_2^2}{\sigma_1^2}(1-\rho^2) + \left(R_2 - \rho\frac{\sigma_2}{\sigma_1}\right)^2\right)^{\frac{1}{2}M}} \qquad \text{(ix)}$$

This is a symmetrical curve of my Type VII. The slope of the regression line varies symmetrically round the value in the sampled population proceeding from plus to minus infinity.

The momental coefficients of this curve are given by the relations

$$\mu_{2s} = \frac{2s-1}{M-(2s+1)} \frac{\sigma_2^2}{\sigma_1^2}(1-\rho^2)\mu_{2s-2}, \qquad \mu_{2s+1} = 0, \qquad \text{(x)}$$

Accordingly,

$$\sigma_{R_2} = \frac{1}{\sqrt{M-3}} \frac{\sigma_2}{\sigma_1}\sqrt{1-\rho^2}, \qquad \text{(xi)}$$

$$\beta_2 = 3\frac{M-3}{M-5}, \qquad \beta_4 = 15\frac{M-3}{M-5}\frac{M-3}{M-7}, \quad \&c$$

Thus as $M \to \infty$, we have $\beta_2 = 3$, $\beta_4 = 15$, etc., or the normal values, or the regression coefficient tends with increasing size of the sample to a normal distribution, and we have for the standard deviation the value

$$\sigma_{R_2} = \frac{1}{\sqrt{M}} \frac{\sigma_2}{\sigma_1}\sqrt{1-\rho^2} \qquad \text{(xii)}$$

This is the usual value deduced for large samples, irrespective of the nature of the sampled population, on the assumption that it has linear regression. It seems probable, accordingly, that the result (xi) may extend further than for normal distributions of the sampled population.

The determination of the frequency of R_2 within any given range depends upon a knowledge of the integral

$$\int_0^\theta \cos^{M-2}\theta\, d\theta,$$

i.e., on

$$\tfrac{1}{2}\int_0^x x^{-\frac{1}{2}}(1-x)^{\frac{1}{2}(M-3)}\, dx, \quad \text{if } x = \sin^2\theta,$$

or

$$\tfrac{1}{2}B_x\left(\tfrac{1}{2}, \tfrac{1}{2}(M-1)\right).$$

Thus it reduces to a knowledge of the incomplete B-function, tables of which are in preparation and will be shortly published.

(5) *The Distribution of the Mean of the Array of y-Variates for a Given Value of the x-Variate.*—We will represent this quantity by $\bar{y}_x$ to be determined not from the individuals observed in that array in the given sample, but from the regression straight line of the sample. In other words, we take

$$\bar{y}_x - \bar{y} = r\frac{\Sigma_2}{\Sigma_1}(x - \bar{x}). \tag{xiii}$$

It is clear that $\bar{y}_x$ involves all the five constants $\bar{x}$, $\bar{y}$, Σ_1, Σ_2 and r of the sample. Accordingly, we shall need to use the two parts of the five-variate surface (ii).

We may write —

$$\bar{y} - m_2 = \bar{y}_x - m_2 - \mathrm{R}_2(x - m_1 - (\bar{x} - m_1))$$

and throw this into the form :—

$$\bar{\mathrm{Y}} = \bar{\mathrm{Y}}_x - \mathrm{R}_2(\mathrm{X} - \bar{\mathrm{X}}),$$

where $\bar{\mathrm{Y}} = \bar{y} - m_2$, $\bar{\mathrm{Y}}_x = \bar{y}_x - m_2$, $\mathrm{X} = x - m_1$, $\bar{\mathrm{X}} = \bar{x} - m_1$ and $\mathrm{R}_2 = r\Sigma_2/\Sigma_1$ as before. Here X is an absolute constant from sample to sample, and we have $d\bar{x} = d\bar{\mathrm{X}}$, $d\bar{y} = d\bar{\mathrm{Y}}$ and $= d\bar{y}_x$ if we transform for $\bar{y}$ to $\bar{y}_x$ keeping the variates R_2 and X constant. The first portion of our surface (ii) may be written

$$z = z_0 e^{-\frac{1}{2}\frac{\mathrm{M}}{(1-\rho^2)}\left(\frac{\bar{\mathrm{X}}^2}{\sigma_1^2} - \frac{2\rho\bar{\mathrm{X}}\bar{\mathrm{Y}}}{\sigma_1\sigma_2} + \frac{\bar{\mathrm{Y}}^2}{\sigma_2^2}\right)} \quad [d\bar{\mathrm{X}}\, d\bar{\mathrm{Y}}].$$

Transform this to $\bar{\mathrm{X}}$ and $\bar{\mathrm{Y}}_x$, and after somewhat lengthy rearranging we find :—

$$z = z_0 e^{-\frac{1}{2}\frac{\mathrm{M}}{1-\rho^2}\left\{\left(1 - \frac{2\rho\sigma_2}{\sigma_1}\mathrm{R}_2 + \frac{\sigma_2^2}{\sigma_1^2}\mathrm{R}_2^2\right)\frac{\bar{\mathrm{X}}'^2}{\sigma_1^2} + \frac{(\bar{\mathrm{Y}}_x - \mathrm{R}_2\bar{\mathrm{X}}')^2(1-\rho^2)}{\sigma_2^2\left(1 - 2\rho\frac{\sigma_2}{\sigma_1}\mathrm{R}_2 + \frac{\sigma_2^2}{\sigma_1^2}\mathrm{R}_2^2\right)}\right\}} \quad [d\bar{\mathrm{X}}'\, d\mathrm{Y}_x],$$

where

$$\bar{\mathrm{X}}' = \bar{\mathrm{X}} - \frac{\sigma_1(\mathrm{Y}_x - \mathrm{R}_2\mathrm{X})\left(\rho - \frac{\sigma_1}{\sigma_2}\mathrm{R}_2\right)}{\sigma_2\left(1 - 2\rho\frac{\sigma_1}{\sigma_2}\mathrm{R}_2 + \frac{\sigma_1^2}{\sigma_2^2}\mathrm{R}_2^2\right)}. \tag{xiv}$$

Keeping R_2 and $\bar{\mathrm{Y}}_x$ constant we can integrate out for $\bar{\mathrm{X}}'$ and the limits will be the same as for $\bar{\mathrm{X}}$, and so for $\bar{x}$, i.e., from plus to minus infinity. The result of the integration is

$$z = z_0' \frac{e^{-\frac{1}{2}\frac{\mathrm{M}\bar{\mathrm{Y}}_x'^2(1-\rho^2)}{(1-\rho^2)\sigma_2^2\left(1 - 2\rho\frac{\sigma_1}{\sigma_2}\mathrm{R}_2 + \frac{\sigma_1^2}{\sigma_2^2}\mathrm{R}_2^2\right)}}}{\sqrt{1 - 2\rho\frac{\sigma_1}{\sigma_2}\mathrm{R}_2 + \frac{\sigma_1^2}{\sigma_2^2}\mathrm{R}_2^2}} \quad [d\bar{\mathrm{Y}}_x'], \tag{xv}$$

where

$$\bar{\mathrm{Y}}'_x = \bar{\mathrm{Y}}_x - \mathrm{R}_2\mathrm{X}.$$

We have now to combine this with the second part of (u)

$$e^{-\frac{1}{2}M\left(\frac{\Sigma_1^2}{\sigma_1^2}-\frac{2r\Sigma_1\Sigma_2}{\sigma_1\sigma_2}+\frac{\Sigma_2^2}{\sigma_2^2}\right)}\Sigma_1^{M-2}\Sigma_2^{M-2}(1-r^2)^{\frac{M-4}{2}} \quad [d\Sigma_1\, d\Sigma_2\, dr]$$

But if we change our variables in this from Σ_1, Σ_2, r to Σ_1, Σ_2 and R_2, and integrate out Σ_1 and Σ_2, we know from section (4) the answer This can be done because (xv), while it contains R_2, does not contain Σ_1 and Σ_2 directly. The result is then :—

$$z = z_0'' \frac{e^{-\frac{1}{2}\frac{M}{(1-\rho^2)}\frac{\bar{Y}_x'^2(1-\rho^2)}{\sigma_2^2\left(1-2\rho\frac{\sigma_1}{\sigma_2}R_2+\frac{\sigma_1^2}{\sigma_2^2}R_2^2\right)}}}{\left(1-2\rho\frac{\sigma_1}{\sigma_2}R_2+\frac{\sigma_1^2}{\sigma_2^2}R_2^2\right)^{\frac{1}{2}(M+1)}}\,[d\bar{Y}_x'\,dR_2]. \qquad \text{(xvi)}$$

Now

$$\begin{aligned}\bar{Y}'_x &= \bar{Y}_x - R_2X\\ &= \bar{y}_x - m_2 - \rho\frac{\sigma_2}{\sigma_1}(x-m_1) - \left(R_2-\rho\frac{\sigma_2}{\sigma_1}\right)(x-m_1)\\ &= y_x' - R_2'(x-m_1),\end{aligned}$$

where $\bar{y}_x'$ and R_2' are the array mean and the regression coefficient measured from their respective mean values Hence we have :—

$$z = z_0''' \frac{e^{-\frac{1}{2}M\frac{(\bar{y}_x'-R_2'(x-m_1))^2}{\sigma_2^2(1-\rho^2)}\frac{\sigma_2^2(1-\rho^2)}{\sigma_1^2(1-\rho^2)+R_2'^2}}}{\left(\frac{\sigma_2^2}{\sigma_1^2}(1-\rho^2)+R_2'^2\right)^{\frac{1}{2}(M+1)}} \quad [d\bar{y}_x'\,dR_2'] \qquad \text{(xvii)}$$

as the correlation surface between $\bar{y}_x'$ and R_2' This surface is a somewhat complicated one in R_2'. We note, however, that for R_2' constant, $\bar{y}_x'$ follows a normal distribution with a linear regression, *i.e.*,

$$\text{Mean}\quad \bar{y}_x' = R_2'(x-m_1)$$

but the system is heteroscedastic with a standard deviation given by

$$\sigma_{\bar{y}_x'} = \frac{\sigma_2\sqrt{1-\rho^2}}{\sqrt{M}}\sqrt{1+\frac{R_2'^2}{\frac{\sigma_2^2}{\sigma_1^2}(1-\rho^2)}}.$$

The distribution of R_2' for a given $\bar{y}_x'$ is less easy of interpretation.

If we integrate from $\bar{y}_x' = +\infty$ to $-\infty$, we obtain at once the curve already given as the frequency distribution of R_2'. If we could integrate with regard

to R_2' we should obtain the frequency distribution of $\bar{y}_x'$. To simplify the required integral, take

$$R_2' = \frac{\sigma_2}{\sigma_1}\sqrt{1-\rho^2}\tan\theta,$$

and we have

$$z = z_0 {}^{1}e^{-\frac{1}{2}M\left(\bar{y}'_x\cos\theta - \frac{\sigma_2}{\sigma_1}\sqrt{1-\rho^2}(x-m_1)\sin\theta\right)^2}{\sigma_2^2(1-\rho^2)}} \cos^{M-1}\theta\,[d\theta\,d\bar{y}_x'] \qquad \text{(xix)}$$

Accordingly, writing $a = \sqrt{M}\,\bar{y}'_x/\sigma_2\sqrt{1-\rho^2}$ and $b = \sqrt{M}\,\frac{x-m_1}{\sigma_1}$, we have for the required integral:

$$I(a,b) = \int_{-\frac{1}{2}\pi}^{+\frac{1}{2}\pi} e^{-\frac{1}{2}(a\cos\theta - b\sin\theta)^2}\cos^{M-1}\theta\,d\theta. \qquad \text{(xx)}$$

By expanding first the exponential and then the resulting binomials it is possible to express this integral in a double series of complete beta-functions as coefficients of a series of powers of a^2 and b^2 and their products, but the series is not rapidly convergent.*

I have therefore approached the problem from another standpoint. If we multiply the expression in (xix) by $(\bar{y}_x')^p$ and integrate with respect to $\bar{y}_x'$ from $-\infty$ to $+\infty$, and θ from $-\frac{1}{2}\pi$ to $+\frac{1}{2}\pi$, we shall find $N\mu_p$, where N is the number of samples and μ_p the p^{th} moment coefficient about the mean. These integrations are feasible.

Writing $U = \bar{y}_x'\cos\theta - \frac{\sigma_2}{\sigma_1}\sqrt{1-\rho^2}\,(x-m_1)\sin\theta$ and transforming from $\bar{y}'_x$ to U, we have:

$$N\mu_p = z_0 {}^{1}\int_{-\infty}^{+\infty}\int_{-\frac{1}{2}\pi}^{+\frac{1}{2}\pi} e^{-\frac{1}{2}\frac{MU^2}{\sigma_2^2(1-\rho^2)}}\left(U + \frac{\sigma_2}{\sigma_1}\sqrt{1-\rho^2}\,(x-m_1)\sin\theta\right)^p \cos^{M-1-p}\theta\,d\theta\,dU.$$

If p be odd $= 2s+1$, this will depend on integrals of forms which contain either an odd power of U or an odd power of $\sin\theta$; in both cases the integrals vanish or we conclude that $\mu_{2s+1} = 0$; all odd moment-coefficients vanish, or the curve of distribution of $\bar{y}'_x$ is symmetrical.

Professor G. N. Watson kindly sends me the expansion

$$I(a,b) = \sum_{m=0}^{\infty}(-1)^m B(\tfrac{1}{2}M, m+\tfrac{1}{2})(a^2+b^2)^m F\left(-m, -\tfrac{1}{2}(M-1), \tfrac{1}{2}, \frac{a^2}{a^2+b^2}\right)$$

where F is the hypergeometrical series, but as a^2 and b^2 both contain the factor M, usually large, this does not seem likely to work in our case.

If $p = 0$, then:

$$N = 2z_0{}^{M}\sqrt{2\pi}\frac{\sigma_2\sqrt{1-\rho^2}}{\sqrt{M}}\int_0^{\frac{1}{2}\pi}\cos^{M-2}\theta\,d\theta = z_0{}^{M}\sqrt{2\pi}\frac{\sigma_2\sqrt{1-\rho^2}}{\sqrt{M}}\,B\left(\tfrac{1}{2},\tfrac{1}{2}(M-1)\right) \tag{xxi}$$

If $p = 2$, then

$$N\mu_2 = 2z_0{}^{M}\int_0^{\frac{1}{2}\pi}\int_{-\infty}^{+\infty} e^{-\frac{1}{2}\frac{MU^2}{\sigma_1{}^2(1-\rho^2)}}\left(U^2 + \frac{\sigma_2{}^2}{\sigma_1{}^2}(1-\rho^2)(x-m_1)^2\sin^2\theta\right)\cos^{M-4}\theta\,d\theta\,dU,$$

since the odd term in U vanishes. Hence:

$$N\mu_2 = z_0{}^{M}\sqrt{2\pi}\frac{\sigma_2\sqrt{1-\rho^2}}{\sqrt{M}}\left\{\frac{\sigma_2{}^2(1-\rho^2)}{M}\,B\left(\tfrac{1}{2},\tfrac{1}{2}(M-3)\right) + \sigma_2{}^2(1-\rho^2)\frac{(x-m_1)^2}{\sigma_1{}^2}\,B\left(\tfrac{3}{2},\tfrac{1}{2}(M-3)\right)\right\}$$

and hence by (xxi):

$$\mu_2 = \frac{\sigma_2{}^2(1-\rho^2)}{M-3}\left(1 - \frac{2}{M} + \frac{(x-m_1)^2}{\sigma_1{}^2}\right) \tag{xxii}$$

or

$$\sigma_{y'} = \frac{\sigma_2\sqrt{1-\rho^2}}{\sqrt{M-3}}\left(1 - \frac{2}{M} + \frac{(x-m_1)^2}{\sigma_1{}^2}\right)^{\frac{1}{2}}. \tag{xxii^{bis}}$$

This agrees with the usual value for large samples, *i.e.*,

$$\sigma_{y_x} = \frac{\sigma_2\sqrt{1-\rho^2}}{\sqrt{M}}\left(1 + \frac{(x-m_1)^2}{\sigma_1{}^2}\right)^{\frac{1}{2}}$$

The formula indicates that $\sigma_{y'}$ gets larger and larger as we pass away from arrays near the mean.

For $p = 4$

$$N\mu_4 = 2z_0{}^{M}\int_0^{\frac{1}{2}\pi}\int_{-\infty}^{+\infty} e^{-\frac{1}{2}\frac{MU^2}{\sigma_1{}^2(1-\rho^2)}}\left\{U^4 + 6U^2\sigma_2{}^2(1-\rho^2)\frac{(x-m_1)^2}{\sigma_1{}^2}\sin^2\theta + \sigma_2{}^4(1-\rho^2)^2\frac{(x-m_1)^4}{\sigma_1{}^4}\sin^4\theta\right\}\cos^{M-6}\theta\,d\theta\,dU$$

$$= 2z_0{}^{M}\sqrt{2\pi}\frac{\sigma_2\sqrt{1-\rho^2}}{\sqrt{M}}\sigma_2{}^4(1-\rho^2)^2\int_0^{\frac{1}{2}\pi}\left\{\frac{3}{M^2} + \frac{6}{M}\frac{(x-m_1)^2}{\sigma_1{}^2}\sin^2\theta + \frac{(x-m_1)^4}{\sigma_1{}^4}\sin^4\theta\right\}\cos^{M-6}\theta\,d\theta$$

$$= z_0{}^{M}\sqrt{2\pi}\frac{\sigma_2\sqrt{1-\rho^2}}{\sqrt{M}}\sigma_2{}^4(1-\rho^2)^2\left\{\frac{3}{M^2}\,B\left(\tfrac{1}{2},\tfrac{1}{2}(M-5)\right) + \frac{6}{M}\frac{(x-m_1)^2}{\sigma_1{}^2}\,B\left(\tfrac{3}{2},\tfrac{1}{2}(M-5)\right) + \frac{(x-m_1)^4}{\sigma_1{}^4}\,B\left(\tfrac{5}{2},\tfrac{1}{2}(M-5)\right)\right\}.$$

Hence,

$$\mu_4 = \sigma_2^4(1-\rho^2)^2\frac{3}{(M-3)(M-5)}\left\{\left(1-\frac{2}{M}\right)\left(1-\frac{4}{M}\right)+2\left(1-\frac{2}{M}\right)\frac{(x-m_1)^2}{\sigma_1^2}+\frac{(x-m_1)^4}{\sigma_1^4}\right\}$$

$$=\sigma_2^4(1-\rho^2)^2\frac{3}{(M-3)(M-5)}\left\{\left(\frac{(x-m_1)^2}{\sigma_1^2}+1-\frac{2}{M}\right)^2-\frac{2}{M}\left(1-\frac{2}{M}\right)\right\} \qquad \text{(xxiii)}$$

Thus, we have for $\beta_2 = \mu_4/\mu_2^2$,

$$\beta_2 = 3\frac{M-3}{M-5}\left\{1-\frac{\frac{2}{M}\left(1-\frac{2}{M}\right)}{\left(\left(\frac{x-m_1}{\sigma_1}\right)^2+1-\frac{2}{M}\right)^2}\right\}$$

$$\beta_2 - 3 = \frac{6}{M-5}\left\{1-\frac{\left(1-\frac{2}{M}\right)\left(1-\frac{3}{M}\right)}{\left(1-\frac{2}{M}+\left(\frac{x-m_1}{\sigma_1}\right)^2\right)^2}\right\}. \qquad \text{(xxiv)}$$

It is easy to see that the second term in the curled brackets is less than unity, so that $\beta_2 - 3$ is always positive. Hence, the distribution of $\bar{y}'_x$ as far as the first four moments are concerned can be expressed by a leptokurtic curve, Type vii. But an investigation of the higher even moments indicates that the moment-coefficients of the distribution for $\bar{y}'_x$ do not satisfy the intermomental relations for Type vii. If that curve be

$$z = \frac{z_0}{(a^2+x^2)^m},$$

then we have

$$\mu_2 = \frac{1}{n-3}a^2\mu_0, \qquad \mu_4 = \frac{3}{n-5}a^2\mu_2,$$

$$\mu_6 = \frac{5}{n-7}a^2\mu_4, \qquad \mu_8 = \frac{7}{n-9}a^2\mu_6, \text{ and so on.}$$

But for $\bar{y}'_x$ the momental coefficients are:

$$\mu_2 = \frac{\sigma_2^2(1-\rho^2)}{M-3}\left\{1-\frac{2}{M}+\frac{(x-m_1)^2}{\sigma_1^2}\right\},$$

$$\mu_4 = \frac{3\sigma_2^4(1-\rho^2)^2}{(M-3)(M-5)}\left\{\left(1-\frac{2}{M}\right)\left(1-\frac{4}{M}\right)+2\left(1-\frac{2}{M}\right)\frac{(x-m_1)^2}{\sigma_1^2}+\frac{(x-m_1)^4}{\sigma_1^4}\right\},$$

$$\mu_6 = \frac{3 \cdot 5 \cdot \sigma_2^6 (1-\rho^2)^3}{(M-3)(M-5)(M-7)} \left\{ \left(1-\frac{2}{M}\right)\left(1-\frac{4}{M}\right)\left(1-\frac{6}{M}\right) + 3\left(1-\frac{2}{M}\right)\left(1-\frac{4}{M}\right)\frac{(x-m_1)^2}{\sigma_1^2} + 3\left(1-\frac{2}{M}\right)\frac{(x-m_1)^4}{\sigma_1^4} + \frac{(x-m_1)^6}{\sigma_1^6} \right\},$$

$$\mu_8 = \frac{3 \cdot 5 \cdot 7 \cdot \sigma_2^8 (1-\rho^2)^4}{(M-3)(M-5)(M-7)(M-9)} \left\{ \left(1-\frac{2}{M}\right)\left(1-\frac{4}{M}\right)\left(1-\frac{6}{M}\right)\left(1-\frac{8}{M}\right) + 4\left(1-\frac{2}{M}\right)\left(1-\frac{4}{M}\right)\left(1-\frac{6}{M}\right)\frac{(x-m_1)^2}{\sigma_1^2} + 6\left(1-\frac{2}{M}\right)\left(1-\frac{4}{M}\right)\frac{(x-m_1)^4}{\sigma_1^4} + 4\left(1-\frac{2}{M}\right)\frac{(x-m_1)^6}{\sigma_1^6} + \frac{(x-m_1)^8}{\sigma_1^8} \right\}, \text{ and so on.}$$

If we put $\phi^2 = 1 - \frac{2}{M} + \frac{(x-m_1)^2}{\sigma_1^2}$ we have

$$\mu_2 = \frac{\sigma_2^2(1-\rho^2)}{M-3}\phi^2, \qquad \mu_4 = \frac{3\sigma_2^4(1-\rho^2)^2}{(M-3)(M-5)}\left\{\phi^4 - \frac{2}{M}\left(1-\frac{2}{M}\right)\right\},$$

$$\mu_6 = \frac{15\sigma_2^6(1-\rho^2)^3}{(M-3)(M-5)(M-7)}\left\{\phi^6 - \frac{6}{M}\left(1-\frac{2}{M}\right)\phi^2 + \frac{8}{M^2}\left(1-\frac{2}{M}\right)\right\},$$

and so on.

Thus, as M increases, the dominant term in the series of curled brackets is the first, and the momental coefficients approach closer and closer to a curve of Type VII, or the distribution of $\bar{y}'_x$ will follow then with considerable accuracy the curve of Type VII:

$$z = \frac{z_0}{\left(\sigma_2^2(1-\rho^2)\left(1-\frac{2}{M}+\frac{(x-m_1)^2}{\sigma_1^2}\right)+\bar{y}'^2_x\right)^{\frac{1}{2}M}} \qquad \text{(XXV)}$$

and will ultimately pass over into the normal distribution

$$z = z_0 e^{-\frac{M}{2}\frac{\bar{y}'^2_x}{\sigma_2^2(1-\rho^2)\left(1+\left(\frac{x-m_1}{\sigma_1}\right)^2\right)}} \qquad \text{(XXV}^{\text{bis}}\text{)}$$

It is, perhaps, desirable to remind the reader that the actual value of the mean of the x array of y's is:

$$\bar{y}_x = \bar{y}_x' + m_2 + \rho\frac{\sigma_2}{\sigma_1}(x-m_1).$$

I have not succeeded—except as a double summation—in showing what the frequency curve for $\bar{y}'_x$ is whatever be the value of M. That remains a problem for the mathematician who can exhibit in a compact form the result of integrating

$$I(a, b) = \int_{-\frac{1}{2}\pi}^{+\frac{1}{2}\pi} e^{-\frac{1}{2}(a\cos\theta - b\sin\theta)^2} \cos^{M-1}\theta \, d\theta.$$

The object of this paper has been to indicate how regression lines far from straight, and correlation surfaces far from normal,* may arise in the case of compound characters even if we are sampling from a normal population. Thus we see how readily the old theory of "probable errors" may mislead us.

Further Spectroscopic Studies on the Luminous Vapour Distilled from Metallic Arcs.

By Lord Rayleigh, F R S

(Received June 8, 1926)

Plates 1–3

This paper continues the investigation of a previous one† entitled "Luminous Vapour from the Mercury Arc, and the Progressive Changes in its Spectrum" Several points (it is hoped) are cleared up, and new phenomena are described Needless to say, much remains to be done. The present work is an instalment only.

§ 1. *Conditions for the Appearance of Higher Members of Spectrum Series.*

It was found‡ that the lines of the diffuse series from M = 12 upwards, $1p_1 - 12d$, $1p_1 - 13d$, etc, were seen in the distilled mercury vapour, but not in the arc from which the distilled vapour came. This point has now been examined more closely

In the first place the spectra in question have been photographed with a

* For example (xxv) or (xxv^{bis}) above when we treat x and $\bar{y}'_x$ as our variates. I have dealt with the regression and scedasticity of surfaces of the type of (xxv) in an earlier paper, 'Biometrika,' vol XV, pp 231–244 (1923)

† 'Roy. Soc. Proc,' A, vol. 108, p. 262 (1925).

‡ *Loc. cit.*, p. 266.

larger quartz spectrograph instead of the small one used before. The point is brought out still more clearly. See Plate 1. I is the distilled vapour spectrum, and II the arc spectrum. The diffuse series lines are indicated on the strip separating the two.

To examine more closely the transition between the arc, in which these lines do not appear, and the jet of luminous vapour in which they do, a special arrangement was set up (fig. 1). The arc was produced in a porcelain tube A of 1 cm. inside diameter. The top of a barometric column B formed the cathode as usual The anode was a cap of steel tubing C, 0 75 mm thick, with a side hole to the left 1 mm. diameter. The cap was kept cool with water as shown It was desired to make the metal wall immediately round the hole the effective anode The porcelain tube was cut away under this portion, to expose it, and it alone, to the vapour column. The end of the porcelain tube was covered with a mica disc The whole was assembled in a T tube of silica D, the joints being made with indiarubber cemented on The mercury vapour issued through the small hole into the side silica tube E where its luminosity could be observed. Near the hole it was concentrated, but broadened out in a distance comparable with the diameter of the tube until it filled the latter The appearance of the self-luminous vapour is indicated as well as may be in figs. 1 and 2. E (fig. 1) was attached to a vessel for catching distilled mercury, and to the air pump

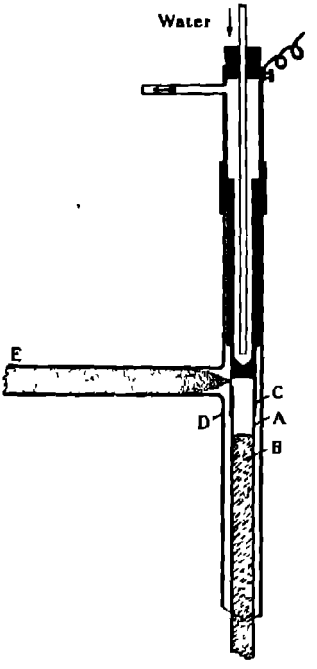

Fig. 1

The advantage of the arrangement was that there was no trouble from stray light. The porcelain tube containing the arc was sufficiently opaque, at any rate in the ultraviolet, and the only place where the light of the arc could issue was the small hole. Observing as near as possible to the hole, and across the horizontal issuing jet of vapour, the light from the latter was not appreciably contaminated with light from the arc The spectroscope slit was vertical, and

the jet was focussed upon it by a quartz-fluorite achromat Thus the central part of the length of each spectrum line came from the core of the luminous jet, and the extremities of this line from the expanded and much less intrinsically luminous vapour around this core see fig. 2, which shows the image of the issuing jet of vapour and the wall of the steel tube (*c*, fig. 1) as depicted on the plane of the spectroscope slit

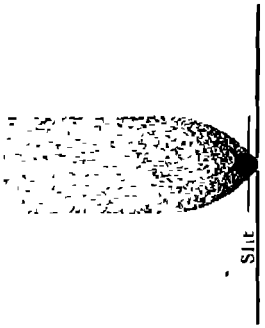

Fig 2.

The result is instructive. It is seen (Plate 1, No. III) that the lines of the diffuse series $1p_1 - 9d$ upwards are very broad at the centre, and fine out above and below The central broadening is not due to photographic over-exposure This is clear if we compare these lines with, *e g.*, the line 2576·29 $1p_2 - 3s$. The latter, though more intense, is narrower. It is certain, therefore, that the broadening of $1p_1 - 9d$, etc , is real.

The breadth increases as we go up the series, and at $1p_1 - 11d$ upwards the breadth has become so great that the successive lines tend to encroach on one another

It seems pretty clear that the broadening is due to the Stark effect, increasing as it does as we proceed up the series The case is interesting because here we have no external electric field at all, and the effect must be due solely to the interatomic fields In accordance with this it diminishes as the luminous vapour expands, and the luminous centres get further apart

It appears then that the failure of these high members of the diffuse series to appear in the arc is simply due to the fact that at the high concentration of luminous vapour, which prevails there, they are broadened to the point of becoming unrecognisable, the higher members actually overlapping one another. It is therefore impossible to resolve them

In the case of the second members of the diffuse triplets, of the type $1p_2 - md$, the same broadening may be observed in the more concentrated region of the distilled glow In the expanded vapour the series can be traced on my negatives 7 or 8 members further than in the arc.

The same cause of broadening and consequent enfeeblement of the lines acts in the case of the sharp series, but less powerfully, and here the distilled vapour has not so great an advantage over the arc in bringing up the higher members.

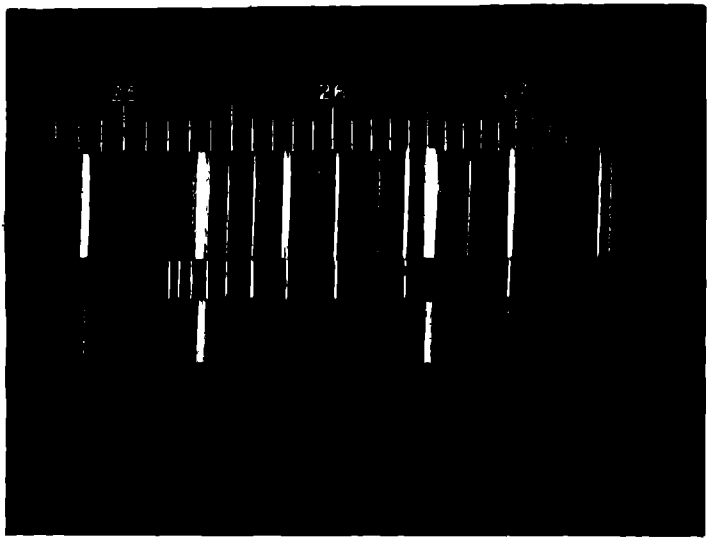
I
II

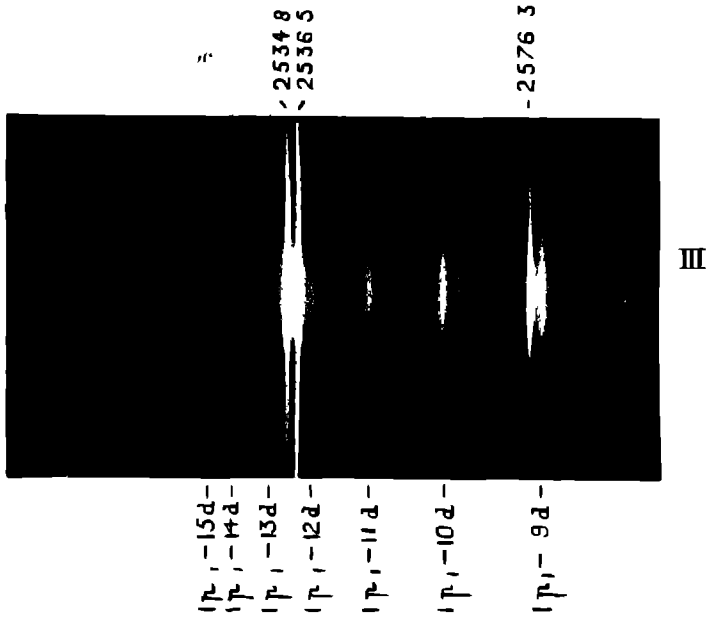
2534 8
2536 5
2576 3
III
$^1P_1 - 15d$
$^1P_1 - 14d$
$^1P_1 - 13d$
$^1P_1 - 12d$
$^1P_1 - 11d$
$^1P_1 - 10d$
$^1P_1 - 9d$

The same phenomenon may be seen at the limits of the principal triplets, and of the diffuse and sharp singlets. It appears to be general.

§ 2. *Appearance of enhanced lines in the vapour jets from mercury, magnesium and calcium. Relative duration of these and of the arc lines. Relative duration of resonance lines.*

In the investigation of last year* certain lines were listed as present in the arc but apparently absent in the distilled vapour. I recapitulate the list, partly because there were some errors in it, and partly because further search of the literature has enable me to add notes about the character of the lines.

3984 Enhanced (Steinhausen).
3860 Belongs to many lined spectrum (Stiles).
3820 Enhanced (Steinhausen).
3770 Enhanced (Steinhausen). Many lined spectrum (Stiles).
3752 Enhanced (Steinhausen).
3561 Enhanced (Steinhausen)
3544 Enhanced (Steinhausen).
3390 Enhanced (Steinhausen).
3382 Not traceable in tables
3278 Many lined spectrum (Stiles)
2848 Enhanced (Steinhausen). Subordinate series of spark spectrum (Carrol).
2820 Enhanced (Steinhausen). Many lined spectrum (Stiles).
2775
2791
2686 Many lined spectrum (Stiles)
2003
1974
1943 Principal series of spark spectrum (Carrol).†

That the intensity of the lines listed above is at any rate very small in the distilled glow is clear from the reproduction in the former paper. These show spectra of the arc and of the distilled glow in comparison. The triplets are of equal intensity in each, but the lines of the above list are apparently limited to the arc, and do not noticeably distil out of it The experimental arrangement

* *Loc. cit.*, p. 266.

† References in above:—Steinhausen's paper is in 'Zeits f. Wissen.,' Phot 3, p. 45 (1905). Stiles in 'Astroply. J.,' vol. 30, p. 48 (1909) Carrol's classification of spark lines is referred to by Turner and Compton, 'Phys. Rev.,' vol 25, p. 613 (1925).

of fig 1 allowed of a sharp isolation of the spectrum of the distilled vapour without ambiguity from stray light This made possible a more searching test for some of the above lines in the light of the distilled vapour without ambiguity from stray light of the arc. An exposure of about 1 hour was made on the brightest part of the issuing vapour, near the hole The plates were oiled with "Nujol" for sensitiveness in the extreme region of the quartz spectograph. The latter was put close to the silica tube, so that the source was approximately in focus, and the bright part of the glow only produced short spectrum lines as in photograph No III, though in the present case no lens was used The shortness of a spectrum line gave confirmatory evidence that the bright issuing vapour was really its source, since the limits corresponded in the vertical direction

The series line 1850 (1S — 1P) of the arc spectrum came out very definitely. This is important, since in the former paper it was found to weak be in the vapour.

The lines 1974, 1943, 2003 also came out strongly, in the above order of intensity, different from the order of intensity in the arc, in which 1943 is the strongest

Judging by these examples, it would seem that there is no absolute distinction between lines which appear in the arc only, and those which appear in the distilled vapour as well These lines in the remote part of the spectrum were only obtained when the exposure was so prolonged that the region of the strong series triplets was fogged by diffused light. It would therefore be more difficult to extend the test to the less refrangible lines in the above list.

Mercury is not a very suitable metal for this particular part of the investigation, because the enhanced lines are not very strong, and are not situated in a very accessible part of the spectrum Experiments have therefore been carried out with magnesium and calcium The arrangement used for observing the jet of luminous vapour will be described in § 3 of this paper, in another connection Here it is enough to say that it was similar in principle to the arrangement used for mercury, except that the vapour expanded into an open space, instead of being led along a silica tube

The photograph No. IV shows the spectrum of the magnesium jet focussed on the slit of the spectrograph, the vertical magnification of the reproduction being twofold as compared with the actual height of the vapour jet. It will be seen that the pair of enhanced lines 2795–2802 due to ionised magnesium appear at the base of the jet The arc triplets are marked at the top of the photograph by their series designation and by the wave length of the middle

member It will be seen that as compared with these the enhanced pair quickly fade out as the vapour moves up.

It is remarkable that the resonance lines (flame lines) of the magnesium spectrum 2852 (1S — 1P) and 4571 (1S — $1p_2$) fade out quickly, like the enhanced lines.

In the case of 2852 (1S — 1P) this is seen in No IV, though with the small dispersion used, the line is somewhat involved with the triplet $1p$ -- $4d$ Nevertheless on the original negative it is quite clear that 2852, less refrangible than the triplet, is the line which quickly fades out.

The same is seen without complication in the case of 4571 (1S — $1p_2$) See V from another part of the same negative, showing 4571 in contrast with the diffuse series of singlets.

The behaviour of 1S — 1P and 1S — $1p_2$ of magnesium is surprising, in the first place because the diffuse triplets and singlets, which are intermediate between the resonance lines and the spark lines in facility of excitation, yet persist longer than either of them In the second place, it is surprising because mercury shows most strongly the opposite behaviour. The resonance line 1S — $1p_2$ of mercury 2537 grows continuously in intensity relative to all the mercury lines as the vapour moves away from the orifice *

In the case of calcium, the enhanced lines H and K are conspicuous in the distilled vapour They do not die out quickly like the enhanced lines of magnesium, but maintain their intensity approximately *pari passu* with the triplets of the arc spectrum. The resonance line 4227 (1S — 1P) also dies down at about the same rate as the above. On the other hand, the resonance line 6572 (1S — $1p_2$) gains intensity relative to all the above, behaving in this respect like the corresponding mercury line

It would seem that these facts must ultimately prove important, but they do not fall into any obvious generalisation at present.

§ 3 *Excitation of a Metallic Vapour by Contact with Another previously excited.*

The importance was early recognised of determining whether other metallic vapours, introduced into the jet of glowing mercury, would be excited to luminosity, and if so, under what limitations This question was considered in 1914, but, owing to the circumstances of the time, no experiments were then made. Since then, the advance of knowledge has put the whole subject in a much more definite light. The theoretical considerations of Klein and

* *Loc. cit.*, pp. 267–269.

Rosseland* indicated that collisions " of the second kind " should occur between excited atoms and electrons, resulting in the transfer of energy from the excited atom to the electron, with gain of kinetic energy by the latter. An extension of this conception lead Franck and his school to the idea of direct excitation of one atom by another previously excited. The experiments of Franck and Cario† showed that mercury vapour emitting resonance radiation under the influence of λ2537 could excite the line emission of thallium vapour mixed with it. The lines excited had, however, in some cases a greater excitation potential than the 4 86 volts which the excited mercury atoms could afford. To explain this, supplementary hypotheses were made

Finally, Saha and Sur‡ suggested that active nitrogen derived its power of exciting the spectra of other substances by this mechanism They regarded active nitrogen as a molecule energised to the extent of about 8·5 volts §

The experiments so long contemplated have been recently carried out. Luminous mercury vapour distilled from the arc in a silica tube apparatus (somewhat as shown in ' Roy Soc Proc ,' A, vol 108, p 264) was passed over a piece of sodium As soon as the tube was heated so as to raise sodium vapour, a strong yellow glow was observed, starting from the sodium and proceeding down stream. It was observed visually that lines of the diffuse and sharp series were present as well as the D line. Similar experiments were made with magnesium and cadmium instead of sodium.

This experimental arrangement, though it showed conclusively and at once that the effect sought for really occurs, was not very convenient for its further study ; for it was not well applicable to obtaining a jet of luminous vapour from metals other than mercury · and the quartz tube was obscured by formation of an amalgam of the metal under investigation , thus only an intermittent and unsatisfactory view was obtained.

I have previously described|| a method of observing these luminous jets with the more volatile metals in general The arc was produced in a silica or quick-

* ' Zeits f Physik.,' vol 4, p. 46 (1921)

† ' Zeits f. Physik.,' vol 17, p 202 (1923).

‡ ' Phil. Mag ,' vol. 48, p. 421 (1924).

§ The view taken by Saha and Sur is interesting and suggestive, but I cannot regard it as free from serious difficulty. In particular, attention may be drawn to some experiments which I described in 1912 (Strutt, ' Roy Soc. Proc.,' A, vol 86, p 264 (1912)) These experiments show that active nitrogen emits its energy most rapidly when compressed to a small volume. It is difficult to explain this except on the view that a bimolecular reaction is taking place, or at least that collisions determine the emission of light.

|| Strutt, ' Roy Soc Proc ,' A, vol 90, p. 364 (1914)

lime tube with a metal cap as anode The vapour raised by the heat of the arc was allowed to rush out through a hole in the anode into an evacuated bell jar, in which the silica tube was mounted. In returning to the study of the luminous jets, various improvements of technique have been made, and the methods are worth recording, though no doubt capable of further improvement The following description should be read with the help of the three

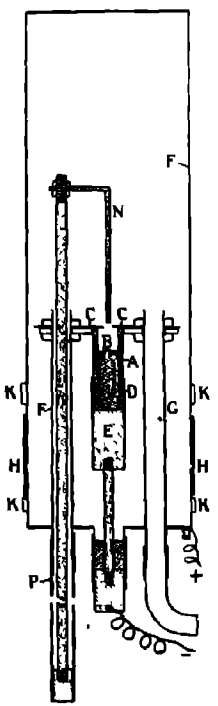

Fig 3

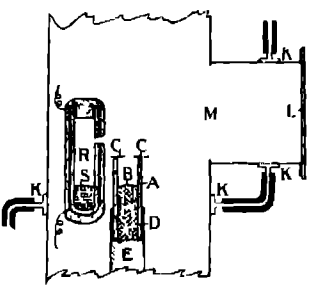

Fig 4

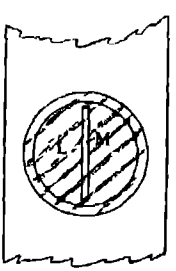

Fig 5

diagrams, figs 3, 4, 5 (one-quarter actual scale). Fig 3 shows a section through a vertical diametral plane of the apparatus.

Fig. 4 shows a section through a diametral plane at right angles to the former

Fig. 5 shows the elevation in the same aspect as fig. 3.

The arc is produced in a silica or alundum tube A, figs 2 and 3. This tube contains the metal under investigation B, the surface of which serves as cathode. The nickel plate CC serves as anode. A rests in the steel tube D,

into which it is packed with mica D fits on to a solid steel cylinder E, from which the cathode connection is led out airtight and insulated as shown. C is supported by the tubular brass pillars F and G (fig 3) and the anode connection is made to the body of the apparatus The latter is in two parts, united by a rubber sleeve H (fig. 3) This is made airtight by rubber solution and by thin steel wires. Each wire takes one complete turn round it, and is kept in tension by elastic bands attached to fixed supports (not shown) The metal casing is kept cool by three ring water-jackets KKK A stream of cold water goes through these in series The vacuum is maintained by exhaustion through G. The luminous vapour issues through the hole in C into the space above It is observed through the silica window L, fastened on with soft cement At M there is a slit in the main vessel, affording only limited access to the side tube carrying the window L This is designed to avoid the obscuration of L by a film of deposited metal, and succeeds fairly well in most cases. The rod N, fig 3, serves to strike the arc For this purpose it is pulled down for a moment into the discharge tube B, to make contact between cathode and anode The rubber tube P, kept from collapsing by a spiral spring, can be stretched to allow of this movement N is tipped with tungsten to prevent the end fusing into a knob It is turned aside when out of use, so as not to interfere with the issuing vapour. Light is reflected into the apparatus with a piece of mirror glass when using the striker

This completes the arrangements when the glowing jet from any one metal is to be examined (see above, p. 16) The electric resistance furnace R (fig 4) is to afford the (non-luminous) vapour of a second metal S, which issues transversely from the small hole and mixes with the luminous vapour of the first metal B In some cases the spectrum of S is excited thereby. The furnace R is made on an alundum tube, and the nichrome winding is lagged with alundum cement

It will be noticed that indiarubber was freely used in the apparatus, and it greatly facilitated the work. Any vapour that comes out of it is of small consequence compared to the large quantity of gas that comes out of the metals vaporised in the experiment. A Gaede rotating mercury pump was used and served the purpose, though more pumping power would sometimes have been desirable for rapidly removing this gas. The vacuum required in the experiments is not high. About ·2 mm. of mercury is quite good enough. A glass spectrum tube connected with the pumping system, and excited by a small induction coil, forms a convenient gauge of this, and gives warning by the spectrum whether air is leaking in.

The soldered joints of the metal vessel were coated with rubber solution to protect them when mercury was evaporated in the apparatus.

To control the amount of the metal S evaporated from the furnace R (fig 2) the furnace was weighed before and after the experiment

If an experiment of this kind apparently gives a positive result, anxiety is naturally felt as to whether the vapour of the metal S or condensed metallic particles from it have not gained admission to the discharge tube A If this happened, the result would be made ambiguous, because the arc would pass through the vapour of the metal S mixed with the vapour of B and S would be subject to direct electrical excitation

After trying various methods, I came ultimately to keeping the arc running continuously in the discharge tube throughout an experiment This ensured a constant outward stream of the vapour of B, and seems to afford satisfactory security that the vapour of S could not enter the discharge tube to any appreciable extent. The latter vapour was only generated by closing the current in the heating circuit of the furnace *after the arc was started*

In some cases it was possible to check the success of these precautions by observing or photographing the spectrum of the arc in the discharge tube simultaneously with that from the glowing vapour above it in the external vessel. This could be done when the metal B was zinc cadmium or mercury, for in these cases the arc was produced in a translucent silica tube, which was not chemically attacked, and allowed the arc to be observed through it in conveniently reduced intensity. The absence of lines of the metal S was then observed in the discharge tube, combined with their presence in the space above the lines of metal B showing in comparable intensity in each In other cases when the walls of the discharge tube were opaque, it was impossible to apply this test But it always proved reassuring in the cases where it could be applied See the photograph No VI, which shows the spectrum of the cadmium arc below (intensity reduced by the translucent silica tube) and the luminous cadmium vapour jet above, into which zinc vapour is introduced, and which shows the zinc lines in addition Cadmium wave lengths are marked below, zinc wave lengths above

In carrying out the experiments there was a danger of missing the opportunity when vapour of the metal S was coming off in the most favourable quantity for its lines to be excited strongly. To avoid this, successive exposures were taken continuously during the experiment. Each exposure was usually of one or two minutes' duration, though in some cases more. Visual examination of the spectrum often indicated when the conditions were right, but with a

continuous photographic watch, this was merely supplementary. It does not, of course, show what is happening in the ultraviolet region, which is often the most important

The photographs were taken with a small size Hilger quartz spectrograph, using a quartz-fluorite achromat to produce on the slit a reduced image of the issuing jet of luminous vapour The reduction was about fivefold, and allowed nearly the entire height of the jet as limited by the window (5 cm.) to be projected on the slit if necessary. It was often more convenient, however, to limit the length of the spectrum lines to the bright part of the glow.

Each experiment was continued from 10 to 20 minutes, and in most cases there was no difficulty in maintaining the luminous jet for so long. Obscuring of the window by deposited metal was a residual source of trouble; the arrangements for mitigating it were usually adequate, but least so when sodium was in use

It was not desirable to let the vacuum in the apparatus become too good, since in that case the jet becomes very large and diffuse, and its intrinsic brightness is diminished. Moreover, there is danger of parasitic discharges taking place outside the discharge tube proper By checking the pumping when necessary, the jet would be limited to a height of 1 or 2 cm. It was then very bright and well defined, and this was the condition best suited to the experiments The arc current was usually about 10 amperes, which was necessary to maintain the evaporation In the special case of mercury much less is desirable

The following tables give the lines observed to be excited in the various cases, together with the calculated excitation potentials. They are arranged so as to bring together the results for the metal S (in the nomenclature used above) when the metal B distilled from the arc is varied.

The various triplets of magnesium calcium and mercury are denoted each by its middle member but it is to be understood, of course, that when this was present its companions were present as well.

Excitation of Sodium.

Exciting Metal	Ionisation Potential of Same	Principal Doublets	Diffuse Doublets	Sharp Doublets
Cadmium	8 95 volts	to $1\sigma - 4\pi$ λ 2680 4 60 volts	to $1\pi - 5\delta$ λ 4066 4 72 volts	to $1\pi - 5\sigma$ λ 4750 4 09 volts
Mercury	10 4 volts	to $1\sigma - 3\pi$ λ 2953 4 32 volts	to $1\pi - 4\delta$ λ 4960 4 57 volts	—

Excitation of Magnesium

Exciting Metal	Ionisation Potential of Same.	$1S - 1p_2$ λ 4571 2 70 volts	$1S - 1P$ λ 2832 4 33 volts	Diffuse Triplets	Sharp Triplets	Diffuse Singlets	Spark Spectrum 2795 2802 12 0 volts
Sodium	5 13 volts	—	Masked, if present	—	—	—	—
Cadmium	8 95 volts	—	Masked, if present	to $1p - 5d$ λ 2734 7·20 volts	to $1p - 4s$ λ 2278 7 13 volts	to $1P \cdot 6D$ λ 4167 7 28 volts	Present 12 0 volts
Mercury	10 4 volts	—	Present 4 33 volts	to $1p - 3d$ λ 3093 6 67 volts	to $1p - 1s$ λ 5172 5 07 volts	—	—

Excitation of Calcium

Exciting Metal	Ionisation Potential of Same.	$1S - 1p_2$ λ 6572 1 89 volts	$1S - 1P$ λ 4226 2 92 volts	Diffuse Triplets	Sharp Triplets	Spark Spectrum 3934 K 3968 H 9 19 volts
Magnesium	7 61 volts	—	Present 2 92 volts	to $1p - 3d$ λ 3631 5 26 volts	—	—
Cadmium	8 95 volts	Present 1 89 volts	Present 2 92 volts	to $1p - 5d$ λ 3215 5 71 volts	to $1p - 3s$ λ 3475 5 43 volts	Present 9 19 volts
Zinc	9·35 volts	Not examined	Present 2 92 volts	$1p - 2d$ λ 4435 4 65 volts	—	9 19 volts
Mercury	10 4 volts	Not examined	Present 2 92 volts	$1p - 2d$ λ 4435 4 64 volts	—	Present 9 19 volts

Excitation of Zinc.

Exciting Metal	Ionisation Potential of Same	$1S - 1p_1$ λ 3076 4 01 volts	$1S - 1P$ λ 2139 5 77 volts	$1P - 2D$ λ 6362 7 69 volts	$1p - 2d$ λ 3302 7 74 volts	$1p - 3s$ λ 2684 8 60 volts.
Sodium	5 12 volts	—	—	—	—	—
Magnesium	7 61 volts	—	—	—	—	-
Cadmium	8 95 volts	Present 4 01 volts	—	—	—	Doubtful
Mercury	10 4 volts	Present 4 01 volts	Present 5 77 volts	Present 7 69 volts	Present 7 74 volts	Present 8 60 volts

Excitation of Cadmium

Exciting Metal	Ionisation Potential of Same	$1S - 1p_1$ λ 3261 3 78 volts	$1S - 1P$ λ 2288 5 30 volts	$1P - 2D$ λ 6438 7 30 volts	Diffuse Triplets to $1p - 4d$ λ 2677 8 38 volts	Sharp Triplets to $1p - 3s$ λ 2775 8 22 volts
Sodium	5 12 volts	Present 3 78 volts	—	-	—	—
Magnesium	7 61 volts	Present 3 78 volts	Present 5 30 volts	Present 7 30 volts	Present 8 38 volts	Present 8·22 volts
Zinc	0 35 volts	Present 3 78 volts	Present 5 39 volts	Present 7 30 volts	Present 8 38 volts	Present 8 22 volts
Mercury	10 4 volts	Present 3 78 volts	Present 5 39 volts	Present 7 30 volts	Present 8 38 volts	Present 8 22 volts

Excitation of Mercury

Exciting Metal	Ionisation Potential of Same	$1S - 1p_1$ λ 2537 4 86 volts	$1s - 1p$ λ 4358 7 70 volts	$1p - 2d$ λ 3130 8 80 volts
Sodium	5 12 volts	—	—	—
Magnesium	7 61 volts	—	—	—
Cadmium	8 95 volts	—	Present 7 70 volts	—
Zinc	0 35 volts	Present 8 46 volts	Present 7·70 volts	Present 8 80 volts

In addition, it has been found that neither hydrogen nor helium shows any visual line when introduced into the mercury vapour jet. Hydrogen requires

more than 15 volts to excite it, while helium requires more than 20 volts Singly ionised mercury can only supply 10·4 volts,

It will be noticed that so far as lines of the arc spectrum are concerned, the excitation potential of the observed lines rarely exceeds the ionisation potential of the exciting metal. It is natural, therefore, to regard the excitation as due to single collisions with ionised or excited atoms of the latter metal

There was, however, one distinct exception In the case of cadmium the series triplet $1p - 4d$ requiring 8 38 volts was excited by magnesium, which has an ionisation potential of 7·61 volts only.

The data of the present investigation are not adequate to settle the explanation of this. Franck and Cario (*loc cit*) have given reasons for believing that the kinetic energy of translation of the interacting atoms should be added to the energy of the exciting atom in order to determine the total energy available Having regard to the temperatures involved, this cause would probably be enough to contribute the energy of less than one volt which is needed to make up the deficiency. There is, however, another possible explanation, the emission of the Mg^+ lines 2795 and 2802 shows that some of the magnesium atoms carry an energy of 12 volts, and if these come into action their energy is, of course, more than enough to satisfy the requirements

The question arises, how much stress can be laid on negative results as a general confirmation of the point of view that excitation is determined by the ionisation potential of the exciting metal It is difficult to give any definite answer. If excitation is not observed, the possibility always remains that longer exposure or more favourable experimental conditions might have brought it out. and the technique of the present work, so far as developed at present, hardly admits of a variation of, *e g.*, the densities and relative proportions of the interacting metals over wide limits. In this work we have no evidence so satisfactory as, for instance, the abrupt appearance of a line at a certain excitation potential, which gives definite significance to its non-appearance below that potential

Speaking generally, if the spectrum of the metal B (fig 4) comes out very strongly on the plate, and if a gram or more of the metal S has been evaporated into the luminous jet, the absence of *any* of the lines of S is probably a fairly reliable indication that no excitation has taken place. It must be admitted, however, that in certain cases when the conditions are apparently favourable, the excitation is by no means strong. For example, the excitation of mercury by the cadmium jet is very feeble, though quite definite both by visual and photographic observations. It would not seem that this faintness can easily

be brought into relation with the excitation potentials. For the resonance line $1_1S - 1p_2$ (2537) of low excitation potential was not seen at all. Yet it is ordinarily as intense as the triplet of much higher potential actually observed. Indeed, it was expected that this resonance line would readily appear alone, that is to say in the absence of other mercury lines, when a metal like sodium of low ionisation potential was used to give the luminous jet: but this was never observed with mercury The analogous experiment with cadmium did succeed, however, as the table shows. The experiments using a sodium jet were less satisfactory and less often repeated than I could wish, owing to lack of adequate air pumps to carry off the large quantities of gas given off by this metal. Many attempted experiments failed from this cause.

In certain cases enhanced lines of the metals are excited. Thus it was observed that the magnesium lines 2795 and 2802 were excited by cadmium, and that the H and K lines of calcium were excited by either cadmium or mercury It seems impossible that the magnesium line mentioned could be excited by collision of the normal atom of magnesium with the singly ionised atom of cadmium unless the latter had itself undergone further excitation; but the spectrum obtained with cadmium alone does not show any of the (strong) spark lines of this metal. It would seem, therefore, that we are thrown back on the alternative of ionisation and further excitation of the magnesium in two separate stages. There are, however, difficulties in understanding the appearance of the enhanced lines in the luminous jet of magnesium alone, which appear to aggravate those dwelt upon last year (*loc. cit.*, p. 277). I cannot help thinking that we have much more to learn before the theory of metastable states can be considered to be on a satisfactory basis.

My assistant, Mr R Thompson, has given valuable help in carrying out these experiments.

§ 4. *Summary.*

In this paper observations are described on the jets of luminous vapour distilled from metallic arcs further to those in 'Roy. Soc. Proc.,' A, vol. 108, p. 262 (1905).

It is shown that the appearance of high series members in the luminous vapour is due to their narrowness In the arc these lines are so broad as to overlap one another. As the vapour emerges and expands, they become narrow and can be resolved.

Enhanced lines occur in the distilled vapour though in diminished intensity relative to the arc lines. In some cases, *e.g.*, magnesium, they fade out very rapidly compared with the arc lines.

2630
1P-7d
2668
1P-6d
2733
1P-5d
2778
1P-4s
2848
1P-4d
2938
1P-3s
IV
2782
2779
2795
2802
Mg+
2852
1S-1P
3832
1P-2d
4057
1P-7D
4167
1P-6D
4352
1P-5D
4703
1P-4D
5173
1S-1P
V
4571
1S-1P2

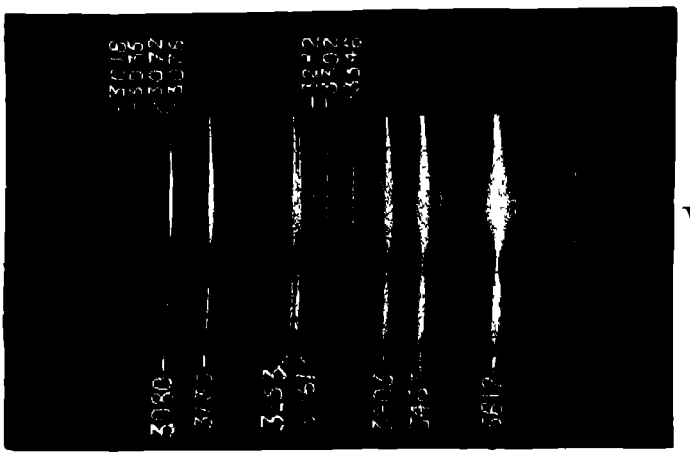

VI

(*Facing p. 29*)

The resonance line of mercury $1S - 1p_2$ gains intensity relative to all other lines as the vapour matures. The same is true of calcium, but the corresponding line of magnesium behaves in the opposite manner, dying out more quickly than the series lines in general.

A luminous jet of one metallic vapour is able in many cases to excite the vapour of another metal injected into it. As a rule such excitation does not take place unless the ionisation potential of the first metal exceeds the excitation potential of the spectrum line in question. There are, however, some exceptions to this rule, and possible explanations are discussed.

DESCRIPTION OF PLATES.

Plate 1

I.—Spectrum of mercury vacuum arc

II.—Spectrum of mercury vapour distilled from the arc. Lines of the diffuse series $1p_1 - md$ are marked on the strip between I and II. Note development of higher member of the series in the vapour

III.—Spectrum of glowing mercury vapour. The middle of the length of each spectrum line is from the dense vapour immediately it has left the arc. The ends of the lines are from the expanded vapour. Note the diminishing breadth of lines of the diffuse series

Plate 2

IV.—Spectrum of a jet of glowing magnesium vapour as it emerges from the arc into a field free space. The spectrum is in focus with the jet itself Note that the spark lines die out much more quickly than the series triplets. Vertical magnification about twofold.

V.—Another region of the same spectrum Note the short extension (and therefore duration) of the resonance line $1S - 1p_2$.

Plate 3

VI.—Excitation of zinc vapour by injecting it into cadmium vapour previously excited. The arc spectrum below. Cadmium lines marked The distilled vapour spectrum above. Zinc lines marked.

The Freezing of Gelatin Gel.

By T Moran.

(Food Investigation Board of the Department of Scientific and Industrial Research and Low Temperature Research Station, Cambridge)

(Communicated by Sir William Hardy, F R S —Received June 10, 1926)

[Plate 4]

"Ash-free" gelatin supplied by the Eastman Kodak Company was used throughout The actual content of ash was found to be 0 05 per cent of the dry weight To prepare gels of known strength, the requisite amounts of gelatin and water were left together overnight and then heated at 60° to 80° C on a water-bath for the least time required to produce a homogeneous solution When dissolved in distilled water, the hydrogen-ion content of the gel was found to be $10^{-4\cdot7}$ gram ions per litre (*i e*, $p_H = 4\cdot7$), which is the iso-electric point for gelatin.

Save where the contrary is stated, discs of gel as nearly as possible 1·5 cms in diameter and 0 3 cm in thickness were used

The behaviour of the gels on freezing and thawing was examined from three standpoints . —

(1) The micro-structure produced by freezing

(2) The quantitative determination of the ice which separates

(3) The volume changes.

No assumptions were made as to the structure of the gels, although a certain amount of evidence was obtained as to the molecular nature of the individual gelatin-water complexes.

1 *Micro-Structure produced by Freezing.*

As is well known, freezing and thawing alter the configuration of colloidal systems whether gels or sols, and the resulting structure depends upon the rate of freezing. Stiles* has summarised the work of previous investigators. The structure is due to the fact that on freezing a gel ice separates, leaving relatively dehydrated gel, and on thawing all the water is not at once or indeed readily reabsorbed

* Special Report No. 7 of the Food Investigation Board." Published by H M. Stationery Office (1922).

Only a qualitative study of the subject was attempted under this heading Cooling was not measured, but was broadly classified as very rapid when the freezing agent was liquid air or in air at — 19° C, as medium in air at — 11° C, and slow in air at — 3° C The structure produced was found to depend upon the rate of freezing and the strength of the gel, the latter is given in percentages, namely, grams dry gelatin in 100 grams gel

Sections were cut at the freezing temperature (— 3°, — 11° or — 19°), save when liquid air was used, all the implements being at this temperature, and were then at once dropped into 40 per cent. formaldehyde at the freezing temperature.

After freezing by dropping the discs into liquid air they were removed to — 11° C and sections cut at that temperature The following is a brief description of the results obtained –

Gel 12 per cent –(*a*) Frozen in air at — 11° C (fig 1). In the interior of the gel are a number of irregular spaces each of which contains a sponge of gel Between these spaces is homogeneous gel Freezing obviously must have started at a relatively small number of centres in the interior Freezing also starts on the surface of the gel because it was found to be covered by a thin shell of ice

(*b*) Frozen in liquid air (fig 2) The interior of the gel is now occupied by a large number of clear spherical spaces each about 3μ* in diameter and arranged in rows Each space represents a distinct centre of crystallisation. No detectable quantity of ice formed on the surface of the gel

(*c*) Frozen in air at — 3° C No spaces are found in the interior Freezing takes place wholly on the surface, where a thick shell of ice forms which encloses a core of dehydrated gel

These observations prove that there are two groups of possible centres of crystallisation, external and internal, and that the former are prepotent because, when the degree of overcooling is not too great, they alone function The external centres may be supposed to be situated in a layer of insensible thickness of very dilute solution of gelatin covering the surface.

At medium rates of cooling the external and a few only of the internal centres function.

* The diameter of the gelatin masses between these ice spaces is roughly of the same order of magnitude. It is interesting, therefore, to cite the observation of Hardy ('Roy Soc Proc.,' vol 66, p. 95 (1900)) He dissolved 13 5 grams of gelatin in 100 c.c. of 50 per cent. alcohol and found that on cooling fluid droplets appeared of the order of 3μ which later went solid and linked up in linear rows.

Freezing at − 19° C. in air was found in effect to be very rapid cooling, the resulting structure resembling that given by liquid air.

It should be mentioned that whereas the appearance shown in figs. 1 and 2 persisted for some days at least in the thawed state, the core of the disc frozen at − 3° C. was perfectly clear and transparent and readily reabsorbed water until its concentration was again 12 per cent., in other words, it was completely reversible.

Gels weaker than 12 *per cent.*—The important difference was that at − 3° C. some internal centres were active, the appearance being that shown in fig. 1. Therefore the weaker the gel the slower must the rate of cooling be wholly to suppress internal centres of crystallisation.

Strong Gels—38 *per cent* —Frozen in air at − 11° C. An entirely new form of freezing now appears The irregular growth of ice crystals resulting in the irregularly shaped spaces, shown in fig. 1, with their contained sponge is replaced by a regular disposition of shells of alternate ice and gel disposed concentrically about the original centre of crystallisation. The spheres so formed are shown in fig 3.

The structure of a sphere was detected by dissecting out one whilst still frozen, fixing it with 40 per cent. formaldehyde, and cutting sections, the whole operation being carried out at − 11° C The concentric layers of ice and gel are shown in fig. 4

The effect of rate of cooling upon the growth of these larger spheres is complicated Another sample of the same gel was kept at − 11° C. until the spheres just began to appear. It was then transferred to − 3° C. to complete the freezing. The spheres now no longer had the structure shown in fig. 4. There was presumably a central nucleus of concentric shells of ice and gel as described above, and no doubt formed at the higher rate of cooling, and about this a thick shell of continuous ice. The arrangement of concentric shells therefore appears to need for its formation a rate of cooling lying within certain limits. At the lower rate it was replaced by continuous ice formation.

Rohonyi* obtained by an artifice concentric shells even in dilute gels (2 to 5 per cent.). In his experiments the gel was transferred alternately from − 10° C. to + 1° C

Fig. 5 gives a clue to the mode of formation of these rings. It represents the changes in volume of 6·56 grams of a 43·7 per cent. gel which supercooled to − 11° C. and finally froze at the same temperature, giving the same ice formation as in fig. 3. The progress of the freezing was followed dilato-

* 'Biochem. Z.,' vol. 53, p. 210 (1913).

Fig 1
(106 diams)

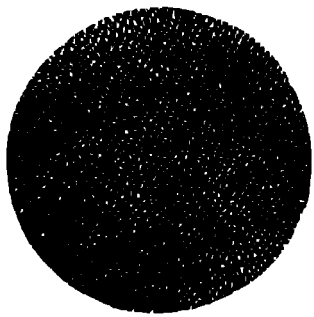

Fig 2
(× 106 diams)

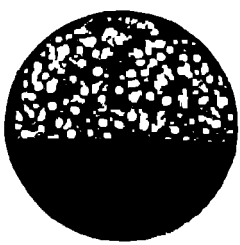

Fig 3
(× 0 7 diam)

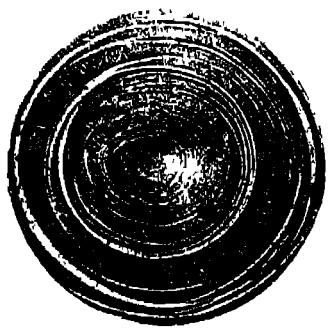

Fig 4
(× 27 diams)

(*Facing p* 32)

metrically (the technique of which is described later) and the ordinates represent capillary readings. It will be observed that complete equilibrium was only

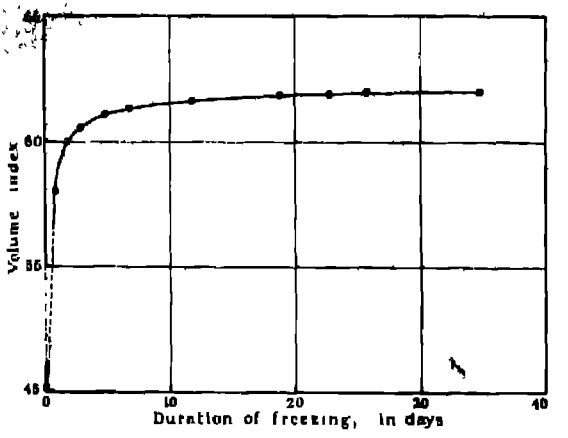

FIG. 5.

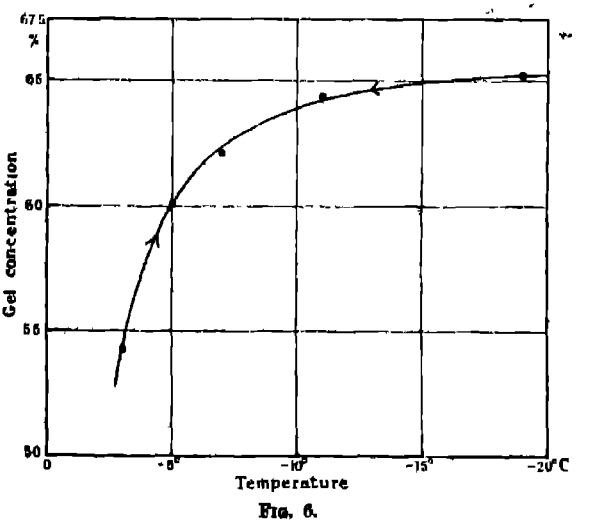

FIG. 6.

attained twenty-six days after freezing had begun. Let it be supposed that a heterogeneous mass of small ice crystals and particles of concentrated gel forms about each internal centre of crystallisation. As is shown in the next section,

the concentration of the gelatin particles will be greater the lower the temperature

Owing to the low diffusivity of the gel and the latent heat of fusion, the temperature at which the mixture of gel and ice forms will be higher than the external temperature (— 11°) Let us suppose that it is as high as — 1° C. The curve in fig 6 shows that, at this temperature, the concentration of gel in equilibrium with ice is approximately 50 per cent., whilst at — 11° the equilibrium concentration is 64·4 per cent. Now let the mass cool to — 11°. More ice will separate from the gel particles, and in this way, by alternate warming and cooling, shells of ice will form

The spheres (fig 3) gradually disappear on thawing, leaving behind in each case a small hole in the gel

Gels from 12 per cent to 40 per cent.—Frozen in air at — 3° C , ice was formed only on the surface Moreover, it was found that this surface ice formation is independent of the external medium and was obtained when the discs were immersed and frozen in organic solvents such as benzene and toluene It does not depend, therefore, on chance seeding by crystals of ice floating in the air.

2 *Phase Equilibrium between Ice and Gel*

The fact that with discs of gel frozen at — 3° C containing not less than 12 per cent gelatin, ice separated only at the surface on freezing was used to determine the ice-gel phase equilibrium at various temperatures. At concentrations of gelatin between 12 per cent and 40 per cent , with gels at the iso-electric point, it was found that on slow freezing in air at — 3° C water passed into the external shell of ice until the gel had reached a constant composition of 54 3 per cent gelatin When equilibrium had been reached at this temperature, some of the discs were transferred to lower temperatures, when more water moved from the core to the shell In this way the equilibrium concentrations of gelatin were obtained for different temperatures, and the results are plotted in fig 6.

The actual experimental figures are given in the following table :—

Table I

Temperature	Gel Concentration.
C	Per cent
- 3°	54 3
- 5°	60 1
— 7°	62 1
—11°	64 4
—19°	65 2

Each point on this curve is the mean of eight separate analyses and represents a true equilibrium value for the analyses, which for any one temperature extended over a period of days, showing no evidence of a trend, and the same point was reached whichever way it was approached along the curve. For example, several discs of an 18 6 per cent. gel were frozen at — 3° C and stored at that temperature for five days. Six were then transferred gradually to each of the temperatures —5°, —7°, —11° and —19° for seven days Another six were plunged into liquid air for a few minutes The discs were then all brought back to — 3° C for 24 hours. The ice layer was then removed and the gelatin cores analysed. The core in every case was 54·3 per cent within the experimental error. The drying of gelatin gel between 54·3 per cent and 65 5 per cent seems to be truly reversible The lower limit of concentration is presumably that gel in which free water appears first, *i e* the gel which on further swelling suffers no contraction of volume. Taffel* has shown that the contraction per 1 gram of gelatin is as complete in a 25 per cent as in a 2 per cent gel. The concentration is therefore greater than 25 per cent It is shown later that in a 52 1 per cent. gel which is reversible on freezing the last ice portion thaws at —0 8° C. Presumably the minimum concentration of gel which is reversible on freezing with no hysteresis is approximately 50 per cent, in which case the complete form of the curve in fig. 6 is S-shaped.

The curve reaches a constant level at a concentration of 65 to 66 per cent gelatin, therefore when the water content falls to 35 to 34 per cent, there is no separation of ice at any temperature. This was confirmed by immersing a 65·5 per cent. gel in liquid air, when it remained clear and transparent, showing that no ice had been formed All gels of lower concentration become white and opaque in liquid air

This undoubtedly suggests that water is present in the gel in two states, which may be distinguished as "bound" water and "interstitial" water. Bound water is merely water which is incapable of being frozen. It is possible that the bound water is held by the gelatin molecules to form molecular complexes, and that the spaces between these act as capillaries.

This theory has been applied to the silica molecule by Patrick† and his co-workers to explain many of its properties, particularly its adsorptive power towards various gases and organic solvents. On the same basis, that water in a gelatin gel which freezes below 0° C would be the capillary water. There

* 'J. Chem. Soc.,' vol 121, p. 1971 (1922)

† 'J. Amer. Chem. Soc.,' vol 42, p. 946 (1920); vol 44, p. 1 (1922); 'J Phys Chem.,' vol. 29, p. 1 (1925); vol. 29, p. 220 (1925).

is, however, no evidence that a gelatin gel has a capillary structure. Thus in a gel of concentration 65·5 per cent., presumably the capillaries are already in existence, and yet this gel will not absorb organic solvents. Until, therefore, more definite evidence is brought forward, the most satisfactory concept is to figure the gelatin molecule or aggregate being surrounded, first, by an envelope of combined water, and then by successive layers of non-combined water up to a critical distance depending upon temperature and the presence of other solutes, i.e. upon the dielectric constant of the aqueous phase. This is virtually the micellar hypothesis of Nageli (1858).

Taffel* comments on the striking curve obtained by Sheppherd and Sweet† for the relationship between the setting point and concentrations of gelatin gels. Between 0 and 65 per cent. the curve is hyperbolic to the axis of concentration, but at a concentration of gel between 65 and 70 per cent. there is a sudden change of direction in the curve, due, as he suggests, to the gelatin-water complexes touching one another and bringing into play force fields of considerable magnitude. He also cites the observation of Shroeder,‡ who exposed a strip of dry gelatin to saturated water vapour for 20 days and found that its weight increased from 0·904 to 1·318 grams, in other words, 1 gram of dry gelatin absorbs 0·414 gram of water to form a 70·0 per cent. gel. This water might be presumed to be the absorbed or bound water. The difficulty, however, in this type of experiment is to maintain the vapour in the saturated state. Unless most elaborate precautions are taken to ensure constancy of temperature, the humidity is often below the saturation point. Moreover, it is not at all certain that the system had reached equilibrium in 20 days.

The hypothesis that chemically held water or water of true hydration may be put as high as 0·53 gram per 1 gram gelatin raises many difficulties. There is evidence for putting it much lower, namely, at about 0·08 gram. Svedberg§ has measured the contraction in volume that occurs when 1 gram of gelatin in gels of various concentrations is dissolved in 100 c.c. of water. The curve, fig. 7, has been constructed from his figures. It shows the contraction in cubic millimetres per gram of gelatin when different weights of water are dissolved in it ($t = 35{\cdot}2°$ C.). The curve shows a sharp change of direction at about 0·08 gram water per 1 gram gelatin equal to a 92 per cent. gel.

Moreover, if discs of a 65·5 per cent. gel are immersed in anhydrous acetone

* *Loc. cit.*

† 'J. Ind. Eng. Chem.,' vol. 13, p. 423 (1921).

‡ 'Z. physikal. Chem.' vol. 45, p. 75 (1903).

§ 'J. Amer. Chem. Soc.,' vol. 46, p. 2673 (1924).

(which is continually replaced), they rapidly lose water, but eventually reach equilibrium at a concentration of gel in the neighbourhood of 94 per cent.

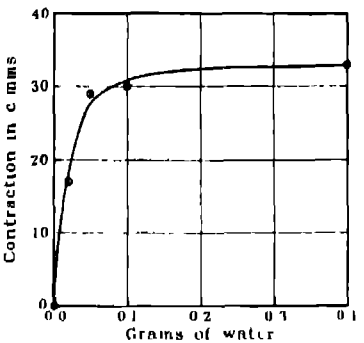

FIG. 7

A set of actual figures are shown in Table II

Table II

Number of days in acetone	Weight of gel disc
	grams
0	0 2468
2	0 1742
6	0 1732
12	0 1716
15	0 1716

Likewise, ordinary Kodak gelatin (water content = 16 4 per cent) under the same conditions gives a critical gel concentration of approximately 92 per cent. (Table III)

Table III

Number of days in acetone	Weight of gel disc
	grams
0	0 2154
2	0·2021
7	0·1966
10	0 1967

Fisher* also states that the rate of drying of gelatin gels is a linear function of the gel concentration until the water content has been reduced to less than 10 per cent. (*i.e.* a gel concentration > 90 per cent.).

It is in the very earliest stages of absorption of water that the greater part of the heat of mixing of gelatin and water is given off. Katz† has calculated that at the initial moment of swelling the heat liberated by 1 gram of gelatin for 1 gram of water absorbed is equal to 230 calories, whilst Wiedemann and Ludeking‡ found experimentally that the average heat of swelling at 18 4^{d} C. is 5·7 calories per gram.

Possibly water combines with the large gelatin molecule at more than one point, as Jordan Lloyd§ suggests, and that each has its own heat of combination and its own effect upon the specific volume.

3. *Changes in Volume of Iso-Electric Gels on Freezing and Thawing*

An attempt was made without much success to settle some of the difficulties raised in the last section by measurements of volume.

An ordinary glass bulb-capillary stem dilatometer was used with liquid paraffin (sp. gr. 0·880) as the displaced fluid. The capillary height could be read to 0·05 cm., and as 1 cm. of capillary had on the average a volume of 0·015 c.c. the volume measurements were accurate to 0·0007 c.c.

The expansion and contraction of the liquid paraffin was perfectly linear between + 15° and − 11° C., but increased more rapidly between − 11° C. and 19° C., so that 1 gram of liquid paraffin at − 19° C. contracted 0·00118 c.c. more than that given by extrapolating the straight line characteristic of the temperatures between + 15° C. and − 11° C. The cooling and warming curves were completely reversible, and there was no evidence whatever of capillary "creep."

Figs. 8 and 9 are the curves obtained with 23·5 per cent. and 52·1 per cent. gels respectively. The arrows indicate whether temperature was falling or rising. Starting at A, the volume falls uniformly until freezing begins in the super-cooled gel at B. Part of the water in the gel then freezes, accounting for the expansion BC. When the freezing is complete the volume again falls uniformly to D, the lowest temperature available for prolonged exposure. With a 23·5 per cent. gel D appears to be a true equilibrium point easily reached. No change of volume occurred in four days. With a 52·1 per cent. gel there is

* 'Roy. Soc. Proc.,' A, vol. 103, p. 673 (1923).
† 'Koll. Chem. Beihefte,' vol. 9, p. 1 (1917).
‡ 'Wied. Annalen,' vol. 25, p. 145 (1885).
§ 'Biochem. J.,' vol. 14, p. 147 (1920).

a slow increase in volume at $-19°$ C, which appears in figure as DD′ The increase in volume took 18 days for completion. D′ is now a true equilibrium

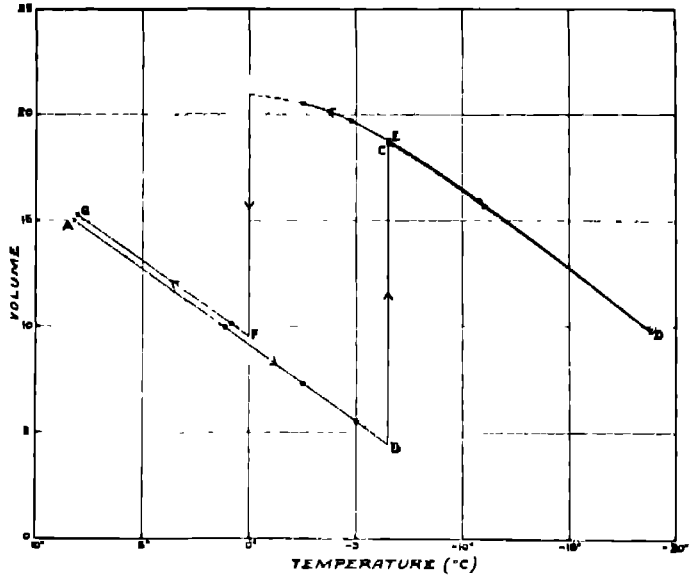

Fig. 8.

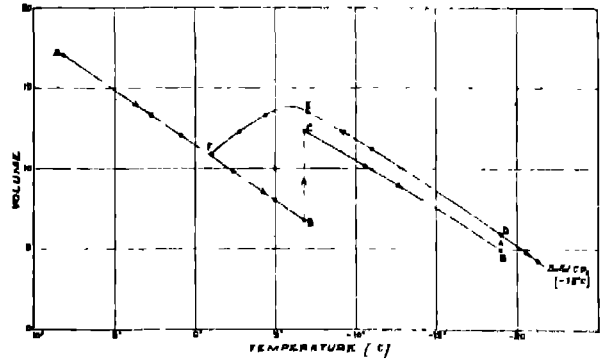

Fig. 9.

point, for on placing the bulb of the dilatometer in solid carbon dioxide (temperature $= -78°$ C) for a few hours, the same volume was attained on

re-warming to $-19°$ C This slow approach to equilibrium with colloids has not been realised sufficiently hitherto, but it is clearly an obvious point of criticism in all work of this nature, particularly static investigations. Thus, as already noted, true equilibrium was attained at $-11°$ C. with a small sample of a 43·7 per cent. gel in not less than 26 days

The storage time at each temperature for the two concentrations 23·5 per cent. and 52 1 per cent are given in the following table :—

Table IV.

Approximate temperature	Storage time	
	23 5 per cent	52 1 per cent
C	Days	Days
8°	2	2
1	1	1
- 3°	1	1
— 5°	1	1
- 7°	11	12
-11°	5	2
- 19°	4	19
11°	2	2
- 7°	2	3
- 5	3	4
— 3°	1	2
— 1°	—	1
+ 1°	2	—
8'	4	3

At each temperature constant volume readings were obtained a few hours (or days) earlier than the stated storage time

The reverse curve in figs. 8 and 9 at first diverges slightly from the freezing curve, *i e* DE and D'E are not parallel to CD This has been observed for different substances by other investigators, notably Foote and Saxton,* and is ascribed to the rupture of capillaries in the freezing process, with consequent increase in volume of the system as a whole

It will also be observed from the thawing portion (D'EF) of the curve in fig 9 that the bulk of the ice formed in a very concentrated gel (52·1 per cent) commences to thaw once a temperature of approximately $-6·5°$ C is reached. This is in agreement with the general shape of the curve in fig. 6, which steepens suddenly at about this temperature.

A second effect of concentration appears on thawing When the concentra-

* 'J. Amer. Chem Soc ,' vol. 38, p. 588 (1916), vol. 39, pp 627, 1103 (1917).

tion is high (*e.g.* 52·1 per cent. gel), the curve EF meets and fuses with the curve AB, but when it is low there is an increase in volume which persists into the fully thawed state. This volume increase, which is presumably the result of structural breakdown, may be regarded as a measure of the irreversible changes in the gel 52·1 per cent. and 43·7 per cent. gels showed no visible alterations as a result of the freezing cycle, and for these gels the increases in volume per 1 gram of gelatin are 0 and 0 0009 c.c. respectively The 11·5 per cent. and 23·5 per cent. were white and opaque on thawing, and, as would be expected, showed the greatest increase, namely, 0·0070 c c per 1 gram of gelatin in each case. This measure of the irreversible change merits further analysis. Apart from the concentration, the only other variable is the rate of freezing. With concentrated gels freezing proceeds at a very slow rate, whereas with the more dilute gels equilibrium is reached quickly The obvious question therefore arises as to whether, other factors being constant, the rate of freezing determines the extent of irreversibility in gelatin gels. To test this, discs of gel containing 5·25 per cent , 9·58 per cent. and 11·5 per cent. gelatin were prepared and weighed and kept for 2 days, some at $-3°$ C, others at $-5°$, $-7°$, $-11°$, $-19°$ C , and some in liquid air ($-190°$ C) for three minutes.

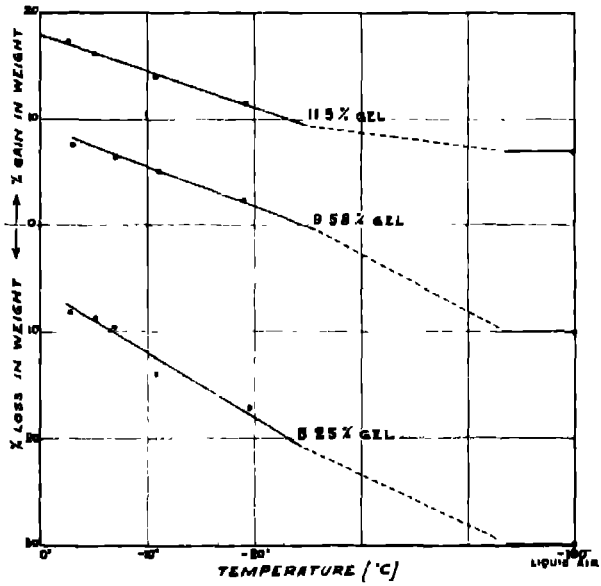

Fig. 10.

The discs at $-3°$ and $-5°$ C. were seeded with ice as soon as they were cooled to ensure freezing. All were then restored to $-3°$ C. for 24 hours and thawed in distilled water of p_H 4·9 at room temperature, the 5·25 per cent. and 11·5 per cent. gel discs for three days and the 9·58 per cent gel discs for two days. Each disc was then weighed after having loosely attached water rapidly blotted off with filter paper. The gain in weight then represents water absorbed by the gel, and this is plotted as a percentage against the temperature of freezing in fig. 10. The experiment was carried out, when necessary, under antiseptic conditions. The curves show that the more rapid the rate of freezing the slower was the uptake of water, *i.e.* the greater the freezing rate the greater the damage to the gel as determined by its subsequent affinity for water. A further point of notice was that in all cases the discs of gel which had been frozen at $-3°$ C. and thawed were quite transparent and apparently unchanged, whereas those which had been frozen in liquid air were densely white and opaque. The obvious suggestion, omitting a capillary hypothesis, is that in some way part of the bound water is removed by rapid freezing with a consequent increase in volume of the system, as opposed to the decrease in volume during normal solution. The reabsorption of this bound water, which will take appreciable time in the gel state, evidently precedes the further swelling of the gel. The validity of this suggestion is borne out by a detailed examination of the dilatometer curves.

Analysis of Dilatometric Results.—It has already been suggested that the bound water in iso-electric gels is approximately 0·53 gram per 1 gram of gelatin and that all the free and pseudo-free water is frozen out at $-19°$ C. Accordingly, an attempt was made to confirm these conclusions by calculating from the volume changes the amount of water unfrozen at $-19°$ C. The physical constants employed are all taken from Landolt-Bornstein Tabellen.

The density of ice at 0° C. is 0·9168, *i.e.* at 0° C. 1 gram of water in changing to ice increases in volume by 0·0907 c.c. This, however, is not true at $-19°$ C., since water and ice possess different co-efficients of expansion. Mohler gives the specific volume of water as low as $-13°$ C. Extrapolating, the specific volume of water at $-19°$ C. is 1·00563. Further, from Roth's data, the density of ice at $-19°$ C. = 0·9181, *i.e.* specific volume = 1·0892. Therefore, the increase in volume when 1 gram of water changes to ice at $-19°$ C. = 0·0836 c.c.

Table V shows in detail the results obtained with four concentrations of gel.

The apparent increase in volume (column 6) was read off from the curves, and is the difference in capillary height between AB produced and D (or D′) multiplied

Table V.

Conc of gel Per cent.	Total grams of water in gel.	Total grams of dry gelatin (a)	Grams of liquid paraffin.	Volume of 1 cm. length of capillary	Total increase in volume at $-19°$ C in c.c.	Increase in volume due to removal of water from gel ($a \times 0\ 026$)	Increase in volume due to water freezing (b)	Grams of water frozen out $\frac{b}{0\text{-}0836}$	Grams of water unfrozen.	Grams of water unfrozen per 1 gram of gelatin.
11 5	3 328	0 432	19·28	0 01515	0 2848	0 0112	0 274	3 278	0 050	0 12
23·5	2·923	0·898	14 06	0 01576	0·2396	0·0234	0 216	2·584	0 339	0·38
43·7	3 693	2 866	17 35	0 01331	0·2461	0·0745	0 172	2 057	1·636	0 57
62 1	2 046	2·224	11 53	0 01496	0 1258	0 0578	0 068	0 813	1 233	0 55

by the volume of 1 cm of capillary. To this is added a correction due to the expansion of the liquid paraffin ceasing to be linear with temperature.

Svedberg,* moreover, has shown that at 35° C. the contraction in volume when a 65·5 per cent gelatin gel containing 1 gram of gelatin is dissolved in a large excess of water is equal to 0 020 c c., *i.e.* this volume represents the contraction of interstitial water per 1 gram of gelatin at 35° C In the present experiments the gel froze between −7° C and −11° C., but no data are available as to the contraction in this region Taffel† gives 0 065 and 0·073 c c. at 32° C. and 15° C respectively as the total contraction when 1 gram of gelatin enters into solution. Assuming a similar proportionality for the contraction of interstitial water, it is concluded that its value at − 7° C is 0·026 c c. The factor, mass of dry gelatin × 0 026, is the volume in c.c to be subtracted from the observed increase in volume (column 6) to obtain the increase in volume due to the water freezing It will be noted that for the purposes of calculation it was first assumed that the unfrozen gel would be of concentration 65·5 per cent.

The table shows that with the 43·7 per cent and 52 1 per cent gels the average amount of bound water per 1 gram of gelatin is 0·56 gram, which compares well with the previously obtained value of 0 53 On the other hand, with the 11·5 per cent. and 23 5 per cent. gels, the amount of bound water is distinctly less It is inconceivable on a mass action basis that the extent of bound water should decrease with decreased concentration of gelatin. Some other factor is responsible It is suggested that during the freezing of the interstitial water in these two concentrations of gel, a portion of the more loosely bound water is mechanically torn away from the gelatin molecule Incidentally, this would explain the relatively large increase in volume of these two gels on thawing.

4. *Effect of the H-Ion Content upon Ice Separation.*

Gels containing 20 per cent gelatin with varying quantities of hydrochloric acid were moulded into discs, frozen at −3° C., the external sheet of ice removed, and the concentrated gel dried to constant weight at 105° C The time of storage in the frozen state varied from five to ten days, and constant analyses were obtained over the whole period In calculating the weight of gelatin, the combined acid was allowed for on the assumption that 10 grams of gelatin combine with 9 c c. of N . HCl.

In fig 11 the water per 100 grams of gelatin which does not freeze is plotted against the number of cubic centimetres of normal acid in the gel per 10 grams of

* *Loc. cit.*

† *Loc. cit.*

gelatin. At 9 c.c. of normal acid the curve turns sharply upwards and, according to the figures given by Harris,* Hitchcock† and others, all the acid up to

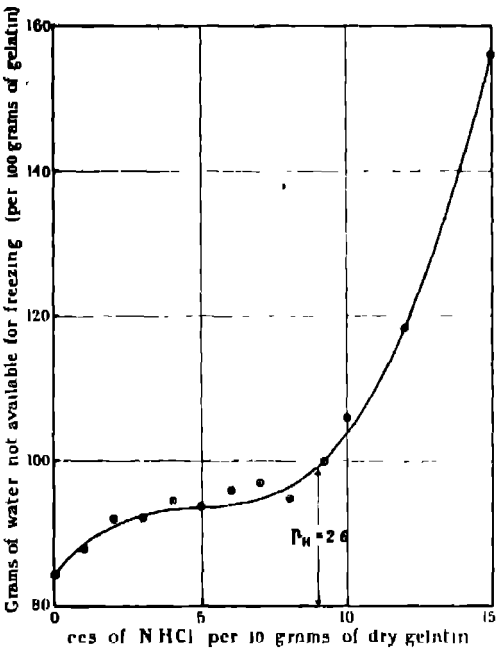

Fig 11.

this point will have combined to form gelatin hydrochloride. Along the ascending part of the curve there was, therefore, excess acid, and the decreasing availability of water for freezing may be ascribed to the lowering of the freezing point by the free acid.

So long as the acid is not in excess, the quantity added has relatively little effect upon the availability of the water. The availability of water is greatest at the iso-electric point.

If the available water be identified with the interstitial or free water of the gel, this result is in sharp contrast to the conclusions of Callow,‡ who found the velocity of crystallisation least at the iso-electric point and greatest at p_H 2 6

* 'Roy. Soc Proc.,' B, vol. 97, p 364 (1925).
† 'J of Gen. Physiol.,' vol 4, p. 733 (1922).
‡ 'Roy Soc. Proc.,' A, vol. 108, p. 307 (1925).

which corresponds to the inflexion point in the curve fig. 11. He concludes from this that the amount of available water is least at the iso-electric point.

Callow measured the rate of advance of the tips of the advancing ice face along a cylinder of gel cooled to — 3° C. and seeded with ice at one end. It cannot be supposed that there was equilibrium between ice and gel at these points On the contrary, behind the levels observed by Callow there would be left a mixture of ice and gel in which ice formation would continue The velocity recorded by him would therefore have little relation to the time required to convert all the available water into ice and cannot be used to determine when the available water is greatest or least. His velocities probably depended upon differences in the gel structure due to variations in the state of aggregation of the gelatin-water complexes.

In conclusion, I wish to express my thanks to my assistant, Mr. H. P. Hale, for his help in the experimental work

Summary

I. The freezing rate and gel concentration determines (*a*) the disposition of the ice in the frozen gel, (*b*) the extent of structural deformation in the gel.

II. When gels above a concentration of 12 per cent are frozen slowly, there is a clear-cut separation into ice and more concentrated gel, and the concentration of the latter is determined by the temperature.

III The existence of this phase equilibrium between ice and gel has been used to determine the state of the water in iso-electric and acid gels.

A Microscopic Study of the Freezing of Gel.

By Sir William B. Hardy, F.R.S.

(Department of Scientific and Industrial Research, Low Temperature Research Station, Cambridge.)

(Received June 10, 1926)

[Plate 5]

The curious spheres described by Moran, consisting as they do of a succession of shells, afford unmistakable proof that the formation of the ice phase inside a gel may not only vary in rate but actually intermit. This study was undertaken in the hope of throwing some light upon this phenomenon. It has revealed two unexpected facts, namely, that, save in very dilute gels, the course of internal freezing is usually intermittent, and that, instead of pure ice, a solid solution of gelatin and ice separates. Pure ice can and does sometimes form in the shape of rounded crystals scattered throughout the gel, but in the common type of freezing, by spheres or rays spreading from centres of crystallisation, it is always a solid solution which separates.

The current conception that the spongy structure found in gels after being frozen and thawed is due to crystals of ice is wrong. It is due to the de-solution on rise of temperature and fall of pressure of the solid solution mentioned above. Actually, so far as my observations go, when crystals of pure ice melt, the water is re-absorbed at once by the surrounding gel, leaving only a tiny cleft.

Neither the optical properties nor the behaviour on thawing of the ice phase support Moran's suggestion that it is at any stage a mixture of ice crystals and particles of dehydrated gel.

Part 1.—Microscopical Observations.

Freezing was watched under the microscope in cold chambers at $-7°$, $-11°$ and $-12{\cdot}7°$ respectively. All appliances and reagents were at the temperature of the chamber. With the exception of numbers 1, 2, 8 and 9, the figures are from free-hand sketches made as carefully as the rigorous conditions permitted of.

The process was followed in plates of gel, roughly 0·5 mm. thick, prepared by placing a drop of melted gel on a slip of glass, covering it with a very thin sheet of glass, and allowing it to set at room temperature. Ordinary medicinal

paraffin was run round the edge to prevent evaporation, and the preparations were stored at 0° for a few days before use

The following types of freezing were found :—

(1) Circles.
(2) Rays
(3) Disseminated.

Circles were undoubtedly the equivalent of the spheres observed by Moran. Each was about 0·5 mm. in diameter, and consisted of a central circular area surrounded by rings (fig 1) With high magnification the rings were seen to be

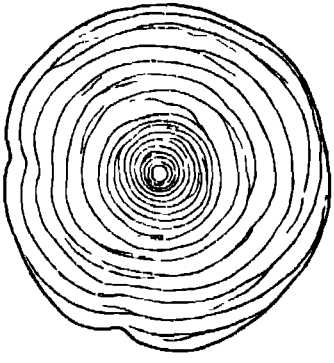

FIG. 1.

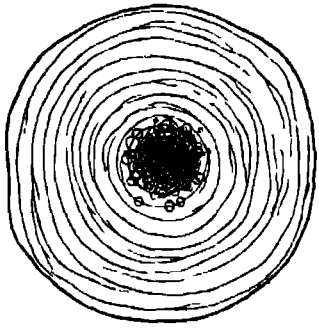

FIG. 2.

40 per cent. gel, frozen at −11° (× 100 diameters, from photographs).
FIG. 1.—A circle FIG. 2.—Secondary areas forming in central part of a circle.

separated from one another by membranes (fig. 3(*a*)), about 0·5μ thick, of dense gel, which were curved in a vertical plane. The structure, therefore, was that which would be produced by compressing one of Moran's spheres between two planes. The membranes separated zones of optically homogeneous material

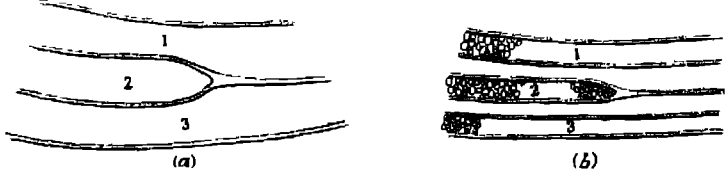

FIG. 3.—38 per cent. gel, frozen at − 11°. Part of a circle highly magnified · (*a*) before, (*b*) after, rapid thawing. To save time, the secondary areas, which now completely occupy zones 1, 2 and 3 were sketched in only in places

which appeared to be pure ice (fig. 3 (*a*)), but which, on thawing, was found to be a solid solution of ice and gelatin (fig. 3 (*b*)). Freezing obviously had been intermittent.

Rays, like circles, were always products of intermittent freezing, being divided by curved membranes into compartments filled by homogeneous solid solution (fig. 5). Circles formed at first rapidly and then slowly In the first period, growth was too rapid, and in the second too slow, to be followed. Rays, however, advanced at a rate which allowed the process to be followed under a high power with ease.

Rays and circles are merely minor variants of the same type of freezing Sometimes a circle would stop growing when the diameter had become about 0·5 mm. Others at or near this limit would continue growing by rays, which often advanced with the same velocity, so as to preserve the circular contour. The membranes of the circle could be seen bulging into the base of the rays (fig. 6)

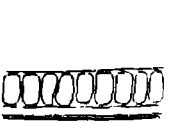

Fig. 4.

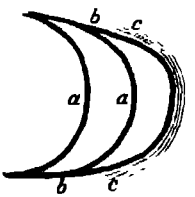

Fig. 5.

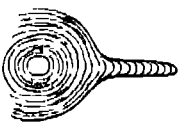

Fig. 6.

Fig. 4.—40 per cent gel, frozen at — 11°. Transferred to 3° to allow secondary areas to develop fully

Fig. 5.—Tip of a ray showing membranes (*a*), luminous zone (*b*), and fine etched lines (*c*)

Fig. 6.—Sketch of a circle with a single ray growing from it.

Disseminated freezing was of two types :—(1) The gel was everywhere closely studded by crystals with rounded edges very regular in size, each being about 20μ in diameter. Each crystal was of pure ice, and each began as a minute sphere whose growth was rapid in very dilute gels, and too slow to follow in gels from, say, 20 per cent. upwards. Freezing did not appear to be intermittent.

Sometimes circles, with or without rays, would form at a few centres, say, 6 to 10, and after a while cease growth. Eight or more days later the remainder of the gel would be found to be occupied by crystals.

(2) The gel was occupied by minute spheres, all of the same size, namely, about 3μ in diameter (see Moran's fig. 2). This kind of freezing was found by

Moran only at temperatures below — 19°, when cooling was very rapid. Probably in this second form of disseminated freezing ice began to form during the fall of temperature, but ceased when the viscosity became too great, in which case the two types are merely different stages in the same process.

Nothing is known as to the nature of the centres of crystallisation, but it is clear that they were in two classes, a few (not more than, say, a dozen in a square centimetre) which became active with moderate cooling and gave rise to circles and rays, and others, many hundreds in number, which in strong gels became active with moderate cooling only after a long latent period lasting for days and at once with great cooling (—19° or more). The less the degree of cold, the fewer of this second class became active.

Prolonged study would be needed to evaluate all the variables, especially as some unknown factor operates. All the preparations from the same mass of gel, for example, do not give the same results Thus, in ten preparations of 15 per cent gel exposed to — 11° for one day, there was no freezing at all in one preparation, and circles, with or without attached rays, from two to five in number, in all the others. The following conclusions, however, appear to be certain —

Freezing is intermittent, with separation of a solid solution in gels from 2 per cent. to 40 per cent (the latter the strongest used) when exposed to temperatures from — 6° to — 13·5°.

Freezing is always disseminated and very rapid, with separation of a multitude of crystals of pure ice, in gels of less than 2 per cent. This same type of disseminated freezing may occur in stronger gels, but it takes a week or more to appear.

Exposed to —19° C in gels between 15 per cent. and 40 per cent., freezing was always disseminated, and only minute spheres of ice were formed. Weaker gels were not tried.

At — 2·6° to — 3°, no spontaneous freezing occurred.

Callow found that when he removed gels in which spheres had begun to form at — 11° to — 3°, pure ice was deposited about them; therefore a solid solution separates only at temperatures below — 3°. It will appear later that the solid solution is unstable at — 3°.

It might be supposed that the separation of a solid solution depended upon the rate of cooling. Slow cooling was tried, ten days being occupied in the change from 0° to — 10·4°. Freezing was intermittent, and a solid solution separated. Owing to the capacity for overcooling, however, slow cooling does not imply slow freezing.

Membranes.—The end of a ray has a smooth rounded contour suggesting a surface moulded by surface tension. The gel ends in a luminous zone (*b*, fig. 5), which may be a diffraction halo or may be a zone of denser gel. It is about 0·5μ wide. Beyond it in the gel are finely etched lines (*c* in the figure). Sometimes lines appear also to be within the luminous zone, but this appearance is probably due to the curvature of the surface in the vertical plane Fine etched lines, similar to those described above, are also found in the gel at the outer edge of circles.

As growth proceeds membranes may be seen to become detached, so as to divide the ray into compartments (figs. 5 and 6), each of which is filled completely by optically homogeneous transparent material

It might be supposed that each compartment represented a single block of solid solution and that the appearance of membranes is really due to diffraction halos at the surfaces separating them. This is negatived by the fact that the membranes are singly refractive, while the contents are uniformly doubly refractive. With crossed Nicols the former are dark against a luminous background The membranes also persist on thawing.

Sufficient cause is found in Part 2 why freezing should be intermittent, the pauses being due either to an increase in the internal friction, or to the concentration of the gel at the ice face increasing until it is in equilibrium with the ice phase The microscope shows, however, that when a pause occurs freezing starts again, not at the original face but at a new face within the gel, thus leaving the characteristic membrane of dehydrated gel behind

The explanation probably is simple. During intermittence the temperature at the face will fall and the hydration of the gel rise. The fine lines described above show that cleavage occurs in the gel owing to uncompensated stresses, and each cleft will be the locus of a thin layer of dilute solution. Such a solution will have a higher freezing point than that of the concentrated gel on either side, and therefore freezing will start in it. The layer of dilute solution will, like the layer of fluid of insensible thickness on the surface of overcooled gel referred to by Moran, be the locus of centres of crystallisation of higher potential than any in the interior of the gel. The clefts at the end of a ray are seen as they appear after thawing in the photograph (fig. 9).

Thawing.—By a simple device it was possible to raise the temperature of a preparation on the stage of the microscope either quickly or slowly, and thus watch the changes.

Two distinct events happen—distinct because the first can happen without the second. They are a separation of the solid solution into ice or water and

concentrated gel at about $-6°$, and a violent transference of water from the sponge of concentrated gel so formed to the surrounding gel, which occurs at about 0° C. The sponge commonly described in the interior of gels which have been frozen and thawed is due to the first of these changes of state, and the final volume occupied by the sponge when thawing is complete is very much less than the volume of the ice phase, owing to the second process. Neither process is arrested by the use of strong fixatives such as formaldehyde. Some years ago* I drew attention to the artifacts caused by fixatives. No more striking instance could be furnished than the false picture given by strong fixatives of the process of freezing in gels, even when used as Moran used them, in the most favourable fashion.

As temperature slowly rises, small spheres appear in the solid solution, which slowly increase in size. In circles they appear first in the central area. Fig. 1 shows a circle at $-11°$, and fig. 2 a circle in which small droplets are beginning to appear at the centre owing to a slow rise of temperature.

As the word "sphere" has been used to denote an entire system, it will help to avoid confusion if these spherical droplets are called secondary areas. The secondary areas are smaller and more numerous the more rapid the rise of temperature. One has therefore in the solid solution, as in entire mass of gel, a great number of centres or nuclei, of which the number which become active is determined by the rate of change of temperature. Secondary areas can be developed to their limit of size by taking a gel from, say, $-11°$ and keeping it for a day at $-3°$. They are then found to occupy the whole distance between the membranes (fig. 4).

Figs. 3 (*a*) and 3 (*b*) illustrate the effect of more rapid warming. Very rapid warming or flooding with 40 per cent. formaldehyde or absolute alcohol—of course, after removal of the cover glass—produces a fine-grained structure composed of a multitude of secondary areas not more than $0{\cdot}1\,\mu$ in diameter. The variation of the size of the areas with the rate of warming proves that they are not preformed.

Secondary areas do not appear to communicate with one another—a fact which makes it difficult to understand the expulsion of water which takes place on further rise of temperature. It is impossible to follow this process; it takes place with such startling rapidity. The quantity of water lost is considerable—rays shrink by 30 to 50 per cent. of their volume, and the water so lost is at once taken up by the surrounding gel. Figs. 7 (*a*) and 7 (*b*) show the appearance

* 'Journal of Physiology,' vol. 24, p. 158 (1899).

of rays before and after rapid thawing. The serrated edges indicate where the membranes have folded together.

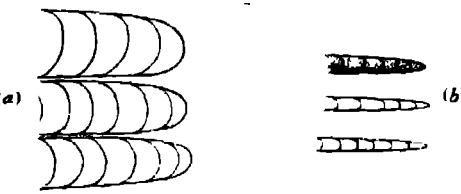

FIG. 7.—15 per cent. gel, frozen at — 11°. Rays before thawing (*a*), and after rapid thawing (*b*). The fine grained structure produced by rapid thawing is indicated in only one of the latter

Expulsion of water from the solid solution occurs also in circles, but a large part is trapped between the concentric layers. The result is that the membranes are split. This is clearly shown in figs. 3 (*a*) and 3 (*b*), which show part of a circle highly magnified before and after thawing.

The capacity of the gel for re-absorbing water is shown also in the case of disseminated freezing. Each ice crystal disappears, and in its place is left a small cleft. The space occupied by the crystal therefore vanishes almost entirely, but, as might be expected, the collapsed walls do not join together. It is to be observed, however, that such extensive re-absorption of water occurs only when the gel is fairly concentrated (20 per cent. and upwards); when it is very dilute (under 2 per cent), the spaces occupied by the crystals round up on thawing, with but little decrease of volume. The result is an open sponge, the spaces in which, however, do not appear, at any rate at first, to communicate with one another.

Polarised Light.—Before any freezing occurs, the gel is singly refractive, even though it has been overcooled for some days. When freezing has taken place, that part of the plate unoccupied by circles, rays or crystals is doubly refractive; the solid solution is also doubly refractive; the membranes are singly refractive. After the formation of secondary areas their walls of concentrated gel are singly refractive.

Even when thawing is complete the plate of gel remains doubly refractive. The molecular structure imparted by freezing therefore persists. Whether it ultimately vanishes was not determined.

These observations suggest an explanation of a striking fact discovered by Callow.* He seeded cylinders of gel overcooled to — 3° at one end and observed

* 'Roy. Soc. Proc.,' A, vol. 108, p. 307 (1925).

the rate of advance of the ice. Up to a concentration of 2 per cent. the velocity was of the order found in pure water. At 2 per cent. it suddenly dropped from 960 cm /hr to 40 cm /hr. My own observations were made entirely upon spontaneous freezing, but they showed that at some low concentration of the gel intermittent freezing appeared and disseminated freezing with separation of pure ice became very infrequent. The drop in velocity noted by Callow may therefore have been due to intermittent freezing replacing a continuous process.

These observations throw some light upon Moran's dilatometer curve (fig. 9)* which shows that as temperature rises there is a sudden contraction at between $-6°$ and $-7°$. This is the temperature at which secondary areas appear; it is, therefore, a decrease of volume due to de-solution of the solid solution. When thawing is complete, the volume does not always return to its original value—there is persistent slight increase. This is probably due to the persistence of that molecular pattern into which the gel is thrown by the stresses set up about the places where actual separation of an ice phase takes place, and which is manifested by the persistence into the thawed stage of double refraction.

Attempts were made to determine whether the separation of a solid solution was due to the rate of freezing by exposing gels to $-3°$. They were not successful owing to the overcooling. Gels from 2 per cent to 40 per cent. failed entirely to freeze at $-3°$. Callow obtained considerable nodules of ice in the interior of a large mass of gel in a test tube, but each was deposited about a minute sphere which had previously formed at $-11°$

My acknowledgments are gladly given to Mr. Hale for microphotographs taken under most trying conditions, and for making all the preparations of gel needed

Part 2.—Theoretical.

Moran distinguishes between internal and external centres of crystallisation and points out that ice formation is confined to the latter when the overcooling is not too great.† He also finds that when ice forms wholly on the surface of the gel a true phase equilibrium between ice and gel is reached in what is, for the colloidal state, a short time.

Phase equilibrium of the kind described is so rare in the case of colloidal systems (I cannot recall another instance) as to deserve some thought. It is no doubt conditional equilibrium and not the absolute equilibrium which simple solutions exhibit, because it will certainly depend upon the previous history of

* *Vide supra*, p. 39. † *Vide supra*, p. 42.

the gel upon, for example, the temperature at which the gelatin was dissolved and the rate at which gelation took place, since such things influence the structure of gels. The point is that when the structure had been finally established the phase relations with ice became a pure function of temperature and, as will appear later, of pressure.

Moran took care to assure himself that the phase relations observed by him were between pure ice and gel. The interface was effectively plane, for, in the thin discs employed, the curvature of the rim was small and its area only a small fraction of the whole surface.

Consider the formation of ice on the surface of one of his thin discs. The ice face would advance inwards at a rate equal to the mass of ice (m) deposited in unit time multiplied by its specific volume (S_i). The gel face would retreat at a rate equal to the same mass multiplied by the specific volume of water (S_w) if the minute contraction which occurs when gels of medium strength absorb water be neglected. Since S_i is greater than S_w a pressure would be set up which would crack the shell of ice at the edges of the thin discs, and Dr. Moran tells me that the shell of ice always was found so cracked. We may therefore take it that the equilibrium obtained was not only at a plane face but also sensibly under constant pressure.

When ice is being formed we may, following H. A. Wilson, suppose that the water is being driven from the gel to the ice by a pressure A which is equal to the difference in the internal pressure W_g of the water in the gel and of the ice W_i. That is, $A = (W_g - W_i)$. This is the pressure which is equal in magnitude to that which would have to be applied to a piston impermeable to ice to stop freezing. For small values of A it may be put equal to the difference in the vapour pressures of gel and ice at the interface multiplied by a constant.*

The pressure A may be supposed to drive water on to the ice face through a layer of gel of depth σ proportional to the range of molecular forces, against a frictional resistance η. The velocity of ice formation V will then be

$$V = \frac{A}{\sigma\eta}, \qquad (1)$$

which, for small overcooling, may be put $= C(\theta_0 - \theta)$.

The effect of an external pressure upon the internal and vapour pressures of a gel is not, so far as I am aware, known, but, save perhaps for very concentrated gels of gelatin in which all the water is absorbed with considerable evolution of

* H. A. Wilson, 'Proc. Camb. Phil. Soc.,' vol. 10, p. 25 (1898)

heat and contraction of volume, increase of pressure is certain to have much the same effect as it has on water. Therefore, if both ice and gel are subjected to an external pressure P instead of a pressure applied only to the ice, W_g will be increased, but not to the same extent as W_i. Therefore, though P can stop ice formation, it will have to be much greater than A to do so.

The pressures A and P are the only ones which have to be considered if either ice or gel, or both, are free from external constraint, as they would be, for example, if they were contained in a cylinder with frictionless walls open at one end This condition is practically realised when a cylinder of gel enclosed in a test tube is seeded at one end if the gel be dilute, because then its adhesion to the glass will be slight. This is the condition which obtained in Callow's measurements of the velocity of ice formation.*

When both ice and gel are under external constraint, as they would be if they were enclosed in a rigid envelope, there is a third pressure π normal to the ice face and due to the expansion of water on freezing. This pressure will diminish the effective overcooling by lowering the freezing point until freezing ceases, when the ice phase will be in equilibrium with gel at the temperature θ and the pressures P and π.

When freezing occurs in the interior of the gel these conditions are realised, except that the interface is no longer plane and the rigid walls are replaced by the elastic mass of gel. Freezing must be stopped at some point by the elastic compression of the ice by the surrounding gel unless the latter is fractured, which it never seems to have been. As a matter of observation, with moderate overcooling freezing did start at only a few centres in the interior, and after a relatively short time ceased.

When ice forms from water the direct influence of the ice face may be supposed to end at the distance a measured along the normal. When it forms from gel, however, owing to the fact that the interface is impermeable or only slightly permeable to gelatin, a diffusion column is formed beyond the limit a.

Let us call the layer of depth a next to the ice M and the diffusion column N. The movement of water in the latter is due to a gradient in the internal pressure so that the velocity through any elementary layer is given by

$$V_w = \frac{dW_g}{dx}\frac{1}{\eta} \qquad (2)$$

when η is the frictional resistance reckoned at the layer.

* *Loc. cit.*

The expression $V = \frac{A}{a\eta}$ differs from the similar expression for the freezing of water in two particulars; the quantity A is a function not only of the degree of overcooling and the pressures P and π, but also of the concentration of gelatin in the layer M. This follows from the phase relations found by Moran

The resistance η also is a function of concentration as well as of the degree of overcooling and pressure.

The internal pressure of water in the gel W_g is also a function of temperature, pressure and concentration, but the coefficient dW_g/dx in equation (2) is either independent of temperature and pressures or is not the same function as the other quantities.

This must not be taken to mean that if the magnitude of A is changed by, for example, a fall of temperature, the diffusion column N will not change It means simply that if the gradient of concentration dc/dx be everywhere kept constant throughout N and the temperature or pressure alone changed, there is no evidence to show that the gradient of internal pressure will change. We may therefore assume that dW_g/dx is a pure function of dc/dx.

Let $\theta_0 - \theta$ be the overcooling, c' the concentration of gelatin in the layer M. We have then:

$$A = \frac{\phi'(\theta_0 - \theta)}{\phi''(c', P, \pi)}, \tag{3}$$

$$\eta = F[(\theta_0 - \theta), c', P, \pi], \tag{4}$$

$$\frac{dW_g}{dx} = f\left(\frac{dc}{dx}\right). \tag{5}$$

Let the efficiency of the diffusion column have its obvious meaning, namely, the rate at which water is brought to the layer M. It is easy to see that the velocity of freezing will depend not only upon expression (1) but also upon the efficiency of the diffusion column It is also obvious that if one of the variables, temperature or pressure, be altered, the result will depend upon the rate of change of different processes such as the rate of addition of water to and of its removal from the layer M, it is therefore the second differentials taken with respect to time which are of importance

The intermittent character of the freezing is expressed algebraically by saying that dV/dt is not always positive. Moran's study of the phase relations shows that at these low temperatures it may even have a negative value. The value will be zero when the concentration of gel in layer M is high enough to be in equilibrium with the ice phase at the local temperature and pressure, but

expressions 1 and 2 show also that it may become sensibly zero if the quantity η becomes large enough.

Consider, for example, the effect of a sudden increase in the degree of overcooling. The change would, by increasing η, decrease the efficiency of the diffusion column It would also, if not too great, increase the rate of removal of water from the layer M and the result of the two processes would be a rapid rise in the concentration of the gel in M.

The chief cause of accumulation of gelatin in the layer M with consequent rise of concentration is, however, the impermeability, or relatively slight permeability, of the interface to this substance It is easy to see that by reason of this impermeability a plane face of ice would not advance along a cylinder of gel at a constant rate. Callow (*loc. cit.*), it is true, found the velocity of crystallisation to be remarkably constant, but what he observed was the rate of advance of the ends of rays of ice along a cylinder of gel seeded at one end and not the total ice formation. The gels he used were of low concentration and the overcooling slight. Probably owing to the low concentration the growing points of the rays pushed aside the accumulated gelatin. The ice face also was curved and the efficiency of a diffusion column is greater over a curved than over a plane surface.

The quantity η is an important one in the theory of freezing. The form of the curve connecting the velocity of crystallisation with the degree of overcooling is determined mainly by it H. A. Wilson* points out that in one-component systems the pressure term A increases more rapidly than η for small overcooling, but when overcooling is great η becomes so large as to stop freezing.

In a single component system η is the pressure needed to drive unit mass of the fluid at unit velocity through itself. For a gel it is the pressure needed to drive unit mass of water through the gel in layer M at unit velocity. In reckoning the quantity, however, regard must be had to the movement of the framework of the gel which the movement of the water brings about. Owing to the impermeability of the interface to gelatin, the internal pressure A is called upon actually to compress the framework. η obviously is a more complex term than it is in single component systems, and in any complete analysis it would probably be necessary to express the frictional resistance by two terms.

Since η is taken to include the resistance of a solid framework built of enormous hydrated molecules of gelatin, it is likely to increase rapidly with fall of temperature; it is therefore not a matter of surprise that, save in dilute gels

* *Loc. cit.*

containing much free water, freezing ceases at a very early stage when the overcooling is only as much as 19°.

The framework of gels is not a purely passive structure. In some gels, such as those of silica or fibrin, the framework spontaneously shrinks and water is expelled. Graham gave to this process the name synæresis. Let us call the synæresis of such gels positive. In other gels synæresis is negative, up to a point—that is to say, in contact with water such gels imbibe water and increase in volume. A gel of gelatin has negative synæresis.

The sign of its synæresis must be an important factor in the freezing of a gel, as is obvious if dehydration and hydration are taken in two stages. Let the gel first lose water to the ice. If synæresis is positive, rehydration by absorption from neighbouring gel will be resisted. Synæresis acts like an internal friction which may be very great.

Over the range of concentrations we are considering the synæresis of gelatin gel may be taken to be negative. Nothing is known of the effect of temperature upon it, but the extraordinary rapidity with which water is reabsorbed on thawing shows that it can by no means be neglected.

In any case the framework of a gel with no synæresis is not one which offers no resistance to change of form, because synæresis is a measure only of the intrinsic capacity for spontaneous change.

The internal pressure of water W_σ in the layer M next the ice face is a function of the concentration σ' of the gel in that layer, but for dilute gels in which some of the water is "free" it will be independent of concentration, and become dependent only for more concentrated gels. The limit between dilute and concentrated, however, is unknown, but Moran's observations appear to fix it at about 50 per cent. All the gels used in this enquiry were below that concentration, but we cannot conclude that A was independent of concentration because the value referred to is the local concentration in the layer M at the face. All we can say is that it would be difficult or perhaps impossible for local accumulation of gelatin seriously to decrease the quantity W_σ when the concentration of the general mass of gel is very low, and this, no doubt, is one of the reasons why intermittent freezing was not found in very dilute gels.

Two of the observed relations seem susceptible of simple explanation. The prepotency of the centres of crystallisation on the surface of a gel can be accounted for by the presence there of an insensible layer of very dilute solution, and to the absence of the normal pressure π; and the separation of a solid solution in the interior within certain limits of concentration and temperature is due to the pressure π and the degree of overcooling, since Moran found pure ice deposited at $-3°$ on the surface only where $\pi = 0$, but at lower temperatures pure ice was deposited on the surface and at the same time, as his figures show, solid solution in the interior, and the only difference between surface and interior was that π was zero at the surface and had a

positive value in the interior. If, however, the specimen was removed from, say, $-11°$ to $-3°$, pure ice was deposited in the interior about the spheres of solid solution.

Freezing at a Spherical Surface.—Let a sphere of the ice phase form inside a mass of gel large enough for the distribution to be symmetrical about its centre. The pressures at the surface of the sphere are A and $(P + \pi)$. P is the atmospheric pressure. The pressure π gives rise in the gel to a radial pressure and a circumferential tension, both of which vary inversely with the cube of the radius.

Since the internal pressure of water in the gel is increased by pressure, the effect of this distribution of radial pressure will be to decrease the steepness of the gradient of internal pressure of water in the diffusion column about the sphere of ice, so that, if the gradient of concentration remained unchanged, the effect of introducing the radial pressure would be to decrease the rate at which water moved to the ice face. On the other hand, the velocity of the diffusing water through each shell required to keep the rate at which it arrives at the ice face constant varies inversely with the square of the radius. We therefore have as a consequence of the form of the surfaces two effects of opposite sign, that with the negative sign being some function of the inverse cube, and that with the positive sign varying with the inverse square of the radius.

Whilst the ice phase is forming heat will be liberated at the surface of the sphere. If the quantity formed in unit time were constant, and loss of heat by radiation be neglected, the sphere would be at a constant temperature. If the rate of formation of ice varied about a mean value, the sphere would act as a reservoir of heat, so that oscillations of temperature due to variations of the rate would decrease as its radius increased.

The gradient of falling temperature about the sphere will have an important effect upon the efficiency of the diffusion column. Let a given diffusion column at uniform temperature deliver water on to the ice face at a certain rate. Now let the external temperature be varied so that, whilst the temperature at the ice face remains constant, a gradient of temperature falling from the ice face outward is set up. The result will be to increase the fricional resistance η everywhere except at the ice face. From geometry it is obvious that the gradient $d\eta/dr$ so produced about a spherical face will be greater than $d\eta/dx$ at a plane surface if the diffusivity of the gel is the same.

If the diffusivity of the gel were very low, enough heat might accumulate in the sphere to stop freezing until some of it was dissipated. This possibility was explored. Mr. Adair was good enough to measure for me the effect of

FIG 8.—40 per cent gel. Frozen at −9. A circle which has formed rays early. Note secondary areas appearing at about −6.

FIG 9.—21 per cent gel. Top of ray after complete thawing. Note cleavage lines in the gel. Mag. about 150 diams.

(*Facing p.* 61)

concentration upon the diffusivity of the gel, and found it to be the same as that of still water over the range of concentration examined.

Probably the most important effect of curvature of the ice face lies in its effect upon the redistribution of gelatin The framework of the gel is being pushed back by the ice face and is also retreating owing to the transference of water to the surface of the sphere. Therefore, when any shell in the gel expands from r_1 to r_2, there will be motion of the molecules of gelatin both radially and tangentially Since the greater part of the gelatin is contained in a solid framework, the rate of redistribution will be rather that of a solid than of a fluid, therefore, unless the rate of ice formation is very low, low enough to permit of redistribution of the stresses, actual fracture of the structure is likely to occur. The microscope shows that fracture does occur Clefts in the gel appear about the ice face (figs 8 and 9) and, much more rarely, radial clefts appear as fine radial lines

Moran found that gels in which the concentration was greater than 65 5 per cent. could not be made to freeze. His phase curve becomes horizontal at this concentration. From this he infers that at this concentration none of the water in the gel is available for freezing because it is bound chemically to the gelatin There is an alternative explanation It is stated in text books on colloids that the freezing point of water absorbed in swelling may be lowered as much at 100°. The statement has no particular significance unless it means that at, say,— 100° ice has been found to separate It is certain, however, that, in the strict sense of the word, the freezing point of water in gels of high concentration is lowered considerably At the same time the internal friction η increases as concentration increases and as temperature falls, it is possible, therefore, that freezing ceases at high concentrations because the forces tending to form ice are not able to overcome the internal friction and that all the points on Moran's curve are determined by this equation If this were the case, however, since η is of the nature of a friction, one would not expect the complete reversibility which he found

Studies in Adhesion.—I.

By Sir William Hardy, F.R.S., and Millicent Nottage.

(Report to the Lubrication Committee, Department of Scientific and Industrial Research)

(Received June 11, 1926)

Friction measures the tangential reaction at an interface to external forces, and certain relations to time, temperature, pressure and chemical constitution have been described in earlier papers. It seemed worth while to examine the relations of the normal reaction, but nothing has been attempted beyond a preliminary survey of what has proved to be an interesting field.

For the purposes of this paper the word adhesion means simply the normal force needed to detach completely a cylinder from a plate. Measurements of this force are described in an interesting paper by Budgett,* which will be referred to later.

The difficulty in discovering the laws of adhesion lies in the fact that, when the lubricant is fluid, anything between zero and a high value can be obtained by varying the time relation and the method of placing the cylinder and lubricant on the plate. To get comparable values one has to seek out mechanically "corresponding" states, to borrow the convenient notation of chemists. One of these states is dealt with in this paper.

Static friction, strictly speaking, is the tangential force per unit area which just fails to cause slipping. It cannot be observed because, owing to the fallibility of our senses, a certain rate of slip enters into all observations. What actually is observed in experiments upon static friction is the force which produces a certain tangential acceleration and it is noticeable that the acceleration varies widely for different lubricants. As a broad rule, it is high when the molecular weight of the lubricant is low, and low (merely a gentle slide) when the molecular weight is high.

Let R_0 be the reaction to the traction just before slipping occurs, then the observed reaction is

$$R = R_0 + \int_0^v \frac{dR}{dv}\,\delta v$$

v might be called the velocity of release.

As nothing exact is known of boundary conditions in kinetic friction we cannot

* 'Roy. Soc. Proc.,' A, vol. 86, p. 25 (1911).

say whether R_0 really does carry over from the static to the kinetic state It may, however, be worth while enquiring what happens if it does The second term on the right then becomes, with the sign changed, the force producing acceleration.

R_0 therefore (= minus the true static friction) would, on this assumption, be less than R (observed) for lubricants of low molecular weight, and the two, R and R_0, tend to equality as the molecular weight rises The enquiry cannot be carried further without more knowledge derived from experiment

The fact that the observed static friction is independent of the quantity of lubricant on the plate, of whether the lubricant is solid or fluid, and of temperature within the limits explored, is perhaps assurance that the observed value is very close to the limiting value No such assurance, however, is forthcoming for studies of adhesion It is difficult to settle what exactly is being measured, save in one group of cases, namely, when a solid lubricant is employed, when the force needed to break the cylinder away from the plate without doubt measures the tensile strength of the joint, so that, though acceleration comes in as it does in static friction, the theoretical reaction is clear.

Any value can be obtained for the adhesion produced by a fluid lubricant, for any normal force given time enough will, if it be sufficient to overcome the relatively slight resistance offered by the surface tension of the lubricant, lift the cylinder When the normal force reaches a certain value, however, the break away occurs instantaneously, and this is a true limiting value because any addition to the force fails to alter the result. As it is a limiting value, it is identifiable. It is not the only identifiable value, that given by solid lubricants, for example, is another. Under certain circumstances it becomes a corresponding value which we will call Value A.

Value A.

Methods —Both cylinders and plates were ground to " optical " faces Each cylinder, no matter of what material it was made, weighed 5·6 grammes, and had a diameter of 1 cm. A normal force was applied by a cord attached to the cylinder in such a way that the force was central, and led over a light pulley to a pan for carrying weights The normal force is the weight in the pan less the weight of the cylinder. The pressure between the faces was varied by placing weights on the top of the cylinder, these weights, with that of the cylinder itself, are called the load Unfortunately it was necessary to remove the added weights before a measurement could be taken and, as adhesion decreases when the load is reduced, the recorded value is somewhat less than the true one The measurements were carried out in a chamber filled with clean dry air

The lubricant was added in one of two ways: a large pool was made on the plate and the cylinder then put into it, or the cylinder was first put on the plate, a little fluid then placed touching its edge and, when fluid had ceased to be drawn underneath by capillary forces, and when therefore fluid was visible all round the edge, more was added to form a large pool.

G. I Taylor has calculated the rate of fall of a flat disc through fluid on to a flat plate and his equation shows that it would take infinite time to get within molecular distance of the plate * This equation is abundantly verified by these experiments. If sufficient time were allowed the cylinder placed in a pool would fall until its weight was borne by the Leslie pressure† due to the attraction of the solid faces for the fluid.

This equilibrium position can, however, be reached quickly by starting from the other end, that is to say, by placing the cylinder on the plate, and allowing the fluid to run underneath The capillary forces then are enormous and equilibrium is reached in a few seconds. *Value A was taken always from this equilibrium position—it is therefore the force needed to break the cylinder away instantaneously when the thickness of the layer of lubricant is such that the Leslie pressure carries the load* For all the loads employed, this thickness includes hundreds, if not thousands, of molecules, as is proved by the fact that if the temperature be allowed to fall sufficiently to freeze the lubricant, and the cylinder be then broken away, the layer is found to be of sensible thickness to be measured in fractions of a millimetre rather than in μ even for the heaviest loads employed. This alone is proof, if further proof be needed, that the attraction field of the solids modify the state of the lubricant throughout a layer many hundreds or thousands of molecules in thickness.

The Latent Period is the interval which elapses between placing the cylinder in the pool, or forming the pool about it, and the time when adhesion attains a steady value It may be the time taken by the cylinder in falling or rising in the pool; or the time occupied in the orientation of the molecules of the lubricant in the attraction fields of the solids When the cylinder is falling the value increases, and the opposite when it rises. The latent period of orientation is always a period of increasing values ‡

The latent period of orientation can be obtained by following the normal

* 'Roy. Soc. Proc.,' A, vol. 108, p 12 (1925).

† *Loc. cit*

‡ The latent period in friction is discussed in 'Roy. Soc. Proc.,' A, vol. 104, p. 25 (1923), and A, vol. 108, p. 9 (1925).

procedure, namely, placing the cylinder in position and allowing the fluid to run under. The following values were obtained —

Table I —Load 5 6 grammes

Latent Period of Orientation

—	Minutes	Viscosity
Octane	0	0 0054 at 20
Cyclohexane	0	0 0089
p-Cymene	0	
Methyl Ethyl Ketone	20	0 0042 at 20°
Acetophenone	20	
Cyclohexanone	20	0 0280 at
1-3 Methyl Cyclohexanone	20	
1-4 ,, ,,	20	
Ethyl Alcohol	20	0 0108 at 25°
Butyl ,,	20	0 0200 at 25
Octyl ,,	20	0 07215 at 25°
Benzyl Alcohol	25	0 0528 at 25°
1-2 Methyl Cyclohexanol	30	
1-3 Cresol	40	0 1878 at 20°
Carvacrol	40	
Heptylic Acid	60	0 0435 at 20
Caprylic ,,	60	0 0575 at 20

It might be supposed that some part of this latent period was occupied by the flowing of fluid between the surfaces, but it must be remembered that the pool was not formed and the measurement was not taken until fluid had ceased to be drawn in A similar latent period was also found in the study of friction.

Octane, in which both ends of the carbon chain are alike, and the saturated ring compound cyclohexane, gave no latent period of orientation, that is to say, the first value obtained was always the same as that found after an hour, no matter what the load might be Why paracymene should show no measurable polarity must be left to chemists to discuss.

The latent periods of orientation for static friction of the three 8-carbon compounds are reproduced here for comparison Octane, none, Octyl alcohol, 15 minutes, Caprylic acid, 60 minutes

The latent period seemed to increase slightly with increase in load, but this might be due to the defective experimental procedure which involved removal of added weights before a measurement could be taken.

Paracymene was chosen for the study of the latent period due to rise or fall in the pool, because it gave no measurable latent period of orientation. A pool was first made on the glass plate, a steel cylinder placed in it, and after a known interval the force needed to detach it instantaneously was measured. Cylinder

and plate were then cleaned and another measurement made after a longer interval. In this way the curves were obtained for loads 5·6, 115·1, and 259·6 grammes. The values of A for these loads—that is, the value which would have been reached had the cylinder had time to fall to its equilibrium position—are plotted at the end of the dotted lines It is obvious from the form of the curves that it would take a very long time to reach these steady values, these curves, therefore, are completely in accord with G. I. Taylor's equation

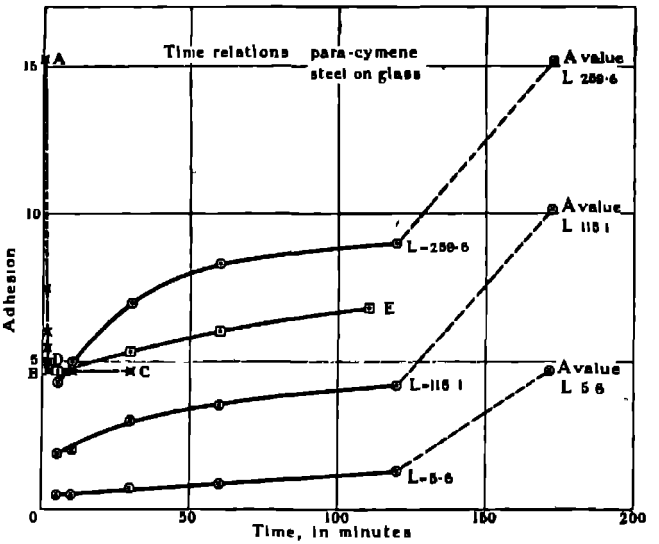

FIG 1

A relation of great theoretical importance which confirmed a similar relation found in the study of friction was got by starting from the equilibrium condition and varying the load.

Steel on glass . *p*-cymene.

Load 259·6 grs. Loaded cylinder placed on the plate, fluid then run under, and a pool formed: 254 grs. then *removed* and reading taken after the interval shown in the first column. Force needed to detach in right-hand column.

As quickly as possible ..	15·2 grs	= A for a load of 259·6 grs.
30 seconds	7·5 ,,	
60 ,,	6·0 ,,	
90 ,,	5·5 ,,	
2 minutes	5 0 ,,	
3 ,, . .	4 7 ,,	
10 ,,	4·7 ,,	
30 ,, ..	4 7 ,,	= A for a load of 5 6 grs

The figures are plotted in curve ABC, fig 1. The cylinder moved from one equilibrium position to the other, rising in the pool, in 3 minutes.

Cylinder in place, fluid run under as before and pool formed Load then *increased* from 5·6 to 259·6 grs. and readings taken (curve DE, fig 1) :—

As quickly as possible ..	4·7 grs.	= A value for a load of 5 6 grs
30 minutes .. .	5 3 ,,	
60 ,, .. .	6 0 ,,	
120 ,, .	6·8 ,,	

Value of A for load 259·6 grms. is 15 2 grs. If π is the Leslie pressure, and P the normal pressure (load divided by area) the condition at the beginning of the first case was $P - \pi = -\frac{254}{\cdot 8} = -317 \cdot 5$ grs, and of the second $P - \pi = +317 \cdot 5$ grs., why, then, should equilibrium be reached so rapidly when the cylinder rose and so exceedingly slowly when it fell? The answer offered is the same as that given in the papers upon friction*—that when the cylinder rises fluid of low viscosity is drawn in, when it falls it presses out lubricant whose molecules are locked in place by the attraction fields of the solids. It is the difference between drawing in a light spirit and expressing a jelly. If this view be correct, the viscosity η in G. I Taylor's equation must be treated as a variable which is a function of time and the distance between the solid faces.

The time taken for the cylinder to rise to the top of the pool and break away depends, as might be expected, upon the normal force. For example —

* 'Roy. Soc. Proc.,' A, vol. 104, p. 27 (1923).

Octyl Alcohol.

Steel cylinder placed on glass plate, the fluid then run under and a pool formed. Load 5·6 grs.

Normal Pull.	Time
0·4 grs.	Rose slowly to top of pool in 30 seconds.
2·4 ,,	Rose slowly and broke away in 23 seconds
4·4 ,,	Broke away in 9 seconds.
6·4 ,,	,, ,, 5 ,,
9·4 ,,	,, ,, 2 ,,
14·4 ,,	,, ,, 1 second
15·9 ,,	,, ,, 1 ,,
[21·2 ,,	,, ,, instantaneously.]

The last of these is the A value

With the help of a telescope magnifying 10 diameters, the rise of the cylinder was followed under small normal pulls It moves at first very slowly, but rapidly accelerates until the final break away occurs The impression is that of a pause followed by rapid movement At the limiting value there is no apparent pause, and this gives the curious impression that there is no resistance on the part of the cylinder This apparent disappearance of resistance is characteristic of the A value and of great value in experiments by marking a sharp end point

The A value probably is not a measure of the tensile strength of the lubricant. Worthington found the tensile strength of alcohol to be 8,165 grammes per square centimetre The A value for ethyl alcohol for a load of 5·6 grs. was only 9 grs per square centimetre The elastic give of the lubricant appears to be sufficient to allow of a tangential flow being established before rupture takes place The A value in that case is a measure of the viscosity of the lubricant, the time value being arbitrarily fixed by the condition "instantaneous." This question can be more profitably pursued, however, when the adhesion produced by solid lubricants has been described

Steady Values.

The A value for a number of substances with different solids and loads are given in grammes in Table II The viscosity of the lubricant in mass at a temperature of 20° C is given in the second column, the figures being taken from various sources. In the third column are the loads in grammes.

The value > 110 means that the adhesion was higher than the apparatus would measure.

Table II.—Value A

Temperature 18° except where mentioned			Steel on Glass	Steel on Steel	Copper on Glass	Copper on Steel	Copper on Copper
	σ	L	A	A	A	A	A
Octane	0 005	5 6	1 2	1 1			
		115 1	3 0	2 8			
		259 6	3 8	3 3			
Ethyl alcohol	0 009	5 6	7 2	5 2	2 7	1 7	
		115 1	22 1	14 2	7 7	4 7	
		259·6	33 9	23 2	12 2	7 2	
Butyl alcohol	0 024	5 6	11 7	9 7		6 5	3 7
		115 1	30 2				
		259 6	42·9				
Undecyl alcohol	5 6			26 2		23 2	20 2
Octyl alcohol	0 064	5 6	21 2	18 7		15 7	13·0
		115 1	44 9	36 2			
		259 6	61 9	50 9			
Heptylic acid	0 043	5 6	12 7				
		115 1	50 9				
		255 6	54·9				
Caprylic acid	0 057	5 6	25 9	18·9			
		115 1	99 9	73 9			
		259 6	>110	97 9			
Cyclohexane	0 009	5 6	3 7	3 5			
		115 1	7 7	7 4			
		259 6	11 7	11 2			
Undecane (51°)		5 6		1 5			
Nonadicane (51°)		5·6		8 2			
Tetracosane (51°)		5 6		12 7			
Me Et Ketone	0 004	5 6	1 5	1 3	1 0		
		115 1	3 9	3 2	2 7		
		259 6	7 0	5·7	4 6		
p-Cymene		5 6	4 7	4 2			
		115 1	10·2	9 2			
		259 6	15 2	13 7			
Acetophenone		5 6	4 2	3 9	3 5		
		115·1	8 0	7 2	6 8		
		259 6	12 7	11 5	10 2		
Cyclohexanone		5 6	16 7				
		115 1	25 2				
		259 6	31 2				
1–3 Methyl Cyclo-hexanone		5 6	17·7				
		115 1	26 9				
		259 6	37 9				

Table V—(continued).

Temperature 18° except where mentioned	η	L	Steel on Glass A	Steel on Steel. A	Copper on Glass. A	Copper on Steel. A	Copper on Copper, A
1-4 Methyl Cyclo-hexanone		5·6	5·2				
		115·1	24·9				
		259·6	34·9				
					9·7		
Benzyl alcohol	0·046	5·6	14·7	12·2	19·9		
		115·1	34·9	27·2	27·9		
		259·6	48·9	38·2			
1-2 Methyl Cyclo-hexanol		5·6	68·9	66·9			
		115·1	>110	101·9			
		259·6		>110			
					89·9		
1-3 Cresol	0·187	5·6	74·9	67·9	83·9		
		115·1	>110	94·9	94·9		
		259·6		>110			
					90·9		
Carvacrol		5·6	105·9	98·9			
Cyclohexanol	0·500	5·6	>110	>110			
Glycol	0·173 25°	5·6	>110	>110			
Glycerol	3·413 25·6°	5·6	>110	>110			

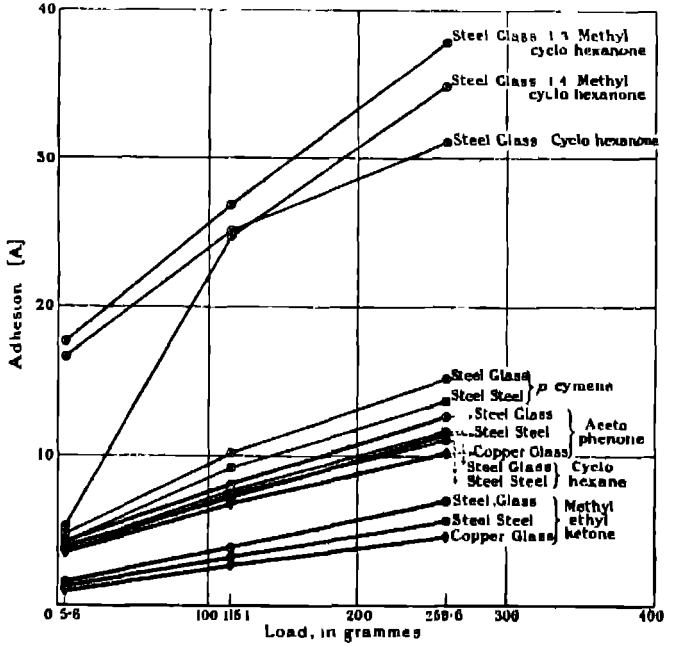

FIG. 2.—Load and Adhesion (*vide* Table II)

Effect of the Pressure —Static friction when both faces are plane increases with the pressure (that is load ÷ area) but not so fast as the pressure. When the latter reaches a certain value the friction varies with the pressure so that the coefficient μ (= tangential force ÷ load) becomes constant. This was attributed to the thinning of the layer of lubricant until a layer of great mechanical stability alone remained *

In these experiments on adhesion it was not possible to reach the pressures found necessary to make μ independent of the load, all values, therefore, lie in the region of varying μ.

The curves in fig 3 show that the coefficient α (= A ÷ load) decreases as

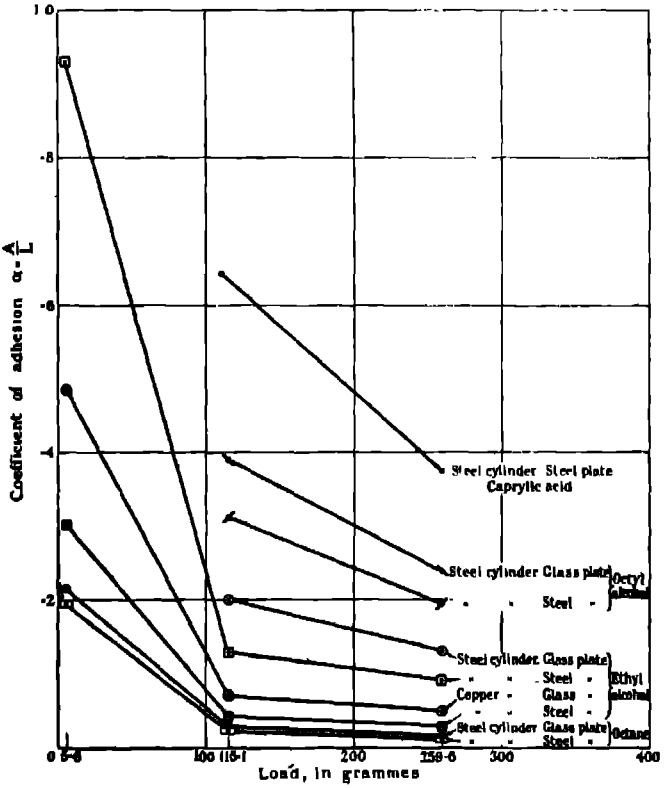

FIG. 3.

* 'Roy. Soc. Proc.,' A, vol. 108, p. 1 (1925).

the load increases. Whether it would become independent of the load at higher pressures must be left uncertain.

Effect of the Nature of the Solid.—The value of A depends not only upon the chemical constitution of the lubricant but also upon that of the solids. The following order was always found glass > steel > copper

In the case of friction the effect of a change in the nature of the solids was merely to shift the curve for μ and molecular weight parallel to itself, and the curve for two different solids was half-way between the curves for each solid by itself.* These same relations seem to hold for the A value, as the curves in fig. 4 show. The equation for the coefficient α (A ÷ load) is

$$\alpha = \frac{(r_1 + r_2)}{2} - sM,$$

where r is a function of the nature of the solid, the load, and the temperature, s a function of the chemical series, and M the molecular weight.

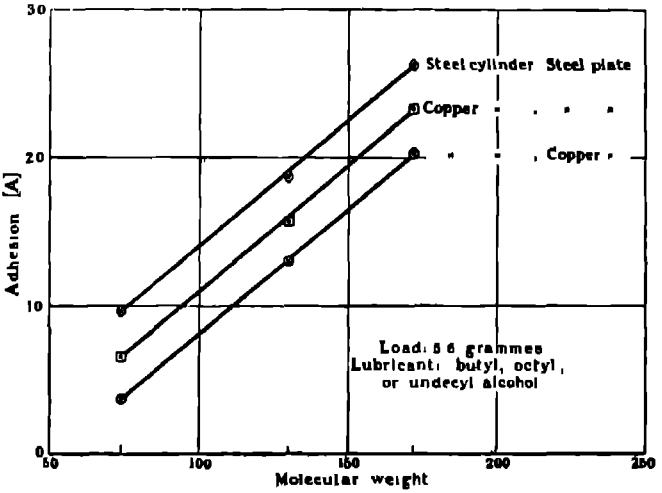

Fig. 4.

The influence of the nature of the solid wall is so striking as to make it a matter of surprise that it is not taken into account in certain of the standard methods of measuring the viscosity of fluids.

Effect of Molecular Weight.—The values for the normal alcohols and normal

* 'Roy. Soc. Proc.,' A, vol. 100, p. 563 (1921–22).

paraffins are plotted against their molecular weight in figs. 5 and 6 The relation, like the similar one in static friction, is linear for the same chemical series.

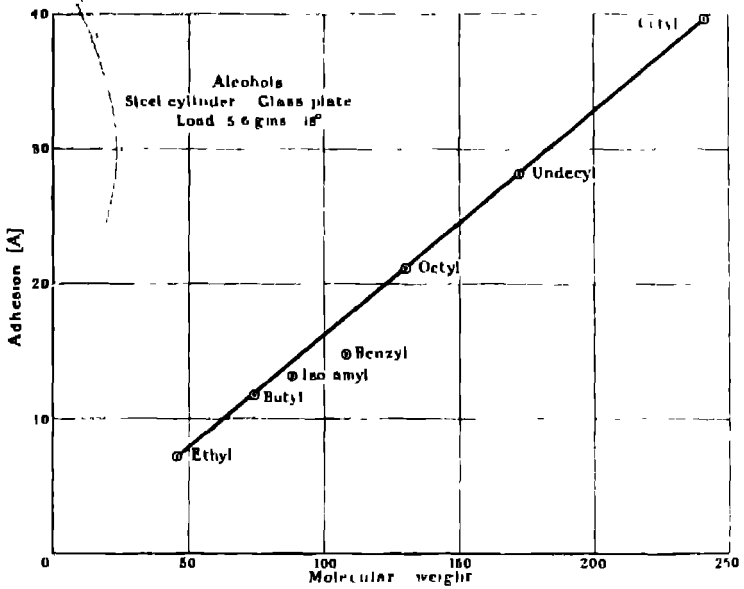

Fig 5

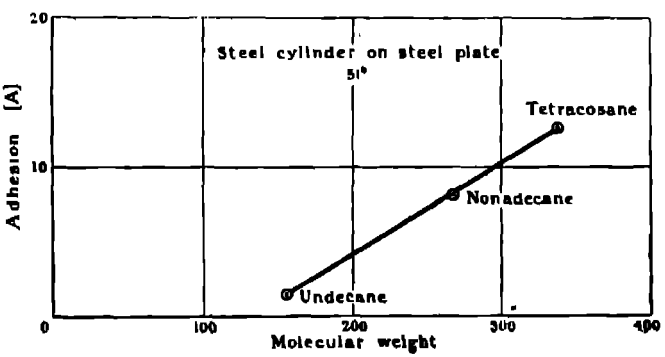

Fig. 6.

The value for cetyl alcohol was calculated from measurements made at 51° and 75° by using the linear relation to temperature. Since these measurements

were made with steel on steel it was necessary to apply a correction to bring the value to that for steel on glass. The value plotted for cetyl alcohol is therefore for the *fluid* state

Effect of Temperature.—The value of A for octyl and cetyl alcohols at different temperatures are given in Table III and plotted in the curves fig. 7.

Table III.

Temp.	Cylinder.	Plate	Load 5·6 grs	115 1 grs	259 6 grs.
			Octyl Alcohol		
18°	Steel	Steel	18 7	36 2	50 9
18°	Copper	,,	15 7	26 3	35·9
35°	Steel	,,	16 9	31 9	45·9
35°	Copper	,,	12 2	22 2	30·9
51°	Steel	,,	12 2	27·9	41·9
51°	Copper	,,	9 2	18·2	26·2
75°	Steel	,,	8 2	22 7	34 9
75°	Copper	,,	4 2	13 2	19 7
			Cetyl Alcohol.		
51°	Steel	Steel	30·7	36 9	78 9
51°	Copper	,,	28 7	46 9	63 9
75°	Steel	,,	25·7	50 9	71·9
75°	Copper	,,	22 2	40 9	55·9

It will be seen that the curves for different solids are parallel, but the position of the curve for the same solid varies with the load The slope of the curves depends upon temperature and the load. The curves are linear.

The equation therefore is

$$A = \alpha - \beta\theta,$$

where α is a function of the nature of the solid and the load and where β is a function of temperature and load.

These relations are similar to those found for friction in the comparable region where the pressure was not great enough to make the coefficient of friction independent of the load. When that coefficient is independent of the load it is also independent of temperature *

* 'Roy. Soc Proc.,' A, vol. 103, p. 16 (1925), and A, vol. 101, p. 487 (1922).

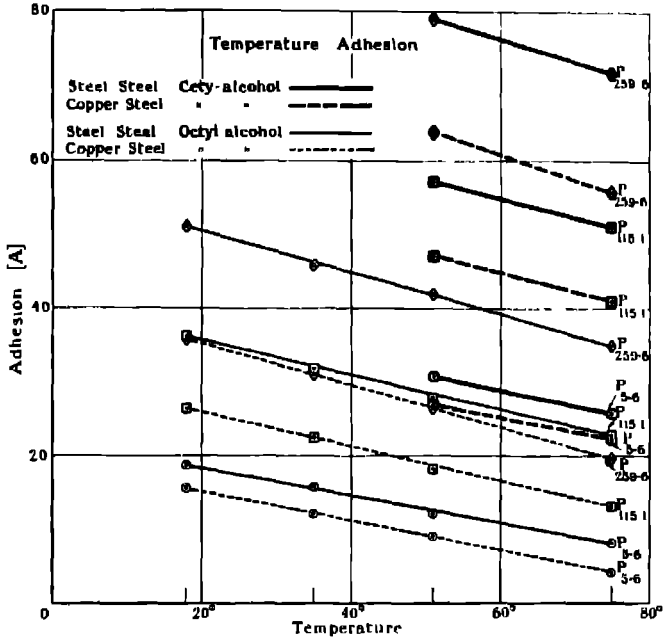

FIG 7

Summary

1 Any force, if it be great enough to overcome the slight resistance offered by the surface tension of the lubricant, can lift a cylinder standing in a pool of lubricant upon a plate, certain values of adhesion are, however, identifiable, and one of these is the normal pull required to break the cylinder away instantaneously. Adhesion here means simply this normal pull

2. In order that the value shall be comparable, cylinder, plate and lubricant must be in a mechanically corresponding relation. One such is when the load is in equilibrium with the Leslie pressure. To the identifiable value for this corresponding state the name A value is given.

3 The latent period which elapses before this state is reached is due either to orientation of the molecules of the lubricant or to the cylinder rising or falling in the pool.

4. The A value is a function of the chemical constitution of the lubricant and of the solids, of the load, and of temperature

Atomic States and Spectral Terms.

By Prof. J. C McLennan, F.R.S., Mr. A. B. McLay, M.A., and Mr. H Grayson Smith, Ph.D., University of Toronto.

(Received June 24, 1926.)

Through the recent brilliant work of Pauli,* Heisenberg† and Hund‡ the foundations have been laid for the interpretation of spectra in terms of atomic states, and it appears that we can now predict, almost with certainty, the structure and chief characteristics of any optical spectrum of the atom of any element when the extra-nuclear electronic configuration that gives rise to it is known. Conversely, if the characteristics of any optical spectrum of an atom be known, it is possible likewise definitely to describe the extra-nuclear electronic states of the atom involved in the production of such spectrum.

The writers were engaged recently in a study of the optical spectra of a number of the elements, including manganese, gold, platinum and palladium, and by applying the ideas of Heisenberg and Hund succeeded in unravelling the arc spectra of each of these elements, and also, in part, those of a number of other elements. In the course of this work we had the advantage of several consultations with Dr Laporte during a visit he very kindly made to the Physical Laboratory at Toronto, and we wish to acknowledge here our appreciation of his help.

The present communication§ is intended primarily as an introduction to the papers that follow, dealing with the chief characteristics of optical spectra of the elements of gold and palladium. The main features of the theory expounded are wholly due to Heisenberg and Hund, and the paper in so far as it deals with these contains nothing original. Certain details in the method of applying the theory appear to us to be novel, and have been found by us to be extremely helpful in dealing with complex spectra. Some simplifications in the notation have also been introduced which seem to be desirable.

During the study referred to above we found it of interest to seek to determine, if possible, the specific spectral term that corresponded to what, from the

* Pauli, 'Zeit. für Phys.,' vol. 31, p. 765 (1925).

† Heisenberg, 'Zeit. für Phys.,' vol. 32, p. 841 (1925).

‡ Hund, 'Zeit. für Phys.,' vol. 33, p. 345 (1925).

§ We wish to note here that after this communication was prepared our attention was drawn to a paper by Fowler and Hartree in the 'Roy. Soc. Proc.,' vol. 111, p. 83 (May, 1926), in which an outline is given of the Heisenberg-Hund theory.

experimental data then available, appeared to be the most stable electronic configuration of the atom of each element.

The results of this application of the Heisenberg-Hund method are given in Table I. A similar table in slightly different form was published recently by

Table I

Element	At No	Atomic Weight	Extra Nuclear Electronic Configurations							Lowest Spectral Term
			K 1_1	L 2_1 2_2	M 3_1 3_2 3_3	N 4_1 4_2 4_3 4_4	O 5_1 5_2 5_3 5_4 5_5	P 6_1 6_2 6_3 6_4 6_5 6_6	Q 7_1 7_2 7_3	
H	1	1 008	1							$^2S_{1}$
He	2	3 99	2							$^1S_0$
Li	3	6 94	2	1						$^2S_{1}$
Be	4	9 1	2	2						$^1S_0$
B	5	10 0	2	2 1						$^2P_{1/2}$
C	6	12 0	2	2 2						$^3P_{012}$
N	7	14 01	2	2 3						$^4S_{3/2}$
O	8	16 0	2	2 4						$^3P_{012}$
F	9	19 0	2	2 5						$^2P_{1/2}$
Ne	10	20 2	2	2 6						$^1S_0$
Na	11	23 0	2	2 6	1					$^2S_{1/2}$
Mg	12	24 32	2	2 6	2					$^1S_0$
Al	13	27 1	2	2 6	2 1					$^2P_{1/2}$
Si	14	28 3	2	2 6	2 2					$^3P_{012}$
P	15	31 04	2	2 6	2 3					$^4S_{3/2}$
S	16	32 06	2	2 6	2 4					$^3P_{012}$
Cl	17	35 46	2	2 6	2 5					$^2P_{1/2}$
A	18	39 88	2	2 6	2 6					$^1S_0$
K	19	39 1	2	2 6	2 6	1				$^2S_{1/2}$
Ca	20	40 07	2	2 6	2 6	2				$^1S_0$
Sc	21	44 1	2	2 6	2 6 1	2				$^2D_{2\frac{1}{2}}$
Ti	22	48 1	2	2 6	2 6 2	2				$^3F_{234}$
V	23	51 06	2	2 6	2 6 3	2				$^4F_{2\frac{3}{2}45}$
Cr	24	52 0	2	2 6	2 6 5	1				$^7S_3$
Mn	25	54 93	2	2 6	2 6 5	2				$^6S_{5/2}$
Fe	26	55·84	2	2 6	2 6 6	2				$^5D_{01\frac{1}{2}34}$
Co	27	58 97	2	2 6	2 6 7	2				$^4F_{2\frac{3}{2}45}$
Ni	28	58 68	2	2 6	2 6 8	2				$^3F_{234}$
Cu	29	63 57	2	2 6	2 6 10	1				$^2S_{1/2}$
Zn	30	65·37	2	2 6	2 6 10	2				$^1S_0$
Ga	31	69 9	2	2 6	2 6 10	2 1				$^2P_{1/2}$
Ge	32	72 5	2	2 6	2 6 10	2 2				$^3P_{012}$
As	33	74·96	2	2 6	2 6 10	2 3				$^4S_{3/2}$
Se	34	79 2	2	2 6	2 6 10	2 4				$^3P_{012}$
Br	35	79·92	2	2 6	2 6 10	2 5				$^2P_{1/2}$
Kr	36	82·92	2	2 6	2 6 10	2 6				$^1S_1$
Rb	37	85·45	2	2 6	2 6 10	2 6	1			$^2S_{1/2}$
Sr	38	87·63	2	2 6	2 6 10	2 6	2			$^1S_0$
Y	39	89·0	2	2 6	2 6 10	2 6 1	2			$^2D_{2\frac{1}{2}}$
Zr	40	90·6	2	2 6	2 6 10	2 6 2	2			$^3F_{234}$

Table I—(continued).

Element	At No	Atomic Weight	Extra-Nuclear Electronic Configurations							Lowest Spectral Term.
			K 1_1	L 2_1 2_2	M 3_1 3_2 3_3	N 4_1 4_2 4_3 4_4	O 5_1 5_2 5_3 5_4 5_5	P 6_1 6_2 6_3 6_4 6_5 6_6	Q 7_1 7_2 7_3	
Cb	41	93 5	2	2 6	2 6 10	2 6 4	1			$^6D_{12345}$
Mo	42	96 0	2	2 6	2 6 10	2 6 5	1			$^7S_3$
Ma	43		2	2 6	2 6 10	2 6 6	1			$^6D_{12345}$
Ru	44	101 7	2	2 6	2 6 10	2 6 7	1			$^5F_{12345}$
Rh	45	102 9	2	2 6	2 6 10	2 6 8	1			$^4F_{2345}$
Pd	46	106 7	2	2 6	2 6 10	2 6 10				$^1S_0$
Ag	47	107 88	2	2 6	2 6 10	2 6 10	1			$^2S_1$
Cd	48	112 40	2	2 6	2 6 10	2 6 10	2			$^1S_0$
In	49	114 8	2	2 6	2 6 10	2 6 10	2 1			$^2P_{12}$
Sn	50	118 7	2	2 6	2 6 10	2 6 10	2 2			$^3P_{012}$
Sb	51	120 2	2	2 6	2 6 10	2 6 10	2 3			$^4S_2$
Te	52	127 5	2	2 6	2 6 10	2 6 10	2 4			$^3P_{012}$
I	53	126 92	2	2 6	2 6 10	2 6 10	2 5			$^2P_{12}$
Xe	54	130 32	2	2 6	2 6 10	2 6 10	2 6			$^1S_0$
Cs	55	132 81	2	2 6	2 6 10	2 6 10	2 6	1		$^2S_1$
Ba	56	137 37	2	2 6	2 6 10	2 6 10	2 6	2		$^1S_0$
La	57	139 0	2	2 6	2 6 10	2 6 10	2 6 1	2		$^2D_{23}$
Ce	58	140 25	2	2 6	2 6 10	2 6 10 1	2 6 1	2		$^3H_{456}$
Pr	59	140 6	2	2 6	2 6 10	2 6 10 2	2 6 1	2		$^4K_{67897}$
Nd	60	144 3	2	2 6	2 6 10	2 6 10 3	2 6 1	2		$^5L_{678910}$
Il	61		2	2 6	2 6 10	2 6 10 4	2 6 1	2		$^6L_{5678910}$
Sa	62	150 4	2	2 6	2 6 10	2 6 10 5	2 6 1	2		$^7K_{45678910}$
Eu	63	152 0	2	2 6	2 6 10	2 6 10 6	2 6 1	2		$^8H_{23456789}$
Gd	64	157 3	2	2 6	2 6 10	2 6 10 7	2 6 1	2		$^9D_{23456}$
Tb	65	159 2	2	2 6	2 6 10	2 6 10 8	2 6 1	2		$^8H_{23456789}$
Ds	66	162·5	2	2 6	2 6 10	2 6 10 9	2 6 1	2		$^7K_{45678910}$
Ho	67	163 5	2	2 6	2 6 10	2 6 10 10	2 6 1	2		$^6L_{5678910}$
Er	68	167 4	2	2 6	2 6 10	2 6 10 11	2 6 1	2		$^5L_{678910}$
Tu	69	168 5	2	2 6	2 6 10	2 6 10 12	2 6 1	2		$^4K_{6789}$
Yb	70	173 5	2	2 6	2 6 10	2 6 10 13	2 6 1	2		$^3H_{456}$
Lu	71	175 0	2	2 6	2 6 10	2 6 10 14	2 6 1	2		$^2D_{23}$
Hf	72	178 0	2	2 6	2 6 10	2 6 10 14	2 6 2	2		$^3F_{234}$
Ta	73	181 5	2	2 6	2 6 10	2 6 10 14	2 6 3	2		$^4F_{2345}$
W	74	184 0	2	2 6	2 6 10	2 6 10 14	2 6 4	2		$^5D_{01234}$
Re	75		2	2 6	2 6 10	2 6 10 14	2 6 5	2		$^6S_2$
Re	75		2	2 6	2 6 10	2 6 10 14	2 6 6	1		$^6D_{12345}$
Os	76	190 0	2	2 6	2 6 10	2 6 10 14	2 6 6	2		$^5D_{01234}$
Os	76		2	2 6	2 6 10	2 6 10 14	2 6 7	1		$^4F_{12345}$
Ir	77	193 1	2	2 6	2 6 10	2 6 10 14	2 6 7	2		$^4F_{2345}$
Ir	77		2	2 6	2 6 10	2 6 10 14	2 6 8	1		$^4F_{2345}$
Pt	78	195 2	2	2 6	2 6 10	2 6 10 14	2 6 8	2		$^3F_{234}$
Pt	78		2	2 6	2 6 10	2 6 10 14	2 6 9	1		$^3D_{123}$
Pt	78		2	2 6	2 6 10	2 6 10 14	2 6 10			$^1S_0$
Au	79	197·2	2	2 6	2 6 10	2 6 10 14	2 6 10	1		$^2S_1$
Hg	80	200 6	2	2 6	2 6 10	2 6 10 14	2 6 10	2		$^1S_0$

Table I—(continued).

Element	At No.	Atomic Weight	Extra-Nuclear Electronic Configurations						Lowest Spectral Term
			K 1_1	L 2_1 2_2	M 3_1 3_2 3_3	N 4_1 4_2 4_3 4_4	O 5_1 5_2 5_3 5_4 5_5	P 6_1 6_2 6_3 6_4 6_5 6_6	Q 7_1 7_2 7_3	
Tl	81	204 0	2	2 6	2 6 10	2 6 10 14	2 6 10	2 1		$^2P_{1/2}$
Pb	82	207 2	2	2 6	2 6 10	2 6 10 14	2 6 10	2 2		$^3P_{012}$
Bi	83	208 0	2	2 6	2 6 10	2 6 10 14	2 6 10	2 3		$^4S_{3/2}$
Po	84	210 0	2	2 6	2 6 10	2 6 10 14	2 6 10	2 4		$^3P_{012}$
Eka-Iod	85		2	2 6	2 6 10	2 6 10 14	2 6 10	2 5		$^2P_{1/2}$
Rn	86	222·0	2	2 6	2 6 10	2 6 10 14	2 6 10	2 6		$^1S_0$
Eka-Caes	87		2	2 6	2 6 10	2 6 10 14	2 6 10	2 6	1	$^2S_{1/2}$
Ra	88	226 0	2	2 6	2 6 10	2 6 10 14	2 6 10	2 6	2	$^1S_0$
Ac	89	227 0	2	2 6	2 6 10	2 6 10 14	2 6 10	2 6 1	2	$^2D_{2\frac{1}{2}}$
Th	90	232 15	2	2 6	2 6 10	2 6 10 14	2 6 10 1	2 6 1	2	$^3H_{456}$
Th	90		2	2 6	2 6 10	2 6 10 14	2 6 10	2 6 2	2	$^3F_{234}$
Ux	91	230 0	2	2 6	2 6 10	2 6 10 14	2 6 10 2	2 6 1	2	$^4K_{6789}$
Ux	91		2	2 6	2 6 10	2 6 10 14	2 6 10	2 6 3	2	$^4I_{5345}$
Ur	92	238 2	2	2 6	2 6 10	2 6 10 14	2 6 10 3	2 6 1	2	$^5L_{678910}$
Ur	92		2	2 6	2 6 10	2 6 10 14	2 6 10	2 6 4	2	$^1S_{01234}$

Dr. Paul D. Foote* in a paper in the 'Transactions of the American Institute of Mining and Metallurgical Engineers.' In Dr Foote's paper the classification of the electronic orbits adopted was according to the scheme of Stoner† and Main Smith,‡ while in ours the classification is limited, it will be seen, to the orbital types usually designated by 1_1; 2_1, 2_2, 3_1, 3_2, 3_3, 4_1, 4_2, 4_3, 4_4, etc. In Dr. Foote's paper no details are given regarding the method by the use of which he obtained his results

In order that the arguments presented in our papers on the spectra of gold and palladium may be apprehended more easily, we propose giving in what follows a few notes illustrating the manner in which we applied the method to obtain the results indicated in the table. It will be seen that in Note III. we have given full details of the determination of the basic terms involved in the structure of the arc spectrum of oxygen The manner in which these terms were found and the way they are arranged will serve to show how the basic terms of the arc spectrum of any element are evolved from the deepest terms in the first spark spectrum of such element.

Since Table I was formulated its validity has been confirmed by experimental

* Paul Foote, 'Trans of the Am. Inst. of Mining and Metal. Eng.,' p. I, No. 1547 D (February, 1926).

† Stoner, 'Phil. Mag.,' vol. 48, p. 719 (1924)

‡ Main Smith, 'Chemistry and Atomic Structure,' Van Nostrand (1924).

data obtained by different investigators with a number of elements In no case as yet, in so far as we are aware, has the type of the fundamental term recorded in the table for any element been found to be incorrect

The only features of the table about which there is a lack of complete definiteness is in connection with the elements, Thorium, Uranium X and Uranium, and in connection with the group Rhenium, Osmium, Iridium and Platinum. Alternative "deepest" terms are given for each of the three elements, Thorium, Uranium X and Uranium, based (1) on the assumption that these elements are, respectively, homologues of Hafnium, Tantalum and Tungsten, and (2) on the assumption that they are homologues of Cerium, Prascodymium and Neodymium respectively Which of these alternatives is the correct one will probably be ascertained shortly from a study of the arc spectrum of either Thorium or Uranium As regards each of the other four elements experiment must decide which of the configurations given in the table is the most stable one The table, it will be seen, gives only the deepest term involved in the structure of the arc spectrum of an element, but in the case of many of the elements the deepest terms involved in their successive spark spectra are given by the result recorded in the table for each of the elements lighter than and immediately successively preceding the one under consideration.

In cases where the fundamental term involved in the structure of any spark spectrum of an element is not directly obtainable from the table, it can be found quite easily by the application of the same method as that used in working out the fundamental term of the arc spectrum of the element.

Without going into any theoretical development, it will suffice to give here a few rules on which the method of determining the lowest spectral terms involved in the structure of the arc spectrum or in that of any spark spectrum of the atom of an element is based

Rules.

1 Orbit types are to be considered as defined by the total, and azimuthal quantum numbers n and k respectively. For purposes of calculation in connection with spectral term determination the quantum number "j," usually designated as "inner," is to be considered as the vector sum of two subsidiary quantum numbers j_a and j_b It is necessary also in some cases to take into consideration the effect of the orientation of orbits with respect to an imaginary small magnetic field, and such orientation involves a fourth quantum number m, which in turn is itself composite and is equal to the vector sum of two subsubsidiary quantum numbers m_a and m_b.

2 Spectral terms are to be designated in the usual way as follows :—S, P, D,

F, G, H, J, K, L, M, N, O, P, Q . . . corresponding to the values 1, 2, 3, 4, 5, 6, 7, 8, 9, 10, 11, 12, 13, 14, . . . for a spectral term quantum number denoted by "l" The manner in which "l" can be evaluated in any selected case is illustrated in the examples given later in this paper.

3 The quantum numbers j_a and j_s are given respectively by $j_a = l - 1$ and $j_s = \frac{r-1}{2}$, where l is the quantum number referred to in Rule 2, and r signifies the multiplicity involved The number m_a is to be considered as having the following values $- j_a, j_a - 1, j_a - 2, \ldots - (j_a - 2), - (j_a - 1), - j_a$, and the number m_s the values $j_s, j_s - 1, j_s - 2 \ldots - (j_s - 2), - (j_s - 1), - (j_s)$. The possible j values associated with a term of any multiplicity are given by the j_s and j_a, corresponding to the term with j max. $= j_a + j_s$ and j min $= j_a - j_s$ or $j_s - j_a$

4. A single electron by itself is to be considered as possessing intrinsically, when occupying an orbit, a doublet character, a feature that is marked by assigning to its corresponding spectral term the multiplicity $r = 2$, which gives $j_s = \frac{1}{2}$ The designation of such corresponding spectral term is determined by the quantum number "l," whose numerical value in such a case is that of the orbit quantum number "k" that defines the type of orbit in which the electron under consideration revolves.

5. No two electrons can occupy identical orbits. If the orbits of two electrons should be characterised by the same values of the quantum numbers n and k, both the associated quantum numbers m_a and m_s cannot have the same values for the two orbits.

6. In determining the energy states (and corresponding term values) for an atom we must take into consideration the resultant effect of all the extra nuclear electrons of the atom in question.

7. If the total number of electrons that can occupy an orbit type, characterised by the same total and azimuthal quantum numbers n and k, be N, the number N is given by $N = 2(2k - 1)$. Such a number is 2 for an orbit of the n_1 type, and 6, 10, 14 for orbits of the n_2, n_3, n_4 .. types respectively.

8 If there are X electrons occupying orbits having the same n and k (equivalent orbits so-called) where $X \equiv N$, the resultant action of X electrons is equivalent to that of $N - X$ electrons, so that the resultant term types will be the same in both cases.

9 If the number of electrons in equivalent orbits is X and if $X \equiv \frac{N}{2}$ the components of any one of the resultant terms will be in the normal order—

that is, the component with the smallest "j" value will be the "deepest." But if $X > \frac{N}{2}$ the term components will be inverted, *i.e.*, the component with the largest "j" value will be the "deepest."

10. By Rule 8 it can be shown that the resultant action of N electrons in equivalent orbits, *i.e.*, orbits having the same value for "n" and "k," is equal to that of no electrons. Therefore, if an orbit type has its complete quota of electrons given by N and forms part of a given electron configuration of an atom, it can be neglected when deriving term types corresponding to that configuration.

11. If in a group of terms that result from a given electron configuration there are terms having the same "l" values but with different multiplicities, the one with the highest multiplicity will be the "deepest." For example, if in such a group there is a ^{4}F term and a ^{2}F term, the ^{4}F term will be deeper than the ^{2}F term.

12. If in a group of terms that result from a given electron configuration there are terms of the same multiplicity, but with different values of "l," that with the highest "l" value will be the deepest. For example, a ^{4}F term will be deeper than a ^{4}D term, a ^{4}D deeper than a ^{4}P, and a ^{4}P deeper than a ^{4}S term.

13. If $\bar{m}_s$ and $\bar{m}_l$ represent the resultants of the m_s and m_l values arising from a set of electron orbits characterised by the same "n" and "k," then $\bar{m}_s$ will be considered as given by $\bar{m}_s = \Sigma m_s$ and $\bar{m}_l$ by $\bar{m}_l = \Sigma m_l$.

14. The multiplicities of the spectral term system of an element are either all even or all odd.

Procedure.

In order to show how the results given in the table were obtained, and also to make clear the procedure to be followed in determining the term type corresponding to a given electron configuration, we append herewith a few illustrative notes.

Note I. *Carbon.*—In the case of carbon the orbits 1_1 and 2_1 are full. The lowest spectral term must therefore be determined by the electrons in the 2_2 orbits.

For the spectral term corresponding to each of these electrons $r = 2$, therefore $j_l = \frac{1}{2}$ and $j_a = l - 1 = k - 1 = 1$. Consequently $m_l = \frac{1}{2}$, $-\frac{1}{2}$ and $m_a = 1$, 0, -1. But the two electrons cannot have the same m_l and also the same m_a, so that we have the following six possibilities:—

m_l =	$\frac{1}{2}$	$\frac{1}{2}$	$\frac{1}{2}$	$-\frac{1}{2}$	$-\frac{1}{2}$	$-\frac{1}{2}$
m_a =	1	0	-1	1	0	1

By adding the above values of m_s and m_a in pairs we can obtain in all fifteen values of $\bar{m}_s$ and $\bar{m}_a$. These are as follows :—

$\bar{m}_s$	1	1	0	0	0	1	0	0	0	0	0	0	−1	−1	−1
$\bar{m}_a$	1	0	2	1	0	−1	1	0	−1	0	−1	−2	1	0	−1

and they can be arranged in three groups as follows —

I.	II	III.
$\bar{m}_s$ 0	1 1 1 0 0 0 −1 −1 −1	0 0 0 0 0
$\bar{m}_a$ 0,	1 0 −1 1 0 −1 1 0 −1,	2 1 0 −1 −2

i e, we have the following types represented —

	$\bar{m}_s$	$\bar{m}_a$				
I.	0	0	$\therefore \bar{j}_s = 0$	$\bar{j}_a = 0$	$r = 1, l = 1$	$^1S_0$
II.	1, 0, −1	1, 0, −1	$\bar{j}_s = 1$	$\bar{j}_a = 1$	$r = 3, l = 2$	$\therefore {}^3P_{012}$
III.	0	2, 1, 0, −1, −2	$\therefore \bar{j}_s = 0$	$\bar{j}_a = 2$	$r = 1, l = 3$	$\therefore {}^1D_2$

i e., there are three possible types for the lowest term involved in the carbon arc spectrum, namely, a singlet S, a singlet D, and a triplet P. According to Rules 11 and 12, ^3P is the lowest term, since it has the highest multiplicity, ^1D is the next lowest, and ^1S next. As the inner quantum numbers j for a triplet P term are 0, 1, 2, and as X, i e, 2, is $< N/2$ i e, < 3, it follows that $^3P_0$ is the deepest component. The lowest term involved in the carbon arc spectrum is therefore $^3P_{012}$, the figures in italics giving the deepest component. This result, it may be stated, is a prediction and has yet to be verified experimentally

In the case of one 2_s electron orbit and one 3_s orbit, where the value of each k is 2, and consequently by Rule 4 each l is 2, our problem is to combine two ^3P terms, and the procedure is as follows —

$$m'_a = 1, 0, -1 \qquad m'_s = \tfrac{1}{2}, -\tfrac{1}{2}$$
$$m''_a = 1, 0, -1 \qquad m''_s = \tfrac{1}{2}, -\tfrac{1}{2}$$

By addition, taking two values at a time, we have then the following possibilities :—

$\bar{m}_a =$

2	1	0
1	0	−1
0	−1	−2

i.e., 2, 1, 0, −1, −2
1, 0, −1
0

$\bar{m}_s =$

1	0
0	−1

i.e, 1, 0, −1
0

i e, $\bar{j}_a = 0, 1$ and $2 \therefore l = 1, 2, 3$
$\bar{j}_s = 0, 1 \quad , \quad r = 1, 3$

The term types involved are therefore

$$^1S_0 \quad ^1P_1 \quad ^1D_2$$
$$^3S_1 \quad ^3P_{012} \quad ^3D_{123}$$

which differs from the case of all the electrons being in equivalent orbits in that the terms ^3S, ^3D, ^1P are retained.

This last result might have been obtained more simply by using the vector magnitudes j_a and j_s directly, for we have for the two ^2P terms

$$j'_a = 1 \qquad j'_s = \tfrac{1}{2}$$
$$j''_a = 1 \qquad j''_s = \tfrac{1}{2}$$
$$\bar{J}_a \text{ max} = 2\bar{J}_a \text{ min} = 0 \text{ or } \bar{J}_a = 0, 1, 2 \quad \therefore l = 1, 2, 3$$
$$\bar{J}_s \text{ max} = 1\bar{J}_s \text{ min.} = 0 \text{ or } \bar{J}_s = 0, 1 \quad \therefore r = 1, 3$$

The term types involved are therefore

$$^1S_0 \quad ^1P_1 \quad ^1D_1$$
$$^3S_1 \quad ^3P_{012} \quad ^3D_{123}$$

Note II. *Nitrogen.*—With nitrogen the lowest spectral term must be determined by the three electrons in the 2_s orbits.

With nitrogen, as with carbon, we have the following possible combinations for m_s and m_a:—

	(a)	(b)	(c)	(d)	(e)	(f)
m_s	$\frac{1}{2}$	$\frac{1}{2}$	$\frac{1}{2}$	$-\frac{1}{2}$	$-\frac{1}{2}$	$-\frac{1}{2}$
m_a	1	0	-1	1	0	-1

Our problem is: In how many ways can we combine these six sets of corresponding values of m_s and m_a, taking three sets at a time. Clearly the number of ways is $\frac{6, 5, 4}{1, 2, 3} = 20$, and they are the following:—

abc	acd	ade	aef
abd	ace	adf	
abe	acf		
abf			
bcd	bde	bef	
bce	bdf		
bcf			
edc	cef		
cdf			
def			

These give the following three groups of values for $\overline{m}_s$ and $\overline{m}_a$ —

	I.	II.	III
$\overline{m}_s$	$\frac{1}{2}$, $-\frac{1}{2}$	$\frac{1}{2}$, $-\frac{1}{2}$	3/2, 1/2, $-\frac{1}{2}$, $-3/2$
$\overline{m}_a$	1, 0, -1	2, 1, 0, -1, -2	0

Group I gives $\overline{J}_s = \frac{1}{2}$ $\therefore r = 2$ $\therefore$ the term $^2P_{12}$

$\overline{J}_a = 1$ $\therefore l = 2$

Group II gives $\overline{J}_s = \frac{1}{2}$ $r = 2$ $\therefore$ the term $^2D_{23}$

$\overline{J}_a = 2$ $l = 3$

Group III gives $\overline{J}_s = 3/2$ $r = 4$ $\therefore$ the term $^4S_2$

$\overline{J}_a = 0$ $\therefore l = 1$

The deepest term in the spectral system of nitrogen I is $^4S_2$, the next deepest is $^2D_{23}$, and the next to that is $^2P_{12}$. If, however, we should have two electrons in 2_s orbit and one in a 3_s, a 4_s or a 5_s, etc., orbit, the following is the procedure to follow —

Two electrons in a 2_s orbit give us the terms $^3P_{012}$, $^1D_2$, $^1S_0$. One electron in a 4_s orbit gives us the term $^2P_{12}$ We must therefore find the result of combining separately $^2P_{12}$ with each of the terms $^3P_{012}$, $^1D_2$ and $^1S_0$ This is worked out in the following manner —

Combination.

I.

$^3P_{012}$ $\begin{cases} j_s = 1 & j_s \text{ max.} = 3/2 \cdot \quad r \text{ max} = 4 \\ j_a = 1 & j_a \text{ min} = 1/2 \cdot \quad r \text{ min} = 2 \end{cases}$ or $r = 2$ or 4 by Rule 14.

$^2P_{12}$ $\begin{cases} j_s = \frac{1}{2} & j_a \text{ max} = 2 \\ j = 1 & j_a \text{ min} = 0 \end{cases}$ $\cdot \begin{cases} l = 3 \\ l = 2 \\ l = 1 \end{cases}$

The term types involved are therefore

$^4D_{1234}$	$^4P_{123}$	$^4S_2$
$^2D_{23}$	$^2P_{12}$	$^2S_1$

II.

$^1D_2$ $\begin{cases} j_s = 0 & j_s \text{ max.} = \frac{1}{2} \\ j_a = 2 & j_a \text{ min.} = \frac{1}{2} \end{cases}$ $\therefore r = 2$

$^3P_{12}$ $\begin{cases} j_s = \frac{1}{2} & j_a \text{ max.} = 3 \\ j_a = 1 & j_a \text{ min} = 1 \end{cases}$ $\therefore l = 2, 3, 4$

The term types involved are

$$^2P_{12} \quad ^2D_{23} \quad ^2F_{34}$$

III

$$^1S_0\begin{cases} j_s = 0 & j_s \text{ max } = \frac{1}{2} \\ j_a = 0 & j_a \text{ min. } = \frac{1}{2} \end{cases} \therefore r = 2$$

$$^2P_{12}\begin{cases} j_s = \frac{1}{2} & j_s \text{ max } = 1 \\ j_a = 1 & j_a \text{ min. } = 1 \end{cases} \therefore l = 2$$

or the type of term involved is $^2P_{12}$

An important feature is brought out by the calculations just given, namely, that the arc spectrum of nitrogen involves spectral terms that can be resolved into three groups, each of which originates in a special type of term that is representative of the carbon like singly charged nitrogen ion This is a feature that applies generally in working out the term systems for atoms of nearly all elements A second feature that is brought out by the calculation is that the term types obtained are the same when the outermost electron of the nitrogen atom is in any one of the 3_2, 4_2 . . . n_2 orbits. This feature is the one that provides for the existence of spectral series and series terms.

Note III. Oxygen.—With oxygen the lowest spectral term will be determined by the four electrons in the 2_2 orbits

For possible combinations we again have

	(a)	(b)	(c)	(d)	(e)	(f)
$m_s =$	$\frac{1}{2}$	$\frac{1}{2}$	$\frac{1}{2}$	$-\frac{1}{2}$	$-\frac{1}{2}$	$-\frac{1}{2}$
$m_a =$	1	0	-1	1	0	-1

and our problem is to combine the corresponding values of m_s and m_a, *i.e.*, a, b, c, d, e, f, in as many ways as possible taking four at a time, *i.e.*, $\frac{6543}{1234} = 15$, and to obtain possible values for $\overline{m}_s$ and $\overline{m}_a$. These combinations are as follows :—

abcd	acde	adef
abce	acdf	
abcf		
bcde	bcef	
bcdf	bdef	
abde	abcf	cdef
abdf	acef	

These groupings give us for $\overline{m}_s$ and $\overline{m}_l$ the following :—

	I.	II.	III.
$\overline{m}_s$	0	0 0 0 0 0	1 1 1 0 0 0 −1 −1 −1
$\overline{m}_l$	0	2 1 0 −1 −2	1 0 −1 1 0 −1 1 0 −1

Group I gives $\overline{j}_s = 0$, $r = 1$; $\overline{j}_l = 0$, $l = 1$ } ∴ the term $^1S_0$

Group II gives $\overline{j}_s = 0$, $r = 1$; $\overline{j}_l = 2$, $l = 3$ } ∴ the term $^1D_2$

Group III gives $\overline{j}_s = 1$, $r = 3$; $\overline{j}_l = 1$, $l = 2$ } ∴ the term $^3P_{012}$

Of the three terms $^1S_0$, $^1D_2$, $^3P_{012}$ we see by Rules 11 and 12 that the deepest is $^3P_{012}$, the next deepest $^1D_2$, and the next to that $^1S_0$

Further, since the number of electrons in 2_2 orbits is 4, *i.e.*, $> \frac{N}{2}$ or > 3, we see that the usual order by Rule 9 is inverted, and of the components of the term ^3P that with the largest j value is the deepest, namely, $^3P_2$; the deepest term with our system of designation is then $^3P_{012}$.

The complete spectral term scheme for oxygen as it has been built up from the three fundamental terms of nitrogen, $^4S_{\frac{3}{2}}$, $^2D_{2\frac{1}{2}}$ and $^2P_{1\frac{1}{2}}$ is given in Table II.

Table II.

Nitrogen

n_s	l_1	2_1	2_2	3_1	3_2	3_3	Terms		
2	2	3	—	—	—	$^4S_{\frac{3}{2}}$	$^2D_{2\frac{1}{2}}$	$^2P_{1\frac{1}{2}}$	

Oxygen

A								B								
n_s	l_1	2_1	2_2	3_1	3_2	3_3	Terms			n_s	l_1	2_1	2_2	3_1	3_2	3_3	Terms		
2	2	3	—	—	—		$^4S_{\frac{3}{2}}$			2	2	3	—	—	—		$^2D_{2\frac{1}{2}}$		
2	2	4	—	—	—		$^2P_{012}$			2	2	4	—	—	—		$^1\overline{D}_2$		
2	2	3	1	—	—		$^4S_{\frac{3}{2}}$	$^4S_{\frac{3}{2}}$		2	2	3	1	—	—		$^4\overline{D}_{1\frac{1}{2}}$	$^1D_2$	
2	2	3	—	1	—		$^4P_{1\frac{1}{2}}$	$^2P_{012}$		2	2	3	—	1	—		$^4F_{\frac{3}{2}\frac{5}{2}}$	$^2\overline{D}_{1\frac{1}{2}}$	$^3P_{012}$
2	2	3	—	—	1		$^4D_{\frac{1}{2}\frac{3}{2}\frac{5}{2}}$	$^2D_{2\frac{1}{2}}$										$^1F_2$	$^1\overline{D}_2$	$^1P_1$
										2	2	3	—	—	1		$^4G_{2\frac{1}{2}}$	$^2\overline{F}_{2\frac{5}{2}}$	$^2D_{2\frac{1}{2}}$
																	$^2\overline{P}_{012}$	$^3S_1$	$^1G_4$
																	$^1F_3$	$^1D_2$ $^1\overline{P}_1$	$^1S_0$

Table II.—(continued.)

C

n_2	l_1	2_1	2_2	3_1	3_2	3_3	Terms		
	2	2	3	—	—	—	$^3P_{11}$		
	2	2	4	—	—	—	$^1\overline{S}_0$		
	2	2	3	1	~	-	$^3\overline{P}_{012}$	$^1\overline{P}_1$	
	2	2	3	-	1	—	$^3\overline{D}_{123}$	$^3P_{012}$	$^3\overline{S}_1$
							$^1\overline{D}_2$	$^1P^1$	$^1\overline{S}_0$
	2	2	3	—	—	1	^3F	^3D	$^3\overline{P}$
							^1F	^1D	$^1\overline{P}$

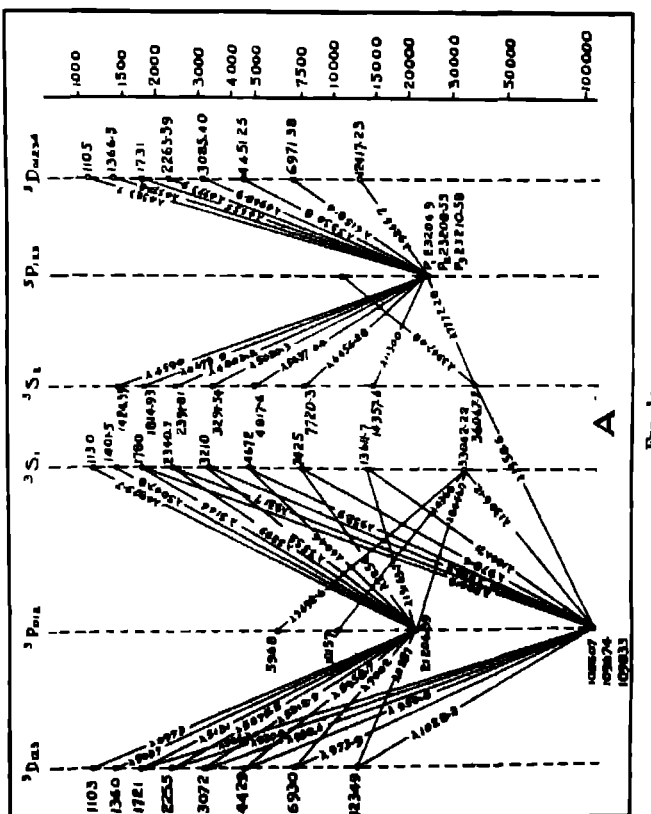

FIG 1A.

These terms are all shown graphically in fig. 1. From this diagram it will be seen that the Triplet-Quintet scheme of terms A includes practically all of the

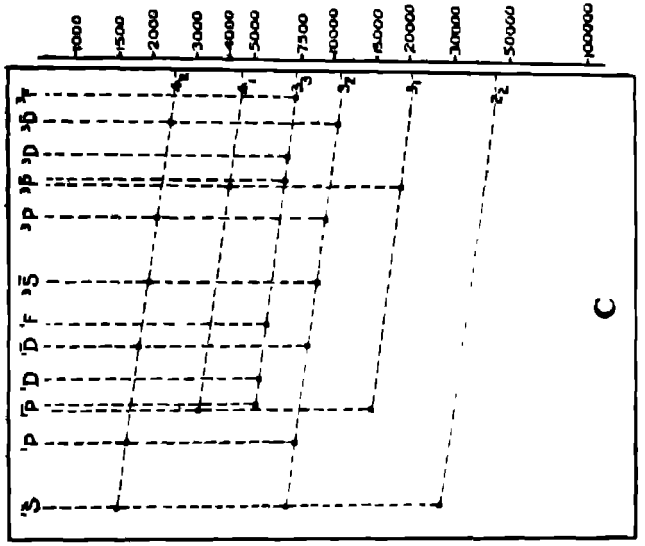
4000
4500
5000
6000
7000
8000
9000
10000
15000
20000
30000
50000
100000
^1S ^1P ^1D ^1D ^1F ^1F ^1G ^3S ^3P ^3D ^3D ^3F ^3F ^3G
$^4S_2$ $^4P_1$ $^3S_1$ $^3P_2$ $^3P_1$ $^3D_3$ $^3D_2$ $^3D_1$ $^3F_4$ $^3F_3$ $^3F_2$ $^3G_5$ $^3G_4$ $^3G_3$
B

Fig. 1b

4000
4500
5000
6000
7000
8000
9000
10000
15000
20000
30000
50000
100000
^1S ^1P ^1D ^1D ^1F ^1F ^3S ^3P ^3D ^3D ^3F ^3F ^3G
$^4S_2$ $^4P_1$ $^3S_1$ $^3P_2$ $^3P_1$ $^3D_3$ $^3D_2$ $^3D_1$ $^3F_4$ $^3F_3$ $^3F_2$ $^3G_5$ $^3G_4$ $^3G_3$
C

Fig. 1c

known series lines in the spectrum of atomic oxygen. The single-triplet schemes B and C, however, provide systems of levels for two groups of series lines whose possible existence has not been suspected hitherto. It has been suggested by one of the writers that the Auroral Green line λ 5577·35 A may find its place in one or other of the term schemes B and C set forth above. It is possible, too, that some spectral lines hitherto unidentified and others assigned to so-called "coronium" or to so-called "nebulium" may ultimately be identified as originating in the term schemes provided in B and C or in similar schemes of terms that can be worked out for nitrogen or others of the elements.

The method by which the terms in A, B and C have been worked out will be seen from the following three examples :—

Scheme A (see last row).

Combine the terms $^4S_2$ and $^2D_{23}$.

We have $^4S_2$, giving $j_a = 0$ j_a max $= 2$; $j_s = 3/2$ j_a min. $= 2$ $\Big\}$ $j_a = 2$

$^2D_{23}$, giving $j_a = 2$ j_s max. $= 2$; $j_s = \frac{1}{2}$ j_s min. $= 1$ $\Big\}$ $j_s = 1$ and 2,

$\therefore$ $l = 3$ and $r = 3$ and 5.

$\therefore$ the terms $^5D_{1234}$ and $^3D_{123}$.

Scheme B (see last row)

Combine the terms $^3D_{23}$ and $^2D_{23}$.

We have $^3D_{23}$, giving $j_a = 2$ j_a max $= 4$; $j_a = \frac{1}{2}$ j_a min $= 0$ $\Big\}$ $j_a = 01234$ $\therefore$ $l = 12345$

$^2D_{23}$, giving $j_a = 2$ j_s max. $= 1$; $j_s = \frac{1}{2}$ j_s min $= 0$ $\Big\}$ $j_s = 0, 1$ $\therefore$ $r = 1$ and 3

$\therefore$ the terms

$^3G_{345}$ $^3F_{234}$ $^3D_{123}$ $^3P_{012}$ $^3S_1$

$^1G_4$ $^1F_3$ $^1D_2$ $^1P_1$ $^1S_0$

Scheme C (see last row)

Combine $^4P_{12}$ with $^2D_{23}$

We have $^4P_{12}$, giving $j_a = 1$ j_a max. $= 3$; $j_s = \frac{1}{2}$ j_a min. $= 1$ $\Big\}$ $j_a = 1, 2, 3$ $\therefore$ $l = 2, 3, 4$

$^2D_{23}$, giving $j_a = 2$ j_s max $= 1$; $j_s = \frac{1}{2}$ j_s min. $= 0$ $\Big\}$ $j_s = 0, 1$ $\therefore$ $r = 1, 3$

The terms are therefore

$$^3F_{234} \quad ^3D_{123} \quad ^3P_{012}$$
$$^1F_3 \quad ^1D_2 \quad ^1P_1$$

Note IV. Neon.—Here we have the configuration $\begin{matrix} n_1 & 1_1 & 2_1 & 2_2 \\ 2, & 2, & 6 & \end{matrix}$

For each of the six 2_2 electron orbits the corresponding spectral term is $^2P_{12}$.

$^2P_{12}$ gives $j_s = 1 \quad m_s = 1 \; 0 \; -1$

$j_s = \frac{1}{2} \quad m_s = \frac{1}{2} \quad -\frac{1}{2}$

or

m_s	m_s		
1	$\frac{1}{2}$	From $\overline{m}_s = 0$ we have $j_s = 0 \quad \therefore l = 1$	$^1S_0$
0	$\frac{1}{2}$		
−1	$\frac{1}{2}$	$\overline{m}_s = 0 \quad \therefore \quad j_s = 0 \quad \therefore l = 1$	
1	$-\frac{1}{2}$		
0	$-\frac{1}{2}$		
−1	$-\frac{1}{2}$		
$\overline{m}_s =$ 0	$\overline{m}_s = 0$		

i.e., the lowest term involved in the neon spectrum is a singlet S term, i.e., $^1S_0$.

This is a result that recently received a remarkable verification through the investigations of Hertz *

Note V. Titanium, Nickel, Zirconium, Hafnium and possibly Thorium.—With these five elements the lowest spectral term is determined by two n_3 electron orbits That this is so will be seen from the following table :—

	n_k	1_1	2_1 2_2	3_1 3_2 3_3	4_1 4_2 4_3 4_4	5_1 5_2 5_3 5_4 5_5	6_1 6_2 6_3 6_4 6_5 6_6	7_1 7_2
Titanium	=	2	2 6	2 6 2	2 – – –	– – – – –	– – – – – –	– –
Nickel	=	2	2 6	2 6 8	2 – – –	– – – – –	– – – – – –	– –
Zirconium	=	2	2 6	2 6 10	2 6 2 –	2 – – – –	– – – – – –	– –
Hafnium	=	2	2 6	2 6 10	2 6 10 14	2 6 2 – –	2 – – – – –	– –
Thorium ?	=	2	2 6	2 6 10	2 6 10 14	2 6 10 – –	2 6 2 – – –	2 –

To determine the term corresponding to the combination of an n'_3 orbit and an n''_3 orbit where n' is not equal to n'', we may proceed as follows —

* Hertz, 'Zeit. für Phys.,' vol. 32, p. 933 (1925).

For an n_3 orbit we have the doublet term $^2D_{23}$ and are therefore required to combine two $^2D_{23}$ terms

$^2D_{23}$ gives $j_a = 2$ j_a max. $= 4$

$\therefore l = 12345$

$j_s = \frac{1}{2}$ j_a min. $= 0$

$^2D_{23}$ gives $j_a = 2$ j_a max $= 1$

$\therefore r = 1$ or 3.

$j_s = \frac{1}{2}$ j_a min $= 0$

The resultant terms are therefore ^5G, ^3F, ^3D, ^3P, ^3S and ^1G, ^1F, ^1D, ^1P, ^1S. Certain limitations are imposed, however, when $n'_3 = n''_3 = 4_3$ for example, and to find these, as we have seen before, it is necessary to take into account the quantum numbers m_a and m_s

Since $j_a = 2$ it follows that $m_a =$ 2 1 0 −1 −2 and

since $j_s = \frac{1}{2}$,, $m_s = +\frac{1}{2}$ $-\frac{1}{2}$ from which we have

$m_s =$	$\frac{1}{2}$	$\frac{1}{2}$	$\frac{1}{2}$	$\frac{1}{2}$	$\frac{1}{2}$	$-\frac{1}{2}$	$-\frac{1}{2}$	$-\frac{1}{2}$	$-\frac{1}{2}$	$-\frac{1}{2}$
$m_a =$	2	1	0	−1	−2	2	1	0	−1	−2

There are 45 ways in which we can select two out of the ten sets of values for m_s and m_a and these give for $\bar{m}_s$ and $\bar{m}_a$ the following groups of values :—

	I.	II.	III.	IV.	V.
$\bar{m}_s$	0	1, 0, −1	1, 0, −1	0	0
$\bar{m}_a$	43210 −1 −2 −3 −4	3210 −1 −2 −3	1, 0, −1	210 −1 −2	0

Group I gives $\bar{j}_s = 0$ $\therefore r = 1$

$\therefore$ the corresponding term is $^1G_4$.

$\bar{j}_a = 4$ $\therefore l = 5$

Group II gives $\bar{j}_s = 1$ $\therefore r = 3$

$\therefore$ the corresponding term is $^3F_{234}$

$\bar{j}_a = 3$ $\therefore l = 4$

Group III gives $\bar{j}_s = 1$ $\therefore r = 3$

$\therefore$ the corresponding term is $^3P_{012}$

$\bar{j}_a = 1$ $\therefore l = 2$

Group IV gives $\bar{j}_s = 0$ $\therefore r = 1$

$\therefore$ the corresponding term is $^1D_2$

$\bar{j}_a = 2$ $\therefore l = 3$

Group V gives $\bar{j}_s = 0$ $\therefore r = 1$

$\therefore$ the corresponding term is $^1S_0$.

$\bar{j}_a = 0$ $\therefore l = 1$

We see, then, that with two n_3 orbits we may have one or other of the spectral terms ^3F ^3P ^1G ^1D ^1S, of which ^3F is the deepest In the case of Titanium, Zirconium, Hafnium and Thorium the component of ^3F that is deepest is $^3F_2$, while with Nickel it is $^3F_4$. This follows from Rule 9.

Note VI. Neodymium, Uranium and Tungsten.—In order to find the lowest term in the arc spectrum of Neodymium and possibly also of Uranium, we must find the resultant spectral term corresponding to a combination of three 4_4 orbits and one 5_3 orbit

To do this we must first of all find the deepest spectral term corresponding to three 4_4 orbits. In all, there are 14 types of 4_4 orbits and of these we can select three at a time in $\frac{14\ 13\ 12}{1\ 2\ 3} = 364$ ways.

To a 4_4 orbit there corresponds the term $^2F_{34}$ and $^2F_{34}$ gives

$$j_a = 3$$
$$j_a = \tfrac{1}{2}$$

for m_s and m_a we have the following sets of values –

$m_s =$	$\frac{1}{2}$	$\frac{1}{2}$	$\frac{1}{2}$	$\frac{1}{2}$	$\frac{1}{2}$	$\frac{1}{2}$	$\frac{1}{2}$	$-\frac{1}{2}$	$-\frac{1}{2}$	$-\frac{1}{2}$	$-\frac{1}{2}$	$-\frac{1}{2}$	$-\frac{1}{2}$	$-\frac{1}{2}$
$m_a =$	3	2	1	0	−1	−2	−3	3	2	1	0	−1	−2	−3

By inspection we see on considering these pairs of values in groups of three that the highest multiplicity involved is given by $\bar{m}_s = 3/2$ with the corresponding value of $\bar{m}_a$ given by $\bar{m}_a = 6$. This shows that the deepest term three 4_4 orbits can give rise to is a quartet J, *i e*, $^4J_{6678}$.

The complete list of terms that corresponds to three 4_4 orbits we have found to be ^4J, ^4G, ^4F, ^4D, ^4S, ^2L, ^2K, ^2J, ^2H, ^2H, ^2G, ^2G, ^2F, ^2F, ^2D, ^2D, ^2P, with $^4J_{6678}$ the deepest

We must now combine the term ^4J with a term $^2D_{23}$ and we have

^4J or $\bar{j}_s = \frac{3}{2}$ $\therefore$ j_s max. $= 2$
$\therefore r = 3$ and 5

$\bar{j}_a = 0$ $\quad$ j_a min. $= 1$

^2D or $\bar{j}_s = \frac{1}{2}$ $\quad$ j_a max $= 8$
$\therefore l = 5\ 6\ 7\ 8\ 9.$

$\bar{j}_a = 2$ $\quad$ j_a min. $= 4$

The corresponding terms are therefore ^5L, ^5K, ^5J, ^5H, ^5G and ^3L, ^3K, ^3J, ^3H, ^3G, and of these the deepest by Rule 9 is ^5L. Of its five components $^5L_6$ is the deepest, which agrees with the term designation given for Neodymium in the table, namely, $^5L_{678910}$. This type of term may possibly turn out

to be the lowest involved in the structure of the arc spectrum of Uranium as well, but certain considerations lead one to the view that with Uranium the lowest term should be the same as that involved in the structure of the arc spectrum of Tungsten, namely, $^5D_{0123\frac{1}{2}}$ This it can be easily shown is the term equivalent of four 5_2 orbits and is obtained by combining four $^2D_{2\frac{1}{2}}$ terms Reverting to the case of Neodymium it may be stated that we found that the complete list of terms resulting from a combination of a term $^2D_{2\frac{1}{2}}$ with each of the terms ^4J, ^4G, ^4F, ^4D, ^4S, ^2L, ^2K, ^2J, ^2H, ^2H, ^2G, ^2G, ^2F, ^2F, ^2D, ^2D, ^2P, numbers 158. It is given in Table III.

Table III —Lowest Terms involved in the Structure of the Neodymium Arc Spectrum

I	^5L ^5K ^5J ^5H ^5G ^3L ^3K ^3J ^3H ^3G	II	^5J ^5H ^5G ^5F ^5D ^3J ^3H ^3G ^3F ^3D	III	^5H ^5G ^5F ^5D ^5P ^3H ^3G ^3F ^3D ^3P
IV	^5G ^5F ^5D ^5P ^5S ^3G ^3F ^3D ^3P ^3S	V	^5D ^3D	VI	^5N ^5M ^5L ^5K ^5J ^1N ^1M ^1L ^1K ^1J
VII	^5M ^5L ^5K ^5I ^5H ^1M ^1L ^1K ^1J ^1H	VIII	^5L ^5K ^5J ^5H ^5G ^1L ^1K ^1J ^1H ^1G	IX	^5K ^5J ^5H ^5G ^5F ^1K ^1J ^1H ^1G ^1F
X	^5K ^5J ^5H ^5G ^5F ^1K ^1J ^1H ^1G ^1F	XI	^5J ^5H ^5G ^5F ^5D ^1J ^1H ^1G ^1F ^1D	XII	^5G ^5F ^5D ^5P ^5S ^1G ^1F ^1D ^1P ^1S
XIII	^5H ^5G ^5F ^5D ^5P ^1H ^1G ^1F ^1D ^1P	XIV	^5H ^5G ^5F ^5D ^5P ^1H ^1G ^1F ^1D ^1P	XV	^5G ^5F ^5D ^5P ^5S ^1G ^1F ^1D ^1P ^1S
XVI	^5G ^5F ^5D ^5P ^5S ^1G ^1F ^1D ^1P ^1S	XVII	^5F ^5D ^5P ^1F ^1D ^1P		

With such a number of "deep" terms available, it is easily seen that Neodymium should possess an arc spectrum of great complexity.

From the illustrations given above the method of determining the type of spectral term that corresponds to any selected configuration for the electronic orbits of an atom will be evident. The experimental data still required to completely test the validity of the scheme as set forth are not extensive and are likely to be forthcoming soon. With the validity of the scheme of orbits set forth in Table 1 established, we shall be in the position of being able to predict all optical spectra including both the arc and the spark spectra of the atoms of all the elements We shall be able also to make some progress in the determination of the characteristics of the spectra of atoms of hypothetical elements heavier than Uranium.

We desire to state here that one of us (A. B McLay) was enabled to collaborate in the investigation leading up to this communication through the award to him of a fellowship by the National Research Council of Canada.

On the Structure of the Arc Spectrum of Gold.

By Prof. J. C. McLennan, F.R.S., and A. B. McLay, M.A.

(Received June 10, 1926.)

I. *Introduction.*

The first successful attempt to find series relationships among wave-lengths of the gold arc spectrum was that made by Thorsen* in 1923. In his paper he classified two sets of wave-lengths into a sharp and a diffuse subordinate doublet series, the first pair of the sharp series providing the first pair of the corresponding principal doublet series. In a communication† by us a year ago some absorption experiments were described that were carried out with the normal vapour of gold in the quartz and fluorite spectral regions. In this communication it was shown that we confirmed Thorsen's selection of the first pair of the principal series, and that we were able to extend this series so as to include the second pair as well. In addition, two other interesting features of the spectral structure were pointed out that at the time were not completely understood. The first of these was concerned with the existence of a deep metastable inverted doublet D term, and the second with a pair of terms that were characterized by features similar to those of doublet terms of the P type. This pair did not seem to belong, however, to the regular series of doublet P terms. In the communication referred to we also pointed out that our term scheme did not permit us to classify a number of strong lines that were known to belong to the gold arc spectrum, and that included many of the wave-lengths found to be absorbed by Miss Buffam and Mr. H. J. C. Ireton‡ in experiments on the underwater spark spectrum of gold. To account in a general way for many of these wave-lengths we suggested that they might possibly be found to belong to a quartet or to a sextet system, the features of which we were not at the time able to develop.

Recently, through the brilliant work of Pauli§, Heisenberg‖ and Hund¶ on the interpretation of spectra, we have been furnished with a means of predicting with considerable accuracy the structure of any spectrum. By this theory,

* 'Naturw.,' vol. 25, p. 500 (1923).
† 'Roy. Soc. Proc.,' A, vol. 108, p. 571 (1925).
‡ 'Trans. Roy. Soc. Can.,' vol. 19, III, p. 113 (1925).
§ 'Z. f. Physik,' vol. 31, p. 765 (1925).
‖ 'Z. f. Physik,' vol. 32, p. 841 (1925).
¶ 'Z. f. Physik,' vol. 33, p. 345 (1925).

with some modifications and extensions, we can now predict the structure of the gold arc spectrum, and as a consequence are able to carry out a more systematic investigation of its features The significance of the two unusual features found by us in our earlier work and mentioned above is now more clearly understood. We shall proceed to explain these features and to develop the structure of the spectrum more fully in the discussion following in Sections IV and V

II. *Absorption Experiments and Wave-length Measurements.*

As a further aid to the present investigation, absorption experiments were repeated in the quartz spectral region, both by the method of normal vapour absorption and by that of the underwater spark. Table III contains all the wave-lengths found to be absorbed by gold vapour in these experiments, and they are classified according to our subsequent analysis of the spectrum

A few wave-lengths, not previously recorded in either the arc or the spark spectrum of gold, have been measured by us either from our plates of absorption spectra or from some plates of the emission arc spectrum taken by us for the purpose. These wave-lengths are noted by an asterisk in the tables. All other values used in this paper were obtained from Kayser and Konen's 'Handbook, Vol. VII, with the exception of the three wave-lengths λ 1833 26 (I vac.), λ 1665 52 (I vac.) and λ 1646·50 (I vac.) which were measured by Bloch.* Certain of the wave-lengths, however, that had been observed previously only in the spark spectrum were found by us to be really arc lines. The intensities of such wave-lengths were estimated by us from our arc spectrum plates.

We have adopted Sommerfeld's values for the quantum numbers and Russell's notation for the term designations throughout. For example, the designation 1^2D_3 represents the component of the "deepest" term of the doublet D type, having the inner quantum number $j = 5/2$

III *Theoretical Considerations.*

It has been shown by Pauli, Heisenberg, and Hund in their treatment of the interpretation of spectra, referred to in Section I of this communication, that in order to determine the energy states of an atom involved in the emission of any of its spectra, the resultant action of all the electrons of the atom in question must be considered Without going into the theoretical development in any detail, we will merely give here a few rules that it will be necessary to refer to later. Certain of these rules are based on theoretical considerations and certain

* 'J. Physique et Rad.,' vol. VI, 4–5, pp. 105 and 154 (1925).

of them were given by Hund in his paper and were derived by him from empirical relations found to exist in a number of known cases.

1. If the total number of electrons that can occupy an orbit type, characterized by the same total and azimuthal quantum numbers n and k, be N, the number N is given by $N = 2(2k - 1)$. Such a number is 2 for an orbit of the n_1 type, and 6, 10, 14 . . for orbits of the n_2, n_3, n_4 ... types respectively

2. If there are r electrons occupying orbits having the same n and k (equivalent orbits) where $r \equiv N$, the resulting action of r electrons is equivalent to that of $N - r$ electrons, and so the resultant term types would be the same in either case.

3. If the number of electrons in equivalent orbits is r, and if $r \equiv \frac{N}{2}$, the components of any one of the resultant terms should be in the normal order, that is, the component with the smallest "j" value should be the "deepest" But if $r > \frac{N}{2}$ the term components should be inverted, that is, the component with the largest "j" value should be the "deepest."

4 By rule 2 it can be shown that the resultant action of N electrons in equivalent orbits is equal to that of no electrons. Therefore if an orbit type has its complete quota of electrons, given by N, and forms a part of a given electron configuration of an atom, it can be neglected when deriving the term-types corresponding to that configuration.

5. If in a group of terms that result from a given electron configuration there are terms having the same "l" values but of different multiplicities, that with the highest multiplicity should be the "deepest." For example, if in such a group there is a ^4F term and a ^2F term, the ^4F term should be "deeper" than the ^2F term.

6. If in a group of terms that result from a given electron configuration there are terms of the same multiplicity but with different values of "l," that with the highest "l" value should be the deeper. For example, a ^4F term should be deeper than a ^4D term, a ^4D deeper than a ^4P and a ^4P deeper than a ^4S term.

We will now proceed to develop the theoretical structure of the gold arc spectrum according to the methods furnished by Pauli, Heisenberg and Hund, before discussing the results of our empirical analysis of its features.

Hund has shown in his paper that we can most easily predict the terms belonging to the arc spectrum of any element by first considering the "deep" terms of the spark spectrum that correspond to all stable and metastable electron

configurations possible for the atom when in the singly ionized state Passing then to the terms of the arc spectrum we obtain these by adding an electron that is supposed to occupy an orbit of any type not already possessing its complete quota of electrons

Table I gives the three possible electron configurations that represent the most stable energy states involved in the emission of the Au II spectrum, *i.e.*, the first spark spectrum of gold.

If now we add an electron in various possible ways and calculate the resultant terms, we arrive at the term types given in Table II. In this table only those configurations are given that determine the most important energy states involved in the emission of the Au I spectrum, and that are necessary for the discussion of our empirical analysis of its features. The added electron is bracketed in each configuration of Table II It should be pointed out that from each configuration in Table II only the first member of a term series can be determined Higher series members result when the added electron occupies an orbit of higher total quantum number, n, than that given

When the gold atom is in any one of the states in Table II, say in 1A, 2A, or 3A, its arc spectrum is characterized by ^2S, ^2P and ^2D terms respectively. If the bracketed electron in 1A, 2A, or 3A, Table II, is removed entirely, the atom will then in each case be in the ionized state 1A in Table I, and its first spark spectrum while in this state will be characterized by a "deep" term of the ^1S type This means that the "deep" ^1S terms of the spark spectrum is the common limit of the ^2S, ^2P and ^2D series of the arc spectrum, the first members of which are indicated in 1A, 2A, or 3A, Table II. In the same way the limit of any other term series belonging to the arc spectrum can be shown to be one of the "deep" terms of the spark spectrum given in Table I In Table II the series limits are indicated in the right-hand column.

It will be seen from Table II that the gold atom cannot get directly from any one of the states in a certain class 1, 2 or 3 to any other state in the same class without involving a violation of the selection rule for the azimuthal quantum number, "k," of an orbit, *i.e.*, that in a transition "k" may change only by ± 1. Neither can the atom get directly from either of the states in class 1 to either of those in class 3 without a violation of this selection rule. But the selection rule would permit certain transitions between a state in class 2 and certain states in class 1 or certain states in class 3. Hund, however, says that the atom can get directly from any of the states in class 2 to any of those in class 1 or to any of those in class 3. If this is correct, there must be two kinds of transitions possible, (*a*) those for which a single electron jumps

Table I.—Au II—Deep Terms.

	Class / n_k	Electron Configurations																Deep Terms.
		1_1	2_1	2_2	3_1	3_2	3_3	4_1	4_2	4_3	4_4	5_1	5_2	5_3	5_4	5_5	6_1	
I	A	2	2	6	2	6	10	2	6	10	14	2	6	10	—	—	—	$^1S_0$
	B	2	2	6	2	6	10	2	6	10	14	2	6	9	—	—	1	$^3D_{3,2,1}$ $^1D_2$
	C	2	2	6	2	6	10	2	6	10	14	2	6	8	—	—	2	$^3P_{2,1,0}$ $^3F_{4,3,2}$ $^1D_2$ $^1G_4$

Table II.—Au I—Term Types

Class	n_2	1_1	2_1	2_2	3_1	3_2	3_3	4_1	4_2	4_3	4_4	5_1	5_2	5_3	5_4	5_5	6_1	6_2	6_3	6_4	6_5	6_6	Term Types.	Series Limit Au II Term
1	A	2	2	6	2	6	10	2	6	10	14	2	6	10	—	—	(1)	—	—	—	—	—	^2S	^1S
	B	2	2	6	2	6	10	2	6	10	14	2	6	9	—	—	1(1)	—	—	—	—	—	^2D	^3D
2	A	2	2	6	2	6	10	2	6	10	14	2	6	10	—	—	—	(1)	—	—	—	—	^2P	^1S.
	B	2	2	6	2	6	10	2	6	10	14	2	6	9	—	—	1	(1)	—	—	—	—	$^4P\ ^4\overline{D}\ ^4F$ $^2P\ ^2\overline{D}\ ^4F$ $^2P\ ^2\overline{D}\ ^2F$	^3D ^1D
	C	2	2	6	2	6	10	2	6	10	14	2	6	8	—	—	2	(1)	—	—	—	—	$^4\overline{D}\ ^4F\ ^4\overline{G}$ $^2\overline{D}\ ^4F\ ^2\overline{G}$ $^4\overline{S}\ ^4P\ ^4\overline{D}$ $^2\overline{S}\ ^2P\ ^2\overline{D}$ $^2F\ ^2\overline{G}\ ^2H$ $^2P\ ^2\overline{D}\ ^2F$ ^2P	$^3\overline{F}$ $^3\overline{P}$. ^1G ^1D. ^1S
3	A	2	2	6	2	6	10	2	6	10	14	2	6	10	—	—	—	—	(1)	—	—	—	^2D	^1S
	B	2	2	6	2	6	10	2	6	10	14	2	6	9	—	—	1	—	(1)	—	—	—	$^4S\ ^4\overline{P}\ ^4D\ ^4\overline{F}\ ^4G$ $^2S\ ^2\overline{P}\ ^2D\ ^2\overline{F}\ ^2G$ $^2S\ ^2\overline{P}\ ^2D\ ^2\overline{F}\ ^2G$	^3D. ^1D

from an orbit with k to one with $k \pm 1$, in accordance with the selection rule, and (*b*) those for which two electrons jump simultaneously one from an orbit with k_1 to an orbit with $k_1 \pm 1$ and the other from an orbit with k_2 to an orbit with $k_2 \pm 2$ where k_1 and k_2 may be equal or unequal For example, if the atom is to get from 2A to 1B one electron must jump from a 6_2 orbit to a 6_1 orbit, the other electron from a 5_2 orbit to a 6_1 orbit. Our empirical analysis shows that such a transition does occur in the emission of certain wave-lengths of the gold arc spectrum, so that double electron groups, governed by the rules in (*b*) above, must be possible for the un-ionized atom of gold They have been known to occur in the atoms of a number of other elements also, and were found originally by Russell and Saunders* to be an important characteristic of the emission of the arc spectra of the alkaline earth elements

IV.—*Discussion of Empirical Results*

The results of our empirical analysis of the gold arc spectrum are given in the energy diagram Fig. 1 and in Tables IV and V. Table IV contains the

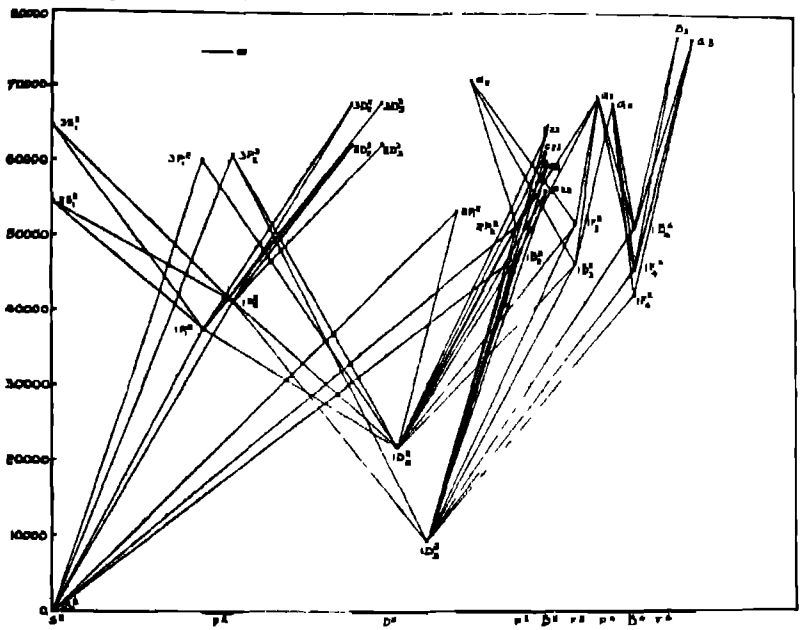

FIG. 1.—*Note.*—To keep the notation uniform with the text, nX_r' of this diagram should be read as n^rX_r throughout, *e.g.* $3S_1'$ as 3^2S_1, etc

* 'Astrophys J.,' vol 61, p. 38 (1925)

values of all the terms we have been able to find The terms have been grouped so that each group corresponds to a certain configuration of the electrons of the un-ionized atom of gold The configurations (of the 11 outer electrons only) are given in the right-hand column in such a way that $(5_3)^{10}\,6_1$, for instance, indicates that there are 10 electrons occupying 5_3 orbits and one occupying a 6_1 orbit. Table V contains the wave-lengths that we have been able to classify as combinations between pairs of the terms in Table IV.

Our absorption experiments show that the deepest term of the whole arc spectrum of gold is that designated as $1\,^2S_1$, for all the wave-lengths in Table III that we found to be absorbed by the normal vapour of gold involve this term. To it, therefore, we have assigned the value zero It corresponds to the ^2S term predicted in Table II, 1A, and is the first member of a doublet S series, two higher members of which have also been identified. The terms designated as $1\,^2P_{1,2}$ and $2\,^2D_{2,3}$ correspond to those predicted in Table II, 2A and 3A respectively They are the first members of a doublet P and of a doublet D

Table III —Absorbed Wave-lengths

I	λ (I A)	ν (vac).	Combination	Method
8	3122 78	32018·5	1^2D_2—1^2P_1	U W
8r	3029·22	33002 2	1^2D_2—1^2F_3	U W.
6	2748 26	36375 9	1^2D_2—1^2F_4	U.W
4	2700 90	37013 7	1^2D_2—1^2D_3	U W.
10R	2675·95	37358 8	1^2S_1—1^2P_1	U W ; N V
4	2641 49	37846 1	1^2D_2—1^2D_2	U W.
10R	2427 98	41174 0	1^2S_1—1^2P_2	U.W ; N V
5	2387·75	41867·6	1^2D_2—1^2D_2	U W.
4	2376 25	42070 3	1^2D_2—2^2P_2	U W.
6	2352 65	42492·2	1^2D_2—1^2F_3	U W.
2	*2129·40	46945·4	1^2D_2—$a_{1,2}$	U W
2	*2126 62	47008·2	1^2S_1—1^2D_2	U W , N V
4	2110·60	47364 9		U.W
4	2082·00	48015·3		U.W.
3	*2021 40	49454 6	1^2D_2—$b_{2,2}$	U.W.
3	*2012 02	49685·2		U W.
2	2000 68	49966 9		U W.
3	1991 15	50205 8		U W
4	1977 32	50557·1		U.W.
3	1951·21	51233 4	1^2S_1—2^2P_2	U W. ; N V.
2	*1938 52	51567·7	1^2D_2—3^2P_2	U W.
4	1918 92	52095 5	1^2D_2—$c_{1,2}$	U.W
3	1879 13	53198 4	1^2S_1—2^2P_1	U W. ; N V.
	λ (I vac).			
1	1665 52	60041 2	1^2S_1—3^2P_1	N V
2	1646 50	60734 9	1^2S_1—3^2P_2	N V.

* Measured by the authors

series, and we have found one higher member of each series as well The common limit of each of these term series we have shown in Section III to be the "deep" ^1S term of the Au II spectrum, given in Table I, 1A The calculated value of the limit is 74,461 cm.$^{-1}$, and is indicated in fig 1 by the horizontal line with the infinity symbol at the right of it.

Table IV.

"j" value	Term Designation	Term Value	Term Separation	Configuration of Outer Electrons
1/2	1^1S_1	0		$(5_2)^{10}6_1$
5/2	1^3D_3	9160 8	12274 0	$(5_2)^9\ (6_1)^1$
3/2	1^3D_2	21434 8		
1/2	1^1P_1	37358 6	3815 6	$(5_2)^{10}6_2$
3/2	1^1P_2	41174 2		
7/2	1^1F_4	42163 0		$(5_2)^{10}6_1 6_2$
7/2	1^3F_4	45836 7		
5/2	1^3D_3	46174 5	832 5	
3/2	1^3D_2	47007 0		
7/2	1^3D_4	51038 4	6116 4	
3/2	2^3P_2	51231 0	1977 3	
5/2	1^3F_3	51653 1		
1/2	2^3P_1	53208 3		
3/2 or 5/2	a_{32}	56105 2		
3/2 or 5/2	b_{32}	58616·2		
3/2 or 5/2	c_{32}	61255 4		
3/2 or 5/2	d_{32}	63712 9		
1/2	2^1S_1	54484 8		$(5_2)^{10}7_1$
1/2	3^3P_1	60032 5	695 7	$(5_2)^{10}7_2$
3/2	3^3P_2	60728 2		
3/2	2^3D_2	61951 5	82 4	$(5_2)^{10}6_2$
5/2	2^3D_3	62033 9		
1/2	3^1S_1	64742 4		$(5_2)^{10}8_1$
3/2	3^3D_2	67469·1	41·8	$(5_2)^{10}7_2$
5/2	3^3D_3	67510 9		
7/2	a_4	67810 8		$(5_2)^{10}6_1 6_2$
5/2	a_3	68704 6		
3/2	a_2	70652 7		
9/2	a_5	76731 5		
9/2	β_5	76829 2		

Table V

I.	λ (I A.).	ν (vac.)	Combination
5	7510·74	13310·6	$1^3P_2-2^3S_1$
4	6278·18	15923 8	$1^3D_3-1^3P_2$
1u	5956 98	16782 4	$1^1D_2-a_4$
1u	5862 94	17051 6	$1^3F_3-a_3$
4	5837·40	17126 2	$1^3P_1-2^3S_1$
0	*5721 26	17473 8	$2^3P_2-a_3$
1	5655 76	17070 2	$1^1D_2-a_2$
1	*5201 82	18999 6	$1^3F_2-a_2$
1	*5147 39	19421 9	$2^3P_2-a_4$
2u	5004 02	19739 4	$1^3D_3-1^3P_2$
4u	4811 61	20777 3	$1^3F_3-2^3D_3$
8	4792·00	20859 7	$1^3P_2-2^3D_3$
0	*4020 70	21635 7	$1^3D_2-a_4$
4	4007 35	21698 4	$1^3D_2-a_2$
4	4488·26	22274 1	$1^3F_4-a_4$
4	4437·28	22530 0	$1^3D_3-a_3$
1	4315 11	23167 9	$1^3F_4-a_3$
2u	4241 84	23568 2	$1^3P_2-3^3N_1$
1u	4084 14	24478·1	$1^3D_3-a_2$
0	4066 08	24592 8	$1^3P_1-2^3D_2$
2	4040 95	24739 7	$1^3D_2-1^3D_2$
2	3909 39	25572 2	$1^3D_3-1^3D_3$
4	3807 88	25647 7	$1^3F_4-a_2$
1	3889 45	25703 3	$1^1D_2-a_3$
1	3875 08	25800 8	$1^1D_2-\beta_3$
1	*3801 97	26294 7	$1^3P_2-3^3D_3$
4	3795·90	26336·7	$1^3P_2-3^3D_2$
3	3650 74	27383 8	$1^3P_1-3^3S_1$
2	3355 18	29796 1	$1^3D_2-2^3P_2$
2	3320 14	30110 6	$1^3P_1-3^3D_2$
2	3308 31	30218 3	$1^3D_3-1^3F_3$
4u	3204·74	31194 7	$1^3F_4-a_3$
4u	3194 73	31292 5	$1^3F_4-\beta_3$
1	3146 37	31778·5	$1^3D_2-2^3P_1$
8	3123 78	32013 5	$1^3D_3-1^3P_2$
8u	3029 22	33002·2	$1^3D_3-1^3F_4$
4	2891 96	34588 5	$1^3F_4-a_2$
3	2883 46	34670 4	$1^3D_2-a_{11}$
6	2748 26	36375 9	$1^3D_3-1^3F_4$
4	2700 90	37013 7	$1^3D_2-1^3D_2$
4	2688 72	37181 4	$1^3D_2-b_{12}$
10R	2675 95	37358 8	$1^3S_1-1^3P_1$
4	2641 49	37846 1	$1^3D_2-1^3D_2$
4	2590 05	38597·7	$1^3D_2-3^3P_2$
4	2544 20	39293·4	$1^3D_2-3^3P_1$
4	2510 50	39820 6	$1^3D_2-c_{11}$
10R	2427 98	41174·0	$1^3S_1-1^3P_2$
5	2387 75	41887 6	$1^3D_2-1^3D_2$
4	2376 25	42070·3	$1^3D_2-2^3P_2$
4	2364·57	42278 1	$1^3D_2-d_{11}$
6	2352 65	42492·2	$1^3D_2-1^3F_4$
2	*2129 46	46945 4	$1^3D_2-a_{10}$
2	*2126 62	47008 2	$1^3S_1-1^3D_2$
3	*2021·40	49454 6	$1^3D_2-b_{10}$

* Measured by the authors.

Table V.—(continued)

I	λ(I.A.)	ν (vac.)	Combination
3	1951·21	51233 4	$1^2S_{\frac{1}{2}}$—$2^2P_{\frac{3}{2}}$
2	*1938 52	51567 7	$1^2D_{\frac{3}{2}}$—$3^2P_{\frac{3}{2}}$
4	1918 02	52095 5	$1^2D_{\frac{5}{2}}$—$\ldots_{\frac{3}{2}}$
3	1879 13	53198 5	$1^2S_{\frac{1}{2}}$—$2^2P_{\frac{1}{2}}$
	λ (I vac.)		
2	1833 26	54547 0	$1^2D_{\frac{3}{2}}$—$d_{\frac{3}{2}}$
1	1665 52	60041·3	$1^2S_{\frac{1}{2}}$—$3^2P_{\frac{1}{2}}$
2	1640 50	60734 9	$1^2S_{\frac{1}{2}}$—$3^2P_{\frac{3}{2}}$

The term designated as $1^2D_{3\frac{1}{2}}$ corresponds to the ^2D term given in Table II, 1B. The term values in Table IV show that it is another "deep" term of the spectrum, but that it is not so "deep" as the 1^2S_1 term. Our absorption experiments also confirm this view, for all the wave-lengths in Table III that involve the component 1^2D_3 were absorbed by the excited vapour in the under-water spark but not by the normal vapour of gold. The energy provided by the under-water spark was, therefore, sufficient to raise the gold atoms to the state represented by the term 1^2D_3, but was probably not sufficient to raise them to the 1^2D_2 state. This would explain why we did not find any absorptions involving the term 1^2D_2. As the term $1^2D_{3\frac{1}{2}}$ does not combine with the term $1^2S_{\frac{1}{2}}$, it must, therefore, represent a metastable state of the un-ionized atom of gold.

The values of the components of the $1^2D_{3\frac{1}{2}}$ term show that the term is inverted, that is, the component 1^2D_3 is "deeper" than the component 1^2D_2. This feature is in conformity with certain rules given in Section III. For the term represents the resultant action of the 11 outer electrons of the un-ionized atom of gold, when nine of them occupy 5_3 orbits and two of them 6_1 orbits. The 6_1 orbit type is by rule 1 thus filled and therefore by rule 4 can be neglected, while the 5_3 orbit type contains nine electrons and this number is greater than N/2 where N = 10 for this type. Therefore by rule 3 the term should be inverted and this we have shown to be the case. The significance of the metastable inverted doublet D term, found by us a year ago, is thus made clear.

It should be noted, however, that the term here designated as 1^2D_3 is not the same as the one we selected in our earlier work as 1^2D_3 ($5\delta_1$ in the previous notation). Our identification of the $5\delta_1$ term last year was based chiefly on a wave-length given by Quincke,* namely λ 4623·26A having the estimated

* Kayser and Konen, 'Handbook,' vol VII.

intensity 6v. A close inspection of our plates of the emission arc spectrum of gold failed to reveal any line of this wave-length in the spectrum.* Our previous evaluation has therefore probably no significance. The discovery of the correct value of the term 1^2D_2 has made possible the advances recorded in this communication.

The most important of these advances is represented by the group of twelve terms at the right of fig 1, beginning with that designated as 1^2F_4 and going on to that designated as d_{23} All these terms are new with the exception of those designated as 2^2P_2 and 2^2P_1, which constitute the irregular terms of the P type found by us in our earlier work and mentioned above in Section I Although we have been able to identify only eight of the twelve terms referred to, it seems fairly certain that all the twelve correspond to certain components of the group $^4F\,^4\bar{D}\,^4P\,^2F\,^2\bar{D}\,^2P$ that result from the electron configuration 2B in Table II. This group, as the table shows, has the ^2D term of the Au II spectrum as a common series limit Of the terms in this group the quartet terms should be "deeper" than the doublet terms of the same type by Rule 5 in Section III. But from the arrangement of the eight components that we have identified it would seem that in this case there is a contradiction to the rule, *i e*, that the ^2F term is deeper than the ^4F term, the $^2\bar{D}$ term is deeper than the $^4\bar{D}$ term, and that the ^2P term is deeper than the ^4P term We will proceed to discuss our arrangement of the group, first empirically and then from a theoretical standpoint

We have shown in Section III that the gold atom can get directly from the state 2B to the state 1A in Table II. Consequently the terms $^4F\,^4\bar{D}\,^4P\,^2F\,^2\bar{D}\,^2P$ can combine with the term 1^2S_1 subject to the selection rule for the inner quantum number "j," associated with any term component, *i e*, "j" may change only by ± 1 or 0 in a transition. The selection rule for "j" limits the number of possible combinations to eight, namely, those from the components $^4F_2$, $^4\bar{D}_2$, $^4\bar{D}_1$, $^4P_2$, $^4P_1$, $^2\bar{D}_2$, $^2P_2$ and $^2P_1$ to the term 1^2S_1 The three doublet components $^2\bar{D}_2$, $^2P_2$ and $^2P_1$ should combine with the term 1^2S_1 more readily than the five components of the quartet terms. It will be seen from fig. 1 and Tables IV and V that only three of the eight possible combinations with the terms 1^2S_1 occur. We have, therefore, been led to the view that the three wave-lengths λ 2126 62A, λ 1951·21A and λ 1879·13A result from the three

* Table VI contains a number of wave-lengths, given by Quincke, that we were not able to detect in the emission arc spectrum of gold.

combinations between the doublet components $^2\bar{D}_2$, $^2P_2$ and $^2P_1$ and the term 1^2S_1, and as a consequence we have identified the terms designated as $1^2\bar{D}_2$, 2^2P_2 and 2^2P_1. The three other doublet components designated as $1^2\bar{D}_3$, 1^2F_4 and 1^2F_3 were then selected so as to be in agreement with Rules 3 and 6 in Section III. The terms designated as 1^4F_4 and $1^4\bar{D}_4$ were identified by the fact that they are the only components of the group $^4F^4\bar{D}^4P$ that have the inner quantum numbers, "j" = 7/2, and, as Table IV shows, each of them has this value for "j". As we have arranged them, 1^4F_4 is deeper than $1^4\bar{D}_4$, but we cannot be certain of this. The remaining four terms of the group of twelve probably are other components of the group $^4F^4\bar{D}^4P$ as well, but we have not sufficient evidence to enable us to identify any of them, and so we have designated them as a_{23}, b_{23}, c_{23} and d_{23} for the time being. The double subscripts 2 and 3 in each case indicate that the inner quantum number "j" belonging to each term may have either of the values 5/2 or 7/2.

If our identification of the terms discussed in the last paragraph be correct, we have shown that in this case the doublet terms of the group $^4F^4\bar{D}^4P^2F^2\bar{D}^2P$ must be "deeper" than the quartet terms of the same type. The question of the series limits involved probably has some bearing on the theoretical significance of this feature. We have indicated in Table II that the terms of the group $^4F^4\bar{D}^4P^2F^2\bar{D}^2P$ have as series limit the ^3D term of the Au II spectrum, but the ^3D term is threefold, and by Rule 3 in Section III should be inverted. The question then is, of the 17 component terms in the group, which ones have the component $^3D_1$ as limit, which ones have the component $^3D_2$ and which ones have the component $^3D_3$.

The question of series limits was treated recently in an extended way by Hund in a special paper.* As an example of spectra characterized by doublet and quartet systems with a threefold limit, Hund discusses the structure of the arc spectra of the elements of the fifth column (N, P, As, Sb, Bi). We give in fig. 2 a diagram of the term structure of the arc spectra of these elements, taken from Hund's paper. By means of the rules given by him we have constructed fig. 3 to represent the arrangement of the group of terms $^4F^4\bar{D}^4P^2F^2\bar{D}^2P$, that we are discussing, in the Au I spectrum. In fig. 2 the components of the limiting term ^2P of the spark spectrum are in the normal order, and as a consequence the components of the term types in the arc spectrum are in the normal order as well. Also quartet terms are deeper than doublet

* 'Z. f. Physik,' vol. 34, p. 296 (1925).

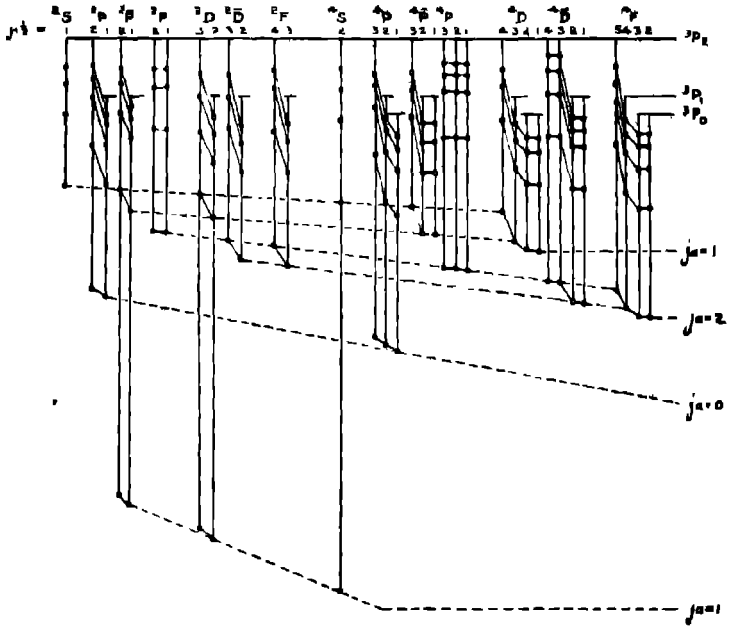
^2S ^2P $^2\bar{P}$ ^2P ^2D $^2\bar{D}$ ^2F ^4S ^4P $^4\bar{P}$ ^4P ^4D $^4\bar{D}$ ^4F
$^3P_2$
$^3P_1$
$^3P_0$
j=1
j=2
j=0
j=1

Fig. 2

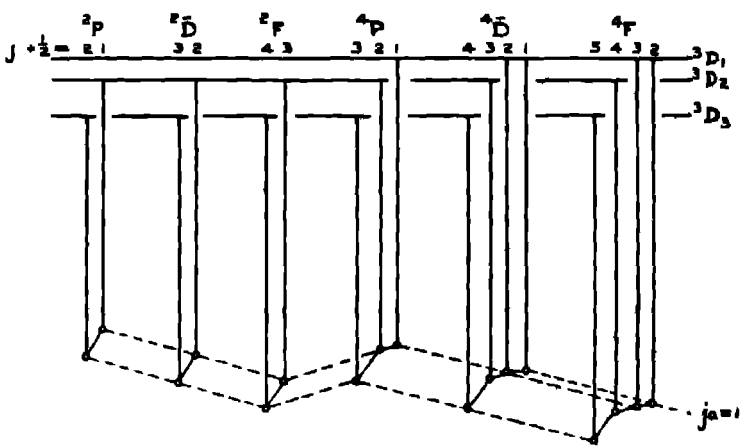
^2P $^2\bar{D}$ ^2F ^4P $^4\bar{D}$ ^4F
$^3D_1$
$^3D_2$
$^3D_3$
j=1

Fig. 3

terms of the same type. But in fig. 3 the limiting term ^3D of the Au II spectrum has its components inverted, and the components of terms of the arc spectrum having the ^3D term as limit are therefore inverted. In order to explain the fact that the doublet terms of the group $^4F^4\bar{D}^4P^2F^2\bar{D}^2P$ in the Au I spectrum are deeper than the quartet terms of the same type, we now put forward the view that the inversion of the components of any term, when the limit is inverted, is accompanied in some cases by an inversion of the relative depth of doublet and quartet terms of the same type, so that the doublet term of any type would be the "deeper".

Table VI.—Wave-lengths of Doubtful Origin recorded by Quincke as belonging to Au I.

I	λ (I.A.)	Origin ?	I	λ (I.A.)	Origin ?
2	6101 65		6U	3092 85	Al I
6w	4623 26		1w	3038 91	
1	4543 74		1	3034 13	Sn I
6R	*3927·57		1w	3024 34	
1	3902 27		2U	2973 25	
1w	3673 59		2	2970 41	
3R	3641·93		2	2963 75	
3	3377·59		1U	2961 91	
2	3242 69	Pd I	1w	2943 04	Ga II
1w	3181 30	Ca I	1w	2913 30	In II
4w	3117 01		1w	2894 29	

* A faint line at this wave-length was observed in our plates.

The only terms in fig. 1 that we have not yet discussed are the high ones designated by Greek letters. These are probably components of the group resulting from the electron configuration 3B in Table II, but we have not been able to show that any of these terms correspond to components of any of the predicted types.

Our analysis of the Au I spectrum has not furnished more than the first member of any series that has the ^3D term of the Au II spectrum as limit. We therefore cannot calculate the values of any of the components of the ^3D term.

V.—*Conclusion*

In the foregoing analysis we have been able to classify by our term scheme nearly all the wave-lengths known to belong to the gold arc spectrum. The most important wave-lengths that have not yet been classified are six, given in

Table III, that were found to be absorbed by the vapour in the under-water spark of gold. These wave-lengths undoubtedly involve the metastable term 1^2D_3 and will probably be found to lead to the identification of certain of the terms of the group $^2P^2\overline{D}^2F$ with the limit of ^1D in Table II, 2D, or to certain of those of the groups in Table II, 2c. But we have not any further evidence in support of this view. Zeeman effect experiments will probably furnish the best means of definitely settling this question and any other features of the arc spectrum of gold that are not yet clear.

The authors wish to thank Misses Allin, Cohen, McDonald and Sutton, and Mr. M. J. Liggett for assistance in taking photographs of spectra. Acknowledgment should also be made to the National Research Council of Canada, for the award of a fellowship to Mr. A. B. McLay, which enabled him to collaborate in this investigation.

On the Series Spectra of Palladium.

By Prof. J. C. McLennan, F.R.S., and H. Grayson Smith, Ph.D.
(Department of Physics, University of Toronto.)

(Received June 10, 1926.)

Introduction.

In a previous paper the authors have given a preliminary analysis of the arc spectrum of palladium.* This has now been extended and brought into better agreement with the theoretical considerations of Hund. In addition, some progress has been made in the analysis of the second or spark spectrum of palladium. The work on the arc spectrum has been made possible by the study of the Zeeman effect of the palladium arc by Beals,† by the experiments of McLennan and Cohen, and McLennan and Liggett‡ on the absorption spectrum of normal palladium vapour, and by the measurements of Meggers§ of the lines of the palladium arc in the region from 4500 to 9000 A.

* 'Trans. Roy. Soc. Can.,' Sec. III (1926).
† 'Roy. Soc. Proc.,' A, vol. 109, p. 369 (1925).
‡ Papers to appear in 'Trans. Roy. Soc. Can.,' Sec. III (1926).
§ 'Bureau of Standards Sci. Papers,' p. 499 (1925).

The Ground Terms of Palladium I.

On the basis of his experiments on the Zeeman effect, Beals assigned most of the strongest lines of the arc spectrum to combinations between a group of low terms designated by $^1S_0$, $^3D_{321}$, $^1D_2$ (in the notation of Russell) and a group of singlet and triplet P, $\bar{D}$ and F terms. This has been generally confirmed, although it has been necessary to rearrange the PDF group slightly in order to bring it into agreement with the theoretical grouping of these terms The new arrangement of the lines involved is shown in Table I, and is supported by consideration of the relative intensity. Those lines for which the agreement between observed and calculated Zeeman effect is particularly good are not affected by the changes Table I also contains other lines due to combinations with the low group, some of which have been identified as the second members of series of which the lines given by Beals are the first members The nature of the other terms combining with the low group has not been ascertained Table II contains lines due to combinations between the P$\bar{D}$F group and two

Table I.—Combinations with Low-Lying Terms

Term.	j	1^1S	1^1D	1^1D		
		0	2	1	2	3
1^1F	2		27089 88 (20R)	28717 90 (50R)	31056 60 (3)	—
	3		25671 84 (20)		29638 56 (30R)	30820 48 (100R)
	4					29303 78 (100R)
1^1F	3		23729·53 (20R)		27606 43 (100R)	28887 22 (50R)
1^1D	1	40837 33 (8R)	29116 98 (20R)	30744 72 (30)	33083 91 (3)	
	2		29049·62 (20R)	30677 30 (30)	33016·15 (20)	34207 08 (10)
	3		28136·49 (50R)		32102·98 (30)	33294·06 (10)
1^1D	2		25256 15 (20)	26881 98 (15)	29220 93 (50R)	30411 85 (10)
1^1P	0			27094 02 (30R)		
	1	36180 08 (15R)	24458 74 (10)	26086 53 (10)	28425 52 (100R)	
	2		22346 79 (15)	23974 94 (5)	26313 80 (10)	27504 90 (200R)
1^1P	1	40368·33 (8R)	28646 80 (15)	30274 64 (30R)	32613 51 (20)	
2^1D	1	58001 (abs.)		47934 (uws)		
2^1P	1	56709 (abs.)	—	46001 (uws)	—	
α	1	57630 (abs.)	45948 (uws)	47581 (uws)	—	
β	1	45484 (abs.)	—	35395 4 (1)	—	
γ	3		39188 56 (1)		43155·40 (1)	44347 25 (1)
δ	1	50530 (abs.)	44797 9 (1)	—	48764 (uws)	
ϵ	3?		—		56954 (abs.)	58129 (abs.)

abs. = absorption. uws = under-water spark reversal

Table II.—Combinations with b^2F

Term	j	b^2F 3	b^2F 4
1^3F	2	—	
	3	—	12292 44 (6)
	4	—	10826 55 (1)
1^3D	2	12557 72 (4)	
	3	11644 64 (1)	14757 08 (12)

Table III.—Lines absorbed by Normal Palladium Vapour.

Wave-length I.A	Absorption Intensity	Frequency cm $^{-1}$	Combination
3634·684	5	27504·90	$1^3P_2 - 1^3D_3$
3609·548	5	27696 43	$1^1F_3 - 1^1D_2$
3516 903	2	28425·52	$1^3P_1 - 1^3D_2$
3460 751	3	28887 22	$1^3F_3 - 1^3D_2$
3421 227	6	29220 93	$1^1D_2 - 1^1D_2$
3404 583	10	29363 78	$1^3F_4 - 1^3D_3$
3378 018	4	29638 56	$1^3F_3 - 1^3D_2$
3302 147	6	30274 64	$1^3P_2 - 1^3D_2$
3287 248	6	30411 85	$1^1D_2 - 1^1D_2$
3258·803	4	30677·30	$1^3D_3 - 1^3D_3$
3251·657	3	30744·72	$1^3D_1 - 1^3D_1$
3242 716	10	30829 48	$1^3F_3 - 1^3D_3$
3114 075	5	32102·98	$1^3D_3 - 1^3D_3$
3065·326	4	32613·51	$1^1P_1 - 1^1D_2$
3027·942	4	33016·15	$1^3D_2 - 1^3D_2$
3002 666	2	33294 06	$1^1D_2 - 1^1D_2$
2922 518	1	34207 05	$1^3D_3 - 1^3D_3$
2763·091	10	36180 68	$1^3P_1 - 1^1S_0$
2751·87	1	36328·1	
2476 441	10	40388 33	$1^1P_1 - 1^1S_0$
2447·998	8	40837 33	$1^1D^2 - 1^1S_0$
2272 2	1*	43997	
2251·470	2	44401·63	
2247 7	2*	44476	
2232 85 ?	2	44797 9	$\delta_1 - 1^1D_2$
2197·9	2*	45484	$\beta_1 - 1^1S_0$
1824 7	1	54804	
1769 0	4	56530	
1763 4	4	56709	$\delta_2 - 1^1S_0$
1755 8	2	56954	$2^3P_1 - 1^1S_0$
1747 4	1	57228	$\epsilon_2 - 1^3D_2$
1734 6	4	57650	
1724 1	2	58001	$\alpha_1 - 1^1S_0$
1720·3	2	58129	$2^3D_1 - 1^1S_0$
1715 6	1	58292	$\epsilon_3 - 1^3D_3$

* Lines not identified with emission lines in the palladium arc

new low terms designated as $b^3\overline{F}_{1,2}$. These are the lowest members of a theoretical group for which the remaining combinations would lie in the infra-red beyond the range of the measurements of Meggers.

Table III contains the lines which were observed by McLennan and Cohen and McLennan and Liggett in the absorption spectrum of normal palladium vapour. These show very clearly that the term designated as $^1S_0$ represents the normal state of the palladium atom, all the lines due to combinations with it being very strongly absorbed. Most of the lines due to combinations with $^3D_3$ are also absorbed, and some of those due to combinations with $^3D_{2,1}$ showing that the triplet D term represents a metastable state of low energy of the palladium atom. It is also evident that there can be no other terms as low or lower than these. This is in agreement with the assignment of the low terms by Bechert and Catalan *

Theoretical and Observed Groups of Terms

F Hund† has recently given a theory by means of which it is possible to predict the arrangement of the terms of the spectrum for an atom containing any number of electrons The effective quantum number (l) that defines the spectral term corresponding to a given configuration of extra-nuclear electrons in an atom is given by $l = \bar{j}_a + 1$, where $\bar{j}_a$ is the vectorial resultant of the quantum numbers $j_a = k - 1$ representative of all the individual electrons outside the last previous rare gas shell. The quantum number $\bar{j}$, determines by the relation $\bar{j} = \frac{1}{2}(r - 1)$ the multiplicity of such spectral term: it also is a vectorial magnitude, being the resultant of the quantum numbers (j_s) of all the individual electrons, each of which is taken to be intrinsically of a doublet nature with its $j_s = \frac{1}{2}$. In this way each possible arrangement of the electrons in orbits (n_k) of given total and azimuthal quantum numbers can be associated with a group of spectral terms.

When two or more electrons are in "equivalent orbits," that is, in orbits having the same values of n and k, account must also be taken of their orientation with respect to an imaginary small magnetic field. No two electrons may actually occupy the same orbit, and so if they have the same values of n, j_a and j_s, one or both of the vectors j_a and j_s must be differently oriented with respect to the field. This limits the number of electrons which may occupy equivalent orbits of quantum number k to $N = 2(2k - 1)$, and also limits the number of

* 'Z. f. Physik,' vol. 35, p 449 (1926); also 'Roy. Soc. Proc.,' *supra*, p. 76.

† 'Z. f. Physik,' vol. 33, p. 345 (1925).

possible ways of combining them to give the quantum numbers l and j, of the terms. In this connection it was shown by Hund that a combination of $N - x$ equivalent electrons (where $x < \frac{1}{2}N$) gives rise to the same group of spectral terms as a combination of x electrons. In the former case it is found empirically, however, that the multiple terms are "inverted," that is, that the term with the highest value of the inner quantum number (j) is the lowest of each multiple term. Hund also gives the empirical rules, that, of such a group of terms, those of largest multiplicity should be the lowest, and that of terms of equal multiplicity that with the largest value of l should be the lowest. The last-mentioned rules are apparently strictly obeyed by the low terms of a series system, but other effects may cause them to break down for the higher terms.

In the case of palladium (atomic number 46) there are ten electrons outside a krypton-like core, and these are to be distributed in the 4_2, 5_1 and higher orbits. The most important configurations to be considered are those in which all ten electrons are in 4_2 orbits, which will be denoted by $(4_2)^{10}$, and those in which there are nine electrons in 4_2 orbits and one in a higher orbit, denoted by $(4_2)^9\ 5_1$, etc. These give the ordinary series system, in which the lines are due to transitions of a single "series electron." The configuration $(4_2)^{10}$ represents a completed shell, and gives rise to the low term $^1S_0$ only, so that it must be the normal configuration of the palladium atom. In order to find the terms due to the other configurations, the j_a and j_c of the tenth electron must be combined with the term resulting from the nine 4_2 electrons, which is a term ^2D. Thus $(4_2)^9\ 5_1$ gives rise to the metastable terms $^3D_{321}$, $^1D_2$, and $(4_2)^9\ 5_2$ to the group $^3\bar{F}\ ^3D\ ^3P\ ^1\bar{F}\ ^1D\ ^1P$ observed by Beals. In accordance with the rule mentioned above, all these terms are inverted. In Table IV the observed terms of the palladium arc spectrum are given, grouped according to the electronic configurations to which they are supposedly due. The first column gives the configuration, the second the predicted terms which should arise from it, and the third the values of the corresponding observed terms. Some terms whose nature has not been determined appear at the bottom of the table. These all combine with the terms of the lowest groups, and may be part of the group due to the configuration $(4_2)^8\ 5_1 5_2$ and so involving double electronic transitions.

The selection principle for the azimuthal quantum number ($\Delta k = \pm 1$) should be applied to the electron concerned in the transition, and not to the effective quantum number (l) of the terms. Thus any term of the group $(4_2)^9\ 5_2$ may combine with the low terms, or with any term of the group $(4_2)^9 5_2$, subject always to the selection principle for the inner quantum number ($\Delta j = \pm 1, 0$).

However, transitions in which l changes by 2 or 3 give rise to lines of small intensity compared with those for which l changes by 1 or 0. According to the usual practice, bars have been used to distinguish terms which combine with ordinary terms of the same value of l. Table V shows the observed combinations between the group $(4_3)^9 5_1$ and the higher terms The rules of intensity are on the whole obeyed for combinations with the $\bar{D}$ and P terms, and justify the arrangement of the upper terms so as to agree with the predictions The intensities of all the combinations with the F terms are rather irregular

Table IV —Terms of the Palladium Arc Spectrum.

Configuration	Terms (predicted)	j	Value of observed term	Separation.
$(4_3)^{10}$	1^1S	0	0 00	
$(4_3)^9 5_1$	1^3D	3	6564 02	
		2	7754 98	1190 96
		1	10093 93	2338 95
	1^1D	2	11721 72	
$(4_3)^9 (5_1)^2$	$b^3\bar{F}$	4	25101 12	
		3	28213 53	3112 41
		2	—	
	$b^3\bar{P}$	2 1 0	Combinations due to these terms would be in infra-red	
	b^1G	4		
	b^1D	2		
	b^1S	0		
$(4_3)^9 5_1$	1^3F	4	35927 75	
		3	37393 53	1465 78
		2	38811 71	1418 18
	1^1F	3	35451 25	
	$1^1\bar{D}$	3	39858·14	
		2	40771·29	913 15
		1	40838·67	57·38
	$1^1\bar{D}$	2	36975 82	
	1^3P	2	34068 80	
		1	36180 46	2111 66
		0	38088 02	1907 56
	1^1P	1	40368·58	
$(4_3)^9 6_1$	2^1D	2	49019·49	
				215 28
	2^3D	3	48804 21	
		2	52587 70	3783 49
		1	52336 31	— 251·39

Table IV—(continued).

Configuration	Terms (predicted).	j	Value of observed term.	Separation.
$(4_2)^2\ 5_2$	a^1G	4	54811 30	
				5 22
	a^1G	5	54806 08	
		4	58064·05	3257 97
		3	58348 92	284·87
	$a^1\overline{F}$	3	55012·19	
				12 97
	$a^3\overline{F}$	4	55025·16	
		3	58561 70	3536·54
		2	58555·78	— 5·98
	a^1D	2	54998 52	
				50 81
	a^3D	3	54947·71	
		2	58448·54	3500·83
		1	58408 07	— 40·47
$(4_2)^2\ 5_3$	a^1P	1	54822 65	
				2 03
	$a^3\overline{P}$	2	54820 62	
		1	58195 26	3374 64
		0	58681 34	486 08
	a^1S	0	55372 99	
				798·90
	a^3S	1	54574 09	
$(4_2)^2\ 6_2$	$2^1\overline{F}$	3	—	
	2^3F	4	—	
		3 2	—	
	$2^1\dot{D}$	2	—	
	$2^1\overline{D}$	3 2	—	
		1	58028	
	2^1P	1	—	
	2^3P	2	—	
		1	56695	
		0	—	
$(4_2)^2\ 7_1$	3^1D	2	58138 33	
	3^3D	3	—	
		2	61638 60	
		1	61002 82	35·78
$(4_2)^2 5_1 5_2$?	α	1	57650	
	β	1	45489 3	
Terms not identified	γ	3	51040 92	
	δ	1	56519 6	
	ϵ	3?	64701	

Table V.—Combinations between Upper Terms.

Term.	j	1^1F.	1^3F.		
		3	4	3	2
2^1D	2	13568 21 (15)		11626 99 (2)	—*
2^3D	3	13352·94 (7)	12876 44 (12)	11410·65 (2)	—*
	2	17036 46 (2)		15094 14 (4)	13676 02 (3)
	1				13524 59 (8)
a^1G	4	19360 09 (40)	18883 53 (7)	17417 76 (7)	
a^3G	5		18876·53 (50)		
	4	22612·73 (2)	22136 32 (10)	20670 61 (4)	
	3	—	—	—	19537 23 (20)
a^1F	3	19560·94 (15)	19084 46 (2)	17618 60 (3)	16200 49 (5)
a^3F	4	19573 88 (1)	19097 44 (20)	17631·02 (30)	
	3	—	—	21168·20 (1)	—
	2	—		21182 55 (6)	19744 09 (10)
a^1D	2	19547 28 (8)		—	16186 85 (5)
a^3D	3	19496·47 (7)	19019 98 (10)	17554 16 (20)	16136 00 (2)
	2	—		—	—
	1				19596·37 (3)
a^1P	1				16011·03 (3)
a^3P	2	19369·36 (5)		17427 04 (12)	16008 95 (1)
	1				19383 63 (0)
a^3S	1				15762 40 (1)
3^1D	2	22686 52 (4)		20744·77 (2)	—
3^3D	2	—		—	22826 80 (1)
	1				22791 10 (2)

* In infra-red

Table V—(continued)

Term	j	$1^1\overline{D}$	$1^3\overline{D}$		
		2	3	2	1
2^2D	2	12043 71 (5)	—*	—*	—*
2^3D	3	11828 37 (0)	—*	—*	
	2	15511 91 (2)	12629 43 (7)	11716·45 (2)	11469 11 (2)
	1	15360 50 (6)		11565 03 (1)	11497 67 (1)
a^1G	4		14953·15 (2)		
a^3G	4		—		
	3	21373·16 (8)	18490 82 (5)	17577·58 (3)	
a^1F	3	18036·43 (30)	15154·04 (1)	—	
a^3F	4		15167 03 (3)		
	3	21585·86 (25)	18703·54 (10)	17790·38 (12)	
	2	21579 99 (3)	18697 62 (2)	17784·46 (3)	17717 06 (8)
a^1D	2	18022·70 (20)	15140 39 (1)	14227 09 (1)	14159 83 (5)
a^3D	3	17971 90 (3)	15089 54 (4)	14176 39 (2)	
	2	—	15090 43 (3)	17677 26 (10)	17609·84 (1)
	1	21432 36 (0)		17636 72 (3)	17569 40 (8)
a^1P	1	17846·94 (8)		—	13983 91 (6)
a^3P	2	17844 00 (2)	14962 44 (3)	14049 30 (3)	—
	1	—		17428 92 (4)	17356 55 (4)
	0				17542 64 (4)
a^1S	0				14584 37 (2)
a^3S	1	17598·38 (2)		13802·83 (2)	13735·43 (2)
3^1D	2	21162 55 (6)	—	—	17299 69 (1)
3^3D	2	—	21780 46 (3)	20867 31 (2)	20799 93 (1)
	1	—		20831 75 (1)	20764·15 (1)

* In infra-red.

Table V.—(continued).

Term		1^1P.	1^3P.		
	j	1	2	1	0
2^1D	2	—*	14950·74 (3)	12838 93 (7)	
2^3D	3		14735 38 (50)		
	2	—	18418·94 (4)	16307 16 (8)	
	1	11967·69 (2)	18267 56 (1)	16155 80 (6)	14248 32 (8)
a^3F	3		—		
	2	18187·20 (6)	—	- -	
a^1D	2	14629 93 (8)	20929 82 (4)	16818 06 (12)	
a^3D	3		20878 94 (20)		
	2	18079·97 (5)	—	22267 68 (5)	
	1	18039·42 (1)	—	22227 57 (3)	20320 09 (8)
a^1P	1	14454 07 (9)	20753 94 (9)	18642 19 (15)	16734 49 (0)
a^3P	2	14451 98 (2)	20751·53 (30)	18640 21 (4)	
	1	17826 67 (7)	—	22014 80 (10)	20107 24 (9)
	0	18312 76 (2)		22500 92 (3)	
a^1S	0	15004·43 (4)		19192·57 (10)	
a^3S	1	14205 52 (3)	20505 30 (20)	18393·62 (7)	16485·99 (1)
3^1D	2	—	—	21957 84 (4)	
3^3D	2	21270 12 (1)	—	—	
	1	21234 25 (2)	—	—	23514 57 (1)

* In infra red

The Series Limits.

Series of terms, following approximately formulæ of the Rydberg or Ritz type, will be produced by configurations with the electrons in orbits of the same azimuthal quantum numbers, but with increasing values of the total quantum number of one of the electrons. For example, the successive configurations $(4_3)^9 5_1$, $(4_3)^9 6_1$, $(4_3)^9 7_1$, etc., of palladium give rise to series of triplet and singlet D terms of which the metastable D terms are the first members. When the series electron is completely removed, there remains a singly charged palladium ion with its nine outer electrons in the configuration $(4_3)^9$. The energy of this configuration, expressed in frequency units, must therefore represent the limit of the series. But at the same time it represents a possible configuration of the spark spectrum, and so in this way the limits of the series of the arc spectrum can be associated with the low terms of the spark spectrum.

In the case of palladium the configuration $(4_2)^9$ gives rise to a low doublet D term of the spark spectrum, and either $^2D_2$ or $^2D_3$ may be the limit of a particular series of the arc. In a recent paper Hund* has considered this question and has shown how to distinguish between the series which proceed to either member of a double limit. In the case of triplet and singlet D terms it is found that the series $^3D_{12}$ converge to the limit $^2D_2$, and $^3D_3$ $^1D_2$ to the limit $^2D_3$. Three members of these series have been found in palladium, and the limits have been calculated approximately by means of Rydberg formulæ. They are found to be 70902 and 67387 cm.$^{-1}$ respectively. The difference between these limits is 3515 cm.$^{-1}$ and should be equal to the frequency difference of the low doublet D term of the spark spectrum, which we have found to be 3512·4 cm.$^{-1}$.

In the case of the series arising from the configurations $(4_2)^9 n_2$, $^3F_{23}$ $3\bar{D}_{12}$ $^3P_{01}$ should converge to the upper limit, $^2D_2$ of the spark spectrum, and $^3F_4$ $^1F_3$ $^3\bar{D}_3$ $^1\bar{D}_2$ $^3P_2$ $^1P_1$ to the limit $^2D_3$. Of the second members of this group we have been able to identify only $^3\bar{D}_1$ and $^3P_1$, both of which combine with $^1S_0$ to give lines which are absorbed by the normal vapour. The existence of the double limit shows in the term separations of the group $(4_2)^9 5_3$, which is divided into two distinct sub-groups according to the particular limit of the series of which these terms are the first members. The multiplicity of the limit will also explain the irregular separations of the P$\bar{D}$F group, and the fact that the singlet $\bar{D}$ and F terms are lower than the corresponding triplets. Since the spark term corresponding to the limit is inverted, all the singlet terms are converging to the lower limit, and when the separation of the limits becomes large compared with the difference to be normally expected between the triplets and singlets, the latter become the lower, and Hund's rule for the order of the terms breaks down.

In the energy diagram (see fig. 1) the terms found in the regular spectrum represented by the configurations $(4_2)^9 n_4$ have been plotted. Terms which arise from the same configuration are connected by broken lines, the two lines for each group representing the two possibilities $^2D_{23}$ for the nine 4_2 electrons. The vertical lines on the diagram represent possible series of terms, and terminate in the particular limit to which the series should converge.

* 'Z. f. Physik.,' vol. 34, p. 296 (1925).

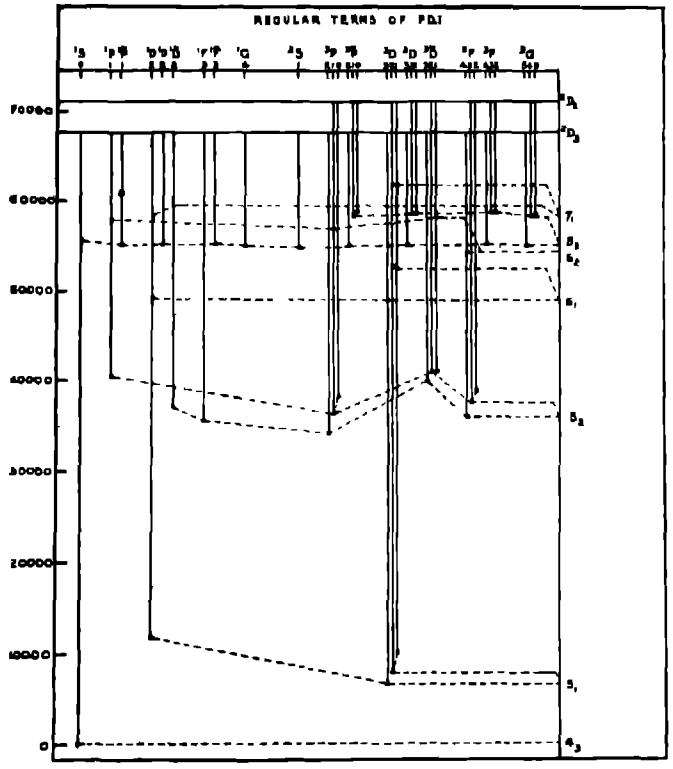

FIG. 1.

The Spectrum of Palladium II.

The values of the wave-lengths for the investigation of the spark spectrum of palladium have been taken from Dhein* for the region of wave-length longer than 2000 A., from Kail† for the region from 2000 to 1850 A., and from the recent measurements of McLennan and Liggett‡ for the Schumann region The analysis is necessarily incomplete, since many of the important lines lie in the latter region, where not much reliance can be placed on the accuracy of the frequency differences.

The first attack on the spark spectrum was made by looking for frequency differences approximating to the value 3515 cm.$^{-1}$ which had been found for the difference between the two limits of the arc spectrum, and it was soon found

* 'Z. f. wiss. Phot.,' vol. 11, 10, p. 317 (1913).

† 'Wien Akad. Wiss. Sitzb.,' IIA, vol 123, p. 1267 (1914). ‡ *Loc. cit.*

that 3512·4 cm.$^{-1}$ was an important frequency difference in the palladium spark. This was subsequently found to be the difference between the lowest term and a term with a value of j one unit smaller, and was accordingly taken to be the inverted doublet D term predicted for the configuration $(4_3)^9$. Other terms, only slightly higher, have been identified with most of those predicted for the configuration $(4_3)^8\ 5_1$

Table VI.—Terms of Palladium II

Term	j	Value	Term	j	Value
(Configuration $(4_3)^9$)			Middle terms		
^2D	5/2	0 0	A	5/2	41549·2
	3/2	3512 4	B	5/2	42437 0
			C	3/2	42558 3
			D	3/2	45369 6
			E	5/2	48482 0
(Configuration $(4_3)^8\ 5_1$)			F	5/2	48665 5
			G	7/2	49027 6
^4F	9/2	—	H	5/2	50482 7
	7/2	1284 9			
	5/2	1946·4	J	5/2	60378 4?
	3/2	2316·9	K	3/2	61969 2?
			L	5/2	62189 4
^2F	7/2	4649·3	M	7/2	62808·6?
	5/2	5362·4	N	3/2	63266 9
			P	7/2	63452 4
^4P	5/2	2909 9	Q	7/2	63489 6
	3/2	4694 0	R	7/2	63687·4
	1/2	—	S	5/2	63971·0
			T	5/2	64265 1
^2P	3/2	6222·9	U	5/2	64401 1
	1/2	—	V	5/2	64484 4
			W	5/2	64570 7
^4Q	9/2	6050·5	X	5/2	64690 0?
	7/2	8625 3	Y	7/2	64841 8
			Z	5/2	65129·1
^2D	5/2	9005 1	AA	5/2	65158·2
	3/2	9691·0?	BB	3/2	66188 8
			CC	5/2	66844 2?
^2S	1/2	—	DD	5/2	67063 3
			EE	3/2	67160·5?
			FF	3/2	67232·9
			GG	1/2	69822·4?
(Configuration $(4_3)^8\ (5_1)^2$)			High terms		
a	3/2	6258·0			
b	5/2	10174·4	α	5/2	89468·9?
c	9/2	12197 2?	β	3/2	92589·1
d	3/2	16484 8	γ	3/2	95309·9
e	3/2	18389 5	δ	3/2	100599·0
f	9/2	20462·7?	ϵ	5/2	101775·0
g	7/2	21425·7?	ζ	5/2	101853·8
h	5/2	22237·6	η	7/2	103400·6
j	3/2	22657·9	θ	3/2	103726·5
k	7/2	22912 4	λ	5/2	104125·7
m	5/2	23374 0	μ	5/2	105851·4
n	5/2	24904·0	ν	5/2	105977·4
p	1/2	29367·8?	π	1/2	107073·1

All the terms found are collected in Table VI, and the lines arising from combinations between them in Table VII. We have not been able to determine the nature of the remaining low terms, or of the higher terms, and they have been denoted by letters. Small letters have been used for the unknown low terms, capitals for the middle terms which combine with these, and Greek letters for the high terms which combine with the middle terms, and which have served principally as a check on the values of the other terms It is probable that the low terms which have not been identified form part of the group due to the configuration $(4_3)^7(5_1)^2$, the predicted terms for which would be $^1\overline{F}$ $^1\overline{P}$, $^1\overline{H}$ ^3G ^1D ^1S, ^3D

Table VII —Lines Identified in the Spectrum of Palladium II

Wave-length	Intensity.	Frequency	Combination
3882·98	1	25746 1	β_3 — OC_3 ?
3843 26	1	26012 2	B_0 — d_3
3842·61	1	26016 6	α_3 — P_4
3825·41	1	26133 6	C_2 — d_2
3670 073	0	27239 69	F_1 — g_2
3311 13	w	30192 5	E_2 — e_2
3243·131	2	30825 54	γ_2 — V_3
3105 349	1	32193 19	H_1 — e_1
3041 664	2	32867 21	C_2 — b^1D_2
2949·075	2	33899 06	N_2 — p_1
2833·18	w	35410·6	δ_1 — AA_3
2774·779	4	36028 20	ϵ_2 — W_3
2751·4	1	36334	G_2 — $^3P_1$
2714 347	3	36830 37	G_4 — c_1
2709·215	1	36900 14	A_2 — $^1F_3$
2696·460	0	37074 68	B_2 — $^3F_3$
2687·675	3	37195 85	C_2 — $^3F_3$
2677·857	2	37332 27	β_2 — N_3
2659 458	0	37590 48	ζ_2 — T_3
2633 218	1	37965 04	FF_2 — p_1
2628·247	10	38036 64	A_2 — a^3D_2
2605·658	0	38366 57	ζ_2 — Q_3
2602·770	3	38409 14	β_2 — L_3
2587·271	0	38639 22	A_2 — $^3P_2$
2584 166	0	38685 64	α_2 — Q_3
2577·141	4	38791 08	E_2 — b^3D_2
2575·531	2	38815 33	L_2 — m_1
2568 298	0	38924 62	B_2 — a^1D_2
2565·527	6	38966 77	κ_2 — M_3
2564·236	0	38986·29	α_2 — H_1
2560·323	1	39045 87	C_2 — a^1D_2
2554 445	0	39135 71	γ_2 — T_3
2553·728	0	39146 70	D_2 — $^3F_2$
2553·128	0	39155 90	β_2 — W_3
2546 017	1	39265·25	θ_2 — U_3
2545·345	0	39277 06	L_2 — k_1
2532 372	0	39476 81	E_2 — b^1D_2
2529 154	1	39527·03	B_2 — $^3P_2$
2525·407	2	39585·68	α_2 — L_3
2520 88	w	39657·2	U_2 — κ_3

Table VII—(continued).

Wave-length.	Intensity	Frequency	Combination.
2520 66	x	39660 2	$F_3 - b^3D_3$
2515 588	1	39740 18	$x_1 - FF_1$
2513 890	1	39766·87	$W_3 - x_3$
2512 529	1	39788 56	$x_4 - BB_1$
2508 224	0	39856·84	$E_3 - {}^3G_4$
2505 742	15	39896·32	$M_4 - k_4$
2502 493	0	39948·05	$x_5 - P_1$
2497 843	0	40022·48	$G_4 - b^3D_3$
2496 75	0	40040·0	$F_2 - {}^3G_4$
2489·617	3	40154 70	$\lambda_3 - S_2$
2484 243	0	40241 36	$C_3 - {}^1F_3$
2480 1	w	40309	$H_3 - b_3$
2479 115	2	40324·80	$Z_3 - n_3$
2471 153	3	40454·71	$GG_1 - p_1$
2466 03	1	40540·1	$P_4 - k_4$
2461 748	1	40609 25	$N_4 - j_4$
2458 474	1	40663 33	$\mu_3 - AA_3$
2457 732	3	40675 61	$D_4 - {}^1P_4$
2454 753	3	40724·96	$R_4 - k_4$
2452 426	0	40763 60	$L_3 - g_4$
2450 031	2	40803 45	$a_3 - F_3$
2446 715	8	40858 74	$\lambda_3 - N_3$
2437 716	2	41009·56	$\mu_3 - Y_4$
2436·534	2	41029 46	$N_4 - h_3$
2433 103	8	41087·31	$U_4 - m_3$
2431 96	1	41109·7	$V_3 - m_3$?
2430 248	1	41135 58	$r_3 - Y_4$
2426 797	1	41211 04	$x_4 - L_3$
2423 378	0	41269 18	$Q_4 - h_3$
2419 564	0	41317 20	$\lambda_3 - M_4$
2415 618	1	41384 69	$BB_1 - n_3$
2415 287	1	41390 36	$\mu_3 - U_4$
2414 735	2	41399 82	$R_4 - h_3$
2410·207	0	41477 59	$H_3 - b^3D_3$
2406·754	1	41537 09	$\theta_3 - L_3$
2406 053	0	41549 19	$\left\{\begin{matrix} A_3 - a^3D_3 \\ U_4 - k_4 \end{matrix}\right.$
2391·53	1	41801 9	$U_4 - j_4$
2388 345	3	41857·23	$\left\{\begin{matrix} D_3 - a^3D_3 \\ H_3 - {}^3G_4 \end{matrix}\right.$
2385·172	1	41913 90	$W_3 - j_3$
2378 712	0	42026·73	$P_4 - g_4$
2377 948	2	42040·23	$CC_1 - n_3$
2374 101	0	42106 74	$\beta_3 - H_3$
2367·989	5	42217 01	$Z_3 - k_4$
2366 327	1	42246 66	$V_4 - h_3$
2365 621	1	42259 57	$\left\{\begin{matrix} E_3 - {}^3P_3 \\ DD_1 - x_3 \end{matrix}\right.$
2364 695	1	42275 81	$AA_3 - k_4$
2361 503	0	42332·95	$W_4 - h_3$
2360·788	0	42345 77	$M_4 - f_3$
2357 369	1	42407·18	$F_3 - a_3$
2355·713	1	42436·99	$B_3 - a^3D_3$
2350 83	w	42525·1	$r_3 - P_4$
2348·996	0	42558·38	$C_3 - a^3D_3$
2347·538	1	42584·56	$x_3 - N_3$
2346·465	1	42604·23	$Y_4 - h_3$
2336 105	0	42977·10	$G_4 - {}^3G_4$
2323·42	x	43026·8	$Q_4 - f_4$

Table VII—(continued).

Wave-length.	Intensity.	Frequency.	Combination.
2332·579	1	42842 35	$\mu_3 - M_4$
2308·589	2	43303 15	$F_3 - {}^1F_3$
2296·503	2	43531 03	$BB_3 - j_3$
2288·183	1	43689 29	$DD_3 - m_3$
2283·029	0	43787 91	$E_3 - {}^4F_3$, $\nu_3 - L_3$
2282·075	3	43806 22	$\pi_3 - N_3$
2275 980	w	43923 52	$\beta_3 - F_3$
2274·42	1	43953 6	$J_3 - d_3$
2271 27	1	44016 0	$F_3 - {}^3F_4$
2266·905	0	44099 34	$a_3 - D_3$
2264·256	1	44150 92	$DD_3 - k_4$
2260 472	0	44224 82	$H_3 - a_3$
2252·624	0	44378 88	$G_4 - {}^3F_4$, $Y_4 - f_4$
2223 030	1	44969 62	$E_3 - a^3D_3$
2214 005	3	45152 90	$F_3 - a^3D_2$
2203 427	1	45369 65	$D_3 - a^3D_3$
2190 480	0	45637·78	$DD_3 - g_4$
2165 458	1	46165 07	$E_3 - {}^4F_3$
2165·148	1	46171 67	$U_3 - e_4$
2148 209	1	46535 70	$E_3 - {}^4F_3$
2134 809	1	46827 77	$\gamma_3 - E_3$
2131 622	1	46897·77	$AA_3 - e_3$?
2128 330	1	46970 30	$H_3 - a^3D_2$
2119 571	1	47164·38	$GG_4 - j_4$
2117·098	0	47219 46	$\beta_3 - D_3$
2081 096	0	48036 28	$U_3 - d_3$
2071 65	w	48255 2	$X_3 - d_3$
2061·955	0	48462 09	$E_3 - a^3D_3$
2059·649	0	48536 36	$H_3 - {}^4F_3$
2054·193	0	48665·26	$F_3 - a^3D_3$
2045 544	0	48871 00	$EE_3 - e_4$
2039 011	0	49027 56	$G_4 - a^3D_3$
2031 956	2	49197 76	$H_3 - {}^4F_4$
2001·745	0	49940 09	$\gamma_3 - D_3$
1998·11	2	50031 0	$\beta_3 - C_3$
1994 71	1	50116 3	$\beta_3 - H_3$
1990·23	2	50482 6	$H_3 - a^3D_3$
1948 97	1	51292 3	$Q_4 - c_4$, $\pi_3 - H_3$
1945·90	1	51373 2	$J_3 - b^3D_3$, $\zeta_3 - H_3$
1939 87	1	51532 8	$GG_4 - e_3$
1934 89	2	51933 8	$\delta_3 - F_3$
1931·88	8	52015 1	$L_3 - b_3$
1928·90	2	52644 6	$Y_4 - c_3$
1920·69	3	52873 1	$\gamma_3 - E_3$
1886 73	2	52964 1	$K_3 - b^3D_3$
1879·62	1	53184 4	$L_3 - b^3D$
1879·41	1	53190 3	$\epsilon_3 - F_3$
1876·32	2	53277·9	$P_4 - b_3$
1864·3	2	53639	$\lambda_3 - H_3$
1860·2	0	53758	$\gamma_3 - A_3$
1856·5	2	53907	$M_4 - b^3D_3$
1842·8	2	54265	$N_3 - b^3D_3$
1842 2	6	54283	$S_3 - b^3D_3$, $U_3 - b_3$
1839·2	2h	54371	$w_3 - G_4$

Table VII—(continued).

Wave-Length	Intensity	Frequency	Combination.
1832·4	0	54573	$T_2 - b^3D_3$
1829 2	2A	54669	$Y_4 - b_3$
1820 9	0	54918	$\eta_3 - E_2$
1817 6	3	55018	$J_1 - {}^3F_2$
			$AA_3 - b_3$
1810 7	1	55227	$\delta_3 - D_2$
1803 3	1	55454	$U_3 - b^3D_3$
1802 5	1	55479	$V_3 - b^3D_2$
1796 0	2	55679	$X_3 - b^3D_1$
1794 4	3	55729	$J_2 - {}^3F_4$
1790 1	1	55863	$V_3 - {}^3G_4$
1781 8	6	56123	$Z_3 - b^3D_2$
1779·8	2	56186	$AA_3 - b^3D_1$
1772 8	2	56408	$\epsilon_3 - D_2$
1764 7	4	56667	$CC_3 - b_3$
1759 8	0	56825	$\mu_3 - G_3$
			$L_1 - {}^3F_3$
1748 7	1A	57185	$\mu_3 - F_3$
			$BB_3 - b^3D_2$
1742·2	3	57399	$P_4 - {}^3G_4$
1741 0	6	57438	$Q_4 - {}^3G_5$
1739 2	2	57496	$\nu_3 - E_3$
			$L_2 - {}^3F_2$
1736 0	1	57584	$R_4 - {}^3G_5$
1731 6	2	57750	$S_2 - {}^3P_2$
1727·0	2A	57904	$N_2 - {}^3F_3$
1722·4	4	58059	$J_2 - {}^3F_2$
			$DD_3 - b^3D_3$
1721 4	2	58092	$P_3 - {}^3F_4$
1719 6	4	58153	$EE_3 - b^3D_2$
1716 1	3	58272	$R_3 - {}^3F_3$
1714·4	0	58329	$GG_3 - b^3D_1$
1710 0	2	58480	$K_1 - a^3D_2$
1707 3	4	58572	$N_2 - {}^3P_2$
1706 3	1	58606	$S_3 - {}^3F_3$
1704 3	6	58675	$L_2 - a^3D_3$
1701 0	4	58708	$Y_4 - {}^3G_5$
1699 5	3	58841	$Q_3 - {}^3F_4$
1697·8	4	58900	$T_2 - {}^3F_3$
1697 6	2	58907	$Z_2 - {}^3P_2$
1696 8	1A	58934	$AA_3 - a_3$
1695 3	1	58987	$R_4 - {}^3F_4$
1693 4	6	59053	$\beta_3 - A_2$
1692·1	1A	59098	$U_2 - {}^3F_3$
1691·3	3	59126	$V_3 - {}^3F_3$
1686 5	1A	59294	$\zeta_3 - C_2$
1685 8	1	59319	$S_3 - {}^3F_4$
			$X_3 - {}^3F_3$
1685 2	0	59340	$\sigma_3 - B_2$
1683 0	3	59418	$\zeta_3 - B_3$
1673·3	2	59762	$U_2 - {}^3P_2$
1671 9	1	59812	$U_3 - {}^3F_4$
1671·4	0	59830	$AA_3 - {}^3F_2$
1668·8	1A	59923	$W_3 - {}^3F_4$
1667 6	7	59966	$BB_3 - {}^3P_2$
1665 8	1	60031	$X_3 - {}^3F_2$
1661·4	1	60190	$Y_3 - {}^3F_4$
1660 8	2	60212	$\rho_3 - A_2$
1658 2	3A	60306	$\zeta_3 - A_1$

Table VII—(continued)

Wave-length.	Intensity	Frequency	Combination.
1656 3	2h	60376	$J_3 - a^3D_3$
1654 6	3	60438	$Z_3 - {}^4P_3$
1654 1	1	60456	$S_3 - a^3D_2$
1653·4	3	60481	$Z_2 - {}^4F_4$ $\mu_3 - D_3$
1653 0	1	60496	$AA_2 - {}^4P_2$
1651 8	2h	60540	$P_4 - {}^4P_3$ $AA_3 - {}^4F_4$
1651 1	0	60566	$CC_2 - a_1$
1646·1	1h	60750	$T_2 - a^3D_2$
1644 0	4h	60827	$BB_3 - {}^2F_3$
1642·0	1	60901	$L_3 - {}^4F_4$ $EE_2 - a_1$
1640 8	4	60946	$U_3 - a^3D_3$
1640 0	1	60976	$V_3 - a^3D_2$
1637 8	1	61058	$S_3 - {}^4P_3$ $W_3 - a^3D_2$
1634·9	0	61166	$\theta_4 - C_2$
1631 3	3	61301	$\theta_3 - B_3$
1629 9	2	61353	$T_3 - {}^4P_3$
1626 5	2	61482	$CC_3 - {}^2F_3$
1625 8	5	61508	$P_4 - {}^4F_3$
1622 9	1h	61618	$Z_3 - a^3D_2$
1621·9	1	61656	$S_3 - {}^4F_4$
1621 1	1	61687	$A_3 - B_3$
1620 7	1	61702	$DD_3 - {}^2F_3$ $\pi_1 - D_1$
1618 2	2h	61797	$EE_3 - {}^2F_4$
1614·2	2	61950	$T_3 - {}^4F_4$
1614·7	0	61931	$Y_3 - {}^4P_3$
1613 7	4	61969	$FF_3 - {}^2F_3$
1613 2	1	61989	$K_3 - a^3D_3$
1609 0	1	62150	$CC_3 - {}^4P_3$
1608 3	2	62177	$\theta_3 - A_3$
1607 9	2	62193	$L_3 - a^3D_3$ $CC_1 - {}^2F_4$
1607 6	4	62205	$Q_4 - {}^4F_4$
1606 2	2	62259	$W_3 - {}^4F_3$
1605·6	0	62282	$AA_3 - {}^4P_3$
1604·8	2	62313	$T_3 - {}^4F3$
1603 8	2	62352	$R_4 - {}^4F_4$
1602 2	2	62414	$DD_3 - {}^2F_4$
1599 0	2	62539	$V_3 - {}^4F_3$
1596 8	5	62625	$W_3 - {}^4F_3$
1595·5	1	62676	$BB_3 - a^3D_3$
1594 0	1	62735	$X_3 - {}^4F_3$
1592 0	2	62814	$Z_3 - {}^4F_3$
1590·6	0	62869	$AA_3 - {}^4F_3$
1582·3	1	63199	$V_3 - {}^4F_4$
1580 5	1	63271	$N_3 - a^3D_3$
1579 0	0	63331	$OC_3 - a^3D_3$
1577 3	0	63399	$X_3 - {}^4F_4$
1576 0	2	63452	$P_4 - a^3D_3$
1575 0	1	63492	$R_4 - a^3D_3$
1571 2	2	63646	$EE_3 - a^3D_3$
1567·0	2	63816	$FF_3 - a^3D_3$
1566·3	1	63845	$Z_3 - {}^4F_4$
1564·8	0	63906	$AA_3 - {}^4F_4$
1563 2	1	63971	$S_3 - a^3D_3$

Table VII—(continued).

Wave-length	Intensity.	Frequency.	Combination
1556 1	2	64263	$T_3 - a^4D_4$
1550 1	3	64512	$x_1 - C_2$
1548 6	2	64574	$W_3 - a^4D_3$
1544 6	1	64742	$DD_2 - {}^4F_3$
1535 4	1	65130	$Z_3 - a^4D_2$, $GG_1 - {}^4P_2$

Conclusion.

The regular arc spectrum of palladium, involving disturbances of a single electron outside a core of nine 4_3 electrons, includes very nearly all the strong lines of the arc, and most of the faint lines of wave-length longer than 3400 A. In the region of shorter wave-lengths there are also a large number of faint lines, apparently belonging to the arc spectrum, for which no place can be found in the regular series system, since all the predicted for the prominent electronic configurations have been found, and any terms due to additional possible configurations would give lines in the infra-red or extreme ultra-violet. These faint lines can probably be ascribed to a secondary series system, the terms of which arise from configurations of the type $(4_3)\ {}^5D_1 n_2$. The analysis of the spark spectrum has shown that $(4_3)\ {}^5D_1$ and $(4_3)^9$ are of almost equal stability, and consequently terms of this type should occur with considerable prominence in the arc spectrum, but might not combine very readily with the regular terms. An attempt to find a clue to this part of the spectrum by means of the inter-combinations has been quite unsuccessful, and no serious effort has been made to analyse it separately. Similar configurations are also likely to be prominent in the spark spectrum, accounting for the very large number of lines, only a small fraction of which have been included in the present analysis.

In conclusion, the authors wish to express their gratitude to Dr. O. Laporte for his assistance in the interpretation of the recent theories and for his very valuable suggestions, and to Mr. A. B. McLay for his interest and suggestions in the course of the work.

The Equilibrium of Heterogeneous Systems including Electrolytes. Part I.—Fundamental Equations and Phase Rule.

By J A. V. Butler, M.Sc., University College of Swansea.

(Communicated by Prof. F G Donnan, F.R S —Received February 17, 1926)

Introduction

In his well-known memoir on the equilibrium of heterogeneous substances Willard Gibbs obtained the conditions of equilibrium in heterogeneous systems * The equations he obtained have been the basis of most subsequent applications of thermodynamics to material systems, and not a great deal of fundamental importance has been added. In one respect alone his results were comparatively meagre, namely in the case of electrolytes The reasons for this were given by Gibbs himself in a letter to Prof. Bancroft, which is printed in the Collected Papers. He there remarks : " The meagreness of the results obtained in my E H.S in the matter of electrolysis has a deeper reason than the difficulty of evaluation of the potentials. In the first place, cases of true equilibrium (even for open circuit) are quite exceptional Thus the single case of unequal concentration of the electrolyte cannot be one of equilibrium, since the process of diffusion cannot be stopped. . . . Again, the consideration of the difference of potential in electrolyte and electrode involves the consideration of quantities of which we have no apparent means of physical measurement, while the difference of potential in ' pieces of metal of the same kind attached to the electrodes ' is precisely one of the things we can and do measure "†

The first of these reasons is no longer valid since many cases of electrode equilibria have been measured with as great or greater precision than equilibria of other types. It is still true that no reliable means of determining the single potential difference between two phases has been discovered, but it will be found to be of importance to proceed with the formulation of the conditions of equilibrium in cases in which such differences of potential must be taken into account, for these are essential factors determining equilibrium not only in galvanic cells but between phases containing electrolytes in general. In this paper the method of Gibbs is employed to obtain the general conditions of equilibrium in systems containing electrolytes Although a number of partial

* " Trans. Conn. Acad.,' vol. 3, p. 108 (1876) ; *id.*, p. 343 (1878) ; ' Scientific Papers,' vol. 1, p. 55.

† ' Scientific Papers,' vol. 1, p. 429. Also ' Jour Phys. Chem .,' vol. 1, p. 416 (1903).

expressions are to be found in the literature,* a complete statement does not appear to have been attempted before.

It must first be observed that the phase rule has been widely applied to systems containing electrolytes without any reference to the electric forces at phase boundaries, the components being taken to represent every possible variation in the matter of the system, provided each phase remains electrically neutral. Although it will ultimately be shown that this is justified, we shall not at first make any restriction as to the electric neutrality of parts of the system We shall take as components the least number of substances, in terms of which every possible variation in the matter of every part of the system may be expressed, disregarding this limitation. Those components whose motion is accompanied by electric flux may, in conformity with common usage, be called *ions*. In addition to its temperature and pressure and the chemical potentials of its components, every portion of matter in the system will be characterised by an electrical potential, *i.e.* the electrical work done in bringing unit positive charge from a standard position (or from infinite distance) to a point within the matter in question

Conditions of Equilibrium of Heterogeneous Masses.

Consider the system as made up of a number of parts each of which is homogeneous with regard to the masses of its components and at the same electrical potential throughout. The parts which fulfil this condition may be finite or only infinitesimal in size. Let S_1, $S_2 \ldots S_g$ be neutral components, the quantities of which in a given homogeneous part of the system are Dm_1, $Dm_2 \ldots Dm_g$; $S_h \ldots S_n$ components which are ions, whose amounts in the same mass are $Dm_h \ldots Dm_n$, and let $a_h \ldots a_n$ be the quantities of (positive) electricity associated with unit masses of $S_h \ldots S_n$ respectively.

Then, if De, $D\eta$, Dv be the energy, entropy and volume of the mass in question and V its electrical potential, variations in its energy will be given by the equation :

$$dDe = td\mathrm{D}\eta - pd\mathrm{D}v + \mu_1 d\mathrm{D}m_1 \ldots + \mu_g d\mathrm{D}m_g + \mu_h d\mathrm{D}m_h \ldots + \mu_n d\mathrm{D}m_n + (a_h d\mathrm{D}m_h \ldots + a_n d\mathrm{D}m_n)\mathrm{V}. \quad (1)$$

* J. J van Laar, 'Versl. Kon Akad. v. Wet.,' vol. 5, p. 431 (1903); 'Sechs Vorträge über das Thermodynamische Potential,' Braunschweig, 1906, p. 103; Herzfeld, Article on "Physikalische und electrochemie," in 'Encyc. der math. Wissenschaft,' vol. 5, t. 1, part ii. Conditions (8) below are given by Milne as a generalisation from Gibbs, 'Proc Camb Phil. Soc.,' vol. 22, p 493 (1925) *Cf* also Tolman, 'J Amer. Chem Soc,' vol. 35, pp. 307, 333 (1913), and Rice, 'J. Phys Chem ,' vol 30, p. 189 (1926).

Applying the general condition of equilibrium

$$(\delta\epsilon)_\eta \geqq 0$$

we have

$$d\mathrm{D}\epsilon' + d\mathrm{D}\epsilon'' + d\mathrm{D}\epsilon''' \ldots \geqq 0 \quad \ldots \tag{2}$$

for all possible variations in the state of the system which do not alter its total entropy and do not conflict with the other equations of condition, *i e* equations representing the constancy of the total mass of each component and of the total volume of the system. Therefore summing equations (1) for all parts of the system we have :

$$\begin{aligned} &t'd\mathrm{D}\eta' - p'd\mathrm{D}v' + \mu_1'd\mathrm{D}m_1' \quad + \mu_s'd\mathrm{D}m_s' \\ &\quad + (\mu_h' + a_h\mathrm{V}')\,d\mathrm{D}m_h' \quad \ldots + (\mu_n' + a_n\mathrm{V}')\,d\mathrm{D}m_n' \\ &\quad + t''d\mathrm{D}\eta'' - p''d\mathrm{D}v'' + \mu_1''d\mathrm{D}m_1'' \quad + \mu_s''d\mathrm{D}m_s'' \\ &\quad + (\mu_h'' + a_h\mathrm{V}'')\,d\mathrm{D}m_h'' \ldots + (\mu_n'' + a_n\mathrm{V}'')\,d\mathrm{D}m_n'' \ldots, \text{ etc} \geqq 0. \end{aligned} \tag{3}$$

for all variations which satisfy the equations of condition, viz. :—

$$\Sigma d\mathrm{D}\eta = 0, \qquad \Sigma d\mathrm{D}v = 0, \qquad \Sigma d\mathrm{D}m_1 = 0 \ldots \Sigma d\mathrm{D}m_n = 0 \tag{4}$$

It is therefore necessary and sufficient for equilibrium that

$$t' = t'' \quad \ldots = t^\nu \tag{5}$$

$$p' = p'' \quad \ldots = p^\nu \tag{6}$$

$$\left.\begin{aligned} \mu_1' &= \mu_1'' \quad \ldots = \mu_1^\nu \\ \mu_s' &= \mu_s'' \quad \ldots = \mu_s^\nu \end{aligned}\right\} \tag{7}$$

$$\left.\begin{aligned} \mu_h' + a_h\mathrm{V}' &= \mu_h'' + a_h\mathrm{V}'' \ldots = \mu_h^\nu + a_h\mathrm{V}^\nu \\ \mu_n' + a_n\mathrm{V}' &= \mu_n'' + a_n\mathrm{V}'' \quad \ldots = \mu_n^\nu + a_n\mathrm{V}^\nu \end{aligned}\right\}. \tag{8}$$

Thus for every part of the system we have :—

$$t = \mathrm{T}; \quad p = \mathrm{P}, \quad \mu_1 \geqq \mathrm{M}_1, \text{ etc}; \quad (\mu_h + a_h\mathrm{V}) \geqq \mathrm{M}_h, \text{ etc}, \tag{9}$$

in which the equality applies to actual components of a given portion, the inequality to possible components

The relation between the potentials of the substances taken as components, when some can be formed out of others, can be obtained by the general method of Gibbs.* We need only consider the case in which a neutral component S_s is formed from the ions S_h, S_j, S_k, etc., according to the equation,

$$a\mathrm{S}_s = h\mathrm{S}_h + j\mathrm{S}_j + k\mathrm{S}_k \ldots \tag{10}$$

The condition of the constancy of the total mass of the system is now satisfied by variations which are in accord with the equation :

$$\Sigma d\mathrm{D}m_s . \mathrm{S}_s = \Sigma d\mathrm{D}m_h . \mathrm{S}_h - \Sigma d\mathrm{D}m_j . \mathrm{S}_j \ldots = 0, \tag{11}$$

* "Scientific Papers," vol. 1, p. 69.

in addition to those which come within the equations of condition (4). For such variations,

$$\mu_a'dDm_a' + \mu_a''dDm_a'' \quad . \quad + (\mu_h' + a_hV')dDm_h' + (\mu_h'' + a_hV'')dDm_h'' \quad . \quad .$$
$$+ (\mu_j' + a_jV')dDm_j' + (\mu_j'' + a_jV'')dDm_j'' \quad ., \text{ etc }, \equiv 0. \qquad (12)$$

Since equilibrium must still be maintained when variations come within conditions (4),

$$\mu_a' - \mu_a'' \quad . \quad . \quad = M_a$$
$$(\mu_h' + a_hV') = (\mu_h'' + a_hV'') \quad . \quad . \quad = M_h$$
$$(\mu_j' + a_jV') = (\mu_j'' + a_jV'') \quad . \quad = M_j$$

as before, therefore (12) requires that

$$M_a\Sigma dDm_a + M_h\Sigma dDm_h + M_j\Sigma dDm_j \quad . \quad = 0. \qquad (13)$$

Hence by comparison with (10) and (11)

$$aM_a = hM_h + jM_j \quad . \quad . \quad . \qquad (14)$$

or

$$a\mu_a' = h(\mu_h' + a_hV') + j(\mu_j' + a_jV'). \qquad (15)$$

Since S_a is electrically neutral,

$$a_hh + a_jj + a_kk \quad = 0,$$

therefore

$$a\mu_a' = h\mu_h' + j\mu_j' + k\mu_k' \quad , \qquad (16)$$

i.e. in every part of the mass the chemical potential of a neutral salt is related to the chemical potentials of its ions by an equation similar to that which relates the masses of these substances.

Conditions of Neutrality.

Hitherto, no condition with regard to the electrical neutrality of the system, or any part of it, has been made. We will now postulate that the system is neutral as a whole This condition is fulfilled by all systems which can be handled practically. The different phases of which such a system is composed may contain an excess of one or other kind of electricity, in fact, if the phases are at different electrical potentials, a corresponding separation of electricities must necessarily occur.

It has been shown that for each ion the quantity $\mu + aV$ is constant throughout those parts of the system in which it is an actual component. It follows that $d\mu + adV = 0$ for any part in which the state of the mass varies continuously. In a homogeneous mass μ is constant, hence V is also constant. The charge of any phase must therefore be located in the non-homogeneous parts in the

vicinity of surfaces of discontinuity If the mass of the system is large in comparison with the mass of the non-homogeneous portions near the interfaces, the contribution of these to the total energy, entropy, etc , may be neglected. Under these conditions it is only necessary to consider the conditions of equilibrium of neutral phases in contact with each other.

For a homogeneous phase we may write (1) in the form

$$de = td\eta - pdv + \mu_1 dm_1 \ldots + (\mu_h + a_h V)\, dm_h \ldots + (\mu_n + a_n V)\, dm_n \ldots \quad (17)$$

By integration

$$e = t\eta - pv + \mu_1 m_1 \ldots + (a_h + a_h V)\, m_h \ldots + (\mu_n + a_n V)\, m_n \ldots \quad (18)$$

But since the mass is neutral

$$a_h m_h + a_j m_j \ldots + a_n m_n = 0 \quad \ldots \quad (19)$$

Therefore

$$e = t\eta - pv + \mu_1 m_1 \ldots + \mu_g m_g + \ldots + \mu_n m_n \quad (20)$$

and

$$\zeta = e - t\eta + pv = \mu_1 m_1 \ldots + \mu_g m_g \ldots + \mu_n m_n. \quad (21)$$

Differentiating (20) generally and comparing with (17), we obtain for neutral masses the usual equation.

$$\eta dt - vdp + m_1 d\mu_1 \ldots + m_h d\mu_h \ldots + m_n d\mu_n = 0. \quad (22)$$

Co-Existent Phases

In (17) there are $2n + 6$ variable quantities, including the electrical potential Between these variables there are $n + 2$ differential equations of the type $\frac{\partial \eta}{\partial e} = t$, which together with (17) make $(n + 3)$ known relations There are also in each phase one equation (22) and one equation (19) expressing electrical neutrality. There are thus $(n + 1)$ independent variables in each phase

In r phases there are $(n + 1)r$ independent variables, but one electrical potential may be left unspecified without affecting the conditions of equilibrium, leaving $(n + 1)r - 1$ to be determined. The conditions of equilibrium between the phases require $(n + 2)(r - 1)$ equations (5) — (8) between these variables, hence the number of degrees of freedom of the whole system is

$$F = (n + 1)r - 1 - (n + 2)(r - 1) = n - r + 1. \quad (23)$$

In the application of the phase rule to systems containing electrolytes, the number of components taken, having regard to the condition of electrical neutrality, is less by one than the number appearing in the above equations. If the

number of components reckoned in the first way be N, $N = n-1$ and the number of degrees of freedom is $N - r + 2$.*

We shall now consider the variability of systems of co-existent phases when all components are not actual components of each.

In the first place, suppose that all parts of phases are in contact with each other. Then, for each component missing in any phase, there is one independently variable quantity less in that phase But there is also one equation missing in (7) or (8), so that the number of degrees of freedom is not altered

If, however, all pairs of phases are not in contact with each other, the number of degrees of freedom may be greater Consider the case of phase I in contact with two others, II and III, which are not in contact with each other. If every component is an actual component of each phase, every equation determining the equilibrium between I and II and between I and III involves a similar equation between II and III and there could be no more equations if II and III were in contact with each other Hence, if I is in equilibrium with II and with III, these must be in equilibrium with each other.

But if certain components are present in II and III but missing in I, this is not the case For each component missing in any phase there is one independently variable quantity less in that phase, but for every component missing in the middle phase there are two equations missing Hence the number of degrees of freedom is increased by one for each component present in two phases which are not in contact and absent from the intervening phase.

However, in certain cases the equilibrium of a system in such a varied state is unstable. Thus, if phase III can be formed out of the matter of phases I and II, the conditions of equilibrium with regard to the formation of a new phase may not be fulfilled with respect to it. Applying the condition of equilibrium in the form $(\delta\zeta)_{t,p} \geqq 0$ for all possible changes (where ζ is the free energy of the whole system), it will be seen that if the free energy would be lowered by the formation of a mass of phase III from phases I and II, the system is not in a

* In a recent paper on "The Application of the Phase Rule to Galvanic Cells" ('J Amer Chem. Soc', vol 46, p 2211 (1924)), J A. Beattie has come to the conclusion that for each surface containing a P.D. in a system the number of degrees of freedom is increased by unity. It will be seen from the above that, provided components are reckoned with respect to the condition of electrical neutrality, the number of degrees of freedom is the same as in a similar system of non-electrolytes.

This conclusion may be expressed differently by saying that while the r electrical potentials provide $(r-1)$ extra variables determining equilibrium, the number of components reckoned is also greater by one, giving $(r-1)$ new relations.

The extra degrees of freedom observed in the galvanic cell is due to another cause, as will appear from the considerations which follow.

state of true equilibrium. But on account of differences between the properties of minute quantities of substances and the properties of large masses of the same composition, the condition $(\delta\zeta)_{t,p} \geqq 0$ may be fulfilled for infinitesimal changes and the system will remain in a state of unstable equilibrium.

As soon as a mass of phase III is formed in contact with II, the extra degree of freedom gained by their separation is lost.

Equilibrium in Galvanic Cells.

Cases of equilibrium of this type are met with in galvanic cells. Thus in a system consisting of metallic silver and zinc and an aqueous solution of silver and zinc nitrates, there are five components, viz.:—silver ions, zinc ions, nitrate ions, electrons and water. In the absence of a vapour phase there are three phases, hence if all phases are in contact, the number of degrees of freedom is three. Thus if the temperature, pressure and concentration of silver ions are fixed, the concentration of zinc ions cannot be varied, which is in accordance with experience. But if the zinc and silver are not in contact, there is no condition of equilibrium of electrons between the two metals to be satisfied, and an extra degree of freedom is gained. However, in a varied state which would not be in equilibrium if the zinc and silver were in contact, the equilibrium is unstable, for the free energy of the system would be lowered by the formation of a quantity of silver from the two phases zinc and solution.* It is possible, however, that the formation of an infinitesimally small quantity of silver would raise the total free energy, so that an infinitesimally small displacement would not be sufficient to destroy the equilibrium. A large displacement, causing the formation of silver in quantities having the properties of the massive metal (or the presence of impurities on the surface of the zinc causing local galvanic action), would be sufficient to do so.

The unstable equilibrium in such a galvanic cell can also be maintained when the metals are in contact outside the solution by raising the electrical potential of one of the metals between the parts in contact with the solution and its junction with the other metal by an amount equal and opposite to the sum of the three potential differences taken round the circuit. This amounts to the introduction of a new variable quantity, which makes equilibrium possible.

* For certain proportions of zinc and silver ions in the solution. For others (which are probably not attainable practically) the free energy would be reduced by the formation of zinc from silver and the solution. [*Note added June 27*: Such cases have been realised See a note on the "Deposition of Metallic Zinc on the Positive Pole of a Simple Voltaic Cell," by Humby and Perrin in 'J. Chem Soc.,' vol. 129, p. 959 (1926).]

Summary.

The method employed by Gibbs in his memoir, 'On the Equilibrium of Heterogeneous Substances,' is extended to systems containing electrolytes by the introduction of another variable, the electrical potential. The general condition of equilibrium are obtained and a modified form of the phase rule for neutral masses containing electrolytes is given and its application to galvanic cells discussed.

An Investigation of the Effects of Variations in the Radiation Factor on the Efficiency of Dewar Vessels.

By Bertram Lambert, M.A., Fellow of Merton College, Oxford, and Kenneth Townend Hartley, B.A., B.Sc., Merton College, Oxford

(Communicated by Prof. F. Soddy, F.R.S.—Received March 20, 1926.)

During the course of some work on Dewar vessels, which was carried out by one of us (B. L.) and S. F. Gates for the Oxygen Research Committee, a curious anomaly was noticed in the behaviour of an all-metal Dewar vessel. This was a commercial copper vessel of the usual spherical type with a long narrow neck of an alloy of low heat-conductivity, its capacity was two litres. The rate of evaporation of liquid oxygen stored in this vessel was approximately double that of liquid oxygen stored in a silvered glass flask of like capacity; but, when equal weights of hot water were put into each of the vessels, it was found that the rate of cooling of the water in the copper vessel was actually slower than in the silvered glass vessel. It appeared, then, that the copper vessel was only half as efficient as a silvered glass one of like capacity for the storage of liquid oxygen, whereas its efficiency for the storage of hot water was greater than that of the silvered glass vessel. This investigation arose out of a desire to explain the apparent anomaly.

Previous work on the factors which influence the efficiency of Dewar vessels has been carried out by Dewar ('Proc. Roy. Inst.,' 1898, p. 815), Banneitz, Rhein and Kurze ('Ann. d. Phys.,' 1920, vol. 61, p. 113), and Briggs ('Proc. Roy. Soc. Edin.,' 1920, vol. 51, p. 97). These investigations have dealt with the efficiency of Dewar vessels considered only as containers for liquid air or oxygen, and the above-mentioned anomaly has therefore not been noticed.

Briggs (*loc. cit.*) worked with vessels with the vacuum-adjacent surfaces of polished gilding metal (95 per cent. copper). From his results on the rates of evaporation of liquid oxygen from these vessels, he calculated a value for the emissivity of the polished surfaces which was considerably greater than that anticipated from the usually accepted value for copper. This observation is intimately connected with that of Lambert and Gates and will be referred to later.

The passage of heat to or from the interior of a Dewar vessel is brought about chiefly by (*a*) conduction through the residual gas in the vacuous space; (*b*) radiation across the vacuous space, (*c*) conduction along the neck. Convection effects in the residual gas in the vacuous space are of negligible importance in a well-evacuated vessel, while convection effects in the space above the liquid stored in the vessel are only of importance when open Dewar vessels are used for the storage of hot liquids Another, but usually small, transfer of heat occurs by radiation through the neck aperture.

This work, which is essentially a study of the effects of variations in the radiation factor ((*b*) above) on the efficiency of Dewar vessels, had necessarily to be carried out under such conditions that the effects of the other factors were the same, and unalterable, in each series of experiments This was effected by using vessels of the same size, shape and material, and differing only in the nature of the vacuum-adjacent films and surfaces, by connecting together the vacuum spaces of the vessels to be compared with wide bore tubing and so ensuring that the pressure was identical in all of them; by keeping the external temperature of all the vessels constant throughout the experiments.

In order to get reliable and repeatable comparisons of the effects of different reflecting vacuum-adjacent surfaces, it was found necessary to construct a special type of glass Dewar vessel, of such a nature that the inner and outer vessels could be taken apart in order to attach to the glass and polish the different reflecting surfaces used. Much experience and practice were necessary before the technique was perfected, and it became possible to make a series of vessels such that, after being used to give a set of results, they could be taken down, repolished and reassembled to give the same results. This was regarded as a necessary criterion of the work.

These special vessels (shown in the figure) consisted essentially of two concentric glass cylinders "A" and "B," connected together at the neck by a 4 cm.-long, well-ground and accurately fitting glass junction "C." Each vessel was about 30 cms. high, the capacity of the inner vessel (below the ground joint) being about 250 c.c., its diameter 3 cms., and the thickness of its walls 1 mm.

Each outer vessel had, at the bottom, an exit tube "D" of internal diameter 10 mms.

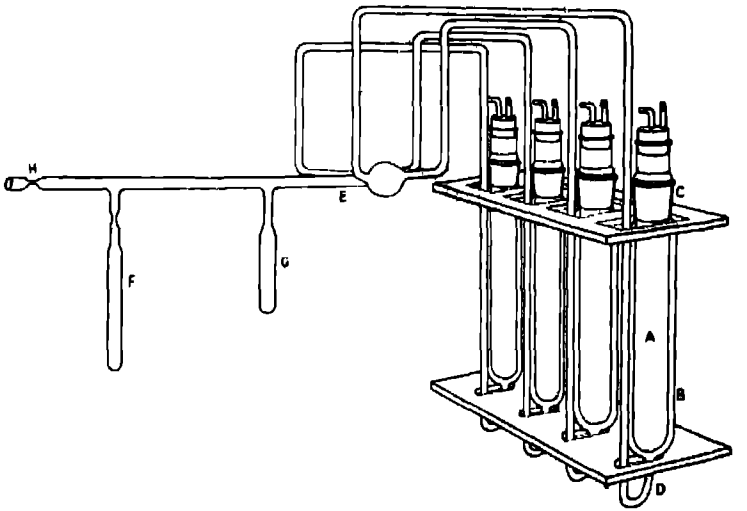

A frame was constructed to hold four of these vessels with their exit tubes sealed into one common evacuating main tube "E," as shown in the figure. The frame and its contents could be clamped firmly in a large constant temperature water bath, so that the Dewar vessels were immersed up to the ground joints. The bath was efficiently stirred and maintained throughout the experiments at a temperature of 18° C. (± 0·01° C.).

Sealed to this system, outside the bath, were two bulbs "F" and "G," each containing about 40 c.cs. of very efficient, "steam-activated" palm-nut shell charcoal in the form of small granules. One of these charcoal bulbs, "F," was connected by a constricted tube so that it could be sealed off from the system when required. The whole system was connected up, through another constricted tube "H," with a mercury pump, a large tube containing phosphorus pentoxide and a vessel containing a supply of pure dry oxygen. With the exception of the constricted tubes necessary for sealing-off purposes, all connecting tubing was of an internal diameter not less than 10 mms. When evacuation was completed, and the apparatus ready for use, there were no constricted connections between any parts of the system.

The following is a brief description of the method of experiment: Four (in some cases three) vessels, with reflecting surfaces prepared, were assembled as

shown in the figure, the ground joints being first thinly lubricated with a heavy grease made from vaseline and rubber, and the parts brought into optical contact with each other. The system was then evacuated by means of an automatic Sprengel pump while the bulbs "F" and "G" were heated by steam jackets. After evacuation had been carried as far as possible—an operation spread over 50 to 60 hours—the system was "washed out" with pure dry oxygen (made by electrolysis of baryta solution and dried for several days over pure phosphorus pentoxide). The process of evacuation and washing out with oxygen was repeated, and the system finally evacuated as perfectly as possible while the bulbs "F" and "G" were heated by steam jackets While these bulbs were still heated, the mercury pump and oxygen supply were sealed off from the system at "H"

The charcoal bulb "F," after being cooled in liquid air for several hours, while "G" was maintained at 100° C., was sealed off. The remaining charcoal bulb "G" was subsequently immersed in liquid oxygen, and kept at this steady temperature for several hours before, and for the whole time during which, the behaviour of the Dewar vessels was under investigation.

While the system was in this controlled condition, the rate of evaporation of liquid oxygen from each of the Dewar vessels was measured and also the rates of cooling of known weights of hot water stored in the vessels All the values obtained were repeated and checked over a period, for each experiment, of 2 to 3 days.

The glass surfaces of the apparatus could not be heated during evacuation, but it was anticipated that repeated slow evacuation, washing out with pure dry oxygen, and long standing in contact with pure phosphorus pentoxide, would result in producing a sufficiently steady residual pressure inside the system. This anticipation proved to be justified, since there was no alteration in the rate of evaporation of liquid oxygen from any of the Dewar vessels after the apparatus had been allowed to stand untouched for several days, and also after hot water had been kept in the vessels for long periods. This proved also that the cooled charcoal in "G" was amply sufficient to take up any vapour given off by the grease used in the lubrication of the ground joints, and any gas given up by the glass and metal surfaces during the course of the experiment. The pressure factor could, then, be considered as controlled at a definite constant value throughout any one experiment. Since the vessels were of the same size, shape and material, the neck conductivity factor was identical in all the vessels.

It was considered desirable to keep the evacuated system as simple as possible,

so no pressure gauge was included in it. For the purpose of this investigation it was necessary only that the pressure should remain unaltered during the course of any one experiment From quantitative work on pressure reductions produced in glass apparatus of known volume, by known amounts of the palm-nut charcoal cooled to the temperature of liquid oxygen, it is calculated that the residual pressure in the system could not be higher than 0 0001 mm. of mercury during the course of any experiment.

The rates of evaporation of liquid oxygen were measured as follows :— All the Dewar vessels of the series under investigation were filled to a level just below the ground junction with liquid oxygen, and fitted with rubber stoppers provided with exit tubes. Each exit tube was connected, for short periods of time, to a calibrated gas meter, and the rates of evolution of gas measured until these rates had settled down to steady values. The gas evolved by each vessel was then measured over short and long periods (up to two hours), and the average rate of evolution of gas was calculated for each vessel It was found that once a vessel had settled down to show a steady rate of evaporation of liquid oxygen, this rate remained unaltered for long periods. The rates of evaporation so determined are expressed in grammes of oxygen lost by evaporation from each vessel in 24 hours Since only comparative values were required, correction for temperature and pressure was not considered necessary, and the volumes of gas were converted (approximately) into grammes per 24 hours by multiplying by the factor $32 \times 24/22 \cdot 4$

The rates of cooling of hot water stored in the Dewar vessels were measured as follows :—A known weight of hot water was poured into each vessel and the vessels were then stoppered to prevent possibly confusing convection effects in the space above the liquids. The temperature of the water in each vessel was taken from time to time and cooling curves were drawn. From these curves, and the known weight of water contained in each vessel, values were calculated showing the loss of heat from each vessel in calories per hour over given ranges of temperature change.

Typical experimental results are given under series A, B, C and D below .—

Series "A."

The original experiment of Lambert and Gates with the two-litre copper and silvered glass vessels was repeated under strictly comparable conditions by the method given above, with the vessels connected together by wide-bore tubing.

The only factors governing the transfer of heat from the outer to the inner vessels which were not identical were, therefore, the radiation factors and the neck conduction factors. The following results were obtained :—

	Rate of evaporation of liquid oxygen in grms / 24 hours	Rate of cooling of hot water in calories per hour, over the temp range 75°–55° C
Copper vessel	600	930
Chemically silvered glass vessel	340	1100

These results confirm the original observation, and it is clear that any explanation of the curious difference in behaviour must be sought for in the radiation factor, since the effects of the neck conduction factors (calculable from the work of Bannertz, Rhein and Kurze (*loc cit*), could not possibly account for the observed differences in behaviour.

Series "B"

The experiments in this series were carried out in order to compare the efficiencies of three Dewar vessels of the same size, shape and material, one with the vacuum-adjacent surface of the inner vessel only silvered, one with the vacuum-adjacent surface of the outer vessel only silvered, and one with both these surfaces silvered. This silvering was done chemically

In the earlier experiments in this series a fourth vessel with both vacuum-adjacent surfaces unsilvered was included, but the rate of evaporation from this vessel was so rapid that it did not settle down to a steady value before the vessel was empty. A trustworthy comparison was thus impossible, and the plain glass vessel was left out in the later experiments of this series. It was found necessary to use much larger vessels in order to make a satisfactory comparison of the efficiencies of silvered and unsilvered Dewar vessels, and this is done in series "C" below.

All the known methods of chemically silvering glass surfaces were carefully tried and the most satisfactory process was found to be that of Brashear as described in "Discussion on the Making of Reflecting Surfaces" ('Phys. and Opt. Soc.,' 1920) This process involves the reduction, at 19° C, of an ammoniacal silver solution with a solution containing cane sugar, nitric acid and alcohol. During the later stages of the process the surface undergoing silvering was gently rubbed with cotton wool in

order to prevent the precipitate (which is always produced) from settling on the silver film and causing "pinholes" in it. The silvered surfaces were washed in turn with distilled water, alcohol and ether and were dried immediately at 100° C. In the earlier experiments in this series it was necessary to polish these silver films with chamois leather and rouge in order to remove the "bloom" from them, but it became possible with experience and the use of "aged" sugar solution, to produce brilliant surfaces free from "pinholes" and needing no polishing whatever

The following are typical results obtained in this series :—

—	Rate of evaporation of liquid oxygen in grms / 24 hours.	Rate of cooling of hot water in cals./hour over temp. range 70°–50° C.
(a) Vacuum-adjacent surface of outer vessel only silvered	279	1940
(b) Vacuum-adjacent surface of inner vessel only silvered	199	1940
(c) Vacuum-adjacent surfaces of both vessels silvered	175	1940

These striking and unexpected results, which were repeated and checked over a period of two days, are discussed later. Separate experiments, with freshly silvered surfaces, afforded substantial confirmation of the accuracy of the results.

Series "C."

The experiments of this series were carried out in order to compare the efficiencies of two glass Dewar vessels of the same shape and size, one with both vacuum-adjacent surfaces silvered and the other unsilvered. As pointed out above, this comparison could not be satisfactorily carried out with the small special vessels used in Series "B" (and "D"). Two spherical glass Dewar vessels were taken, each having a capacity of two litres. One of these had the vacuum-adjacent surfaces chemically silvered, but the silvered surfaces could not be polished or rubbed with cotton wool during deposition of the silver. The experiments afford, however, a comparison applicable to the average chemically silvered and unsilvered commercial Dewar vessels. The flasks were connected together with wide-bore tubing and the method of experiment was exactly the same as in the other series. The factors governing the transfer of heat from the inner vessels were therefore identical in the two flasks with the one exception of the radiation factor. The rates of evaporation of liquid oxygen and of cooling

of hot water were determined and repeated several times, with identical results, as follows :—

—	Rate of evaporation of liquid oxygen in grms./ 24 hours	Rate of cooling of hot water in cals./hour over temp range 70°–50° C
Silvered flask	370	2000
Unsilvered flask	4510	6600

It appears that a chemically silvered glass Dewar vessel is more than 12 times as efficient as a plain glass one of the same shape and size for the storage of liquid oxygen. Dewar (*loc. cit.*) gave a figure 7·4 for this comparison. It is very probable that our figure of 12 would be increased if the chemically silvered surfaces had been prepared under as favourable conditions as those obtaining in the special vessels. The difference between the efficiencies of the two vessels when used for the storage of hot water is very markedly less.

Series "D."

The experiments in this series were carried out in order to compare the effects on the efficiencies of Dewar vessels of polished vacuum-adjacent surfaces of different metals. The surfaces chosen for the comparison were polished silver, gold, platinum, and copper. It was originally intended to put these polished films on the vacuum-adjacent surfaces of both inner and outer vessels of the special type, but it was found impossible to obtain satisfactorily uniform polished metal films on the inner surfaces of the outer vessels, so the experiments were done with the outer vessels of plain glass and with the inner vessels carrying the polished metal films on their vacuum-adjacent surfaces. It is probable that, in these circumstances, a satisfactory comparison is obtained, since each outer vessel had its vacuum-adjacent surface maintained at 18° C., while each inner vessel had its special vacuum-adjacent surface kept at the temperature of the liquid stored within it during the experiment. Again, from the results obtained in Series "B," it is clear that the efficiency of a Dewar vessel with the vacuum-adjacent surface of the inner (containing) vessel silvered and polished is not seriously different in efficiency from a like vessel with both vacuum-adjacent surfaces silvered and polished.

Much time was spent in examining the possibility of forming gold and copper films directly on glass surfaces, by chemical processes, and also of electrically depositing these metals on chemically produced silver films, but the results were

very unsatisfactory. It was finally decided that really reliable and comparable results could only be obtained by coating the glass surfaces with films of platinum, causing these to adhere firmly to the glass, and then electrically depositing silver, gold and copper on these platinum surfaces. The inner vessels were evenly painted on their outside surfaces with a thin film of "liquid platinum" varnish made by Messrs. Johnson and Matthey, London. This film was allowed to dry thoroughly in a dust-free atmosphere at the ordinary temperature. Each vessel was then suspended in an electric tube furnace which was gradually raised to the temperature at which the glass began to soften: at this point the current was immediately turned off and the furnace allowed to cool slowly to the ordinary temperature before the vessel was removed. In this way an even, smooth platinum film was produced and made to adhere to the glass sufficiently firmly to withstand vigorous polishing with rouge and chamois leather. The whole operation was repeated so as to give an adherent platinum film sufficiently thick and even to form a satisfactory base for electroplating. After this operation it was necessary to regrind the joints ("C" in the figure).

The platinised surface of one inner vessel was polished as perfectly as possible, and the surfaces of the three other platinised inner vessels were polished and electroplated with silver, copper and gold respectively. Silver and gold were deposited from cyanide baths and copper from a sulphate bath. Very small current densities (about 50 milliamperes per sq. decimetre) were used in all cases, so as to produce a fine-grain deposit which could be polished with chamois leather and rouge. The polishing proved to be a long and laborious process, but eventually it was carried out so satisfactorily that results which were obtained with the set of vessels could be definitely repeated after taking down the vessels, repolishing and reassembling.

The following are typical results in this series:—

—	Rate of evaporation of liquid oxygen in grms / 24 hours.	Rate of cooling of hot water in cals./hour over temp range 70°–50° C
Inner vessel with polished silver surface	240	2000
Inner vessel with polished gold surface..	250	2000
Inner vessel with polished copper surface	480	2400
Inner vessel with polished platinum surface	340	2900

These results afford a definite confirmation of the peculiar behaviour of Dewar vessels with the vacuum-adjacent surfaces of polished copper. They are discussed below.

Discussion.

The passage of heat by radiation to or from the interior of a Dewar vessel may be investigated (*vide* 'Report of Oxygen Research Committee,' 1923) from the theoretical standpoint as follows :—

Stefan's Law expresses the rate of transfer of heat by radiation from one black body to another as follows —

$$Q = K (T_1^4 - T_2^4), \qquad (1)$$

where Q is the heat in calories per second, per square centimetre of surface ; T_1 and T_2 are the absolute temperatures of the bodies , and K is a constant whose value is taken as $1{\cdot}38 \times 10^{-12}$.

For bodies which are grey—*i. e.*, which emit a constant fraction of the energy which a black body would radiate on the various wave-lengths—the expression is modified thus :—

$$Q = KB (T_1^4 - T_2^4), \qquad (2)$$

where B depends on the emissivity of the grey surfaces. The value of B can be obtained from that of the emissivity as follows —

Let E be the emissivity (the ratio between the heat emitted by unit area of the surface to that emitted by unit area of a black body in the same circumstances) of the (grey) radiating surfaces, in this case the vacuum adjacent surfaces of a Dewar vessel If X is the amount of heat radiated by unit area of a black body, then the amount radiated by unit area of the surface under consideration is XE. This radiation falls on the opposite surface, and a part of it, XE (E), will be absorbed , the remainder, XE (1 — E), is reflected back again to the original surface, where XE (1 — E) (1 — E) is again reflected, and XE (1 — E) E re-absorbed. The reflected portion falls once more on the receiver where XE (1 — E) (1 — E) E is absorbed, so that the net heat transfer by radiation from one surface to the other is given by the sum of the geometric progression :—

$$X [E^2 + E^2 (1 - E)^2 + E^2 (1 - E)^4 + \ldots],$$

which is —

$$\frac{XE^2}{1 - (1 - E^2)} = \frac{XE}{2 - E}. \qquad (3)$$

It has been assumed that the heat transferred between unit areas of two black bodies is X, and therefore $\frac{E}{2 - E}$ is the factor B, and equation (2)

representing the heat transfer between unit areas of two grey bodies may be written .—

$$Q = K \frac{E}{2 - E} (T_1^4 - T_2^4). \quad (4)$$

This argument only holds good if the two surfaces have the same emissivity E. If they are still grey, but have different emissivities E and E′, an argument similar to the above leads to the series .—

$$X [EE' + EE' (1 - E) (1 - E') + EE' (1 - E)^2 (1 - E')^2 \quad . \quad],$$

whence .—

$$B = \frac{EE'}{E + E' - EE'}. \quad (5)$$

Now Maxwell's theory of the relationships between the electrical and optical properties of metals requires that the emissivity of a metal surface, for a given wave-length, shall be proportional to the square root of the absolute temperature, and this has been experimentally confirmed by Haagen and Rubens (' Ann. d. Phys ,' 1903, vol. 11, p 873 , ' Sitz Ber Preuss Akad ,' 1909, vol. 16, and 1910, vol 23) Thus if E is the emissivity of a given surface for room temperature (291° A) and E′ the emissivity at the temperature of liquid oxygen (91° A) ·

$$E' = \sqrt{\frac{91}{291}} E$$

Substituting this value in (5) gives a value for B = E/2 8 — E. In the case under consideration, however, there are probably so many other interfering factors that this refinement may be ignored, further, since E for metals is small, we may write B = E/2 without serious error when both reflecting surfaces are the same, and are metallic

It has been shown above how temperature affects the emissivity of a surface , this value is also affected by the wave-length of the radiation, and this in turn depends on the temperature of the radiator. The wave-length λ_m, on which the maximum energy will be radiated by a black body, at any temperature, is given by Wien's law, which may be expressed in the form .—

$$\lambda_m = \frac{K}{T},$$

where T is the absolute temperature of the body and K is a constant equal to about 2900 Thus for the temperatures concerned in this work—those of hot water, the constant temperature bath and liquid oxygen—370°, 291°, and 91° A., the corresponding wave-lengths are 8 μ, 10 μ and 32 μ. Haagen and Rubens (*loc. cit*),have shown that the metals have almost constant emissivities over a range of wave-lengths 4 μ to 20 μ. Beyond this range there is no experimental

evidence, but it has been assumed that this constancy was maintained over the whole range of long waves concerned in this work—i *e*, 8 μ to 32 μ The values obtained in this work with polished copper surfaces do not justify this general assumption

Before the results obtained in series " B " and " D " can be considered in the light of the above theoretical deductions, the values obtained must be adjusted to allow for the losses due to neck conduction and gas conduction across the vacuous space As explained earlier, these factors were the same for all the vessels in each series

Bannertz, Rhein and Kurze (*loc. cit*) have shown that the rate of evaporation of liquid oxygen due to the neck conduction may be taken as 30 grammes per 24 hours per square centimetre cross section of glass in the neck In all the special vessels the diameter of the neck was 30 mm. and the thickness of the glass 1 mm, so that the cross section of glass in the neck is nearly 1 sq cm, and the rate of evaporation due to neck conduction may be taken as 30 grms per 24 hours.

A method of calculating the rate of evaporation of liquid oxygen due to the conductivity of the gas in the vacuum space is given by Soddy and Berry ('Roy. Soc. Proc,' A, 1909, vol. 83, p 254, and 1911, A, vol 84, p 576, and Briggs (*loc. cit*)). Assuming the residual pressure to be about 0·0001 mm of mercury (see p 140), the rate of evaporation from this cause would amount to 24 grms. per 24 hours Hence the approximate total rate of evaporation due to causes other than radiation is estimated as 54 grms per 24 hours for each vessel.

A proportionate amount must be allowed from the rates of cooling of hot water

Table I, given below, shows the results of the experiments in Series " B," and Table II those of the experiments in Series " D,"

(*a*) with the experimental values adjusted for losses by neck conduction and by gas conduction across the vacuous space,

(*b*) with the values for E of the vacuum-adjacent surfaces (the values for the polished metals are those given by Haagen and Rubens (*loc cit*), and that for glass is taken as 0 75 (Pfund, 'Astrophys. Jl,' 1906, vol. 24, p 25)),

(*c*) with the values of the radiation factor B, calculated from those for E.

Table I.

Vessel.	Adjusted rate of evaporation of liquid oxygen in grms /24 hours	Adjusted rate of cooling of hot water in cals /hr. temp. range 70°–50° C	Values of E.		B
			Outer	Inner	
Vacuum-adjacent surface of outer only silvered	225	1300	0 012	0 75	0 0119
Vacuum-adjacent surface of inner only silvered	145	1300	0 75	0 012	0 0119
Vacuum-adjacent surfaces of both inner and outer silvered	121	1300	0 012	0 012	0 006

Table II

Vessel. (All outer vessels plain glass)	Adjusted rate of evaporation of liquid oxygen in grms /24 hours	Adjusted rate of cooling of hot water in cals /hr temp range 70°–50° C.	Values of E.		B
			Inner	Outer.	
Vacuum-adjacent surface of inner —					
(*a*) Polished silver	186	1330	0 012	0 75	0·0119
(*b*) Polished gold	196	1330	0 019	0 75	0 0190
(*c*) Polished platinum	286	2230	0 045	0 75	0 0443
(*d*) Polished copper	426	1730	0 016	0 75	0·0159

From the theoretical considerations put forward above, it follows that the rate of passage of heat to or from a glass Dewar vessel with either one of the two vacuum-adjacent surfaces silvered, should be approximately double that of a like vessel with both vacuum-adjacent surfaces silvered. The results in Table I show that this is true only if we compare the rate of evaporation of liquid oxygen from a Dewar vessel having the vacuum-adjacent surface of its outer vessel silvered with the rate from one having both vacuum-adjacent surfaces silvered. It is quite certain, however, that a polished silver vacuum-adjacent surface on the inner (or container) vessel has a markedly different effect on the rate of evaporation of liquid oxygen from a similar vacuum-adjacent surface on the outer vessel, and that, for the storage of liquid oxygen, a Dewar vessel with the vacuum-adjacent surface of the inner (or container) vessel silvered is not much less efficient than a similar vessel with both vacuum-adjacent surfaces silvered.

It is most striking that there should be no difference between the efficiencies

of the three vessels when used as storage vessels for hot water in spite of the large differences in their efficiencies for the storage of liquid oxygen

We can offer no satisfactory explanation of these definite experimental results. It seems to be clear, however, that the theory outlined above, of the passage of heat by radiation from one surface of a Dewar vessel, must be regarded as inadequate.

Table II shows that the efficiencies of Dewar vessels with the vacuum-adjacent surfaces of their inner (or container) vessels of polished silver, gold and platinum are (qualitatively) in the order that would be expected from the known emissivities of these metals, and, further, the order is the same whether they are used for the storage of liquid oxygen or hot water.

Note.—That there is not a closer accordance, in these experiments, between the efficiencies and the nominal emissivities of the vacuum-adjacent surfaces probably arises from the differences in the degrees of polish which were given to the metal films Because of the fragile nature of the vessels, all the polishing had to be done by hand, the differences in hardness between the three metal films make it most improbable that the degrees of polish would be the same in all cases

The behaviour of the vessel in the series with the vacuum-adjacent surface of its inner vessel of polished copper places beyond question the anomalous behaviour of polished copper as a radiating surface at the temperature of liquid oxygen.

The copper film, being the hardest of the three electro-deposited films investigated, was polished probably to a less extent than the others, but qualitatively the efficiency of the vessel in which it was used was for the storage of hot water. not seriously out of place in the series

The following explanation of this anomaly is put forward.—

At ordinary and lower temperatures all the heat energy of a metal may be considered to be due to the vibration of its atoms. It appears to be generally accepted that there is, for each element, a "characteristic frequency" with which the atoms themselves vibrate A body will naturally absorb radiation of this frequency very readily—*i.e.*, for the corresponding wave-length, the value of E will be high, and the body will cease to behave as a grey body if radiation of this wave-length falls upon it

In the absence of evidence to the contrary, it has hitherto been assumed that the emissivity of a metal is constant for wave lengths exceeding 4 μ, but when the wave-lengths concerned approach the "characteristic frequency" this assumption obviously cannot hold good.

The "characteristic frequencies" for the metals involved in this work have been calculated from different experimental data by various workers, and average values, with the corresponding wave-lengths, are quoted below.

Metal	Characteristic Frequency	Corresponding Wave-Length.
Silver	$4\ 36 \times 10^{13}$	68 μ
Gold	$3\ 40 \times 10^{13}$	88 μ
Platinum	$4\ 36 \times 10^{13}$	68 μ
Copper	$6\ 7 \times 10^{13}$	45 μ

It has already been pointed out that the wave-lengths primarily concerned in the cooling of hot water and the evaporation of liquid oxygen are about 8 μ and 32 μ respectively. The latter value and the wave-length corresponding to the "characteristic frequency" of copper are relatively close together, and it is therefore to be expected that the emissivity of copper at the temperature of liquid oxygen would be markedly higher for the wave-lengths which preponderate at that temperature than it is for the wave-lengths that are most important when hot water is cooling

In this, therefore, lies a reasonable explanation of the apparently anomalous behaviour of a copper Dewar vessel which led to, and has been verified by, this work It also affords an explanation of the high emissivity of the reflecting surfaces which Briggs (*loc cit.*) calculated for polished gilding metal from his experiments on the rate of evaporation of liquid oxygen from a Dewar vessel made from this alloy

It follows from these results that the efficiency of the commercial copper liquid air containers should be increased by having their polished vacuum-adjacent surfaces of silver instead of copper; an experiment showed that this conclusion was justified.

Two exactly similar 2-litre copper Dewar vessels (one of which was used in Series "A") were returned to the makers. These were taken apart, and the vacuum-adjacent surfaces of one of them silver plated and polished, while the corresponding copper surfaces of the other were simply repolished

The two vessels were connected together by wide-bore tubing and their efficiencies compared under the precise experimental conditions used throughout this work. The factors influencing the passage of heat to or from both vessels were thus identical except for the reflecting surfaces.

The results obtained were as follow :—

Vessel.	Rate of evaporation of liquid oxygen in grms / 24 hours	Rate of cooling of hot water in cals /hour over temp range 70°–50° C
Vacuum-adjacent surfaces of polished copper	525	634
Vacuum-adjacent surfaces of polished silver electroplated on copper	456	634

Silver plating and polishing the vacuum-adjacent surfaces of a 2-litre copper Dewar vessel thus increased its efficiency, when used for the storage of liquid oxygen, by nearly 15 per cent.

The Department of Scientific and Industrial Research has borne the cost of the liquid oxygen and of the copper Dewar vessels used in this work, and we wish to express our thanks for this valuable assistance

---

On the Action of a Locomotive Driving Wheel.

By F. W Carter, M A , Sc D , M.Inst C E., M I E E

(Communicated by Prof A. E H Love, F R S —Received April 15, 1926)

In the appendix to a paper read before the Institution of Civil Engineers,* dealing generally with the subject of the ' Electric Locomotive,' the author discussed the running qualities of locomotives from the point of view of dynamics He based the discussion on the forces set up between wheel and rail, and these forces he referred to the creepage of the surfaces in contact due to elastic deformation of the material in the neighbourhood of the contact, defining " creepage " as the ratio of the distance gained by one surface over the other, to the distance traversed. He later introduced two quantities, f and f', which represented respectively the tractive force per unit creepage, longitudinally and transversely, to the rail. The quantities f and f', which were assumed constant in any particular problem, were not determined at the time, and the present paper is primarily an attempt to compute the first of them.

* See Minutes of ' Proc. Inst. C.E.,' vol. 201, part I, p. 248 See also the author's book ' Railway Electric Traction ' (Arnold, 1922), chap. 2, p. 57, *seq.*

The area of contact between wheel and rail varies with the state of wear of the parts. For a new rail the longitudinal dimension of the contact is in general greater than the transverse dimension; but, as the rail flattens with use, the contact area approximates in shape to a uniform strip transverse to the rail. The final state is assumed herein, the wheel and rail being conceived as cylinders having their generating lines parallel. The problem proposed is accordingly a two-dimensional one. Instead of assuming the problem to be that of a cylinder rolling on a plane, however, we implicitly assume it to be that of two cylinders of like material and of equal and opposite radii, pressed together and rolling on one another, one being subject to a torque and the other to an equal counter-torque. Under this assumption, any state of stress or strain in one member, due to tangential tractive forces only, is matched by an equal reversed state in the other, and the distribution of pressure between the members is unaffected by the traction, since the radial displacements of the surfaces in contact are complementary. We may note also that any conclusion deduced for a driving wheel is true, with reversal of stresses and strains, for a wheel undergoing braking.

The radius of the wheel is large compared with the circumferential extent of the contact area, and, except in the determination of particulars of the contact, may be assumed infinite. The problem is then one of an infinite elastic medium bounded by a plane, on which is a certain local distribution of pressure and tangential traction. The stresses and strains, due to pressure, are known,* and need not be discussed further than as the means of transmitting the tractive effort.

The solution of the two-dimensional problem of an infinite elastic medium, bounded by, and on the positive side of, the plane $y = 0$, in which the portion of the boundary for which x is negative is subjected to a uniform tangential traction parallel to the x-axis, and that for which x is positive is free of externally applied stress, is given by Prof. Love.† Using the same notation as Prof. Love (viz., Δ for dilatation, ϖ for component rotation, λ, μ for elastic constants), the solution is shown to depend on the equation:

$$\frac{d(\xi + i\eta)}{d(x + iy)} = (\lambda + 2\mu)\,\Delta + i2\mu\varpi = C \log (x + iy) \qquad (1)$$

in which $C\pi(\lambda + \mu)/(\lambda + 2\mu)$ is the tangential traction on the half-boundary plane, being directed towards the origin when C is positive and away from it when C is negative. ξ and η are functions defined by the above equation.

* See Love's 'Mathematical Theory of Elasticity,' second edition, chap. VIII, § 138.

† *Loc. cit.*, chap. IX, § 152 (c).

Take the separating line between stressed and unstressed portions of the boundary at $(x', 0)$, and superpose a distribution of tangential stress extending to $(x' + dx', 0)$, and an equal reversed stress extending to $(x', 0)$. We thus obtain the solution of a problem in which the boundary stress extends over a band of width dx' only. Integrating this, in order to obtain the solution of the problem in which the tangential stress—a function of x'—extends over any desired portion of the boundary, we get as fundamental equation

$$\frac{d(\xi + i\eta)}{d(x + iy)} = (\lambda + 2\mu)\Delta + i2\mu\varpi = -\int \frac{C\,dx'}{x + iy - x'}, \qquad (2)$$

the integral being taken over the boundary.

The strain in the direction of the x-axis is, using Prof Love's notation*

$$e_{xx} = \frac{du}{dx}$$
$$= \frac{1}{2\mu}\left[-Y_y + \frac{d\xi}{dx}\right]$$

At the boundary surface, Y_y is zero, and

$$e_{xx} = \frac{1}{2\mu} \cdot \frac{d\xi}{dx}$$
$$= \frac{\lambda + 2\mu}{2\mu}\Delta. \qquad (3)$$

Thus the value of e_{xx} at the boundary is the real part, as y approaches zero, of (see equation 2)

$$-\frac{1}{2\mu}\int \frac{C\,dx}{x + iy - x'} \qquad (4)$$

The values of C with which we shall have occasion to deal are, in form, proportional to $\left(1 - \frac{x'^2}{a^2}\right)^{\frac{1}{2}}$, the limits of x' being $-a$ and a; and

$$\int_{-a}^{a} \left(1 - \frac{x'^2}{a^2}\right)^{\frac{1}{2}} \frac{dx'}{x + iy - x'} = \pi\left\{\frac{x + iy}{a} - \left[\left(\frac{x + iy}{a}\right)^2 - 1\right]^{\frac{1}{2}}\right\} \qquad (5)$$

We discuss the pressure and contact surface between wheel and rail,† taking

* *Loc. cit.*, chap. IX, § 144.

† The matter is here discussed in terms of wheel and rail. For the case of a pair of equal wheels in contact, R should be replaced by R/2 throughout.

the origin at the centre of the contact area, and employing the notation of Prof Love.* If R is the radius of the wheel and P the total pressure

$$\begin{aligned} A &= \frac{1}{2R} \\ &= \tfrac{3}{4}\frac{\lambda+2\mu}{2\pi\mu(\lambda+\mu)}\ P\int_0^\infty \frac{d\psi}{(a^2+\psi)^{\frac{1}{2}}(b^2+\psi)^{\frac{1}{2}}\psi^{\frac{1}{2}}} \\ &= \tfrac{3}{4}\frac{\lambda+2\mu}{2\pi\mu(\lambda+\mu)}\cdot\frac{P}{b}\int_0^\infty \frac{d\psi}{(a^2+\psi)^{\frac{1}{2}}\psi^{\frac{1}{2}}} \text{ if } b \text{ is large} \\ &= \tfrac{3}{4}\frac{\lambda+2\mu}{\pi\mu(\lambda+\mu)}\ \frac{P}{a^2 b}. \end{aligned} \tag{6}$$

The pressure per unit area of contact near the origin is

$$P' = \frac{3P}{2\pi ab}\left(1-\frac{x'^2}{a^2}\right)^{\frac{1}{2}}.$$

Integrating this over the width of the contact, the pressure per unit length of contact is

$$\int_{-a}^{a} P'\,dx' = \tfrac{3}{4}\frac{P}{b}.$$

The equivalent length of the contact is thus $4b/3$, this we call l. Accordingly:

$$\frac{1}{2R} = \frac{\lambda+2\mu}{\pi\mu(\lambda+\mu)}\ \frac{P}{la^2},$$

or

$$a = \left[\frac{\lambda+2\mu}{\pi\mu(\lambda+\mu)}\cdot\frac{2RP}{l}\right]^{\frac{1}{3}}, \tag{7}$$

also

$$P' = \frac{2P}{\pi la}\left(1-\frac{x'^2}{a^2}\right)^{\frac{1}{2}} \tag{8}$$

Assume first that the tangential traction is everywhere proportional to the pressure—an assumption which is only justifiable when the wheel is on the point of skidding. Write its value T_1P'/P, so that T_1 is the maximum available tractive effort. Then

$$C = \frac{\lambda+2\mu}{\pi(\lambda+\mu)}\ \frac{2T_1}{\pi la}\left(1-\frac{x'^2}{a^2}\right)^{\frac{1}{2}} \tag{9}$$

Hence, at the boundary (see equations 4 and 5), when x is in the contact area ($x^2 < a^2$)

$$e_{xx} = -\frac{\lambda+2\mu}{\pi\mu(\lambda+\mu)}\cdot\frac{T_1}{la}\cdot\frac{x}{a} \tag{10}$$

* *Loc. cit.*, chap VIII, §§ 137, 138.

and when x is outside the contact area ($x^2 > a^2$):

$$e_{xx} = -\frac{\lambda + 2\mu}{\pi\mu(\lambda + \mu)} \cdot \frac{T_1}{la} \left[\frac{x}{a} - \left(\frac{x^2}{a^2} - 1\right)^{\frac{1}{2}}\right] \quad (11)$$

We next consider the normal operation of the wheel Assuming it to be running in the positive direction of the x-axis, let A'OA in the figure represent the contact surface, A being the point of first contact, and A' the point of leaving Let ABA' be the curve of limiting tangential traction T_1P'/P The actual curve of tangential traction will follow some line ADCA', starting at A and never exceeding the limiting curve. Over the portion ADC of the curve, the surfaces

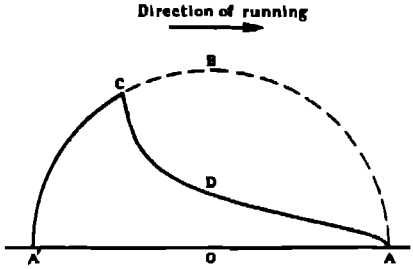

in contact are locked together, and the surface-strain is accordingly constant, for any variation of strain in one member requires an opposite variation in the other member, and this cannot be where the boundaries in contact have no relative movement. Beyond the point C, the pressure between the surfaces is insufficient to support the strain, and the surfaces accordingly slip, with limiting tangential traction The value of the surface strain may be written:

$$e_{xx} = \text{real part of } \underset{y \to 0}{\mathrm{L}} \mathrm{K} \left\{\int_{-a}^{a} \left(1 - \frac{x'^2}{a^2}\right)^{\frac{1}{2}} \frac{dx'}{x + iy - x'} - \int_{c}^{a} \frac{\phi(x')\,dx'}{x + iy - x'}\right\}, \quad (12)$$

in which K is put for the coefficient of $\pi x/a$ in equation 10, and c is the abscissa of the point C in the figure. The function $\phi(x')$ is zero at the limits c and a, and positive between them it is such that, between c and a, e_{xx} is independent of x. The first integral in equation 12 has, however (see equations 5 and 10), been shown to be proportional to x for points within the contact area, the second, accordingly, when $a > x > c$ should be a linear function of x, cancelling the first and leaving a constant

Consider

$$\phi(x') = \frac{a - c}{2a}\left[1 - \left(\frac{x' - \frac{1}{2}(a + c)}{\frac{1}{2}(a - c)}\right)^2\right]^{\frac{1}{2}}.$$

Changing the variable to $y' = x' - \frac{1}{2}(a + c)$, the second integral in equation 12 becomes:

$$\frac{a-c}{2a}\int_{-\frac{1}{2}(a-c)}^{\frac{1}{2}(a-c)}\left[1-\left(\frac{y'}{\frac{1}{2}(a-c)}\right)^2\right]\frac{dy'}{x-\frac{1}{2}(a+c)+iy-y'}$$

This has the same form as the integral in equation 5, and, with $a > x > c$, and $y = 0$, its value is

$$\frac{a-c}{2a}\cdot\pi\frac{x-\frac{1}{2}(a+c)}{\frac{1}{2}(a-c)} = \pi\left[\frac{x}{a}-\frac{a+c}{2a}\right] \tag{13}$$

Hence, with $a > x > c$, equation 12 gives the constant value:

$$e_{xx} = \mathrm{K}\pi\frac{a+c}{2a}. \tag{14}$$

The tractive effort of the wheel is

$$\begin{aligned}\mathrm{T} &= \mathrm{T}_1\left\{1-\frac{2}{\pi a}\cdot\frac{a-c}{2a}\int_{-\frac{1}{2}(a-c)}^{\frac{1}{2}(a-c)}\left[1-\left(\frac{y'}{\frac{1}{2}(a-c)}\right)^2\right]^{\frac{1}{2}}dy'\right\}\\ &= \mathrm{T}_1\left\{1-\left(\frac{a-c}{2a}\right)^2\right\}\end{aligned} \tag{15}$$

Hence c is given by:

$$\frac{c}{a} = 1 - 2\left[1-\frac{\mathrm{T}}{\mathrm{T}_1}\right]^{\frac{1}{2}}. \tag{16}$$

The quantity f is now readily determinable for the case considered. On entering the contact area, and for a certain distance within that area, the surface strain e_{xx} is given by equation 14. Consider a pair of points on the driving and driven wheel-rims respectively, situated an infinitesimal distance δx ahead of A (see figure), and therefore about to enter into contact with one another. The unstrained length of rim represented by δx is $(1 - e_{xx})\,\delta x$ for the driving wheel, and $(1 + e_{xx})\,\delta x$ for the driven wheel. The ratio of angular rotation of driving and driven wheel is therefore as $1 - e_{xx} : 1 + e_{xx}$ or as $1 - 2e_{xx} : 1$. The ratio of rolling rotation is unity, and the quantity $-2e_{xx}$ accordingly represents the creepage as defined above. Writing q for T/T_1, f is then given by:

$$\begin{aligned} f &= \frac{q\mathrm{T}_1}{-2e_{xx}}\\ &= -\frac{q\mathrm{T}_1}{\pi\mathrm{K}}\cdot\frac{a}{a+c} && \text{(eqn. 14)}\\ &= -\frac{\mathrm{T}_1}{2\pi\mathrm{K}}\frac{q}{1-(1-q)^{\frac{1}{2}}} && \text{(eqn. 16)}\\ &= \frac{\pi\mu(\lambda+\mu)}{2(\lambda+2\mu)}la\frac{q}{1-(1-q)^{\frac{1}{2}}} && \text{(eqn. 10)}\\ &= \left[\frac{\pi\mu(\lambda+\mu)}{2(\lambda+2\mu)}\mathrm{RIP}\right]^{\frac{1}{2}}\frac{q}{1-(1-q)^{\frac{1}{2}}}. && \text{(eqn. 7)} \end{aligned} \tag{17}$$

Thus f depends on the tractive effort, increasing in the ratio 1 2 as T falls from T_1 to zero

For the value $T = T_1$, or $q = 1$, and with forces and lengths expressed in ordinary engineering units of the subject, the approximate value of f for steel wheels and rails is as follows :

(1) With forces in kilogrammes and lengths in millimetres

$$f = 93\,[R/P]^{\frac{1}{2}}.$$

(2) With forces in lbs. and lengths in inches .

$$f = 3500\,[R/P]^{\frac{1}{2}}.$$

The effective value of l, the length of contact transverse to the rail is matter for conjecture, and doubtless variable A representative value is perhaps of the order of 25 mm. or 1 in.

On the Specific Heat of Ferromagnetic Substances

By W. Sucksmith, B Sc , and H. H. Potter, Ph D , Lecturers in Physics, University of Bristol

(Communicated by Prof A P. Chattock, F R S.—Received April 28, 1926.)

According to the Weiss theory of ferromagnetism, there is an intimate connection between the specific heat of a body and its magnetisation Weiss* has shown that the magnetic energy per cubic centimetre of a ferromagnetic substance is :—

$$W = -\tfrac{1}{2}HI \qquad (1)$$

where I is the intensity of magnetisation and H is the molecular field Further, it is assumed that

$$H = NI \qquad (2)$$

where N is a constant depending on the material itself Thus

$$W = -\tfrac{1}{2}NI^2$$

and

$$dW/dT = -\tfrac{1}{2}N\,d(I^2)/dT$$

where T is the temperature dW/dT will contribute to the specific heat of the substance which will become equal to

$$S = s + \frac{1}{\rho J}\frac{dW}{dT},$$

* Weiss and Beck, 'Journ de Phys ,' vol. 7, p. 249 (1908).

where s = specific heat neglecting magnetic contribution,

S = total specific heat,

ρ = density,

J = mechanical equivalent of heat,

Therefore

$$S = s - \frac{N}{2\rho J}\frac{d}{dT}(I^2).$$

From consideration of the shape of the magnetisation-temperature curves, Weiss concludes that the specific heat should rise to a maximum at the critical temperature and then decrease discontinuously, owing to the sudden disappearance of the magnetic term.

The first measurements to test this theory were made by Weiss and Beck (*loc. cit*) on nickel, iron and magnetite, using the method of mixtures The mean specific heat between room temperature and the temperature T was determined for increasing temperatures T_1, T_2, T_3, etc The specific heat over the ranges T_2-T_1, T_3-T_2, etc, could then be calculated Other determinations of the specific heat of iron have been made by Harker,* Oberhoffer† and Meuten ‡ These three observers used the Bunsen ice-calorimeter method, but their experiments were not sufficiently detailed for satisfactory theoretical interpretation Further experiments were made by Dumas,§ and Weiss, Piccard and Carrard,|| who elaborated the method of mixtures to secure a higher order of accuracy In these experiments the specimen, which had been heated to a temperature T in an electric furnace, was dropped into a mass of water, the rise of temperature being measured by a platinum resistance thermometer. The mean specific heat S_m between 16° C. and T° C was plotted against T, the curve thus obtained showing a sudden change of slope at the critical temperature From this curve the true specific heat, S, was obtained for various temperatures The results of the experiments were not wholly in agreement with their theory ¶ The best agreement between experiment and theory is obtained in the case of nickel It is interesting to note, however, that nickel shows large deviations from the law of corresponding states,** †† which is a

* Harker, 'Phil Mag.,' vol 10, p. 430 (1905)

† Oberhoffer, 'Metallurgie,' p. 427 (1907).

‡ Meuten, 'Ferrum,' p 1 (1912).

§ Dumas, 'Arch Sci Phys Nat,' 27, pp. 352 and 453 (1909).

|| Weiss, Piccard and Carrard, *ibid*, 42, p. 378 (1916); 43, pp. 22, 113, 199 (1917).

¶ *Cf* Piccard and Carrard, *ibid*, 39, p. 451 (1915).

** Weiss, 'Journ de Phys,' vol. 6, p. 661 (1907).

†† Honda and Ôkubo, 'Phys. Rev.,' vol. 10, p. 738 (1917).

direct result of the Weiss theory of ferromagnetism. Again, to satisfy Lorentz'* equation, it is necessary to assume that the elementary magnet in nickel consists of three atoms.

The experiments themselves were not altogether above criticism for the following reasons —

(*a*) The continued quenching of the specimen may not be without some effect on its physical properties Westgren† has obtained some evidence that the size of the crystal lattice in nickel-steel depends on the temperature of quenching Such an effect is almost certain to influence the specific heat Weiss‡ has found that the magnetic properties of nickel depend on its previous heat treatment

(*b*) The method of smoothed curves was used, the gradient of these curves being used to determine the true specific heat

(*c*) The method requires a high degree of accuracy, as may be seen from the following considerations: To determine the specific heat in the range 350° C to 354° C to 1 part in 100, it is necessary to know the mean specific heats from 16° C to 350° C and 16° C to 354° C to 1 part in 16,000 For nickel, Weiss and his co-workers claim this order of accuracy, which appears to us to be over-estimated

(*d*) In view of the dependence of magnetic properties on heat treatment, it is desirable that magnetic and calorimetric data should be obtained not only for the same specimens, but also simultaneously. In the papers referred to, magnetic data are taken from the earlier experiments of Curie The earlier work of Weiss and Beck has been criticised by Honda and Ôkubo§ on the same grounds They point out that the constant N (equation (2)) varies from one specimen to another so that magnetic and calorimetric data can be compared only if obtained from the same specimens Weiss's theoretical treatment has also been criticised by Ashworth,‖ and difficulties have also been raised by de Waard.¶

In view of the above considerations, experiments by an independent method, enabling specific heat and magnetisation to be measured simultaneously, appeared desirable. The present experiments, besides fulfilling this condition, enable the specific heat to be measured directly over small intervals of temperature.

* Lorentz, 'Revue Scientifique,' p 1 (1912)

† Westgren, 'Journ. Iron and Steel Inst.,' vol 1, p. 241 (1922)

‡ Weiss and Forrer, 'Annales de Phys.,' vol 5, p. 153 (1926).

§ Honda and Ôkubo, 'Phys Rev.,' vol 10, p 738 (1917)

‖ Ashworth, 'Phil Mag.,' vol 43, p 401 (1922).

¶ de Waard, 'Z f Phys.,' vol. 32, p. 789 (1925)

Outline of Method.

The Specific Heat Measurements.—The method used in the present experiments was that of Nernst and Eucken, which has not to our knowledge been used at such high temperatures (up to 410° C.) in any previous work. Heat is supplied by passing a current through a platinum spiral wound on the specimen. The temperature rise of the specimen is measured by the change of resistance of this spiral. Owing to the great increase in the radiation at high temperature, the difficulties of experiment are much greater than those encountered at normal and low temperatures, but we have been able to extend the method to temperatures above the critical points of nickel and Heusler alloy by suspending the specimen in the interior of an evacuated vessel which was in turn enclosed in an electric furnace. The latter could be maintained at any desired temperature T while the specific heat between the temperatures T and T + δT was determined by supplying electrical energy to the specimen so as to raise its temperature by an amount δT. A correction for radiation was applied (see below).

Form of Specimens.—The specimens were made in two parts, the inner portion (fig. 1*a*) being ground into the outer portion (fig. 1*b*). The former had a double screw thread cut on it and into this was wound a spiral of double-silk covered chemically pure platinum wire. The winding was non-inductive, the wire being turned back at the bottom by passing round a tiny glass peg P,

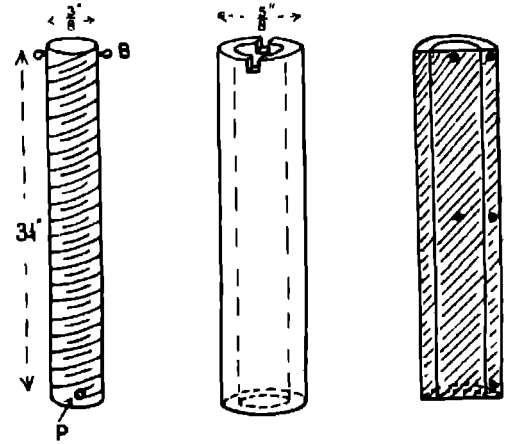

Fig. 1.

embedded in the metal at a place where a small flat had been filed The wire was secured at the top by tying it around a second glass peg B. Before winding the silk insulation was saturated with a paste of china clay, and after winding the wire the screw threads were filled in with more of the paste. On setting, this prevented any movement of the wire and so avoided the possibility of a breakdown of the insulation when the silk covering of the wire became charred. The slots at the top of the outer case (fig. 1*b*) enabled the inner portion to be inserted without damage to the glass peg B. The platinum wire (42 S W.G) was joined to copper leads (35 S.W G.) as close up to the peg B as possible, the copper also being secured to the peg so that the weight of the specimen was not carried by the thin platinum heating coil. The junction was made by binding the platinum wire around the copper and pinching it with a clip made of annealed copper. It was undesirable for obvious reasons to use thick copper leads, but after applying an approximate correction (see page 165) the error resulting from the use of leads of appreciable resistance was negligible.

The specimen itself was suspended in the interior of a double-walled glass vessel shown in fig. 2. The vessel, which was silvered on both walls, was made of " Duroglass " and even when heated to 450° C would withstand the pressure of the atmosphere. It was joined on to the pumping apparatus by means of a glass cap and sealing-wax joint shown at S. A tiny hole in the inner tube at the point D enabled the space between the two walls to be evacuated During the experiments the pressure was maintained at less than 0·01 mm. of Hg. In this way oxidation and loss of heat by convection were eliminated. The copper leads were brought out by the two side tubes TT and were secured at the ends of these tubes by sealing-wax joints. Beyond TT the gauge of the copper was increased to No 18.

The Electric Furnace —The furnace F (fig. 2) consisted of a coil of nichrome tape, wound non-inductively on a copper cylinder to promote uniformity of temperature. The heating current for the furnace was supplied by accumulators which gave a sufficiently steady current to keep the temperature constant to within 0·5° C. at 400° C. for an indefinite period. Such small variations of temperature as did occur would be communicated only very slowly to the specimen on account of the double-walled vacuum vessel. In fact, once equilibrium between the furnace and the specimen had been established, the latter could be maintained for very long periods at temperatures which were constant to within 0·05° C.

The Electrical Connections.—The circuit employed for the measurement of the resistance of the platinum spiral and for the purpose of supplying and

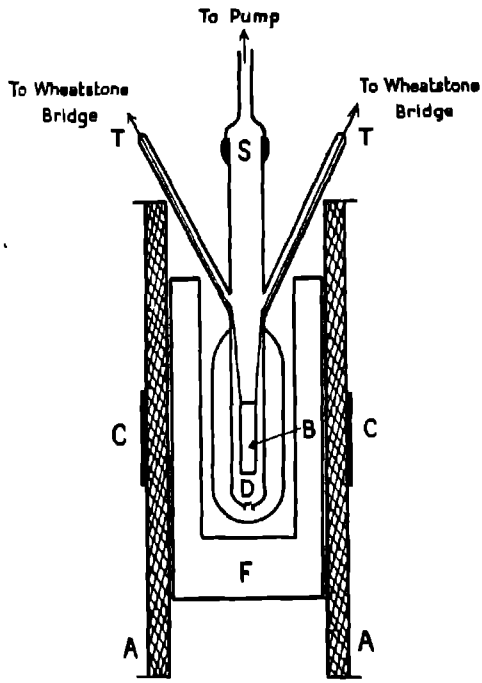

FIG. 2

measuring the heating current was a Wheatstone Bridge modified in such a way that the position of the battery and galvanometer were interchangeable. The circuit is shown in fig. 3.

P represents the platinum spiral, R_1 an open wire manganin resistance of 11·5 ohms, R_2 a variable resistance from a standard resistance box (correct to 0·01 per cent), and R_3 a standard resistance of 2,000 ohms. If the battery is connected at the points B and D and the galvanometer at the points A and C (by throwing switch S_1 to the right and S_2 to the left) then the current through P was so small that the resistance of P could be measured without causing any appreciable rise of temperature If, however, the connections to battery and galvanometer were interchanged (by throwing S_1 to the left and S_2 to the right) the current through P was sufficient to give the rise of temperature required in the measurement of the specific heat. The resistance of P, however, could be measured during the passage of this current (usually about 0·24 ampere)

so that the energy input was known The current was measured with a standard Weston milliammeter A, and a correction applied for fraction of the total current which passed along ADC.

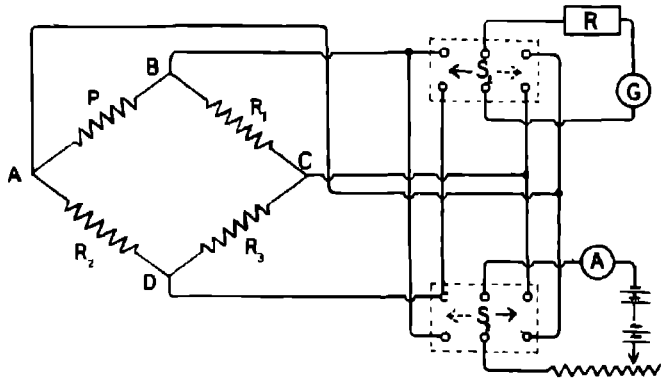

FIG. 3

Estimation of Rise of Temperature δT *on Heating.*—The following procedure was adopted in measuring the specific heat in the range between T and $T + \delta T$.—The furnace current was first adjusted to give the temperature T which was measured very roughly by means of a mercury thermometer. The real object of the thermometer was to indicate variation of furnace temperature and not its absolute value. The specimen was brought into temperature equilibrium with the furnace—the process being expedited by the passage of a current through the spiral in cases where the preceding measurement of the specific heat was made at a temperature considerably less than T and where otherwise the establishment of equilibrium would have taken a long time. Measurements were carried out only after the temperature of the furnace had remained constant to within $\frac{1}{2}$° C. and the spiral to within 1/20° C for at least 10 minutes, and even then corrections were applied for variations in the initial temperature of the specimen. The initial temperature was measured by estimation of the resistance with the battery connected at B and D, then the switches S_1 and S_2 were thrown over to the other position, thus causing sufficient current to pass through the platinum spiral to give a rise of temperature of about 5° C in 4 minutes, after which the switches were thrown back to the original position and the subsequent time-resistance curve taken. The change of resistance was a rather complicated function of the time, rising sharply on switching on the heating current and falling rapidly when the current was stopped. This was due to low thermal

capacity of the spiral, combined with the indifferent thermal contact between the spiral and the specimen A typical resistance time curve is shown in fig. 4.

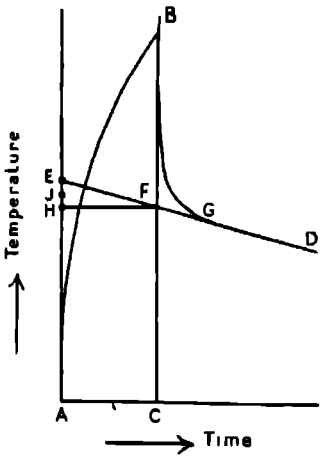

Fig 4.

The portion AB represents the heating part, the current being cut off at B. The portion BG represents the period during which equilibrium is being established between the spiral and the specimen, whilst GD represents the subsequent cooling due to radiation and conduction down the leads The portion GD was, particularly at low temperatures, practically straight and the true rise of temperature was estimated by producing DG back to the axis at the point E The ordinate AE would then give the true rise of temperature if the specimen had all along been cooling at the rate indicated by the slope of DG. This obviously is untrue, but assuming that the rise of temperature was uniform and that Newton's Law of cooling is applicable, it can be assumed that the mean rate of loss of heat during heating was half that given by the slope of DG, and that the true rise was AJ, J being half-way between E and H, and HF being horizontal To test the validity of this assumption, observations were made using various rates and times of heating and various rises of temperature differing by 100 per cent. At room temperature the results agreed to $\frac{1}{2}$ per cent At higher temperatures the experiments were not quite as accurate, due largely to the fact that Newton's Law is not strictly valid, the range over which it holds decreasing as the temperature increases. The result was that at high temperatures GD was not perfectly straight and under these conditions, instead of producing DG backwards, it was necessary to draw a tangent to the curve BGD at some suitable point. The method adopted was to draw the tangent to BGD at a point at a definite time interval (7 minutes) beyond the point B The principal error of experiment undoubtedly lay in drawing this tangent, but by adopting the same method for each experiment any errors introduced would affect different determinations similarly. An attempt to obtain the radiation correction by assuming the fourth power law did not lead to any appreciable increase in the accuracy of experiment. As our principal object was to determine the shape of specific heat-temperature curve, errors of this sort were comparatively unimportant.

Several other factors operated to make the absolute measurement of the specific heat somewhat inaccurate. Firstly, it was assumed that the whole of the platinum was embedded in the specimen and that all the heat generated in it was communicated to the specimen. Actually about 1 cm or 0 7 per cent. of the platinum was outside the specimen. Again, it was assumed that none of the heat generated in the leads was communicated to the specimen. Another inaccuracy lay in the correction for resistance of leads at high temperatures. It was assumed that the mean temperature of the leads was half-way between room temperature and the furnace temperature. This assumption was based on the fact that about half of the leads was in the furnace and the other half was not. The error due to these last two causes must have been very small, as the total lead resistance was about 1 per cent of the whole. Again no allowance was made for the specific heat of the glass, platinum and china clay, but this could hardly have introduced an appreciable error owing to the small mass of these substances concerned

The Magnetic Measurements.—The magnetic measurements were made by the ballistic method The solenoid A shown in fig 2 was so arranged that the specimen B was in a central position. The solenoid was wound in four layers of about 400 turns each, the layers being two in series by two in parallel. The cylinder was of brass, 50 cm. long and 15 cm diameter. To minimise eddy current effects, the brass was split along its entire length by a narrow saw cut, the reclosing of the slot being prevented by the insertion of a strip of asbestos. Thin asbestos paper was used as insulation between the various layers and between the innermost layer and the cylinder. A secondary coil C of 108 turns of 26 S W G. copper was wound in a central position on the solenoid and was insulated from the primary by several layers of oiled silk and one layer of mica. Good insulation is necessary here owing to the large area of contact Owing to the large diameter of the secondary coil, a considerable number of the lines of magnetic induction are ineffective By winding a test coil directly on the specimen, it was found that the lines cut by the secondary were 40 per cent. of the total number of lines of induction This fraction remained constant throughout, and so does not affect our conclusions

Subsidiary coils in series with the primary and secondary windings of the solenoid were so coupled that the reversal of a heavy direct current in the magnetising solenoid produced no deflection of the galvanometer when the specimen was absent. The field obtainable was 20 gauss per ampere, and the maximum current used was 12 amperes.

Heusler Alloy.

Our first results were obtained with Heusler alloy, the original object of our experiments being to extend Weiss's results to a synthetic magnetic alloy whose magnetisation could be varied (by heat treatment).

Preparation of the Alloy.—The difficulty of drilling the large hole through the outer portion (fig. 1*b*) of the specimen in a substance so brittle as the Heusler alloy was met by moulding the portion upon a central core of turned copper. It was then easy to drill out the copper, leaving a hollow cylinder of Heusler alloy. The alloy can be turned and a thread cut in it with high-speed steel tools. The Heusler alloy used was 63 per cent. copper, 25 per cent. manganese and 12 per cent. aluminium melted in a graphite crucible and poured into sand moulds. The inner and outer parts of the specimen were, of course, poured from the same melt. We tried alloys of various constitutions in an attempt to find a specimen with a low critical temperature. (The Nernst-Eucken method is more accurate at low than at high temperatures.) The critical temperatures of alloys of different constitution are given by Take.* Those with low critical temperature we found to be extremely unstable, the critical point rising to about 280° C. after heat treatment of any kind. For specimens of the constitution given above the critical point was very stable, being unaltered by more than a few degrees after quenching from 400° C. or after annealing at 720° C. The critical temperature for these specimens was about 280° C., and it thus appears that the critical temperatures of unstable specimens tend after heat treatment to rise to about the same value as for the stable specimens, although we have not sufficient evidence to verify this point conclusively.

Results.

Heusler Alloy.—The results for Heusler alloy are shown in figs. 5–8. In addition to the specific heat-temperature curves, marked (*a*), the curves connecting I^2 with T (*b*), and $d/dT(I^2)$ with T (*c*), are given. The ordinates of the two last-mentioned are in arbitrary units, the same units being used throughout. In figs. 6 and 8, which deal with Heusler alloy after heat treatment, the scale of the magnetisation curves is increased five-fold. In all cases a complete curve was obtained in one day, the successive points being obtained with increasing temperature.

The specimen of fig. 5 was quenched from about 400° C. and subsequent measurements are given in fig. 6. Both specific heat and magnetisation curves

* Take, 'Ann. der Phys.,' vol. 20, p. 849 (1906).

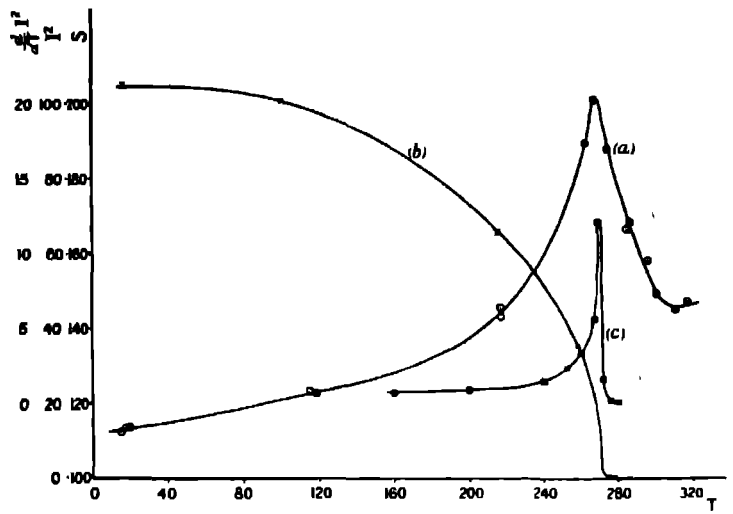

FIG. 5—Heusler 1.

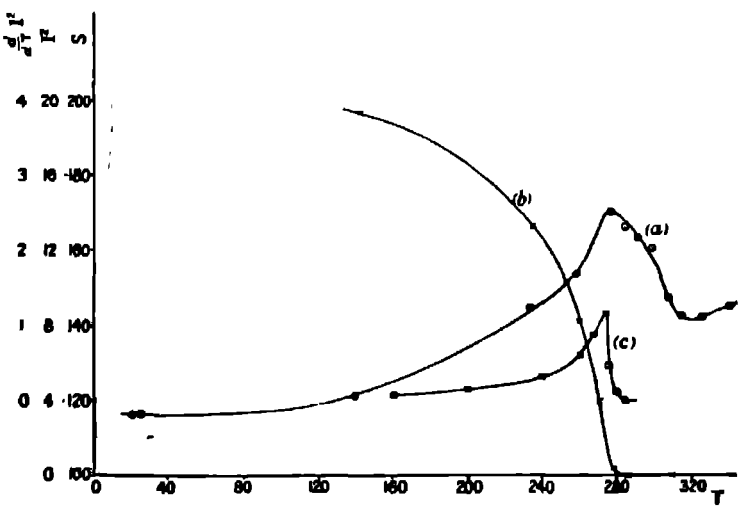

FIG. 6.—Heusler 1 Demagnetised.

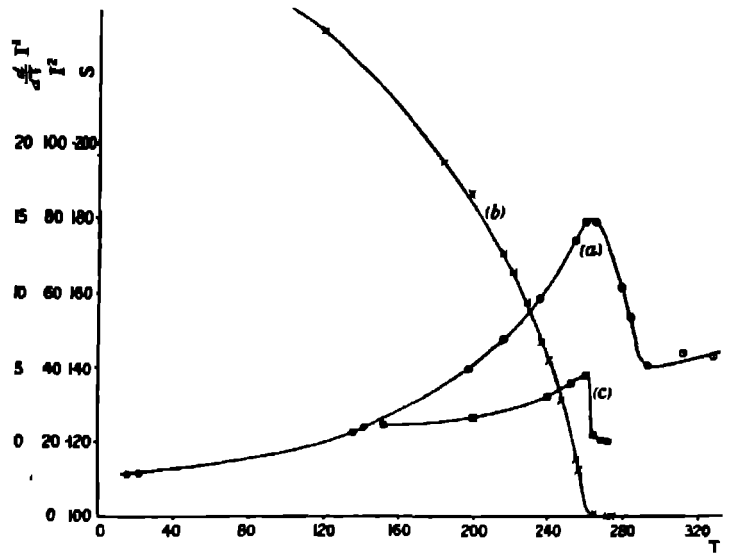

Fig. 7.—Heusler 2

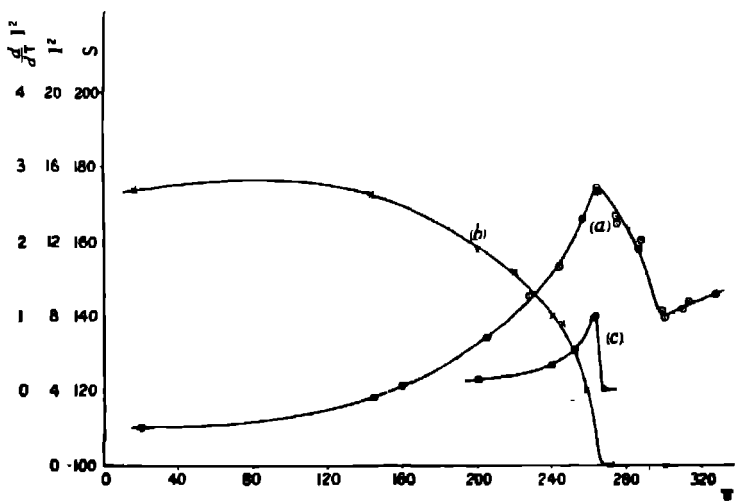

Fig. 8.—Heusler 2 Demagnetised.

indicate a rise of 8° C. in the critical temperature. The fall in the value of the specific heat above the critical temperature was reduced by about 47 per cent., but it is difficult to deduce anything from this owing to the fact that the saturation intensities of magnetisation before and after quenching were not known

The curves for a second specimen of Heusler alloy are given in fig 7, and fig 8 shows corresponding curves for this specimen after annealing at 720° C An examination of the curves for Heusler alloy shows large discrepancies between theory and experiment A full discussion of the results is given below, but one point which concerns Heusler alloy alone will be discussed here In the case of the second specimen the specific heat curves before and after demagnetisation do not show any very great change, whereas the magnetisation in weak fields is greatly reduced This is not a true measure of the reduction of the saturation intensity with which we are concerned in this experiment. We measured the saturation intensity, however, for two pieces of alloy from the same cast as those used in the specific heat measurements referred to One of these pieces was subjected to identical heat treatment to that given to the specimen referred to above The magnetisation was measured by a ballistic method using an electromagnet, and it was found that although the magnetisation in weak fields was vastly different, the saturation intensity (5,000 gauss) of the " demagnetised " specimen was 73 per cent. of that of the original Heusler. Using Weiss's Theorem of Corresponding States,* it can easily be shown that the magnetic contribution to the specific heat in the case of the demagnetised specimen should, according to Weiss's theory of specific heats, be 54 per cent. of that for the normal specimen We found the ratio to be 87 per cent., so that the magnitude of the drop in the value of the specific heat in the neighbourhood of the critical point was affected to a far less extent than would be expected from Weiss's theory

We have assumed here that N (equation 2) remains constant The conflict between theory and experiment could be reconciled if N increased with heat treatment. We made some attempt to measure N by observations on the change of the paramagnetism above the critical temperature.† We were unable to get any satisfactory data on account of the fact that N was continually decreased by heat treatment of the specimen. The curves connecting $1/\chi$ and T (χ = susceptibility, T = temperature) became less and less steep (using

* Weiss, ' Journ. de Phys.,' vol 6, p. 661 (1907), ' Phys. Zeit.,' vol. 9, p. 358 (1908).

† A modified form of the Curie law has been given by Weiss for ferromagnetic substances at temperatures above the critical point, *c.f.* Weiss, ' Phys Zeit.,' vol. 9, p 358 (1908).

$1/\chi$ as ordinate) as the specimen was subjected to heat treatment similar to that used in demagnetising it.

Thus the change in N is in the opposite direction to that demanded if the experimental results are to be brought into line with Weiss's theory. It will be noticed that there is no sudden discontinuity in the value of the specific heat at the critical point. This will be discussed later on in conjunction with the results obtained for nickel.

Nickel.—We were inclined at first to attribute the results obtained with Heusler alloy to the fact that its magnetism is synthetic. This led us to carry out experiments on nickel. Unfortunately it is impossible to obtain "chemically" pure nickel in the form of rods such as are required in this experiment. We therefore used nickel of three grades of purity—ordinary commercial nickel, commercially pure nickel, and Mond electrolytic nickel remelted and drawn into rods by Messrs Johnson and Matthey. Weiss and Piccard used Mond nickel in their measurements, but the analysis they give refers to the nickel before the process of remelting. We give below an analysis* of the three nickels used:—

—	Ordinary Commercial	Commercially Pure.	Mond
	per cent	per cent.	per cent.
Nickel	97·2	98·6	99·46
Iron	0·40	0·80	0·18
Insoluble residue	0·75	trace	—

The Mond nickel was analysed *after* the remelting process. In the case of the commercially pure and Mond nickel the impurity is almost entirely iron. This was not present in a ferromagnetic condition, as examination of the nickel between 450° C. and 600° C. showed that the substance was paramagnetic, and further the susceptibility was independent of field. We could have detected by this method the presence of 0·002 per cent. of ferromagnetic iron. This might be accounted for in several ways, viz., fine division of the impurity, the iron being alloyed with the nickel or present as an oxide. By using nickel of different degrees of purity we have been able to deduce evidence that the results we have obtained are not dependent on the quantity of impurity. The results obtained with nickel are similar to those given by Heusler alloy, and are shown in figs. 9, 10, 11. The experiments are more difficult to carry out.

* Our thanks are due to Dr. Malkin and Messrs. Bull and Pollard, of the Chemistry Department of this University, for the analyses.

on account of the higher temperature at which the ferromagnetism disappears, and also because the changes in the value of the specific heat are not so pronounced in the case of nickel

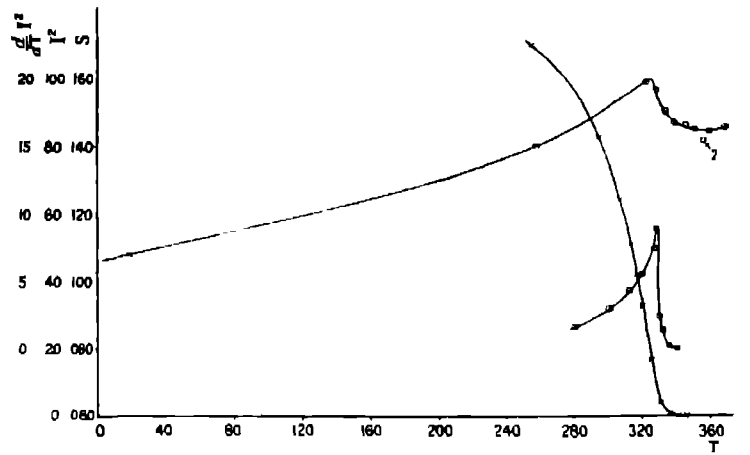

FIG 9.—Commercial Nickel

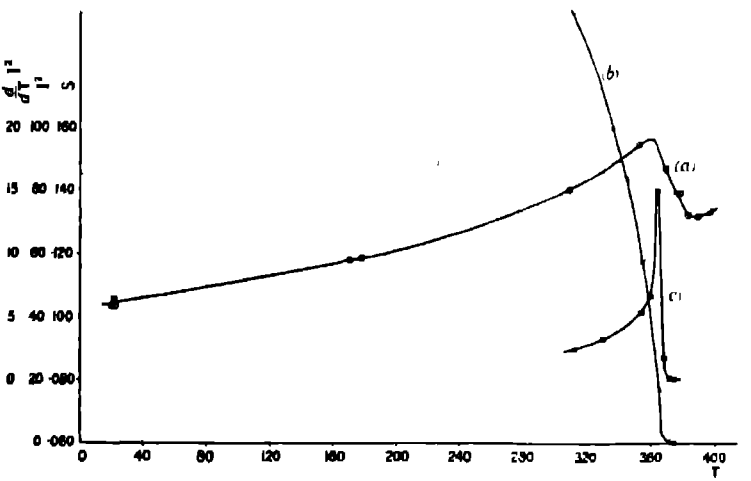

FIG 10.—Commercially Pure Nickel

The most striking feature of the specific heat curves of both Heusler alloy and nickel is the absence of any sudden discontinuity at the critical temperature. The decrease in the value of the specific heat which takes place in the neigh-

bourhood of the critical point is spread over about 40° C. in the case of Heusler alloy and 25° C. in the case of each of the nickel specimens. The curves shown

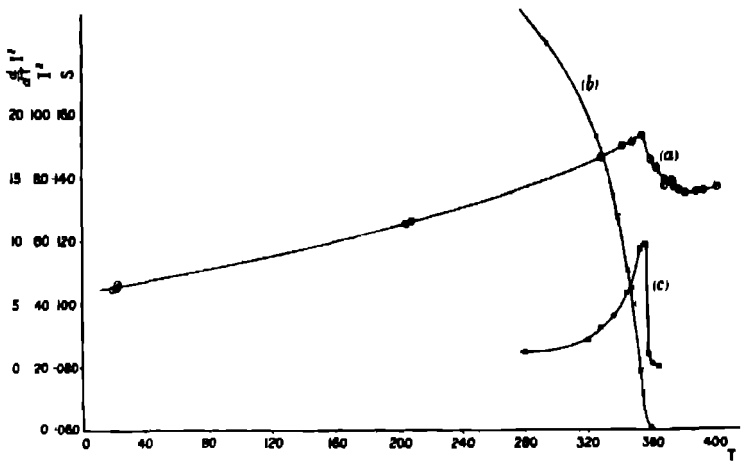

Fig 11 —Pure Nickel

in figs. 5–11 are typical of a number, all of which exhibit the same general features.

Uniformity of Temperature of Specimen.—The "spread" could be most easily explained by a non-uniformity of temperature of the specimen We examined this point by the use of thermo-couples made by securing copper wires to various points of a nickel specimen by means of small nickel screws. For positions of these junctions see fig 1c Any two of the junctions could be used to give the temperature difference between any two points of the specimen. We assured ourselves periodically of the satisfactory working of each thermo-couple by having a subsidiary copper-nickel junction kept in ice Thus the actual temperature as well as the difference of temperature could be measured with any of the thermo-couples. Under the actual conditions of specific heat determinations we were unable to detect any difference of temperature amounting to more than 1 2° C , which is negligible in comparison with the temperature range over which the measured fall in the specific heat takes place.

Discussion of Magnetic Curves.—Whereas the specific heat curves show considerable spread, the $d/dT(I^2) - T$ curves show a much more sudden drop at the critical point, 95 per cent. of the drop in the value of $d/dT(I^2)$ taking place within about 5° C. Our results indicate that the temperature at which

the maximum value of the specific heat is attained coincides with the critical point.* The fact that the curves connecting $d/dT(I^2)$ and T show a more sudden drop at the critical point than the specific heat curves cannot, for reasons stated below, be taken as *conclusive* evidence against the view that under ideal conditions these two curves would be of similar shape

Suppose that the impurity in the nickel is unevenly distributed (We have made three determinations of the iron content for commercially pure nickel, using test specimens from three different portions of the rod. Identical values of the iron content were obtained, but this does not preclude the possibility of uneven distribution in regions small compared with the volume used in chemical analysis)

Such an uneven distribution might give rise to regions of varying critical points. Suppose a volume v_2 is above the critical temperature, whereas a volume v_1 is below the critical temperature and has an intensity of magnetisation I. The measured magnetisation is proportional to $v_1 I$, whereas had the whole specimen been magnetic the measured value would have been $(v_1 + v_2)$ I

The ordinate of the $I^2 - T$ curves is thus reduced in the ratio v_1^2 to $(v_1 + v_2)^2$.

The region v_1 will contribute to the magnetic specific heat a quantity $= v_1 \, d/dT\,(I^2)$, whereas had the whole specimen been magnetic the contribution would have been $(v_1 + v_2)\, d/dT\,(I^2)$. The ordinate of the $I^2 - T$ curve is thus reduced in the ratio $(v_1/v_1 + v_2)^2$, whereas the specific heat curve is reduced in the ratio $v_1/(v_1 + v_2)$.

Another important point is the self-demagnetising action of such small regions The magnitude of this effect can be calculated assuming the regions to be spherical The effect is probably small since the intensity of magnetisation is small in the neighbourhood of the critical temperature, and since, in addition, the intensity reaches saturation for a field of a few gauss There is another effect which operates in the opposite direction and probably is greater than the last-mentioned effect. At room temperature the specimens are very far from saturated in the field available. This is due in some measure to the demagnetising action, reducing the effective field to about 50 gauss Near the critical temperature saturation is almost complete in a very much smaller field, and the actual applied field is greater since the demagnetising effect is smaller.

* The critical point has been defined as the temperature at which spontaneous ferromagnetism disappears, and also that at which $d/dT(I^2)$ reaches a maximum These points differ, however, by about 2° C only. Our experiments are not sufficiently accurate to enable us to discriminate between the two See Honda, 'Sci Rep.,' Tôhoku, I., vol 10, p. 433 (1922).

This has the effect of making the measured slope of the $I^2 - T$ curve less than it should be and also of reducing the ordinates of the curve except near the critical temperature The effect is equivalent to increasing the ordinates of the curve near the critical temperature in proportion to those of the rest of the curve This also accounts for the sharp rise in the value of $d/dT(I^2)$ on the low temperature side of the critical point.

Another factor to be considered is that our magnetisation measurements give values which are proportional to $4\pi I - H_0$, where H_0 is the demagnetising field. The effect of this near the critical point will again depend upon the shape of the small ferromagnetic domains, and the same general considerations as those in the preceding paragraph would apply.

It would thus appear that quantitative relationships between our magnetic and specific heat data cannot be established if we assume uneven distribution of impurity and consequent regions of varying critical points. The difference between the specific heat and the magnetisation curves is very marked, however, and this, combined with the fact that we have obtained similar results with three samples of nickel of different degrees of purity, seems to invalidate this explanation.

Conclusions.

There is considerable discrepancy between the form of the specific heat and magnetisation curves obtained experimentally for nickel and Heusler alloy, and that demanded by Weiss's molecular field theory The difference between the results of Weiss, Piccard and Carrard and those obtained by the present authors for nickel could be entirely accounted for by a change in the neighbourhood of the critical point of about 0 1 per cent. in the *mean* specific heat measurements of the former. The experiments of Dumas (*loc. cit*) do not appear accurate enough to be considered as evidence for Weiss's view as opposed to ours In addition to the difference in the shape of the curve, the decrease in our values of the specific heat for pure nickel is only 60 per cent. of that obtained by Weiss.

There is considerable evidence that the changes in other physical properties are not discontinuous in the neighbourhood of the critical point. This has been discussed in some detail by Benedicks * A paper by Honda and Ogura† is of special interest in this connection. Using Kahlbaum nickel wire they obtained curves connecting the temperature change of magnetisation and electric resistance. Neither curve showed a discontinuity at the critical point.

* Benedicks, 'Journ Iron and Steel Inst.,' II., 1912; I., 1914.

† Honda and Ogura, 'Sci. Rep.,' Tōkohu, vol. 3, p. 113 (1914).

Again, the magnetisation-temperature curves for a field of 160 gauss are very similar to those obtained in our experiments, neither showing such a rapid approach to zero as demanded both by the theory and experiments of Weiss * Weiss's results are strongly criticised by Honda and Ôkubo,† who take the view that what Weiss measured was not an actual specific heat, but a quantity of heat evolved during the transformation at the critical point. The nature of this transformation is somewhat obscure The crystal structure of nickel is a face-centred cube both below and above the critical temperature ‡ Such consideration as Benedicks applies to the case of iron§ could hardly be tenable in the case of nickel, where there is nothing corresponding to the A_3 transformation If a structural change takes place, it must be something other than a change in the arrangement of the atomic centres. That such a change can take place has been indicated by some experiments on the properties of tungsten crystals by the Research Staff of the General Electric Company.|| Our results would point to some such view as that taken up by Honda and Ôkubo. There can be no doubt that the changes in specific heat and magnetisation are closely related, but apparently this relation is not so intimate as that suggested by Weiss. Both, however, are undoubtedly traceable to a common cause It is suggested that the critical point indicates a certain stage in a transition which takes place over a range of temperature of probably some hundred degrees, and which is not complete at the critical temperature.

Summary.

The Nernst-Eucken method of measuring specific heat has been extended to temperatures up to 410° C. The specific heats of the ferromagnetic substances nickel and Heusler alloy have been measured up to temperature considerably above their critical points, and no discontinuities in the values of the specific heat have been found. Magnetic measurements have been obtained simultaneously with those of specific heat in order to investigate relationships between the two effects.

Heat treatment of Heusler alloy resulted in a considerable reduction in the saturation intensity of magnetisation without a corresponding decrease in the value of the specific heat

* Weiss, 'C R.,' vol. 178, p 1671 (1924).

† Honda and Ôkubo, 'Phys Rev.,' vol. 10, p. 740 (1917).

‡ F. Wever, 'Mitt a.d. Kaiser-Wilhelm Inst. f Eisenforschung' (1922).

§ Benedicks, 'Journ. Iron and Steel Inst.,' II., p. 242 (1912).

|| 'Phil. Mag.,' vol. 48, p. 220 (1924).

Evidence that these effects are not due to the presence of impurity nor to inequalities of temperature is presented.

The results of the experiments do not appear to be in agreement with the Weiss theory of specific heats of ferromagnetic substances.

We are indebted to the Colston Research Society of the University of Bristol for a grant towards the expenses of the investigation. Our thanks are due also to Prof. Chattock and Prof Tyndall for valuable suggestions and criticisms.

On the Change of Refractive Index of Linseed Oil in the Process of Drying and its Effect on the Deterioration of Oil Paintings.

By A. P Laurie, M.A , D.Sc.

(Communicated by Sir Arthur Schuster, F R S —Received April 30, 1926)

The following paper is the results of experiments undertaken for the information of the Committee appointed by the Royal Academy to investigate the problems affecting the durability of pictures.

One of the main defects of the modern picture in oil is that in course of years there is a lowering of tone over the whole of the picture—in contrast not only to the early fifteenth-century pictures in oil, but to many of the later schools of painting, such as the Dutch pictures. As the medium—linseed, walnut or poppy oil—is the same, and as the modern painter uses in many cases the same pigments, and in other cases superior substitutes, the cause of this lowering of tone must be found rather in the unscientific methods of using the materials than in the materials themselves This view is confirmed by the fact that an examination of modern pictures—by which I mean pictures painted in the last hundred years—reveals marked differences in the extent to which lowering of tone has taken place The pigments, if properly selected, being permanent under the conditions in a picture gallery, the lowering of tone must be ascribed to the medium This necessitates a study of the properties of the medium with a view to finding out the reasons why lowering of tone takes place

It is well known that oxidised films of all these oils yellow with age, linseed oil films yellowing more than poppy or walnut oil. Such yellowing will alter some pigments more than others—pigments at the green and blue end of the

spectrum more than pigments at the red and yellow end, and a transparent more than an opaque pigment. A pigment, for instance, such as cobalt blue, if painted on thickly, consisting as it does of transparent blue particles, and into the mass of which the light penetrates deeply, will be more affected than an opaque blue pigment

I have seen examples of cobalt blue in oil which have become black in 40 years, exposed to the ordinary light of a studio. A couple of months' exposure in a window, so as to bleach the yellowed oil, restored the colour

Besides the nature of the pigment in the oil, the amount of oil present and the thickness of the painted layer will obviously all have their effect, the oil rising to the surface if a pigment ground in excess of oil is painted on thickly.

The conditions governing this yellowing, the effects of light and time and moisture, are all well worth investigation

There is, in addition to the yellowing, another change which may take place in the oil which would cause lowering of tone. It is known that when the painter has painted over a portion of his picture, in course of time the under-painting shows through, and if a checkboard of white and black squares is painted over with white lead in oil till invisible, it gradually shows through the over-painting in course of time. This has been explained by gradual inter-penetration of the pigment by the dried oil film, causing an increase of translucency, but if that is the explanation, one would expect pigments ground in oil and kept in tubes to grow more translucent, and I am not aware of any evidence to that effect. A more reasonable explanation is that the linseed oil film, which we know is slowly undergoing changes which after the first drying is causing it to increase in density, is at the same time increasing in refractive index.

Pigments may be regarded as transparent bodies of high refractive index.

When light is passing through a transparent medium of low to a transparent medium of high refractive index, part of the light is transmitted and part reflected. The ratio of transmitted and reflected light depends upon the angle of incidence and upon the planes of polarization, and on the difference between the refractive indices of the two media. The well-known equations indicate that an increase in the difference between the refractive indices of two media is accompanied by an increase in the amount of reflected light It is sufficient for our purpose that the greater the difference between the refractive indices of the two media, the more light will be reflected at the interface, and the less transmitted, other conditions being the same.

Abney's researches on pigments show that the light reflected by them

covers the whole of the spectrum, but with an excess in certain portions, or as we might crudely express it:—Vermilion reflects a mixture of red and white light, ultramarine a mixture of blue and white light, and so on

If, then, we are justified in regarding pigments as consisting of transparent particles with the property of absorbing certain parts of the spectrum, we should expect to find their apparent opacity and brilliancy depending on their refractive index and the refractive index of the medium with which they are mixed

That this is so, every painter knows. A chrome yellow, for instance, becomes deeper in tone and less brilliant when air is replaced by water, and still more deep and lowered in tone when water is replaced by oil

In the first place, it seemed to me of interest to take some of the commoner pigments of the artist's palette and mix them in and grind them in media of high refractive index. For this purpose I took bromo-naphthalene, which has a refractive index of 1·65, and methylene-iodide saturated with sulphur, which has a refractive index of about 1·8 White lead mixed with bromo-naphthalene becomes a greyish translucent powder, while the pale yellow, like pale cadmium and pale chrome yellow, becomes orange

The investigations of Breyer, in the study of zinc oxide, and Depew in Ruby and Green, have shown the transparent crystalline nature of white lead and zinc oxide In their experiments the pigments are very highly dispersed and examined with immersion lenses up to 1,500 diameters ('Chemical and Metallurgical Engineering,' vol. xxviii, p. 53) Their examination was made in ordinary media.

In each case I ground the pigment with a muller in the medium, much as would be done in preparing it for use, and examined it under a quarter-inch objective with transmitted light, using the three media, linseed oil, bromo-naphthalene, and methylene iodide

White lead when ground in bromo-naphthalene proves to consist of transparent, doubly-refracting crystals. Zinc oxide is equally transparent With the exception of white lead and lead chrome and vermilion, all the pigments I examined were apparently isotropic. Professor Eibner describes the cadmium yellow as consisting of hexagonal crystals, and in order to decide whether any or all of these pigments are in reality crystalline, it will be necessary to examine them under the higher powers in liquids of much higher refractive index such as a fused mixture of sulphur and selenium

By examining pigments in this way, and finding how high a refractive index was required to make them appear transparent under the microscope,

I have been able to prepare a rough table of order of opacity for the more important bright pigments, starting with those which are transparent in linseed oil and ending up with red oxide of iron, which proves to be opaque, even in methylene iodide saturated with sulphur

The following table shows the pigments arranged both in order of opacity and in order of colour—the pigment at the one corner, namely red oxide of iron, being both opaque and red would be less affected by changes taking place in the linseed oil, while Prussian blue and cobalt blue at the other extreme would be most affected

Red	Yellow	Green	Blue
Madder Alizarine Lakes	Cobalt Yellow	Viridian	Cobalt Blue Prussian Blue
Burnt Sienna	Raw Sienna		Ultramarine
Vermilion.	Chrome Yellow Yellow Ochre	Cobalt Green	Cerulean Blue
Cadmium Scarlet	Cadmium Yellow		
Venetian Indian Red			

It is obvious that such a table, while not pretending to be quantitative, supplies the artist with useful, practical information as to when he should use a pigment for solid painting and when he should use it for thin glazing

The next question which I investigated was—whether a linseed oil film does alter in refractive index. For this purpose I selected a linseed oil which had been prepared for artists' use, by exposing "cold-pressed" oil to air and light over water A film of this oil was painted out on the glass surface of a Herbert Smith refractometer. Its refractive index measured with a sodium flame was 1 480 It was kept in the dark and allowed to dry and measurements taken from time to time The diagram on p. 180 gives the result of these measurements

There is evidently a considerable rise in refractive index during the drying process, and that a lowering of tone takes place during this process is quite evident if we compare pigments freshly ground in oil with the same pigment-oil mixture when the oil is dry But from the point of view of this investigation the interest was whether the rise in refractive index was going to continue On July 15 the refractive index was 1 492, and on July 16—that was two days

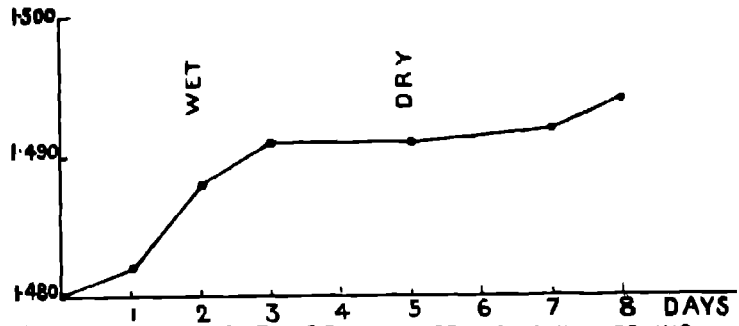

CHANGE IN REFRACTIVE INDEX OF LINSEED OIL WHILE DRYING

Fig 1.

after the film had been surface dry—1 494 From that time onwards the change in refractive index has been slow but continuous

August	7	1 495
August	31	1 496
September	11	1·497
October	24	1 498
January	15	1 499
March	15	1·500

During this time there has been a slight drop in temperature, the temperature being from 17° to 19° C. during the summer months, and now being about 12° C. It was necessary therefore to make a slight temperature correction on these readings, the R I changing 0 001 for a range of 10° C

Judging by these results the film is slowly but steadily increasing in refractive index, and as we know that slow chemical changes, accompanied by increase in density, continue in linseed oil for years, we may, I think, safely assume that this increase in refractive index is going to continue—that consequently the lowering of tone which takes place in oil pictures is due not only to the yellowing of the oil, but also to its increase in refractive index. A change in refractive index from 1·480 to 1·500 causes a perceptible degradation of tone in white lead and makes a pale cadmium yellow appear dull and more orange in tint

The bearing of these experiments on the practice of the oil painter is obvious, and it is of interest to see how far the earlier painters had learned by studio tradition to avoid these dangers.

In the time of the Van Eycks—and considerably later—there is sufficient

evidence, from unfinished pictures, to show that the practice was, beginning with the white gesso panel, to lay in black and white, and even colour, in a low refractive index medium like egg or size, and to glaze thinly with oil pigments over this under-painting. Under these conditions the increase in refractive index of the oil would tend to correct the lowering of tone owing to the yellowing of the oil, as more light would be reflected from a bright tempera surface below A very interesting example of this technique is to be seen in the unfinished picture in the National Gallery by Michael Angelo, No. 790. Later, when the practice of beginning in tempera was dropped, the paintings were still done upon a white gesso and the high lights were painted very thinly on the gesso, as I have shown by actual borings and measurements, so as again to ensure luminosity from the gesso below

It is evident from this brief account of 15th and 16th century methods of painting oil pictures that the painters of that time had thoroughly mastered the possibilities of the oil film, both in the matter of yellowing and of change in refractive index, and there can be no question that under modern conditions of painting in oil, the neglect of these two factors is the explanation of the lowering of tone which so often takes place, and if results as permanent as those of the Old Masters are to be obtained, the painter in oil must take both these changes into account and modify his methods accordingly.

In conclusion, I wish to thank Mr Balsillie of the Mineralogical Department of the Royal Scottish Museum for the assistance he has given me in preparing this paper

The Effect of Occluded Hydrogen on the Tensile Strength of Iron.

By L. B. Pfeil, M.Sc., A.R.S.M.

(Communicated by Prof. H. C. H. Carpenter, F.R.S.—Received May 19, 1926.)

(Plates 6, 7.)

For many years attention has been directed to the embrittling of iron and steel by acid, and it is generally considered that the embrittling is due to the occlusion of hydrogen by the metal.

This subject is of particular importance in those branches of the iron and steel industry where acid is used to remove oxide from the surface of the metal before tinning, galvanizing, wire-drawing, etc. There is also some reason to suppose that certain boiler failures may be connected with the occlusion of hydrogen by the metal. A large number of investigations dealing with various aspects of the subject have been published, notably by Longmuir (1), Andrew (2), Fuller (3), Coulson (4), Parr (5), Watts and Fleckenstein (6), Langdon and Grossman (7) and Edwards (8)

In the above-mentioned papers much interesting quantitative data are available on the effect of hydrogen on the mechanical properties as determined bend tests, impact tests, alternating stress tests, and the Erichsen test. For the purpose of this paper it does not seem necessary to give an account of the results described in these papers, for comparatively little data dealing with the tensile properties of iron have been recorded.

The experimental work carried out during this research may be divided into three sections —

1. Tests on iron in the normal finely crystalline condition.
2. Tests on single iron crystals.
3. Tests on the boundary between two large crystals.

Fig. 1 is included to illustrate the very striking type of result obtained when specimens made up of large crystals are embrittled by hydrogen. The photograph shows a strip of iron 8 inches by 1½ inches by ⅛ inch, mainly composed of crystals about 1 inch in diameter. The strip was pickled for 30 minutes in 20 per cent. sulphuric acid, and was then snapped into pieces with the greatest ease. In the illustration it is clearly evident that fracture took place mainly through the crystal boundaries. Only in one place, near the top of the strip, had the fracture passed through a crystal.

Fig. 1

(*Facing p.* 182)

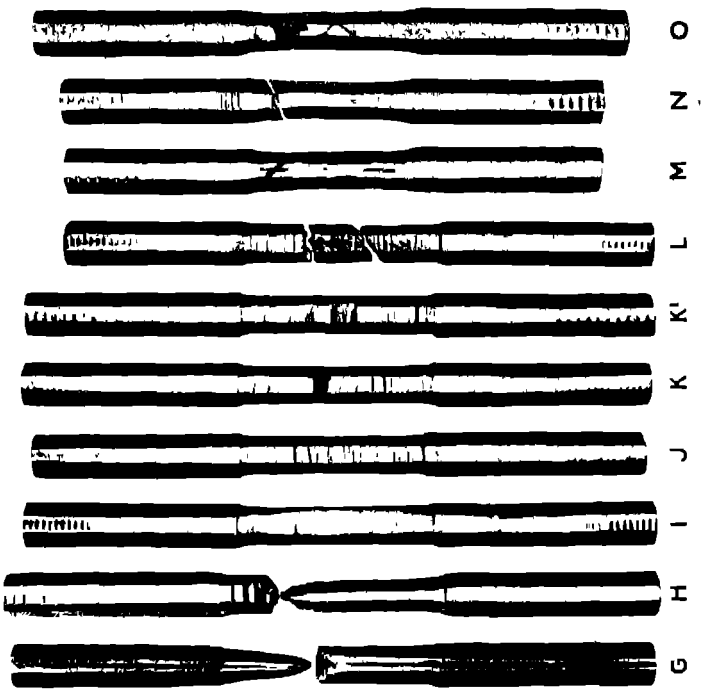

Fig 4

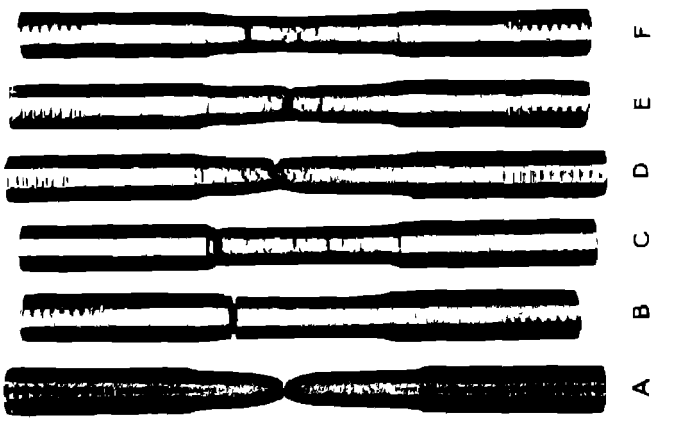

Fig 3

(*Facing p* 18')

It has long been known that ferrous metals embrittled by pickling recover their normal properties on standing, and for this reason quantitative tests can only be satisfactory if this time factor be taken into account It was decided, therefore, to carry out the tensile tests in the first instance while the specimens were actually immersed in the acid. Simple immersion was not satisfactory, for the corrosion occurring during the test greatly decreased the accuracy of the results. Electrolytic pickling was used throughout the experiments to be described, for by this means corrosion was entirely prevented.

The simple apparatus which was employed is illustrated in fig 2 A 2½-inch length of 1¼-inch diameter glass tube (A) was closed at the lower end by a rubber

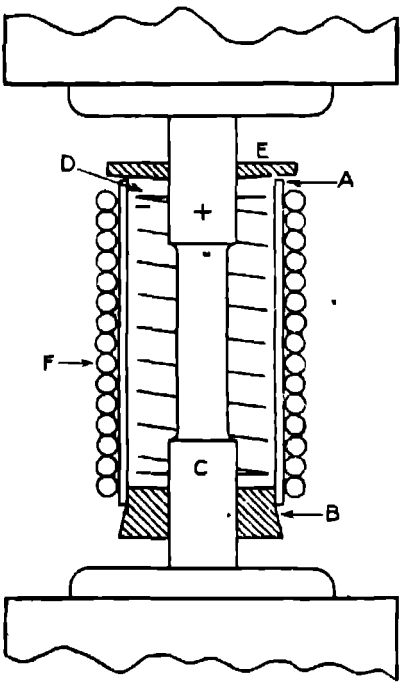

FIG. 2.

bung (B), through which passed one end of the test piece (C). A 1-inch diameter coil of platinum wire (D) within the glass tube formed the anode, and the test piece was made the cathode. The upper end of the test piece carried a rubber disc (E), a loose fit on the top surface of the glass tube to prevent the acid spray

from damaging the testing machine In some experiments a coil of small diameter rubber tubing (F) was wound round the glass tube and carried a stream of cooling water. With the aid of a funnel with rubber tube attached the sulphuric acid electrolyte was introduced after setting up the apparatus in a 10-ton Buckton tensile machine.

The material employed was ½-inch diameter mild steel rod. All the carbon, however, was removed by a prolonged annealing at 750° C. in hydrogen gas, leaving iron of the following composition —

C, nil, Si, 0 064; S, 0 034; Mn, 0·46, P, 0·020 per cent.

Some of the material was tested in the fully annealed, finely crystalline condition as it left the furnace, while the remainder was converted into single crystals by a method adapted from that devised by Carpenter and Elam for converting finely crystalline aluminium into single crystals (9 and 10)

Test pieces were turned to the following dimensions —

Total length	5½ inches
Parallel portion . . .	1½ inches.
Gauge length	1 inch
Diameter of parallel portion .	0 4 inch.

The machining was carried out very carefully so as to avoid any distortion of the material of the test piece. The parallel portion was finished with emery papers down to the 000 grade so as to give a very smooth surface

Tests on Finely Crystalline Iron (150 *Crystals per square mm*)

As a standard for comparison a number of test pieces were broken in the normal manner. The results are given in the following table:—

Table I —Finely Crystalline Aggregate Tested in the Normal Manner.

No. of test	Tensile strength Tons per square inch.	Elongation Per cent. on 1 inch
1	18 15	62 0
2 (A)*	18·30	63 5
3	18·42	62 5
4	18 50	62 0
	Average 18·34	Average 62 5

* Throughout the tables letters indicate specimens illustrated. (See fig. 3, A.)

Some preliminary tests were carried out to determine the most suitable conditions for carrying out the tensile tests during pickling The variables taken into account were :—

1. The strength of the sulphuric acid electrolyte
2. The strength of the electrolysing current.
3. The time the current passed before beginning the loading
4. The diameter of the test pieces
5. The rate of loading
6. The temperature at which the test was made.

1 Acid strengths of 5, 10, 20, 25 per cent concentrated sulphuric acid (by volume) were tried, but no difference in results was observed Ten per cent acid was used in all further tests

2. Tests were carried out using currents from $\frac{1}{2}$ to 4 amperes, equivalent to a current density of 0 2 to 1 6 amperes per square inch of cathode surface No variation was found provided that when the heavier currents were employed a rise in temperature was prevented by water cooling A current of 1 ampere was standardised.

3. Similar test pieces were broken after electrolytic pickling for $\frac{1}{4}$ $\frac{1}{2}$, 1, 2 and 18 hours. A quarter of an hour was insufficient, $\frac{1}{2}$ an hour appeared to be sufficient, but to avoid any uncertainty pickling was continued for 1 hour in all the tests which followed.

No further change could be detected by prolonging the pickling beyond 1 hour

4. Test pieces of the same material, but with three different diameters for the parallel portion, were tested under identical conditions, and gave almost identical results. It was clear, therefore, that the conditions so far determined upon gave a complete penetration of the hydrogen even in the test pieces of larger diameter than those employed in the remainder of the work

5. The time taken from the commencement of loading until fracture occurred was varied from approximately 2 to 30 minutes without any appreciable effect on the final results. An effort was made, however, to keep this time constant at 10 minutes.

6. The temperature at which the experiment was carried out was found to be a factor of considerable importance. Comparatively small variations had a marked influence not only on the tensile strength and elongation, but also upon the actual path of the rupture The influence of temperature will be made clear in what follows.

In Table II the results are given for tests on the finely crystalline aggregate

at a temperature of about 25° C. and under the standard conditions already mentioned (One ampere for 1 hour, 10 per cent sulphuric acid, fracture in 10 minutes)

Table II.—Finely Crystalline Aggregates Tested during Pickling at 25° C.

No. of test	Tensile strength Tons per square inch	Elongation Per cent on 1 inch	Remarks
5	16·10	8·0	Intercrystalline fractures.
6	16·72	10·0	
7 (B)	16·80	11·0	
8	17·14	13·5	
	Average 16·69	Average 10·6	

The tensile strength shows a decrease of 9 per cent, while the elongation is only one-sixth of that obtained in the normal test. The most striking effect of the occluded hydrogen is seen in the nature of the fracture, which passes entirely between the crystals (intercrystalline). The specimens broke suddenly as if made from a hard and brittle metal, the fracture frequently occurring near the shoulder. The fracture was, in fact, similar to that obtained when metals are broken at temperatures near their melting points, in which circumstance an intercrystalline fracture also results (11).

Fig. 3, A, shows ⅔ size a finely crystalline test piece fractured under normal conditions. The specimen shows very marked necking at the fracture. Fig. 3, B, shows a piece of the same metal broken during pickling. The very small elongation and absence of necking are clearly evident.

As the temperature of testing was raised, the tensile strength increased a little, the elongation increased most markedly, and the character of the fracture changed. Figures to illustrate these points are given in Table III.

The tensile strength is intermediate between that obtained in the normal test (18·34 tons per square inch) and that obtained during pickling at lower temperatures (16·69 tons per square inch).

The elongation figures show a progressive increase with increasing temperature, while the fracture changes from intercrystalline to transcrystalline*

* Throughout this report the words "transcrystalline fracture" are used in a rather restricted sense to mean fracture through the crystals after they have drawn down by severe slipping. A sudden fracture through cleavage planes, although in point of fact transcrystalline, is distinguished by being referred to throughout as "cleavage fracture."

Table III.—Finely Crystalline Aggregates Tested during Pickling at Temperatures from 30° C. to 50° C.

No of test.	Temperature of test. ° C.	Tensile strength Tons per square inch	Elongation Per cent on 1 inch	Remarks
9 (C)	30	17 54	22 5	Intercrystalline fractures, with cracks and a tendency to local contraction
10	35	17 62	25 5	
11	35	17 85	26 5	
12 (D)	40	17 80	42 0	Transcrystalline fractures, with cracks and local contraction
13	45	17 93	49 0	
14	50	17 53	44 0	
		Average 17 71	Average 34 9	
15 (F)	40	17 47	29 5	Maximum load reached, but pieces not broken
16 (E)	40	17 61	34 5	

Specimens 9, 10 and 11 broke with an intercrystalline fracture accompanied by a number of small cracks in the parallel portion, and No 11 showed, in addition, a tendency to neck at the fracture Fig 3, C, shows the fracture and cracks in No. 9

In the case of specimens broken at the higher temperatures, the fracture was accompanied by a considerable amount of local contraction, and many cracks were visible The cracks were approximately at right angles to the length of the specimen, as a rule short in length and not very deep Near the fracture the cracks had opened up under the influence of the stress and the fracture itself occurred in the position of the greatest crack. Fig. 3, D, shows a fracture characteristic of this type

A series of test pieces showing stages in the approach of fracture were prepared by intercepting the straining at various loads Two pieces from such a series are illustrated in fig. 3 at E and F In both pieces the maximum load had been reached In F local contraction had scarcely set in, but the cracks may be seen over a considerable portion of the gauge length, and in the actual specimen minute cracks may be seen fairly uniformly distributed over the whole of the parallel part

In E a considerable amount of necking had occurred, some of the cracks had opened out to large fissures. Fracture was about to occur.

Sections through these cracks have been prepared and examined under the microscope. The large cracks were partly intercrystalline and partly cleavage. The smallest cracks (visible only under the microscope) were due to cleavage, each passing in a straight line through or nearly through a crystal.

Sections through the fractures showed that the main part of each was trans-crystalline in character, the minute crystals having drawn down by slip, and in consequence exhibited after etching the darkened surfaces characteristic of cold-worked crystals. As already indicated, the remainder of the fracture passed through the cleavage planes and along the crystal boundaries.

In view of what is stated in the section of this paper dealing with single crystals, it must be pointed out at this stage that the cracks in finely crystalline iron which have just been described were not due to strains set up in the metal during the machining operations

Some tests were carried out to determine for how long the effect of the occluded hydrogen remained after pickling. Specimens were pickled for 1 hour and then rapidly washed in cold water and dried Results are given in Table IV.

Table IV.—Finely Crystalline Aggregate Tested after Pickling.

No of test	Time elapsed since pickling	Tensile strength Tons per square inch	Elongation Per cent on 1 inch	Remarks
17	*	18·17	63 0	A few small cracks
18	15 seconds	18 44	60 5	Normal fractures
19	3½ minutes	18·30	66·5	
20	20 minutes	18 59	62 0	
		Average 18 37	Average 63 0	

* This specimen was not washed, but was broken wet immediately after pickling

It appears from these results that the effect of the hydrogen does not persist for more than a very short time This cannot in reality be true, because shock tests reveal a brittleness which remains long after the end of the pickling It has been shown by other investigators that occluded hydrogen is driven off by cold working and by warming. It seems most probable, therefore, that in the early stages of the tensile test, when pickling has been discontinued, the hydrogen is driven off and the normal properties regained

Tests on Single Crystals.

The results obtained from four single crystal test pieces of circular cross-section broken without pickling are given in Table V.

The method of fracture in these specimens was similar to that obtained by Carpenter and Elam in single aluminium crystals of circular cross-section (12). The crystals flattened in one dimension drawing down finally to a "double knife-edge" or grooved fracture.

Table V.—Single Crystals Tested in the Normal Manner

No. of test.	Tensile strength Tons per square inch	Elongation Per cent on 1 inch.	Remarks.
21	10 22	55 0	Double knife edge or grooved fracture
22 (G)	10 32	57 5	
23	10·46	55 5	
24	10 81	53·0	
	Average 10 45	Average 55 2	

Results obtained from single crystals broken during pickling are given in Table VI.

Table VI —Single Crystals Tested during Pickling at 25° C

No of test	Tensile strength Tons per square inch	Elongation Per cent on 1 inch	Remarks
25	9 44	45 5	Transcrystalline fracture accompanied by cracks.
26 (H)	10 25	46 5	
27	10 25	53 0	
28 (I)	10 32	(39 5)	Stages in the development of the fracture Maximum load reached, but specimens not actually broken
29 (J)	9 62	(26 0)	
30 (K)	10 09	(39 5)	
	Average 10 00	Average, Nos 25 to 27 48 3	

It will be seen from these figures that the tensile strength of the single crystal was scarcely altered by occluded hydrogen, and that the elongation was only reduced by 12½ per cent. The presence of the hydrogen, however, entirely altered the appearance of the fracture Fig. 4, G, shows a single crystal broken in the ordinary manner, while fig. 4, H, shows one broken during pickling. In these two, one-half of each test piece is shown in side elevation and the other half in end elevation Cracks may be seen running across H at right angles to the length, and fracture occurred at a point where one of the largest cracks had appeared

In a number of specimens straining was stopped at various stages in the test and the specimens examined The cracks did not develop until a considerable elongation had occurred, by which time the crystals had flattened The cracks appeared on the broad sides of a crystal and were always at right angles to the length of the test piece. They passed into the crystal approximately at right

angles to the surface, and penetrated to an increasing depth, as the straining was more severe. In fig. 4, I, a single crystal is shown at a stage when the first crack appeared. Fig. 4, J, a later stage, is shown where cracks have occurred throughout the parallel portion, and fig. 4, K, shows one crack opening out at a point where fracture is about to occur. The reverse side of K is shown at K′, where a lens-shaped area may be seen at the point where fracture is about to occur, such as was referred to by Carpenter and Elam in connection with aluminium crystals (13).

In view of the work described in the next section, where it is shown that fracture through cubic cleavage planes may occur at low stresses when crystals are strained in tension during pickling, it was at first thought that the cracks in question were due to incomplete cleavage. The fact that the cracks were always very nearly right angles to the axis of stress made this explanation unlikely, for there was certainly some variation in the orientation of the crystals tested.

Investigation showed that the cracks were not due to cleavage and were not, in all probability, connected in any way with crystallographic planes. A number of crystals were strained until the cracks appeared - that is, until a stage was reached such as that illustrated in fig. 4, J. Sections were cut exactly parallel with the cracks and then polished. Needle point indents were then made on the polished surfaces, and, from the shape of the silhouettes so produced, it was clear that the sections did not all coincide with a cube plane (17) and (18). A further proof that the cracks were not due to cleavage was obtained by subjecting a crystal, in which the cracks had been produced, to a sudden blow before the embrittling effect of the hydrogen had disappeared. Cleavage fracture is readily produced in this manner and fig. 4, L, shows a typical case. In the lower fracture a cubic cleavage plane makes an angle of about 45 degrees with the cracks previously produced; the upper fracture, although it appears to pass straight across, is in reality made up of two cleavages, both at 45 degrees to the cracks.

The only simple explanation for the formation of the cracks which remained was that they were due to the straining of the crystals during the machining. Attention must again be drawn, however, to the great care taken in the turning and the excellent surface finish produced. The view that the cracks were due to straining was supported by some similar tests on single crystals in strip form. These were milled to size, the cutter travelling parallel to the direction of the tensile straining. In these test pieces no cracks developed.

To test this possibility, a further supply of single crystal test pieces were

turned, but they were annealed before the tensile test Annealing for 1 hour at 650° C did not prevent the formation of the cracks during the subsequent testing Annealing for 1 hour at 850° C, however, prevented their formation except for some very small ones in the immediate neighbourhood of the actual fracture.

The appearance of annealed crystals when etched in dilute nitric acid was particularly interesting and instructive Minute crystals had formed, due to recrystallisation, in four bands along the length of the parallel portion Two of these bands were about 1/10 of an inch wide and the other two somewhat less than this The test piece was still essentially mono-crystalline and showed the usual light and shade effects caused by the reflection of light from the facets of the minute etching pits. The bands of minute crystals would, in fact, probably not have been observed had their presence not been expected. The bands were distributed in a symmetrical manner—a broad band at each end of a diameter, and a narrow band at each end of a diameter, but the two diameters were not at right angles

The recrystallisation makes it clear that some surface cold working occurred during the machining The symmetrical arrangement of the recrystallised parts shows that some crystallographic planes (judging from the appearance of the etched crystals, probably either the octahedral or the icositetrahedral planes are more liable than others to be affected by the turning operation (19) Finally, the absence of cracks in single crystals tested after a suitable annealing treatment indicates that the cracks in crystals not so treated were due to machining strains which are intensified in some way by the occluded hydrogen.

Table VII.—Single Crystals Annealed for 1 hour after Machining and Broken during Pickling at 25° C

No of test	Annealing Temperature °C	Tensile strength Tons per square inch.	Elongation Per cent on 1 inch	Remarks
31	650	10 08	48 5	Many cracks
32	850	9 97	54 0	A few small cracks at the actual fracture only
33	890	9 71	57 5	
34	890	9 85	54 0	
35	890	10 48	52 0	
36	890	10 56	54·5	
		Average Nos 32 to 36 10 11	Average Nos 32 to 36 54 2	

In Table VII (p. 191) some results are given for single crystals annealed after machining and broken during pickling. It will be seen that when machining strains are absent occluded hydrogen has no important effect on either the tensile strength or the elongation.

Tests on the Boundary between Two Large Crystals.

Test pieces were prepared from material made up of crystals $\frac{1}{2}$ to $\frac{3}{4}$ of an inch long, most of them occupying the whole cross-section of the rod. The parallel portion of such test pieces consisted of two or three crystals.

These test pieces when broken in the ordinary way always failed by the drawing down of *one* of the crystals to a knife-edge fracture, the tensile strength being practically the same as if the whole parallel portion had been occupied by one crystal. When broken during pickling, however, very different results were obtained. The five following types of fracture have been encountered —

(*a*) The fracture passed entirely through the boundary between two crystals. (Intercrystalline)

(*b*) The fracture passed entirely through one of the crystals exactly as in the case of a single crystal tested during pickling. (Transcrystalline)

(*c*) The fracture passed entirely through cleavage planes (Cleavage)

(*d*) The fracture was partly intercrystalline and partly cleavage.

(*e*) The fracture was partly intercrystalline, partly cleavage, and partly transcrystalline

Tensile strength and elongation figures for one or more of each of these types are given in Table VIII.

Of these specimens, three are illustrated at M, N and O in fig. 4, representing the intercrystalline, the cleavage, and combined intercrystalline and cleavage types respectively O is of particular interest, as it shows, in addition to the type (*d*) fracture, many cracks, both intercrystalline and cleavage, throughout the parallel portion. At the fracture one small crystal broke away and was not included in the photograph

It is of interest to note the very low tensile strength accompanying the intercrystalline type of fracture and the exceedingly low elongation accompanying both intercrystalline fractures and cleavage fractures The tensile strength of specimens showing a purely cleavage fracture was found to be very variable. (The lowest value was 4·96 tons per square inch and the highest 12·64 tons per square inch) It is probable that the angle between the cleavage plane and the axis of stress is the determining factor in this connection, for it was found that the nearer this angle approached 90° the lower was the tensile strength.

Table VIII.—Test Pieces Consisting of Two or More Crystals in the Parallel Portion Broken during Pickling at 25° C.

No. of test.	Tensile strength Tons per square inch.	Elongation Per cent. on 1 inch	Remarks
37	8 84	7 0	Type (*a*) Intercrystalline fracture
38 (M)	9 80	7·0	
39	10 38	40 5	Type (*b*) Transcrystalline fracture
40	11·72	26 0	
41	4 96	1 0	Type (*c*) Cleavage fracture.
42 (N)	12 64	3 0	
43	10 57	8 5	Type (*d*) Intercrystalline and cleavage fracture.
44	10 60	6 0	
45 (O)	11 00	10 0	Type (*d*) With cleavage and intercrystalline cracks
46	8 37	4 0	Type (*e*) Intercrystalline, transcrystalline and cleavage

Consideration of Results

1. Occluded hydrogen has a remarkable weakening effect on the intercrystalline boundary. This applies not only to the boundaries between very large crystals, but also to the boundaries between the very minute crystals of which ordinary iron consists. The strength of the boundary between two single crystals has been shown to be about 8½ tons per square inch and of the boundary between very small crystals about 17 tons per square inch. It is probable that this marked difference is due, not to any real variation in the strength per unit area, but to the difference in the ratio between actual area of fracture and the cross-sectional area of the test piece in the two cases. This ratio is certainly much greater in the case of the aggregate than it is in the case of the two large crystals.

It may be mentioned here that a few experiments which have been made indicate a progressive fall in boundary strength as the crystals are larger. Since the tensile strength of iron obtained in the normal manner is nearly constant over a considerable range of crystal sizes (14), the ratio between tensile strength as normally obtained and boundary strength as obtained by tests during pickling will be found to vary with the size of the crystals in the specimens tested.

2. In addition to its effect on the boundaries, hydrogen decreases the cohesion across the cubic cleavage planes, a pull of 5 tons per square inch applied at right angles to the cleavage plane being sufficient to cause separation

3 Occluded hydrogen does not prevent deformation by slipping on the icosetetrahedral planes of the iron crystal (15) Judging from the behaviour of the single crystals during these tests, it seems improbable that the hydrogen has even any important effect on the resistance to movement along the slip planes.

4 In a single iron crystal certain crystallographic planes or directions are particularly liable to damage during machining operations (16). The surface cold working does not become evident in an ordinary tensile test, but is made very evident when the test is made during pickling

5. The effect of hydrogen on the finely crystalline iron is very much less marked at temperatures a little above room temperature Under these conditions the crystal boundaries are not so greatly weakened. Fracture takes place mainly *through* the crystals after they have drawn down by slipping, but the point at which fracture occurs is determined by cracks which form as a result of a limited cleavage and intercrystalline failure. The cracks probably originate in those crystals so set at the surface of the test piece as to present a cleavage plane at right angles to the stress, these being particularly liable to fracture at low stresses. The minute notches so produced lead to large cracks which, decreasing the effective cross-section of the test piece, cause a low value to be recorded for tensile strength.

6 Unless the pickling were continued during the stressing the effect of the hydrogen was scarcely noticeable in these tests This indicates how limited in value is the tensile test as a means of investigating mysterious failures which sometimes occur in steel structures for which occluded hydrogen is suspected as being responsible

The author wishes to express his gratitude to Prof. C A. Edwards, D.Sc, for allowing this work to be carried out in his laboratories and also for the encouragement which he constantly gave.

REFERENCES.

(1) Longmuir, 'Journal of the Iron and Steel Institute,' No 1, p. 163 (1911)
(2) J H Andrew, 'Transactions of the Faraday Society,' vol 9, p 316 (1913)
(3) T. S. Fuller, 'Transactions of the American Electrochemical Society,' vol 32, p. 247 (1917), and vol. 36. p 113 (1919).

(4) Coulson, 'Transactions of the American Electrochemical Society,' vol 32, p 237 (1917)
(5) S W. Parr, 'University of Illinois, Bulletin No. 18' (January, 1917)
(6) Watts and Fleckenstein, 'Transactions of the American Electrochemical Society,' vol 33, p 169 (1918).
(7) Langdon and Grossman, 'Transactions of the American Electrochemical Society,' vol 37, p. 543 (1920)
(8) C. A Edwards, 'Journal of the Iron and Steel Institute,' No 2, p 9 (1924)
(9) H C. H Carpenter and C F Elam, 'Roy. Soc Proc.,' A, vol. 100, p 329 (1921)
(10) C. A. Edwards and L. B. Pfeil, 'Journal of the Iron and Steel Institute,' No 1, p 129 (1924).
(11) W. Rosenhain and D Ewen, 'Journal of the Institute of Metals,' No 2, p. 119 (1913).
(12) H. C. H. Carpenter and C. F Elam, 'Roy Soc. Proc.,' A, vol 100, pp. 346–347 (1921)
(13) H. C H. Carpenter and C. F. Elam, 'Roy. Soc. Proc ,' A, vol. 100, p. 346 (1921)
(14) C A Edwards and L B. Pfeil, 'Journal of the Iron and Steel Institute,' No. 2, p 100 and p. 106 (1925).
(15) L B. Pfeil, 'Journal of the Iron and Steel Institute, Carnegie Scholarship Memoirs,' 1926.
(16) See Prof. Carpenter's contribution to the discussion of Edwards' and Pfeil's paper, 'Journal of the Iron and Steel Institute,' No. 2, p. 114 (1925)
(17) F Osmond and G Cartaud, 'Journal of the Iron and Steel Institute,' No 3, p 444 (1906)
(18) L. B. Pfeil, 'Iron and Steel Institute, Carnegie Scholarship Memoirs' (1926).
(19) C. F. Elam, 'Journal of the Iron and Steel Institute,' No 2, p 112 (1925)

The Infra-red Secondary Spectrum of Hydrogen.

By T. E. Allibone, M Sc., Physics Department, The University, Sheffield.

(Communicated by Prof. S. R. Milner, F R S.—Received May 19, 1926)

(Plate 8.)

The first observations of the "many lined" spectrum of hydrogen in the infra-red were made by Croze,* who measured the wave-lengths of 72 lines between 6836 A.U and 8027 A U. to the nearest integer on the Rowland system. Porlezza† measured the wave-lengths of 43 lines between H_α and 6963 A.U. with greater accuracy, but failed to observe lines of greater wave-length than 7000 A.U, even though his photographic plates were specially sensitised. Watson‡ had likewise failed to detect lines in the infra-red above H_α, though his plates were treated to record up to 8000 A U Croze§ corrected some of his earlier lines and added some 27 more, but did not extend the further limit beyond 8027 A U., and his later results were still only given to the nearest integer As Merton and Barratt|| had investigated the secondary spectrum only for wave-lengths less than H_α, it was thought desirable to re-investigate the infra-red region, to obtain a more accurate record of the wave-lengths of the lines, and to push the limit, if possible, to longer wave-lengths.

A plain diffraction grating spectroscope fitted with quartz lenses was used. The grating had 14,500 lines to the inch and gave a dispersion of 25 A per mm. An H-shaped vacuum-tube, fitted with aluminium disc electrodes at the heads of the upright stems, contained hydrogen, and to one stem of the tube a large glass bulb was sealed, so that a considerable volume of gas was available at about 2 mm pressure. The capillary tube connecting the stems was 2 mm. internal diameter, and light emerging from the end of this tube parallel to the tube was directed on to the slit of the spectroscope with a quartz lens. In this "end-on" position the intensity of the secondary spectrum was at a maximum

The discharge was excited by an induction coil with hammer break, and it was found that addition of inductance or capacity to the circuit reduced the absolute intensity of the secondary visible spectrum. The intensity was, however, increased by running the coil on a high voltage (60 volts) with rheostats,

* 'C R,' vol 152, p 1574 (June, 1911).
† 'Atti. Accad. Lincei,' vol. 20 (2), p. 176 (August, 1911).
‡ 'Roy. Soc. Proc,' A, vol. 82, p. 189 (1909).
§ 'Ann. Physique,' vol 1, p 35 (1914).
|| 'Phil. Trans.,' A, vol. 222, p 369 (1922).

when the discharge had almost the same appearance at each electrode, and the intensity of the H_α was considerably reduced. The large applied voltage had the additional advantage that the coil worked steadily for hours without attention.

Adjustments of the spectroscope were made with light from the Cu or Fe arc, both possessing strong infra-red spectra. A red filter cut out the second order spectra. The hydrogen spectrum was photographed adjacently to the iron arc, and an exposure of six or eight hours gave a strong succession of lines extending from H_α to 8300 A.U., similar in appearance to the visible secondary spectrum.

It was impossible to focus the whole of this region of the spectrum on one plate, so it was measured in two sections. Visual estimates of intensities (0 to 20) were made on each line, the mean wave-lengths reduced to vacuo, and wave-numbers calculated.

The photographic plates were sensitised according to a formula developed by Mr. L. Wright in this laboratory. Two solutions, A and B, were mixed just previous to use —

Solution A. 0·005 gr. dicyanine dye dissolved in 10 c.cs. methylated spirit.

Solution B. Fifty c.cs. methylated spirit, 50 c.cs. distilled water, and 5 c.cs. ammonia Sp. gr. 0·88.

The first solution had to be freshly prepared for each plate, but the other could be made up in bulk. The plate was immersed in the bath for 10 to 15 minutes, moving the solution continuously over the surface of the plate; then it was dried rapidly in a current of air. As the sensitiveness diminished after about three days, plates had always to be sensitised just previous to use. After exposure, they were bathed in a solution of methylated spirit and water to remove any grains of dye adhering to the surface, but even this did not prevent a "spotting" of the plates occasionally. Ordinary panchromatic developer was used.

Some 320 lines have been observed of wave-length greater than H_α, and these are recorded in Table I, H_α (wave-number $\nu = 15233{\cdot}22$) to 8349·52 A.U. ($\nu = 11973{\cdot}44$), the wave-lengths being referred to the secondary standards of the iron arc.* The spectrum, as stated before, was photographed in two sections, 8349 A.U. to 6921 A.U. and 6963 A.U. to H_α. In the first section two plates were taken, A and B, and the wave-lengths recorded in the table are the mean of calculations on the two plates, each plate having been measured on the comparator twice. In the second section only one plate was taken,

* International Iron Arc Secondary Standards, Burns, 'C.R.,' vol. 156, p. 1612.

but it was measured on the comparator three times. Thus the estimated error can only be given for lines falling in the section 8349 to 6921 A.U. In a few cases lines appeared on plate A which did not occur on plate B, and *vice versâ*, but these lines, without exception, were of intensity 0 or 1, so that, though observed on the one plate they may have been too doubtful to record on the second, these lines have been noted in the tables by the letter A or B. On the whole, the impression on plate B was slightly stronger than on plate A. Four curious anomalies occur which cannot be accounted for: lines 7442·33, 7423·61, 7395 91 and 7394 97 have intensities 1 or 2 in plate A, but 5 or 6 in plate B. The photographs were taken without any change in setting of the apparatus, and, as far as was ascertained, the character of the discharge did not alter. Line 7362·18 in plate B was observed to be a doublet in plate A, 7262·48–7261 91. In succeeding columns in Table I are recorded the wave-lengths in I.Å units, the estimated errors where known, the intensities and the wave-numbers corrected to vacuo. For comparison the wave-lengths of lines found by Croze 8029 to 6836 A.U. (Rowland system), and recorded in his two papers, are given with those of Porlezza, 6962·82 to 6566·92 and Piazzi Smith, 6836·2 to 6567 5. It will be seen that there is very little correspondence between the author's results and those of Croze, both with regard to wave-length and relative intensity of the lines. It is known that the character of the secondary spectrum depends on the conditions of excitation and pressure of the gas, and these factors may account to some extent for the marked discrepancy, but Croze's results published in 1914 differ by as much as 3 A.U. from those published in 1911, and his dispersion was only 185 A.U. per mm., whereas the author used a dispersion of 25 A. per mm. Porlezza's results are in closer agreement, but even here it should be noted that his measurements* of wave-lengths of the lines below H_α in the visible spectrum differ from those of Merton and Barratt by amounts ranging up to 1 A.U. In this region below H_α the author's results agree with the latter's to within 0 1 A.

With regard to the purity of the gas, it was found that in the visible secondary spectrum no lines occurred which are not also recorded by Merton and Barratt. It is possible that helium may have been present to a small extent, but a photograph taken of the discharge in a tube containing helium and showing strong band spectra in the visible region gave no infra-red band spectrum in a six-hours exposure, so that it may be concluded that none of the lines here recorded is due to helium. Furthermore, two other tubes filled with hydrogen prepared electrolytically, and purified by passing through a liquid air trap, produced spectra identical with the first tube.

* Porlezza and Norzi, "Atti. Accad. Lincei," vol. 20 (1), p. 819 (1911).

Table I.

Wave-length, I Å.	Error.	Intensity	Wave-number (Vac.)	Wave-length (Croze, R.A.)		Intensity.
				1911.	1914	
8349 52	0·02	2	11973 44			
B. 30·46		1	12000 84			
8273·26	0·06	2	83 80			
22·67	0·01	1	12158 15			
B. 16 11		0	67 80			
8164·64	0 01	3	12244 58			
B 30 85		1	95 45			
30 58	0·01	1	95 86			
15 10	0 01	2	12319 32			
04·11	0 03	1	36 02			
00·06	0 00	1	42 15			
8094·80	0 00	1	50 20			
01 48	0 00	1	55·29			
54·61	0 07	2	12411 85			
36·47	0·11	1	39 86			
B. 32 25		1	46 30			
				8027	8020	1
18 75	0·00	3	67 35			
13 42	0 01	1	75 64			
B 07 07		0	85 53			
B 00 05		0	96 48			
B. 7994 64		0	12504 94			
91·55	0 00	1	09 77			
B 87 29		1	16 45			
85 76	0 00	2	18 85			
84·10	0 05	2	21 46			
70 13	0 08	3	43 40			
67 24	0 09	1	47 95			
63 23	0 00	1	54 27			
B 59 92		1	59 48			
56·94	0·04	1	64 20			
53 27	0 04	1	70 00			
50 03	0 03	1	75 12		7950	2
B 47 27		1	79 49			
33·29	0 02	3	12601 65			
A. 23·35		1	17 45			
B 22·79		1	18·35			
03 04	0 07	3	49 88			
00 72	0 05	3	54 24			
A 7895 57		0	61 85			
A 86 53		1	76 36			
75 07	0 07	2	94·81			
56·63	0 05	3	12724 01			
29 67	0 01	1	68 41			
					7827	6
12 66	0 00	3	96 21			
				7810	7809	6
04·17	0 01	3	12810·14			
7798 98	0 01	1	18 66			
					7797	3
00 03	0 04	0	33 38			
74·14	0·00	2	59 61			
57·10	0·01	1	87 88			
B. 55·12		1	91 16			
B 45·46		0	12907 24		46	5
39·92	0·08	1	16·47			
32 83	0 01	5	28 32			

Table I.—(continued).

Wave-length, I Å	Error	Intensity.	Wave-number. (Vac.)	Wave-length (Crosse, B.A.) 1911.	1914	Intensity.
B. 7728 79		1	12935·07			
B. 24 28		1	42 62			
21 67	0 05	1	47 00			
19 01	0 08	2	51 45			
06·22	0 00	3	72·96			
A. 04 85		1	75 27		7705	5
B. 03·16		1	78·11			
7698 49	0 05	1	85 98			
92 67	0 12	6	95 81			
90 45	0 10	1	99 56			
85 48	0 00	5	13007·96			
79 42	0 02	2	18 22			
72 91	0 06	1	29 29			
68 97	0 03	1	35 97		7669	8
61 09	0 05	6	49 38	7663	7660	6
54 36	0 00	3	60 85			
50·86	0 02	4	66 82			
47 76	0·09	4	72·14			
B 45·13		1	76 03			
B. 41 87		1	82 21			
					7639	2
35 21	0 01	1	93 61			
31 46	0 00	1	13100 05			
23 17	0 01	2	14 29			
20 76	0·01	2	18 44			
13 94	0 02	2	30 18	7613	7615	9
09 80	0 04	1	37 22			
06 26	0 05	4	43 45		07	8
03 42	0 02	6	48 36			
7597 27	0 01	9	59 01			
93 80	0 01	1	65 02			
					7589	3
84 69	0 04	3	80 82			
					82	5
79 33	0 01	2	90 15			
76·33	0 03	4	95·37		76	5
71 63	0 03	3	13202 50			
A 67 15		0	11 39			
65 32	0 02	1	14 58	7565	7565	3
61 43	0 03	3	21 37			
58·95	0 03	3	25 71			
					7557	4
45·13	0 00	4	49 93	7548	7548	8
42·03	0 02	4	55·37			
38·51	0 03	5	61·56			
37 24	0 01	3	63·79	7536	7536	7
35 00	0 02	2	67·75			
31·75	0 02	2	73·47			
28 40	0 03	1	79·38		7529	8
24·64	0 01	8	80 02			
22 26	0 01	1 *d*	90 22			
				7518	7519	3
14 77	0 06	1	13303 40		16	2
					14	4
12·43	0 04	3	07 61			
07 25	0 02	5	16 78			

d = diffuse

Table I.—(continued).

	Wave-length, I Å.	Error.	Intensity.	Wave-number. (Vac.)	Wave-length. (Croze, R A.) 1911	Wave-length. (Croze, R A.) 1914.	Intensity
	7504·13	0·08	5 *d*	13322 32	7505	7503	5
	7497 89	0 03	1	33·40			
	96 30	0 01	1	36·23	7496	7496	5
	89·46	0·03	2	48·42			
	88·04	0 04	2	50 96		88	2
	84 40	0·03	1	57 45			
					81	80	2
	78·33	0·00	3	68 29			
	74·48	0·01	5	75 17			
	68·46	0·06	8 *d*	85 94	68	67	8
	64·70	0 03	1	92·09			
	63·16	0 03	1	97 26			
	59·44	0 00	6	13402 15			
	55·49	0 01	4	09 25			
						53	6
	49 26	0 02	11	20·46			
A.	44 02		1	29·90	45	44	2
	42 33	0 01	A 1	32·98			
			B 6				
	38 63	0 03	1	39·64			
	34 84	0 02	3	46 48			
	33 89	0 01	3	48 20			
	31 23	0 02	2	53 02			
						28	2
			A. 1				
	23 61	0 05	B 5	66 92			
	21 63	0 02	4	70 42			
					16	17	2
	14 09	0·01	3	84 13			
B	07 81		1	95·55		09	6
	06 20	0 02	1	98 49			
	04 21	0 00	1	13502 11			
	02·49	0 00	0	05 23			
					7401	7399	6
	7398·27	0 03	1	12 95			
	96 91	0 00	A 2	17 26			
			B 6				
	94 97	0 01	A 2	18 97			
			B 6				
					7388	86	5
	84 07	0 03	4	38 92			
					80	80	5
	78 71	0 00	1	48 78			
	76·03	0 02	4	55 54			
	71·82	0·02	4	61·44			
	70 04	0 05	1	64 71			
	68 15	0 04	1	68 20			
	67 01	0 00	1	70 29	68	66	6
	65 42	0·02	2	73 22			
	60 29	0 00	8	82·67			
	57·05	0 00	1	88 06			
	55 96	0·03	3	90·67			
	54·17	0 04	4	93 98			
	50 53	00 0	12	13600·73	46	49	8
	44·85	0·05	1	11·24			
					41	42	4

d = diffuse

Table I.—(continued).

Wave-length, 1 Å	Error.	Intensity	Wave-number (Vac.)	Wave-length. (Crose, R.A.)		Intensity.
				1911	1914	
				7337	7337	4
7333 61	0 03	3	13632 00			
				30	31	4
28·29	0 01	8	41 99			
				25	25	6
				21	21	3
19 72	0·05	3	57 95			
18 29	0 01	2	60 62			
16 96	0 01	2	63 11			
				15	15	8
13 02	0 02	5	70·46			
09 88	0 01	6	76 35			
07 19	0 09	6	81 39			
03 73	0·01	1	87·86	04	04	7
01 76	0 01	1	91·56			
00 20	0 01	4	94·32			
7295 62	0 00	8	13703 08	7296	7297	6
00 88	0 00	2	11 98			
89 18	0 01	6	15 18			
87 66	0 01	2	18 04			
86 56	0 01	1	20 11	86	85	5
84 10	0 02	1	24 74			
80 10	0 03	5	32 28			
75 74	0 01	1	40 50	76	76	7
74 62	0 01	1	42 62			
72 16	0 07	1	47 28			
70 07	0 03	10	51 25	69	70	8
67·04	0 01	7	56 97			
A 62 48		5	65 61			
A. 61 01		5	66 69			
B 62 18		12				
60 05	0 05	4	70 21		58	6
54 20	0 02	10	81 32			
53 41	0 02	10	82·82			
51·12	0 01	6	87 17			
44 35	0 00	10	13800 05	45	43	5
40 60	0 02	12	07 22			
				34	34	5
31 06	0 00	10	25 42			
28 07	0 02	9	31 15			
				26	27	3
25 33	0 02	1	36 39			
22 91	0 04	3	41 02	22	22	5
18 35	0 05	3	48 78			
15 10	0 00	3	56 00	16	16	5
11 09	0 05	1	63 71			
10 25	0 00	7	65·31	08	10	3
05 60	0 06	1	74 27			
03 40	0·00	2	78 50			
01 54	0 02	6	82 08	02	02	5
7198 00	0 03	2	88 93			
95 82	0 00	10	93 13	7195	7196	8
88 67	0 02	1	13906 05			
				86	87	8
84 26	0 02	10	15·48			
79 65	0 00	10	24 41	80	80	5
76 47	0 06	5	30·36			

Table I.—(continued).

	Wave-length, I Å	Error	Intensity	Wave-number. (Vac.)	Wave-length. (Crova, R.A.)		Intensity
					1911	1914	
	7178·13	0 01	4	13037 07			
	70·10	0 00	2	42 96	7171	7171	7
	68 92	0 00	3	45·25			
A	67·59		1	47 84			
	66·79	0 06	1	49 53			
					65	65	5
	60·42	0 01	3	61 83			
	58·83	0 02	4	70 77			
	52 42	0·00	3	77 43	53	53	5
					43	43	5
	39 40	0 07	4	14002·91			
	38 17	0·02	4	05·33			
	34 92	0 01	0	11 70			
B.	29 51		0	23 33	30	28	3
	26·65	0 05	1	27 98			
	24·42	0 05	2	32 37			
	21·65	0 00	1	37 83			
	16·73	0 02	3	47·33	19	16	6
	14 38	0 04	2	52·17			
	12·66	0 00	10	55 56			
					07	07	5
	04 53	0 03	1	71 64			
	7099·61	0 00	1	81 39			
	96 39	0 00	6	89·77	7097	7096	6
	91·36	0 00	2	14117 69			
					80	80	3
	75 29	0 04	0	29 80			
					72	72	10
B	67 13		0	46 11	67	67	2
	63 07	0 03	3	54 24			
	61·50	0·00	3	57 37	61	62	3
A	59 19		0	62 04			
B.	55·79		1	68 84	56	56	9
	53 20	0 13	1	74 66			
	49 88	0 01	10	80·74			
					47	48	8
	46 18	0 02	3	88 18			
	44·98	0 02	3	90 60			
	40·73	0 00	2	99 16			
A	39 39		2	14201 86			
	35·70	0 06	10	09 31	36	37	7
	31·41	0 00	1	17 98			
	27 20	0 03	1	26 49			
B.	24 31		2	32 36			
A	23 93		2	33 11			
	22 38	0 05	1	36 27	21	23	5
						13	4
	10·79	0 04	3	59 80			
	04·15	0 06	1	73 32	05	04	4
	02·27	0 01	1	77 15			
					6995	6993	4
	6988 47	0 05	4	14305·33			
					80	80	4
	78 09	0 05	3	26 03			
					72	72	4
B.	65 61		1	52 29	67	67	6

Table I.—(continued).

Wave-length I.Å.	Error.	Intensity	Wave-number. (Vac.)	Wave-length. (Crose, R.A.) 1911.	1914.	Porlezza.	Intensity
6961·76	0·10	4	14360·22	6962	6962	6962·82	12
55·36	0 06	3	73·43				
				54	54		8
B. 49 40		2	85 76				
A 48 96		2	86 66				
				45	45		6
40·58	0 05	6	14404 05	41	41	40 69	10
36 00	0·05	1	13 56	37	37	36·04	12
				30	30		6
				23	23		11
21 31	0·05	1	44·15				
15 98		1	55·27	16	16		12
12·03		0	63·54				
09 64		1	68 53	08	08	09 76	8
06·35		0	75 05				
					04	03·47	7
02 94		2	82 60	00	00	00 19	4
6899 62		2	89·56				
96 55		2	96 01				
90·90		2	14507 89	6887	6887		6
86 32		1 *d*	17 54	83	83		4
80·87		1	29 03				
77·15		4	36·89			6877 52	7
73 32		4	40·76			74·73	6
				72	72		6
67·68		1	56·95				
				63	63		8
52 09		2 *d*	90 06	52	52		2
41·04		10	14613·63			40·52	0
				Piazzi Smith			
				6830·2			5
34 32		2 *d*	27 99				
31·93		2 *d*	33 07				
				29·5			9
28 28		1	40 94	27·7			6
25 72		2	46 44				
23 90		1	50·34	23·5			5
				21 3			6
20 76		2	57·09	20 2		20·38	4

d = diffuse.

Table I.—(continued).

Wave-length, I.Å.	Intensity	Wave-number, (Vac)	Wave-length. (P. Smith)	Wave-length. (Porlezza.)	Intensity
6818 10	5 *d*	14662·79		6817·74	1
15·43	3 *d*	08 54	6815 4		4
			14 5		5
			11·3		10
			08 4		8
			08·2		7
06·55	12	87 67	06·0	06·20	5
02·76	1	95 85	03 5		0
00 62	1	14700 48	6798 1		10
			96 3		6
6793 85	8	15 12			
				6792 65	0
				90 30	1
			86 2		10
80 70	1	43·68			
			47 7		5
72 36	0	61 92			
71 19	0	64 38	71 4		5
68 44	0	70 37	69 3		8
			66 2		0
65 35	0	77 12	65 1		6
60 48	0	87 76	60 0		4
59 51	0	89 88			
56 41	10	96 06		55 82	3
			54 6		3
			50 6		11
48 01	1	14813 13	49 4		5
			45 1		2
			44 7		1
43·83	1	24 28	43 5		1
42 49	2	27 23		42 54	2
38 03	1	37 04	38 3		8
35 29	1	43 07			
33 52	1	46·97	34 3		5
30 34	0	53 99	30 4		4
28 55	2	57 94			
			27 1		4
			26 0		4
23 80	0	68 43	23 3		4
21 21	2	74 16	20 6		3
19 79	2	77 30	17 8		5
17 85	2	81 60			
16·37	4	84 87	15 0	16 90	6
				14 80	8
				13 10	6
07 67	4	14904 20			
			05 4		6
			04 6		8
01 95	8	16 91		01 73	
6099·45	1	22 48	6099·3	6098·94	8
96 89	10	28·18		96 86	1
94 80	6	32 84	94·1	94 78	9
			92 2		7
			90 6		5
88 03	2	47 05	89 2		6
85 37	1	53 90	85·8		4

d = diffuse

Table I.—(continued)

Wave-length. I Å.	Intensity.	Wave-number (Vac)	Wave-length (P. Smith)	Wave-length (Porlezza)	Intensity.
			6684 4		4
6682 24	1	14960 92	82 0		4
			80 7		4
			78 6		5
77 86	4	70 73	77·9	6677 41	4
			75 9		6
74 98	2	77 19	74 8	75 11	8
			71 1		2
70 49	0	87 27	70 0		2
			69 0		1
			68·3		2
			67 8		1
66 25	0	96 80	67 2		1
			64 0		2
61 30	1	15007 94	61 5		2
			56 8		1
			53 5		2
			52 2		1
			48 7		2
47·28	3	39 58	46 2	47 19	2
43 09	2	49 07	43 2	43 31	2
			41 0		2
			38 7		1
36 74	3	63 48	35 1	36 48	8
33 86	3	70 02	32 7	33 47	6
30·30	4	78 11	29 2		8
28 50	1	82 20	27 5		7
				24 84	1
23 90	6	92 67		23·47	1
22 06	6	95 50	22 8	22·82	8
20 78	0	99 79	21 4	20 77	10
19 81	2	15102 00	20·0	19·24	4
17 62	1	06 99		17·49	4
			16 4		4
14 87	1	13 27	13 3		1
11 82	0	20 24	11 6		2
10 95	0	22·24			
09 21	0	26 21	08 5		2
				04 57	1
01 98	3	42 80	01·3		3
6599 74	1	47 93	00 6	00 77	3
97 96	4	52 02	6598 2	6597 58	4
95 75	2	57 10	94 6		5
			92 0		4
89 05	3	72 50		90 90	4
			88 1		8
85 34	1	81 05		85 98	10
			84 7		1
			84 3		7
				79 73	0
			74 3		5
			72·6	72 08	4
70 00	2	15216 51	70·5	70 11	7
			67·5	66 92	9
H_α 62·82	20	33 15	63 1	63·05	15

Fulcher's First Band.

It has been possible to extend Fulcher's first band into the infra-red, and the wave-numbers of the members of the S_1, S_2 and S_3 bands are given in Table II below. The lines marked with an * are in the infra-red; the others in the visible spectrum are taken from Merton and Barratt's table †

Table II

	S_1		S_2		S_3	
Member.	Wave No	Intens	Wave No	Intens	Wave No	Intens
$m =$ 1	16574·14	(10)	16596 41	(7)	16611 43	(10)
2	16294 53	(8)	16315·64	(9)	16330 66	(10)
3	16025 35	(8)	16046 34	(7)	16060 31	(9)
4	15767·10	(6)	15787 28	(5)	15800 73	(8)
5	15520 05	(3)	15539 43	(2)	15552 41	(5)
6	†15284·93	(6)	†15303 77	(4)	15315 93	(4)
7	*15063·48	(3)	*15082 20	(1)	*15092 67	(6)
8	*14857·94	(2)	*14877 30	(2)	*14884 87	(4)
9	*14668 54	(3)	*14687 07	(12)	*14695 85	(1)
10	*14496 01	(2)	*14517 54	(1)	*14529 03	(1)

† These lines were not included in Fulcher's original band but are given by Curtis, 'Roy Soc. Proc.,' A, vol 107, p 573 Their wave-numbers were calculated from the author's measurements.

The intensities of the lines are given in brackets, but those in the infra-red are not on the same basis of estimate as those of Merton in the visible region

Between the first and second member of the S_1 series there is a frequency difference of, roughly, 280 units; between the second and third a difference of 270 units, between the third and fourth 260 units, and so on. That is to say, the first differences decrease in approximate arithmetical progression Now if we plot in a graph the wave-numbers of the spectrum along a set of horizontal x-axes placed one below the other, and so arranged that the wave-numbers in one row are removed from those of the preceding row by a frequency difference of 280, 270, 260, etc, for the first, second, third, etc, row, then a spectrum series, the first differences of which decrease in arithmetical progression starting with $\Delta\nu = 280$, will appear in this graph as a group of lines extending down the graph parallel to the y-axis. Any extension to this "straight-line" series will be more easily decided upon than one to the original parabolic series, so that this method is of particular value in a complicated spectrum such as that of hydrogen. In fig. 1 all the

† *Loc. cit.*

lines in the spectrum from $\nu = 16611$ to $\nu = 14450$ occurring in the region of the band are plotted, the intensity of the spectral line being represented by the

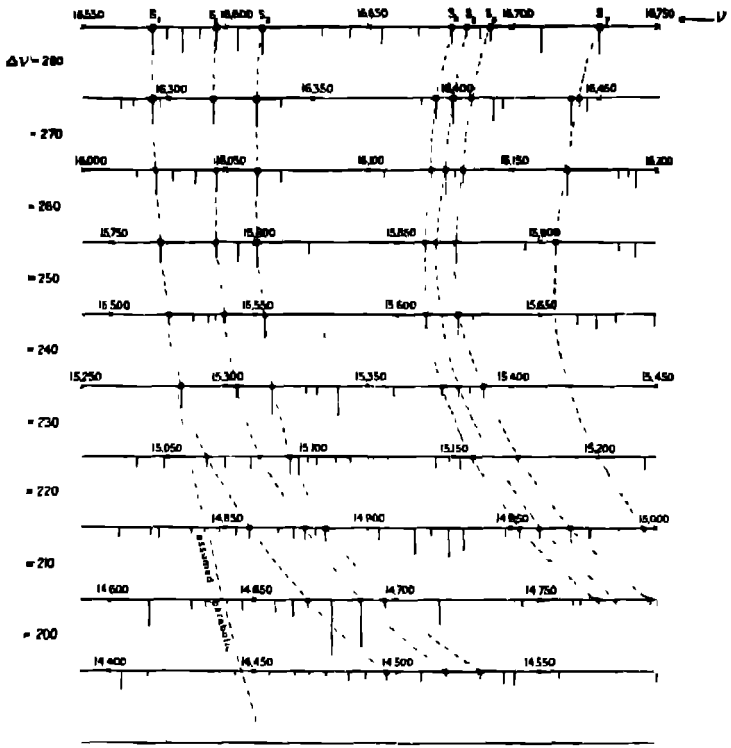

length of the graphed line The members of each of the three series are joined by dotted lines, all three of which are slightly curved, due to the second differences ($\Delta^2\nu \sim 10\ 5$) being not quite equal to the A.P. differences ($d = 10{\cdot}0$) between successive x-axes.

It will be seen upon examination of the graph that even with this simplified representation the choice of an extension is somewhat arbitrary owing to the involved character of the spectrum, and it is necessary to bear in mind the differences—first, second and third—of wave-numbers between successive lines and between corresponding lines in adjacent series. The first six members

in each series have second differences which increase slightly with m (thus 10·4, 10·9, 11·2, 11·9), and Allen* and Curtis† have represented the series by quadratic formulæ in which this small increase has been neglected. The quantum theory of band spectra, in fact, supplies an explanation of the quadratic expression, but it has not yet been extended so as to explain the presence of more complicated terms in the formulæ. A careful examination of the possibility of extending the series, however, shows that extensions in which the parabolic character of the series is maintained are not possible, and that the only extensions possible are such that the second differences continue to increase more and more with m. Hence the whole series from $m = 1$ to $m = 10$ are better represented by formulæ of the type $\nu = A + Bm + Cm^2 + Dm^3$. This formula gives good agreement between observed and calculated values of lines for the S_1 and S_2 series, as shown in Table III, where the "O − C" is given for each line, but it is not so good for the S_3 series, where a fourth term

Table III.—"O − C" for S_1 and S_2 series.

m	− 1	2	3	4	5	6	7	8	9	10
S_1	−0 38	−0 83	−0·29	+0 63	+1·07	+0 59	−0 05	−0·07	−0 06	−0·53
S_2	−1 38	−1 79	−0·10	+1·19	+1·78	+1 36	+0 55	+0 70	−0 92	−1 38

is apparently necessary for the accurate representation of the series. The calculated constants for the S_1 and S_2 series are given in Table IV. The extent of this deviation from the parabolic formula is shown graphically on p. 208

Table IV.—Constants for the S_1 and S_2 series

		A.	B	C	D
Leading line $m = 1$	S_1	16861·97	− 291·22	3·58	0 188
	S_2	16836 92	− 292 06	3 41	0·213

by the dotted line which represents the S_1 series assumed to be purely parabolic.

Passing to the other series $S_4 - S_7$ of the first band, we find again that it is impossible to extend these series in a parabolic form, and the extensions suggested follow the general trend of the earlier series, as shown in the figure. As these are missing lines in the visible and infra-red regions, no formulæ have been calculated; the wave-numbers only are given in Table V.

* 'Royal Soc. Proc.,' A, vol 106, p. 69 (1924).

† 'Roy. Soc. Proc.,' A, vol 107, p. 570 (1925)

Table V.—Extension to First Band

	$m = 10$.		$m = 9$		$m = 8$.		$m = 7$.		$m = 6$		$m = 5$
S_1	14496·01 (2) *21·53*	*172·53*	14668·54 (3) *19·13*	*189·40*	14857·94(2) *19·36*	*205·54*	15063·48 (3) *18·72*	*221·45*	15284·93 (6) *18·84*	*235·12*	15520·05 (3) *19·38*
S_2	14517·54 (1) *11·49*	*170·13*	14687·67(12) *8·18*	*189·63*	14877·30 (2) *7·57*	*204·90*	15082·20 (1) *10·47*	*221·57*	15303·77 (4) *12·16*	*235·66*	15539·43 (2) *12·93*
S_3	14529·03 (1)	*166·82*	14695·85 (1) *75·52*	*189·02*	14884·87 (4) *69·03*	*207·80*	15092·67 (6) *64·43*	*223·36*	15315·93(10) *59·98*	*236·48*	15552·41 (5) *58·59*
S_4			14770·37 (0) *6·75*	*183·53*	14953·90 (1) *7·02*	*203·20*	15157·10 (2)	*218·81*	15375·91 (2) *4·90*	*235·00*	15610·91 (1)
S_5			14777·12 (0) *10·64*	*183·80*	14960·92 (1) *9·81*				15380·81 (2) *9·72*		
S_6			14787·76 (0) *25·37*	*182·97*	14970·73 (4) *26·07*	*201·77*	15172·50 (3)	*218·03*	15390·53 (2)	*231·49*	15622·02 (6)
S_7			14813·13 (1)	*183·67*	14996·80 (0)						

Table V is constructed as an extension to Allen's* table of the Fulcher band, and is introduced for completeness. The last column of his table is reproduced as the first column here, $m = 5$, and the table extends to $m = 10$. The first differences, horizontal and vertical, are given in italics and the intensities in brackets.

The Zeeman Effect on the Secondary Spectrum.

Dufour† examined the secondary spectrum of hydrogen under the influence of a strong magnetic field (H = 11,700 gauss), and found that in the green and yellow region of the spectrum, lines could be grouped into three classes, those showing a separation of 0·12 to 0·18 A.U —a "normal" effect,—those showing a distinct separation but less than 0·12 A, and those in which no effect was visible More recently, Kimura and Nakamura‡ showed that in a field of 7,000 g. there occurred a selective reduction of intensity of the lines—the resolving power was too small to separate any Zeeman components if present—those least affected being those which Dufour stated showed no Zeeman effect

The author applied a field of 7,000 g. transversely to the capillary tube at the end nearest to the spectrograph, the pole pieces of the magnet being 1½ cms apart. The discharge became highly constricted and turned yellowish, the secondary spectrum being reduced in intensity by a half and reduced with respect to H_α. Water was sprayed on to the tube to prevent excessive heating, and the discharge was then increased till the intensity of the secondary spectrum was restored to its former value. A Rochon "double-image" prism separated the beam into two components of almost equal intensity (the non-rotating spectrum showing H_α as a doublet) By turning the prism until the two images were in the same vertical line they could be photographed on the same plate. An exposure of 11 hours was given, but, due to an accident, the rotating image spectrum only received an eight-hour exposure. The region of the spectrum photographed was the 6349 — 6921 A. only.

The effect on the lines was remarkable. Every line increased in intensity at its extremities at the expense of the central portion, showing that the discharge was split into two streams in the field, the one above the other Also the lines of the non-rotating spectrum were widened at their intense portions, whilst the lines of the rotating spectrum remained at constant width. From the photograph it was found that there was no selective action of the field; every line of the non-rotating image was almost equally affected (widened), though

* *Loc. cit.*, p 75.

† 'Phys. Z.,' vol 10, p. 135 (1909).

‡ Kimura and Nakamura, 'Jap. J. of Physics,' vol 1, Nos 9, 10 (1923)

it was impossible to distinguish two separate components of any line. There was no marked relative intensity change between corresponding lines in the two spectra, and a comparison with the plate A showed a similarity of intensity in every line. Thus there was no "normal" Zeeman effect in the region photographed; any "abnormal" effect was masked by a widening shown by every line of the "non-rotating" spectrum.

Summary.

Using specially sensitised plates a large number of lines have been photographed in the many-lined spectrum of hydrogen in the infra-red. Their wave-lengths are recorded in Table I, together with the corrected wave-numbers, and wave-lengths measured by previous investigation. Photographs of the spectrum are reproduced in Plate 8.

An extension has been made to Fulcher's first band in all seven series. To represent these adequately a term Dm^3 is required in the formula. The complete bands are set out graphically in the figure.

The effect of a transverse magnetic field was noted. No selective effect could be detected, but there was a general broadening of all the lines.

In conclusion, the author desires to express his indebtedness to Prof. S. R. Milner for his constant assistance and direction during this work.

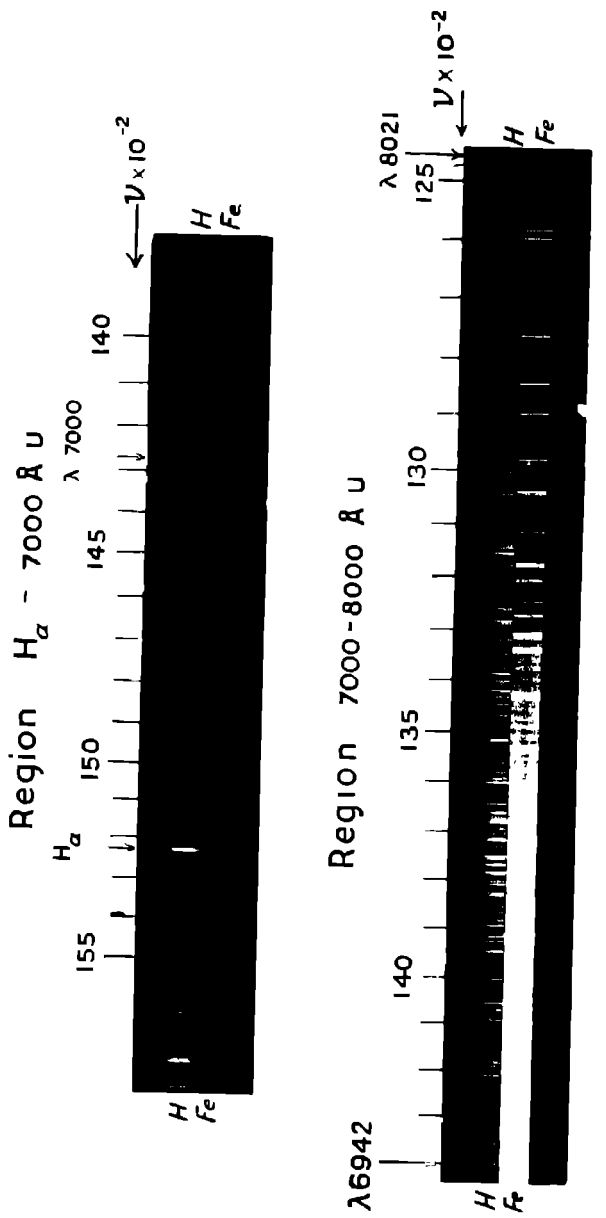
Region H_α - 7000 Å U
H_α
λ 7000
155
150
145
140
$V \times 10^{-2}$
H
Fe
H
Fe
Region 7000-8000 Å U
λ6942
140
135
130
125
λ 8021
$V \times 10^{-2}$
H
Fe
H
Fe

(Facing p. 212.)

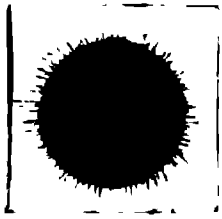

Fig 1

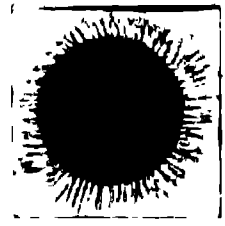

Fig 2

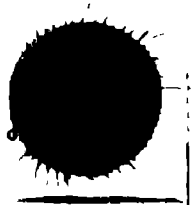

Fig 3

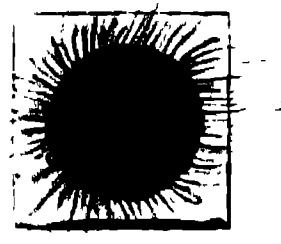

Fig 4

(*Facing p* 211)

A further Note upon "Inter-traction."

By Sir Almroth E. Wright, M D , F R.S.

(Received June 22, 1926)

(Plate 9)

I pointed out in a previous communication* that a mixture of fluids can be brought about not only by the operations of mechanical convection and diffusion, but also by the impulsion of a force which can very rapidly carry down a lighter overlying fluid into a heavier underlying fluid in the form of characteristic pseudopodial streamers, conveying at the same time the heavier underlying fluid into the lighter superjacent fluid in the form of a palisade of ascending streams. I have ventured to call the agency by which this reciprocal in-streaming is produced —*inter-traction*.

These phenomena which I described as occuring when salt, and also sugar, solutions are brought into contact with albuminous solutions can, as Schoneboom† showed, be obtained also with a very wide range of substances; and they have been ascribed by him to the operations of negative interfacial tension, and identified with phenomena theoretically anticipated by Clerk-Maxwell. Adam and Jessop, in a further communication,‡ have insisted that the pseudopodial streaming is attributable to operations of diffusion and resulting changes in specific gravity, and they have stressed the point that the characteristic appearances can be obtained only when the lighter is superposed upon the heavier fluid, and not when the fluids are disposed side by side In view of the fact that the conclusion that horizontal streaming cannot be obtained rests only upon experiments conducted by filling fluids of different specific gravity into adjoining cell compartments, and then removing the dividing wall, it seemed desirable to try for horizontal inter-traction with a technique which would get rid of the complication of the heavier fluid sinking to the bottom and the lighter going to the top of the vessel, and would allow of more accurate and deliberate observation. The quite simple technique now to be described satisfies these desiderata.

A disc of filter paper is fixed, with a minute pellet of plasticine, to the surface

* 'Roy. Soc. Proc.,' B, vol. 92, p. 118 (1921).
† 'Roy. Soc. Proc.,' A, vol. 101, p 531 (1922).
‡ 'Roy. Soc. Proc.,' B, vol 98, p. 206 (1925).

of a cover-glass of larger diameter, and the four edges of the cover-glass are now rimmed with paraffin in such a manner as to permit of the cover-glass with attached disc being conveniently floated upon any desired fluid That done the filter paper is impregnated with an albuminous fluid—such as serum—coloured with an anilin dye, and the cover-glass is now set afloat upon a watch glass of hypertonic salt solution (conveniently a 4·5 per cent solution of NaCl, for this is a little heavier than the serum). The streaming effects which are characteristic of inter-traction now come into view almost immediately, presenting at first the appearance shown in the photographs figs. 1 and 2 The streamers then extend outwards upon the surface until, after about 5 minutes, they stretch out far beyond the limits of the cover-glass (figs. 3 and 4).

The Molecular Fields of Hydrogen, Nitrogen and Neon.

By J. E Lennard-Jones Reader in Mathematical Physics, The University, Bristol, and W R. Cook, B Sc , The University, Bristol.

(Communicated by Prof S Chapman, F R.S —Received May 26, 1926)

§ 1. *Introduction*

Since the publication of some recent papers on molecular fields,* some new experimental information has become available, which permits of further determinations of the forces between molecules Hydrogen, nitrogen and neon are now added to the list of gases whose isotherms have been obtained by the precise methods of Holborn and Otto † The publication of these results for neon is of special interest, because one determination of the molecular field of neon has already been made,‡ and it is valuable to have another independent method of attacking the same problem.

A method of determining molecular fields from measurements of the isotherms of a gas has been described in an earlier paper § It proceeds on the assumption that the molecular field is spherically symmetrical and that it can be expressed in terms of inverse power laws, one to represent the repulsive force and one to

* 'Roy. Soc Proc ,' A, vol. 106, pp. 441, 463, 709 (1924) ; vol. 107, p. 157 (1925) ; vol. 109, pp. 476 and 584 (1925).

† 'Z f. Physik.,' vol. 23, p. 77 (1924) , vol. 30, p 320 (1924) ; vol. 33, p. 1 (1925).

‡ 'Roy Soc. Proc ,' A, vol 107, p 157 (1925).

§ 'Roy. Soc Proc.,' A, vol. 106, p 463 (1924).

represent the cohesive force. The method shows whether any particular model is a suitable one or not, and, when it is, leads to a determination of the force constants.

It is satisfactory to find that the application of this method to the isotherms of neon, as given by Holborn and Otto, leads to results which are almost identical with those found in a former paper from its viscosity and thermal conductivity.

Although the theory of the equation of state is applicable only to fields which are spherically symmetrical, it has been applied to hydrogen and nitrogen It was not expected that there would be agreement between theory and experiment in these cases. The point of interest was rather to examine the extent of the divergence. There proves, however, to be a remarkably close agreement between the two, from which the inference may be drawn that hydrogen and nitrogen can both be adequately represented by spherical fields This result is interesting in view of the theories of the structure of the nitrogen molecule which have recently been proposed to explain its spectral lines *

In view of these results, the evidence of viscosity as to the molecular fields of hydrogen and nitrogen has also been examined. In the case of hydrogen, careful measurements have been made from 20° absolute to 457 3° absolute and these provide a stringent test for any theoretical formula. However, that which corresponds to a spherically symmetrical field of an inverse power type seems adequately to fulfil this test. Furthermore, the theory leads to a value of the force constant which is in remarkable agreement with that found by the othe. method mentioned above A similar agreement was found in the case of helium in an earlier paper †

The viscosity data for nitrogen are not so extensive nor so numerous as those for hydrogen, but they have none the less been used to make theoretical calculations of the repulsive force constants In this case there is not the same agreement between the results obtained from the two methods. The discrepancy, curiously enough, is about the same as that found in the case of argon in earlier papers.‡ It is singular that the two methods should have led to concordant results in the cases of hydrogen, helium and neon, but discordant results in the cases of nitrogen and argon. Reasons are given for supposing that in the latter cases the results obtained from the equation of state are more reliable. All the results about the molecular fields of gases, obtained in this and preceding papers, are here collected and compared.

* Birge, 'Nature,' vol. 117, p. 300 (1926).

† 'Roy. Soc. Proc.,' A, vol. 107, p. 157 (1925).

‡ 'Roy. Soc. Proc,' A, vol. 106, pp. 441 and 463 (1924).

§ 2. *The Equation of State of Neon.*

When an earlier paper was written on the atomic field of neon, there was no satisfactory information available about its equation of state. This need has now been met by the work of Holborn and Otto,* who have extended their accurate pv-measurements of gases to include neon. Their experiments cover the range of temperature $-183°$ C. to $400°$ C. for pressures up to 100 atmospheres. They show that each equation can be represented by an equation of the type

$$pv = A + Bp + Cp^2, \tag{2·01}$$

when the coefficients are suitably chosen. These coefficients, usually referred to as *virial coefficients*, are functions of the temperature only.

It is the coefficient B and its variation with temperature which concerns us in this paper, for a theoretical formula has been obtained for it on the assumption that molecules repel according to the law $\lambda_n r^{-n}$ and attract according to the law $\lambda_m r^{-m}$. According to this calculation,†

$$B_N = \tfrac{2}{3}\pi\nu\left(\frac{\lambda_n}{n-1}\frac{m-1}{\lambda_m}\right)^{3/(n-m)} F(y), \tag{2·02}$$

where ν is the molecular concentration at normal temperature and pressure, and

$$F(y) = y^{3/n-m}\left\{\Gamma\left(\frac{n-4}{n-1}\right) - \sum_{r=1}^{\infty} f(r)y^r\right\}. \tag{2·03}$$

In this expression y is a function of the temperature given by

$$y = \frac{\lambda_m}{(m-1)\,kT}\left(\frac{n-1}{\lambda_n}kT\right)^{(m-1)/(n-1)} \tag{2·04}$$

and the coefficients $f(r)$ are written for

$$f(r) = \frac{3\Gamma\left(\frac{r\sqrt{m-1}+n-4}{n-1}\right)}{r!\,(r\sqrt{m-1}-3)} = \frac{3\Gamma\left(\frac{r\sqrt{m-1}-3}{n-1}\right)}{r!\,(n-1)}. \tag{2·05}$$

The subscript N is added to B to emphasise the fact that it is referred to the concentration at normal temperature and pressure, whereas the coefficient determined by Holborn and Otto refers to a unit of pressure of one metre of mercury. The results of Holborn and Otto can be transformed to the more usual units by means of the formula‡

$$B_N = \frac{lB}{A_0 + B_0 l + C_0 l^2}, \tag{2·06}$$

* Holborn and Otto, 'Zs. f. Phys.,' vol. 33, p. 1 (1925).

† 'Roy. Soc. Proc.,' A, vol. 106, p. 463 (1924).

‡ 'Roy. Soc. Proc.,' A, vol. 106, p. 474 (1924).

where l is the magnitude of an atmosphere in metres of mercury and A_0, B_0, C_0, are the values of the coefficients in equation (2·01) for the isothermal 0° C. For neon, $A_0 = 0{\cdot}99937$, $B_0 = 0{\cdot}625\ 10^{-3}$ and $C_0 = 0\ 49.10^{-6}$. The values of B_N, or rather log B_N, determined in this way from the results of Holborn and Otto (B, in the second column), are given in the following table :—

Table I.—The Virial Coefficients of Neon

T	B 10^3	log B_N
400	0 8060	$\bar{4}{\cdot}7869$
300	0 8080	$\bar{4}{\cdot}7880$
200	0 7660	$\bar{4}$ 7648
100	0 6960	$\bar{4}$ 7232
0	0 6257	$\bar{4}{\cdot}6770$
−50	0 5350	$\bar{4}{\cdot}6089$
−100	0 3786	$\bar{4}$ 4588
−150	0 0058	$\bar{3}$ 6440
−182 6	−0 4800	$\bar{4}$ 5618 (n)

When the laws of force assumed in this paper sufficiently represent actual molecular forces, the graph of log F (y) plotted against log y on a suitable scale becomes identical with that of log B_N plotted against log T. For each pair of values of n and m there is a definite theoretical curve, and a comparison of a series of these curves with the experimental one (the log B_N curve) picks out those values of n and m which can be regarded as suitable. To show how the shape of these curves depends on n and m a number of curves have been given in a former paper *. When agreement is secured between the theoretical and experimental curves, a knowledge of X and Y, the co-ordinates of the parallel transformation necessary to obtain this result, determines λ_n and λ_m, for they are connected by the linear equations†

$$\log \frac{\lambda_n}{n-1} = \frac{n-1}{n-m}X + \frac{n-1}{3}Y - \frac{n-1}{3}\log\frac{2\pi\nu}{3} + \log k \quad (2{\cdot}07)$$

$$\log \frac{\lambda_m}{m-1} = \frac{n-1}{n-m}X + \frac{m-1}{3}Y - \frac{m-1}{3}\log\frac{2\pi\nu}{3} + \log k \quad (2\ 08)$$

The following curves have been found to give good agreement in the case of neon, viz (i) $n = 9$, (ii) $n = 11$, (iii) $n = 14\frac{1}{2}$, and (iv) $n = \infty$ (rigid sphere), with $m = 5$ in each case. As in the case of argon, considered in a former paper, the experimental results allow of considerable latitude in the value of n, the index of the repulsive field. However, by calculating the sum of the squares

* 'Roy. Soc. Proc.,' A, vol. 107, p. 157 (1925).

† 'Roy. Soc. Proc.,' A, vol 106, p 469 (1924)

of the distances of the experimental points from the theoretical curve when the best fit is secured, a definite order of priority is indicated. This places $n = 11$ first, and $n = \infty$ last * The curve for the first model together with the experimental points is shown in fig. 1.

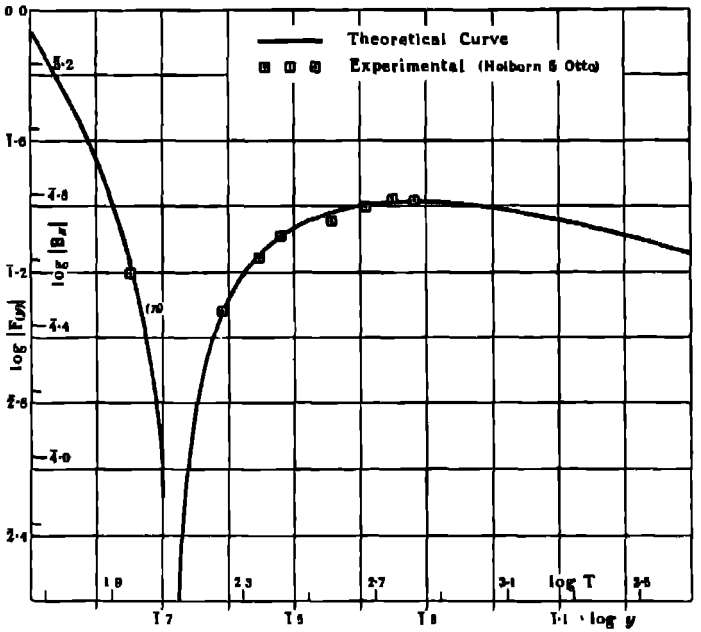

FIG 1.—Theoretical Curve for the Second Virial Coefficient for the Model, $\lambda_a r^{-a} - \lambda_b r^{-b}$, with the Experimental Values for Neon.

The order of accuracy to be expected from the method may be gauged from the following results. These give for two cases the outer limits of X and Y, for which the curves could be said to be in agreement, and the corresponding values of the force constants.

n	X.	Y	λ_a.	λ_m	σ_a 10^8
9	0·725	5·363	$6\ 07\ 10^{-74}$	$2{\cdot}17.10^{-44}$	4·90
	0·733	5 374	$6{\cdot}74.10^{-74}$	$2{\cdot}22\ 10^{-44}$	5 03
∞	1·570	4 897	0	$6\ 82.10^{-43}$	2·41
	1·605	4 916	0	$7\ 85\ 10^{-43}$	2·44

* The sum of the squares of the distances for $n = 9$, 11, 14½ and ∞ were in the ratios 223 : 135 : 144 : 1304.

As a convenient method of comparing the λ_n's, which are of different orders of magnitude, a quantiy σ_n is calculated, as in former papers, from the formula

$$\sigma_n = \left(\frac{2\lambda_n}{3 . \overline{n-1}\ k}\right)^{(1/n-1)} \qquad (2\cdot09)$$

This is called a generalised " diameter " because it corresponds to a diameter in the ordinary sense when $n = \infty$.

The results obtained from the best fits of the curves are given in Table II

Table II.—The Force Constants and " Diameters " of Neon from the Equation of State

n.	X	Y.	λ_n	λ_∞	σ_n 10^8	$\sigma_n \cdot 10^8$ (viscosity).
9	0 729	3 3655	$6\ 32.10^{-74}$	$2\cdot23.10^{-44}$	4 99	5 02
11	0 893	3 2580	$4\ 38.10^{-88}$	1 72	4 29	4 30
14½	1 0578	3·1573	$2\ 22\ 10^{-116}$	1 33	3 70	—
∞	1 588	2 9050	0	0 73	2 42	2 35

In the last column are included the corresponding results of a preceding paper* from viscosity and thermal conductivity The agreement between the two sets of results is striking. It is significant that the agreement is best for that model (viz., $n = 11$) which had previously been decided upon as the correct one by the use of crystal measurements.† The two sets of results are shown graphically in fig. 4, along with the " diameters " of other gases

§ 3 *The Molecular Fields of Hydrogen and Nitrogen*

(i) *The Equation of State.*—Earlier measurements of the isotherms of hydrogen —and there are many—may be regarded as displaced by the precise measurements recently made by Holborn and Otto‡ These range from −183° to 200° C., a wider range than has previously been attempted. The values of the second virial coefficient, as given by them, and the corresponding values for ordinary units§ are given in Table III. In the same table are included the values for nitrogen, also deduced from the work of Holborn and Otto.

* ' Roy. Soc Proc ,' A, vol. 107, p 168, Table VI (1925)

† ' Roy. Soc Proc ,' A, vol 109, p. 485 (1925).

‡ Holborn and Otto, *loc. cit.*

§ *See* preceding paragraph

Table III.—The Virial Coefficients of Hydrogen and Nitrogen.

T.	Hydrogen.		Nitrogen.	
	B 10^3.	log B_H.	B . 10^3	log B_N
400			1·38086	$\bar{3}$·0206
300			1 21257	$\bar{4}$·9642
200	0 02168	$\bar{4}$ 8452	0·90133	$\bar{4}$ 8353
150			0·67717	$\bar{4}$·7112
100	0 01400	$\bar{4}$ 8416	0 38057	$\bar{4}$ 4374
50	0 89000	$\bar{4}$·8300	−0 01514	$\bar{5}$ 0606 (*n*)
0	0·82004	$\bar{4}$·7949	−0 60716	$\bar{4}$ 6638 (*n*)
−50	0 71000	$\bar{4}$·7319	−1 54934	$\bar{3}$ 0706 (*n*)
−100	0 53700	$\bar{4}$ 6106	−3 04600	$\bar{3}$ 3642 (*n*)
−130			−4 68594	$\bar{3}$ 5513 (*n*)
−150	0 17300	$\bar{4}$·1187		
−183	−0 32500	$\bar{4}$·3925 (*n*)		

As the theoretical work referred to in the preceding paragraph refers only to spherically symmetrical fields, it would not be expected to apply to diatomic gases such as hydrogen and nitrogen. The attempt to apply the theory to these gases was in the first place purely tentative, for it was felt that it would be of interest to know to what extent theory and observation could be brought into agreement. The application of the method described in the preceding paragraph leads, however, to a striking agreement in both cases. This is evident from figs. 2 and 3. For hydrogen the molecular models $n = 9$, $m = 5$, and $n = 11$, $m = 5$ are the most suitable, higher values of n involving greater discrepancies.* However, the readings of X and Y are given for the same models as in the case of neon.

Table IV.—Force Constants of Hydrogen from Equation of State.

n	X	Y	λ_n	$\lambda_m 10^{44}$	$\sigma_n 10^8$cms
9	0 7045	$\bar{3}$ 446	$9\ 20\ 10^{-74}$	2 54	3·23
11	0·8640	$\bar{3}$ 3405	$7\ 38.10^{-88}$	1 98	4·52
14½	1 0248	$\bar{3}$ 245	$4\ 89.10^{-114}$	1 56	3·92
∞	1·5380	$\bar{4}$·991	0	0 85	2 59

The limits of accuracy were about the same as those given above for neon. The corresponding results for nitrogen are given in Table V†. In this case the model $n = 9$ is definitely the most suitable.

* The sum of the squares of the distances of the experimental points from the theoretical curves for $n = 9$, 11, 14½ and ∞ were in the ratios 52 : 54 · 98 : 570.

† The sum of the squares in this case for $n = 9$, 11, 14½ and ∞ were in the ratios 15 : 42 : 64 : 343, with the same unit of measurement as used above for neon and hydrogen.

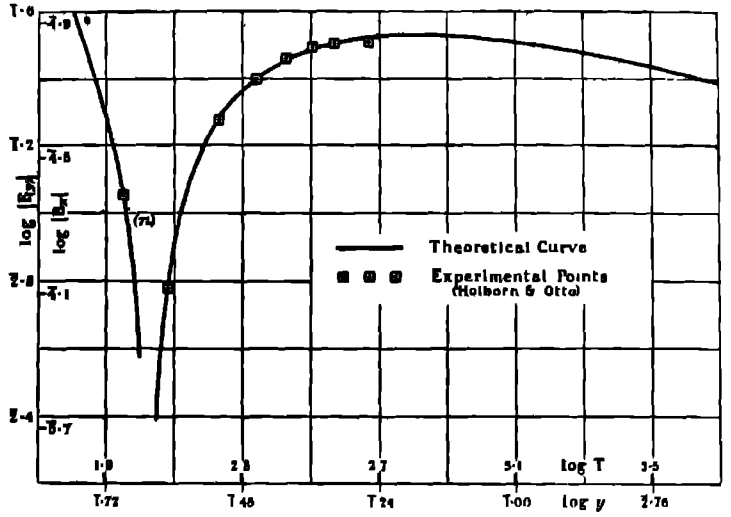

FIG. 2.—Theoretical Curve for the Second Virial Coefficient for the Model, $\lambda_{11}r^{-11} - \lambda_6 r^{-6}$, with the Experimental Values for Hydrogen.

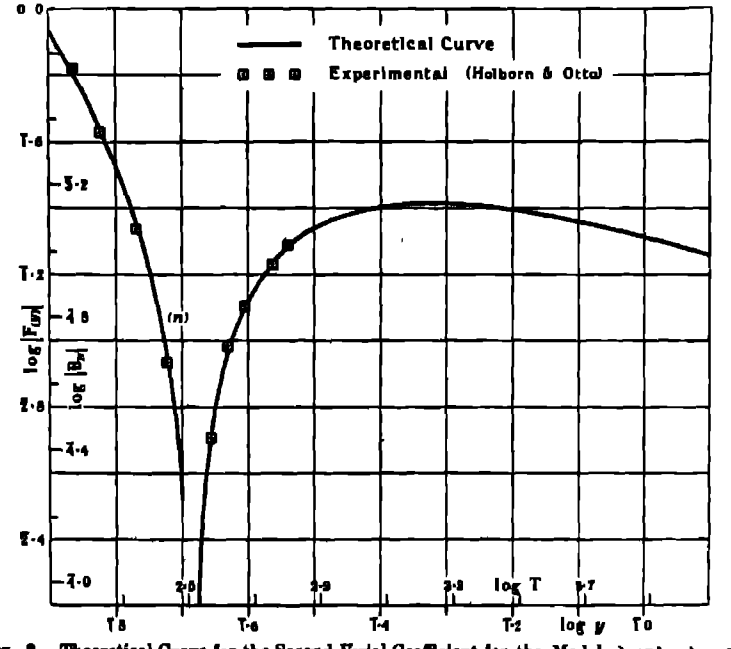

FIG. 3.—Theoretical Curve for the Second Virial Coefficient for the Model, $\lambda_9 r^{-9} - \lambda_6 r^{-6}$, with the Experimental Values for Nitrogen.

Table V.—Force Constants of Nitrogen from Equation of State.

n.	X.	Y.	λ_n.	$\lambda_n \cdot 10^{44}$.	σ_n 10^8 cms.
9	0·941	3 732	$1\ 58\ 10^{-79}$	16 19	7 46
11	1·1528	3·641	$2\cdot28.10^{-97}$	15·06	6 36
14½	1 3615	3 537	$3\cdot16\ 10^{-128}$	12 29	5·42
∞	2 031	3 342	0	7 74	3·38

(ii) *The Viscosity of Hydrogen*.—The observations of Markowski* on the viscosity of hydrogen, supplemented by the joint work of Kamerlingh Onnes, Doraman and Weber† at low temperatures, provide results from 20° absolute to 457·3° absolute. Between these temperatures the viscosity of hydrogen increases its value tenfold and so there is ample experimental information for the testing of any theoretical formula. As Kamerlingh Onnes has shown, this variation of viscosity can be represented to a remarkable degree by the formula

$$\mu = \mu_0 \left(\frac{T}{T_0}\right)^s, \qquad (3\cdot01)$$

with $\mu_0 = 0\cdot844.10^{-4}$ at $T_0 = 0°$ C. and $s = 0\cdot695$. The observed values and those calculated by this formula, together with those calculated from the usual Sutherland formula, are reproduced from the paper by Kamerlingh Onnes in Table VI.

Table VI.—The Viscosity of Hydrogen.

T	μ_{obs} 10^7	$\mu_S 10^7$	$\mu_{calc.}$ 10^7
457 3	1212	1203	1207
373 6	1046	1050	1052
293 95	—	887·2	886
287 6	877	874	875
273 0	844	843	843
261 2	821	814	816
255 3	802	800	803
233 2	760	747	757
212 9	710	697	709
194 4	670	648	666
170·2	609·3	582	608
89 63	392 2	326	389
70 87	319 3	257	329
20·04	105–111	58	137

Although the latter formula was given as an empirical equation, it corresponds

* 'Ann. d. Physik,' vol. 14, p. 742 (1904), also Schmitt, 'Ann d. Physik.,' vol. 30, p. 398 (1909).

† 'Comm. Phys. Lab. Leiden,' No. 134a (1913).

to a theoretical formula for viscosity when molecules repel according to an inverse power law. If this law be $\lambda_n r^{-n}$, the formula is*

$$\mu = \varepsilon_n \frac{B_n \; m^{\frac{1}{2}}}{\lambda_n^{2/(n-1)}} T^{\frac{n+3}{2(n-1)}}, \qquad (3\cdot02)$$

where m is the mass of the molecule, and ε_n and B_n are numbers, depending only on n, the former lying between the narrow limits 1·000 and 1·016,† and the latter being given by

$$B_n = \frac{5\,\pi^{\frac{1}{2}}\,k^{(n+3)/2(n-1)}}{4\,I_3(n)\,\Gamma\left(4-\frac{2}{n-1}\right)2^{(n-3)/(n-1)}} \qquad (3\cdot03)$$

In this expression, k is the usual gas constant ($1\cdot372\,.\,10^{-16}$).‡ $I_3(n)$ is a function of n, its value having been computed for some values of n by Chapman,§ and for others by one of the present authors ||

Since the index s of the empirical formula is related to n by the relation

$$s = \tfrac{1}{2} + \frac{2}{n-1}, \qquad (3\cdot04)$$

we conclude that viscosity results for hydrogen require a value $n = 11\cdot2$.

It is, however, more convenient to have an integral power law, and so we choose $n = 11$. For this value we can find the appropriate value of λ_n from the formula given above The numerical values to be inserted in the formula are $\varepsilon_n = 1\cdot006$, $I_3(n) = 1\cdot0008$, $\mu_0 = 0\;844\;\;10^{-6}$, $T_0 = 273\cdot1$ and $m = 3\cdot32\;\;10^{-24}$ grams. The result proves to be

$$\lambda_n = 7\cdot19\,.\,10^{-29}.$$

This result is in remarkable agreement with that obtained above for the same model by the other method. They are compared in the following table :—

Table VII.—Repulsive Force Constants of Hydrogen for $n = 11$.

—	Equation of State	Viscosity
λ_n	$7\cdot38\;10^{-29}$	$7\;19\;10^{-29}$
"σ_n"	$4\cdot52\;10^{-8}$	$4\;51\;10^{-8}$

* For references, see ' Roy. Soc. Proc.,' A, vol. 107, p. 165 (1925).

† Chapman, ' Phil Trans ,' A, vol. 216, p. 279, Table V (1915).

‡ Jeans, ' Dynamical Theory of Gases,' 3rd edn., p. 119 (1921).

§ ' Memoirs Manchester Lit. and Phil. Soc .' vol. 66, No. 1 (1922).

|| ' Roy. Soc. Proc ,' A, vol. 106, p. 456 (1924).

We conclude, therefore, that a repulsive force of the inverse 11th power type satisfies the requirements of both viscosity and equation of state results. Only the latter method determines the corresponding attractive field. This is found (Table IV) to be of the inverse 5th power with a force constant $\lambda_m = 1 \cdot 98 . 10^{-44}$. The molecular field of hydrogen may therefore be regarded as given by Table VIII, the repulsive force constant being the mean of the two results given in Table VII.

Table VIII —The Molecular Field of Hydrogen

n	m	λ_n.	λ_m	"σ_n."
11	5	$7 \cdot 29 . 10^{-89}$	$1 \cdot 98 . 10^{-44}$	$4 \cdot 52 \cdot 10^{-8}$

The attractive field is evidently small* and presumably has an inappreciable effect on viscosity.

(iii) *The Viscosity of Nitrogen* —The viscosity of nitrogen has been measured at various temperatures by Schmitt,† Vogel‡ and Kia Lok Yen.§ Their results, if plotted as a function of temperature, lie on a smooth curve and are evidently consistent. They are given in Table X below.

The simple theoretical formula, which has been used for hydrogen, is found to be unsuitable for nitrogen, from which we infer that nitrogen cannot be represented by a repulsive field alone A more general formula has, however, been given, which applies to molecules possessing a weak attractive field as well as a repulsive field of the inverse power type. This formula is||

$$\mu = \mu_0 \left(\frac{T}{T_0}\right)^{s/2} \frac{T_0^{\frac{n-s}{2n-2}} + S}{T^{\frac{n-s}{2n-2}} + S}, \qquad (3{\cdot}05)$$

where S is a constant, independent of temperature, which represents the effect of the attractive field

To secure the best fit between theory and experiment, various values of n are chosen, and the values of S, required to give agreement between theory and experiment, are calculated from the observed values of μ. The values of μ at the temperatures 23° C. and 15·4° C. are, however, omitted from this calcula-

* Compare the corresponding attractive force constants for nitrogen in Table V above.

† 'Ann. d. Physik.,' vol. 30, p. 398 (1909).

‡ 'Ann. d. Physik ,' vol. 43, p. 1258 (1914).

§ 'Phil. Mag.,' vol. 38, p. 582 (1919).

|| 'Roy. Soc. Proc.,' A, vol. 106, p. 441 (1924).

tion owing to the small range of temperature between them and the temperature of 0° C., which is taken as standard. The results are given in the next table.

TABLE IX.—Values of the Attractive Constant (S) of Nitrogen.

T.	$n = \infty$	15	11	9
455·8	114·03	20 59	6 509	−0 5058
373 2	108 06	20 67	7 171	0 3296
81 6	101·94	32·24	16 975	11·2172
Value used	108·01	24 50	10 885	3 680

The average values are given at the foot of each column. With these values of S, the viscosity is then calculated from the above formula and the results are given in Table X along with the observed values. The value $n = \infty$ (corresponding to rigid sphere + attractive field) is clearly the most successful. The smaller the value of n, the greater the discrepancy between the observed and calculated values. This is contrary to the requirements of the equation of state considered above. There the smaller values of n were the more successful.

Table X.—The Observed and Calculated Viscosity of Nitrogen.

T	$\mu_{obs.}10^4$	Authority	$\mu_{calc.}10^4$			
			$n = \infty$	15	11	9
455·8	2 458	(1)	2 445	2 479	2 493	2 505
373 2	2·123	(1)	2 123	2 135	2 140	2 144
296 1	1·7648	(2)	1·787	1 787	1 788	1·788
288 6	1 747	(1)	1 751	1 750	1 752	1 753
273 1	1·678	(3)	(1 678)	(1 678)	(1 678)	(1·678)
81·6	0·560	(3)	0·551	0·593	0 612	0 630

(1) Schmitt, *loc cit.* (2) Kia Lok Yen, *loc. cit* (3) Vogel, *loc cit*

The appropriate force constants for these models can be calculated from the formula*

$$\lambda_n^{\frac{2}{n-1}} = \frac{B_n\ m^{\frac{1}{2}}}{\mu_0}\ \frac{T_0^{3/2}}{T_0^{\frac{n-3}{n-1}} + S}, \qquad (3\cdot06)$$

with the same notation as used in equation (3·02) above. The results are given in Table XI.

* 'Roy. Soc. Proc.,' A, vol. 106, p. 441, eqn (7·01), (1924).

A general formula for S, which represents the effect of the attractive field, has not been worked out and so it is not as yet possible to determine the attractive force constants from viscosity data

Table XI —Repulsive Force Constants of Nitrogen.

n	9	11	15.	∞
λ_n	$7\ 59\ 10^{-78}$	$9\ 08\ 10^{-88}$	$1{\cdot}17\ 10^{-117}$	0
$\sigma_n 10^8$ cms.	6·81	5 81	4 84	3·15

The repulsive force constants found by this method are consistently smaller than those found above (Table V).

The relation between the two sets of results can be seen at a glance from fig. 4, where the "diameters" σ_n are plotted as a function of $1/n$. The discrepancy

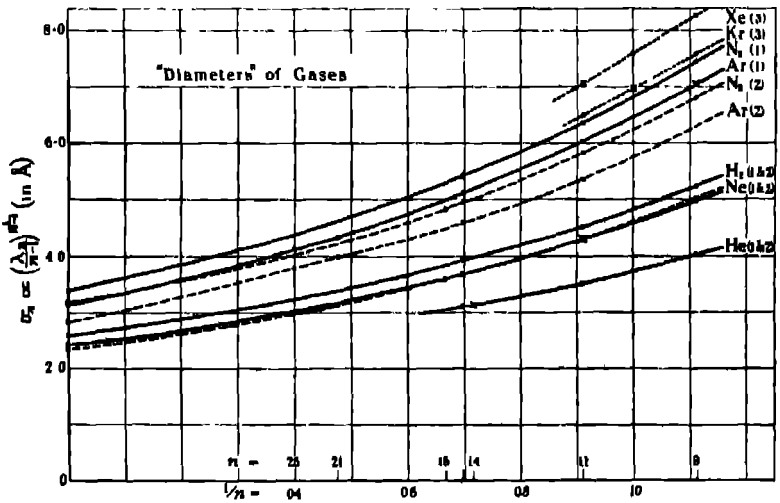

FIG 4.—The "Diameters" of Gases determined from (1) equation of state, (2) viscosity, (3) crystal data The numbers in the figure indicate which of the methods has been used The values of n which have been chosen in the various cases are indicated by crosses.

between them is about the same as that found in the case of argon * Applications of the latter results to crystal calculations have decided in favour of the

* 'Roy. Soc. Proc.,' A, vol. 106, pp 461 and 477 (1914); the first of these sets of results is to be supplamented with the values $\lambda_n = 3\ 92\ .\ 10^{-88}$ and $\sigma_n = 5{\cdot}35\ .\ 10^{-8}$ for $n = 11$. in the second set $\sigma_n = 7\ 053\ 10^{-8}$ and not $7{\cdot}530\ .\ 10^{-8}$ as printed for $n = 9$.

equation of state results.* Whether or not the same conclusion applies to nitrogen cannot at present be decided.

§ 4 *Summary of Previous Results.*

For convenience of reference, the knowledge about molecular fields gained in this and preceding papers from the properties of gases is collected in the following table, the attractive field being assumed in each case to be according to an inverse fifth power law. The corresponding "diameters" are written below the force

Table XII.—Repulsive Force Constants and "Diameters" of Gases

	Method	$n = 9$.	11	14	14½ *	15	21	∞
He	(1)	1 14 10^{-74} 4 03	6 26 10^{-99} 3 53		2 15 10^{-113} 3·10			
	(2)			5·74 . 10^{-113} 3 12				
Ne	(1)	6 32 10^{-74} 4 99	4 38 . 10^{-99} 4 29		2 22 10^{-114} 3 70			— 2 42
	(2)	6 66 10^{-74} 5 02	4 45 10^{-99} 4·30			1 76 10^{-118} 3 60	3 89 10^{-168} 3 153	— 2 35
Ar	(1)	1 01 10^{-73} 7·05	1 31 10^{-97} 6 03		1 64 10^{-114} 5·11		2 34 10^{-166} 4 34	— 3·13
	(2)		3·92 10^{-98} 5 35		3 57 10^{-118} 4 70		2 82 10^{-168} 3 99	— 2·84
Kr	(3)	(n = ∞ 10) 7 34 . 10^{-99} 6 06						
Xe	(3)		6 21 10^{-97} 7 05					
H_2	(1)	9 19 10^{-74} 5·23	7 38 10^{-99} 4·52		4 80 10^{-114} 3 92			— 2 50
	(2)		7 19 10^{-99} 4·61					
N_2	(1)	15·82 . 10^{-74} 7 46	22 45 . 10^{-99} 6·36		3 61 10^{-114} 6 42			— 3 38
	(2)	7 59 10^{-74} 5·81	9·06 10^{-99} 5 81			1 17 10^{-117} 4 84		— 3·15

* This fractional number has advantages in numerical applications of the formula for the equation of state.

(1) From equation of state. (2) From viscosity (3) From crystal data.

* 'Roy. Soc. Proc.,' A, vol. 109, p 476 (1925), *cf.* p. 480, footnote

constants. These are given in Angstrom units, and, being of the same order of magnitude, are convenient in giving a graphical representation of the results. Fig 4 shows these quantities as a function of $1/n$, and gives a convenient summary of the results. It shows that the gaseous properties of a gas do not always of themselves determine the molecular field. They do, however, limit the molecular model to one of a definite series Other methods have then to be employed to select from this series the one of most general utility.

In two cases, viz , hydrogen and helium, the viscosity and equation of state results have themselves fixed the molecular model. In the case of neon, the results from viscosity in conjunction with certain crystal data* have led to a value $n = 11$ It is satisfactory to find that this paper provides additional evidence in favour of this model It shows that this model gives the best agreement between theory and observation in the equation of state. Moreover, the force constants, which this method of this paper determines for this model, is in excellent agreement with that previously found from viscosity. The figure shows the consistency between the two sets of results.

Argon and nitrogen differ from hydrogen, helium and neon in that their gaseous properties do not lead to consistent results The reason for this discrepancy is obscure Table XIII, however, throws some light on the question. This table gives the *attractive* force constants of the respective gases, as deduced from the equation of state. These force constants are all measured in terms of the same unit, since the law of force assumed in each case is according to an inverse fifth power, and so they indicate the relative magnitude of the forces of cohesion for the various gases.† It is to be observed that the gases, for which we have found consistent results from the two methods, possess the *weakest* attractive fields. This is significant because it is to be remembered that all the theoretical formulæ for the coefficient of viscosity are subject to the limitation that the attractive field is weak. It looks, therefore, as though this condition does not apply to argon and nitrogen and that none of the theoretical formulæ for viscosity are strictly applicable to these gases. A rigorous theoretical formula for viscosity, true for attractive fields of any magnitude, might lead to force constants different from those which have now been found. This problem is being considered

The equation of state method has the advantages that it applies to all fields,

* 'Roy. Soc. Proc.,' A, vol. 109, p. 476 (1925).

† The fact that these attractive force constants depend on the law of force assumed for the repulsive field is immaterial. It does not affect the relative orders of magnitude

whether strong or weak, and it determines the forces of attraction as well as those of repulsion. For this reason it is to be preferred.

Table XIII.—The Attractive Force Constants of Gases ($\lambda_m r^{-6}$).

λ_m 10^{60}	$n = 9$	11	14½	∞
He	4 35	2 91	1 90	—
Ne	22 3	17 2	13 3	7 3
H_2	25 4	19 8	15 6	8 8
Ar	162 0	138 0	113 0	70 4
N_2	182·0	151·0	123 0	77 0

The models which appear most suitable in the various cases are indicated by Clarendon type in the tables and by crosses in the figure The cases of krypton and xenon have been dealt with from crystal data alone owing to the lack of experimental data about their gaseous properties.

Finally, as an indication of possible applications of the force constants, we give in Table XIV a quantity ϕ, which represents the work required to separate two molecules to infinity from their positions of equilibrium under the influence of their mutual fields This quantity, which corresponds to a "heat of dissociation," should be an important factor in determining the boiling point of a gas It is satisfactory to find a correspondence between the observed and the calculated quantities.

Table XIV.—The Boiling Points of Gases (T_B)

—	n_1	m	λ_n	λ_m	ϕ_{crys} 10^{16}	T
He	14	5	$5\ 74\ 10^{-118}$	$1\ 93\ 10^{-44}$	3·43	4·3
H_2	11	5	$7\ 38\ 10^{-89}$	$1\ 98\ 10^{-44}$	12 31	20 4
Ne	11	5	$4·38\ 10^{-89}$	$1·72\ 10^{-44}$	13 81	34 1
N_2	9*	5	$1·58\ 10^{-72}$	$1\ 82\ 10^{-42}$	26 14	77·4
A_2	9	5	$1\ 01\ 10^{-72}$	$1·62\ 10^{-42}$	32 70	87 1

* This value has been assumed for nitrogen because of the similarity between its curve of "diameters" and that of argon

The force constants given in this paper should provide a starting point for a more complete quantitative explanation of the boiling points and other properties of these gases than has yet been given.

The Forces between Atoms and Ions.—II.

By J. E. Lennard-Jones, Reader in Mathematical Physics, Bristol University, and Beryl M. Dent, B.Sc., Bristol University.

(Communicated by Prof S Chapman, F.R S —Received June 8, 1926)

§ 1 This note is supplementary to a paper recently published on the same subject.* It extends the results so as to provide a complete table of forces between the monovalent and divalent ions of the inert gas type as well as between the inert gases themselves The method follows that of the previous paper, in which the forces between ions are deduced from the forces between inert gas atoms by the use of published data on ionic refractivities

The table of force constants, which is given, should have numerous applications in theoretical calculations of crystal structures. It should, for instance, be useful in determining parameters in crystal structures, which are difficult to determine from X-ray measurements.

§ 2. Forces between atoms and ions arise from various causes There are between ions *electrostatic forces* of attraction and repulsion owing to their effective electrostatic charges These depend only on the valency of the ions concerned and need not be considered further In addition, there are forces between the neutral cores, just as there are forces between the inert gas atoms to which they are similar From the physical properties of these gases, we learn that at large distances the atoms attract, while at small distances they repel. It is convenient, therefore, to regard the cores as exerting on each other two forces, one attractive and the other repulsive, the former preponderating at large distances, the latter at small. This is virtually what van der Waals did in deducing his well-known equation of state. We may, therefore, conveniently refer to the attractive force as the *van der Waals attractive force*. This distinguishes it from the electrostatic attractive force just mentioned.

The repulsive force was represented by van der Waals as a rigid sphere, but this is now recognised as not being sufficiently general for most purposes. It is replaced in this paper by an inverse power law, which, being a continuous function, is more likely to be in accord with fact This repulsive force between cores may be called the *Intrinsic Repulsive Force*.

There are as well *forces due to polarisation*. Atomic or ionic cores are liable to be distorted by the presence of neighbouring electrostatic charges, so that

* Lennard-Jones, 'Roy. Soc. Proc.,' A, vol. 109, p. 584 (1925).

there is a relative displacement of negative and positive charges This creates an effective dipole at the centre of the core, and the mutual influence between the dipole and the charge producing it gives rise to an attractive force Certain simple assumptions indicate that this is likely to be of the inverse fifth power type.*

The forces just enumerated arise between ions whose electronic structure is similar to that of the inert gases and may therefore be regarded as spherically symmetrical. Unsymmetrical ions or molecules have to be considered differently. These sometimes possess permanent dipoles,† whose mutual influence is to be considered separately from the forces of attraction and of repulsion

§ 3 In crystals of a high degree of symmetry, such as rocksalt, the forces due to polarisation need not be considered A dipole created in an ion by a neighbouring ion is neutralised by the effect of another ion diametrically opposite Nor is it necessary to consider the van der Waals cohesive forces, because these are negligibly small compared with the electrostatic forces of attraction between neighbouring ions ‡ Only in crystals of neutral atoms, such as solid argon, are the van der Waals forces important

The difference in magnitude between the two kinds of attractive forces is indicated by the difference in the physical properties of crystalline argon and rocksalt, in particular by their widely different melting points § For the intrinsic repulsive forces are of the same order in the two cases.

Hence the forces between ions in crystals, such as rocksalt, may be regarded as sufficiently determined when the intrinsic repulsive forces are found It is these forces which are considered in this paper

It has been shown in former papers|| that when the repulsive forces between the inert gases are represented by the law λr^{-n}, neon requires the value $n=11$, argon the value $n=9$, krypton the value $n=10$ and xenon the value $n=11$. These laws of forces are held to be true also for ions of the same electronic structure, so that the laws of force between ions are summarised in the following table .—

* *Cf.* Born and Heisenberg, 'Z. f. Phys.,' vol 23, p 337 (1924)

† Debye, 'Phys. Zeits,' vol 13, p 97 (1912), Smyth and Zahn, 'Journ. Amer Chem Soc.,' vol 47, p. 2501 (1925), Zahn, 'Phys. Rev.,' vol. 27, p 455 (1926)

‡ *Cf* 'Roy. Soc. Proc.,' A, vol 106, pp 715 and 716 (1924).

§ Simon and Simson, 'Z f Physik,' vol 21, p 168 (1924), and vol 25, p 160 (1924).

|| 'Roy. Soc. Proc.,' A, vol. 109, p. 584 (1925)

Table I.—The Laws of Force between Atoms and Ions (the values of n in λr^{-n}).

——	Neon group.	Argon group.	Krypton group.	Xenon group
Neon-like ions	11	10	10	11
Argon like ions	10	9	9	10
Krypton-like ions	10	9	10	10
Xenon-like ions	11	10	10	11

The derivation of the appropriate force constants is facilitated by the use of a quantity $\sigma^{(n)}$, which is proportional to $\left(\frac{\lambda_n}{n-1}\right)^{\frac{1}{n-1}}$ and is of the dimensions of a length. This quantity is regarded as a measure (on an arbitrary scale and for a given law of force) of the size of the outer shells of electrons in ions so that its value for one ion can be derived from that of another ion from a knowledge of their ionic refractivities.

These so called "diameters" are functions of n, as is evident from the following table where they are given for the values $n=9$, 10 and 11.* They are derived from the corresponding quantities for the pure gases, the latter having been determined from the kinetic theory for $n=9$ and $n=11$, and by interpolation for $n=10$.

Table II.—The "Diameters" of Ions ($\sigma^{(n)}$)

n	O^{--}	F^-	Ne	Na^+	Mg^{++}	S^{--}	Cl^-	Ar	K^+	Ca^{++}
9	7 26	6·23	5 02	4 71	4·10	9 77$_5$	6 50	7 05	6 43	5 91
10	6 69	5 74	4 63	4 34	3·78	9·01	7·83	6 50	5 93	5·45
11	6 21	5·33	4 30	4 03	3·51	8·36	7·27	6·03	5 50	5·05
n	Se^{--}	Br^-	Kr	Rb^+	Sr^{++}	Te^{--}	I^-	X	Cs^+	Ba^{++}
9	9 58	8 89	7 58	6·96	6 49	9·66	9·52	8·26	7·61$_5$	7·05
10	8 83	8 19	6 98	6 41	5·98	8·88	8·75$_5$	7 00	7 01	6·48
11	8 20	7 61	6·49	5 96	5 55$_5$	8·24	8 12	7 05	6·50	6·01

* 'Roy. Soc. Proc.,' A, vol. 109, p. 592 (1925)

Table III —The Force Constants of Atoms and Ions

——	O^{--}	F^{-}	Ne	Na^{+}	Mg^{++}	S^{--}	Cl^{-}	Ar	K^{+}	Ca^{++}	Se^{--}	Br^{-}	Kr	Rb^{+}	Sr^{++}	Te^{--}	I^{-}	X	Cs^{+}	Ba^{++}
O^{--}	17 6	8 42	3 30	2 55	1 51	21 0	10 4	4·37	2 94	2·07	18 9	12 9	6 03	4 11	3 04	79·8	73 4	33 8	22 1	14·9
F	8 42	3·81	1·38	1·04	0 58	11 9	5·64	2 23	1·45	1·00	10·7	7 14	3 15	2·09	1 51	42 5	38·9	17 0	10 8	7·07
Ne	3 30	1 38	0 44	0·32	0 17	5 91	2 62	0·95	0 59	0 38	5 25	3 38	1 39	0 88	0 61	19 3	17·5	7 13	4·34	2·73
Na^{+}	2 55	1·04	0·32	0 23	0·12	4·87	2 12	0 74	0·46	0 29	4·31	2 75	1 10	0 69	0 48	15·5	14·1	5·60	3·37	2·09
Mg^{++}	1 51	0 58	0 17	0 13	0 05	3 31	1 39	0 46	0·27	0 17	2 92	1 82	0 70	0 42	0 29	10 1	9·10	3·48	2·03	1·23
S^{--}	21 0	11 9	5·91	4 87	3 31	13 7	8 00	4 13	3 06	2 36	12·7	9 47	5 29	3·96	3 15	67 9	63·8	34 8	25·1	18·6
Cl^{-}	10 4	5·64	2 62	2 12	1·39	8 00	4 49	2 20	1 59	1·19	7·34	5 38	2 87	2·10	1 64	36·7	34 3	17 9	12 6	9 10
Ar	4·37	2 23	0 95	0 74	0 46	4 13	2 20	1 00	0 70	0 51	3·76	2 68	1 35	0·95	0 72	17·4	16 2	7 97	5 43	3·78
K^{+}	2 94	1·45	0 59	0 46	0 27	3 06	1 59	0·70	0 48	0·34	2·78	1·95	0·95	0 66	0 50	12·4	11·5	5·50	3·68	2·53
Ca^{++}	2 07	1 00	0·38	0 29	0 17	2 36	1·19	0 51	0 34	0 24	2 13	1·48	0·70	0·48	0·35	9·22	8·52	3·97	2·62	1·77
Se^{--}	18·9	10·7	5 25	4 31	2·92	12 7	7 34	3 76	2 78	2·13	60 4	43 4	22·3	16 0	12 4	62·0	58·2	31·6	22·7	16·7
Br^{-}	12 9	7 14	3 38	2 75	1·82	9·47	5 38	2 68	1 95	1 48	43 4	30 7	15·4	10 9	8·33	44·5	41 7	22 1	15·7	11·4
Kr	6 03	3 15	1 39	1 10	0 70	5·29	2 87	1 35	0 95	0 70	22 3	15 4	7 28	5 01	3·73	23 0	21 4	10 8	7·43	5 25
Rb^{+}	4·11	2 09	0 88	0 60	0 42	3 96	2·10	0 95	0 66	0 48	16 0	10 9	5 01	3 38	2 49	16·5	15 3	7 53	5·11	3 55
Sr^{++}	3 04	1 51	0 61	0 48	0 29	3 15	1 64	0 72	0·50	0 35	12 4	8·33	3·73	2 49	1 81	12 8	11 8	5 68	3 81	2 62
Te^{--}	79·8	42 5	19 3	15 5	10 1	67·9	36 7	17 4	12 4	9·22	62·0	44 5	23 0	16 5	12·8	297 0	276 0	140 3	97 3	69·4
I^{-}	73·4	38 9	17 5	14·1	9·10	63 8	34·3	16 2	11 5	8 52	58 2	41 7	21 4	15 3	11 8	276 0	256 5	129 7	89 7	63 7
X	33·8	17 0	7·13	5·60	3 46	34 8	17 9	7 97	5 50	3 97	31 6	22 1	10 8	7·52	5 68	140 3	129 7	62·4	41·9	29·0
Cs^{+}	22·1	10·8	4 34	3·37	2 03	25 1	12 6	5 42	3 68	2 62	22 7	15 7	7 43	5 11	3 81	97 3	89 7	41 9	27·7	18 9
Ba^{++}	14 9	7 07	2 73	2 09	1 23	18 6	9·10	3 78	2 53	1·77	16·7	11·4	5 25	3 55	2 62	69 4	63 7	29 0	18·9	12·6

Following the method of the former paper,* the force constants given in Table III are deduced from the "diameters" of Table II. Owing to the fact that these force constants depend on $\sigma^{(n)}$ to a high power (9 or 10), great accuracy cannot be expected. An accuracy of 10 per cent in a force constant is equivalent to an accuracy of 1 per cent. in a diameter as usually understood. Similarly in applications of the force constants to calculate *distances*, an accuracy of 10 per cent in the force constants should yield an accuracy of 1 per cent. in the answer. It is believed that the force constants lie within these limits of accuracy.

Some of these results were given in the preceding paper, but they are given here as well for the sake of completeness They have been recalculated and a few numerical errors have been detected and corrected The results of Table III are to be regarded as displacing any former results where there is a discrepancy

The force constants are given in such units as give the force in dynes when the unit of length is the Ångstrom The table is to be used in conjunction with Table I. For example, to find the force between Na^+ and Cl^- at a distance of 2Å, we note that the law of force is the inverse tenth and that the force constant is 2 12. The force is therefore $(2{\cdot}12)2^{-10}$ dynes, that is 0·002 dynes.

§ 4. Our thanks are due to the Department of Scientific and Industrial Research for a grant to one of us to pursue this investigation and to make the applications to be described in later papers.

* 'Roy Soc Proc,' A, vol. 109, p. 584 (1925).

The Origin of the Electrical Charge on Small Particles in Water.

By Thomas Alty, M.Sc., Ph D., Professor of Physics, University of Saskatchewan.

(Communicated by Sir Joseph Thomson, F R S.—Received June 15, 1926)

Introduction.

The surface of an air bubble is a particularly simple one at which to examine the electrical conditions which attend all small particles when immersed in a liquid. An air bubble may be considered as a type of coarse suspensoid, which, on being immersed in water, acquires a charge and moves in an electric field as if negatively electrified.

The present work is a continuation of that already published ('Roy Soc. Proc.,' A, vol. 106, p 315 (1924)) and deals chiefly with the charge on the bubble immediately after it enters the liquid, this is examined experimentally and also theoretically In addition, a new method of calculating the potential difference between the bubble surface and the interior of the liquid is suggested

For convenience, a few results of the former work must first be mentioned. It was there shown that the gas phase has little or no influence on the surface electrification, so that all the electrical effects may safely be ascribed to the surrounding liquid medium. Experimental evidence indicated that the surface phenomena are due to the selective absorption of ions from the water Furthermore, the mobility of the bubble diminished steadily with increasing purity of the surrounding water. It therefore appears probable that in perfectly pure water the charge would be very small, or even zero

Experimental

The experimental arrangements were as described in the former work A small gas bubble (2 mm in diameter) is introduced into partially air-free water contained in a cylindrical glass vessel which rotates about a horizontal axis. The bubble then takes up a position on the axis and moves along the latter when an electric field is applied between the two ends of the cell The mobility is measured continuously as the bubble is slowly absorbed into the water until it finally disappears. After each reading of the velocity, the total time since the introduction of the bubble into the water is also noted, so that the variation of the electrical conditions with the age of the surface can be investigated. It

has previously been shown that in water of specific conductivity 1×10^{-6} ohms to 2×10^{-6} ohms^{-1} there is a slow and steady "charging up" of the surface, and that for some time after the introduction of the bubble the charge varies continuously until its final equilibrium state is attained. Since the first object of the present work is a complete investigation of this charging up, water of the above-mentioned purity was used

For comparison, the experiments were repeated in water of specific conductivity 6×10^{-6} ohms^{-1}; in this water the charging-up period is very short and the velocity of the bubble increases steadily with decreasing radius until the latter is about 0·05–0·1 mm At about this point the velocity is a maximum and thereafter decreases steadily until the bubble disappears The explanation of the maximum is not clear. It may represent a true change in the electrification of the surface, or it may be due to increased resistance to the motion of the bubble along the axis. At about this size (0 05 mm. diameter) the bubble ceases to be perfectly stable, and if accidentally disturbed it oscillates about the axis before returning to its equilibrium position. This vibration may increase the resistance of the water to the motion and consequently decrease the mobility As this point cannot be definitely settled, only bubbles having diameters greater than this minimum will be considered in what follows.

Further experiments were also performed to investigate quantitatively the relation between the charge on the surface and the rate of absorption of the bubble. Air-saturated conductivity water was used after a very small quantity of air had been removed from it by evacuation. A bubble introduced into such water was therefore absorbed very slowly On completion of this experiment more air was removed from the water and a second bubble introduced This was absorbed more rapidly than the previous one and gave different results. The process was repeated for a series of bubbles until the rate of absorption became so great as to render further observations impracticable.

If now the bubble is assumed to acquire a definite charge, E, by ionic adsorption, then this charge may be calculated by an application of Stokes' Law If X is the intensity of the electric field producing the velocity v, η the coefficient of viscosity of water, and r the radius of the bubble, then

$$XE = 6\pi\eta rv$$
$$\text{or} \quad E = 6\pi\eta rv/X.$$

Thus E may be determined directly from a knowledge of v.

The experimental results were represented graphically by plotting the total charge, as calculated above, against either the bubble radius or the age of the

surface. The total charge at any time t will indicate very directly the state of adsorption at that time.

Fig. 1 shows a graph of charge against age of surface and was obtained in

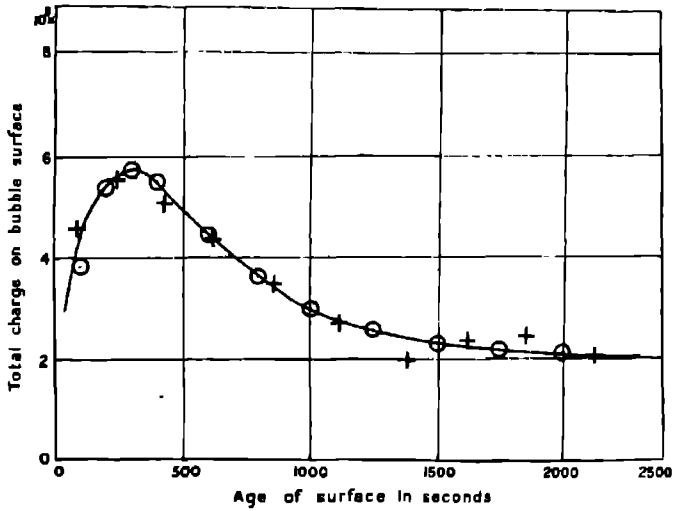

Fig. 1.

very pure, air-saturated water. In this water the size of the bubble changes only very slightly during the experiment. It will be observed that the charge is extremely small at first, increases to a maximum, and then falls to a value of about one-third of this maximum. After this stage, the charge on the bubble surface appears to be independent of the time

These experiments were repeated in water from which some air had been removed so that the diameter of the bubble decreased continuously during the experiment. It was found that the curve obtained was very similar to that in fig 1, and that when equilibrium had been attained the total charge on the bubble remained independent not only of time but also of bubble diameter This is somewhat surprising and appears to indicate that, once an equilibrium state is reached, the surface density of charge must increase inversely as the square of the bubble radius, since the total charge remains practically constant while the bubble area shrinks, sometimes down to about 1/20 of its original size. Fig. 2 illustrates one of these experiments.

The experiments in water of higher specific conductivity test this point

further. In this water the charging-up period is very short so that after the first few readings the equilibrium state is reached, and it might then be expected

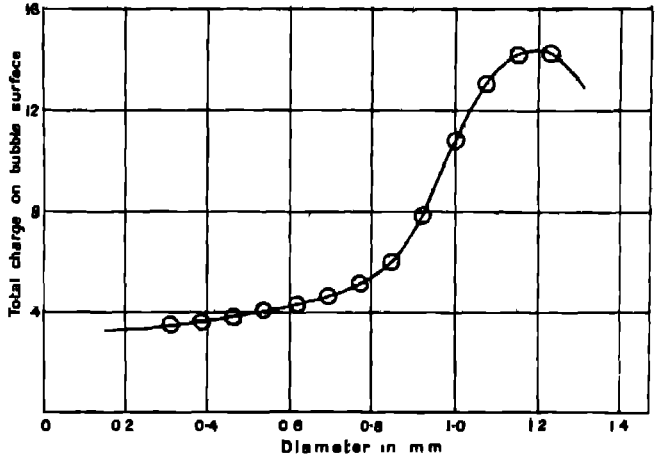

FIG. 2.

from the above that the total charge on the surface would remain independent of the bubble radius and the time. Fig 3 illustrates the results obtained in such water For the whole range of diameters the total charge remains almost constant, decreasing very slightly with decreasing radius

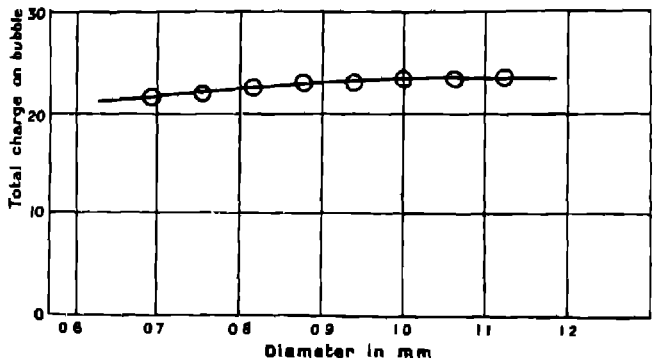

FIG. 3

It was found possible to obtain the above type of graph (fig 3) only when the rate of absorption of the bubble was very slow. If the rate of absorption were great the total charge decreased steadily from the first observation.

Fig. 4 shows the results obtained from two successive experiments in which the water used had the same conductivity but contained a different amount of

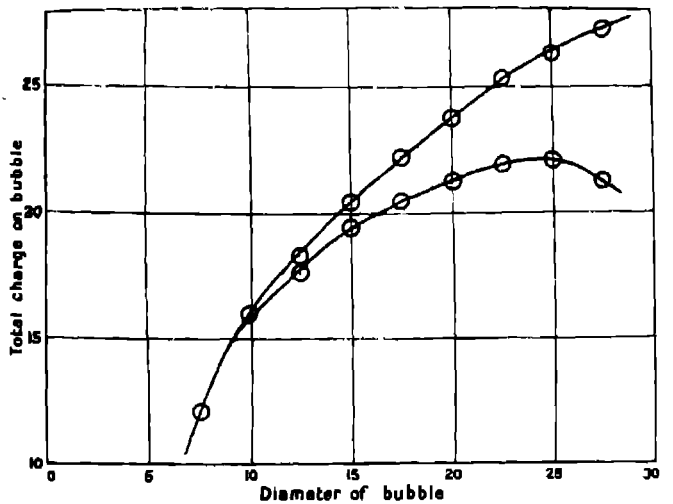

Fig. 4.

air in each experiment. An examination of such curves shows that the greater the rate of absorption the greater the initial equilibrium charge (Fig 3 and fig. 4 together indicate that for zero rate of absorption the total charge is independent of the radius of the bubble.) It will later be shown that there is a quantitative relation between the rate of absorption of the bubble and its charge This is illustrated in fig. 5

In all experiments the velocity of the bubble was measured using two different values of the electric field (X) alternately. In this way the velocity was shown to be proportional to the applied field throughout the charging period as well as through the subsequent history of the bubble.

Theoretical.

The results previously obtained as well as those described above conflict with the usual theories as to the electrical structure of the surface of small particles in water. This being so, an endeavour is made here to account for the whole phenomenon on the basis of adsorption, and the relations deduced are compared with experiment.

When a bubble is first introduced into water, the surface is composed of water molecules, which being polar are all orientated and thus have a resultant electric field Since the bubble acquires a negative charge, this orientation must be such that the surface molecules attract negative and repel positive ions in the water, each molecule thus being a possible point at which a negative ion may be attached to the surface. In this way the surface steadily becomes covered with negative ions At the same time positive ions from the liquid strike the bubble surface. Any such ion striking one of the negative ions already adsorbed may be bound close to the latter and neutralise its charge. Hence the accumulation of the surface charge must consist of two distinct processes; firstly, the adsorption of negative ions on to the bubble surface, and, secondly, the binding of positive ions to some of the negative adsorbed ions. These two processes will continue side by side until equilibrium is attained, the total charge on the bubble at any instant being equal to the charge on the uncovered negative ions on its surface The bound positive ions, being farther from the surface, are held less firmly than the adsorbed negative ions and may be removed by collisions due to the general motion of thermal agitation in the liquid. Equilibrium is therefore attained when the number of positive ions bound per second is equal to the number removed by collision In this state there will be a number of uncovered negative ions as well as a number covered In this connection it is of interest to note that Rinde ('Phil. Mag.,' vol 1, p. 32 (January, 1926)) found that on sulphur particles in an acid solution both Cl' ions and also neutral HCl molecules were adsorbed. The process of adsorption in this case may be very similar to that under discussion, the neutral molecules being due to the covering of the Cl' ions

In these experiments pure distilled water was used so that the ions present would be chiefly H^+ and OH'. In addition, there would be minute traces of electrolytic impurities from the glass of the cell, etc, giving rise to ions which for convenience may be called X' and Y^+. These in comparison with the hydrolytic ions must be extremely few in number, and this number must decrease with increasing purity of the water On the other hand, the hydrolytic ions are still present in relatively large numbers even in water of the greatest purity, the ionisation of pure water yielding about 10^{13} H^+ and OH' ions per c.c. Consequently it is impossible by purification to remove all ions from the water. Nevertheless, it was found that the greater the purity of the water (as measured by its electrical conductivity) the lower the mobility of the bubble, which in some cases was reduced as low as 1 per cent. of its normal value. From these considerations it is evident that the charge on the bubble is *not* produced by

the H^+ and OH' ions, but is due almost entirely to the presence of stray ions X' and Y^+ in the water

The inactivity of the H^+ and OH' ions may possibly be a consequence of the small dimensions of these particles. For being so small, when adsorbed they are very close to each other and to the bubble surface This arrangement will result in intense binding forces which may be sufficiently great to prevent many of the covering ions being removed by the molecular agitation of the liquid Hence, when the adsorption of OH' ions has reached an equilibrium condition, very few of them are left uncovered to give a resultant charge to the bubble At the same time, when equilibrium is attained, these OH' ions do not cover the whole of the bubble surface but only a definite fraction of it Langmuir ('J A C.S.,' vol. 40, p. 1367 (1918)) has pointed out that once equilibrium is established the exact fraction of a surface occupied by any adsorbable molecule may depend on the size and shape of that molecule It may, therefore, be possible for another ion (X'), on account of its different size and shape, to become attached to those points on the surface not occupied by the OH' ions, so that finally the surface is covered mainly by OH' ions but also to some extent by X' ions.

If it is assumed that there are 10^{13} OH' ions per cubic centimetre, and that any one of them striking an unoccupied surface molecule remains attached, then a simple calculation indicates that these ions cover 90 per cent of the surface in about 1/100 sec Since the adsorption of covering H^+ ions proceeds concurrently, only a very brief interval of time is required for the adsorption of both these ions to reach its equilibrium state, and this even in the purest water.

The adsorption of X' ions will be a much slower process owing to their scarcity In exactly the same way as for H^+ and OH' ions, the adsorbed X' ions will be covered in their turn by Y^+ ions from the liquid Since X' and Y^+ are larger than OH' and H^+, they will be unable to approach so closely to each other and the binding forces will therefore be weaker For this reason the Y^+ ions will be more readily removed by the thermal agitation of the surrounding liquid Hence a certain fraction of the adsorbed X' ions when in equilibrium will still be uncovered, and it is to *these* that the bubble owes its charge. In the very pure water the number of such stray ions as X' and Y^+ is small and as a result the equilibrium state is attained but slowly

According to this view the H^+ and OH' ions, although so numerous and occupying a large fraction of the surface, add but little to the bubble charge owing to the tight binding existing between them. Their chief function then

appears to be that of limiting the number of possible points at which other ions can be adsorbed

Since such ions as X' and Y^+ occur simply as impurities in the water and always in very minute concentrations, their exact number would be expected to vary from one experiment to another even when the specific conductivity remains practically constant For this reason the rate at which the bubble acquires its charge in the purest water may vary widely in the different experiments. Such variation is found in practice, the longest charging period being shown in fig 1. In other experiments in water of the same conductivity, the period varied from this value to 100 secs. These variations are observed only in the purest water.

Although the number of X' and Y^+ ions present varies in this way, they are always so scarce that the conductivity of the pure water is chiefly due to the ions H^+ and OH'. Thus the fact that the rate of charging varies while the conductivity remains practically constant (1×10^{-6} ohms^{-1}) is in accordance with the view that the charge is due to stray ions X' and Y^+ and not to the hydrolytic ions

The experiments described show that in equilibrium the number of uncovered ions per square centimetre of surface is inversely proportional to the square of the radius. This relation would hold true if the numbers (N_x) of negative ions and (N_y) of positive ions per square centimetre each varied inversely as the square of the radius. N_x and N_y also depend on the age of the bubble surface so that it may be assumed that

$$\left.\begin{aligned} N_x &= \frac{f(t)}{r^2} \\ N_y &= \frac{g(t)}{r^2} \end{aligned}\right\}, \qquad (1)$$

where $f(t)$ and $g(t)$ are functions of t.

Hence the total charge on the bubble $= 4\pi r^2 . (N_x - N_y) = 4\pi \{f(t) - g(t)\}$, which is independent of r, in accordance with experiment

Making certain assumptions it is now possible to calculate the total charge on the bubble at any time t after its formation For convenience, these assumptions are tabulated as follows :—

1. A fraction α of the bubble surface is alone capable of adsorbing the X' ions from the water. The remaining fraction $(1 - \alpha)$ is occupied by H^+ and OH' ions in loose combination. These prevent the close approach and adsorption of X' ions to the surface.
2. Each adsorbed X' ion is attached to a single surface water molecule.

3. The forces between an X′ ion and the surface molecule to which it is attached are great enough to prevent appreciable re-evaporation of the X′ ions. Hence any such ion striking an unoccupied surface molecule remains attached.

(Evidence of this assumption is given later, p. 246.)

Let there be n_x of the X′ ions per c.c of the liquid

,, v_x be their average velocity of thermal agitation (velocity of mean square)

,, γ be the surface area occupied by one adsorbed X′ ion = area of a surface water molecule

,, α be the fraction of the surface occupied in equilibrium by X′ ions

α then depends on the radius of the bubble and $= \beta/r^2$ (experimental) Let N_x = number of X′ ions adsorbed per unit area at time t. Then the number striking unit area per unit time is $n_x v_x/\sqrt{6\pi}$.

Fraction of the area occupied by OH′ ions $= (1 - \alpha)$

Fraction of the area occupied by X′ ions at time $t = \gamma N_x$

Therefore fraction of the whole surface which is unoccupied at time $t = \alpha - \gamma N_x$ and the number of free X′ ions striking these unoccupied spaces per second

$$= \frac{n_x v_x}{\sqrt{6\pi}} (\alpha - \gamma N_x)$$

If all collisions between surface molecules and free X′ ions result in adsorption and if re-evaporation is negligible, then

$$\frac{dN_x}{dt} = \frac{n_x v_x}{\sqrt{6\pi}} (\alpha - \gamma N_x)$$

The solution of this is

$$N_x = \frac{\alpha}{\gamma}\left(1 + Ce^{-\frac{n_x v_x \gamma t}{\sqrt{6\pi}}}\right)$$

But $N_x = 0$ when $t = 0$. Therefore

$$N_x = \frac{\alpha}{\gamma}\left(1 - e^{-\frac{n_x v_x \gamma t}{\sqrt{6\pi}}}\right) \qquad (2)$$

= number of adsorbed X′ ions at time t.

Let the same symbols as above, with suffix y, refer to the Y^+ ions Since these ions are bound to the surface only when they strike an adsorbed X′ ion, the chance of any Y^+ ion becoming bound is proportional to the fraction of the surface occupied by uncovered X′ ions

Fraction of surface occupied by uncovered X′ ions $= \gamma (N_x - N_y)$

Therefore the increase in the number of Y^+ ions attached to unit area of the surface in time dt

$$= \frac{n_y v_y}{\sqrt{6\pi}} (N_x - N_y)\gamma\, dt.$$

At the same time, some of those already attached are removed by the thermal agitation of the liquid.

Let k = fraction of the positive covering ions removed per second in this manner. Then the equation for N_y is

$$\frac{dN_y}{dt} = \frac{n_y v_y \gamma}{\sqrt{6\pi}} (N_x - N_y) - kN_y, \tag{3}$$

when

$$t = \infty, \quad \frac{dN_y}{dt} = 0 \quad \text{and} \quad N_x = \alpha/\gamma$$

Therefore

$$N_y = \frac{\alpha/\gamma}{1 + \frac{\sqrt{6\pi}\, k}{n_y v_y \gamma}} \tag{4}$$

The number of uncovered negative ions in equilibrium is therefore $(N_x - N_y)$ per square centimetre,

$$= \frac{\alpha}{\gamma}\left\{1 - \frac{1}{1 + \frac{\sqrt{6\pi}\, k}{n_y v_y \gamma}}\right\} = \frac{k\alpha}{\gamma}\left\{\frac{1}{k + \frac{n_y v_y \gamma}{\sqrt{6\pi}}}\right\} \tag{5}$$

= surface density on the bubble when equilibrium is attained.

Returning to equation (3)

$$\frac{dN_y}{dt} + N_y\left(\frac{n_y v_y \gamma}{\sqrt{6\pi}} + k\right) = \frac{n_y v_y \gamma}{\sqrt{6\pi}} N_x.$$

$$= \frac{n_y v_y \gamma}{\sqrt{6\pi}} \cdot \frac{\alpha}{\gamma}\left(1 - e^{-\frac{n_x v_x \gamma}{\sqrt{6\pi}} t}\right) \qquad \text{by equation (2)}$$

Hence

$$N_y = n_y v_y \alpha\left[\frac{1}{n_y v_y \gamma + \sqrt{6\pi}k} - \frac{e^{-\frac{n_x v_x \gamma}{\sqrt{6\pi}} t}}{(n_y v_y \gamma - n_x v_x \gamma + \sqrt{6\pi}k)} + \frac{n_x v_x \gamma e^{-\left(\frac{n_y v_y \gamma}{\sqrt{6\pi}} + k\right) t}}{(n_y v_y \gamma + \sqrt{6\pi}k)(n_y v_y \gamma - n_x v_x \gamma + \sqrt{6\pi}k)}\right].$$

Also

$$N_x = \frac{\alpha}{\gamma}\left(1 - e^{-\frac{n_x v_x \gamma}{\sqrt{6\pi}} t}\right).$$

But the number of uncovered negative ions per square centimetre $= (N_x - N_y)$. Therefore M = total number of uncovered negative ions on surface of bubble $= 4\pi r^2 (N_x - N_y)$

$$= \frac{4\pi\beta}{\gamma}\left[\frac{k}{\frac{n_y v_y \gamma}{\sqrt{6\pi}} + k} + \frac{n_x v_x - \sqrt{6\pi}\frac{k}{\gamma}}{n_y v_y - n_x v_x + \sqrt{6\pi}\frac{k}{\gamma}} e^{-\frac{n_x v_x \gamma}{\sqrt{6\pi}} t}\right.$$

$$\left. - \frac{n_x v_x n_y v_y e^{-\left(\frac{n_y v_y \gamma}{\sqrt{6\pi}} + k\right)t}}{\left(n_y v_y + \sqrt{6\pi}\frac{k}{\gamma}\right)\left(n_y v_y - n_x v_x + \sqrt{6\pi}\frac{k}{\gamma}\right)}\right]. \quad (6)$$

This expression (6) then gives the number of free negative ions on the bubble surface at time t. If the ions X' and Y^+ are monovalent then the charge on the bubble at time t is M.ε e.s.u. (ε = ionic charge)

The constants β and k are evaluated below. Using the values there obtained, equation (6) reduces to

$$M = 1{\cdot}91 \times 10^6[0{\cdot}1096 + 1{\cdot}19\, e^{-3{\cdot}23 \times 10^{-2} t} - 1{\cdot}299 e^{-5{\cdot}44 \times 10^{-4} t}] \quad (7)$$

The values of the total charge as calculated from (7) are shown in fig. 1 by points marked ⊙. The points + are experimental values. It will be seen that the agreement is exceedingly good. This agreement between theory and experiment lends support to the present view of surface electrification.

Evaluation of β *and* k

The constants β and k used in the above expression furnish much information regarding the number of negative and positive ions on the surface at any time. From the measurement of the electric charge at any instant only the *difference* between the number of negative and positive adsorbed ions is obtained. By definition of β the total number of adsorbed negative ions on the bubble when equilibrium is attained is given by

$$4\pi r^2 \frac{\alpha}{\gamma} = \frac{4\pi\beta}{\gamma},$$

and therefore can be obtained directly from a knowledge of β.

In order to evaluate β the above expression for M (equation 6) is applied to the experimental curves. Considering a representative graph (fig. 1), the total charge on the bubble attained a maximum value after 300 seconds, this value being $5{\cdot}66 \times 10^5$ ε. Hence if the adsorbed ions were monovalent, the number

of uncovered negatives at this instant was $5{\cdot}66 \times 10^5$. Finally when equilibrium conditions obtained on the surface the total charge was $2{\cdot}093 \times 10^5$ e. Hence the experimental conditions may be expressed.

$$\left.\begin{aligned} t = 300 \text{ secs} \quad & \frac{dM}{dt} = 0 \quad M = 5{\cdot}66 \times 10^5 \\ t = \infty \quad & M = 2\ 093 \times 10^5. \end{aligned}\right\} \tag{8}$$

In equation (5) there occurs the average velocities of thermal agitation v_x and v_y of the two ions. These are not known accurately owing to the uncertainty of the nature of the ions X' and Y^+, but, since in temperature equilibrium the kinetic energy of a liquid molecule is equal to that of a gaseous molecule, an approximation to the required values may be made from a knowledge of the mean square velocities of gaseous molecules These range in general from 1×10^4 cm /sec. to 5×10^4 cm /sec , so that the desired values must he in this region For the purposes of calculation, therefore, it may be assumed that

$$v_x = 2 \times 10^4 \text{ cm /sec}$$
$$v_y = 3 \times 10^4 \text{ cm /sec}$$

This assumption, while being only approximately correct, will alter only the numerical value of the constants obtained from equation (6) , it cannot affect their order of magnitude, which is of primary interest. It will be shown later that any error here introduced is negligible in the calculation of the potential difference at the surface. On differentiating (6), inserting the above conditions (8) and putting $n_x = n_y = n$, the constants are found to have values

$$n = 7 \times 10^8.$$
$$k = 5{\cdot}96 \times 10^4.$$
$$\beta = 1{\cdot}5 \times 10^{-10}$$

This shows that the ions X' and Y^+, due to chance electrolytic impurity, are very few in number compared with the H^+ and OH' ions.

The constant k gives very useful information as to the binding of the covering Y^+ ions. It appears that only about 6×10^{-4} of these ions are removed per second by impact with surrounding molecules These positive ions are farthest from the water surface and will therefore be least firmly bound to it Hence, in the case of the *negative* ions, which are even more firmly bound, the number removed per second is quite negligible, and the assumption that all the negative ions striking blank spaces remain attached would seem to be justified.

The total number of negative ions on the surface when equilibrium is attained is

$$4\pi\beta/\gamma = 1\ 85 \times 10^6$$

The number of *uncovered* negative ions, as measured by the resultant charge on the bubble is $2{\cdot}09 \times 10^5$. These figures therefore indicate that about 89 per cent of the adsorbed X′ ions are covered by bound positive ions, while only about 11 per cent. are uncovered and thus charge the surface negatively

From these figures the constitution of the surface layer of the bubble may be summed as follows :—

Taking the number of water molecules per square centimetre as equal to 10^{15}, the very great majority of them are covered by H^+ and OH' ions which are bound so tightly to the surface that very few of them "evaporate" to give a resultant charge There are also $2{\cdot}35 \times 10^8$ negative ions of larger size attached per square centimetre and of these 89 per cent. are covered by positive ions which are continually evaporating and recondensing on the negatives, the fraction evaporating per second being $6{\cdot}0 \times 10^{-4}$ In this way a definite resultant charge is given to the bubble by those negative ions which are momentarily uncovered.

Relation between the Charge and the Rate of Absorption of the Bubble

The above adsorption hypothesis is further confirmed by an examination of the bubble charge after the surface is fully formed At this stage the adsorption has reached a state of dynamic equilibrium Hence, from equations (2) and (3), when $t = \infty$, $\frac{dN_y}{dt} = 0$,

$$\therefore \quad N_x = \alpha/\gamma, \qquad \frac{n_y v_y \gamma}{\sqrt{6\pi}} (N_x - N_y) = kN_y.$$

Therefore

$$N_y = \frac{\alpha/\gamma}{1 + \frac{k\sqrt{6\pi}}{n_y v_y \gamma}}$$

The equilibrium charge is therefore

$$4\pi r^2 (N_x - N_y) = \frac{4\pi\beta}{\gamma}\left(1 - \frac{1}{1 + \frac{k\sqrt{6\pi}}{n_y v_y \gamma}}\right)$$

$$= \frac{4\pi\beta/\gamma}{1 + \frac{n_y v_y \gamma}{k\sqrt{6\pi}}} \qquad (9)$$

This is the equilibrium charge when the bubble is *not* being absorbed into the water But when air-free water is used, the gas molecules pass through the surface in a continuous stream. Consequently more positive ions will be

removed by collisions between them and the incoming air molecules. Hence the total charge on the bubble is greater the faster the bubble is absorbed.

The number of positive covering ions removed by the air molecules will obviously be proportional to the number of air molecules passing per second through unit area of the surface, and also to the number of positive ions present per sq cm of surface But the rate of absorption of the bubble is

$$\frac{d(\text{Vol})}{dt} = 4\pi r^2 \frac{dr}{dt}.$$

Therefore the number of air molecules passing through one square centimetre per second is dr/dt Then the equation giving the number of positive ions per square centimetre will become

$$\frac{dN_y}{dt} = \frac{n_y v_y \gamma}{\sqrt{6\pi}}(N_x - N_y) - kN_y - CN_y\frac{dr}{dt}$$

where C is a constant

In equilibrium

$$\frac{dN_y}{dt} = 0 \quad \text{and} \quad N_x = \frac{\alpha}{\gamma}$$

Therefore

$$N_y = \frac{\alpha/\gamma}{1 + \dfrac{\left(k + C\dfrac{dr}{dt}\right)\sqrt{6\pi}}{n_y v_y \gamma}},$$

and the charge per unit area

$$= N_x - N_y = \frac{\alpha}{\gamma}\left\{1 - \frac{1}{1 + \dfrac{\left(k + C\dfrac{dr}{dt}\right)\sqrt{6\pi}}{n_y v_y \gamma}}\right\}$$

$$= \frac{\alpha}{\gamma}\left\{\frac{1}{1 + \dfrac{n_y v_y \gamma}{\left(k + C\dfrac{dr}{dt}\right)\sqrt{6\pi}}}\right\}$$

The total charge is

$$\frac{4\pi\beta}{\gamma}\left\{\frac{1}{1 + \dfrac{n_y v_y \gamma}{\left(k + C\dfrac{dr}{dt}\right)\sqrt{6\pi}}}\right\} = M, \qquad (10)$$

but

$$M_0 = \frac{4\pi\beta}{\gamma}\left\{\frac{1}{1 + \dfrac{n_y v_y \gamma}{k\sqrt{6\pi}}}\right\}$$

= total charge when rate of absorption is zero.

Therefore

$$M - M_0 = \frac{(96\pi^3)^{\frac{1}{2}} n_v v_v \beta C \frac{dr}{dt}}{\left\{\left(k + C\frac{dr}{dt}\right)\sqrt{6\pi} + n_v v_v \gamma\right\}\left\{k\sqrt{6\pi} + n_v v_v \gamma\right\}}$$

and

$$\frac{1}{M - M_0} = \frac{(k\sqrt{6\pi} + n_v v_v \gamma)}{4\pi n_v v_v \beta} + \frac{(k\sqrt{6\pi} + n_v v_v \gamma)^2}{(96\pi^3)^{\frac{1}{2}} n_v v_v \beta C}\frac{dt}{dr}$$

$$= \left(\frac{k\sqrt{6\pi} + n_v v_v \gamma}{4\pi n_v v_v \beta}\right)\left(1 + \frac{k\sqrt{6\pi} + n_v v_v \gamma}{\sqrt{6\pi} C}\frac{dt}{dr}\right)$$

or

$$\frac{1}{M - M_0} = A + B\frac{dt}{dr},$$

where A and B are constants so long as n, v and k are constant

If now a series of bubbles of constant diameter are examined in water of constant conductivity but containing different quantities of air in solution,

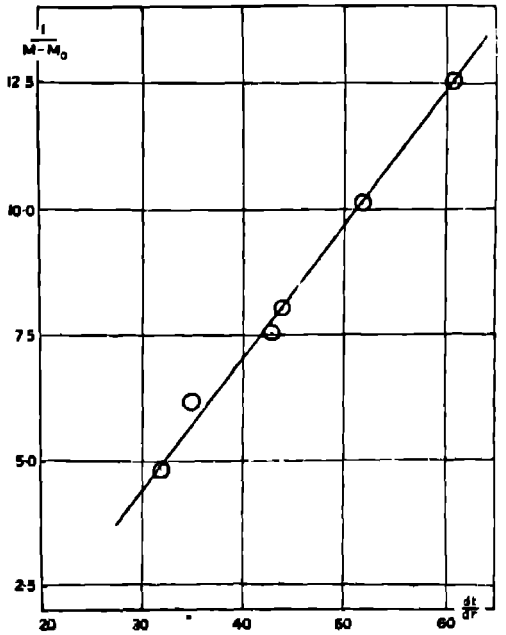

Fig. 5

then n, v and k will be constant and by the above equation there should be a straight line relation between $1/(M - M_0)$ and dt/dr.

This has been examined experimentally. A bubble of 0·05 cm. diameter was used in air-saturated water. The equilibrium charge on this bubble gives the value of M_0. The charge (M) on a bubble of the same diameter was then measured in a series of experiments in water unsaturated by air. By using water of various degrees of air saturation values of M could be determined for various values of dr/dt (measured experimentally). The $1/(M - M_0)$ was then calculated and plotted against dt/dr. The result is seen in fig. 5, which is a straight line graph and offers strong evidence in support of the theory.

Evaluation of the Potential Difference between the Surface and the Interior of the Liquid

Since it is assumed that an air bubble has a resultant charge, Helmholtz' equation may not be applied. On the other hand, the concentration of adsorbed ions on the bubble surface will result in a potential difference between the surface and the interior of the liquid. This potential difference may be determined by the use of the Boltzmann equation

$$m_1 = m_2 e^{-\psi/kt},$$

where m_1 and m_2 are the number of particles in regions 1 and 2 in equilibrium, and ψ is the work done in moving one particle from region 1 to region 2.

Now let m_2 and m_1 be the number of free negative ions per c.c. near the bubble surface and in the interior of the liquid respectively. If there is a difference of potential of V volts between these regions, the work done in moving one ion from the surface into the interior of the liquid will be $Ve/300$ ergs.

Taking $e = 1{\cdot}774 \times 10^{-10}$ e.s.u.

$k = 1{\cdot}372 \times 10^{-16}$

$T = 300°$ A.

$$\frac{e}{kT} = 38{\cdot}65,$$

$$\log_e m_1/m_2 = 38{\cdot}65\ V,$$

or
$$V = \frac{1}{38{\cdot}65} \log_e \left(\frac{m_1}{m_2}\right). \qquad (11)$$

Hence a knowledge of the number of ions per c.c. in the liquid and on the surface will give the value of V. It has been shown above that in one representative experiment, the number of ions per c.c. in the liquid was $7{\cdot}0 \times 10^6$. For the evaluation of m_2 it is only necessary to consider the uncovered negative

ions on the surface, since those having a positive ion attached will exert no repulsion on another negative ion approaching the surface

In equilibrium in the above experiment, the number of such ions on the bubble was $2 \cdot 09 \times 10^5$ Consider the time at which the area of the bubble was 5×10^{-3} square cms

Then the number of ions attached per square cm $= 1 \cdot 18 \times 10^6$ and average distance between these ions $= \left(\frac{1}{1 \cdot 18 \times 10^6}\right)^{\frac{1}{2}}$

$$= 4 \cdot 89 \times 10^{-4} \text{ cm}$$

Hence in a small volume close to the bubble surface the negative ions are $4 \cdot 89 \times 10^{-4}$ cm apart Consequently the number per c.c in this region is $\left(\frac{1}{4 \cdot 89 \times 10^{-4}}\right)^3 = 8 \cdot 55 \times 10^9$,

hence

$$m_1 = 7 \cdot 0 \times 10^8,$$

$$m_2 = 8 \cdot 55 \times 10^9,$$

and therefore by equation (11)

$$V = 0 \cdot 064 \text{ volt},$$

which agrees well with the values determined directly by other observers.

Since it is found that while the bubble shrinks the charge remains constant, m_2 and therefore V must increase as the bubble diameter decreases.

Summary

The electrical charge on an air bubble in water is measured under various conditions and an examination is made of the mode of formation of this surface charge. For bubbles ranging in diameter from 2 0 mm to 0 2 mm. the total charge is independent of the diameter when equilibrium conditions obtain at the surface

The constitution of the surface layer is examined theoretically and a new method of measuring the potential difference between the surface and the interior of the liquid is suggested

In conclusion the writer wishes to express his appreciation of the unfailing kindness of Prof. Sir J J. Thomson, who has interested himself in the work and given much helpful criticism.

The Effect of Superposed Alternating Current on the Polarisable Primary Cell Zinc—Sulphuric Acid—Carbon Part II – High Frequency Current

By A J Allmand, D Sc., and H C. Cocks, Ph D.

(Communicated by Prof S. Smiles, F R.S —Received May 11, 1926)

In Part I of this investigation,* it was shown that, when alternating currents of frequencies between 20 and 400 per second are passed through the primary cell zinc-sulphuric acid-carbon, the depolarisation and increase in current output first observed by Brown,† are essentially due to an effect produced at the carbon electrode, the potential of which becomes more positive by an amount depending on the strength and frequency of the alternating current used The greater this current and the lower its frequency, the greater the effect, a result quite in line with what was already known on the subject of the action of superposed alternating currents on polarised electrodes

Brown had, however, also obtained a marked action when using a current of 12000 periods, and had ascribed it to an effect produced at the zinc electrode The results of Allmand and Puri indicated that such high-frequency currents would be unlikely to depolarise the carbon electrode perceptibly. In addition, the anodic solution of zinc is usually regarded as occurring almost reversibly, although Allmand and Puri had certainly noticed a small depolarising effect caused by their low frequency currents. Consequently, the results reported by Brown with a frequency of 12000 appeared to merit further investigation, and the present paper contains an account of experiments to this end.

The high-frequency current was generated by a valve oscillator of simple design and construction. Three independent coils were used—a grid coil, an anode coil shunted by a condenser, and a tapped coupling coil These were wound with fairly heavy gauge D S C wire on large disc-shaped formers. When the apparatus was in use, the anode coil was placed on the grid coil, and the coupling coil placed on the anode coil, or supported at a small distance above it, according to the output required. The most suitable tapping of the coupling coil for maximum output according to the impedance of the circuit with which it was connected was found by trial.

Three Marconi-Osram L.S 5 valves were used, their grids, anodes and filaments

* 'Roy Soc Proc.,' A, vol 107, p 120 (1925)

† 'Roy Soc Proc.,' A, vol. 90, p. 26 (1914)

being connected in parallel. The grids were given a negative bias of 45 volts by means of a high-tension battery, thus avoiding the use of a grid leak and grid condenser The anode voltage was maintained at 340 volts, and an output of about 4 watts was obtained The anode current was furnished by a 100 volt-500 volt direct current rotary transformer. In order to diminish commutator ripple, it was passed through a " smoothing " unit, consisting of two 20-Henry choke coils (one in the positive and one in the negative lead) and two 2-microfarad condensers (one connected across the input side and one across the output side of the choke coils). The inductance of the anode coil was measured and found to be 0 011 Henry , it was therefore shunted by a condenser of 0 016 microfarad, this being the calculated value for giving a circuit resonant to 12000 cycles. The frequencies actually generated were measured by means of a heterodyne wave-meter, using the usual " zero beat " method. They were found to vary with the output of the oscillator in accordance with the following table - -

Table I

Current in amperes delivered to the cell	Frequency (cycles per second)
0 0	10280
0 1	10300
0 3	10450
0 5	10910
0 7	11110
0 9	11450

Experiments on Current Delivery.

The primary cell consisted of a carbon rod 1 c m in diameter, and a stick of amalgamated commercial zinc of about the same dimensions, these being immersed to varying depths in aqueous sulphuric acid of 1 20 specific gravity. The circuits employed were very similar to those used by Brown. The direct current circuit contained a switch, a moving-coil milliammeter, a choking-coil and a variable resistance The alternating current circuit was composed of the coupling-coil, a hot-wire ammeter, a variable resistance and a 1-microfarad condenser. In each experiment, the direct-current circuit was first closed, and the cell allowed to furnish current, the regulating resistance being adjusted until the amperage had settled down to a pre-determined figure. The alternating current was then switched in, kept running for a minute, and the new value of the direct current read off This was repeated for different alternating-current strengths, the direct current being adjusted to its original figure in

between the alternating-current periods when required. This was seldom necessary, as, in practically every case, the changes in direct current, on switching in and out the alternating current, were abrupt and at once ceased. During all the experiments, the zinc electrode remained coated with bubbles of hydrogen, and no difference in its appearance could be detected when the alternating current was switched in or out.

The lengths of electrode immersed in the different experiments were as follows:—

I.—5 c.m. of zinc rod, 5 c.m. of carbon rod.
II.—5 c.m. of zinc rod, tip of carbon rod.
III.—Tip of zinc rod, 5 c.m. of carbon rod.

In two other experiments, the carbon rod was fully depolarised by immersion in a small porous pot containing strong nitric acid (as in the Bunsen primary cell).

IV.—5 c.m. of zinc rod, 5 c.m. of carbon rod (in HNO_3).
V.—Tip of zinc rod, 5 c.m. of carbon rod (in HNO_3).

The voltages of these cells when furnishing direct current in the normal way were not actually measured, but it will be clear, when it is remembered that the main polarisation is at the carbon electrode, and, in every case, will be greater, the smaller the electrode, that they will stand in the order IV>V>I>III>II. A calculation based on the currents supplied and the approximate values of the series resistances in the different cases points to figures of about 1·6, 1·5, 0·2, 0·1 and 0·04 volt respectively.

The data obtained are plotted in the figure.

The results are, of course, somewhat complex, owing to the fact that, as will be seen later, polarisation is occurring normally at *both* electrodes, and that therefore, if it is relieved at one electrode, the increased cell output is, to a certain extent, nullified by the fact that the greater current density causes increased polarisation at the other electrode. They can, however, be explained on the assumption that, as Brown supposed, the seat of the depolarising effect of the high-frequency current is solely at the zinc, and not at the carbon, electrode. Thus, cells IV and V both give an increased current output. The percentage increase is, however, small, as the cells, to commence with, are only slightly polarised. It is rather greater with V than with IV, where the initial polarisation, owing to the larger zinc electrode surface, is less. With cell I, the effects are much greater, corresponding to the low initial voltage. Curve III rises more rapidly

than I, owing to its originally heavier polarisation. In cell II, the initial polarisation is almost entirely due to the small carbon electrode, and this is not affected

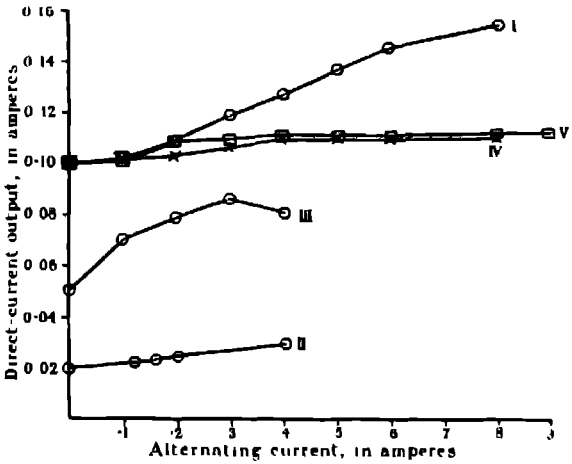

by the alternating current Hence, its increase in output is relatively small, even for a very high ratio of alternating current to initial direct current

Experiments on Electrode Potential

The measurement of electrode potential, however, offers the most certain method of investigating the nature of the effect, and such measurements were next undertaken The general arrangement employed was similar to that used by Allmand and Puri, but the problem was here a simpler one, in that the high-frequency currents allowed of the use of a condenser in the alternating current circuit, any leak of direct current into the latter being thereby eliminated The same carbon electrode was used as in the above experiments, whilst the amalgamated zinc electrode was of the pure metal, 1 × 1 cm. in cross section Both electrodes were immersed in the electrolyte (sulphuric acid of 1 20 S G.) to a depth of 5 cm. The auxiliary electrode for leading in the alternating current was of the same material as the cell electrode under investigation, whilst the choking-coil in the direct-current circuit prevented alternating current from passing through the other cell electrode The circuits were otherwise practically identical with those described above A voltmeter was put across the cell electrodes in order to measure the effect of the superposed alternating current

on the cell voltage The electrode potentials were determined by the usual compensation method, employing a Luggin capillary, metre bridge, and moving coil galvanometer. A normal mercurous sulphate electrode was used as reference electrode, and was connected with the cell electrolyte by a bridge of N H_2SO_4.

In carrying out the experiments, measurements of open circuit E M.F and of electrode potential were first taken. The cell was then allowed to discharge through a suitable resistance in the direct-current circuit until the current was constant (30 minutes to 2 hours), when current, voltage and electrode potential were read Then an alternating current of 0·1 amp. was allowed to flow for five minutes, and a fresh set of readings taken This was followed by an interval of five minutes with direct current only, the same readings as before being taken, after which alternating current of higher amperage was applied for five minutes, and so on The highest alternating current used was 1 ampere, whilst the direct current output of the cell varied between 0·023 and 0 009 ampere.

The results obtained when the high-frequency alternating current was superposed on the carbon cathode are quickly described. Two series of readings were taken, and in neither of them was an alteration in polarisation greater than one millivolt observed when switching in or out the alternating current In 10 out of 14 such changes, there was no perceptible effect Naturally, the cell voltage—read to the nearest millivolt—was equally unaffected. The ratio alternating current . direct current in these experiments varied between 2·2 and 45 We therefore conclude that alternating currents of frequency 10,000–12,000 do not affect the polarisation of a carbon cathode charged with hydrogen, a result to be anticipated from the work of Allmand and Puri.

With the zinc electrode, an effect was obtained, and the data are given in Table II.

It will be noticed, first, that the effect of superposing the high-frequency alternating current on the zinc electrode is to increase considerably the cell current output Thus, with an alternating current of 0·9 amp., the cell current is doubled During the intervals in which alternating current is not flowing, however, it drops below its original value. This is due to the increased polarisation at the carbon electrode, brought about by the heavier current passing during the preceding period. Column 4 shows the corresponding voltage changes, and its last two readings bring out the slow recovery of the polarised carbon electrode after all current has ceased to flow. The chief interest in the table, however, lies in columns 5 and 6 Column 5 shows that an amalgamated zinc anode,

Table II.

Time in minutes from commencement of experiment.	Alternating current in amperes	Direct current in milli-amperes	Voltage of primary cell in volts.	Potential of Zinc Electrode (e_A) in volts.	Change in potential in millivolts due to alternating current
0	0 0	0	1 3	0 740	
30	0 0	50	0 12	0 673	
40	0 1	50	0 115	0 682	— 9
50	0 0	49	0 110	0·673	
55	0·2	52	0 123	0 704	-29
60	0 0	48	0 108	0 675	
65	0 3	60	0·140	0 737	-62
70	0 0	45	0 105	0 673	
75	0 4	70	0·163	0 777	—104
80	0 0	45	0·105	0 672	
85	0 5	80	0 190	0 818	—146
90	0 0	45	0 105	0 672	
95	0·9	99	0 232	0 885	—213
100	0	46	0 109	0 675	
115	0	0	0 74	0 781	
150	0	0	0 91	0 781	

subjected in dilute sulphuric acid to a current density of the order* of 10 milliamps./cm.^{2}, is polarised to the extent of more than 0·1 volt, whilst column 6 shows that high-frequency currents not only lower this polarisation, but, if sufficiently great, completely destroy it, and, eventually, make the electrode considerably less noble than a static zinc electrode Allmand and Puri (who were using a considerably lower direct current than here employed) make no particular reference to any direct current polarisation, whilst the depolarising effect of their low-frequency alternating currents was far less than here recorded (although the maximum *alternating current : direct current* ratio in their case was 200, as against 20 in the above table)

The zinc electrode in this experiment was covered with bubbles of hydrogen. Although no visible change of any kind was noticed when the alternating current was switched on, some connection between the presence of this layer of gas and the unexpected polarisation and depolarising effect appeared possible. Accordingly, experiments were done in which the zinc electrode was placed in a neutral $ZnSO_4$ solution, whilst the carbon electrode was immersed in a dilute solution of sulphuric acid, contained in a porous pot. Using a normal calomel electrode, the influence of the high-frequency current on the potential of the zinc electrode (when the cell was polarised) was again investigated. The effects observed were less, and it suggested itself that they were connected with the diffusion of

* This assumes that only one face of the immersed rod carries the current The real current density will certainly be less than this, and will vary from point to point of the electrode.

acid out of the porous pot surrounding the cathode. Accordingly, the carbon cathode was replaced by one of amalgamated zinc, and the sulphuric acid by neutral $ZnSO_4$ solution, the anode now being polarised by an accumulator placed in the direct current circuit. The result was to reduce both the direct current polarisation (already much less than when the zinc was in the sulphuric acid), and also the effect of the alternating current, down to a few millivolts. On adding sulphuric acid to the electrolyte, both these magnitudes rose to values comparable with those first observed with the acid solution. The actual data are recorded in the paper which follows

Discussion.

It thus appears that high-frequency currents have a very considerable depolarising action on an anode of amalgamated zinc in a solution containing free acid, and that this effect, as suggested by Brown, is the cause of the increased current output in the $Zn-H_2SO_4-C$ cell Both electrodes in this cell contribute to the polarisation, the carbon to a considerably greater extent than the zinc. But whereas low-frequency alternating currents only affect the zinc electrode to a small degree, whilst materially decreasing the polarisation at the carbon, high-frequency currents are without any effect whatever on the carbon, and profoundly influence the zinc electrode The depolarising action of the low-frequency currents on the carbon electrode can be attributed to the partial destruction of the hydrogen charge during the anodic pulse, a reaction which is by no means instantaneous, and therefore the more marked the lower the frequency But the effects at the zinc electrode described in this paper are less easy to analyse. We have investigated them in more detail, and the results are described in the following communication. Here it will only be said that they are apparently in no sense connected with the disruption of a visible film of gas by means of a rapidly alternating electrical stress There is no perceptible change in appearance of the gas-covered zinc anodes when the current is applied. There is no change in appearance or decrease in overvoltage at the carbon cathode under the same circumstances And in the experiments mentioned above, in which the zinc was immersed in a zinc sulphate solution, under conditions which made diffusion of acid from the cathode possible, although both polarisation of the anode and its removal by the high-frequency current were observed, there were no visible bubbles of gas on the zinc.

These experiments were carried out in the autumn of 1925. We are indebted to a fund put at the disposal of the laboratory by Brunner, Mond and Company, Limited, for the purchase of the rotary transformer and the wave-meter.

The Polarisation of Zinc Electrodes in Neutral and Acid Solutions of Zinc Salts by Direct and Alternating Currents.—Part I.

By A. J. Allmand, D Sc, and H. C. Cocks, Ph D.

(Communicated by Prof. S Smiles, F R.S —Received May 11, 1926)

1. *Introductory.*

In the preceding paper* it was shown that an amalgamated zinc electrode made anode in an acid zinc sulphate solution undergoes considerable polarization, and that this polarization can be more than overcome by the superposition of a sufficiently large alternating current of high frequency Further, Allmand and Puri† mention experiments in which a cathode of amalgamated zinc had superposed on it alternating currents of intensities up to 200 times that of the direct current, and of frequencies varying between 20 and 400, the effect being to increase the polarization of the electrode, which became more negative. These results were not to be anticipated from previous work, and it seemed that a closer investigation of the whole subject might not only explain the facts referred to, but perhaps throw fresh light on the mechanism of the electrode processes involved. As possible factors affecting the phenomena could be considered the amalgamation or otherwise of the zinc electrode, the presence or absence of free acid in the solution, the nature of the zinc salt (*e g*, whether sulphate or chloride), duration of electrolysis, temperature, the absolute and relative values of the direct and alternating current densities, and the frequency of the alternating currents The present paper contains an investigation of some of these points. Working at room temperature and with zinc sulphate solutions, potential measurements have been made with amalgamated zinc electrodes in absence and in presence of free H_2SO_4, and with unamalgamated electrodes in neutral solution. Alternating currents and compound currents‡ have been used, and a few experiments made with direct currents Frequencies varying between 50 and 11,000 have been worked with.

2 *Experimental.*

The experimental arrangement used was simple. The electrolysis vessel, a large beaker, was covered with an ebonite plate which carried three zinc

* p. 252 *supra*

† 'Roy. Soc Proc.,' A, vol 107, p 126 (1925).

‡ An alternating superposed on a direct current will be termed a *compound current* in this paper.

electrodes. These were of the purest zinc available (amalgamated or unamalgamated), identical in dimensions (rectangular rods of cross-section 1 × 1 cm.), and were immersed to a depth of 5 cm in the electrolyte Two of the three were placed close together, and the third some distance away. In the compound current experiments, the middle of the three was the one polarized by the compound current and the one the potential of which was measured The adjacent electrode led in the alternating-current, whilst the more distant one acted as the other direct-current electrode In the measurements with alternating or direct current, two only of the electrodes were used The electrolyte was well stirred. The direct current was supplied by accumulators, whilst the low-frequency alternating currents were obtained from the generators described by Allmand and Puri By altering slightly the positions in the circuit of the moving coil milliammeter and the hot-wire ammeter, the arrangement for compound currents used by Allmand and Puri was much improved on (see fig. 1) Although leakage of alternating current into the direct-current circuit and *vice versa* still takes place, the actual readings given by the instruments measure the currents which pass through the electrode under experiment, and require no correction for leakage. When working with high-frequency currents, the generator and arrangement described by the authors in the preceding paper were employed An additional set of coils was made for us by the Research Staff of the General Electric Company, who found that, when they were used under the operating conditions described in the preceding paper, the frequencies of the currents generated were 535 cycles, 1050 cycles and 1950 cycles when the anode coil was shunted by a condenser of 1 microfarad, ½ microfarad and 1/16 microfarad respectively. These frequencies were checked by us when our apparatus was set up by comparing the note heard in a telephone held near the coils with that of known frequency produced by a tuning fork.

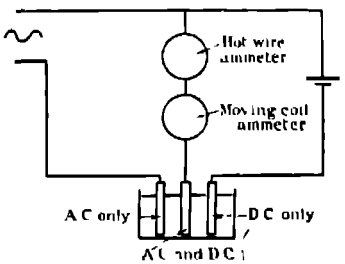

Fig 1

The potential measurements were made in the usual manner, using a normal calomel electrode, with a bridge of 3 N. KCl Precautions were taken to prevent the diffusion of this salt into the electrolysis vessel Occasionally a normal mercurous sulphate electrode was used All potentials in the paper are referred to the hydrogen scale.

3. *Unamalgamated Electrodes in Neutral Normal Zinc Sulphate Solution*

In all these experiments, unless otherwise stated, the electrode under observation was polished with emery cloth before use.

Initial Static Potential.—This was observed on many occasions. The most negative figure obtained was − 0·793 volt (twice), the most positive − 0 777 volt (once), and the mean of 37 recorded readings − 0 784 volt. Usually about 20 minutes were required for these potential differences to become constant.

Cathodic Direct-Current Polarization.—With a current of 50 m a., an initial polarization of nearly 80 m v. was observed. This fell in course of time, and, after an hour, the electrode was about 60 m v. more negative than its original static potential. Higher and lower current densities gave correspondingly greater and smaller polarizations. On cutting off the current, the potential of the electrode immediately became more positive and, after a few minutes, settled down at − 0·795 volt and remained there for hours. This figure, which was always obtained, is more negative than the original static potential. The cathode after electrolysis was covered with a dark grey deposit, semi-crystalline in appearance.

Anodic Direct-Current Polarization.—With the same current of 50 m a., the initial polarization observed was about 20 m v., *i.e.*, considerably less than at the cathode. It fell with time, but only about 4 m v. in the hour, a smaller rate than with the cathode. A change in current density caused a change of polarization in the usual direction. On cutting off the current, the potential at once became more negative, and, on those occasions on which it was read immediately, was found to have passed its original static potential by a few millivolts. This effect, however, was only transitory, and in half-an-hour the original potential had been regained—in fact, the electrode sometimes became more positive than its original figure. The electrodes under anodic treatment roughened slightly and became dark grey.

Alternating-Current Polarization.—Measurements were carried out with frequencies of 50, 450, 1,950 and 11,000 cycles. In general, the potential of the electrode whilst the current was flowing was *more negative* than the static value, but the result was complicated by two facts. The static potential itself, except in the high-frequency experiment, was altered in the negative direction by the passage of the current, and only returned to its original figure comparatively slowly after the current was cut off. Further, the polarization due to the alternating current became less with increased time of electrolysis, whether

referred to the original static potential, or to its intermediate value, determined during the course of the experiment, either immediately before or immediately after the measurement on the polarized electrode.

With the high frequency, the effect produced was small—thus, an alternating current of 0·9 amp. only changed the electrode potential from −0·790 to −0·799 volt. With frequencies of 1,950 and under, care had to be taken to avoid getting spurious results, owing to the time effects mentioned. Measurements were accordingly made in which (*a*) the frequency was kept constant and the alternating current increased by steps, periods of current flow being intercalated with equal periods during which no current was passing, (*b*) an alternating current of constant amperage and frequency was allowed to flow for a considerable time—up to one hour—then cut off, and the rate of return of the electrode potential to more positive values noted, (*c*) experiments similar to those under (*a*) were carried out, except that currents of two frequencies were used alternately, two measurements with a given current density thus being made before going on to a higher current density. The results of these numerous experiments lead us to conclude that an increase in current density causes a slight increase in the effect, and that the influence of frequency within the limits of 50–2,000 is negligible. Table I, which contains the amounts in millivolts by which an electrode becomes more negative than its (intermediate) static potential after current has been flowing for five minutes, supports these conclusions. With the exception of the figures with currents of 0·5 amp., the values given are the average of two to four readings.

Table I

Frequency	Current in Amperes.					
	0·05	0·1	0·3	0·5	0·7	0·9
50	32	32	36	45	38	44
450	—	33	42	—	—	51
1950	31	33	36	40	39	—

In most cases the electrodes were hardly changed in appearance during these experiments, merely becoming somewhat duller. If, however, a sufficiently large number of coulombs at a sufficiently low frequency were passed through the electrode, the surface of the latter became more or less covered with a loose grey powder. The static potentials immediately after cutting off the current

varied between — 0·789 and — 0·791 volt, these figures usually slowly becoming more positive with time, and approaching the original static value.

Cathodic Compound Current Polarization.—Keeping the direct current constant at 0·05 ampere,* the alternating current was increased in steps, with intervening periods during which only direct current was flowing. In some cases, the frequency was kept constant during such a series of measurements, in other cases, two frequencies were used alternately (procedures (*a*) and (*c*) as described for the alternating-current experiments). Complications were present owing to the cathodic direct-current polarization decreasing with time, and the static potential becoming more negative. With the 11,000 frequency, practically no change in potential could be detected on switching in and out the alternating current. With frequencies between 50 and 1950 (measurements were also made with $n = 100$, 240 and 450) and alternating currents of 0·1—0·9 ampere, a depolarizing effect was noticed in every case—that is, the potential became more positive when the alternating current was superposed. The changes observed ranged between 4—23 m.v. Owing to the complications referred to, the measurements were not very reproducible. The figures in Table II give the average differences observed between the *intermediate direct-current cathodic potentials* and the compound-current potentials (one set of readings only for $n = 100$).

Table II

Frequency.	Current in Amperes				
	0·1	0·3	0·5	0·7	0·9
50	13	14	16	9	11
100	13	16	15	12	12
240	15	20	18	16	15
450	12	20	19	16	14
1950	4	9	12	10	—

Frequency would seem to have no influence up to $n = 450$, but the change to $n = 1950$ results in a smaller effect, particularly with lower current densities. There would seem to be, from the table, an optimum current density between 0·3—0·5 amp. This, however, is only apparent, in the sense that, during the electrolysis, the direct-current cathodic polarizations were becoming less (by

* In all the experiments described in this paper with compound, or superposed alternating on direct currents, the direct-current component was kept throughout at 50 milliamperes.

10--20 m v. in the course of a run) and the static potentials more negative (they were — 0·794 to — 0·795 volt at the conclusion of a series of measurements, a change of 13 m v. in the extreme case) It is therefore probable that, *referred to the intermediate static potentials*, which were not measured, the polarization produced by the compound current may continue to decrease still further as the alternating-current component increases If the mean values of the actual measured potentials be considered, thus eliminating changes in direct-current polarization, the maxima already disappear in the case of the three higher frequencies and are made flatter for the lower frequencies

After the electrolysis, the electrode was found to be covered with a dark semi-crystalline deposit when working with low frequencies, and with a dark grey film when using the high frequency

Anodic Compound Current Polarization —The experiments were carried out similarly to those just described The complications encountered when the polarized zinc electrodes were more negative than the static value were here much less important, and the result consequently more reproducible and easier to interpret. Measurements were made with currents of frequency 50, 100, 240, 450, 530, 1050, 1950 and 11,000 The superposition of an alternating current on a polarized zinc anode causes depolarization, which is greater the larger the alternating current and the lower the frequency Currents of $n = 1950$ and 11,000, even of the maximum strength used in these measurements, gave no definite perceptible effect With $n = 1050$, an effect was first noted at 0 3 amp., and with $n = 530$ at 0·1 amp As frequency was still further lowered, so the effect increased, till, with $n = 50$, a current of 0 1 ampere caused a depolarization of 5 m.v or more

Just as in the measurements with direct current, on cutting off the compound current, the electrodes assume for a short time a potential more negative than the initial static value, changing in the course of an hour or so to a figure more positive than the initial value.

4. *Amalgamated Electrodes in Neutral Normal Zinc Sulphate Solution.*

In all experiments with amalgamated electrodes, these were freshly re-amalgamated before use, unless otherwise stated

Static Potential —Some twenty measurements were made on freshly amalgamated electrodes, and a large number after a polarizing current of some description had been cut off The extreme figures noted were — 0·794 and — 0·797 volt. The average of — 0·796 volt is the accepted figure for the potential of the system $Zn/N.ZnSO_4$.

Cathodic Direct Current Polarization.—This was measured for currents between 10 and 100 m a., and found to be small (up to 15 m v). In one case, the polarizations observed decreased with time, being several millivolts less after 10 minutes passage of current than after 5 minutes. Thus, with 50 m a., the initial value of 13 m v. changed to 10 m v. The bright surface of the electrode was afterwards found to be dulled. In another instance, where the polarizations were constant over 10 minutes, they were distinctly lower, and the electrode at the end of the experiment was crystalline in appearance. The polarization for a current of 50 m a. was 7 m.v. in this case. The same figure was obtained in another experiment, and remained constant over an hour. In still another case (see below), the polarization for the same current was only 1 m v., and remained constant during the experiment (15 minutes).

Anodic Direct-Current Polarization.—This was still smaller, and increased linearly with the current density, in one case amounting to 9 m v. at a current of 0·1 ampere. After the experiment, the electrode surface was somewhat dulled.

Alternating Current Polarization.—Measurements were made with currents of frequency 50, 1950 and 11,000. No appreciable time effect was noticeable. The observed polarizations were negative and very small with the two lower frequencies. Thus, with a current of 0·5 ampere and frequency 50, values of 2 and 4 m v. were noted in two different experiments. The figures with $n = 1950$ were practically the same, if anything, rather less. With $n = 11{,}000$, the effect was greater, *e.g.*, 16 m v. for 0·5 ampere. The electrodes became a dull white in appearance during the low-frequency experiments—with 11,000 cycles, no change was noticed.

Cathodic and Anodic Compound Current Polarization.—We used currents of 50, 480 and 11,000 cycles. With the lower frequencies, the effects of superposing an alternating current were small at both anode and cathode. In the former case, within the experimental error of 1 millivolt, whilst, in the cathodic experiments, on one occasion a slight *increase* in polarization apparently took place (not exceeding 2 millivolts with an alternating current of 0·9 ampere) the remaining experiments giving no indication of any effect on the direct-current polarization figures. The intermediate direct-current cathodic polarizations fell throughout the experiments, and were only about 5—6 m v. at the end of a run, whilst the surface of the electrodes became roughened and crystalline in appearance. In one experiment, where the initial figure was abnormally high, a decrease also took place in the anodic direct-current polarization.

With 11,000-cycle currents, no change whatever was noticed when they

were superposed on a cathode, the direct-current polarization of which, however, was only 1 m.v (less than the usual figure). In the anodic experiments, the direct-current polarization was 10 m v (greater than usual) and remained unchanged during the measurements. A definite depolarizing effect was produced in this case, amounting to 10 m v. when the alternating current was 0·9 ampere.

5. *Amalgamated Zinc Electrodes in Acidified Zinc Sulphate Solutions.*

Static Potentials.—About fifteen readings of the potential of an amalgamated electrode in N $ZnSO_4$ + N H_2SO_4 gave values varying between extremes of − 0 791 and − 0·799 volt, the mean of just over − 0·795 volt being practically the same figure as was given by unacidified N $ZnSO_4$. No gas film was visible on the electrodes. On the other hand, in solutions of composition N. $ZnSO_4$ + 7N H_2SO_4, where the zinc electrode became covered with bubbles shortly after immersion, potentials of − 0·811 to − 0·818 volt were observed

Cathodic Direct-Current Polarization —This was considerable, and depended on the concentration of the free acid and the time of electrolysis. With an acid concentration of 1N, and a current of 50 m.a , the polarization, read five minutes after starting the current, was about 70 m v In one case, in which no visible change in the surface of the cathode was caused by the passage of the current, this figure decreased slowly with time, being 61 m.v. at the end of an hour In another case, in which the cathode became coated with minute zinc crystals during the experiment, the fall in potential was far more rapid, the polarization after an hour being only 17 m.v. With the more strongly acid solution (7N) and the same current density, an initial polarization of 0·197 volt was observed in one case, falling to 0 187 volt in 13 minutes , on another occasion, the initial figure was 0 220 volt, dropping to 0·193 volt after 34 minutes. There was a tendency towards slow cathodic evolution of hydrogen from this strongly acid solution, the gas bubbles which coated the electrode in the static condition becoming larger and, in some cases, detaching themselves Nothing of the sort was observed with the less acid electrolyte. On cutting off the current, the polarization immediately disappeared, potentials of − 0·796 volt and − 0·817 to − 0 820 volt being reached within a minute in the weak and strong acid solutions respectively

Anodic Direct-Current Polarization —High initial figures were obtained with the electrolyte N $ZnSO_4$ + N . H_2SO_4, less, indeed, than the corresponding cathodic polarization, but increasing to very high values as electrolysis proceeded. There was no visible alteration of any kind in the electrode. The

nature of these changes in two different freshly amalgamated electrodes is illustrated graphically in fig. 2

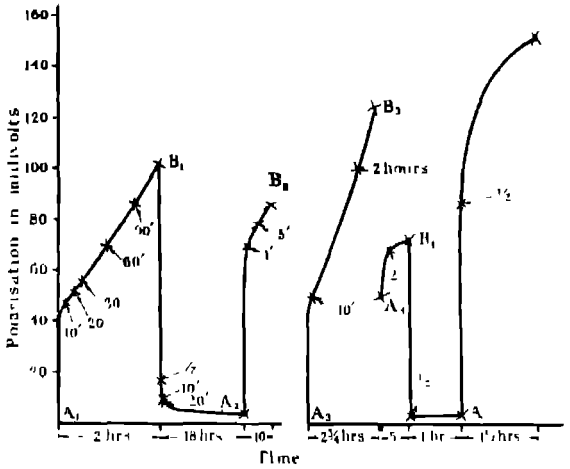

Fig 2

At points A_1A_2 . . , a current of 50 m a. was switched in, and at points B_1B_2. . switched out. Between B_2 and A_4, the electrolyte was changed, the current being interrupted for 30 seconds The polarizations observed are far greater than those given in neutral $ZnSO_4$ solutions, whether with amalgamated or unamalgamated electrodes Attention is drawn to the fact that high polarisation figures are reached far more rapidly after an electrode has been once polarized and allowed an interval for recovery than when a freshly amalgamated electrode is polarized for the first time Further, the recovery of the initial static figure after cutting off the current is much slower than is the case after cathodic polarization

With the solution of composition N $ZnSO_4 + 7H_2SO_4$, still greater initial effects were obtained Thus, with the same current, a polarization of 80 m v. was observed after two minutes and 90 m v after 10 minutes. With continued polarization, the layer of hydrogen bubbles slowly disappeared.

Alternating-Current Polarization —Using the electrolyte N. $ZnSO_4$ + N H_2SO_4, experiments were done with currents of 50, 460 and 1950 cycles. The polarisations observed were negative in all cases, and quickly became constant The figure obtained increased with increase in current density, at first rapidly and then more slowly, but appeared almost independent of frequency within the

limits used On the other hand, it seemed to depend on the initial potential of the electrode, being the greater, the more positive the latter. This is made clear by the data in Table III for $n = 1950$. The polarizations are given in volts. The initial static value of $-0{\cdot}782$ volt was found for an electrode which had not been freshly re-amalgamated before use

Table III

Current	Initial Static Potential		
	− 0 798	− 0·791	− 0 782
0 05 amp	− 0 011	− 0 022	− 0 033
0 5 amp.	− 0 032	− 0 038	− 0·050

After cutting off the current, the electrode potentials reverted to their original static values when these were of the normal figure of $-0{\cdot}795$ to $-0{\cdot}796$ volt With electrodes which were at the start more positive, the final static value lay between the original figure and $-0{\cdot}795$ volt. In all cases, currents of 0·5 amp and over caused the appearance of bubbles of gas on the electrodes.

Similar experiments were done with the more strongly acid solution, using a frequency of 11,000 Negative polarizations were observed, less at low current densities than those recorded above for the lower frequencies and less acid electrolyte, but increasing very rapidly with the current strength. With a current of 1 ampere, there was a slow evolution of gas, immediately ceasing when the current was cut off. The intermediate and final static potentials were within a millivolt of the initial figure

Cathodic Compound Current Polarization.—We used currents of 50 and 470 cycles in the weaker, and 11,000 cycles in the stronger, acid solution. The experimental data were again somewhat difficult to interpret, owing to the decrease of cathodic direct-current polarization with time. Making allowance for this, and for the less important changes in static potential which also took place during the electrolysis if the initial values differed from the average or normal value characteristic of the electrode system, the result is that alternating currents of all frequencies bring about a partial depolarization, i.e., that the electrode potential becomes more positive This effect increases rapidly with current density to begin with, but soon seems to approach a limit A change from 50-cycle to 470-cycle current has no effect. The visible result of superposing the alternating current in the $N.ZnSO_4 + N.H_2SO_4$ solution was to lead

to the appearance of bubbles of gas on the cathode In the case of the more strongly acid solution, the superposition of a higher frequency current of sufficient strength caused an increased rate of disengagement of the hydrogen with which the electrode was covered. This lasted for some minutes after the alternating current had been cut off

Anodic Compound Current Polarization —Similar experiments were done to those just described, and the same difficulties (though less important) were encountered in the interpretation of the results, owing to gradual changes in the direct-current polarization (a slow increase) and in the static potential (a tendency to become more negative) In all cases, a very marked depolarization resulted, and, with the highest currents used, the zinc was dissolved at measured potentials more negative than its static potential, *i.e*, it behaved like a baser metal than zinc. The biggest effects were noted with currents of 11,000 cycles in the solution of composition N . Z_nSO_4 + 7N . H_2SO_4 Our experiments do not yet enable us to say whether the increased acidity or the increased frequency is the essential factor The experiments with the lower frequencies and less acidified solutions indicate, however, a definite, though small, increase of the effect with rising frequency.

6. *Discussion.*

Fig 3 contains the salient numerical data which must be accounted for in any explanation of the phenomena described above. Along the ordinates are plotted the alternating current intensities in amperes. Potential differences expressed in millivolts are plotted vertically In diagrams *a*, *b*, *d*, *e*, *g*, *h*, in order to avoid complications due to changes in direct-current polarization with time during the experiments, the *intermediate potential* at any moment of the electrode polarized with a direct current of 50 m a. is taken as the zero of the scale, *i.e*, the direct-current polarization potential determined either immediately before switching in the alternating current or immediately after cutting it out The differences between this zero line and the various curves then give directly the effect on the potential of superposing for 5 –10 minutes on the direct current an alternating current of a certain frequency and intensity. The distance between the zero line and the heavy horizontal line represents the average value of *direct-current* polarization measured after the current has been passing for 5—10 minutes, and referred to the average *initial* static potential value of the electrode concerned [—0 784 volt for Zn (unamalgamated)/N . $ZnSO_4$; — 0·796 volt for Zn (amalgamated)/N . $ZnSO_4$ and Zn (amalgamated)/ N $ZnSO_4$ + N . H_2SO_4 ; — 0·815 volt for Zn (amalgamated)/N $ZnSO_4$ +

$7N.H_2SO_4$]. In this sense only, the heavy line corresponds to the static potential of the electrode Owing to changes in static potential and polarization

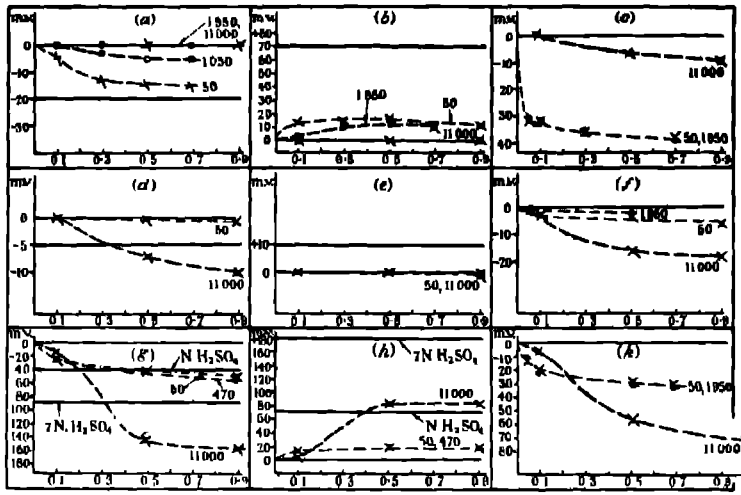

Fig 3

potential difference with time during electrolysis, the differences between this static potential line and the various curves in most cases have only a qualitative significance.

In diagrams *c*, *f*, *k*, the thin horizontal zero line denotes the intermediate *static* electrode potential, and the differences between this line and the various curves represent the immediate effect caused by switching in and out the alternating current.

(*a*) *Unamalgamated Electrodes*

In the case of the well-known anodic and cathodic retardation phenomena exhibited by the ferrous metals, it is generally agreed (although the details of the explanations proposed vary considerably) that the *presence* of oxygen or *absence* of hydrogen in the metal when acting as anode favours a high polarization figure, whilst the *presence* of hydrogen has the same effect in the cathodic process. The solution and deposition of most other metals from their simple salt solutions, on the other hand, have usually been regarded as taking place essentially reversibly, and the observed polarizations (less than with the ferrous metals) as being of the nature of concentration polarization.

A closer examination of the available data, however, shows that the matter is less simple. The cathodic and anodic current density—potential curves given by mercury and lead in their nitrate solutions—are indeed so steep as to be explicable in this way. But other systems—*e.g.*, $Zn/ZnSO_4$ and $Cu/CuSO_4$ behave differently. Thus, for the anodic solution of Hg (in acid $HgNO_3$), Cu (in acid $CuSO_4$), and Ni (in neutral $NiCl_2$) at room temperature and at a current density of 5 m a./cm ^{2}, the respective polarizations are of the order of 5, 20 and 400 m.v.; whilst for the cathodic deposition at the same current density of Hg (from acid $HgNO_3$), Zn (from neutral $ZnSO_4$), and Ni (from nearly neutral $NiCl_2$), polarizations of about 6, 70 and 180 m.v are required.* The obvious suggestion that, with metals like copper and zinc, electrode retardation phenomena occur of the same type as with the ferrous metals, but of smaller magnitude, is supported by the oscillographic work of Le Blanc,† who showed the existence, during both anodic and cathodic processes, of polarization effects too great to be accounted for by concentration polarization. We assume then that the observed polarization phenomena are due to retardations in the actual electrode process, and that these retardations are closely connected with charges of atomic oxygen and hydrogen in the electrode surface layers.

Static Potentials.—The presence of such charges being postulated, it follows that, at electrodes showing static equilibrium potentials, the following equilibria must exist—

$$Zn + 2\,H^{\cdot} \rightleftarrows 2\,H + Zn^{\cdot\cdot}$$

$$Zn^{\cdot\cdot} + 2\,OH' \rightleftarrows O + Zn + H_2O$$

and that the observed electrode potential difference must agree, not only with the figure calculated from the osmotic pressure of the zinc ions and the electrolytic solution pressure of zinc (to use the conventional terminology), but must equally be reconcilable with values derived from the electrolytic solution pressures of H and of O and the $H^{\cdot}$ and OH' osmotic pressures. The presence of O atoms in a zinc crystal lattice will result in a lowering of the electrolytic solution pressure of zinc, and the electrode will exhibit an alloy potential, the value of which will be more positive the higher the oxygen concentration. On the other hand, the presence of H atoms in the surface layer will make the potential more negative—atomic hydrogen is the baser constituent of the

* Förster, 'Elektrochemie wässeriger Lösungen,' pp. 355, 399 (1922). In our experiments with Zn/N $ZnSO_4$, the observed anodic and cathodic polarizations were also about 20 and 70 m.v respectively, which, with a current of 50 m.a., indicates that we had an active electrode area of 10 cm ^{2}.

† 'Abhandlungen der Deutschen Bunsen-Gesellschaft,' No. 3, pp 40 ff., 48 ff (1910).

Zn—H alloy. A zinc electrode in equilibrium with an aqueous solution of a zinc salt will contain then both H and O atoms in its surface layer—*in minute amounts*—and will have a potential which will be more negative the greater [H] and the less [O] The potentials of unamalgamated electrodes in N. $ZnSO_4$ noted by us averaged $-0{\cdot}784$ volt, and varied between $-0{\cdot}793$ and $-0{\cdot}777$. The true potential of Zn/N $ZnSO_4$, unaffected by other factors, is probably $-0{\cdot}796$ volt. We suggest that these electrodes, owing to contact with air, were carrying an O charge rather in excess of what would correspond to equilibrium between electrodes, originally oxygen-free, and an air-free electrolyte

Cathodic Polarization.—$Zn^{\cdot\cdot}$ and $H^{\cdot}$ ions, the latter in very small amount, are discharged, and the electrode becomes covered with a freshly deposited surface containing Zn and H atoms Hydrogen over-voltage at a zinc electrode is high, and this is explained by a slow rate of union of H atoms, deposited in the zinc lattice, to form molecular hydrogen. Consequently, the concentration of H atoms in the surface layer increases in excess of the amount which would correspond to the equilibrium potential of -0 796 volt, and the discharge potential of both $Zn^{\cdot\cdot}$ and $H^{\cdot}$ ions becomes more negative than this equilibrium figure. The polarization noted by us was about 80 m v at the start, but gradually decreased with time A change in appearance of the electrode took place simultaneously—it became covered with a loose greyish deposit It is known that hydrogen over-voltage is less in such a case than at a smooth electrode, owing to the decreased rate at which H atoms are deposited per unit of surface, and possibly owing to the fact that, in a metal lattice at the moment of its formation, the H atoms are less firmly held The same explanation would account for the decrease in zinc deposition polarization noted by us. The rapid fall in potential to the equilibrium figure of $-0{\cdot}795$ volt when the current was cut off is, of course, simply due to the rapid disappearance of the excess of H in the surface layers—either by the reaction $2H \rightarrow H_2$ or by $2H + Zn^{\cdot\cdot} \rightarrow 2H^{\cdot} + Zn$

Anodic Polarization.—We assume provisionally simultaneous formation of $Zn^{\cdot\cdot}$ ions and deposition of O atoms, the latter in small amount, and by the discharge of OH' or SO_4'' ions. The presence of the oxygen in the surface layers not only makes the reversible solution potential of the zinc more positive, but also retards the process $Zn + 2\oplus \rightarrow Zn^{\cdot\cdot}$ — it would seem natural that the presence of electronegative atoms in a metal lattice should restrain the mobility of the metallic atoms—and there is, consequently, an initial polarization of some 20 m v. A fresh metallic surface is being continually uncovered, and if one assumes that O deposition is occurring at a rate too

slow to keep up the O content to the value corresponding to the original air potential, the slow fall in polarization is explicable The slight roughening of the surface may also play a part. After cutting off the current, the potential at once drops to and passes its original value, an effect due to the low O density in the freshly exposed zinc surface But, in course of time, the electrode charges itself up with oxygen until in equilibrium with the atmosphere, and the original potential is reproduced.

Alternating Current Polarization (fig 3 (*c*)) —The potential read is an average figure, which is a complicated function of a large number of variables. Assuming, as here, that the electrodes exhibit polarization with direct currents, the simplest case conceivable is one in which the changes in the electrodes responsible for the setting in and disappearance of such polarization take place rapidly in comparison with the duration of a single unidirectional current pulse In these circumstances, the observed potential should be near the arithmetic mean of the direct-current potentials for this current density. If, on the other hand, some one or more of these processes take place slowly, then a divergence from this mean value may be anticipated. In our case the assumed relations are the formation and disappearance of H and O charges in the electrodes, and a polarization potential rather more negative than this mean value is found For an alternating-current of 0 05 ampere, the observed polarization for frequencies of 50 and 1950, after five minutes' flow of current were — 31 to — 32 m.v., whilst the mean value of the direct-current polarizations after the same lapse of time (anodic + 20 m v., cathodic — 70 m v.) is — 25 m.v This might be taken to signify that the rate of loss of deposited H atoms is so slow that an appreciable fraction still exists in the metal at the end of the cathodic pulse—or perhaps that the discharged OH' or SO_4'' ions had insufficient time to furnish oxygen, or this oxygen to enter the zinc surface This last supposition sounds plausible, for whereas only two steps are involved in the transition from $H^{\cdot}$ ions to a $Zn—H^{\cdot}$ alloy, three would appear to be necessary for OH' (or SO_4'') ions producing a Zn - O alloy

Facts which need explanation are that, whereas, below 2000 cycles the effect reaches a high value with a small current density, only increasing slowly as the current is increased, and is also independent of frequency, with a frequency of 11,000, the effect is far smaller, and is not disproportionately great for small currents. The smaller result produced by high-frequency currents may, of course, simply be due to insufficient time being given in the duration of a single pulse for even the (presumably) more mobile H atoms all to enter the zinc Another aspect of the phenomenon is that which considers to what

extent a single pulse of a certain frequency can affect the metal surface as a whole. A simple calculation will show that whereas one square cm. of zinc surface contains about $16{\cdot}8 \times 10^{14}$ atoms of zinc, a single cathodic or anodic pulse of 11,000-cycle current of 90 m.a./cm.^{2} will only deal with about $0{\cdot}13 \times 10^{14}$ atoms, *i.e.*, will change less than one per cent of the surface. With 50-cycle current, on the other hand, more than a complete layer of atoms is dissolved or deposited, and a larger effect of low-frequency current would thus be anticipated

Another view is that the H and O atoms deposited in succeeding pulses do not disappear as their respective gases, but mutually destroy one another on the reversal of current. In this case a stoichiometric excess of H over O atoms would be responsible for the residual negative polarisation There are clearly other possibilities of explanation, some of them of interest in connection with those theories of anodic solution which ascribe a necessary rôle to intermediate oxygen formation. Nothing is to be gained by discussing them further at this stage.

Compound Current Polarization (fig 3(*a*), (*b*)).—As the ratio of the alternating-current to the direct current increases, so the resultant current, from being a steady direct current, will first become a pulsating direct current, and, when the critical ratio A C · D C $\cdot 1 \cdot \sqrt{2}$ has been passed, will change into an asymmetrical alternating current. The greater the alternating-current component, the more nearly will this asymmetrical current approach a symmetrical one—as far as the *ratio* of the coulombs in the two pulses is concerned. But there will always be a constant *difference* in coulomb figures between the pulses, corresponding to the value of the direct-current component Over the pulsating direct-current range, the effect of the alternating-current superposition will be to lower the direct-current polarization by amounts which will be greater the higher the A C. D C. ratio, and the lower the frequency. The treatment given by Allmand and Puri* for gold anodes in HCl is applicable in such cases, and, although our actual measurements in this paper have been carried out at higher alternating-current densities, the trend of the curves agrees with their deductions.

When considering the effects of larger superposed currents, the residual direct-current component, and the fact that the net result of the electrolysis is the continual formation of a fresh zinc surface by deposition or solution, must be borne in mind. This aspect of the phenomena is particularly important when comparing the anodic compound current polarizations with

* 'Trans. Faraday Soc.,' vol. 21, p. 1 (1925).

the alternating-current polarizations. With an alternating-current component of 0·7 amp. (implying a coulomb ratio for the anodic, compared with the cathodic, pulse of 0·75 : 0·65), the average potential, even with 50-cycle current, a single pulse of which practically changes the whole of the surface layer, is still very far removed from the potential of an electrode polarized with 0·7 amp. of alternating current. On the other hand, the potential of an electrode polarized with a cathodic compound current of the same strength and of not too high a frequency, is within a few m v of the alternating-current electrode potential This difference in behaviour corresponds to the differences in nature of the electrode surface—with the excess anodic polarization, a surface hardly distinguishable from that resulting when using an anodic direct current but, with the excess cathodic polarization, a loose deposit, resembling the surface obtained after polarization for a sufficient time with pure alternating current of sufficiently high intensity and low frequency.

The influence of frequency is interesting, and includes points which cannot at present be satisfactorily explained, but which are clearly of importance in connection with the actual mechanism of the electrode processes. The effects of 1950-cycle current are of this nature Whereas with alternating currents they cannot be distinguished from those of 50-cycle current, in the cathodic compound current experiments, they are distinctly less, particularly at small current densities, and, in the anodic experiments, are indistinguishable from those of 11,000 frequency The small effect of high-frequency currents is readily explicable by the fact that, whereas the *net* result of the compound current is to deposit or dissolve some ten layers of zinc atoms per second (reckoned on the original dimensions of the zinc and assuming 10 cm^2 to be the effective area), a single pulse, even of the largest alternating current of 11,000 frequency used, does not affect as much as 1 per cent of a single layer.

(*b*) *Amalgamated Electrodes in Neutral Solution*

The *static potential* of − 0 796 volt we regard as the true equilibrium potential of Zn/N . $ZnSO_4$, unaffected by the oxygen changes which are made possible in the unamalgamated electrode owing to the constraining effect of the metallic lattice on the mobility of the oxygen atoms In the present case, the electrode will simply contain minute amounts of dissolved O and H atoms in electrolytic equilibrium with the H$^+$ and OH$^-$ concentrations in the electrolyte. The small polarization effects noted on making the electrode the *anode*, we attribute to concentration polarization in the amalgam layer, the actual process Zn + 2 ⊕

$\rightarrow Zn^{\cdot\cdot}$ taking place reversibly at the amalgam surface. The *cathodic* process appears to be slightly retarded, this retardation becoming less as electrolysis proceeds, and the amalgam surface becomes covered with crystals of zinc. As already noted, in one case it was only 1 m.v. with a current of 50 m.a. We suggest that, simultaneously with the $Zn^{\cdot\cdot}$ ions, $H^{\cdot}$ ions are discharged in small number, the H atoms formed dissolving in the mercury. Their rate of combination to form molecular hydrogen lags behind their rate of deposition, with the result that the alloy potential becomes more negative As the electrode becomes covered to an ever greater extent with loose zinc crystals, which replace the amalgam as the actual surface of ionic discharge, so the true current density falls, whilst an increasing fraction of the discharge takes place at the surface of the finely divided zinc. It is considered that both these facts will tend to a lower H concentration in the electrode and hence to a lower polarization.

For the results obtained with alternating and compound currents, we adopt the same views as an experimental working hypothesis In the *alternating-current* experiments (fig. 3 (*f*)) there is no polarization during the anodic pulse. With the smaller frequencies, enough zinc is thrown out on the amalgamated surface during the cathodic pulse to form the crystal layer referred to (the electrodes became a dead white in appearance), and there is consequently only a very small cathodic polarization With the frequency of 11,000, on the other hand, no change in the electrode surface was noted, and the conclusion drawn is that, during the very short cathodic pulse, the small amount of zinc deposited does not crystallize, and is simply redissolved during the succeeding anodic pulse. The H atoms deposited therefore dissolve in the mercury, and are responsible for the net negative polarization observed. With *anodically compounded currents* (fig 3 (*d*)) the conditions are practically the same as far as the cathodic pulse is concerned, and we consequently have, with 11,000-cycle current, but not with low-frequency currents, a negative polarization *superposed* on the concentration polarization in the amalgam due to the residual anodic current. With *cathodically compounded currents* (fig. 3(*e*)) the amalgam surface is being continually covered with crystals, and consequently the small and decreasing polarization due to the cathodic direct-current component is unaffected by alternating currents of any frequency

This view of the phenomena, which is consistent with the experimental facts so far brought to light, will be tested further in several ways.

(c) *Amalgamated Electrodes in Acid Solution.*

Static Potentials.—In accordance with the assumption of the existence of the equilibrium $Zn + 2H^{\cdot} \rightleftarrows 2H + Zn^{\cdot\cdot}$ at the electrode-electrolyte interface, it is clear that the addition of free acid to the neutral zinc sulphate will have as effect an increase of the H concentration at the amalgam surface. According to our measurements, the potential remains unaffected if $[H_2SO_4]$ becomes 1N. This can only mean that the increases in [H] and [H] run parallel up to this acidity. If, however, $[H_2SO_4]$ is made 7N, then the electrode becomes more negative, a change which can be interpreted by assuming that the increase of [H] in the electrode outstrips that of [H$^{\cdot}$] in the electrolyte, and that these concentrations determine the amalgam potential (H, not Zn, will be the most base constituent of the amalgam). The fact that the electrode is coated with a visible gas film indicates that the value of [H] is now so high that the tendency for the reaction $2H \rightarrow H_2$ to take place freely is only held in check by surface tension forces.

This curious rise of the negative value of the potential following the addition of acid obviously needs further elucidation, and experiments will be undertaken to this end. After our measurements had been made, we found that Richards and Dunham* had noticed the same phenomenon, recording even greater potential changes.

Cathodic Direct-Current Polarization.—The cause of this polarization is the same as that observed with neutral $ZnSO_4$, *i.e.*, the simultaneous deposition of H$^{\cdot}$ ions, resulting in an increase in the value of [H] in the electrode surface, and in the potential becoming more negative. The part taken by H$^{\cdot}$ ions in the cathodic discharge is here, however, more important, and the effect correspondingly greater. The slow evolution of hydrogen is to be expected. So is the sudden drop in polarization on cutting off the current, as the H "amalgam" here postulated will be unstable and rapidly decompose in accordance with the equation $2H \rightarrow H_2$. It may be mentioned that observations of Lewis and Jackson† and Dunnill‡, on hydrogen over-voltage phenomena at a mercury electrode, make probable the existence of such transitory amalgams. Further, Mellor§ cites a number of older papers which support this view, and, amongst later workers, Heyrovsky‖ has been led to the same conclusion, as

* 'Jour. American Chem. Soc.,' vol. 44, p. 678 (1922).

† 'Zeit. für physikal. Chem.,' vol. 56, p. 193 (1906).

‡ 'Trans. Chem. Soc.,' vol. 119, p. 1081 (1921).

§ 'Treatise on Inorganic Chemistry,' vol. 4, p. 758 (1923).

‖ 'Trans. Faraday Soc.,' vol. 19, p. 785 (1924).

opposed to the idea of any kind of hydrogen film on the mercury surface. Finally, the fact that the polarization falls with time, and rapidly when zinc crystals appear on the surface, is explained by us in the same way as the corresponding drop in polarization in neutral solutions

Anodic Direct-Current Polarization.—The observations made in this connection (fig 2) are unexpected and remarkable, as the absence of polarization effects would have been anticipated The electrode is assumed to be charged with atomic hydrogen and, according to generally accepted views, the anodic solution of zinc should then take place reversibly. In any case, in the more strongly acid solution, the zinc is on the point of dissolving spontaneously. Further, although anodic solution of the unamalgamated metal in neutral $ZnSO_4$ exhibits considerable irreversibility, with amalgamated zinc there is only small polarization

A tentative series of assumptions is necessary to account for the observed facts We suggest that direct ionization of hydrogen dissolved in the mercury occurs with difficulty or not at all—in fact, that the H is passive The anodic passivity of hydrogen under other circumstances is well known, though usually ascribed to a different cause. It is further necessary to explain why the zinc does not ionize readily. This we suggest may be due to mere mechanical hindrance, or a displacement of Zn atoms from the surface layer by H atoms. As then neither Zn nor H atoms can ionize reversibly, anionic discharge will take place to a certain extent, followed by oxygen deposition. It is assumed that the oxygen formed dissolves in the mercury and reacts with the H atoms present, but comparatively slowly, subsequently accumulates, and that this is the cause of the remarkable rise in potential observed. The removal of the dissolved hydrogen facilitates the direct ionization of zinc and, in addition, the reaction $Zn + 2\,H^{\cdot} \rightarrow 2H + Zn^{\cdot\cdot}$ will then take place, tending to restore the H concentration in the surface layer. The comparatively slow rate of return of the anodically polarized electrode to the static potential is ascribed to slow disappearance of the dissolved oxygen--it would seem that a solution of O atoms in mercury (or in zinc amalgam) is more stable than a solution of H atoms.

Experiments involving Alternating Currents - The above assumptions being made, a plausible mechanism for the remaining phenomena is not difficult to imagine. With *alternating currents* (fig. 3 (*k*)) the anodic pulse involves appreciable polarization and the deposition of a little oxygen. During the cathodic pulse, this oxygen is destroyed owing to the momentary high concentration of deposited H atoms, the excess of which causes, in its turn, considerable cathodic polarization The net result is a residual negative

polarization of the electrodes, accompanied, at high current densities, by incipient evolution of hydrogen and solution of zinc, whilst the O atoms are not afforded an opportunity of accumulating in the electrode.

With *cathodic compound currents* (fig 3 (*h*)) the phenomena differ only in degree. The polarizations observed are more negative, corresponding to the excess of the cathodic component and, at high current densities, obviously approach those given by pure alternating currents The result reported by Allmand and Puri—viz , that superposition of an alternating current on an amalgamated zinc cathode in acid zinc sulphate solution causes an *increase* in polarization and in the electrolysing voltage—now falls into line They were using electrodes of the same dimensions as we were, but a cathodic direct current of only 10 m a —one-fifth of our figure—whilst their alternating currents varied between 0·5 and 2·0 amps The polarizations they were measuring would then be practically alternating-current polarizations, and of the order of 30—40 m v , judging from our figures Their results were rather irregular, and were not quoted by them They are available to us, and show that, for frequencies between 60 and 400, the average amount by which the cathodic potential difference became more negative for 0 5 amp of superposed alternating current was 16 m.v , and for 2 0 amp , 22 m v This would lead to a direct-current cathodic polarization of about 15- 20 m.v in their experiments, which appears a reasonable figure (We got 60 m v with five times the current density.)

With *anodically compounded currents* (fig. 3(*g*)), the same general view accounts for the facts. The H atoms deposited in quantity (comparatively speaking) during the cathodic pulse react with the oxygen (or a proportion of it) liberated during the anodic pulse, the result being that the polarization during this pulse becomes less The cathodic pulse giving a negative polarization in any case, the resultant effect is that the average potential actually measured rapidly becomes more negative with increase in current density Eventually, the alternating-current polarization value is approached This appears more slowly with anodically than with cathodically compounded currents, as the slow increase observed in the intermediate direct-current polarization values shows that some of the deposited oxygen escapes reaction with the H atoms during the cathodic pulse

The work described above was carried out between December, 1924, and December, 1925. It will be extended further, not only in respect of those points mentioned in the course of the paper, but also by means of oscillographic measurements.

A Method of Studying the Behaviour of X-Ray Tubes.

By R. C. Richards, M.Sc., Carey Foster Laboratory, University College, London

(Communicated by Prof. A. W. Porter, F.R.S.—Received May 1, 1926.)

Introduction.

A quantitative study of the radiation output from an X-ray tube, in relation to the voltage applied and current flowing, would appear to be important both from the theoretical point of view and that of designing tubes of greater steadiness and efficiency. In this sense, of course, the tube itself is not the only determining factor, the operation of the break and coil must be taken into account as well, and in what follows the term "system" will be used to denote coil, break and tube collectively.

There are two methods to approach this problem, the three variables, current (C), voltage (V), and radiation output (I), might be measured over the period of a single break of the coil by, for example, an oscillographic method, as in the work of Taylor Jones, although a serious difficulty arises in the measurement of the very small quantity of radiation available for examination. Alternatively, one might find the average for a large number of breaks of instantaneous values of these variables; this is the method to be described here.

The former of these two methods, ignoring for a moment the difficulty of measuring the radiation—is obviously the only one which could be reasonably applied in the case of gas tubes, in which the internal conditions are continually varying, but even then the information gained would not be very reliable in extrapolation to lengthy periods of operation. The method has yielded elegant results in the hands of Taylor Jones* as far as the measurement of C and V are concerned, but for the measurement of I a photographic method has to be employed with the attendant difficulty of interpreting the "density" of a photographic image.

For a Coolidge tube, on the other hand, an average of instantaneous values is applicable, since, after it has been running for a short period, the hardness remains constant, provided suitable safeguards are introduced to ensure the constancy of the filament heating current. As will be seen, too, in this method, the difficulty of measuring small quantities of radiation is avoided.

* Taylor Jones, "The Theory of the Induction Coil" (Pitman).

2. *General Description of Method*

The system in the following description consists of a 10-inch induction coil, a rotary jet mercury interrupter, and an ordinary Coolidge tube In essence, all that happens is that the interrupter "makes" and "breaks," producing voltages in the secondary of the coil, the latter of which causes a current to flow in the tube, producing an output of radiation This cycle is repeated over and over with reasonable constancy if the break is clean and smoothly operated.

Suppose we describe the process of the make and break by some such expression as ωt, by which is meant that at the instant $t = 0$, the interruption is on the point of "making," and at some later instant, $t = t'$ say, the process of "break" is first completed. Then for every value of t between 0 and t', there will be a corresponding instantaneous value of the following quantities, some of which, of course, may be zero owing to the rectifying power of the tube :—

primary current,	tube current (C),
secondary voltage (V),	X-ray output (I)

The method consists in selecting a particular value of t (i.e of a certain instant in the interruption) and for a large number of successive cycles, examining the corresponding instantaneous values of V, C and I. At once it will be seen that the method avoids measuring small quantities of radiation, since as much radiation as one wants may be had by observing over a sufficiently large number of cycles.

Now by altering the selected value of t, the variables may be measured again, and so on over the whole series of values of t comprised in a complete discharge Thus we shall obtain what perhaps may be called an average instantaneous value of the variables in relation to the "phase" of the break, against which they may be plotted.

3 *The Apparatus*

The experimental method is essentially stroboscopic A heavy flywheel, 9 inches in diameter, is geared to the driving shaft of the mercury break, and rotates twice during one revolution of the latter. The flywheel is provided with a small radial slit near its circumference Behind the wheel is a lead box containing the Coolidge tube, the radiation from which escapes through a slit in the box and impinges normally on the rotating wheel. This radiation is completely stopped by the wheel at all times, except when the radial slit passes in front of the slit in the X-ray box.

Thus, only radiation escapes which is characteristic of a particular phase of the break, and it is received in a long ionisation chamber containing methyl iodide vapour, where it is measured by the usual method with a quadrant electrometer, by finding the rate at which the instrument charges up.

The measurement of the instantaneous value of the voltage across the tube calls for special arrangements In theory it could be arranged that the rotating wheel carried contacts which connected the ends of the secondary of the induction coil to a measuring instrument for an instant at the identical time at which the X-ray beam is escaping through the radial slit into the ionisation chamber. Owing to the high value of the voltage, this is impracticable, and a means of stepping down this voltage must be employed.

This is accomplished by a system of condensers in series. The total voltage drop will be distributed in the condensers in inverse ratio to their capacities, and the voltage across one of these condensers can be measured by the method suggested above, that is, by instantaneous contact on the flywheel and a quadrant electrometer.

In order to simplify this procedure, the tube is operated with one end earthed; the final condenser in the series is merely the quadrant-system of the electrometer, one pair of quadrants being earthed. The first condenser in the series, across which the greater part of the voltage is taken up, consists of an earthed metallic box (shown in section fig 1) through the opposite ends of which are well-insulated supports carrying carefully polished spherical balls, one of which is relatively close to the earthed wall of the box.

The direct technical difficulty in this voltage measurement is the tendency of the high potential leads to "splutter" This was overcome by heavy insulation, and where this was not practicable, by careful polishing and the elimination of points In a similar way the current flowing through the tube can be measured A non-inductive coil of 10,000 ohms resistance was placed in series with the tube, and leads from the ends of the resistance were led to a quadrant electrometer, by way of a contact on the revolving wheel, so arranged that contact was made at the same instant as the X-ray beam escaped through the radial slit. The electrometer measured the instantaneous value of the potential across this coil, and provided a measure of the current flowing, since the coil was constructed of wire with negligible temperature-resistance coefficient. The coil was placed at the "earthed" end of the tube for obvious reasons.

It remains to show how we may obtain values for V, C and I, corresponding to the several values of the break phase. The interrupter was mounted bodily

on a turn-table which could be turned about a vertical axis corresponding with the axis of rotation of the break spindle. The turn-table was graduated in degrees, and the body of the interrupter could be clamped at any position on the scale If we imagine the break spindle and, consequently, the flywheel to be stationary in the position in which the radiation escapes through the radial slit, the instantaneously measured quantities V, C and I will be characteristic of the angle ϕ, denoting the break phase Now, if the body of the break, and in consequence its contacts, be rotated through a small angle α, and clamped, the variables in a succeeding experiment will be characteristic of a break phase $\phi \mp \alpha$, according to which way the rotation took place Thus we can find values of V, C and I corresponding to various settings of the interrupter on the turn-table.

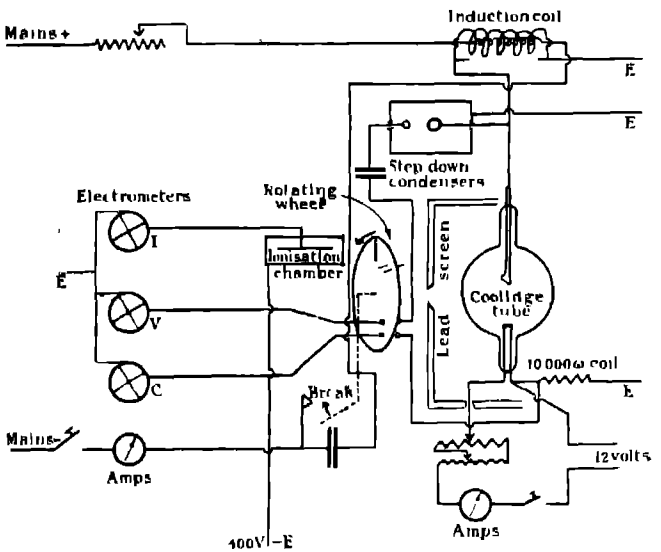

FIG. 1 —Diagram of Connections

4. *Measuring Instruments.*

For the ionisation and current measurements, Dolezalec electrometers were used , the potential was measured by an ordinary quadrant electrometer, of relatively large capacity, acting as it does as the last member in the chain of

series condensers used to step down the potential across the tube. Three main difficulties arise in the measurements :—

(i) due to induction effects from the high-tension system,

(ii) due to frictional electrification arising from the revolving flywheel,

(iii) due to insulation leaks.

The first is overcome by very thorough shielding of all insulated leads, etc., by earthed shields.

Frictional effects are inherent in the system, but can be minimised by reducing sliding contacts and earthing the flywheel. Imperfection in insulation was eliminated by trial and error, till the electrometers, connected up to their leads and the contacts on the flywheel, showed no appreciable leak.

The greatest difficulty in the experiment was to find suitable contacts, which "made" on the projecting points on the rotating wheel at the instant when the variables were examined. With the flywheel rotating about 1500–2000 times a minute, a considerable blow was given to these contacts, and they soon broke off. After a great deal of trouble it was found that a flexible wire, made of cotton thread wound over with a very thin spiral of copper, stood up to the wear very well, and at the same time made a reliable contact.

5. *Method of Operation.*

The interrupter, which was driven by an electric motor, was set in rotation, and with it the flywheel. After a time the speed became constant. This constancy was determined by a stroboscopic method originally, the control being a reed vibrating laterally, but it was found that constancy of speed was very well indicated by the constancy of the current flowing in the driving motor, or by the pitch of the note emitted by the gearing between the break spindle and flywheel. The observer became very sensitive to any speed variation, as indicated by a change in pitch of this note. The instruments were then examined to see if any charges were accumulating due to friction, and if this was satisfactory, the primary coil current was switched on. So far only small primary currents have been used, in the region of 3 amperes. The Coolidge tube was thus set in operation, and the electrometers measuring V and C at once show deflection. The whole system was then allowed to run for fifteen or twenty minutes until the V and C deflections remained steady. The ionisation chamber and its corresponding electrometer were then thrown into the circuit, and provided that the particular phase at which the interrupter is set is suitable, the instrument will start to charge up, the rate of charging being determined by the rate at which the spot of light reflected from the mirror on

the needle passed over a transparent scale. When a satisfactory series of values of this rate had been obtained, the deflections of the instruments measuring C and V were read, thus giving the values of C, V and I for their particular setting of the break.

Without disturbing the apparatus, the break was moved forward a degree on the turn-table, and the above process repeated again and again till the period of the break had been passed When this happens, the ionisation and current values drop to zero, but the voltage generally indicates considerably higher values than during the conducting part of the cycle, owing to the inverse voltage on make, and the lack of any conduction in the tube.

6 *Tube Control*

In order to keep sufficient control over the heating current in the filament of the tube, two rheostats, one a high resistance one, were used in parallel, and a sensitive ammeter was placed in the circuit The filament end of the tube was earthed, and the 12-volt battery supplying the heating current carefully insulated, so that no tube current got to earth via the batteries, instead of flowing through the measuring coil.

During the operation of the apparatus strict watch was kept on the ammeter mentioned above, and if necessary the rheostat was touched from time to time to restore the filament current to the chosen value. The whole system is very sensitive to any variation in this heating current

7. *Contact Adjustment*

Extreme importance must be attached to the adjustment of the contacts made once per revolution of the flywheel, connecting the current and voltage electrometers into the system These contacts must be adjusted so as to operate at the exact moment at which the radial slit transmits radiation into the ionisation chamber

In order to test a particular setting of the contacts, the wheel was turned until its projecting points were just touching both pairs of the external contacts, and a piece of bromide paper was placed behind the radial slit, on the side of the flywheel remote from the X-ray tube. The filament of the tube was then heated to whiteness by a current, and the light was reflected from the anode through the slit in the lead box on to the surface of the wheel If now the contacts are correctly set, the light will pass through the radial slit and produce a latent image on the bromide paper. Adjustment was carried on until a clear image was produced on the paper, with the flywheel set so as to give contact with the current and potential measuring instruments.

8 *Experimental Results*

Following the method of section 5 above, tests were carried out to determine the manner in which I, C and V varied during a complete break.

In the first experiment here recorded, only two of the variables, namely, ionisation output and potential difference, are recorded (fig. 2).

The first point which is noticed in this graph is that the break of the ionisation curve does not correspond with that of the voltage curve. It is this important point which led to the careful photographic method of adjusting the contacts. So far as can be examined, the phase difference indicated here is purely instrumental, and, as is seen in subsequent graphs, it disappears with rigorous adjustment by the method indicated. This graph also shows the inverse potential, produced at make This rises to a high value owing to the fact that the tube is non-conducting for this particular part of the cycle

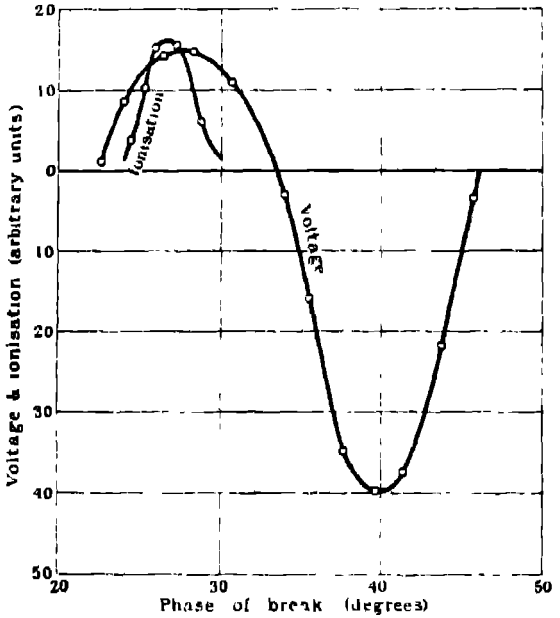

FIG 2.

This curve, which was one of the first to be obtained when the initial difficulties of the method were overcome, is included chiefly to show the inverse potential Conditions inside a rotary mercury break must necessarily depart very

considerably from the simple make-and-break conception, which leads to the conclusion that the "make" potential will be small compared with that at break An arc at "break" may have a relatively low resistance, such as would render the rate of fall of primary current not greatly different from its rate of rise on completing the circuit This view seems to derive support from this curve

Fig 3 represents the type of curve which is obtained by the method described, when rigid phase adjustment is carried out. It is plotted only over that part of the cycle during which the tube is conductive.

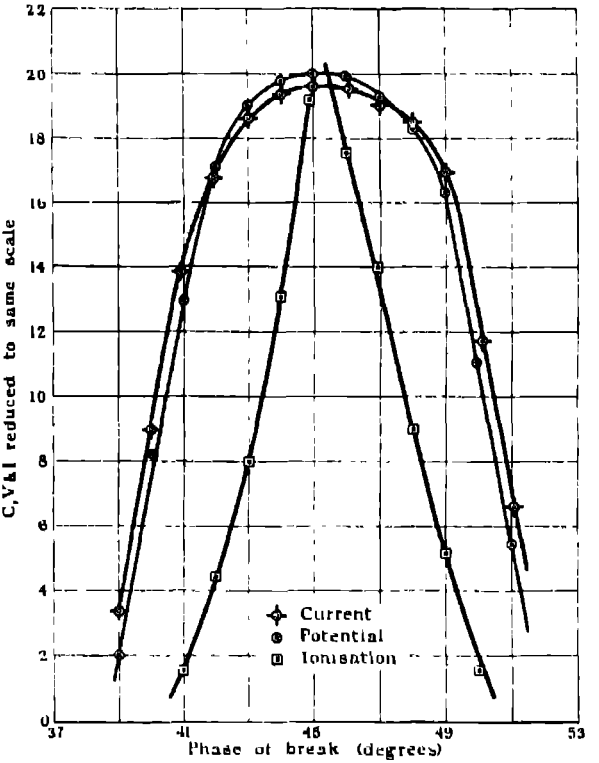

Fig 3

9 *General Observations*

Stress must be laid on the point that these results are of a preliminary nature, and are quoted in order to show that the method described above is

an effective one. With this reservation, however, we can make a few general observations The curves in fig. 3, which are typical, show that there is little, if any, difference of phase between the variables C, V and I. It is possible, however, that inductance and capacity effects balance one another, with the system arranged as at present. It is the subject of future work to test this question of phase in greater detail.

Another noticeable feature is that the ionisation output is concentrated in a narrow region coinciding with the current and potential maximum Seven or eight degrees of a break cycle are alone fruitful in producing radiation, in a break provided with four contacts, therefore, only about one-tenth of the time of operation is spent in producing reasonable quantities of X radiation This observation is in agreement with one of Taylor Jones, as shown by the photographic method, in which he showed a darkening of the photographic plate just underneath the secondary potential break, not extending to any great distance on either side of the central line.* This radiation, it must be remembered, is the actual radiation detected in the ionisation chamber, and as such is subject to various influences, so that its relation to the observed values of C and V may be obscure, or, at least, very complicated. Mention may be made of absorption at the wall of the tube and the aluminium window of the ionisation chamber as two of these disturbing effects What the curves do show is the extent of useful radiation, in relation to C and V, in a qualitative fashion.

The X-ray tube was operated on an alternative spark gap of 12 cms. between points in such a way that the secondary potential is in the neighbourhood of 80 kilovolts. The anti-cathode of the tube is of tungsten, which requires bombardment by cathode rays which have fallen through a potential drop of 13 kilovolts to produce the characteristic L radiation and 95 kilovolts to produce its K radiation † It follows, therefore, that our particular system will, in addition to producing white radiation throughout the cycle, give tungsten L radiation for parts of the cycle in which the voltage is greater than 13 kilovolts This will have the effect of concentrating the observed, or useful, radiation into a peak, as shown by the graphs.

The writer desires to express his indebtedness to Prof. A W Porter, F.R.S., for suggesting this line of work and for his continued help and advice; to the Royal Society for a grant to enable the purchase of apparatus; and to Mr Stephen Northeast, B Sc, formerly of this Laboratory, who designed the step-down condenser used in the potential measurement, and was closely associated with the preliminary stages of the work.

* Taylor Jones, *ibid*, p. 159
† Kaye, 'X-Rays,' p 127

Tensile Tests of Large Gold, Silver and Copper Crystals

By C. F. Elam, D.Sc. (Armourer's and Brasier's Research Fellow).

(Communicated by Prof H. C H Carpenter, F R S —Received July 6, 1926)

Large crystals of a number of metals have been made by Bridgman* by slowly lowering a tube containing the metal through a furnace so that it cools from one end. By using a graphite tube Davey† succeeded in making copper crystals by this method. He obtained crystals over six inches long and up to nearly one inch in diameter.

The present paper describes some tensile tests on gold, silver and copper crystals which have been made by this method Rods of the metal were melted in graphite tubes 0 25 inch diameter and 10 inches long, tapered at one end These were slowly lowered by clockwork through a platinum-wound electric tube furnace, the middle portion of which was maintained at 100° C. above the melting-point of the metal Nitrogen was passed slowly through the tube to prevent oxidation. In some cases the whole rod (about eight inches long) consisted of one crystal. It does not seem to be essential that the graphite tube should be tapered, as it was sometimes found that a crystal growing from the point stopped a short distance up the rod, and that a new crystal beginning here occupied the whole cross-section of the rod for the length that remained

The crystals were free from blow-holes if prepared in this way, but if rods of the metal were melted in the tubes and allowed to cool down with the furnace they were frequently very unsound This occurred even when the metal was melted *in vacuo*, and, in fact, a copper rod melted three times *in vacuo* still contained large blow-holes Apart from this, cooling started from both ends, with the result that the rod consisted of two or more crystals, with unsoundness in the middle.

Great care is required in removing the crystals from the tubes to avoid bending The bore of the tubes was not always uniform, and slight irregularities in the surface were filled by the molten metal, which, when solidified, prevented the rod from slipping out easily. On one occasion, in pulling a tube off a gold crystal, the whole crystal was twisted into a spiral showing three complete turns. The spiral only made its appearance on etching, the rod appearing

* 'Proc. Amer. Acad. Sci.,' vol. 60, Nos. 6, 7 and 8.

† 'Phys. Rev.,' vol. 25 (February, 1925).

quite normal when extracted from the tube. The crystals of all three metals required great care in handling.

The gold was kindly furnished by the Goldsmith's Company, through the courtesy of Mr Prideaux. The silver was the purest available assay silver The copper, in the form of rod made from electrolytic copper, was kindly given by the Broughton Copper Company, and after remelting in nitrogen was almost entirely free from oxide

The orientations of the crystals were determined by means of X-rays. Davey* has stated that a cubic axis was always parallel to the axis of the cylinder in copper crystals, and Bridgman† also noticed that certain directions were favoured, and concluded that the growth of the crystal was easier in some directions than others A diagram illustrating the position of the axis of the rod, relative to the principal crystal axes of eight copper crystals, is given in fig 1 This represents part of a stereographic diagram of a cubic crystal, the dots in the triangle being the positions of the axes of the rods of the various crystals. A full description of this diagram and the means of using it has been described already ‡ According to Davey the points should be near the pole of the (010) plane No crystals of copper, silver or gold have so far been obtained in this position Actually the orientations vary considerably, as this and subsequent diagrams show

Tensile tests were carried out with these crystals and the crystal axes determined at each stage. As it was impossible to machine them there were small variations in the cross-section, and often the rod was slightly tapered. Sometimes these irregularities increased as the test proceeded; sometimes the rods became more uniform Errors due to this cause show in the X-ray measurements, as the extension, measured over two inches, included regions which were sometimes more and sometimes less than the average, with corresponding variations in the positions of the crystal axes.

The rods became elliptical on stretching, showing the lens-shaped figure found in aluminium and breaking with a double-wedge fracture. Slip-bands were observed on all the crystals They were more noticeable during the early stages of extension, and tended to become almost obliterated later One set of planes was usually observed until near the end of the test, when two sets were visible No attempt was made to measure the position of the planes,

* *Loc cit.*

† *Loc. cit.*

‡ Taylor and Elam, 'Roy. Soc. Proc.,' A, vol. 108.

owing to the roughness of the surface and to the fact that they were not clearly marked all round the specimens

Copper, silver and gold resemble aluminium in that their crystals have a face-centred cubic lattice It is therefore to be expected that they should show the same type of distortion in tension The process of distortion of aluminium crystals is now well known, and it has been shown that it is due to slip on an octahedral (111) plane in the direction of the pole of one of the three (110) planes *† It was also shown* how the slip-plane and direction of slip could be predicted from the position of the axis of the test-piece relative to the crystal axes. If, therefore, it can be shown that the axis of the test-piece changes in respect to the crystal axes in the gold, silver and copper crystals, in the same way as was found for aluminium, the conclusion can be drawn that the distortion is all of the same type, although no distortion measurements are made. This can best be shown by means of diagrams. By the method previously described the positions of the axis of the test-piece in reference to the crystal axes is plotted for each extension on the stereographic diagram. Part of this diagram showing the points is shown in figs 2, 3, 4, 5 and 6, which refer to one gold crystal, two silver crystals, and two copper crystals respectively The figures refer to the elongation per cent. on two inches of the original crystal The diagrams show that, as in the case of aluminium, the points lie very nearly on a great circle (drawn in dotted lines), through the original point, *i e* the axis with 0 extension, and the pole of the (110) plane, until this line cuts the great circle through the poles of the (010) and (111) planes At this point two octahedral planes make equal angles with the axis, and it was shown previously that slip then occurs on both planes, the axis now moving along this line towards the pole of the (121) plane The diagrams all show a tendency for the axis to move in this direction Irregularities in the rods have already been mentioned as probable sources of error which may cause the points to be off the line. Other errors occur in the measurements of the extensions, in the X-ray measurements, and also in the possibility that the loading of the testing pieces was not axial The main direction of the movement of the axes resembles that found for aluminium so closely that there is every reason to suppose that the distortion of these metal crystals is actually of the same character Fig. 6 is particularly interesting. The crystal axes of this copper crystal were in such a position that double-slipping should occur from the beginning of the test, and as it was very close

* Taylor and Elam, 'Roy. Soc. Proc.,' A, vol 108

† Taylor and Elam, 'Roy. Soc. Proc.,' A, vol. 102,

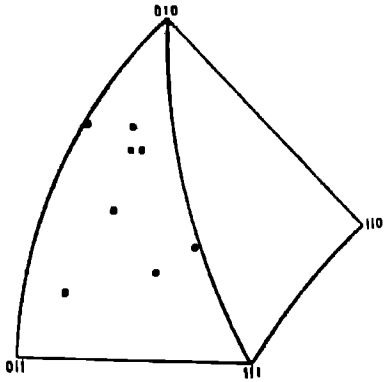

Fig. 1.—Position Diagram.

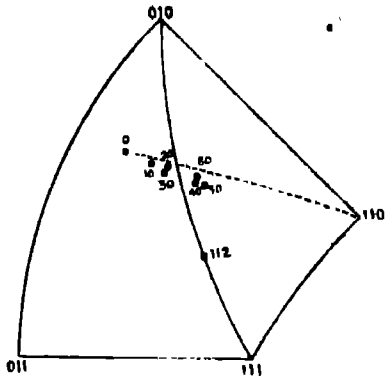

Fig. 2.—Gold.

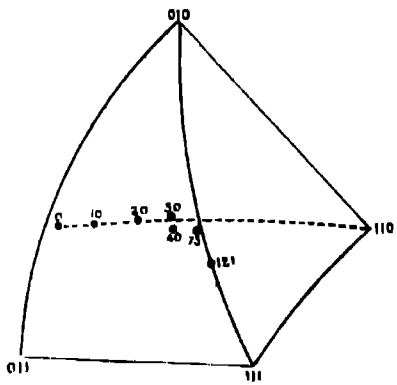

Fig. 3.—Silver II.

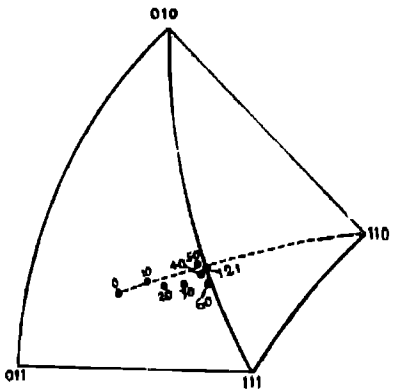

Fig. 4.—Silver III.

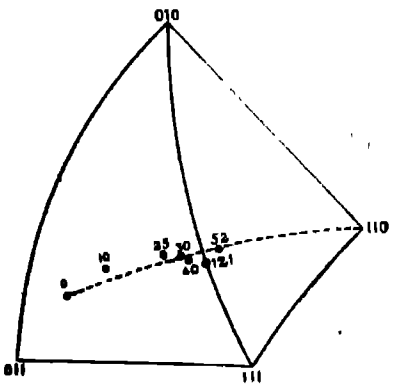

Fig. 5.—Copper XI.

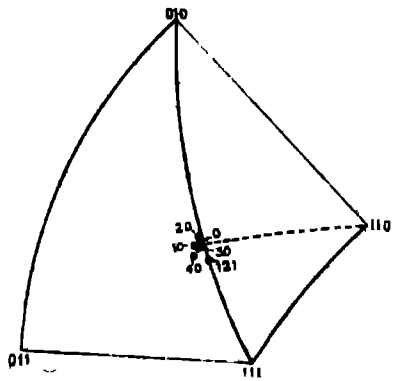

Fig. 6.—Copper X.

to the pole of the (121) plane, very little movement of the test-piece axis was to be expected. The diagram shows that the position of the axis remained practically unaltered throughout the extension A similar crystal of aluminium showed the same result.*

In Table I the inclinations of the slip-planes are given, and it will be seen that these all tend to reach the same value as in aluminium The limiting value should be 61° 52′.

Table I.

	ϵ	Load	Area	θ	η	S
		lbs	inches	° ′	° ′	lbs sq ins
Gold .	1 00	—	0 0501	49 50	8 40	—
	1·10	248	0 0456	53 40	6 40	2,575
	1 20	379	0 0418	55 50	5 0	4,195
	1 30	433	0 0385	56 40	6 40	5,125
	1 40	478	0 0359	60 0	3 10	5,760
	1 50	490	0 0342	61 30	3 10	6,000
	1 60	500	0 0329	60 50	4 20	6,465
Silver II . .	1 00	—	0 0504	48 30	15 20	—
	1 10	105	0 0455	52 40	12 40	1,095
	1 20	198	0 0418	55 30	12 40	2,150
	1 30	338	0 0386	58 0	12 0	3,850
	1 40	483	0 0363	60 30	11 0	5,495
	1 50	557	0 0340	61 20	10 0	6,645
	1 60	609	0 0319	62 30	12 40	7,640
Silver III	1 00	—	0 0492	40 13	4 20	—
	1 10	95	0 0452	44 13	4 0	1,051
	1 20	144	0 0414	50 36	3 20	1,702
	1 30	248	0 0383	54 55	1 50	3,450
	1 40	353	0 0355	58 40	4 0	4,405
	1·50	544	0 0346	59 30	4 0	6,845
Copper XI	1 00	—	0 0492	42 03	18 0	—
	1 10	287	0 0447	47 0	12 10	3,230
	1·25	683	0·0373	55 30	10 0	8,430
	1 30	764	0 0341	56 46	10 0	10,250
	1 40	815	0 0317	58 40	10 40	11,200
	1 52	857	0 0278	63 20	8 40	12,220
Copper X	1 00	—	0 0490	62 0	0 0	—
	1·10	512	0 0450	—	—	4,665
	1 20	810	0 0300	—	—	8,325
	1 30	934	0 0370	—	—	10,380
	1 40	979	0 0327	—	—	12,270
	1 50	987	0 0298	—	—	13,580

The load required to stretch the crystals at each stage, and the cross-sections were measured. The slip-plane and direction of slip were deduced and the

* *Loc. cit.*, No. 24, fig. 9, p. 44.

tangential component of shear stress calculated for each extension. This is given by the formula—

$$S = T/A (\cos\theta, \sin\theta, \cos\eta)$$

where T = total load,

A = cross-sectional area,

θ = angle between the normal of the slip-plane and the axis of the test-piece,

η = angle between direction of slip and the direction of maximum slope of the slip-plane.

Table I gives the measurements and values calculated for S in lbs. per square inches In fig 7 these are plotted against the ratio of the extended to the

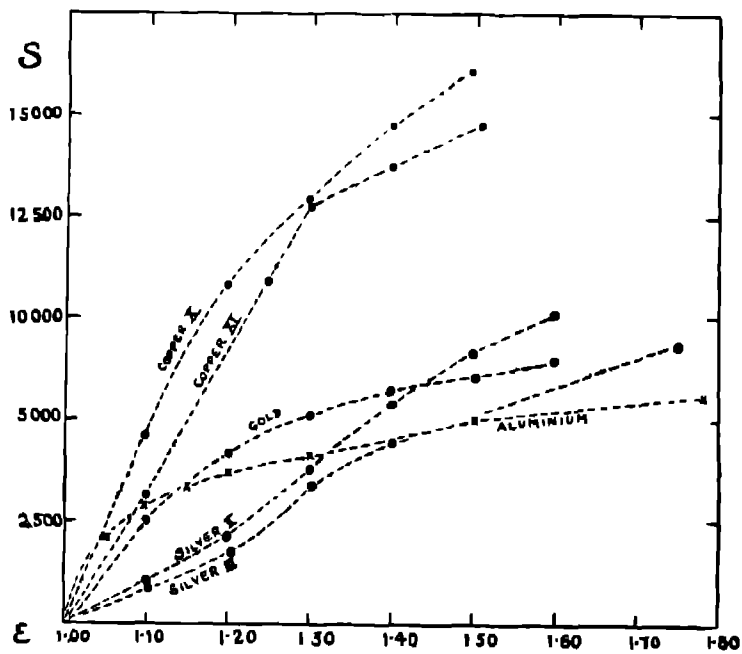

Fig. 7.

initial length of the specimens, ϵ. All of the crystals were extended until they began to neck, so that the final figure represents approximately the shear stress at fracture. A curve obtained from an aluminium crystal is

included for comparison. This is taken from the previous paper, where other curves and figures for aluminium are given *

It is interesting to note that, although the aluminium hardens more rapidly at first than gold or silver, it finally becomes the weakest and is passed by both gold and silver. Similarly the gold begins by being stronger than the silver, but in the final stages of the tests this order is reversed. It will be seen on reference to figs. 5 and 6 that copper crystal No X began straight away to slip on two planes, while No. XI only began double-slipping between 30 and 40 per cent. The curve of the former is smooth, whereas that of the latter shows a sharp change of direction at about this point Similar breaks in the curves for the other metals have not been observed.

The shapes of the curves for the four metals are entirely different, although the distortion is of the same type If the hardening were due solely to bending and breaking up of the crystal during the process of slipping, it would be expected that the curves would have a similar shape Those of the two copper crystals and the two silver crystals are nearly parallel, and it was found that all the crystals of aluminium showed approximately the same values for the same extensions. Therefore the differences observed must be considered as being due to specific properties of the several metals.

It might be suggested that this effect is due to the influence of impurities. That such is not the case, however, is evident from the fact that the gold, silver and copper are of a high degree of purity, while the aluminium is relatively impure. (The aluminium contains 0·2 per cent iron and 0·2 per cent. silicon.)

A few of the properties of these metals most likely to influence the mechanical properties are compared in Table II. The dimensions of the space-lattices of

Table II.

	Gold.	Silver	Copper.	Aluminium.
Melting-point	1,064° C	960° C	1,084° C.	659° C
Atomic weight	197 2	107 88	63 57	27 1
Density†	19 31	10·51	8 952	2 583
Side of elementary cube in "Ångström" units‡	4 08	4 00	3 60	4 01

* *Loc. cit.*

† Landolt and Börnstein.

‡ Bragg. 'X-rays and Crystal Structure.'

gold, silver and aluminium are almost identical, while the value for copper is considerably lower The other properties do not appear to bear any relation to the mechanical properties. It is impossible to draw any conclusions from these observations in the present state of our knowledge, but it is significant that the metal whose atoms are nearest together shows a greater proportional increase in hardness on deformation.

My thanks are due to Prof. H C H Carpenter, F.R.S , and to Prof. G. I. Taylor, F.R S , for advice during the course of this work, and to Prof W. E. Dalby, F.R S., for his kindness in allowing me the use of a testing machine in the City and Guilds Engineering College.

The Absorption of Gases by Charcoal —I.

By R Angus Smith, Ph.D , F R.S.

(Received December 27, 1862 —Read January 29, 1863)

[In June, 1926, the Council of the Royal Society considered an application from Mr S Lenher for permission to print certain parts of Dr. R A. Smith's paper on " The Absorption of Gases by Charcoal " on account of their historical interest. The paper had been formally read before the Society in January, 1863, but, acting on the advice of a referee, Council had published only a summary of the paper (' Proceedings,' vol 12, p 424 (1863)), consigning the main manuscript to the Archives Mr. Lenher wrote that " Dr Smith's paper is of such historical importance for adsorption work that the printing of a considerable part of the original is now warranted," and suggested publishing the material from Dr Smith's paper in the form of an historical note. Council felt that if the paper were to be published at all, it should appear in their own ' Proceedings,' for which it had been originally submitted in 1862. Prof. Donnan and Mr Lenher accordingly selected such parts as seemed to them most suitable for publication, and these appear herewith, followed by a short note by Mr. Lenher

An examination of the original manuscript of the paper makes it clear that it was hardly suited for publication in the form in which it was submitted No attempt was made to tabulate or summarize the results of the different groups of experiments, and the manuscript looks rather like a laboratory note-book. One of the experts to whom the paper had been referred spoke of the experiments as being " presented in a crude form which is far from attractive," and continued " The theoretical deductions at the end of the paper possess more interest, although rather vague and general ; but they are borne down by the heavy matter with which they are associated " Doubtless it was this report which led Council originally to print only the summary with which the original paper ended.- J H J.]

" . . . I had several reasons for beginning these experiments. Some years ago I had given general opinions on the oxidizing powers of porous bodies, and had made some experiments obtaining interesting results I was therefore desirous of knowing the details more fully. I had reason also to consider the subject of the purification of liquids, and I believed that the study could only be prosecuted by beginning with the rudimentary actions of the substances employed. Thirdly, I have had still more occasion to consider the purification of air and the peculiar action of charcoal on some gases and vapours which are found to be noxious or disagreeable

" I have paid little attention to the absolute quantity of gas absorbed, believing that enough had been done on this part of the subject ; for the same reason I have neglected the nature of the wood , beech and oak were used indifferently, and the hardest were found to be the most active . ."

Charcoal and Atmospheric Air.

" The mode of experimenting was that adopted by others and actually suggested by the circumstances of the case The charcoal was heated to redness to the very centre, and when in this state was plunged instantly under mercury. It must not be allowed to reappear on the surface, but must be transferred at once to the eudiometer. The charcoal becomes very heavy, being thoroughly penetrated with mercury . . Tubes for absorption were from one-half to three-quarters of an inch in diameter. The pieces of charcoal were one and one-half inches in length and about one-half inch in diameter. I give only a few results among many dozen. . . " [Four experiments are chosen from a considerable number recorded in the original MS]

Volume of air used.		Volume after absorption		Volume of gas absorbed
No 1.	58 30 { 12 12 O 46 18 N	37 99 { 0 06 O 37 93 N		12 12 0 06
No 5	80 85 { 16 74 O 63 76 N	64 50 { 0 74 O 63·76 N		16 00 0 00
No 7	115 0 { 23 92 O 91 08 N	72 02 { 3 75 O 68 45 N		19 35 22 68
No. 9.	80·67 { 16 76 O 63·91 N	42 36 { 0 00 O 42·36 N		16 76 21 55

" These experiments were repeated until the results became familiar . . .

" Finding that charcoal absorbed oxygen rapidly, leaving nitrogen untouched,

I expected to obtain a constant stream of the former by alternate heating and cooling. I found that I could obtain little else than carbonic acid The rapidity with which some charcoal absorbs oxygen is marvellous In this we see readily the cause of its spontaneous combustion The rapid condensation of the gas itself produces heat which, if retained as has been shewn to be the case in great aggregations of charcoal, increases until combination takes place. This combination, however, seems to take place without the aid of this accumulated heat and certainly as low as the boiling point of water.

"The absorption of oxygen is not merely the filling up of the pores craving by their emptiness a supply of particles but it is caused by a power capable of making a selection, removing all the oxygen from the air, even ejecting the nitrogen from the pores of the charcoal to make room for the gas more readily condensible, and most readily absorbed. The absorption seems not to be in relation to the specific gravity of the gas, as I always find that hydrogen expels nitrogen. We know nothing of the condensibility by mere pressure of oxygen, nitrogen and hydrogen so as to make a comparison. . "

Oxygen on Charcoal.

[Tables given for the absorption of hydrogen, carbonic acid, and oxygen on charcoal over a period of a month.] "In these experiments we find that hydrogen is not absorbed by charcoal except for a very short time . The numbers shew an amount of gas almost constant during the whole period, and leading us to conclude that so little is hydrogen inclined to condense in the pores of the charcoal that even with some increase of pressure there was no tendency. On the other hand, a diminution of temperature has a certain marked effect in causing condensation . "

Displacement of Nitrogen in Charcoal

"The displacement of nitrogen in charcoal by other gases was very conspicuous; nearly all the charcoal even after being heated and plunged into mercury still contained this gas, but when surrounded with an atmosphere of oxygen the nitrogen was removed and the oxygen took its place

"When the charcoal containing nitrogen was introduced into any gas, the nitrogen might reasonably be expected to mix with the external gas, either until a homogeneous mixture was made or until a mixture took place depending on the amount and specific gravity of each gas as is the case over liquids The first does not take place, as I have shewn by proving the elective action of charcoal when oxygen is present, nor does the second occur as a main result, although

I think it probable that it will occur as a secondary action after the counterbalancing part of the attraction has been satisfied The amount of attraction for the gas diminishing outwards from the surface of the charcoal, a time will come when it will be no greater than the amount of its solubility in water or its diffusibility in air or other gas Still, the first apparent result is very different from anything here imagined When the charcoal containing nitrogen is put into any other gas the nitrogen flows out If the gas in the tube be rapidly absorbed, the flow of nitrogen is not observed, but if the gas be hydrogen and the charcoal not very absorbent, there will be a flow of nitrogen out of the charcoal so as gradually to lower the mercury below the external level The same occurs with other gases and nitrogen according to the qualities of the charcoal When this action is finished the absorbing action is again observed on the remaining gas by the rise of mercury and at last even on the ejected nitrogen itself

"If the charcoal be previously saturated with a gas such as nitrogen or hydrogen, the amount which escapes on passing it into another gas is very great. It requires no diminution of pressure to remove it but the pressure only of another gas which will cause it to flow out against pressure and with so much force that the mercury in the tube has been depressed about three-quarters of an inch below the outside level. After suffering this depression the absorption begins to be apparent.

"We may suppose either that the gas in the charcoal is given out before the absorption of the external gas begins or that it is given out more rapidly than the rate of absorption. With a greater pressure and without a membrane we have one gas flowing into another with such a force as to depress the mercury more than the atmosphere, recalling to mind the saying of Dalton to explain diffusion, that one gas acts as a vacuum to another. And this is practically true to some extent

"This same gas will not entirely leave the charcoal even in a vacuum, in those cases, however, where there is a depression of the inside mercury, the gas in the charcoal was so great that much of it would have left readily on a diminution of the pressure. We see then that the pressure of another gas acted exactly like a diminution of pressure. . . ."

Table.—[A Summary of the Data given by the Author.]

Gas with which the charcoal was originally saturated	Gas into which the charcoal was introduced.
Nitrogen	Oxygen
,,	Hydrogen
,,	Carbonic acid.
Hydrogen.	Oxygen
,,	Carbonic acid
,,	Nitrogen.
Carbonic acid.	Oxygen
,,	Hydrogen
,,	Nitrogen
Oxygen	Hydrogen.
,,	Carbonic acid
,,	Nitrogen

Theoretical Considerations.

"We are obliged to view chemical union as the most complete case of contact known to us And as yet the subject is not without its difficulties, and experiments occasionally suggest doubts. Dr. Andrews found that 1500 atmospheres did not render oxygen a liquid, and Vatterer speaks of 3600, and yet at less specific gravity it comes before us in many compounds in a condensed state. We may view the atoms or molecules of a gas as separate or independent, refusing contact with each other until affinity begins to act The first result will be a close contact; this we have been accustomed to call physical only and to look on as cohesion, but there are grades of this contact; one substance holds and is held more powerfully than another Platinum finely divided retains oxygen powerfully. Silica finely divided retains oxygen less powerfully and iron seizes it with such force that if the division be fine enough the physical boundary is rapidly passed and chemical affinity results in chemical union. But in what way can we separate the action of affinity resulting in manifest combination from the action which tends to retain the oxygen in the pores of the powdered metal? The tendency to unite is begun by the tendency to remain in firm physical contact.

"If the distance of atoms be at the smallest when they are in a state of chemical union, then chemical affinity acts at distances greater than those between the atoms chemically united. This then leads us to conclude that a force acts beyond the boundary of the atom itself If the atoms are nearer after combination, force must pass between them causing them to combine. And at what distance does this force act? (This phrase will be objected to,

but the objections must come from other grounds than any known to me before I can pay much attention to them I do not know what a force is and can find no teacher, and by changing its name I feel no wiser.)

"The distance at which chemical affinity first manifests itself is not a smaller one than ordinary physical contact. Bodies to unite chemically are brought into ordinary physical contact. Is this always the same or are there variations in the closeness of contact? When charcoal is put in a tube of air over mercury the air is absorbed; more is absorbed when the pressure is great. If by removing the pressure of the atmosphere, the whole air were extracted, we might be inclined to give little heed to the force exerted, but this extraction does not take place.

"Let us suppose that on the entrance of the oxygen into the pores of the charcoal the surface is covered with a coating of gas disposed in thin layers of atoms or molecules When this attraction is satisfied and force is still exerted beyond this thin layer, there will be a second layer formed, but it will be held with less power, being farther distant from the charcoal than the first layer Afterwards a third layer will be formed, and so on In this way there will be a succession of layers of oxygen each held by a different amount of affinity. Now this appears to me to agree thus far with the facts of the case.

"There would also be a tendency to unite the first layer of oxygen with the carbon. It is extremely probable that the affinity of every layer would contribute towards compelling the carbon to unite with the nearest particles of oxygen, because the affinity appears to stretch through a certain number of layers of oxygen This will give a reason why pure oxygen should act more rapidly than when mixed with another gas, besides the fact of a larger surface being exposed.

"If there were only one layer there would be an equal attraction over all the surface and there would be no reason why one portion of the gas should be removed by removal of pressure more than another A succession of layers is indispensable and as a consequence a continuation of affinity or rather attraction through them, or, in other words, at distances greater than those which form chemical combination and also at various stages of distances It is extremely probable that these stages are exactly in proportion to the size of the molecule, that there is not a stage at any pressure we choose to assume but a series of steps as distinct as atomic weights and depending on the same cause If we could measure these steps by fine measurements of pressure we could measure the size of atoms The atom I speak of may more properly be called a molecule,

but it is an atom to us, not in the sense of a thing that *cannot* be divided but of one that *is not* divided by any of our operations The chemistry of bodies smaller than Dalton's atoms is yet to come

"If there be an attraction at the surface of bodies or in porous bodies closely resembling the affinity called chemical on the one side and that called physical on the other, we may expect that it will be elective as chemical affinity is and have the faculty of choosing from various substances in preference to others Accordingly, when we introduce active charcoal into common air the oxygen is taken up first and afterwards if the charcoal is capable of taking up more gas it absorbs the nitrogen This choice is very strikingly shewn when the charcoal contains nitrogen, as it almost always does, not only is the oxygen taken up but the nitrogen is expelled The same takes place when hydrogen is used, the hydrogen is absorbed, although to a smaller extent, and the nitrogen is expelled. Here we may have chemical affinity acting in a manner which we are accustomed to call physical it is chemical affinity at distances greater than we have been accustomed to, it is also chemical affinity active as an agent between bodies which do not combine, shewing a wider interrelation and dependence of substances than we have hitherto recognized

"But may we not view the chemical and the physical as at this point one I call it physical because combination is not produced, I call it chemical because election is made. This elective nature may however entirely depend on the compressibility of the gases as we find that carbonic acid is very much compressed and condensed . When charcoal is saturated with mercury and is then moistened with water or dipt into it, the mercury is instantly driven out, water taking its place How far combined oxygen may be inclined to exercise its affinities we do not know, all we know is that its capacity for combining farther is bounded we have only to believe that the capacity for uniting and the inclination to unite are different and the matter becomes clearer

"In this view of the case when there is a condensation of volume or an attraction shewn by compression or otherwise, we cannot separate the terms chemical and physical The term chemical commences when a true union is formed The two attractions are one, however, in quality To illustrate this, charcoal may have an attraction for oxygen when the oxygen is in a state of combination with carbon, but it cannot combine simply because combination has already taken place on the part of the oxygen We have somewhat confounded attraction, affinity, and combination. I see only one attraction which is both chemical and physical, resulting in chemical combination when opportunities are fitting The action of mass is readily explained by this mode of

representation, but this is scarcely a place for giving more than a brief account of ideas which I hope more fully to elaborate "

Note -An editor's footnote in a paper by John Hunter (' Jour Chem Soc ,' vol 18, p 285 (1865)) calls attention to the work of R. Angus Smith on the absorption of gases by charcoal (' Roy Soc Proc ,' vol 12, p 424 (1863)) The paper in the Proceedings of the Royal Society is merely a short abstract of a paper which Dr Smith read before the Royal Society on January 29, 1863 , but brief as it is the account seemed of such historical importance that a perusal of the original manuscript was warranted. A study of Dr Smith's original paper in the Archives of the Royal Society (a document of some 38 pages of experiments, tables, and theoretical considerations) confirmed the belief that attention should be drawn to this excellent and much neglected work No mention of the early work of Dr Smith is made in the literature of adsorption and absorption after the footnote in Hunter's paper of 1865

Bancroft (' Applied Colloid Chemistry ' (1921)) remarks on some of the later work of Smith (' Report of the Brit Ass for the Adv. Science,' Norwich, 1868, Abstracts, p 44 , ' Chem News,' vol 18, p 21 (1868) , ' Roy Soc Proc ' vol 28, p 22 (1879)) which is of little value at present , and until this time Dr Smith's pioneer work in adsorption has been forgotten and neglected Dr Smith's experiments and conclusions are of such excellence, showing as they do how far ahead of his contemporaries he was in the field of adsorption, that a fuller rendering of the material in his paper seems justified - S LENHER

A Comparison of the Records from British Magnetic Stations Underground and Surface.

By C. Chree, Sc.D., LL.D., F.R.S., and R. E. Watson, B.Sc.

(Received June 16, 1926.)

§1. During nearly six years a weekly statement of 2-hourly declination values was issued from Kew Observatory for the benefit of mining engineers. This helped to bring to the front the question of how far data from an observatory in the S.E. of England apply to the British coalfields. So far as we know, the only previous investigation in which continuous records were obtained from neighbouring underground and surface magnetographs was carried out in 1906 near Dortmund, in Germany. In a short preliminary account, Prof. Ad. Schmidt,* of Potsdam, stated that only trifling differences had been observed between the surface and underground stations, and that doubts existed as to whether their cause was natural or artificial. No further discussion seems to have been published.

In 1920 the question of special observations in a mine was raised by Mr. T. G. Bocking, M.I.Min.E., of Birmingham, and this led eventually to the present investigation. The scheme having been approved by the Director of the Meteorological Office, Mr. Bocking secured the co-operation of Mr. H. W. Hughes, General Manager of the Diamond Jubilee Pit at the Sandwell Park Colliery, West Bromwich (52° 5′ N. lat.), and accommodation was provided for magnetographs. Two old eye-reading declinometers in stock at Kew Observatory were transformed into magnetographs by Mr. R. E. Watson, and some changes were made to a Kreyness H (horizontal force) magnetograph to render it more sensitive. Messrs. Bailey, of Birmingham, a firm of mining engineers in which Mr. Bocking is a partner, kindly arranged that the immediate charge of the instruments should be undertaken by Mr. S. W. Howarth, one of their assistant surveyors, and they afforded facilities at their office for the development of the photographic traces. The instruments were set up by Mr. Watson near the end of March, 1923, the H magnetograph and one of the D (declination) magnetographs being underground and the second D instrument at the surface. Records were taken until the middle of the following November, but operations were suspended during July and August and part of September. The

* 'Terrestrial Magnetism,' vol. 11 (1906), and 'Met. Zeit.,' p. 130 (1907).

underground and surface D instruments were interchanged in September as a precaution against instrumental uncertainties

§2. Magnetographs housed in a mine are exposed to special dangers, and from one cause or another there was a considerable loss of trace It was clearly desirable to limit the comparison of D results in general to days in which complete records were obtained from both the D instruments at Sandwell Park It was finally decided to select for each month two groups of days not exceeding five in each group, one group representative of quiet, the other of "disturbed" conditions The international quiet and disturbed days were used when records were available Diurnal inequalities were derived from these two groups of days, non-cyclic corrections being applied in the usual way. It was clearly desirable to include in the comparison a more northern as well as a more southern observatory The elements regularly recorded at Eskdalemuir of late years have been N and W (north and west components), not D and H. Diurnal inequalities can be calculated for D and H from N and W curves, but irregular changes can be satisfactorily measured only for the elements actually recorded. A third declinometer was accordingly transformed by Mr Watson into a declination magnetograph, and installed at Eskdalemuir

While the reduction of the observations was in progress, the magnetic curves obtained during 1923 at the new observatory at Lerwick in the Shetlands were sent to Kew for examination, and it was decided to utilize them as well Hourly tabulations had already been made in Scotland, so the extra labour entailed was not very serious

§3 In addition to the inter-comparison of the regular diurnal inequalities at the different stations, a comparison was made of the amplitude of irregular short period changes What was measured was the difference of ordinate at successive turning points (crests and hollows). In general there is no difficulty in identifying corresponding movements in the same element at British stations, even when so far apart as Kew and Eskdalemuir The selection of suitable movements was based mainly on a study of the Kew curves During the busy hours of the local electric railways artificial disturbance was too large at Kew to permit of the satisfactory measurement of minor movements This consideration alone would have restricted the choice mainly to the night hours, but this was desirable in any case, because the instruments at Sandwell Park also suffered sensibly from artificial disturbances during the day These seemed to be due, not to the electrical power used in the mine, but to electric tramways at some distance

Only D irregular movements were available at Eskdalemuir This was one

of the reasons for the use of the Lerwick curves, because the magnetographs in use there recorded D and H

The direct comparison of underground and surface phenomena at Sandwell Park was necessarily limited to D Such comparisons are not so simple as may appear at first sight Assuming the regular diurnal variation to be due to the varying action of some electric current, the changes in declination depend not only on the direction, distance and intensity of the current, but also on the local value of H In the present case complete observations of H were not taken, but the time of swing of a magnet was measured at both stations, as well as at Kew Observatory The value of H thus deduced for the surface station from the known value at Kew was intermediate between the values obtained by Rücker and Thorpe and by Mr G W Walker at stations a few miles away, due allowance being made for secular change. The value obtained at the underground station was the larger by about 100γ, or 0 5 per cent This is not much in excess of the probable error of observation, but several observations were taken and all agreed as to the sign of the difference Supposing the result exact, it would imply a reduction of 0·5 per cent in the amplitude of the D changes underground, as compared with those at the surface, provided the depth of the underground station 1,800 feet or 0 55 km roughly, is negligible compared with the distance of the currents to which the diurnal inequality is due

§ 4 In considering the amplitude of the diurnal inequality, attention was given to the A D (numerical mean of the 24 hourly departures from the mean value of the day) as well as to the range

In the case of the quiet day D inequalities, in four months out of five, both the range and the A D were larger for the surface than for the underground station, the average difference in the case of the range representing about 3 per cent of the surface value But in the disturbed day inequalities the excess in the range at the surface averaged only 1 per cent , and in the case of the A.D the excess vanished In the case of the quiet day inequalities the difference between the amplitudes is in the direction we should expect from the enhanced values of H underground, but is greater than the enhancement in the value of H would account for In the case of the disturbed day inequalities the difference might be accounted for by the difference in the underground and surface values of H

The irregular D movements used for the comparison of the underground and surface stations were taken from seven months, the number varying from 13 in March to 106 in October Every month gave an excess for the amplitude of the surface movement. In three months the excess represented

only 1 per cent, but on the aggregate of the 348 movements measured it represented 4 per cent Additional confidence in the reality of the excess may be derived from the fact that it appears both prior and subsequent to the interchange of instruments

The facts that the irregular movements showed a clear excess at the surface, and that the A D of the regular diurnal inequality on disturbed days did not, may appear contradictory But the results obtained at the various surface stations showed that there is no recognisable relation between the regular and irregular changes

In the case of H no certain conclusion can be drawn as to a difference between inequalities underground and at the surface All that can be said is that on an average of five months the ratio borne by the range or A D from the disturbed day inequality to the range or A D from the quiet day inequality was very nearly the same for the underground station as for Kew Observatory As regards the irregular changes in H, the phenomena observed were at least consistent, as in the case of D, with a small reduction in the amplitude of the movements underground, but no certain conclusion can be drawn

The results are consistent with the view that in a coal mine, where local disturbance is absent or very small, declination changes may for practical purposes be treated as identical with those at the surface. During the time of the observations at Sandwell Park there was no instance where the difference between an irregular movement recorded underground and the corresponding surface movement was sufficient to catch the eye There were small differences in amplitude, according to the measurements made, but no difference was noticed in the type of any irregular movement We should not, however, be justified in assuming that differences visible to the eye never occur 1923 was a very quiet year, and contained few disturbances of any size, and there were no conspicuously large rapid oscillations. Such oscillations constitute the conditions under which a difference between surface and underground phenomena would seem most likely to arise This limitation is practically unimportant, because no observations taken during a magnetic storm should be employed for engineering purposes.

It is, perhaps, only proper to add that the conditions were not favourable for the detection of *minute* differences The curves did not in general possess the sharpness of outline which can be secured with first-class magnetographs at a first-class observatory, and the artificial disturbances at the underground and surface stations were not identical

§ 5 The second main question, how far results from a station in S E England are applicable elsewhere in the British Isles, has an even wider interest It is not a new question, but deserves more attention than it has received The first important occasion when it arose in modern times was in connection with Rücker and Thorpe's survey * In their reduction of field observations Rücker and Thorpe acted on two assumptions, the hypothetical character of which they explicitly recognised :—(1) That the regular diurnal inequality is independent of disturbance, and may be treated as identical over the British Isles, provided allowance be made for the difference in local time, (2) that irregular movements may be treated as identical over the same area Accepting the truth of these hypotheses, they were justified in applying everywhere a correction for the diurnal inequality based on quiet day inequalities from Kew Observatory, and in making an allowance for irregular disturbances based on the curves of the same station

Even in Rücker and Thorpe's time it would have been possible to check the truth of these assumptions by comparing corresponding records from Kew and Stonyhurst This, however, does not seem to have been done A possible explanation is that Rücker and Thorpe may have been aware of a comparison instituted by Dr Balfour Stewart† and the Rev W Sidgreaves, S J , which—owing, apparently, to a confusion over scale values‡—led to the erroneous conclusion that the less rapid irregular movements at Kew and Stonyhurst were practically equal in amplitude The next comparison between British stations was more exhaustive, but it was between Kew and Falmouth,§ observatories both in the south of England, and was confined to quiet day inequalities In that case the results were, on the whole, not unfavourable to Rücker and Thorpe's first hypothesis.

The question arose again in connection with Mr G W. Walker's re-survey for the epoch 1915 Eskdalemuir had then been recording for several years, and sufficient intercomparison had been made of Kew and Eskdalemuir to show that disturbance tended to be larger at the more northern station. Mr. Walker|| was aware, as he explicitly states, that neither of Rücker and Thorpe's hypotheses was true, but he thought it best to follow their procedure, relying this time on Greenwich as a base station.

* 'Roy Soc Phil. Trans,' A, vol 181, p 53 (1890)
† 'Roy Soc Proc ,' vol 17, p 236 (1869)
‡ *Cf* 'Inst Electrical Engineers' Journal,' vol 57 p 593 (1919)
§ 'Roy Soc Phil Trans ,' A, vol 204, p 373 (1905).
|| 'Roy Soc Phil Trans.,' A, vol. 210, p 9 (1910)

It is obviously impossible even now to reduce field observations taken in different parts of the British Isles as satisfactorily as if there were in existence additional magnetic observatories in South-Western England or Wales, Western Ireland and North-Western Scotland But this does not mean that no better course is possible than that followed by Rücker and Thorpe and by Walker The rest of this paper may be regarded as helping to elucidate this point The Sandwell Park D data it utilizes are those from the surface station

§ 6 Taking first the D regular diurnal inequality on quiet days, it was found that the differences between the ranges or A D 's at Kew Sandwell Park and Eskdalemuir were small in all months There was a slight tendency in the range, and still more in the A D , to increase as we go north, but even in the case of the A D the excess at Eskdalemuir over Kew, on an average from the five months May, June, September, October and November, was only 8 per cent of the Kew value

Results for Lerwick were more complicated Even in the south of England the amplitude of the regular diurnal inequality on quiet days has a large annual variation, with a pronounced minimum at midwinter But at Lerwick this annual variation is further developed In June the range at Lerwick was 11 per cent and the A D was 35 per cent larger than at Kew, but in October the range and A D were actually smaller at Lerwick than at Kew

The results obtained for quiet days for H differ considerably from those obtained for D If we take an average from April, May and June, the ratio borne by the range of the regular diurnal inequality to that at Kew was 1·15 for Sandwell Park, 1 37 for Eskdalemuir, and 1 48 for Lerwick , while, if we take a mean from October and November, the ratio was 1·10 for Sandwell Park, 0 91 for Eskdalemuir and 0 80 for Lerwick The tendency to increased amplitude as we go north in summer, and the tendency to a reduced amplitude at the more northern stations in winter, are thus shared with declination, but to an enhanced degree.

§ 7. When considering disturbed day inequalities, it is important to remember that the five most disturbed days may represent a much higher absolute standard of disturbance in one month than in another 1923, a year of sunspot minimum, was a quiet year Also, owing to breakdowns, the disturbed days selected were not always the most disturbed of the month Thus the differences found here between quiet and disturbed day inequalities are not unlikely to be less than the differences to be encountered in an average year

In the case of D the ratio borne by the range of the diurnal inequality from the selected disturbed days to the range of the inequality from the selected quiet

days varied at Kew from 1 38 in June to 2 42 in November at Sandwell Park it varied from 1 34 in June to 2·47 in November, at Eskdalemuir it varied from 1 43 in May to 3 07 in November, and at Lerwick it varied from 1 25 in May to 4 63 in November These ratios, if Rücker and Thorpe's hypotheses had been true, should all have been 1 00.

On an average from five months, the ratio borne by the disturbed day D inequality range to the quiet day range was 1 82 for Kew, 1 87 for Sandwell Park, 2·06 for Eskdalemuir, and 2 61 for Lerwick The tendency in the ratio to increase with increase of latitude was not shown in May and June, and it became less prominent when the A D. was substituted for the range.

In the case of H, if we omit Lerwick, we find less difference between the different stations and the different months The ratio borne by the range of the disturbed day inequality to the quiet day inequality, on an average of five months, was 1 44 at Kew, 1·42 at Sandwell Park and 1 41 at Eskdalemuir The extreme values of the ratio in individual months if we include the three stations were 1 09 and 1 68 There was no decided tendency in the ratio to increase with latitude When, however, we pass to Lerwick, we encounter a totally different state of matters The ratio borne by the disturbed day inequality range to the quiet day range varied from 1 46 in June to 6 49 in October, and on an average of five months it was no less than 3 33 It was found, moreover, that the diurnal inequality on disturbed days at Lerwick in the later months was quite different in type from that at the other stations To make sure that the phenomenon was not an accident of the special days selected, the Eskdalemuir and Lerwick tables for the international quiet and disturbed days of all months of 1923 were consulted These put the matter beyond a doubt. On quiet days at Lerwick 11 h. or 10 h appears to be the normal time of the minimum the whole year round, as at Eskdalemuir or Kew At the more southern stations there seems no difference in this respect between disturbed and quiet days But at Lerwick on disturbed days, at least in 1923, the principal minimum in the equinoctial and winter seasons appeared near midnight This happened even in one summer month June, and the influence of the equinoctial and winter months was so great that even in the mean diurnal inequality for the year the minimum fell at 2 h. Analysis in Fourier series showed that for September and October on disturbed days there was a difference approaching 180° in the phase angles of the 24-hour waves for Lerwick and for the three more southern stations.

In view of its high latitude, 60° N., Lerwick may appear a somewhat extreme station for the British Isles. But Eskdalemuir, on the other hand, is in the

south of Scotland, and there may be a large part of Scotland where the conditions approach as closely to those of Lerwick as to those of Eskdalemuir.

§ 8 Irregular D movements were measured on about 90 nights at Kew, a few highly disturbed, a few quiet, and the majority moderately disturbed The practice adopted was to take the sum of the amplitudes of all the movements measured on a single night at each station, and compare it with the corresponding aggregate for Kew. The measurements were made in millimetres, the curves from the different stations being similarly dealt with, but independently, and the results should be quite unprejudiced Readings were taken to 0·1 mm., but accuracy cannot be secured to 0·1 mm except under very favourable conditions.

On a few of the more highly disturbed nights, some of the D movements selected at Kew could not be identified with movements at Lerwick, and this was even true in a few cases at Eskdalemuir In such cases only the movements, the identification of which was undoubted, were taken into account when comparing the two stations

On every single night when comparisons were made the aggregate of the D movements was greater for Eskdalemuir than for Sandwell Park or Kew, and greater for Lerwick than for Eskdalemuir. Out of a total of 66 nights used, there were only 5 when the aggregate movement was larger for Kew than for Sandwell Park, and on each of the 5 occasions the aggregate was small, and the apparent excess trifling From the grand aggregates of all the irregular movements measured, the ratios borne to the Kew movement by the corresponding movements at Sandwell Park, Eskdalemuir and Lerwick were respectively 1·12, 1·48 and 2·09. The values obtained for the ratio Lerwick . Kew in seven separate months varied only between 1·92 and 2·26.

The ratio borne by the representative irregular D movement at Lerwick to the corresponding movement at Kew is much larger, especially in the summer months, than the ratio borne by the range of the regular D diurnal inequality on disturbed days at Lerwick to the corresponding range at Kew

§ 9. An analogous comparison was made of irregular H movements at Kew, Sandwell Park and Lerwick Here, again, D and H do not behave alike In every month the aggregate of the H movements was substantially greatest at Lerwick, but there was quite a considerable number of individual nights when the aggregate for Lerwick was similar to or even less than the corresponding aggregate for Kew. On some of these occasions there was a fall in the amplitude in passing from Kew to Sandwell Park, and a further fall in passing from Sandwell Park to Lerwick There was not any decided tendency, such as

appeared in the case of D, for the amplitude of the irregular movement to be larger at Sandwell Park than at Kew In fact, taking the aggregate of 514 movements measured, there was a deficiency of 1 per cent in the amplitude at Sandwell Park This may, of course, be due to the station being underground. As the H inequality range from disturbed days at Sandwell Park was, on an average, from five months, 13 per cent in excess of the Kew range, it is clear that the phenomenon can hardly be due to any error in scale values

As already stated, there were nights when the equivalents of some of the irregular D movements measured at Kew could not be identified at Lerwick, but such occasions were few In the case of H, however, there were a good many such occasions, whole nights, in fact, when satisfactory identifications could not be made. On one of these nights the H range at Lerwick exceeded 900 γ, while the corresponding range at Kew was only about 140 γ On another occasion, when identification did seem possible for 12 movements, the aggregate of the H movements at Lerwick was 4 8 times the corresponding aggregate at Kew. This occasion and one or two others of a like kind were treated as exceptional Omitting them the ratio of the representative irregular movement at Lerwick to that at Kew, based on an aggregate from 344 movements, was only 1 35 This is much less than the corresponding result obtained from the D irregular movements, even when the latter are converted into their force equivalents so as to allow for the lower value of H at Lerwick

§ 10 The cases where it was difficult or impossible to identify corresponding irregular movements in H at Kew and Lerwick were examined individually, and a comparison was made which was based on *mean* hourly values of D and H The changes from hour to hour measured in this way are not as accurate as the amplitudes of individual irregular movements, but the stations differed so widely that the accuracy sufficed to bring out the salient features

In the case of D, even on highly disturbed days, the sign of the change from hour to hour was in general the same at the different stations, and the amplitude of the change, whether easterly or westerly, increased pretty regularly with the latitude For example, on the night of September 26–27, one of the most disturbed, the change in D shown by the mean hourly values was continuously easterly from 19 h to 23 h on the 26th, and the aggregate movement was 20′·9 at Kew, 23′·7 at Sandwell Park, 28′·5 at Eskdalemuir and 36′·3 at Lerwick, while on the morning of the 27th from 1 h to 3 h. the movement was westerly, the aggregate change being 13′ 7 at Kew, 16′·1 at Sandwell Park, 20′ 9 at Eskdalemuir and 44′ 2 at Lerwick

In the case of H the changes were sometimes of the same sign at all the

stations, but the increase with latitude was often extraordinarily pronounced Taking again the night September 26–27, the aggregate change from 19 h of the 26th to 1 h. of the 27th was a fall at all the stations, but it amounted to 43γ at Kew, 37γ at Sandwell Park, 114γ at Eskdalemuir and 340γ at Lerwick , while from 1 h. to 4 h on the 27th there was a rise amounting to 30γ at Kew, 41γ at Sandwell Park, 109γ at Eskdalemuir, and 247γ at Lerwick On these occasions it was only at Eskdalemuir and Lerwick that the fall or rise in the successive hourly means appeared absolutely unbroken

On other occasions changes in H from one hour to the next were such as the following .—

Kew	Sandwell Park	Eskdalemuir	Lerwick
+28γ	+17γ	+ 4γ	−269γ
+ 8γ	+ 7γ	22γ	−130γ
− 1γ	+ 4γ	+17γ	+228γ
−22γ	−20γ	−13γ	+ 39γ

With the Lerwick data before us, we can recognise an orderly progression in the changes at the three more southern stations An influence dominant at Lerwick was apparently in opposition to an influence which prevailed in the south of England

It is sufficiently obvious that in any of the above cases any corrections based, like Rücker and Thorpe's, on Kew data alone would be absolutely futile, so far at least as northern Scotland is concerned In such cases the best course may be to disregard any field observation taken at a distance from a magnetic observatory

The results of the present paper are based on a very large amount of data which it is hoped to present adequately in a Geophysical Memoir to be published by the Meteorological Office

We have pleasure in acknowledging the great assistance given us by Mr Bocking, Messrs Bailey and Mr Howarth, and by the manager and staff of the Sandwell Park Colliery. Without the active assistance of these gentlemen the work would have been impossible

On the Gyration of Light by Multiplet Lines.

By C. G Darwin, F R S

(Received June 22, 1926)

1. In the last few years there has been a great development of the theory of the intensities of spectral lines, and in its turn this theory has reacted on the general theory of spectra, so that any experimental method which throws new light on the subject has a great importance It has not apparently been explicitly noticed that a study of the dispersive effect of the rotation of polarized light by a vapour can be made to yield information on the second approximations to the intensities of the ⊥ Zeeman components Since the difficulties of direct intensity measurement and of obtaining strong magnetic fields must always be very great, there would seem to be an advantage in having a method of attack which is, it is true, difficult, but only with the difficulty of a very well-known technique, the study of polarized light

The present work is a theoretical investigation of some of the properties that may be expected to be found. In a recent paper* the present writer worked out some results on the subject using the purely mechanical models of the type discussed by Voigt, and obtained the result that any atom which exhibits the Paschen back effect should show a similar effect in a *weak* magnetic field in regard to the gyration of light, provided that *the frequency of this light is not too close to the lines of the multiplet* (Of course light in the immediate neighbourhood will not be affected in this way, but will exhibit the actual Zeeman effect inversely.) In other words, the equation of Becquerel† relating the gyratory constant V with the refractive index n

$$V = \frac{e}{2mc^2} \lambda \frac{dn}{d\lambda}$$

will give the normal value of e/m, and all trace of the anomalous Zeeman effect will disappear. If this result is true for a single multiplet, it will remain true in regions where more than one contribute sensibly to the refraction, and will only fail for light of frequency very close to that of one of the multiplets of the spectrum.

The purely mechanical model for which this result was found has, of course,

* 'Phil. Mag.,' vol. 1, p. 161 (1926).

† 'C. R.,' vol. 125, p. 679 (1897).

many weaknesses, but it does have some of the features of the "electron and core" model, for it can be thrown into a form where one electron is solely responsible for emission and exhibits the normal Larmor rotation, while the electron is loosely linked with others which are "blind" and have anomalous rotation It therefore seemed very probable that the result could be proved as a result of the electron and core model, and it was the main object of the present work to see if this were so, by attacking the problem by the use of Kramers' and Heisenberg's dispersion theory * The expected result is verified, and some progress is made in evaluating the second order terms in the intensities.

There can be no doubt that the proper approach to the problem is through the New Mechanics of Heisenberg applied to the rotating electron of Uhlenberg and Goudsmit, but little has yet been published about the rotating electron, and the New Mechanics has many more fundamental problems to dispose of first, so that it is perhaps still not out of place to make what proves to be an exceedingly unambiguous application of the Correspondence Principle The present work is carried out only with the model which is used for the simpler types of spectra, indeed the theory of intensities of more complex lines is still too imperfect to carry the result farther

What is practically the same subject as the present work was discussed in a recent paper by Frenkel.† He was engaged in an examination into the "paramagnetic gyration" which Ladenberg‡ suggested should arise from the unequal numbers of atoms orientated in the various directions He appears to the present writer to have made an oversight so that he did not calculate the changes in intensities of the Zeeman lines, and in consequence his results are largely vitiated

2 The gyration of light by a mass of gas is readily expressed as an atomic effect by methods which are practically those of Lorentz An atom is in a magnetic field along z and is exposed to light going along z and polarized along x. Then it acquires electric moment of components σE_x, $i\rho E_x$ along x and y We shall call σ and ρ, respectively, the *refraction* and the *gyration* of the atom. The result is a scattering of waves which causes unequal refraction for right- or left-handed circularly polarized light, according to the equation $\frac{3(n^2-1)}{n^2+2} = 4\pi N(\sigma \pm \rho)$, where N is the number of atoms in unit volume If

* 'Z. f. Physik,' vol. 31, p 681 (1925).
† 'Z f Physik,' vol 36, p. 215 (1926).
‡ 'Z. f. Physik,' vol 34, p. 898 (1925).

n', n'' are the two solutions, the plane of polarization rotates an angle $\pi(n' - n'')/\lambda$ per unit length. As long as we are studying light not very close to a spectral line ρ is much smaller than σ and we write $n' - n'' = 2\rho \Big/ \left(\frac{d\sigma}{dn}\right)$ where n is the mean refractive index If the atom exhibits the normal Larmor rotation 0_L, it is not hard to show that

$$\rho = 0_L \frac{d\sigma}{d\nu} = \frac{0_L}{c} \frac{\lambda^2}{2\pi} \frac{d\sigma}{d\lambda}, \tag{2 1}$$

and hence in this case we get a rotation per unit length

$$\frac{0_L}{c} \lambda \frac{dn}{d\lambda},$$

which is Becquerel's result

Thus for our purposes all that is necessary is to calculate σ and ρ for the models adopted, and these are determined by the methods of Kramers and Heisenberg We quote their result, excluding the emissive terms which are necessary for the complete correspondence, but which will not practically concern us A_s is a vector associated with frequency* ω_s of which the classical analogue is the coefficient of $e^{i\omega_s t}$ in the Fourier expansion of the electric moment Then under electric force which is a vector $Ee^{i\nu t}$ the atom acquires an excited moment proportional to

$$\mathbf{M} = \Sigma_s \left\{ \frac{\bar{\mathbf{A}}_s (\mathbf{E}\mathbf{A}_s)}{\omega_s - \nu} + \frac{\mathbf{A}_s (\mathbf{E}\bar{\mathbf{A}}_s)}{\omega_s + \nu} \right\} e^{i\nu t}. \tag{2.2}$$

Here $\bar{\mathbf{A}}_s$ is the complex quantity conjugate to $\mathbf{A}_s$ We are only concerned with the $\perp$ Zeeman components and the ω's fall into two classes r and l, where ω_r, ω_l correspond to the emission of light which is polarized respectively in right- and left-handed circles For the right-handed we have $A_r^y = -iA_r^x$, and for the left, $A_l^y = iA_l^x$

Then under the stimulus of an electric force $\mathbf{E}_x$ the moment is

$$\begin{aligned} \mathbf{M}_x &= \sigma \mathbf{E}_x e^{i\nu t}, \\ \mathbf{M}_y &= i\rho \mathbf{E}_x e^{i\nu t}, \end{aligned} \tag{2.3}$$

where

$$\begin{aligned} \sigma &= \Sigma_r |A_r^x|^2 \left(\frac{1}{\omega_r - \nu} + \frac{1}{\omega_r + \nu} \right) + \Sigma_l |A_l^x|^2 \left(\frac{1}{\omega_l - \nu} + \frac{1}{\omega_l + \nu} \right), \\ \rho &= \Sigma_r |A_r^x|^2 \left(\frac{1}{\omega_r - \nu} - \frac{1}{\omega_r + \nu} \right) - \Sigma_l |A_l^x|^2 \left(\frac{1}{\omega_l - \nu} - \frac{1}{\omega_l + \nu} \right), \end{aligned} \tag{2 4}$$

and our problem is solved when we have evaluated these quantities

* Throughout this paper *frequency* will mean the number of vibrations in 2π secs., so as to avoid the perpetual recurrence of the factor 2π which has disfigured the printing of so much recent work

We shall refer to $|A^x|^2$ as the intensity of the line at ω. Strictly speaking, this is ambiguous because the relative intensities of lines of different frequencies will differ according to whether we consider absorption or emission, in other words, whether we are discussing the Einstein A or B. Fowler* shows good reason to regard B as the proper one to take, and shows that with the simple Larmor rotation it will be invariant—that is, $|A_r|^2 = |A_l|^2 = |A_0|^2$, he also conjectures that this should be true for the anomalous Zeeman effect, but we shall see reason to differ from this view. In any case, our $|A|^2$ is the quantity which will be called intensity in the New Mechanics, and it is therefore unnecessary to go further into the question.

3. We shall now assume a result obtained later by the Correspondence Principle. When a line is broken into its Zeeman components, the corresponding members r and l on the opposite sides of the zero are not exactly equal in intensity, but one is slightly increased and the other is diminished to exactly the same extent. If 0_L is the Larmor rotation and if β is a parameter measuring the separation of the members of the multiplet, then the intensities of the r and l members are, respectively, changed in the ratio $1 + a0_L/\beta$, $1 - a0_L/\beta$, where a is a numerical constant of order unity depending on the quantum numbers of the switch and also on the ratio of the separations of the two sets of terms concerned in the multiplet.

We require to add together a large number of rather complicated expressions, and the handling of the process is very materially simplified by using the following notation. In the first place, the symbol ϕ means ± 1. The introduction of this symbol enables us to take together the r and l components without writing out separately the expressions for them. Let ω be the centre of gravity of the multiplet, then the zero position of one of its members is $\omega + b\beta$, where b is of the order unity. A Zeeman component has frequency $\omega + b\beta + \phi c0_L$, where c is the factor giving the magnetic anomaly for the component—of the order unity. This line has intensity $I(1 + \phi a0_L/\beta)$. The refraction of the pair of lines is

$$\Sigma_\phi I(1 + \phi a0_L/\beta)\left[\frac{1}{\omega - \nu + b\beta + \phi c0_L} + \frac{1}{\omega + \nu + b\beta + \phi c0_L}\right] \quad (3.1)$$

We are only considering values of ν far from the multiplet, so that this may be written

$$\Sigma_\phi I(1 + \phi a0_L/\beta)\left[\left(\frac{1}{\omega - \nu} + \frac{1}{\omega + \nu}\right) - (b\beta + \phi c0_L)\left(\frac{1}{(\omega - \nu)^2} + \frac{1}{(\omega + \nu)^2}\right)\right]. \quad (3.2)$$

* 'Phil. Mag.,' vol. 1, pg. 1079 (1925).

To evaluate the gyration we must write $\frac{1}{\omega - \nu} - \frac{1}{\omega + \nu}$ and $\frac{1}{(\omega - \nu)^2} - \frac{1}{(\omega + \nu)^2}$, and must subtract the r and l members instead of adding. This subtraction can be done by multiplying each of the terms by ϕ and then adding. Both the required results can be found together by setting down the expression

$$I(1 + \phi a 0_L/\beta)[P - Q(b\beta + \phi c 0_L)]. \tag{3 3}$$

Then the term independent of ϕ gives the value of the refraction,* if P is taken to mean $\frac{1}{\omega - \nu} + \frac{1}{\omega + \nu}$ and Q $\frac{1}{(\omega - \nu)^2} + \frac{1}{(\omega + \nu)^2}$, and the gyration is given by taking the coefficient of ϕ, with P meaning $\frac{1}{\omega - \nu} - \frac{1}{\omega + \nu}$ and Q $\frac{1}{(\omega - \nu)^2} - \frac{1}{(\omega + \nu)^2}$. In all our work the summation for ϕ can be left to the very end, so that no confusion arises on account of this dual meaning of P and Q, but when we require to distinguish them we shall write P_σ, Q_σ, P_ρ, Q_ρ. We observe that

$$Q_\rho = \frac{\partial P_\sigma}{\partial \nu}.$$

If we multiply out (3 3), we obtain

$$I[P(1 + \phi a 0_L/\beta) - Q(b\beta + \phi c 0_L + \phi a b 0_L)], \tag{3.4}$$

and this is to be summed over the multiplet.

Experiments will always consist in a comparison of gyration with refraction. Since ω has been chosen as the centre of gravity of the multiplet, $\Sigma I b = 0$ and we shall have $\sigma = P_\sigma \Sigma I$. This is the natural way in which it would be expressed, corresponding to a pure Lorentz formula for the refractive index, without a correction term in Q_σ. The gyration will be

$$\rho = 0_L \Sigma I[- P_\rho a/\beta + Q_\rho(c + ab)], \tag{3.5}$$

and it is clear why the second order terms in the intensities must be known, for a comes in twice over in terms which are certainly not negligible. The result we are to prove consists in showing that if taken over the whole multiplet the sum (3.4) will contain no term in $P\phi$, and that the sum of all the terms in $Q\phi$ will add up to an amount exactly corresponding to the Larmor rotation. In other words, the sum of all the term of (3 4) reduces to

$$(P - Q\phi 0_L)\Sigma I. \tag{3.6}$$

* Strictly speaking, the value should be doubled, but as we are only concerned with the ratio of gyration to refraction, this is immaterial.

4. As a consequence of temperature certain other cases arise which deserve discussion A multiplet is constructed out of the differences of two sets of levels, the term-multiplets, and in evaluating frequencies and intensities these play entirely similar roles But here we are not concerned with emission or absorption, but only with refraction, and the atoms are all present in only one set of levels—the other set having a purely potential existence We shall call the states of the atom which are really present the "actual states," the others the "potential" Any temperature effect will only be concerned with these actual states, and to this extent the refractive effect of the multiplet may be quite unsymmetrical in the two sets of levels that concern its formation

Ladenburg* has called attention to a phenomenon which he calls "paramagnetic gyration," as opposed to the ordinary diamagnetic gyration The magnetic energy of some initial states is greater than that of others, and consequently there are unequal probabilities of the atoms being found in these states Hence, he predicts a type of gyration which will depend on the temperature We may usefully review this question from a rather more general standpoint, as several cases arise. In the first place the magnetic energy ΔW_m is always small, so that at any reasonable temperature we can expand the expression $\exp. - \Delta W_m/\kappa T$ as $1 - \Delta W_m/\kappa T$ But it will also be necessary to allow for the fact that the different states of the actual term-multiplet have different energies and therefore different probabilities of occurrence, and here we must discriminate between the cases of high and low temperature Low temperature will mean that practically only one actual state of the atoms will be present (of course, split into its magnetic levels), and high that all are present with probability factor $1 - \Delta W_j/\kappa T$

In the case of low temperature there cannot be more than three lines active ($j \rightarrow j \pm 1$ and $j \rightarrow j$, starting from one initial j) It will be proper to expand the effect in terms of a P and Q corresponding to the centre of gravity of the lines present, in order that there should be no Q-term in the refraction. The temperature effect will be represented by a factor $1 - mg\phi_0 h/2\pi\kappa T$ (in Landé's notation) attached to each line issuing from the state of quantum number m, and the result is that (3 4) must be multipled by a quantity of the form, $1 - \frac{h}{2\pi\kappa T} d\phi_0$, and then summed over the three or less lines present The complete formula will be

$$\Sigma I\left[P - Q\phi_0 (c + ab) - P\phi_0 \left(\frac{h}{2\pi\kappa T} d - \frac{a}{\beta}\right)\right].$$

* *Loc. cit.*

Of the three terms in the gyration, that in Q will predominate at points near the multiplet. As ν gets farther away, this term will bear to the P-term a ratio of the order $\beta Q/P$ or $\beta/|\omega - \nu|$, so that the P-term will become the more important at distances greater than the separation of the multiplet. Of the two P-terms the paramagnetic is much the more important—unless $\kappa T > \beta h$, and this would contradict our assumption of low temperature. We also observe that the paramagnetic term can be calculated without knowing the second orders in the intensities, but that these must be known for both the other terms.

In the case of high temperature we have to sum the effect of the complete multiplet, and $\Delta W/kT$ will contain β as a factor, so that we shall have to allow for the influence of the second order terms on the paramagnetic effect. We shall work out this problem for the classical case, and shall find that the paramagnetic gyration, like the diamagnetic, is entirely independent of the magnetic anomaly and the multiplet separation. The result brings out in an interesting manner the distinction between the actual and the potential states.

We may here remark that the interest in the case of high temperature, including the purely diamagnetic gyration which corresponds to infinite temperature, is mainly theoretical, in that it enables us to obtain information by the Correspondence Principle as to the values of the second orders in the intensities. These are required in order to know the gyration of an actual substance, but except in very close multiplets only one actual state will be present at manageable temperatures. In § 11 examples will be given, showing how it is possible to give the expressions for low temperatures from a knowledge of those at high.

5. In general terms the result that we have to prove can be put in the following form. The atom is composed of two loosely linked systems A and B, and β is a small parameter measuring the closeness of the linkage. A is acted on by an external force which is without *direct* effect on B. Then the reaction of A to this force will only be effected by B to the order β^2—putting it loosely, one β arises because the effect has to pass in to B, and the second because it comes back to A before appearing in the outer world. This result is easy to prove quite generally provided that there is no degeneracy present, but in the actual systems for which we require it B causes secular perturbations in A, and the theorem becomes much more complicated. As we want to know not merely the behaviour of the whole multiplet but also of its separate members, we shall take a specific model and work with that, merely noting that the rather elaborate way in which the terms cut out suggests that the theorem would probably be true for a far more general class of model.

The model we shall use is that which explains the ordinary classes of multiplet

where the multiplicity is the same for both of the terms out of which the spectrum is constructed.* We shall summarize its properties A single electron, which alone is affected by external forces, has principal quantum number n and angular momentum k_0 directed in the direction K A core which is blind (unaffected by the radiation) has angular momentum r_0 in the direction R, and the resultant angular momentum is j_0 in the direction J (which lies in the plane through KR) m_0 is the component of j_0 along Z the direction of the magnetic force These constitute a canonical system of co-ordinates provided their conjugates are taken as

w_k^0 = the angle between JK and the apse of the motion of the electron

w_r^0 = similarly for the core

w_j^0 = the angle ZJK

w_m^0 = the angle XZJ.

w_n^0 = the " mean anomaly " in the orbital motion

The energy of the system is composed of

(i) $H_k(n, k_0)$ the energy of the electron

(ii) $H_r(r_0)$ the energy of the core, involving other degrees of freedom which play no part in the process

(iii) the mutual energy To agree with the ordinary separation of multiplets this must be proportional to cos KR. We shall take it as $k_0\beta$ cos KR, where β itself will depend on k_0 (being in fact, for many lines, proportional to $1/k_0^3$) Also $\cos \mathrm{KR} = \dfrac{j_0^2 - k_0^2 - r_0^2}{2k_0 r_0}$

(iv) the magnetic energy of the electron. As the electron exhibits the normal Larmor rotation this is $0_L k_0$ cos KZ.

(v) the magnetic energy of the core. The core has anomalous rotation of amount which we shall call $0_L + \varepsilon$ though as a fact ε itself is equal to 0_L This contributes an amount $(0_L + \varepsilon) r_0$ cos RZ

Adding these together we have as energy

$$H = H_k(n, k_0) + H_r(r_0) + \beta \frac{j_0^2 - k_0^2 - r_0^2}{2r_0} + m\left(0_L + \varepsilon \frac{j_0^2 - k_0^2 + r_0^2}{2j_0^2}\right) - \varepsilon k_0 \sin \mathrm{KJ} \sin \mathrm{ZJ} \cos w_j^0 \qquad (5.1)$$

The actual energy is given by omitting the last term, since it fluctuates. But the presence of this term means that the co-ordinates are not true angle variables, suitable for the dispersion theory, and we must make a small

* See for example Pauli, ' Z. f. Ph .' vol. 20, p. 371 (1924).

transformation to remove it We shall submit the system to the canonical transformation generated by

$$S = kw_k^0 + rw_r^0 + jw_j^0 + mw_m^0 + \frac{\epsilon}{\beta}\frac{kr}{j}\sin\overline{KJ}\sin\overline{ZJ}\sin w_j^0 \qquad (5\,2)$$

We are supposing throughout that the magnetic field is weak, so that $\epsilon \ll \beta$. Here $\sin\overline{ZJ}$, $\sin\overline{KJ}$, are the same functions of k, r, j, m as $\sin ZJ$, $\sin KJ$ of k_0, r_0, j_0, m_0 A great deal of our work is concerned with these angles $\overline{ZJ}$ and $\overline{KJ}$, which we shall write as Z and K Thus

$$\cos Z = m/j \qquad (5\,3)$$

$$\cos K = (j^2 + k^2 - r^2)/2jk. \qquad (5\,4)$$

The transformation has the effect of not altering k, m, r, but

$$j_0 = j + \frac{\epsilon}{\beta}\frac{kr}{j}\sin K\sin Z\cos w_j. \qquad (5\,5)$$

The result is that to the order ϵ, the energy is

$$H = H_k + H_r + \beta\frac{j^2 - k^2 - r^2}{2r} + m\left(0_k + \epsilon\frac{j^2 - k^2 + r^2}{2j^2}\right) \qquad (5\,6)$$

6 Let us suppose that a pair of axes ξ, η are drawn through the apse and at right angles in the plane of the orbit Then with regard to these axes the electric moment is

$$\xi = \sum_{T=-\infty}^{\infty} a_T e^{iTw_r}, \qquad \eta = -i\sum_{T=-\infty}^{\infty} b_T e^{iTw_r}, \qquad (6.1)$$

a_T, b_T are functions of n, k_0 only and $a_{-T} = a_T$, $b_{-T} = -b_T$.

If we transform successively to (1) a set of axes with pole at K and with one of the others in the plane of KJ (2) axes with pole at J and one in the plane of JK (3) to x, y, z, we get for the moment along x an expression which may be written

$$\begin{aligned} M_x = -\sum_T \frac{a_T + b_T}{8} e^{i(Tw_r + w_j^0)}\{&e^{i(w_j^0 + w_m^0)}(1 + \cos KJ)(1 + \cos ZJ) \\ &- e^{i(w_j^0 - w_m^0)}(1 + \cos KJ)(1 - \cos ZJ) + e^{i(-w_j^0 + w_m^0)}(1 - \cos KJ)(1 - \cos ZJ) \\ &- e^{i(-w_j^0 - w_m^0)}(1 - \cos KJ)(1 + \cos ZJ) + 2\sin KJ\sin ZJ\,(e^{iw_m^0} + e^{-iw_m^0})\} \\ &+ \text{a similar expression involving } (a_T - b_T)\,e^{-iw_j^0}. \end{aligned} \qquad (6\,2)$$

As the second expression involves a different change of k it belongs to a different multiplet, and so here falls out of consideration. The coefficients that have been written down are those from which the intensities of the Zeeman components are ordinarily determined, but to obtain the second order terms they must be submitted to the transformation (5.2).

In what follows the work is much shortened by an extension of the notation of §3. θ and ϕ both represent ± 1 Then

$$\mathbf{M}_x = -\Sigma \frac{a_T + b_T}{8} e^{i(1\omega_+ + i\omega_+^0)} \Big\{ \sum_{\theta,\phi} (1+\theta \cos \mathrm{KJ})(\phi + \theta \cos \mathrm{ZJ}) e^{i(\theta w_j^0 + \phi i w_m^0)} + \sum_{\phi} 2 \sin \mathrm{KJ} \sin \mathrm{ZJ}\, e^{i\phi i w_m^0} \Big\}. \quad (6\,3)$$

$\mathbf{M}_y$ is derived from $\mathbf{M}_x$ by writing $w_m^0 - \pi/2$ for w_m^0, which can be conveniently done by multiplying each term by $-i\phi$ before summing.

It is next necessary to apply the transformation (5.2), which modifies not only j_0 and through it KJ and ZJ, but also w_k^0, w_j^0, w_m^0 We must also remember that β is a function of k_0, so that the modified terms will involve $d\beta/dk$ which we shall write as β' The presence of the term in $\sin w_j^0$ in the generating function means that, so to speak, intensity is transferred from the components of the $j \to j$ lines to the $j \to j \pm 1$ and vice versa, while there appear new lines $j \to j \pm 2$ We need not give the work nor even set down its results, since it is the squares of the coefficients in $\mathbf{M}_x$ that are required These are given in the next section

7 The intensities (Einstein B's) are obtained by applying (5 2) to (6 3) and squaring the coefficients We write $|a_T + b_T|^2/16 = \mathrm{M}$ a function of n, k only, and for convenience we give the frequency of each line also

$$\mathrm{I}_{2\theta,\phi} = \tfrac{1}{16} \mathrm{M} \sin^2 \mathrm{K} \sin^2 \mathrm{Z} (1 + \theta \cos \mathrm{K})^2 (\phi + \theta \cos \mathrm{Z})^2 \frac{\epsilon^2}{\beta^2} \frac{k^2 r^2}{j^4} \Big(1 + \theta \frac{\beta'}{\beta} j\Big)^2$$

$$\omega_{2\theta,\phi} = \omega + \beta' \frac{j^2 - k^2 - r^2}{2r} - \beta \frac{k}{r} + 2\theta \Big(\beta \frac{j}{r} + m\epsilon \frac{k^2 - r^2}{j^3}\Big) + \phi \Big(0_L + \epsilon \frac{j^2 - k^2 + r^2}{2j^2}\Big)$$

$$\mathrm{I}_{\theta,\phi} = \tfrac{1}{4} \mathrm{M} (1 + \theta \cos \mathrm{K})^2 (\phi + \theta \cos \mathrm{Z})^2 \Big[1 + 2\frac{\epsilon}{\beta} \frac{r}{j^2} \theta \Big\{ \frac{\beta'}{\beta} kj (1 - \theta \cos \mathrm{K})(\phi - \theta \cos \mathrm{Z}) - (\phi - \theta \cos \mathrm{Z})(j - k \cos \mathrm{K}) + k \cos \mathrm{Z} (1 - \theta \cos \mathrm{K}) \Big\} \Big]$$

$$\omega_{\theta,\phi} = \omega + \beta' \frac{j^2 - k^2 - r^2}{2r} + \beta \frac{j\theta - k}{r} + \phi 0_L + \frac{\epsilon}{j} [(\phi - \theta \cos \mathrm{Z})(j - k \cos \mathrm{K}) - k \cos \mathrm{Z} (1 - \theta \cos \mathrm{K})]$$

$$\mathrm{I}_{0,\phi} = \mathrm{M} \sin^2 \mathrm{K} \sin^2 \mathrm{Z} \Big[1 + \frac{\epsilon}{\beta} \frac{r}{j^2} \Big\{ -\frac{\beta'}{\beta} kj (\phi \cos \mathrm{K} + \cos \mathrm{Z}) + (2j - 5k \cos \mathrm{K}) \cos \mathrm{Z} - k\phi \Big\} \Big]$$

$$\omega_{0,\phi} = \omega + \beta' \frac{j^2 - k^2 - r^2}{2r} - \beta \frac{k}{r} + \phi 0_L + \frac{\epsilon}{j} [\phi (j - k \cos \mathrm{K}) - k \cos \mathrm{Z}] \quad (7.1)$$

An exactly similar process gives the z component of electric moment and thus the intensities of the $\parallel$ lines. We omit their frequencies, since these are obtained by putting $\phi = 0$ in the corresponding expressions for the $\perp$ lines.

$$I_{2s,0} = \tfrac{1}{4} M \sin^2 K \sin^4 Z (1 + \theta \cos K)^2 \frac{\varepsilon^2}{\beta^2} \frac{k^2 r^2}{j^4} \left(1 + \theta \frac{\beta'}{\beta} j\right)^2$$

$$I_{s,0} = M (1 + \theta \cos K)^2 \sin^2 Z \Big| 1 + 2 \frac{\varepsilon}{\beta} \frac{r}{j^2} \cos Z \Big\{ -\frac{\beta'}{\beta} kj (1 - \theta \cos K) + (j - k \cos K) + k\theta (1 - \theta \cos K) \Big\} \Big|$$

$$I_{0,0} = 4M \sin^2 K \Big| \cos^2 Z + \frac{\varepsilon}{\beta} \frac{r}{j^2} \cos Z \Big\{ \frac{\beta'}{\beta} kj \sin^2 Z - 2 \sin^2 Z (j - k \cos K) + k \cos K (1 - 3 \cos^2 Z) \Big\} \Big| \quad (7.2)$$

We may now make a partial interpretation into the terms of the quantum theory. A simultaneous change of ϕ into $-\phi$ and $\cos Z$ into $-\cos Z$ means a comparison of the s and t lines at equal distances from the zero position of a member of the multiplet. This change leaves the main terms in the intensities unaltered, but changes the sign of the second order terms. Thus what one gains in intensity the other loses. The same is true for the $\parallel$ components. It follows that the whole line remains unpolarized to the second approximation.

The ordinary summation rule fails. For this requires that $I_{s,1} + \frac{1}{2} I_{s,0} + I_{s,-1}$ should be independent of m, but it is actually for $j \to j - \theta$

$$M (1 + \theta \cos K)^2 \left\{1 + 2 \frac{\varepsilon}{\beta} \frac{r}{j^2} \theta k (1 - \theta \cos K) \cos Z\right\},$$

and for $j \to j$

$$2M \sin^2 K \left\{1 - 2 \frac{\varepsilon}{\beta} \frac{r}{j^2} k \cos K \cos Z\right\},$$

both of which depend on m through $\cos Z$. On the other hand, if we add these sums together for the three switches of j we have simply $4M$, so that we have another summation rule

If we add together the intensities of all switches from given j and m, the result will be independent of j and m. This rule is pointed out by Kronig* and by Fowler.† We shall examine some of its consequences later.

The new lines $j \to j \pm 2$ have intensity of the order $(\varepsilon/\beta)^2$, and so will play no part in our work. We may, however, note that each of them is unpolarized and that its intensity contains as chief factors the intensities of the lines

* 'Z. f. Ph.,' vol. 31, p. 885 (1925).

† *Loc. cit.*

generating it, that is, the line $j \to j$ | 2, $m \to m + 1$ will have as factors the product of the intensities $j \to j$ + 1, $m \to m + 1$ and $j \to j$, $m \to m + 1$. But, of course, when the quantum numbers are put in, it may be necessary to alter the factors by a unit or so

We must also observe the occurrence of j in the denominator We do not expect this to lead to any infinity in the case $j = 0$ because the same factor does not do so for the frequencies, but we should conjecture that the difference of intensities of the r and l components would be most marked with the lines of small quantum number j

8. In accordance with the principles described in §§ 2, 3, we now apply the Kramers-Heisenberg formula for refraction and gyration For the line $j \to j - 0$ the term $1_{\theta\phi}$ contributes

$$\{T\frac{\partial}{\partial n} + \frac{\partial}{\partial k} + 0\frac{\partial}{\partial j} + \phi\frac{\partial}{\partial m}\}1_{\theta\phi}\left\{\frac{1}{\omega_{\theta\phi} \quad \nu} \pm \frac{1}{\omega_{\theta\phi} + \nu}\right\} \tag{8 1}$$

We have to sum the influences of all the lines of the multiplet, but shall do it in two stages so as to determine in passing the gyration of a single line We therefore write

$$\omega_\theta{}^j = \omega + \beta' j^2 - k^2 - r^2 + \beta^j \theta \quad k, \tag{8 2}$$

and take

$$P_\theta{}^j = \frac{1}{\omega_\theta{}^j - \nu} \pm \frac{1}{\omega_\theta{}^j + \nu}, \quad Q_\theta{}^j = \frac{1}{(\omega_\theta{}^j - \nu)^2} \pm \frac{1}{(\omega_\theta{}^j + \nu)^2}, \tag{8 3}$$

where the ambiguous sign is positive for refraction and negative for gyration Then

$$\frac{1}{\omega_{\theta\phi} - \nu} \pm \frac{1}{\omega_{\theta\phi} + \nu} = P_\theta{}^j - Q_\theta{}^j\left\{\phi 0_L + \frac{\epsilon}{j}[(\phi - 0\cos Z)(j - k\cos K) - k\cos Z(1 - 0\cos K)]\right\} \tag{8 4}$$

The contribution of all the Zeeman components will be given by summing over m between $\pm j$—in the classical problem, this, of course, means an integration *

* There can be no doubt that this is the proper process, but it may be left open whether the averaging is really over the orientations of separate atoms For example, in the $1S$—$2p_1$ Hg line (though this is not a case in point here) the single atom is isotropic, whereas our model necessarily implies that a single atom should have a gyratory effect But as we are considering radiation which is coherent from the different atoms, it makes no difference whether we sum over different atoms or over the phase space of a single atom.

We thus require

$$\int_{-j}^{j} dm \Big(\mathrm{T}\frac{\partial}{\partial n}+\frac{\partial}{\partial k}+\theta\frac{\partial}{\partial j}+\phi\frac{\partial}{\partial m}\Big)\tfrac{1}{2}\mathrm{M}(1+\theta\cos\mathrm{K})^2(\phi+\theta\cos\mathrm{Z})^2$$
$$\times\Big[1+2\frac{\epsilon}{\beta}\frac{r}{j^2}\theta\Big\{\frac{\beta'}{\beta}kj(1-\theta\cos\mathrm{K})(\phi-\theta\cos\mathrm{Z})$$
$$-(\phi-\theta\cos\mathrm{Z})(j-k\cos\mathrm{K})+k\cos\mathrm{Z}(1-\theta\cos\mathrm{K})\Big\}\Big]$$
$$\times\Big[\mathrm{P}_s^{j}-\mathrm{Q}_s^{j}\Big\{\phi 0_L+\frac{\epsilon}{j}[(\phi-\theta\cos\mathrm{Z})(j-k\cos\mathrm{K})$$
$$-k\cos\mathrm{Z}(1-\theta\cos\mathrm{K})]\Big\}\Big]. \qquad (8.5)$$

The evaluation is very much simplified by the fact that

$$\int_{-j}^{j} dm\Big(\mathrm{T}\frac{\partial}{\partial n}+\frac{\partial}{\partial k}+\theta\frac{\partial}{\partial j}+\phi\frac{\partial}{\partial m}\Big)(\phi+\theta\cos\mathrm{Z})\,\mathrm{F}(n,k,j,m)$$
$$=\Big(\mathrm{T}\frac{\partial}{\partial n}+\frac{\partial}{\partial k}+\theta\frac{\partial}{\partial j}\Big)\int_{-j}^{j} dm\,(\phi+\theta\cos\mathrm{Z})\,\mathrm{F}(n,k,j,m), \qquad (8.6)$$

since the differentiation of the limits of integration by j exactly gives the term in $\phi\frac{\partial}{\partial m}$. We thus obtained as the sum

$$\Big(\mathrm{T}\frac{\partial}{\partial n}+\frac{\partial}{\partial k}+\theta\frac{\partial}{\partial j}\Big)\tfrac{1}{2}\mathrm{M}(1+\theta\cos\mathrm{K})^2\ \tfrac{1}{2}j\Big\{2(\mathrm{P}_s^{j}-\mathrm{Q}_s^{j}\phi 0_L)$$
$$+\mathrm{P}_s^{j}\phi\,2\frac{\epsilon}{\beta}\frac{r}{j^2}\theta\Big[\frac{\beta'}{\beta}kj(1-\theta\cos\mathrm{K})+k\theta-j\Big]+\mathrm{Q}_s^{j}\phi\frac{\epsilon}{j}(k\theta-j)\Big\}. \qquad (8.7)$$

In the similar calculation for $j\to j$ we use P_0^{j}, Q_0^{j} formed with

$$\omega_0^{j}=\omega+\beta'\frac{j^2-k^2-r^2}{2r}-\beta\frac{k}{r}.$$

The same simplification comes in, for on account of the factor $\sin\mathrm{Z}$ the term involving $\phi\frac{\partial}{\partial m}$ falls right out and we get

$$\Big(\mathrm{T}\frac{\partial}{\partial n}+\frac{\partial}{\partial k}\Big)\mathrm{M}\sin^2\mathrm{K}\ \tfrac{1}{2}j\Big\{(\mathrm{P}_0^{j}-\mathrm{Q}_0^{j}\phi 0_L)$$
$$+\mathrm{P}_0^{j}\phi\frac{\epsilon}{\beta}\frac{r}{j^2}\Big[-\frac{\beta'}{\beta}kj\cos\mathrm{K}-k\Big]-\mathrm{Q}_0^{j}\phi\frac{\epsilon}{j}(j-k\cos\mathrm{K})\Big\}. \qquad (8.8)$$

Since the differential operator lies in front of the whole expression, the interpretation goes exactly as in Kramers' and Heisenberg's paper. We can say that, for both $j\to j\pm 1$ and $j\to j$, there will be a P-term in the gyration, so that

it will fall off according to $\frac{2\nu}{\omega^2 - \nu^2}$, not $\frac{4\omega\nu}{(\omega^2 - \nu^2)^2}$ for frequencies far from the line

9 We next sum the effects of all the lines ν must now be right outside the multiplet We can again simplify the procedure by putting the differential operator outside For

$$\int_{|k-r|}^{k+r} dj \left(\mathrm{T} \frac{\partial}{\partial n} + \frac{\partial}{\partial k} + \theta \frac{\partial}{\partial j} \right) (1 + \theta \cos \mathrm{K})\, \mathrm{F}(n, k, j)$$

$$- \left(\mathrm{T} \frac{\partial}{\partial n} + \frac{\partial}{\partial k} \right) \int_{|k-r|}^{k+r} dj\, (1 + \theta \cos \mathrm{K})\, \mathrm{F}(n, k, j) \qquad (9\,1)$$

This result is true whether k is greater than r or less, for in either case the differentiation of the limits of integration by k exactly yields the term in $\theta \frac{\partial}{\partial j}$ Similarly

$$\int_{|k-r|}^{k+r} dj \left(\mathrm{T} \frac{\partial}{\partial n} + \frac{\partial}{\partial k} \right) \sin \mathrm{K}\, \mathrm{F}(n, k, j)$$

$$= \left(\mathrm{T} \frac{\partial}{\partial n} + \frac{\partial}{\partial k} \right) \int_{|k-r|}^{k+r} dj \sin \mathrm{K}\, \mathrm{F}(n, k, j) \qquad (9\,2)$$

So we add together the terms under the integral sign This is best done in two stages, first taking together the three terms issuing from one j We have $\mathrm{P}_0{}' = \mathrm{P}_0 - \mathrm{Q}_0 \beta \frac{\theta}{r}$ and with sufficient accuracy $\mathrm{Q}_0{}' = \mathrm{Q}_0$ Then the three lines together give

$$\frac{4}{3} j \mathrm{M} \left\{ 2 (\mathrm{P}_0 \quad \mathrm{Q}_0 \phi 0_k) - 2\mathrm{Q}_0 \beta \frac{l}{r} \cos \mathrm{K} - \mathrm{P}_0 \phi \frac{\varepsilon}{\beta} \frac{r}{j^2} 2 \cos \mathrm{K} (j - k \cos \mathrm{K}) \right.$$

$$\left. + \mathrm{Q}_0 \phi \frac{\varepsilon}{2j} \left[- 2 \frac{\beta'}{\beta} kj \sin^2 \mathrm{K} - j + 3j \cos^2 \mathrm{K} - 2k \cos^3 \mathrm{K} \right] \right\} \qquad (9\,3)$$

In setting this down it has, of course, been necessary to include terms which result from multiplying $\mathrm{Q}\beta$ by ε/β

Next we change the point of reference from $\omega_0{}'$ to ω This involves writing

$$\mathrm{P}_0{}' = \mathrm{P} - \mathrm{Q} \left[\beta' j^2 - \frac{k^2 - r^2}{2r} - \beta \frac{k}{r} \right], \quad \mathrm{Q}_0{}' = \mathrm{Q},$$

where

$$\mathrm{P} = \frac{1}{\omega - \nu} \pm \frac{1}{\omega + \nu}, \qquad \mathrm{Q} = \frac{1}{(\omega - \nu)^2} \pm \frac{1}{(\omega + \nu)^2} \qquad (9\,4)$$

The result is

$$\frac{4}{3}\jmath M\Big\{2(\mathrm{P}-\mathrm{Q}\phi 0_1)-2\mathrm{Q}\beta'\frac{\jmath^2-k^2-r^2}{2r}$$
$$-2\mathrm{Q}\beta\frac{\jmath\cos\mathrm{K}-k}{r}-\mathrm{P}\phi\,\frac{\epsilon}{\beta}\frac{r}{\jmath^2}\,2\cos\mathrm{K}\,(\jmath-k\cos\mathrm{K})$$
$$+\mathrm{Q}\phi\,\frac{\epsilon}{2\jmath}\Big[2\,\frac{\beta'}{\beta}\Big\{\frac{(\jmath^2-k^2-r^2)\cos\mathrm{K}\,(\jmath-k\cos\mathrm{K})}{\jmath}-\jmath k\sin^2\mathrm{K}\Big\}$$
$$-\frac{4k\cos\mathrm{K}\,(\jmath-k\cos\mathrm{K})}{\jmath}-\jmath+3\jmath\cos^2\mathrm{K}-2k\cos^3\mathrm{K}\Big]\Big\}. \qquad (9\,5)$$

This is to be integrated over all values of $\jmath$ from $|k-r|$ to $k+r$, and we shall show that all the terms except the first will vanish.

First

$$\int_{|k-r|}^{k+r}\jmath\,d\jmath\;(\jmath^2-k^2-r^2)=\tfrac{1}{4}(\jmath^2-k^2-r^2)^2\Big|_{|k-r|}^{k+r}=0$$

Also

$$\jmath\cos\mathrm{K}-k=(\jmath^2-k^2-r^2)/2k.$$

The vanishing of these two terms proves that we have taken the centre of gravity of the multiplet rightly. The remainder of the terms are best reduced without expressing them directly in terms of $\jmath$ by using the relation $\jmath-k\cos\mathrm{K}=\jmath k\dfrac{\partial}{\partial\jmath}\cos\mathrm{K}$. At the upper limit $\cos\mathrm{K}=1$, and also at the lower if $k>r$, but if $k<r$, $\cos\mathrm{K}=-1$ at the lower limit. In either case $\jmath\cos\mathrm{K}=k-r$ at the lower limit. We thus have

$$\int_{|k-r|}^{k+r}\jmath\,d\jmath\,\frac{2\cos\mathrm{K}}{\jmath^2}(\jmath-k\cos\mathrm{K})=k\cos^2\mathrm{K}\Big|_{|k-r|}^{k+r}=0$$

$$\int_{|k-r|}^{k+r}d\jmath\Big\{\frac{(\jmath^2-k^2-r^2)\cos\mathrm{K}\,(\jmath-k\cos\mathrm{K})}{\jmath}-\jmath k\sin^2\mathrm{K}\Big\}$$
$$=\tfrac{1}{2}k\Big[(\jmath^2-k^2-r^2)\cos^2\mathrm{K}-\jmath^2\Big]_{|k-r|}^{k+r}=0$$

$$\int_{|k-r|}^{k+r}d\jmath\,\{-\jmath+3\jmath\cos^2\mathrm{K}-2k\cos^3\mathrm{K}\}=\Big[-\tfrac{1}{2}\jmath^2+\jmath k\cos^3\mathrm{K}\Big]_{|k-r|}^{k+r}=0.$$

Thus, finally, we get as the whole refractive effect

$$\Big(\mathrm{T}\frac{\partial}{\partial n}+\frac{\partial}{\partial k}\Big)\frac{16}{3}k r\mathrm{M}\,(\mathrm{P}-\mathrm{Q}\phi 0_1), \qquad (9.6)$$

which means that

$$\sigma = \left(\mathrm{T}\frac{\partial}{\partial n} + \frac{\partial}{\partial k}\right)\frac{32}{3}krM\left[\frac{1}{\omega - \nu} + \frac{1}{\omega + \nu}\right]$$

$$\rho = 0_L\left(\mathrm{T}\frac{\partial}{\partial n} + \frac{\partial}{\partial k}\right)\frac{32}{3}krM\left[\frac{1}{(\omega - \nu)^2} - \frac{1}{(\omega + \nu)^2}\right] = 0_L\frac{\partial\sigma}{\partial\nu}$$

The magnetic anomaly and the separation of the multiplet have entirely disappeared and we are left with the exact Lorentz expression for the gyration It is evident that this can be taken over by the Correspondence Principle, so as to give the same result in the quantum theory Thus for a frequency far from the multiplet we have

$$\rho = 0_L\frac{\partial\sigma}{\partial\nu},$$

which is the chief theorem we set out to prove

10. We now work out the clasical value for the paramagnetic gyration, supposing that the temperature is so high that the whole of the "actual' term-multiplet is present This means that before summation the expression for the refractive effect is to be multiplied by

$$-\frac{1}{\kappa\mathrm{T}}\left[\beta\frac{j^2 - k^2 - r^2}{2r} + m\left(0_L + \epsilon\frac{j^2 - k^2 + r^2}{2j^2}\right)\right], \qquad (10\,1)$$

which represents the second term in $\exp\ -\frac{1}{\kappa\mathrm{T}}(\Delta\mathrm{W}_j + \Delta\mathrm{W}_m)$

As pointed out in § 4, there are two effects acting inseparably, the first corresponding to the energy of the zero position of the level, the second to the magnetic energy This second effect by itself can be calculated without knowing the second order terms in the intensities, but the first cannot, because the β will multiply terms in ϵ/β and make contributions that cannot be disregarded We thus must work out

$$-\frac{1}{\kappa\mathrm{T}}\int_{|k-r|}^{k+r} dj\int_{-j}^{j} dm\left[\beta\frac{j^2 - k^2 - r^2}{2r} + m\left(0_L + \epsilon\frac{j^2 - k^2 + r^2}{2j^2}\right)\right]$$

$$\sum_{\theta = \pm 1,\,0}\left(\mathrm{T}\frac{\partial}{\partial n} + \frac{\partial}{k} + \theta\frac{\partial}{\partial j} + \phi\frac{\partial}{\partial m}\right)\mathrm{I}_{\theta\phi}\mathrm{P} \qquad (10\,2)$$

It is easy to see that to the required order there will be no Q-term The work follows much the same course as before and the final result is (including the ordinary gyration for comparison) :

$$\left(\mathrm{T}\frac{\partial}{\partial n} + \frac{\partial}{\partial k}\right)\frac{16}{3}krM(\mathrm{P} - \mathrm{Q}\phi 0_L) - \frac{\phi 0_L}{\kappa\mathrm{T}}k^3\left(\mathrm{T}\frac{\partial}{\partial n} + \frac{\partial}{\partial k}\right)\frac{8}{3}r\mathrm{MP} \qquad (10.3)$$

We observe that the magnetic anomaly and the multiplet separation have again completely disappeared from the expression

The interpretation of this formula in the quantum theory is complicated by the presence of h^2 in front of the differential operator Since this operator is interpreted as giving rise to an expression symmetrical in the two states of the atom, it is rather natural to attribute the presence of the outside term to the asymmetry discussed in § 4 By the discussion of a few examples we shall make a conjecture as to its exact form

11 We shall now apply the results obtained to a few special cases The summation rule and our gyration rule are quite insufficient to fix the second order terms in general (the polarization rule gives no help at all), and this gives some interest to the particular cases where they do suffice In the *sp* and *ps* doublets the summation rule determines the mutual ratios of all the second order terms, but is, of course, powerless to fix their relation to the first order. The gyration rule, however, provides us with exactly the necessary extra information required

sp Doublet.—The following scheme gives the system of the lines The first column shows the two sets of values of the quantum numbers j, m, normalized as in Sommerfeld's Atombau In the second column ω is the centre of gravity of the doublet and β the separation In the third column the quantities A E are known by the summation rule and the polarization rule They are A = 3, B = 1, C = 2, D = 2, E = 1—the $\|$ components here used are half the values frequently set down

j, m $\quad$ j, m	Frequency	Intensity	Polarization
$\frac{1}{2}, \frac{1}{2} \to \frac{1}{2}, \frac{1}{2}$	$\omega + \frac{1}{4}\beta + 0_L$	A $(1 + a0_L/\beta)$	$\perp, r$
$\frac{1}{2}, \frac{1}{2} \to \frac{1}{2}, -\frac{1}{2}$	$- \frac{1}{3}0_L$	D $(1 - d0_L/\beta)$	$\|$
$\frac{1}{2}, -\frac{1}{2} \to \frac{1}{2}, \frac{1}{2}$	$- \frac{5}{9}0_L$	B $(1 - b0_L/\beta)$	$\perp, l$
$\frac{1}{2}, -\frac{1}{2} \to \frac{1}{2}, -\frac{1}{2}$	$+ \frac{5}{9}0_L$	B $(1 + b0_L/\beta)$	$\perp, r$
$\frac{1}{2}, -\frac{1}{2} \to \frac{1}{2}, \frac{1}{2}$	$+ \frac{1}{3}0_L$	D $(1 + d0_L/\beta)$	$\|$
$\frac{1}{2}, -\frac{1}{2} \to \frac{1}{2}, -\frac{1}{2}$	$- 0_L$	A $(1 - a0_L/\beta)$	$\perp, l$
$\frac{1}{2}, \frac{1}{2} \to \frac{1}{2}, \frac{1}{2}$	$\omega - \frac{3}{4}\beta - \frac{3}{9}0_L$	E $(1 - e0_L/\beta)$	$\|$
$\frac{1}{2}, \frac{1}{2} \to \frac{1}{2}, -\frac{1}{2}$	$- \frac{4}{9}0_L$	C $(1 - c0_L/\beta)$	$\perp, l$
$\frac{1}{2}, -\frac{1}{2} \to \frac{1}{2}, \frac{1}{2}$	$+ \frac{4}{9}0_L$	C $(1 + c0_L/\beta)$	$\perp, r$
$\frac{1}{2}, -\frac{1}{2} \to \frac{1}{2}, -\frac{1}{2}$	$+ \frac{3}{9}0_L$	E $(1 + e0_L/\beta)$	$\|$

The summation rule for the upper levels gives

$$A(1+a0_L/\beta) = D(1-d0_L/\beta)+B(1+b0_L/\beta) = B(1-b0_L/\beta)+D(1+d0_L/\beta)$$
$$= A(1-a0_L/\beta) = E(1-e0_L/\beta)+C(1+e0_L/\beta) = C(1-e0_L/\beta)+E(1+e0_L/\beta),$$

and for the lower levels

$$A(1+a0_L/\beta)+D(1-d0_L/\beta)+B(1-b0_L/\beta)+E(1-e0_L/\beta)+C(1-e0_L/\beta)$$
$$= B(1+b0_L/\beta)+D(1+d0_L/\beta)+A(1-a0_L/\beta)+C(1+e0_L/\beta)+E(1+e0_L)/\beta),$$

and taking account of the values of A , these give

$$a = 0, \quad b = 2d, \quad e = 2c, \quad b + 2c = 0$$

Next we set down the refractive effect This will be

$$A(1+\phi a0_L/\beta)[P - Q(\tfrac{1}{3}\beta + \phi 0_L)]$$
$$+ B(1+\phi b0_L/\beta)[P - Q(\tfrac{1}{3}\beta + \phi\tfrac{2}{3}0_L)]$$
$$+ C(1+\phi c0_L/\beta)[P - Q(-\tfrac{1}{3}\beta + \phi\tfrac{1}{3}0_L)] \qquad (11\,1)$$
$$= P[6 + (3a + b + 2c)\phi 0_L/\beta] - Q\phi 0_L[\tfrac{1}{3} + \tfrac{1}{9}(3a + b - 4c)]$$

As the gyration is to be normal this must reduce to $6[P - Q\phi 0_L]$ The summation rule makes the P-term correct For the Q-term we require that

$$3a + b - 4c = -4$$

This fixes all the coefficients and we have

$$a = 0, b = -\tfrac{1}{3}, \quad c = \tfrac{1}{6}, \quad d = -\tfrac{2}{3}, \quad e = \tfrac{1}{3}$$

We may remark that both for the $\perp$ and the $\parallel$ components these results imply a decrease in the intensities of the outermost members of the multiplet and an increase in the inner ones These changes in intensity will contribute toward the gradual establishing of the Paschen Back effect, quite apart from the modifications of wave length

The values a e can also be used to determine the gyration of a *ps* line when the actual state is, say, p_2 with p_1 absent In this case we refer P, Q to the one line at $\omega + \frac{1}{3}\beta$ Then the refractive effect is

$$A(1+\phi a0_L/\beta)[P - Q\phi 0_L] + B(1+\phi b0_L/\beta)[P - Q\phi\tfrac{1}{3}0_L]$$
$$= 4P(1 - \phi\tfrac{1}{3}0_L/\beta) - Q\phi\tfrac{1}{3}0_L,$$

so that the refraction being $\frac{2\omega}{\omega^2 - \nu^2}$ the gyration is

$$\tfrac{1}{3}\frac{0_L}{\beta}\frac{2\nu}{\omega^2 - \nu^2} + \tfrac{8}{9}0_L\frac{4\nu\omega}{(\omega^2 - \nu^2)^2} \qquad (11\,2)$$

Evidently at frequencies for which $|\omega - \nu| > \beta$ the first term will be the

important one We shall see, however, that if the temperature is low enough to suppress p_1, there will be present a paramagnetic P term which far outweighs it

Next we examine the paramagnetic gyration, when the " actual " state is s This requires that the three terms in (11.1) shall be multiplied by the respective factors (depending on the m of the actual states)

$$1 - \phi\frac{0_L h}{2\pi\kappa T}, \quad 1 + \phi\frac{0_L h}{2\pi\kappa T}, \quad 1 + \phi\frac{0_L h}{2\pi\kappa T}.$$

It is evident that there is no paramagnetic effect at all

Now take a ps line at such a high temperature that both p_1 and p_2 are present. The energies are composed of two parts, one for the multiplet difference, the other for the Zeeman effect In the latter we must multiply the m of each p level by the appropriate " g-factor," $\frac{4}{3}$ for p_2 and $\frac{2}{3}$ for p_1. Thus the terms of (11.1) are to be multiplied respectively by

$$1 - (\tfrac{4}{3}\beta + \phi 20_L)\frac{h}{2\pi\kappa T}, \quad 1 - (\tfrac{1}{3}\beta + \phi\tfrac{1}{3}0_L)\frac{h}{2\pi\kappa T}, \quad 1 - (-\tfrac{2}{3}\beta + \phi\tfrac{1}{3}0_L)\frac{h}{2\pi\kappa T}.$$

Multiplying out we find that the whole result is

$$6\left[\mathrm{P} - \mathrm{Q}\phi 0_L - \mathrm{P}\phi\frac{0_L h}{2\pi\kappa T}\right],$$

so that compared to a refraction $\frac{2\omega}{\omega^2 - \nu^2}$ we get a gyration

$$0_L\left[\frac{4\omega\nu}{\omega^2 - \nu^2} + \frac{2\nu}{\omega^2 - \nu^2}\frac{h}{2\pi\kappa T}\right]. \qquad (11\,3)$$

In addition to the above case I have examined the sp and ps lines in the triplet and quartet systems, and the pd and dp lines in the doublet system. In all these cases the summation rules give the $\parallel$ components in terms of the $\perp$, and also certain relations between the $\perp$ components These relations make the P-term in the gyration vanish ; it should not be hard to prove this generally The gyration rule fixes partially the absolute values of the second order terms, but is quite insufficient to determine them completely. The paramagnetic gyration (at high temperatures for the sp triplet vanishes like the doublet and for the ps lines bears to the ordinary gyration exactly the relation given by (11 3) This result is also evidently general for ps lines

The case of a pd or dp doublet merits fuller discussion, because a not very rash conjecture enables us to discover the gyration of each of its three lines, and the result could be tested experimentally. The following scheme gives

the frequencies and intensities of the $\perp$, r components β is the separation of the p-terms, γ of the d-terms, ω is the frequency of the centre of gravity

p_2d_3	p_1d_2	p_1d_1
$\omega+\frac{3}{4}\gamma-\frac{1}{4}\beta+0_\perp$ 90 $(1+a)$	$\omega-\frac{3}{4}\gamma-\frac{1}{4}\beta+\frac{1}{5}0_\perp$ 6 $(1+e)$	$\omega-\frac{3}{4}\gamma+\frac{3}{4}\beta+\frac{1}{4}0_\perp$ 75 $(1+h)$
$+\frac{1}{3}0_\perp$ 54 $(1+b)$	$+\frac{1}{4}0_\perp$ 8 $(1+f)$	$+\frac{1}{4}0_\perp$ 25 $(1+j)$
$+\frac{1}{5}0_\perp$ 27 $(1+c)$	$+\frac{1}{5}0_\perp$ 6 $(1+g)$	
$+\frac{1}{4}0_\perp$ 9 $(1+d)$		

The unknowns a, b . . will be of the form $a=\left(\frac{a'}{\beta}+\frac{a''}{\gamma}\right)0_\perp$, etc., as is indicated by the requirement of symmetry and the presence of $d\beta/dk$ in (7 1) Applying the summation rule we find

$$a=0$$

$$54b+9d+6e+6g+75h=0$$

$$27c+8f+25j=0$$

and the gyration rule gives

$$\gamma\,(54b+27c+9d)+\beta\,(75h+25j)=-\tfrac{3}{5}0_\perp.$$

Since β and γ need not be commensurable this gives

$$54b'+27c'+9d'=0,\quad 75h''+25j''=0,$$

$$54b''+27c''+9d''+75h'+25j'=-\tfrac{3}{5}, \qquad (11\,4)$$

and all the necessary conditions are now fulfilled

We next evaluate the paramagnetic gyration at high temperature For pd (p the " actual " state) we find for the total refractive effect

$$300\,(\mathrm{P}-\mathrm{Q}\phi 0_\perp)-\frac{h}{2\pi\kappa\mathrm{T}}\,\mathrm{P}\phi 0_\perp\left\{\tfrac{550}{5}-(75h'+25j')\right\} \qquad (11.5)$$

and for dp

$$300\,(\mathrm{P}-\mathrm{Q}\phi 0_\perp)-\frac{h}{2\pi\kappa\mathrm{T}}\,\mathrm{P}\phi 0_\perp\,(486+(54b''+27c'+9d'')) \qquad (11\,6)$$

The paramagnetic terms cannot be evaluated, but their difference can, and gives

$$300\,\frac{h}{2\pi\kappa\mathrm{T}}\,\mathrm{P}\phi 0_\perp.$$

Now our treatment of the classical problem indicated that associated with

$$\left(\mathrm{T}\frac{\partial}{\partial n}+\frac{\partial}{\partial k}\right)\frac{16}{3}kr\,\mathrm{M}\,(\mathrm{P}-\mathrm{Q}\phi 0_k),$$

we should have

$$-\frac{k^2}{\kappa\mathrm{T}}\left(\mathrm{T}\frac{\partial}{\partial n}+\frac{\partial}{\partial k}\right)\frac{8}{3}r\mathrm{MP}\phi 0_k,$$

k, etc., here are dynamical and require multiplication by $h/2\pi$ to reduce them to numbers. The expression under the differential operator is to be symmetrical in the two terms of the multiplet, but the k^2 in front presumably represents the asymmetry attached to the "actual" state. Thus we say that to an ordinary effect A $(\mathrm{P}-\mathrm{Q}\phi 0_k)$ will correspond a paramagnetic effect

$$-\frac{h}{2\pi\kappa\mathrm{T}}\,\mathrm{F}(k)\,\frac{\mathrm{AP}\phi 0_k}{f(k,k')},$$

where k and k' refer to the actual and potential states, and $\mathrm{F}(k)\sim k^2$ as $k\to\infty$, while f is symmetrical in k, k' and $\sim 2k$. We know the exact values for sp, ps and the difference for pd and dp, and these suffice to determine the forms of F and f—at least assuming them to be simple. They take their simplest form with the normalisation in which $k=0,\ 1,\ 2\ldots$ for $s,\ p,\ d\ldots$ and we get as the whole refractive effect

$$\mathrm{A}\left[\mathrm{P}-\mathrm{Q}\phi 0_k-\frac{h}{2\pi\kappa\mathrm{T}}\,\frac{k^2}{k+k'}\,\mathrm{P}\phi 0_k\right]$$

If this assumption is correct we have

$$75h+25j=\frac{250}{3}\,\frac{0_k}{\beta}$$

$$54b+27c+9d=-86\,\frac{0_k}{\gamma},$$

and therefore

$$6e+8f+6g=86\,\frac{0_k}{\gamma}-\frac{250}{3}\,\frac{0}{\beta}\,.$$

These results suffice to determine the gyration of the multiplet at low temperatures, and we shall conclude by giving the gyrations at low temperatures for all doublet systems issuing from any p-level. They are compared to refraction $2\omega/(\omega^2-\nu^2)$ where ω is the frequency of the centre of gravity of the *active* lines. As usual

$$\mathrm{P}=\frac{2\nu}{\nu^2-\omega^2},\quad \mathrm{Q}=\frac{4\nu\omega}{(\nu^2-\omega^2)^2}$$

$$p_1{}^3 \qquad 0_L\left[\frac{4}{3}Q - P\left(\frac{2}{3}\frac{1}{\beta} + \frac{1}{3}\frac{h}{2\pi\kappa T}\right)\right],$$

$$p_2{}^3 \qquad 0_L\left[\frac{7}{6}Q + P\left(\frac{1}{3}\frac{1}{\beta} - \frac{5}{3}\frac{h}{2\pi\kappa T}\right)\right],$$

$$p_1{}^1 \qquad 0_L\left[\frac{5}{6}Q + P\left(-\frac{5}{6}\frac{1}{\beta} + \frac{1}{6}\frac{h}{2\pi\kappa T}\right)\right],$$

$$p_2{}^1 \qquad 0_L\left[\left(\frac{2}{3} + \frac{3}{8}\frac{\gamma}{\beta}\right)Q + P\left(\frac{5}{12}\frac{1}{\beta} + \frac{5}{6}\frac{h}{2\pi\kappa T}\right)\right].$$

The first term in P has been set down for the sake of completeness, but if it is not negligible the assumption that there is only one actual level present will be violated. A rough calculation shows that at 500° abs. for a multiplet in the visible spectrum the P-term will exceed the Q at distances greater than 100 A.U. from the lines. It would be very hard to observe the gyration of a metallic vapour at all at such distances, so that we conclude that experiment must be mainly occupied with an investigation of the Q-terms.

Here we shall leave the matter, though it would seem probable that a more "refined" application of the Correspondence Principle might determine the second order terms precisely. In view of the expectations based on the New Mechanics it seems unnecessary to enter on this rather laborious process.* What we have already obtained should suffice to show the general features to be anticipated in any experimental attack on the subject.

Summary

A general discussion shows that when light passes through the vapour of a substance possessing a multiplet spectrum, its gyration cannot be predicted without a knowledge of the second approximations in the intensities of the lines that the substance would emit.

The "electron and core" model is applied so as to find these approximations. They are shown to bear ratios of the order $0_L/\beta$ to the first order terms (0_L Larmor rotation, β multiplet separation). Of a pair symmetrically placed about the zero position of a line, one is increased and the other diminished to an equal extent, so that the whole line is unpolarized to the second order. It is verified that the sum of all the intensities issuing from given j and m is independent of j and m.

* Just as this paper was completed there has appeared a work by Heisenberg and Jordan ('Z. f. Ph.,' vol. 37, p. 263) which fulfils this expectation. They have obtained the complete formula for the doublet system at all strengths of field, and their result confirms those here set down.

Using the methods of Kramers and Heisenberg, a classical calculation is made of the gyration due to the whole multiplet, when the incident light *has frequency not very close* to it. It is shown that there is an effect rather like that of Paschen-Back, in that the gyration corresponds to a normal and not an anomalous Zeeman effect, this result is true, however weak the magnetic field

A similar calculation is carried out allowing for the effect of temperature. Taking the temperature as so high that a first approximation will suffice, it is shown that the gyration is again independent of the magnetic anomaly and the multiplet separation, but that it now contains a "paramagnetic" term inversely proportional to the temperature

These rules can be interpreted in the quantum theory, and a few cases can be solved by their means For lines issuing from an s-level, there is no paramagnetic effect, and the gyration of light far from the multiplet will be exactly that given by a simple Lorentz di-pole. Formulæ are given for the gyration corresponding to any of the lines issuing from either p-level in the doublet system These would be applicable to a substance where the doublet separation is so large that at practicable temperatures the substance is all at one level. The gyration is composed of two terms, one "paramagnetic" proportional to $\frac{0_1}{T}\frac{2\nu}{\omega^2-\nu^2}$, the other "diamagnetic" proportional to $0_1\frac{4\omega\nu}{(\omega^2-\nu^2)^2}$ (ν frequency of incident light, ω mean frequency of multiplet).

The Distortion of Iron Crystals.

By G. I Taylor, F R S , and C. F Elam, D Sc

(Received July 28, 1926)

(Plates 10–12)

Experimental Methods

In recent years several attempts have been made to determine what happens to iron crystals when they are strained and various conflicting statements have been made as to the connection between the crystal axes and the nature of the strain No reliable results have been obtained, however, partly because the largest crystals available were too small for accurate experiment, partly because workers have assumed that planes of slip coincide with crystal planes—an assumption which the experiments to be described prove to be erroneous—but chiefly because the analysis of strain has not been carried out in a systematic manner so as to obtain all information possible from external measurement of strained crystals

The work of Prof Edwards and Mr. Pfeil has now enabled us to obtain crystals sufficiently large for the purpose, and, in fact, all the material used in the experiments now to be described was cut from specimens very kindly supplied by them

Two different methods were used for producing distortion In the first the material was cut in the form of a uniform bar of rectangular cross section, usually about 2 mm. square The length was about 10 cm , of which some 4 cm. in the middle was occupied by a single crystal Specimens of this type were marked with fine scratches and pulled in a tensile testing machine. The distortion was measured in the manner described in our Bakerian Lecture.*

In the second method circular discs about 6 mm diameter × 1 4 mm thick were cut from a crystal and compressed between polished steel plates. The distortion was measured by methods previously described †

Though the methods used were identical with those developed for dealing with aluminium crystals, the difference in the material necessitated small changes

* 'Roy Soc Proc.' A, vol 102, p 643 (1923)

† Taylor and Farren, "Distortion of Crystals of Aluminium under Compression," 'Roy. Soc. Proc ,' A, vol. 111, p. 529 (1926).

in the procedure In the first place great care had to be taken to ensure that the depth of the surface layer to which the crystal lattice is distorted by grinding and polishing was as small as possible The specimens were sawn with a fine saw or milled with a fine cutter They were then ground down on emery paper of successive degrees of fineness till at least 0 2 mm had been removed from each cut surface Finally all flat faces were polished till a mirror surface was obtained The holder used for grinding and polishing the tension specimens was made, at the suggestion of Mr A Woodward, from stainless steel kindly supplied to us by Dr W H Hatfield

Owing to the small size of the specimens it was necessary to use special methods for marking them The tension specimens were mounted on an adjustable table which could slide on a bed similar to a lathe bed A cutter consisting of a safety razor blade broken across the middle was mounted so that it pressed, with a weight of 10 grammes, on the specimen as it passed under it. In this way a fine mark of very uniform width could be made The specimens were marked with a longitudinal scratch down the middle of each face and cross scratches on all four faces spaced at intervals of 5 mm

The marks on the compression discs had to be slightly deeper and a weight of 50 grammes on a sharpened gramophone needle was employed, the specimen being mounted on the traversing cone of our measuring microscope

Measurements —The most difficult measurement to make with the necessary accuracy was the angle between the faces of the tension specimens For this purpose the lines down the middle of each face were used The angle between the planes passing through pairs of marks on opposite faces was measured by a method previously described * But the smallness of the specimen necessitated the use of a very good goniometer, which was kindly lent to us by Dr A. Hutchinson, F R S With this instrument measurements of the angle between pairs of opposite faces could be relied on to 20 minutes of arc

Methods of Calculation —The method adopted for representing the distortion was the same in the tension and the compression specimens. The cone containing all lines of particles which remained unstretched after the crystal had been distorted was determined. The difference in shape between the two types of specimen, however, necessitated some difference in the formulæ used for deducing the equation of the unstretched cone from the external measurement

* Taylor and Elam, "The Plastic Extension and Fracture of Aluminium Crystals," 'Roy Soc Proc ,' A, vol 108, p 33 (1925)

Equation to Unstretched Cone for Tension Specimens

In the case of tension specimens rectangular co-ordinates were chosen so that one edge was the axis OZ and one face (called face 1) was the plane $y = 0$. The scheme is shown in fig 1

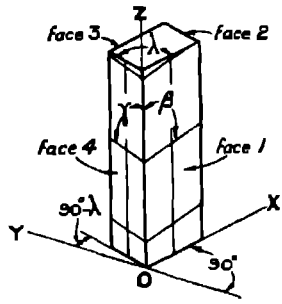

Fig 1

The measured quantities were

λ the angle between the faces 1 and 4

b the width of faces 1 and 3

c the width of faces 2 and 4

β the angle between ruled scratches across face 1 and the axis OZ

γ the angle between ruled scratches across face 4 and axis OZ

d the distance between successive marks parallel to the axis of the specimen.

Using suffixes 0 and 1 to denote the conditions before and after stretching, the ratio of the final to the initial length is $\frac{d_1}{d_0} = \varepsilon$, and let $f = \frac{b_1}{b_0}$ and $g = \frac{c_1}{c_0}$ If (x_1, y_1, z_1) are the co-ordinates in the strained material of a particle whose co-ordinates in the unstrained material were (x_0, y_0, z_0), the formulæ of transformation are

$$\left.\begin{aligned} x_1 &= fx_0 + ly_0 \\ y_1 &= my_0 \\ z_1 &= px_0 + qy_0 + \varepsilon z_0 \end{aligned}\right\}, \tag{1}$$

where

$$\left.\begin{aligned} l &= g\frac{\cos\lambda_1}{\sin\lambda_0} - f\cot\lambda_0 \\ m &= g\frac{\sin\lambda_1}{\sin\lambda_0} \\ p &= -\varepsilon\cot\beta_0 + f\cot\beta_1 \\ q &= \varepsilon\cot\beta_0\cot\lambda_0 - f\cot\beta_1\cot\lambda_0 + g\frac{\cot\gamma_1}{\sin\lambda_0} - \varepsilon\frac{\cot\gamma_0}{\sin\lambda_0} \end{aligned}\right\}. \tag{2}$$

The unstretched cone is given by

$$x_0^2 + y_0^2 + z_0^2 = x_1^2 + y_1^2 + z_1^2, \tag{3}$$

and eliminating x_1, y_1, z_1 from 1 and 3 the equation of the unstretched cone becomes

$$x^2(f^2 + p^2 - 1) + y^2(l^2 + m^2 + q^2 - 1) + z^2(\varepsilon^2 - 1) + 2xy(fl + pq) + 2zx(\varepsilon p) + 2yz(\varepsilon q) = 0. \tag{4}$$

If spherical polar co-ordinates are used, θ being the angle which the direction concerned makes with the axis of z and ϕ the angle which its projection on the plane $z = 0$ makes with the axis of x, then

$$\left.\begin{aligned} x/z &= \tan\theta\cos\phi \\ y/z &= \tan\theta\sin\phi \end{aligned}\right\}, \tag{5}$$

so that the equation of the unstretched cone in its first position before stretching the material is

$$\begin{aligned}&\{(f^2+p^2-1)\cos^2\phi + 2(fl+pq)\cos\phi\sin\phi \\ &\quad + (l^2+m^2+q^2-1)\sin^2\phi\}\tan^2\theta \\ &\quad + \{2\varepsilon p\cos\phi + 2\varepsilon q\sin\phi\}\tan\theta + \varepsilon^2 - 1 = 0 \end{aligned} \tag{6}$$

To find the unstretched cone in its second position, in the stretched material, the simplest method is to reverse all the formulæ, replacing measurements made before extension by corresponding ones in the stretched material and *vice versa*.

The formulæ of tranformation are then :—

$$\left.\begin{aligned} x_0 &= f_1 x_1 + l_1 y_1 \\ y_0 &= m_1 y_1 \\ z_0 &= p_1 x_1 + q_1 y_1 + \varepsilon_1 z_1 \end{aligned}\right\}, \tag{7}$$

where $l_1 = -\dfrac{1}{g}\dfrac{\cos\lambda_0}{\sin\lambda_1} - \dfrac{1}{f}\cot\lambda_1$, etc.,

and the equation to the unstretched cone in its second position is identical with (6) except that each of the symbols inside the brackets has a suffix 1.

Equation of Unstretched Cone for Compression Specimens

The scheme of marking specimens and the methods of measurement are described in a previous paper by one of the authors * A photograph of one of

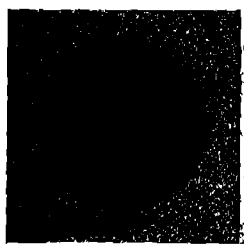

Fig 2

Fig. 3

Fig 4

Fig. 2.—Iron crystal Fe 8c before compression. Fig 3.—Fe 7c after compression to $\varepsilon = 0{\cdot}397$. Fig 4.—Fe 3c after compression to $\varepsilon = 0\ 840$.

* Taylor and Farren, *loc. cit*

the specimens before compression is shown in fig. 2. Figs 3 and 4 are photographs taken after compression of specimens which were marked originally with six scratches in the square pattern shown in fig 2 A rectangular system of co-ordinates was chosen so that the origin was at the central point o of the nine points where the scratches intersect The axis OZ was vertical and perpendicular to the face of the specimen OX was along one of the central scratches and OY was perpendicular to it The directions of the axes are shown in fig 5

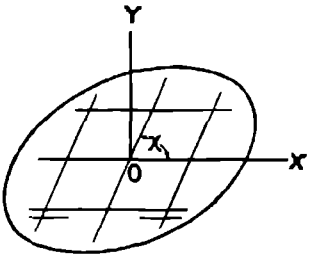

Fig 5

Measurements were made of the amount the material had stretched in the directions of the two sets of scratches. The ratios of the final to the initial length in these two directions are called α and β* respectively If the final and initial thickness of the specimen between its plane faces are t_1 and t_0, the compression is measured by $\gamma = t_1/t_0$. The angle between the two sets of scratches is χ_0 before, and χ_1 after, compression The co-ordinates of the central mark on the under-side of the specimen are $(X_0, Y_0, -t_0)$ before and $(X_1, Y_1, -t_1)$ after compression The formulæ of transformation are

$$\left.\begin{aligned} x_1 &= \alpha x_0 + l y_0 + \mu z_0 \\ y_1 &= m y_0 + \nu z_0 \\ z_1 &= \gamma z_0 \end{aligned}\right\}, \tag{8}$$

where

$$\left.\begin{aligned} l &= \beta \frac{\cos \chi_1}{\sin \chi_0} - d \cot \chi_0 \\ m &= \beta \frac{\sin \chi_1}{\sin \chi_0} \\ \mu &= \frac{X_1 - \alpha X_0 - l Y_0}{-t_0} \\ \nu &= \frac{Y_1 - m Y_0}{-t_0} \end{aligned}\right\}. \tag{9}$$

* This notation is the same as that adopted in the previous work on compression tests. It uses some symbols which have already been used in other senses in this paper in connection with tensile specimens, but no confusion need arise.

The equation of the unextended cone in its first, or unstrained, position is

$$\{(\alpha^2 - 1)\cos^2\phi + (m^2 + l^2 - 1)\sin^2\phi + 2\alpha l \cos\phi \sin\phi\}\tan^2\theta + \{2\alpha\mu\cos\phi + 2(l\mu + m\nu)\sin\phi\}\tan\theta + \gamma^2 + \mu^2 + \nu^2 - 1 = 0, \quad (10)$$

where θ and ϕ are spherical polar co-ordinates which bear the same relation to the rectangular co-ordinates x, y, z as they did in the case of the tension specimens (see equations 5)

The most convenient method for finding the equation to the unextended cone in its second position in the compressed material is to replace in formulæ 8, 9 and 10 measurements made before compression by those made after and *vice versa* As in the case of tension specimens, suffixes are added to the coefficients in the transformation formulæ These then become —

$$\left.\begin{aligned} x_0 &= d_1x_1 + l_1y_1 + \mu_1z_1 \\ y_0 &= m_1y_1 + \nu_1z_1 \\ z_0 &= \gamma_1z_1 \end{aligned}\right\} \quad (11)$$

In Table 1 is given a list of the data used in calculating the unextended cones for three extension and four compression specimens In the case of Fe 1, the first of our tension specimens, the methods of calculation described in our Bakerian Lecture were used In the case of all the other specimens we used the methods described in the present paper

Representation of Unstretched Cones

The unstretched cones are represented by means of a stereographic diagram of which the centre is the axis of Z ($\theta = 0$). The axis of x ($\theta = 90$ degrees, $\phi = 0$) is represented by a radius marked in each of figs. 6 to 15

The symbols common to all diagrams are explained in fig 1. Points on the cone are found by taking values 0, $\pm$ 30 degrees, $\pm$ 60 degrees and 90 degrees for ϕ and calculating the two corresponding values of θ from the equation to the cone

Measurement of Orientation of Crystal Axes.

The orientation of the crystal axes was determined by the methods used previously in the case of aluminium crystals.*

The α radiations from an iron anticathode were reflected from dodecahedral {110} planes in the crystal, the angle of reflection being 28·9 degrees. In the

* See Müller, 'Roy. Soc Proc.,' A, vol. 105, p. 500 (1924), and Taylor and Farren, "Distortion of Crystals of Aluminium under Compression," 'Roy. Soc Proc.,' A, vol. 111, p 529 (1925)

case of aluminium, where reflections were obtained from {111} and {100} planes, two were sufficient to determine the orientation of all the axes, but in the case of iron two planes are not sufficient to determine the rest completely unless they are at right angles to one another When two {110} planes making an angle of 60 degrees have been found, they determine a {111} plane, but there are two alternative positions for the crystal lattice, and in this case it is necessary to find another {110} plane, not in the same {111} plane as the first two In the case of the tension specimens it was not always possible to get reflections from three crystal planes owing to the limitations of the apparatus, but the ambiguity was resolved by cutting the specimen and polishing a plane perpendicular to the axis, after the test was finished It was always possible to get a reflection from this new face and so to remove the ambiguities in the case of the distorted material Since the motion of the {110} planes relative to the surface of the specimen during the distortion was not large and was moreover, related to the distortion no difficulty was encountered in identifying planes in the distorted specimen with those measured in the specimen before distortion In this way the ambiguity was resolved in every case

Results of Extension Tests

Three specimens were stretched, Fe 1 was extended 15 per cent, Fe 3 and Fe 4 each about 9 per cent It was found that they do not stretch very uniformly, a variation of 1 per cent or even 2 per cent in a total of 9 per cent being found between the extension in successive 5 mm lengths of the specimen In order to make the best use of the measurements two or three sections 5 mm long were taken in the part of the specimen where the stretching appeared to be most uniform The measurements in these sections were averaged and used in the calculations The figures given in Table 1 are derived from these averages In each case the unstretched cone was calculated for both positions, *i e*, before and after stretching. The orientations of the crystal axes were likewise determined before and after stretching

In figs 6 to 11 the unstretched cones are represented on stereographic diagrams, each of the calculated points being shown by a round dot. On examining these diagrams it was found that the unstretched cones in every case coincided almost exactly with two planes In each of the diagrams the pair of planes which passes most nearly through the calculated points is shown by means of two great circles

This type of distortion was already familiar to us. It can be caused by uniform shearing or slipping parallel to either of the two unstretched planes

in a direction at right angles to their line of intersection * Accordingly the point on each of the planes which corresponds with a possible direction of slip was marked on the diagram with a cross and the pole of each possible plane of slip was marked also

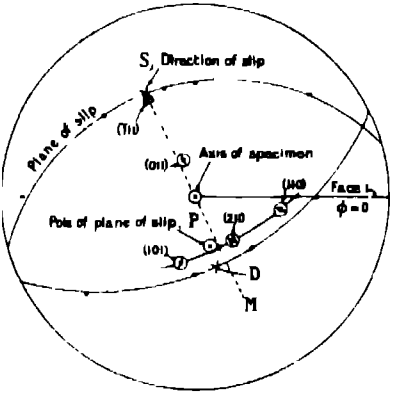

Fig 6 —Fe 1 $\epsilon = 1\ 0$

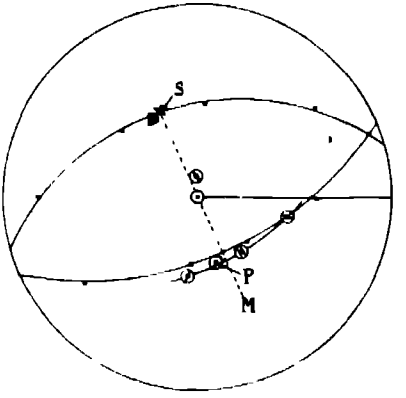

Fig. 7 —Fe 1 $\epsilon = 1\ 150$

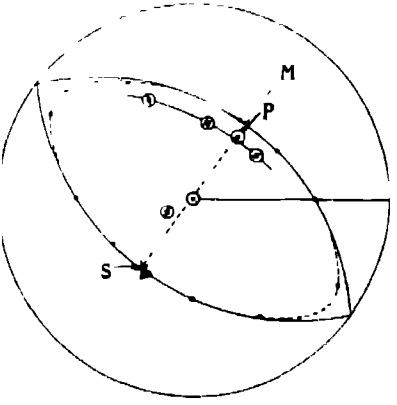

Fig. 8 —Fe 3 $\epsilon = 1\ 0$

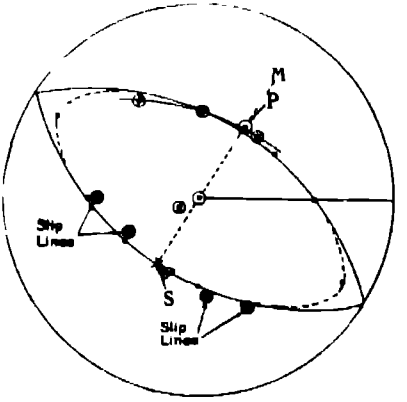

Fig 9 —Fe 3 $\epsilon = 1\ 0915$.

The positions of the crystal axes were next determined from the X-ray measurements and marked on the stereographic diagrams From inspection of six diagrams similar to those shown in figs 6 to 11 the following deductions were drawn :—

* Bakerian Lecture, *loc. cit.*, p. 657

(*a*) In each case one of the two alternative possible directions of slip was close to the pole of a {111} plane The spherical polar co-ordinates of the pole

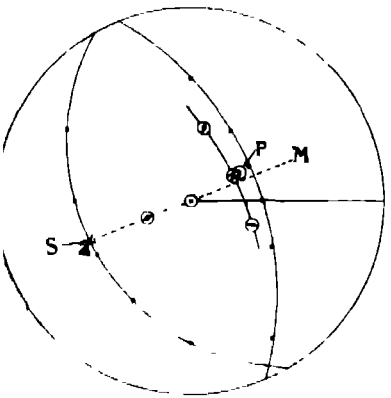

Fig. 10.—Fe 4 $\epsilon = 1\ 0$

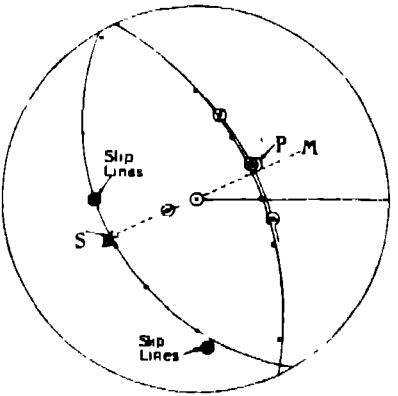

Fig. 11.—Fe 4 $\epsilon = 1\ 0879$

of the {111} plane and the corresponding possible direction of slip are given in Table II, and are marked in each figure by means of the symbol ▲* and the direction of slip is represented by a cross X

The second possible direction of slip that marked at D in fig. 6, but not marked in the rest of the diagrams—seemed to bear no relation to the crystal axes.

(*b*) The crystal axes move during the distortion so that they are nearly fixed relative to that one of the pair of unstretched planes which contains the pole of the {111} plane mentioned in (*a*) They move in the opposite direction to the other unstretched plane

The material behaves therefore both in regard to the motion of the crystal axes and in regard to the total distortion as though this distortion were due to slipping on a crystal plane and in a direction parallel with the perpendicular of a {111} plane It remains to discover how the plane of slip is related to the crystal axes In an attempt to solve this question the pole of the plane determined by distortion measurements was marked on each diagram These are shown at P in figs 6 to 11 and an arc representing a portion of the $(\bar{1}11)$ plane, which is nearly perpendicular to the direction of slip determined by distortion measurements, is also drawn The plane contains the poles of three {110} planes and three {112} planes In each diagram the poles of two {110} planes,

* In fig. 6 the particular octahedral plane referred to is given the symbol $(\bar{1}11)$ in order to conform to the conventions of crystallography

(101) and (110) in fig. 6, one either side of P, are represented by the symbol ⓓ and the pole of the intermediate {112} plane, (211) in fig. 6, is represented by the symbol Ⓗ. It will be seen that in the case of Fe 4 the pole of the plane of slip coincides almost exactly with the (211) plane so that the plane of slip coincides with this plane. On the other hand, in the case of Fe 1, the pole of the plane of slip is 14 degrees away from the pole of the (211) plane, i.e., almost exactly half-way between the poles of the (101) and (211) planes. In the case of Fe 3, P is nearer to the pole of the (101) plane than to the pole of the (211) plane.

It appears therefore that the distortion is such as can be produced by slipping parallel to a plane of particles in the material and that the direction of slip has a definite relation to the crystal axes, but that the plane of slip is not a definite crystal plane at all. On the other hand, the plane of slip does appear to be related to the distribution of stress. The pole of the slip plane lies close to the plane which contains the axis of the specimen and the direction of slip. In each of the diagrams figs. 6 to 15 the straight line which represents this plane is shown as SM. If it were accurately true that P in every case lies, as it does in fig. 8, on SM, then it would mean that of all possible planes through the given direction of slip, slipping occurs on the one for which the direction of slip lies along the line of greatest slope in the slip plane, the axis of the specimen being supposed vertical.

Metallurgists are familiar with the conception of a plastic material which yields by slipping or shearing on a plane parallel to the plane of maximum shearing stress, and they have recently become familiar with the conception of a plastic crystal which yields by slipping on a crystal plane and in the direction of a crystal axis, the choice among crystallographically similar types of slipping being determined by the stress distribution. The conception now put forward is quite different from either of these. The direction of slipping is a crystal axis and the plane of slipping is determined chiefly by the stress distribution.

Compression Experiments.

Before going on to consider how this kind of plastic yielding could arise we shall describe further experiments in which the question is examined by means of a method which permits of much greater accuracy than was possible in the experiment we have so far described. The chief sources of error in the extension experiments were attributable (*a*) to the fact that the stretching of the specimens was not uniform, and (*b*) to the difficulty of determining the position of the specimen relative to the X-ray spectrometer in which it was fixed when measuring the orientation of its crystal axes. In regard to (*b*) the accuracy

of the X-ray determinations relative to the spectrometer can be judged by the fact that the angle between two crystal axes never differed by more than 2 degrees and seldom by more than 1 degree from the angle required by the cubic symmetry of the crystal The accuracy of the distortion measurements can be gauged from the accuracy with which the points of the unstretched cone line on two planes and from a comparison of the volume of the specimen before and after stretching It is improbable that the calculated direction of slip is in error by more than 3 degrees On the other hand, there seems to be a possibility that an error of 5 or 6 degrees may occur in determining the position of a tension specimen in our X-ray spectrometer This position is determined either by rotating the specimen till the line of sight lies along one face when looking through the holes which confine the beam of X-rays or else by adjusting the X-ray spectrometer till the axis of rotation of the table is in the plane passing through the vertical scratches on opposite faces The accuracy of both these methods depends on the smallest dimension of the cross section of the specimen, which, for various reasons could not be greater than about 1 5 mm The first method is also liable to inaccuracy owing to the rounding of the faces due to polishing and to the unevenness of the surface when the material has been stretched The second method depends on a high degree of accuracy in the axis of the turn-table of the spectrometer With our X-ray spectrometer this source of error was appreciable, but the measurements of λ used in our distortion calculations were made with a first-class goniometer the axis of which was quite good enough for our purpose

The use of compression specimens reduces these sources of error till they are less than the other errors to which both types of specimen are liable. In the first place, the diameter of the flat faces on which the measurements are made are three times as great as the thickness of the largest tension specimen we are able to use In the second place, the conditions of the experiment kept the faces flat and parallel during compression This last point is important because it was sometimes found possible to obtain extraordinary uniformity of distortion through the whole volume of a compression specimen The photographs shown in figs, 2, 3 and 4 illustrate this Fig 2 shows a specimen before distortion marked in squares Fig 3 shows Fe 7c after compression till its thickness was $^*\epsilon = 0\ 897$ of its initial thickness, ϵe, a compression of about 10 per cent

* The symbol ϵ is here used to denote a state of the material, ϵe, the total amount of compression the crystal has undergone since it was formed The symbol γ is used to denote the ratio of the thickness at the end of any experiment to that at the beginning, so that if t_0 is the unstrained thickness, t_1 that after one compression and t_2 that after a second compression, t_2 is the value of γ used in calculating the unstretched cone for t_1 the second compression After the first compression $\epsilon = t_1/t_0$ and after second compression $\epsilon = t_2/t_0$

It will be seen that after compression the ruled lines remained straight. Fig. 4 shows a specimen Fe 3c in which the ruled scratches were so straight and so nearly parallel after compression to 84 per cent. of its initial thickness that we were unable to detect any want of uniformity.*

In some of the compression specimens the distortion was not quite uniform, the ruled scratches becoming slightly bent or curved. In some of these cases it was possible to say that the want of uniformity arose from imperfections in the crystal which only came to light when the specimen was compressed. In all cases where there was an obvious lack of uniformity in distortion (three out of the nine specimens tried) the specimen was rejected after compression. In order to save the great waste of time which the determination of the crystal axes of the rejected specimens would have entailed, the orientation of the crystal axes was not measured before compression. The crystal axes of the four specimens Fe 3c, Fe 5c, Fe 6c and Fe 7c were determined after compression and the second (distorted) position of the unextended cone was calculated in each case. The equations to the cones and also the data used in calculating them are given in Table I.

Table I.—Measurements and data from which unstretched cones were calculated

Extension Tests

$\varepsilon, f, g, l, m, p, q$ are non dimensional. $\beta_0, \beta_1, \gamma_0, \gamma_1, \lambda_0, \lambda_1$ are angles, and are expressed in degrees.

Fe 1.—$\varepsilon = 1{\cdot}150, f = 0{\cdot}9894, g = 0{\cdot}9000$. $\beta_0 = 90{\cdot}0$ degrees, $\beta_1 = 92{\cdot}9$ degrees, $\gamma_0 = 89{\cdot}9$ degrees, $\gamma_1 = 85{\cdot}5$ degrees, $\lambda_0 = 90{\cdot}0$ degrees, $\lambda_1 = 84{\cdot}3$ degrees.

Fe 3.—$\varepsilon = 1{\cdot}0915$, $f = 0{\cdot}9748$, $g = 0{\cdot}9481$, $\beta_0 = 90{\cdot}0$ degrees, $\beta_1 = 89{\cdot}8$ degrees, $\gamma_0 = 90{\cdot}0$ degrees, $\gamma_1 = 89{\cdot}8$ degrees, $\lambda_0 = 89{\cdot}9$ degrees, $\lambda_1 = 94{\cdot}0$ degrees.

$l = -0{\cdot}0679$, $m = 0{\cdot}9460$, $p = 0{\cdot}0034$, $q = 0{\cdot}0033$.

Unstretched cone in first position is—

$$(0{\cdot}0498\cos^2\phi + 0{\cdot}1325\cos\phi\sin\phi + 0{\cdot}0992\sin^2\phi)\tan^2\theta + (-0{\cdot}0074\cos\phi - 0{\cdot}0072\sin\phi)\tan\theta - 0{\cdot}1914 = 0.$$

* This specimen was originally circular, but three flats were ground on its curved edge for a reason which will be explained later, so that the plan form is not elliptical, as is always the case when a circular disc is compressed.

Table I –(continued)

In second position it is—

$$(0\ 0525 \cos^2\phi + 0\ 1508 \cos\phi \sin\phi + 0\ 1229 \sin^2\phi) \tan^2\theta + (-0\ 0059 \cos\phi - 0\ 0062 \sin\phi) \tan\theta - 0\ 1606 = 0$$

Fe $4 - \varepsilon = 1\ 0879$, $f = 0\ 9379$, $q = 0\ 9856$, $\beta_0 = 90\ 0$ degrees, $\beta_1 = 93\ 4$ degrees, $\gamma_0 = 90\ 0$ degrees, $\gamma_1 = 90\ 9$ degrees, $\lambda_0 = 90\ 0$ degrees, $\lambda_1 = 93\ 6$ degrees

$l = -0\ 0618$, $m = 0{\cdot}9836$, $p = -0\ 0552$, $q = -0{\cdot}0147$

Unstretched cone first position is—

$$(0\ 1173 \cos^2\phi + 0{\cdot}1144 \cos\phi \sin\phi + 0\ 0275 \sin^2\phi) \tan^2\theta + (0\ 1202 \cos\phi + 0\ 0320 \sin\phi) \tan\theta - 0\ 1835 = 0$$

In second position it is—

$$(0\ 1397 \cos^2\phi + 0\ 1446 \cos\phi \sin\phi + 0\ 0381 \sin^2\phi) \tan^2\theta + (0\ 0992 \cos\phi + 0\ 0314 \sin\phi) \tan\theta - 0\ 1551 = 0$$

Compression Tests

X_0, Y_0, X_1, Y_1, t_0, t_1 are expressed in millimetres α, β, γ, l, m, μ, ν are non-dimensional

Fe 3c.—First compression from $\varepsilon = 1\ 0$ to $\varepsilon = 0\ 908$.

$\alpha_1 = 0\ 9117$, $\beta_1 = 0\ 9988$, $\gamma_1 = 1\ 1022$, $X_0 = 0\ 118$, $Y_0 = +0\ 111$, $X_1 = -0\ 069$, $Y_1 = +0\ 114$, $l_1 = +0\ 0207$, $m_1 = +0\ 9994$, $\mu_1 = +0\ 0385$, $\nu_1 = +0\ 002$, $t_0 = 1\ 630$, $t_1 = 1\ 479$

Second position of unstretched cone is—

$$(0{\cdot}1690 \cos^2\phi - 0\ 0378 \cos\phi \sin\phi + 0\ 0008 \sin^2\phi) \tan^2\theta + (-0\ 0702 \cos\phi - 0\ 0056 \sin\phi) \tan\theta - 0{\cdot}2162 = 0.$$

Total compression from $\varepsilon = 1\ 0$ to $\varepsilon = 0\ 840$

Fe 3c.—$\alpha_1 = 0\ 8460$, $\beta_1 = 0\ 9954$, $\gamma_1 = 1\ 1915$, $X_0 = -0\ 118$, $Y_0 = +0\ 111$, $X_1 = -0\ 078$ $Y_1 = 0\ 116$, $l_1 = +0\ 0172$, $m_1 = +0{\cdot}9971$, $\mu_1 = +0\ 8417$, $\nu_1 = -0\ 004$, $t_0 = 1\ 630$, $t_1 = 1\ 368$

Second position of unstretched cone is—

$$(0\ 2843 \cos^2\phi - 0\ 0798 \cos\phi \sin\phi + 0\ 0030 \sin^2\phi) \tan^2\theta + (-0\ 0701 \cos\phi - 0\ 0119 \sin\phi) \tan\theta - 0\ 4214 = 0.$$

Fe 5c.—Compression from $\varepsilon = 1\ 0$ to $\varepsilon = 0\ 888$

$\alpha_1 = 0\ 9966$, $\beta_1 = 0\ 8898$, $\gamma_1 = 1{\cdot}1268$, $X_0 = -0\ 042$, $Y_0 = +0\ 002$, $X_1 = -0\ 051$, $Y_1 = -0{\cdot}119$, $l_1 = -0\ 0346$, $m_1 = +0{\cdot}8903$, $\mu_1 = -0\ 0038$, $\nu_1 = -0\ 0825$, $t_0 = 1{\cdot}475$, $t_1 = 1\ 309$

Table I—(continued)

Second position of unstretched cone is—

$$(0\ 00677\ \cos^2\phi + 0\ 0689\ \cos\phi\ \sin\phi + 0\ 2064\ \sin^2\phi)\ \tan^2\theta + (0\ 0076\ \cos\phi + 0\ 1466\ \sin\phi)\ \tan\theta - 0\ 2665 = 0$$

Fe 6c —Compression from $\epsilon = 1\ 0$ to $\epsilon = 0{\cdot}902$

$\alpha_1 = 0\ 9951$, $\beta_1 = 0\ 9078$, $\gamma_1 = 1\ 1083$, $X_0 = -\ 0\ 036$, $Y_0 = -0{\cdot}171$, $X_1 = -\ 0\ 045$, $Y_1 = -0\ 226$, $l_1 = +\ 0\ 0275$, $m_1 = +0\ 9082$, $\mu_1 = -\ 0\ 0106$, $\nu_1 = -\ 0\ 0243$, $t_0 = 1\ 575$, $t_1 = 1\ 421$

Second position of unstretched cone is —

$$(0\ 0098\ \cos^2\phi - 0\ 0548\ \cos\phi\ \sin\phi + 0{\cdot}1744\ \sin^2\phi)\ \tan^2\theta + (0\ 0211\ \cos\phi + 0\ 0447\ \sin\phi)\ \tan\theta - 0\ 2290 = 0,$$

Fe 7c —Compression from $\epsilon = 1{\cdot}0$ to $\epsilon = 0\ 897$

$\alpha_1 = 0\ 997$, $\beta_1 = 0\ 894$, $\gamma_1 = 1\ 115$, $X_0 = -0\ 016$, $Y_0 = -0\ 027$, $X_1 = -0\ 025$, $Y_1 = -0\ 113$, $l_1 = +0\ 0204$, $m_1 = +0\ 894$, $\mu_1 = -0{\cdot}009$, $\nu_1 = 0\ 072$ $t_0 = 1\ 340$, $t_1 = 1\ 202$

Second position of unstretched cone is —

$$(0{\cdot}006\ \cos^2\phi - 0{\cdot}041\ \cos\phi\ \sin\phi + 0\ 201\ \sin^2\phi)\ \tan^2\theta + (0\ 018\ \cos\phi + 0\ 129\ \sin\phi)\ \tan\theta - 0\ 248 = 0$$

Results of Compression Tests

Stereographic diagrams for the compression tests similar to those used in the case of extension specimens are shown in figs. 12 to 15 It will be seen that they give the same result as the tension tests In each case the point S, which represents the direction of slip deduced from the distortion measurements, lies very close to the triangle which marks the position of a pole of a {111} plane determined by X-rays The improvement in the accuracy of the measurements has produced a corresponding improvement in the agreement between these two directions This is shown in the second half of Table II, where it will be seen that the maximum angle between them is only 1½ degrees Figs 12 to 15 and the third column of Table III show also that the plane of slip is not a definite crystal plane, but that, as in the case of the tension specimens, it is nearly perpendicular to the vertical plane which passes through the direction of slip and the axis of the specimen In the diagrams this plane is represented by a dotted line SM It will be seen that for each of the four compression specimens the pole of the plane of slip is inclined through a small angle away from the

plane SM towards the pole of the nearest {112} plane and therefore away from the pole of the nearest {110} plane The measured values of this small angle

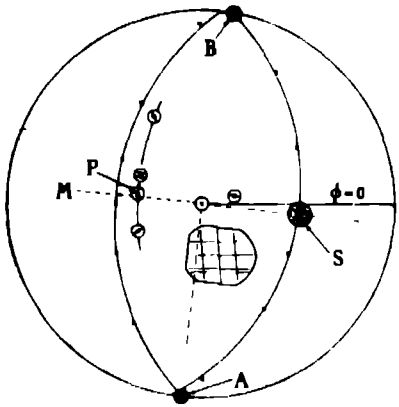

Fig 12.—Fe 3c $\epsilon = 0\ 840$

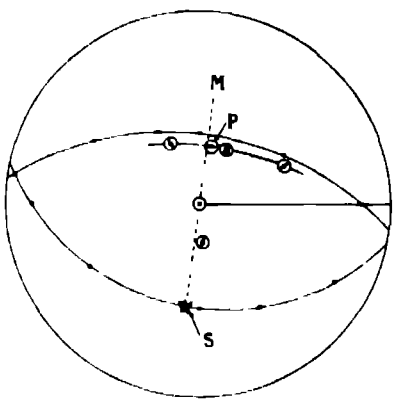

Fig 13 —Fe 5c $\epsilon = 0\ 888$

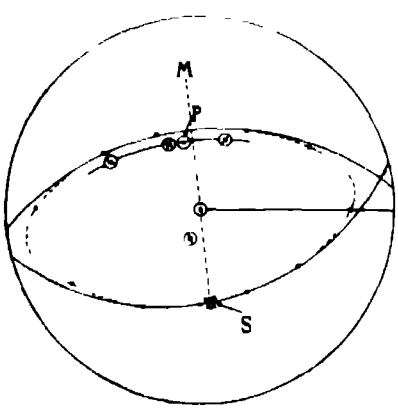

Fig 14 —Fe 6c $\epsilon = 0\ 902$

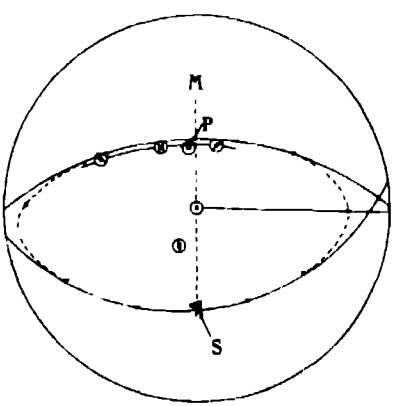

Fig 15 —Fe 7c $\epsilon = 0\ 897$

are given in column 4 of Table III Its maximum value is only $4\frac{1}{2}$ degrees, but, on the other hand, an error of this magnitude could not have occurred in our measurements, so that the effect represented by it must be a real one

The conclusions to be drawn from these results are that slip can occur on any plane, not necessarily a crystal plane, which passes through the normal of a {111} plane The fact that the pole of the slip plane is so close to the plane

Table II.—Co-ordinates of direction of slip and normal to {111} plane.

Extension Specimens

	Fe 1		Fe 3.		Fe 4	
	θ	ϕ	θ.	ϕ	θ	ϕ
Before stretching—						
Direction of slip	61	116	48	233½	58½	202
Normal to {111} plane	58	117	49½	235½	62	205½
After stretching—						
Direction of slip	52	114½	43	238	52	204
Normal to {111} plane	50½	120	44½	240	53	206

Compression Specimens

	Fe 3c		Fe 5c		Fe 6c		Fe 7c	
	θ	ϕ	θ	ϕ	θ	ϕ	θ	ϕ
After compression—								
Direction of slip	53	350	56	262	51½	270	55	272
Normal to {111} plane	53½	355	56½	261	51½	276	54	271

Table III

—	—	Angle between pole of {112} plane and pole P of slip plane	Angle between P and axial plane SM through direction of slip
	Degrees	Degrees	Degrees
Fe 3c	53	9½	2
Fe 5c	56	8	3
Fe 6c	51½	8	4½
Fe 7c	55	14	4

SM seems to show that the resistance to shear does not vary much, as the plane of slip takes up different positions round the pole of the {111} plane The fact that the pole of the plane of slip is inclined through a small but measurable angle away from the plane SM and towards the pole of the nearest {112} plane seems to indicate that the resistance to slipping is rather less on planes near {112} planes than it is on those in the neighbourhood of {110} planes

Mechanism of Slip in Iron Crystals

The question now arises how it can happen that a material can slip parallel to a crystal axis but on a plane which is related to the direction of stress rather than to the orientation of the crystal axes. Where slipping occurs on a crystal plane, as it does in all metals which have been examined in the past, the distortion may be represented by a model consisting of a pack of cards capable of sliding over one another, the cards being ribbed or grooved so that they can only slide on one another in one direction. A corresponding model for representing the distortion of iron crystals might consist of a bundle of rods or pencils, and in order that there may be three-fold symmetry about their axes they might be hexagonal in section *

Another way in which we could conceive the distortion of iron taking place is by slipping on two crystal planes which both pass through the normal of the {111} plane, the direction of slip on each of them being parallel to their line of intersection. Such planes might be two {110} planes or two {112} planes. By adjusting the ratio of the amount of slip on one plane to that on the other the total distortion can be equivalent to slip on any given plane through their line of intersection.

It is impossible to distinguish between these two hypotheses by distortion or X-ray measurements. On the other hand, an examination of the slip lines which appear on a polished surface of the crystal when it is strained seems to furnish the clue required. In each of the tensile specimens these slip lines appeared. They were not straight, but, on the other hand, they appeared to run in a definite direction, and measurements of this direction could frequently be repeated in different parts of the same face with a probable error of about 2 degrees. Figs. 16, 17 and 18 show typical examples of the lines in parts of the specimens where they are free from imperfections in the crystal. In many parts these imperfections make measurement of slip lines impossible, but some reasonably good measurements were obtained in the case of crystals Fe 3 and Fe 4. The orientation of the slip lines on two faces of Fe 4 and on two faces and two extra flats ground on the corners in Fe 3 are represented by the symbol ● in figs. 9 and 11 †. It will be seen that they lie close to the plane of slip in each case. In Table IV are given the measured values of the angle between

* Such a model cannot without modification fully represent the crystal because a cubic crystal like iron has no hexagonal axis of symmetry, but only trigonal, *i.e.*, axis through diagonal of cube which is threefold. For the present purpose, however, this point is immaterial.

† These two flats are not those referred to later, p. 358.

the axis of the specimen and (*a*) the slip lines, (*b*) the trace of the plane of slip determined by distortion measurements on the face of the specimen, (*c*) the trace of the nearest {110} plane, (*d*) the trace of the nearest {112} plane, (*e*) the trace of the second unstretched plane determined by distortion measurements It will be seen that the maximum angle between the slip lines and the trace of the plane of slip is 4 degrees This is less than the errors of measurement in the case of slip lines on the face of tension specimens On the other hand, the maximum angle between slip lines and the traces of crystal planes are 31 degrees in the case of the nearest {110} plane and 26 degrees in the case of the nearest {112} plane

Table IV

	Fe 3		Fe 4	
	Face 1	Face 2	Face 1	Face 2
Inclination to axis of specimen of–	Degrees	Degrees	Degrees	Degrees
(*a*) Slip lines	125	127	124	105
(*b*) Trace of plane of slip*	121	131	124½	100
(*c*) Trace of nearest {110} plane	126	115	133	74
(*d*) Trace of nearest {112} plane	90	132	123	109
(*e*) Trace of second unstretched plane*	81	50	37	62

* From distortion measurements

It appears, therefore, that the slip lines mark the intersection of the plane of slip determined by distortion measurements with the surface of the specimen They have no relation to the crystal planes except, as in the case of Fe 4, where the plane of slip happens to coincide with a crystal plane owing to an accidental element of symmetry in the original orientation of the crystal axes in the specimen It will be seen later that this result is confirmed with considerable accuracy in the compression experiments

It is worth noticing that the slip lines confirm our identification of one of the two unstretched planes determined by distortion measurement as the plane of slip This is shown clearly by the figures in rows *a*, *b* and *c* in Table IV, where row *e* shows the position of the trace of the second unstretched plane on the surface of the specimen It seems, therefore, that if we had no X-ray measurements, we should still be able to make our choice by observing slip lines In fact, the information furnished by rough indications of slip lines on the curved surfaces of the compression discs were used in our later measurements to guess which of the two planes was the slip plane and so to limit the range of setting

angles employed during our search for positions of the specimen in which X-ray reflections could be obtained Much labour was saved in this way, the search for these positions being very laborious

Interpretation of Results

We are now in a position to interpret our results In the first place, we can reject the hypothesis that the distortion is due to slipping on two or more crystal planes passing through the normal of a {111} plane This hypothesis would explain the nature of the distortion and the position of the crystal axes in relation to the slip phenomena, but it is contrary to previous experience with other metals In the cases of aluminium, copper, silver and gold,* planes of slipping which are crystal planes have been proved to exist when a bar of the material is stretched The material slips on one crystal plane only till the change in orientation of the crystal axes, as the distortion increases, brings another crystallographically similar plane into such a position that the two planes are symmetrically placed with respect to the direction of stress Slipping then occurs on both planes In the case of iron, the two planes of slip required in the hypothesis we are discussing would not, except in special accidental circumstances, be similarly orientated in relation to the axis of the specimen, so that the shearing stress on one plane would be different from that on the other We should, therefore, expect slipping on one plane only, namely, that for which the shear stress was the greatest

On occasions when slipping on two planes has been proved to exist, *i.e.*, when the two planes are symmetrically placed, we have sometimes been able to observe slip lines and in each case there have been two sets of lines crossing one another. Observations of this kind have also been made in the case of single crystals under alternating stresses †

Among our iron crystals we had one example in which the axis of the specimen lay very nearly in a {100} plane so that the normals of two {111} planes, *i.e.*, two possible directions of slip, were equally inclined to the axis of the specimen. On stretching this crystal two sets of slip lines appeared crossing one another. It appears therefore that double slipping occurs in iron when the shear stress is equal on two possible planes of slip, and that when it does occur two sets of slip lines appear on the surface In all cases where the crystal axes were not

* The case of aluminium is treated in our Bakerian Lecture, *loc cit* The cases of copper, silver and gold which have lattices similar to aluminium will be treated in a paper by one of us which will be published shortly

† Gough, Hanson and Wright, 'Phil Trans' (1925).

symmetrically placed with respect to the axis of the specimen, only one set of slip lines was observed, and that set did not coincide with any crystal plane

The weight of evidence is therefore strongly against the hypothesis that the distortion is due to slip on two crystal planes

There remains the hypothesis that the crystal does not divide itself into sheets when a shearing stress is applied but into rods or pencils It is clear that any uniform distortion of such a system due to slipping of the rods on their neighbours must be a uniform shear with a plane of slip which contains the direction of the length of the rods, but may be in any orientation round this direction If these rods were of molecular dimensions and if the shear were uniform right down to molecular dimensions, so that every rod bore exactly the same relation to its neighbours as every other rod, any marks or slip lines which could appear on the surface of a strained crystal would depend on the shape of the rods and their relative positions, not on the direction of the plane of slip. This can be easily understood by thinking of a model Fig. 19 is a photograph, taken from above, of a bundle of hexagonal rods standing with their axes vertical These rods pack together so as to fill a volume without interstices The ends of the rods are all cut square (i e, at right angles to their axes) and before distortion they were all at the same level so that the end of the bundle was a plane perpendicular to the axes of the rods Owing to the fact that the rods were accurately made, the outline of the hexagonal ends could not be seen before distortion. The bundle was given a uniform shear by sloping the board on which it was standing. The direction of the trace of the slip plane on the plane of the ends of the rods is shown as a line below the photograph The whole bundle was lighted obliquely so as to show up the projecting parts of the surfaces of slip. It will be seen that the "model slip lines" which appear on the surface are traces of crystal planes on the plane end of the bundle The orientation of the plane of slip which would be determined by external distortion measurement may affect the relative brightness of these "model slip lines," but not their direction.

As a matter of fact, the distortion of which fig 19 is a model cannot occur because it would involve an alteration in the spacing of the atoms in the crystal lattice, which X-ray analysis shows does not occur. In any distortion large bundles of rods must stick together. When they slip they must slip at least one atomic distance along the direction of slip—they may slip much more.

In the model one atomic distance is represented by a given fraction of the diameter of each rod In order, therefore, to see what the model looks like when it is forced to shear in such a way that the slip of each rod on its neighbour is

one atomic distance at every point where there is any slip, the sloping board which produced the effect shown in fig 19 was replaced by a pile of drawing-boards the thickness of each of which represented one atomic distance These were arranged in steps so that the slope of the plane which touched the edges of all the steps was the same as that used in the first experiment The model was then placed on the steps with the rods vertical and they were pressed down as far as they would go Fig 20 shows a side view of the model in this position

Fig. 21 is a top view of the bundle of rods in the same position as they occupied when the photograph for fig 20 was taken The point of view, the method of illumination, the amount of shear and the orientation of the plane of slip are identical with those applicable to fig 19 It will be seen that the "model slip lines" are very different from those shown in fig. 19 In general they run parallel to the trace of the plane of slip which is marked below the photograph. Neglecting the details of their structure in general direction, they are straight lines which have no connection with crystal planes, but when examined in detail they have a jagged appearance It has been known for a long time that slip lines on the surface of iron crystals are not straight in detail We have found that when single crystals are strained so that the shear is uniform throughout a finite volume, the general direction of the slip lines can be found with fair accuracy, and this direction is constant over the whole of a flat surface ground and polished on the outside of a crystal. We have already shown that this direction coincides with the trace of the plane of slip derived from distortion measurements It appears, therefore that our model does in fact reproduce with remarkable accuracy all the facts connected with the distortion of iron crystals which we have brought forward

Prediction of Variation in Character of Slip Lines with Orientation of Plane of Slip to Surface of Specimen.

The success of our model in fitting together the known facts about slipping in iron crystals naturally led us to consider whether it would enable us to predict any hitherto unknown properties of iron The prediction which seemed most suitable for immediate verification was a possible variation in the character of the slip lines with changes in the orientation of the surface of the specimen in relation to the direction of slip. It will be seen that whatever the form of the bounding surface of the individual rods of the model may be (in our model they were hexagonal, but that is not essential) the jagged elements of the lines of slip will flatten out and approximate to the general direction of the slip lines which will therefore become almost straight when the surface of the

specimen is nearly parallel to the direction of slip In the limit when the direction of slip is in the surface of the specimen, the slip lines should appear quite straight provided that the surface is flat and that the lines can be made visible Conversely, the most jagged slip lines may be expected when the surface of the specimen is most nearly at right angles to the slip lines.

In order to test this prediction one of the extension specimens, Fe 3, for which the orientation of the direction of slip had already been worked out from distortion measurements, was taken, and two of its edges were ground down in such a way that two new faces were formed Both were parallel to the axis of the specimen and one of them was also parallel to the direction of slip The second was perpendicular to the first, so that it made the greatest possible angle with the direction of slip The specimen became therefore a prism whose section was an irregular hexagon Referring to fig 9, it will be seen that the dotted line SM represents the orientation of the first of these new faces This line makes an angle of 57 degrees with face 1, which corresponds with the axis $\phi = 0$ Accordingly the new faces were ground at angles of 57 degrees and 147 degrees with face 1 The faces were then polished and the specimen again extended. Fig 22 shows the appearance of the slip lines on the new face cut parallel to the direction of slip, while fig 23 shows the slip lines in the face cut at 174 degrees to face 1 It will be seen that our prediction is verified in a most striking manner The slip lines in fig. 22 are remarkably continuous, they are also straighter than any others we had obtained before, as can be seen by comparing fig 22 with figs 16, 17 and 18 The vertical lines in figs 22 and 23 are due to irregularities in the surface of the specimen which we attribute to somewhat inexpert polishing It will be seen that the small wobbles in the slip lines shown in fig 22 are associated with these grinding and polishing marks. If the surface had been flatter, the slip lines would have been even straighter

The slip lines shown in fig 23 are, as we predicted they should be, more jagged or curved than any of the others In order to confirm this result we ground new faces on another specimen—this time a compression disc, Fe 3c. The specimen was first compressed to $\epsilon = 0{\cdot}908$ The distortion at this stage was calculated and the direction of slip in the distorted specimen found Its co-ordinates were $\theta = 52$ degrees, $\phi = 354$ degrees. Three flat faces were then ground on the curved surface of the specimen so that they were all parallel to the normal to its upper and lower faces. Two of them were parallel to the direction of slip, i.e., they were parallel to the plane $\phi = 354$ degrees The third was cut at right angles to these so that its equation was $\phi = 84$ degrees These extra flat faces are seen in the photograph fig 4, and the relation between

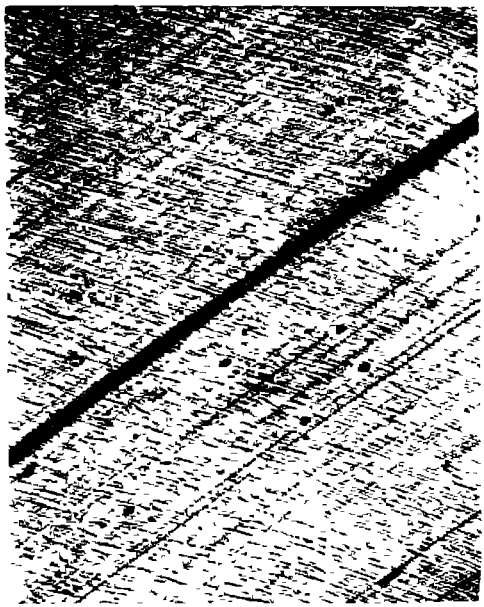

FIG. 16

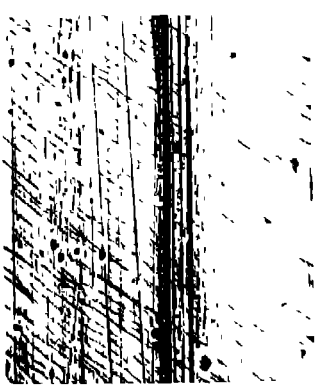

FIG. 17

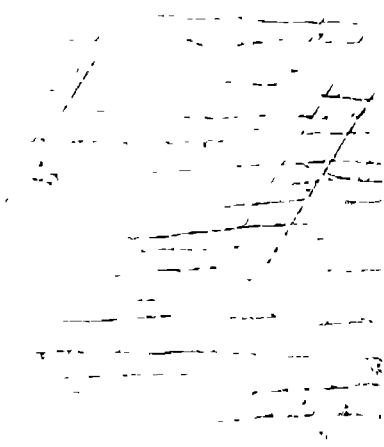

FIG. 18

Fig. 21

Fig. 20

Fig. 19

×150

FIG 22

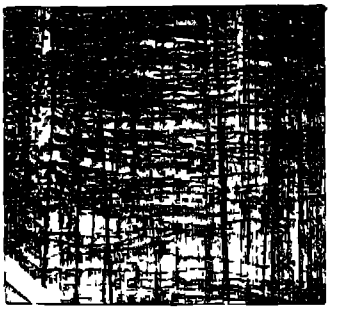

×150

FIG 23

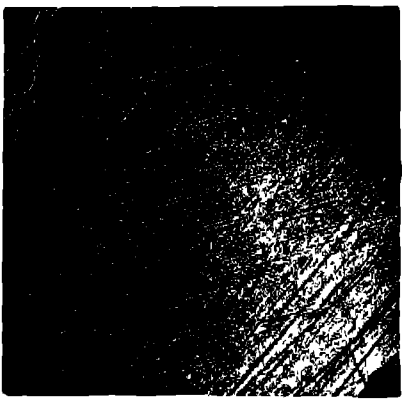

×150

FIG 24

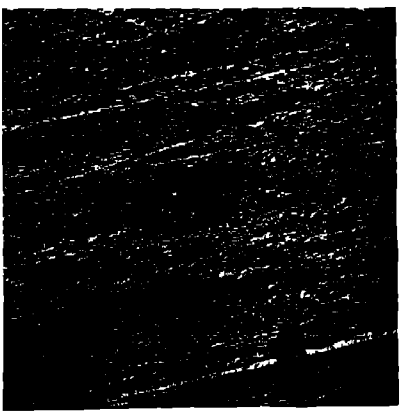

×150

FIG. 25

×150

FIG. 26

them and the co-ordinate axes is shown in fig 12, where an outline copy of fig 4 is shown in position on the stereographic diagram representing the distortion of Fe 3c

The specimen was next compressed to $\epsilon = 0{\cdot}840$ Fig 24 shows the appearance of the surface ground parallel to the line of slip Some difficulty was experienced in showing any slip lines at all on this surface and careful arrangement of the top illumination was necessary It will be seen that the slip lines are extraordinarily straight Their direction can be measured to 0 5 degree. The inclination of the slip lines to the trace of the flat top of the specimen was found to be 37 degrees, so that their inclination to the normal to the flat top was 53 degrees This direction is shown in fig. 12 as the shaded circle S. The inclination of the direction of slip is given in Table II. It is 53 degrees, so that there is perfect agreement between the slip lines and the trace of the slip plane

Fig 25 shows the slip lines on the flat face $\phi = -84$ degrees It will be seen that they are jagged or curved as our theory led us to predict, but that it is possible to measure their general direction with a probable error of about 4 degrees. This direction happened to be parallel to the trace of the flat top of the specimen Its position is represented by the point A in fig 12.

Fig 26 shows the slip lines which appear on the top surface of the specimen (the surface which had been in contact with the sheet plates during compression). It will be seen that here again they are very much bent, but that their general direction can be determined with a probable error of about 3 degrees. This direction, which was measured as $\phi = 80$ degrees, is marked on the stereographic projection of fig 12 at B Again, the plane of slip coincides to the limit of accuracy of our measurements with the general direction of the slip lines.

Conclusion.

The final result of this work is to show that the mechanism of distortion in iron crystals is subject to laws which are quite different from those which govern the slip phenomena in any metal hitherto investigated The particles of the metal stick together along a certain crystallographic direction and the resulting distortion may be likened to that of a large bundle of rods which slide on one another The rods stick together in groups, or smaller bundles of irregular cross section, and the slip lines which appear on a polished surface are the traces of these bundles on that surface When the distortion of the crystal in bulk is a uniform shear these bundles stick together to form plates of irregular thickness, but lying in general with their planes parallel to the plane of slip determined by external measurements of the surface. The plane of these plates

is determined by the direction of the principal stress. It has no direct relationship with the crystal axes

This conception was arrived at entirely as a result of external measurements of the specimens and measurements of the orientation of their crystal axes. The fact that it appears to explain the nature of the slip lines is therefore remarkable. The slip lines, which are curved in detail, preserve a general direction which can be measured in cases where the distortion is uniform, and this direction coincides with the trace on the polished surface of the specimen of the plane of slip determined by external measurements The slip lines appear to have no direct relationship with any of the principal crystal planes.

Perhaps the most telling point in favour of the theory is that it has enabled us to predict the hitherto unknown fact that if the crystal is cut with a polished surface parallel to the direction of slip the slip lines are all straight. When there is an appreciable angle between the polished surface and the direction of slip the slip lines are jagged or curved, and the greater this angle the more jagged they become, but even so they preserve a general direction which is easily measured and is in agreement with the distortion measurements

Bearing of these Conclusions on Previous Work

This completes the work up to a definite stage Before concluding, it may be of interest to bring out the connection between our results and those of previous workers. Nearly all our predecessors* have assumed that the crystal has a plane of slipping which is a crystal plane, and in most cases they have attempted to correlate the slip lines with traces of crystal planes If the work described in this paper is accepted, it is clear that that method was foredoomed to failure. One notable exception, however, is to be found in the work of Osmond and Cartaud,† who point out that among the slip lines which occur when an iron crystal is strained, curved ones predominate. They were unable to find any relationship between these curved lines either as a whole or in their detail and the crystallographic planes. In order to produce slip lines which are straight as a whole, though curved in their details, it is essential in the light of our work here described to subject a single crystal to a *uniform* distribution of stress It was only after a careful study of the methods by which a uniform strain can be produced that we were able to discover the relationship between slip lines and distortion.

* Rosenhain and Ewing, 'Phil Trans.,' A, vol. 93 (1900); Howe, 'Metallography of Steel'; Polanyi, 'Z. f. Kristallographie,' vol 61, p. 49 (1925); Weissenberg, *ibidem*, p. 58, Mark, *ibidem*, p 75

† Osmond and Cartaud, 'Journ. Iron and Steel Institute,' No. 111 (1906).

In conclusion, we should like to express our thanks to Sir Ernest Rutherford for allowing the work to be carried out in the Cavendish Laboratory, to Prof. Carpenter for the use of his laboratory in which the micro-photography and most of the X-ray work was done, to Dr A Hutchinson for allowing us to use several of his crystallographic measuring instruments, and to Prof Inglis for allowing us the continuous use of a Buckton compression machine in his laboratory We also wish to express our gratitude to Prof Edwards and Mr. Pfeil for supplying the large crystals of iron with which the work was carried out, and to Mr W. S. Farren for much help in designing special apparatus for marking, holding and measuring our specimens

DESCRIPTION OF PLATES

Plate 10

Fig 16.—Slip lines on polished surface of iron crystal Magnification 100 The lines parallel to the broad black line which is a scratch made by a razor blade are marks made in polishing

Fig 17.—Slip lines magnification 45, polish marks vertical

Fig 18.—Slip lines (horizontal in photograph) Polish marks at angle of about 60 degrees to slip lines Magnification 350.

Plate 11

Fig 19.—Top view of model, showing appearance where no rods stuck together during distortion

Fig 20.—Side view of model showing hexagonal rods standing vertically on slope of steps.

Fig. 21.—Top view of model showing appearance when rods slip a definite amount or not at all

Plate 12

Fig 22.—Slip lines on face of Fe 3 cut parallel to direction of slip Magnification 150

Fig 23.—Slip lines on face of Fe 3 cut at maximum possible angle with direction of slip. Magnification 150.

Fig 24.—Slip lines on vertical face of Fe 3c cut parallel to direction of slip Magnification 150.

Fig. 25.—Slip lines on vertical face of Fe 3c cut at maximum angle (53 degrees) to direction of slip Magnification 150

Fig. 26.—Slip lines on flat top of iron crystal These were not actually taken on Fe 3c, because the specimen got too much scratched, but they were taken on another almost identical specimen Angle to direction of slip, 37 degrees Magnification 150. Slip lines parallel to bottom of photograph

The Structure of Thin Films. Part VIII.—*Expanded Films*

By N. K Adam, M A , Royal Society Sorby Research Fellow, and G Jessop, Ph D

(Communicated by Sir William Hardy, F R S - Received June 14, 1926)

The present paper describes a closer investigation than has hitherto been possible of the "expanded" state of surface films and of the relation of the films in this state to the condensed films on the one hand, and the gaseous on the other. The expanded films were first reported by Labrouste (1) and examined more closely by one of us (2, Parts III to VI). They are formed from the close-packed condensed films by rise of temperature, the change being complete in a few degrees at constant pressure, and being of much the same nature, whatever the substance. It has been established in previous papers that the temperature of the expansion is raised regularly by an increase in the length of the chain of the molecule, the amount of this rise being practically the same in all homologous series where there is only one chain in the molecule , the absolute temperature of expansion depends, however, on many factors, not yet understood Evidently the expansion is a partial overcoming of the cohesion between the molecules in the condensed film

In the expanded films, however, there is still much cohesion In Part VII we have shown that some of the expanded films possess, at low surface pressures, a definite vapour pressure of a few tenths of a dyne per cm , this region ending in a state of the films which is analogous to a gas in two dimensions In the gaseous film, there is very little cohesion between the molecules. When there is a definite surface vapour pressure between the expanded film and the gaseous, we must clearly regard the expanded film as "liquid." We propose to call the expanded films which end in this vapour pressure region "liquid expanded films."

The results of this paper, as well as some of those of Part VII, show that films must often be regarded as belonging to the "expanded" class, even though they may not behave as liquids and do not show phenomena of evaporation in the surface Such films we shall call "vapour expanded films", they pass without discontinuity into the gaseous films as the surface pressure is diminished By analogy with matter in three dimensions, we consider the liquid expanded films as liquids below their critical point , the vapour expanded as above the critical point. The main difference between substances

which form "liquid" and those which form "vapour" expanded films seems to be that with the former the critical evaporation temperature is above the expansion temperature at which the condensed film changes into the expanded, in the latter, the critical temperature is below the expansion temperature

The apparatus used for measuring low surface pressures is that described in Part VII, for pressures from about 0·5 dyne per cm upwards we have used another instrument on the same principle, actually a preliminary model of the sensitive apparatus, without covers for protection against draughts, with a thicker torsion wire giving a force of 0 256 dyne per cm for one degree rotation of the head, and without the vernier on the torsion head The silk fibres connecting the float to the rest of the instrument were replaced by silica fibres; and to allow of the use of the instrument at higher temperatures, these have been fixed by solder instead of resin cement Both for convenience, and in accuracy, this instrument is a great improvement on the earlier arrangement with the balance and air jets, and the thin gold ribbons at the ends of the float are adequate to prevent leaks at any surface pressure.

Temperature has been controlled by immersing the trough to within a few millimetres of the brim in a very large water-bath with thermostat, up to 35°, above 35° we have used small burners under the trough. The water-bath changed temperature so slowly that the thermostat was usually unnecessary

Liquid Expanded Films

Fig. 1 shows the pressure-area isothermals on myristic acid, on N/100 HCl, from 2 5° to 34°. The three curves inset show the variation of area with temperature at the three pressures of 1 4, 5 0, and 15 0 dynes per cm. The curves replace figs 1 and 2 of Part III *

* We estimate the accuracy of these curves as follows, the pressures are probably correct to 0·1 dyne, except above 10 dynes, the temperatures from 7° to 20°, to 0 1°; outside these limits there may be error of 0 3° The accuracy of the areas per molecule is limited by the precision with which drops can be dropped from a fine pipette, rather rapidly, since the solvents must be volatile In single experiments of a series it is sometimes possible to detect over 5 per cent error, the curve being shifted laterally parallel to itself. We have selected curves for reproduction in which no such lateral shift was visible.

In calibrating the dropping pipette, a correction for the evaporation of the volatile solvent is necessary and was made as follows:—The pipette charged with the solution is fitted loosely into a small test tube by a cork and weighed It is then removed and twenty drops delivered at about one per second, the pipette being steadied (as in use on the trough) in a vertical position. The pipette is immediately replaced in the tube and re-weighed.

Fig 2 gives similar data for the α-bromo-acids of different lengths of chain. The 14, 15, 17 and 18 carbon acids were Dr. Le Sueur's specimens, 16 and a

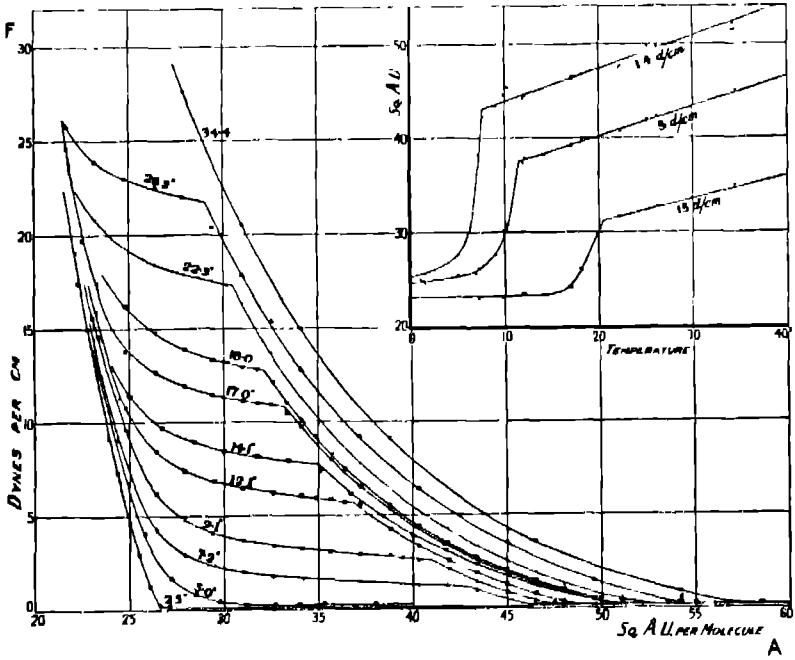

FIG 1.—Myristic Acid.

duplicate specimen of 18, giving practically identical results, were made here. The 18 carbon acid was examined at 26·2°, as it is a condensed film at room temperature, the other measurements were made at room temperature.

Figs. 1 and 2 show that (1) the shape of the isothermal of the expanded film

The loss of weight is the actual amount of solution which falls from the pipette, plus the evaporation from the drops during formation, plus the evaporation from the test tube during the whole period of weighing. The weight required is the sum of the first and second of these quantities. The weight of the solvent evaporating from the test tube during weighing was determined in a blank experiment, care being taken that the times of the blank and the dropping experiment were approximately equal. With petroleum ether of 60°–70° boiling point, the correction to be subtracted from the first weight was about 5 per cent of the whole. Between 13° and 18°, temperature made no difference to the weight delivered outside the error of dropping.

Probably the areas per molecule given in the curves are correct to 3 per cent.

is nearly independent of the length of the chain when the film is examined not far above the temperature of expansion, (2) the transition from the

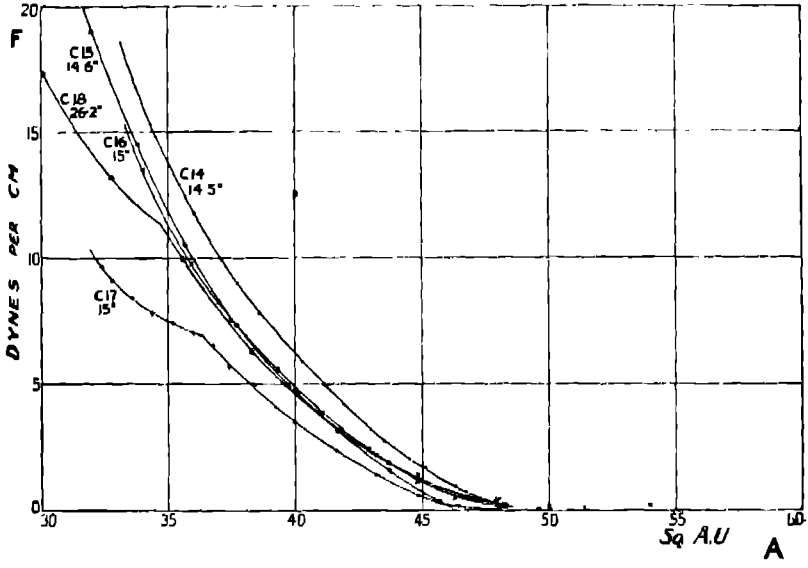

Fig 2.—α-Bromo-Acids

expanded to the condensed state gives a curve nowhere strictly horizontal, with a sharp change at the expanded end and a very gradual change at the condensed end of the transition region It is difficult to say where the condensed curve is reached, indeed, there may be a very slight increase in area of the condensed film with increasing temperature It should be recalled that the condensed curve of myristic acid is not one of the closest possible packing, but is on this solution one of close packed heads, in which compression causes the heads to pack more closely by rearrangement

The discontinuous passage of the expanded curve into the transition region was masked in the curves obtained with the balance and air-jet apparatus, we believe it now to be general, and have observed it also on elaidic amide, hexadecyl alcohol, and margaric nitrile.

The films of myristic acid are not quite free from hysteresis, there is an appreciable delay in attaining pressure equilibrium when the barrier is set at a given area of the surface This is most marked in the flattest regions of the curve, where the expanded film is turning into the condensed. The

pressures recorded are after about half a minute, when they are practically steady. The hysteresis is so small in amount that in this case it will be difficult to make an exact investigation of it, we have not yet attempted to do so.

The myristic acid (at any rate at room temperature and slightly above) and the bromo-acids are definitely liquid expanded films, showing a surface vapour pressure. As the surface vapour pressure is never more than a few tenths of a dyne, and the expanded curve approaches the vapour pressure region fairly steeply, it is possible to extrapolate the expanded curve to no compression fairly accurately It is a very remarkable fact that with the liquid expanded films, the area extrapolated to no compression (with the single chain molecules) is almost a constant. The following table gives the areas at no compression, and the surface vapour pressures, at the temperatures indicated, which, except in the case of oleic acid, are fairly close to the expansion temperature:—

—	Substance	Area at no compression	Temperature of half expansion, at 1·4 dynes per cm	Surface pressure vapour	Temperature of measurement of area and vapour pressure.
		Sq. Å U.	°C.	Dynes per cm.	°C.
Myristic acid	C_{14}	50	9	0·16	room (13–15)
Bromo-acids	C_{14}	48·5	(− 17)	0·05	,,
	C_{13}	46·5	(− 7)	0·04	,,
	C_{12}	48	3	0·02	,,
	C_{11}	46·5	13	0·013	,,
	C_{10}	48·5	22	—	26
Elaidic acid	C_{18}	50	(− 0·5)	0·09	room
Erucic acid	C_{22}	50	4·5	0·015	,,
Elaidic amide	C_{18}	49	—	—	,,
Erucic amide	C_{22}	50	—	—	,,
Oleic acid	C_{18}	55	(− 30)	0·08	,,
Palmitic nitrile	C_{16}	45	6·5	0·15	,,
Hexadecyl urea	C_{16}	47	48·5	—	51
Hexadecyl alcohol	C_{16}	47	46	—	53
Hexadecyl phenol	C_{16}	49	55	—	60
Palmitic amide	C_{16}	47	36	—	43·5

All the areas are so close to 48 sq. Å U. that the difference is possibly experimental error, except with palmitic nitrile and oleic acid The palmitic nitrile was collapsing to some extent, and the observed area may be too small, the oleic acid was probably nearly 50° above its expansion temperature, while the other substances were nearly all within 15°, and mostly within 8°, of the expansion temperature It thus appears that the areas, at no compression, of the liquid expanded films are very close to 48 sq. Å U. per molecule when the temperature is close to the expansion temperature.

Earlier papers gave the result that at a constant surface pressure, after the change from the condensed to the expanded film is complete, there is a slow further increase in area with rise of temperature, of the same order of magnitude as the thermal expansion of a gas The present experiments confirm this, the magnitude of the thermal expansion of the expanded film is, however, difficult to determine with less than about 100 per cent error

The surface vapour pressures in the table decrease with increasing length of chain, becoming very small in the 22 carbon series These vapour pressures have no relation to the temperatures of expansion beyond the general one that vapour pressures decrease with length of chain, and in any one series the expansion temperature is raised by lengthening the chain

Fig. 3 is of oleic acid, on dilute acid with and without permanganate, the curves on acid only being taken at two temperatures, and showing the thermal

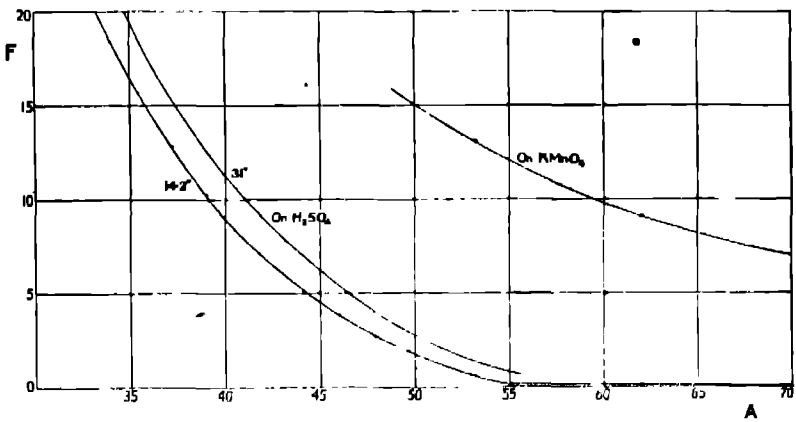

FIG 3 —Oleic Acid.

expansion of the expanded film This film at 14° is definitely "liquid expanded," although it is probably about 45° C. above its expansion temperature

Expanded Films with more than One Chain

Fig. 4 gives curves of lecithin and triolein Triolein tends to an area of 135 at no compression; we have also made measurements with the older apparatus on tripalmitin and tristearin, obtaining about 115 sq A.U. at 60°, that is, just above the expansion temperatures Therefore in these compounds with three chains, the film in the liquid expanded state occupies about 2 4 times the area of the corresponding compound with a single chain.

Lecithin, with one saturated, and one unsaturated chain, but with the bulky choline and phosphoric acid groups at the head of the molecule, occupies about

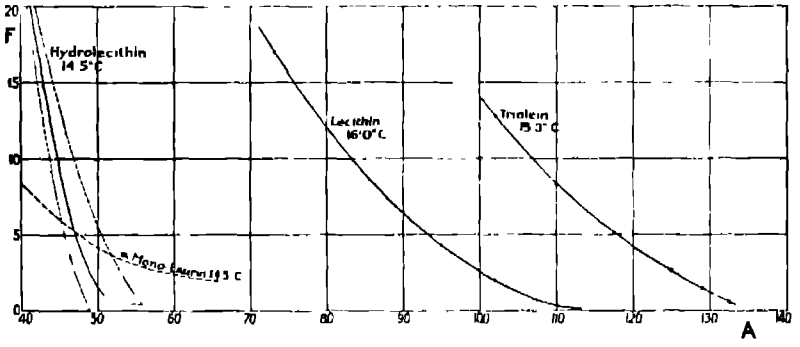

Fig 4

114 sq. Å U. at no compression, a greater area than that proper to two similar chains singly, in the expanded state In other respects these curves resemble the expanded curves of single chain substances *

The equation of state proposed by Cary and Rideal (3, p 309), on the basis of their experiments on the spreading of films from crystals, does not fit the data for any of these substances Their equation

$$F = k\left(\frac{1}{A} - \frac{1}{A_0}\right)$$

would require that F plotted against 1/A should be a straight line. The slope of the curve with F as ordinates and 1/A as abscissæ actually increases steadily

* Fig 4 also shows α-monolaurin and hydrolecithin, the latter is a condensed film, expanding at about 28° under 1 4 dynes compression to an expanded curve similar to that of lecithin The curve for the monolaurin is only approximate, the film collapsing, probably dissolving, very rapidly.

Hydrolecithin shows a great deal of hysteresis If sufficient time is allowed for the film to settle down, the full curve is given, if the area is contracted rapidly, the right-hand dotted curve may be obtained, if the area is increased rapidly from a high compression, the left-hand curve may be found. If the area is set suddenly to a given amount, from a low compression, the observed compression is at first high, falling gradually to the equilibrium curve, if suddenly decompressed, the film shows a low pressure, rising to the equilibrium The time for attainment of equilibrium pressure is several minutes At room temperature, the rise or fall to the equilibrium pressure is not exponential, but the rate falls off more rapidly than if it were exponential at first. Further investigation of this hysteresis is needed, it is doubtless to be ascribed to the very complicated heads taking time to pack closely. The cross section of the head is about 52 sq. Å.U.

as the pressure increases from small values up to 16 dynes or more, and in some cases is more than doubled in this range It is not surprising that this equation proves to be incorrect, as it is based on the assumption that the pressure is proportional to the number of molecules in excess of the number $1/A_0$ required to pack the film to the area at no compression Since the film can certainly not pack more closely than to about 20 sq A.U, we should expect the pressure to increase more rapidly with decreasing area than would be required by this equation

Vapour Expanded Films

Typical instances of films which expand from the condensed state into a state which passes without discontinuity into the gaseous films are the ethyl esters Fig 2 of Part VII shows that none of the esters give a horizontal vapour pressure region, except when the liquid surface phase is a condensed film Earlier papers, and figs 5 and 6 of this paper, show that the expanded

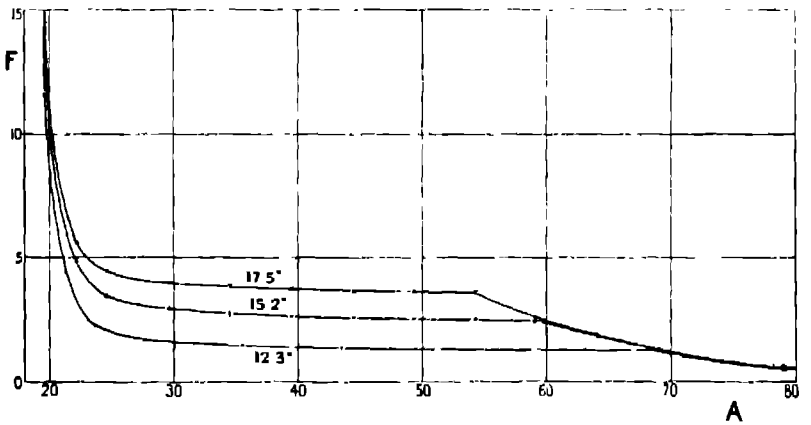

Fig. 5 —Ethyl Palmitate.

curve passes into the condensed in much the same way as with the liquid expanded films just considered, there is the same discontinuity at the expanded end of the transition region and gradual change at the condensed end, the chief difference being that the area of the expanded film is greater with the ethyl esters than with the liquid expanded films.

While it is true that none of the esters show a region of constant vapour pressure between the expanded and the vapour regions of the curves, still

ethyl palmitate at 15° and ethyl pentadecylate at 7·5° show a fairly sharp change of direction between 100 and 150 Å U. at about 0 25 dyne per cm This area is of the same order of magnitude as that of the molecules lying flat on the surface. Fig 6 shows clearly the influence of temperature on the isothermals of these esters. The temperatures of half expansion, under 1·4 dynes per cm, are ethyl palmitate, 13°, ethyl pentadecylate, about 5°, ethyl myristate, below 0°, probably about — 5°. The curves of ethyl palmitate at 15° and of ethyl pentadecylate at 7·5° are nearly identical, these may be taken as typical of the ethyl esters just above their expansion temperature The curves of ethyl pentadecylate at 17·5° and of ethyl myristate at 15° show the influence of a rise of 12° and of 20° above the expansion temperature, the angle at the lowest point of the curves is very much blunted at even 12° above the expansion temperature Twenty degrees above the expansion temperature the film is evidently a long way above the two-dimensional critical evaporation temperature.

A few experiments have been done on the methyl esters, which give vapour expanded films, very much like the ethyl esters The expansion temperatures of the methyl esters are roughly 10° above those of the ethyl esters

The methyl ketones R CO CH_3 also form vapour expanded films Fig 6 shows the FA–F curve for tridecyl methyl ketone on distilled water at 12·5° C.

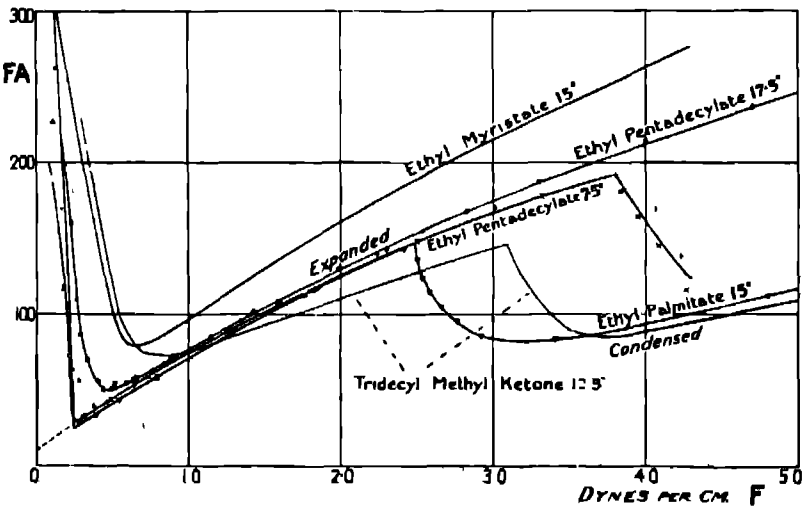

Fig. 6.

It condenses at about 3 dynes per cm , at this temperature, to a film giving the characteristic curve of close-packed chains Heptadecyl methyl ketone gives a condensed film with close packed chains expanding above 40° The condensed films are liquid, not solid

Methyl Ketones.

Substance	Area of condensed film at no compression (sq A.U)	Temperature of half expansion, under 1 4 dynes per cm
Tridecyl methyl ketone	(21)	10
Heptadecyl methyl ketone	20 5	42 5

The Influence of Permanganate on Unsaturated Linkages

An attempt has been made to apply a definite attraction towards the water, in the neighbourhood of the middle of the chain of the molecule, by dissolving reagents in the water which might be expected to act on a double bond in this part of the molecule Mercuric chloride, acid potassium bichromate, and hydrogen peroxide were found to have no appreciable action on the films Potassium permanganate, in 0 85 per cent concentration, or in ten times this concentration, with N/10 sulphuric acid, always caused the films which had a double bond in the middle of the chain to become "gaseous" Fig 7 shows

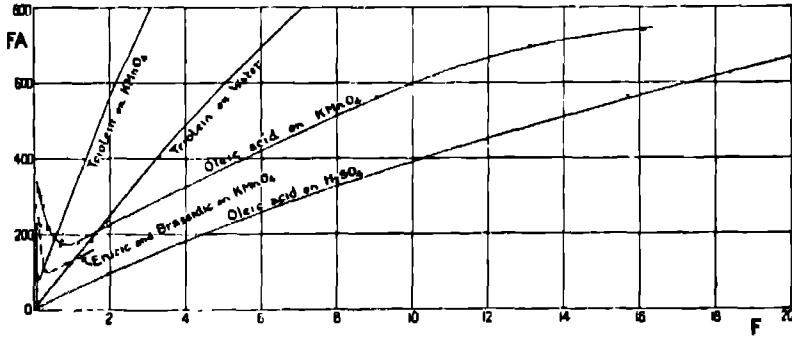

FIG 7 —Influence of Permanganate.

the effect on oleic acid, triolein, and erucic and brassidic acids, the curves for the last two being dotted, as but few points were obtained. Elaidic acid on permanganate gives a curve almost identical with that on oleic up to 2 dynes

per cm. Comparison of these curves with those obtained by Schofield and Rideal (4) on the absorbed films of the soluble fatty acids (RT being equal to 400, very nearly) shows that the cohesion between the film molecules has been reduced to a very small amount for oleic acid on permanganate, with erucic and brassidic acids, which have four more carbons in the chain, there is rather more cohesion, but the films are far above their critical temperature

The same effect has also been found on films of ethyl brassidate, erucic and elaidic amides, and on lecithin, which has one saturated and one unsaturated chain Permanganate has no such action on films of ethyl pentadecylate, palmitic nitrile, α-monolaurin, and barely perceptible action on the iso-oleic acid, which has the double bond in the αβ position to the carboxyl. On tetradecyl alcohol the film was not a gaseous film, but there was evidence that the CH_2OH group was undergoing oxidation to myristic acid, as the curve slowly changed from that proper to the alcohol towards that of the acid at the same temperature This change is to be further investigated

It is quite clear that permanganate turns the film into a gaseous film only when the double bond is in the middle of the chain, it appears that the action is simply to make the molecules lie flat We have other evidence that the molecules of the shorter chain acids lie flat on the surface in the adsorbed films of the soluble acids, and the flat position appears to be characteristic of the gaseous state of the films

Discussion of the Structure

The experimental evidence described above shows that the *liquid expanded* state is a definite intermediate stage between the gaseous and condensed films Its stability depends very much on the nature of the head of the molecule, the free carboxyl group, and the bromo-acid head, favouring the formation of liquid expanded films, while in no case has a liquid expanded film been obtained with an ester or a methyl ketone The area at no compression is limited and is with one chain, 48 sq A.U, being independent both of the length of chain and the nature of the head. This area ϕ is much too small for the molecules lying flat and much too large for the vertical close packed orientation

In addition, there is considerable compressibility, which decreases with increasing compression, and a large coefficient of thermal expansion. The change from the expanded to the condensed films has some resemblance to a change of state, but requires a few degrees interval of temperature for completion.

We suggest that the molecules are coiled down in helices, with vertical axis, and are closely packed by their cohesion, even without external compression.

The compressibility may be due to the chains being straightened out by lateral compression and forced vertical Owing to the tendency of the valencies between carbon atoms to form the tetrahedral angle with each other, the cross section of this helix should be about the same as the maximum section of cyclohexane or cyclopentane by a plane parallel to the ring Direct evidence as to the dimensions of these rings does not appear to exist, a possible basis for an estimate is found in Bragg's measurements on crystals of naphthalene and anthracene (5). The area in the plane of the ring occupied by one molecule of naphthalene, as packed in the crystals, is $8\cdot34 \times 8\cdot69 \sin 57^\circ 11' = 61$ sq. A U ; the corresponding area of anthracene is $8\cdot7 \times 11\cdot6 \sin 55^\circ 36' = 83\cdot1$. Now the difference between benzene and naphthalene is the same as that between naphthalene and anthracene, therefore benzene should have an area, in the plane of the ring, of about 39 sq A U It is well known that additional hydrogens greatly increase molecular dimensions, so that 48 sq A U does not seem an unreasonable value for the cross section of a helix with vertical axis

The high co-efficient of thermal expansion may be analogous to the high co-efficients observed with liquefied gases not far below their critical point

The *vapour expanded* state is not a definite phase in the surface, but if the films are not far above the critical evaporation temperature, the properties of the vapour expanded films are not very different from those of the liquid expanded Probably the vapour expanded films are homogeneous mixtures of molecules coiled down and lying flat, as the temperature is raised, or pressure lowered, the proportion of those lying flat is increased

In the following paper some instances will be given of films which expand straight from the condensed state into a state fairly closely resembling perfect gases; in these the molecules must be nearly all lying flat These molecules have polar groups at each end

Since the fatty acids generally form liquid expanded films, but the esters and methyl ketones form vapour expanded films, it appears that the lateral attraction between the coiled-down molecules is much increased if the heads have plenty of residual affinity Possibly far the most important factor determining whether a substance forms a liquid or a vapour expanded film is the amount of the additional cohesion given to the coiled-down molecules by the adhesion between adjacent heads. It would appear that the contribution to the total cohesion, made by the adhesion between heads, is much greater in the coiled-down configuration than in the vertical close packed arrangement of the condensed films. This would account for the comparative independence

between the value of the surface vapour pressure and the temperature of expansion.

If the hypothesis that the chains are coiled down is incorrect, we are forced to fall back on some special kind of vibration, which is so controlled by the cohesive forces that the area in the liquid expanded films becomes definitely limited at 48 sq Å U There seems little hope of developing a working hypothesis on such assumptions

Summary

1. The expanded state of the films of fatty acids, bromo-acids, esters, methyl ketones, and other compounds possessing one chain only in the molecule, and of several compounds with more than one chain, has been re-investigated with improved apparatus.

2 Two types of expanded film exist—the liquid expanded, which exhibits a constant vapour pressure in the surface, and a discontinuous transition into the "gaseous" film, and the "vapour expanded," which passes continuously into the gaseous film The liquid expanded films show a definitely limited area at no compression, which is very close to 48 sq. Å U per molecule, and is independent both of the nature of the head and of the length of the chain, within the range of substances investigated. The vapour expanded films have no limiting area, as the temperature is raised and the pressure lowered they gradually approach the gaseous condition Some vapour expanded films give, near the temperature of expansion, pressure-area curves fairly closely resembling those of the liquid expanded films

The structure of the liquid expanded films may be that the long chains are coiled down in helices with the axis vertical, the molecules being close packed in this orientation by their mutual cohesion. The two-dimensional evaporation in the surface will then be a separation of the molecules, followed by uncoiling and lying flat The liquid expanded state can only exist when there is sufficient adhesion between the molecules in the coiled-down state It appears that the adhesion between the heads of the molecules is an important factor in conferring the necessary adhesion in this configuration The esters and methyl ketones formed only vapour expanded films, the acids and most of the other compounds liquid expanded films

3. Acid potassium permanganate in the water acts on ethylenic linkages *in the middle of the chain* in such a way as to make films gaseous, which would be either condensed, or very far removed from the gaseous state, in the absence of this reagent Permanganate does not act on saturated chains nor on one in

which the ethylenic linkage is next to the head of the molecule. The action is probably simply that the extra attraction on the middle of the chain causes the molecule to lie flat

4 The methyl ketones form condensed films with close-packed chains, the heads packing to less than 21 sq. A U

5. Hydrolecithin, in the condensed state, requires some minutes to reach its final pressure in the films; a similar hysteresis, though more rapid and much smaller in amount, probably occurs also with a simple fatty acid. The hysteresis may be due to slowness of the molecules in taking up their final packings

We are indebted for the lecithin and hydrolecithin to Prof Leathes, the specimens being prepared by Dr. P A. Levene, of New York Messrs J. Crosfield and Sons, Ltd., kindly gave us the α-monolaurin, and Mr W B Savile the methyl ketones

REFERENCES

(1) Labrouste, 'Ann. de Phys,' vol 14, p. 164 (1920)
(2) Adam, 'Roy Soc Proc,' Parts I to V. A, vol. 99, p. 336; vol 101, pp 452, 516, vol. 103, pp 676, 687 Adam and Dyer, Part VI, vol 106, p. 694 Adam and Jessop, Part VII, vol. 110, p. 423.
(3) Cary and Rideal, 'Roy. Soc. Proc,' A, vol. 109, p. 309 (1925).
(4) Schofield and Rideal, 'Roy. Soc. Proc,' A, vol 109, p 67, vol. 110, p 170
(5) Bragg, 'Phys Soc Proc.,' vol. 34, p 33 (1921).

The Structure of Thin Films. Part IX.—*Dibasic Substances.*

By N. K. Adam and G. Jessop.

(Communicated by Sir William Hardy, F.R.S.—Received June 14, 1926.)

We have been anxious for some time to examine mono-molecular films of long chain molecules with a polar group at each end. In 1924, Mr. Dyer prepared specimens of the acid $COOH(CH_2)_{16}COOH$, and of its mono- and di-ethyl ester, but the publication of the results obtained on these has been deferred until a more extended series of compounds were available. Now Dr. D. A Fairweather, who has prepared a long series of compounds of this series, including many new compounds, has most kindly placed at our disposal specimens of the acids 16, 20, 24 and 32*; of the di-ethyl esters 10, 11, 16, 20 and 32; and of the mono-ethyl ester $COOH(CH_2)_{16}COOC_2H_5$. Films of these compounds have been examined by the methods of the preceding paper.

The esters gave films of fair stability and easy to work with; figs. 1 and 2 show the F—A and FA—F curves. The shorter chain substances are gaseous films at room temperature; below 2 dynes per cm they approach much more closely to the perfectly gaseous condition than any insoluble films yet studied. The minimum for FA is about 330, the theoretical for a perfect gas being 1·372 T. or about 400. Variation of temperature from 1° to 15° made no difference appreciable within the accuracy of experiment, the fact that the curve for 10 appears below that for 11 is probably due to the former being so volatile that the molecules leave the film too rapidly for exact measurements. Above 2 dynes per cm. the correction to the gaseous state due to the size of the molecules causes the curves to take a form similar to those of the adsorbed films of the slightly soluble acids (reference 4 of preceding paper).

At 1° the ester 11 changes to a condensed film.

The ester 16, in the gaseous state, shows more cohesion, the minimum for FA being just above 200. The three middle curves show the influence of temperature on the transition from the gaseous to the condensed state. This resembles the transition from the vapour expanded to the condensed state in the case of the ethyl esters, but there is no discontinuity at the gaseous end of the transition region.

The ester 20 is condensed up to 40°, expanding at higher temperatures to a

* The substances will be designated by a number indicating the number of CH_2 groups in the molecule.

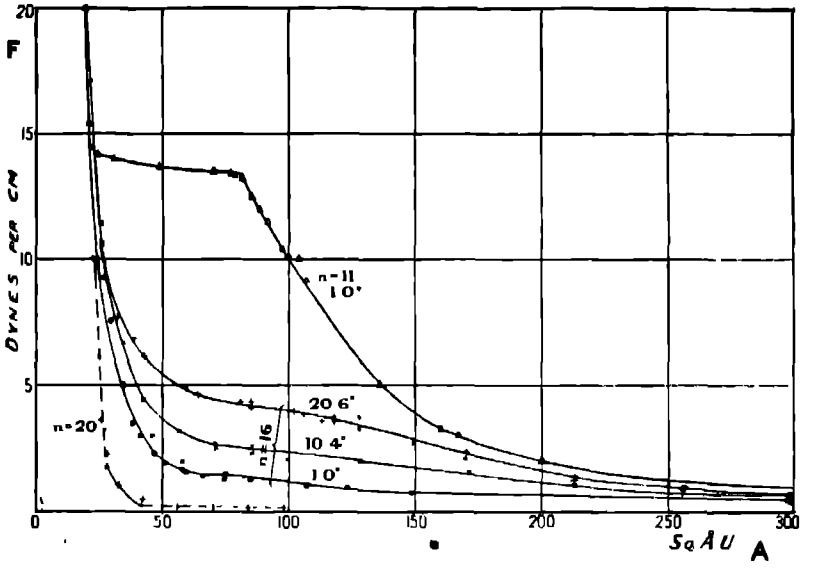

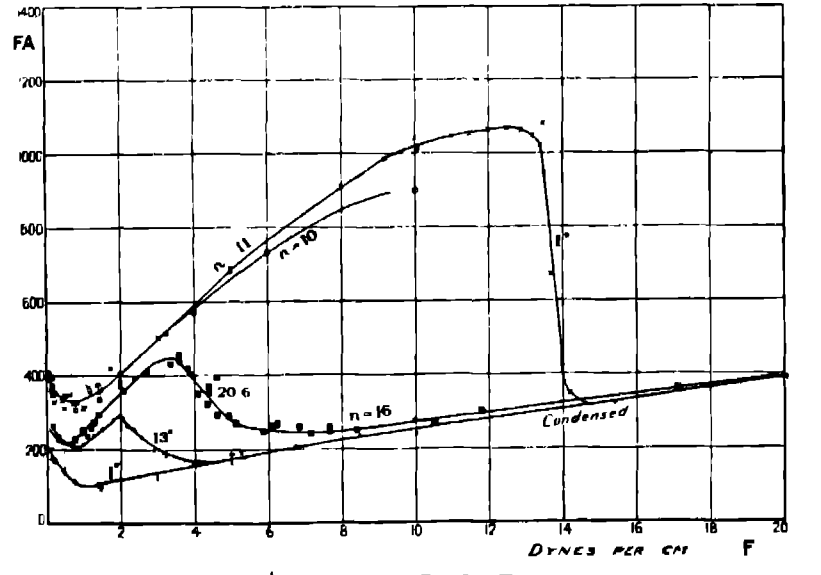

FIGS. 1 and 2. — Di-ethyl Esters.

gaseous film resembling those of the lower esters. The ester 32 forms a condensed film at all temperatures we could employ.

The mono-ethyl ester 16 was examined on dilute HCl. Its behaviour is very similar to that of the di-ethyl ester, corresponding curves to those of fig 1 being found at a temperature three or four degrees lower

The condensed curves all end, above 10 dynes per cm., in a steep curve of area 20 to 21 sq A.U., *i e* the cross section of chains close packed This shows that under moderate compressions the molecules stand vertically with only one end in the water Films in this state were found to be solid, except with the ester 11, which was so viscous as to be nearly solid. In most cases there was a fairly rapid collapse above 10 dynes per cm.

The question arises whether any sign can be detected of a packing in which both polar ends of the molecules are in the water, the chains forming an arch between the molecules. In such a packing the two ends would occupy an area of at least 40 and the arch might easily require considerably more, owing to the impossibility of bending a hydrocarbon chain very sharply; since there is no such definite area, we conclude that this packing is never found. But below 10 dynes per cm. the condensed films do have a greater area than that of close packed chains. The curve for the condensed film, produced from 2 dynes, where there is a sharp bend, cuts the abscissa at about 28 sq. A.U, this area being rather variable in successive experiments It seems possible, therefore, that a proportion of the molecules are adhering by both ends to the water surface, these being entangled among a greater number in an upright position, and being themselves forced upright by compressions of 10 dynes per cm

The marked tendency of these dibasic esters to form gaseous films is no doubt due to the strong attraction for water at both ends, this makes it easy for the molecules to lie flat, and difficult for them to stand upright. The molecules probably lie flat in all gaseous films, in condensed films they are upright, closely packed, and held together by the lateral adhesions of the chains All the previous work on these films shows that thermal agitation tends to disrupt the lateral cohesion between the upright molecules, and favour either a less definite or a horizontal orientation.

The temperatures of half expansion from the condensed to the gaseous films under 1·4 dynes per cm. compression are as follows:—The curve of change of area was very much like the usual change from condensed to expanded films, and the change required several degrees for completion.

Temperatures of Half Expansion

Substance	°
Di-ester 16	7
,, 20	44
,, 32	Above 65
Mono-ester 16	10 5

The acids formed rather unstable films In the condensed state areas from 6 to 18 sq Å U. per molecule were obtained with a great deal of contraction. We do not think these low areas can be taken as evidence that the molecules form films two or three molecules thick on the surface, as the areas were not reproducible in successive experiments if the temperature was varied, and very frequently not when all conditions were apparently constant, the contraction was so great that it was difficult to select any one area as correct It should be said, however, that the acids 24 and 32 very frequently ceased contracting almost completely at an apparent area of 12, and that the acid 20 had a tendency to cease contracting about 8 sq Å U We think the most probable explanation is that much of the material had been forced away from the surface, a tendency to cease collapsing when a part of the film is left, as if part of the film was more stable than the rest, has been noticed before (Part I) It was easy to see visible aggregates on the surface after collapse had proceeded some way. The free carboxyl groups which would be exposed at the surface of the film, if the molecules were standing upright as in the condensed films of the esters, would form natural points for the adhesion of fresh molecules in the proper positions for building up crystals in bulk and would facilitate collapse

The acids 16, 20, and 24 were found to form gaseous films, of rather smaller area than the esters At 2 dynes per cm. the areas were roughly two-thirds of those of the di-ester 16 in the gaseous state. There is thus a greater cohesional correction in the gaseous state of the films of acids than in those of the esters, it is probable that this is due to the attraction between the COOH groups of neighbouring molecules in the film.

Summary.

The dibasic esters $C_2H_5OOC(CH_2)_nCOOC_2H_5$ form mono-molecular surface films of the gaseous and condensed types. The cohesional correction to the gaseous films increases with the length of the chains, the films of the esters, in which n has the values 10 and 11, being the closest approach to the perfectly gaseous state yet found with insoluble films.

In the condensed films the only stable state is one with the molecules adhering to the water by one end only and packed closely in an upright position The transition from the condensed to the gaseous films is of the same nature as that from the condensed to the expanded films described in previous papers; but the condensed films expand in all cases to films of the "vapour" type.

The behaviour of the acids of the series, and of the mono-ethyl ester, for which n is 16, is generally similar.

The Number of Particles in Beta-Ray Spectra.—II. *Thorium* B *and Thorium* (C + D).

By R W. Gurney, Ph.D, Trinity Hall, Cambridge.

(Communicated by Sir Ernest Rutherford, Pres R S —Received June 30, 1926)

1. *Introduction.*

Measurements of the number of particles emitted with different velocities in the beta-ray spectra of Radium B and Radium C have been recently described by the writer.* In the present paper the measurements have been extended to the spectra of Thorium B and Thorium (C+D). As before, portions of the magnetic spectrum were focussed into a Faraday cylinder, and the number of electrons determined in absolute magnitude

The conclusion reached in the previous paper was that in the case of both Radium B and Radium C there is, underlying the beta-ray lines, a continuous spectrum similar to that of Radium E, and of the same magnitude—that is, containing one electron per atom breaking up. This leaves little doubt that in these three bodies it is the nuclear electrons ejected in the disintegration with varying velocities which form the continuous spectra. If this is true of other bodies we expect to find in the Thorium series also large continuous spectra containing one electron from every disintegrating atom. The measurements of the spectrum of Thorium (B+C+D) by Pohlmeyer† showed, however, that the continuous spectrum was feeble in comparison with the beta-ray line Hρ 1398. But since an ionisation method was used, no determination of the absolute number of particles was possible.

* 'Roy. Soc. Proc.,' A, vol. 109, p. 540 (1925).

† 'Z. f. Physik.,' vol. 28, p. 216 (1924).

In the present investigation the gamma-ray activity of each of the sources was measured on an electroscope and the number of atoms disintegrating in a source of known gamma-ray activity was afterwards determined by counting the number of alpha particles emitted, as described below.

2. *Apparatus and Method.*

The radioactive material was deposited on metal plates 8 mm. long by 3·5 mm wide, which were tilted at an angle in the usual way, so that the beta particles left the surface at angles approaching grazing incidence The sources of Thorium (B + C + D) were obtained on aluminium by exposure to the emanation, those of (C + D) were obtained on nickel by deposition from solution.

The method was the same as before, except that the residual gamma-ray effect was balanced out by means of the leak in an ionisation chamber, to the walls of which about 1/30 of a volt was applied. Reference should be made to the previous paper for the precautions that were taken to ensure that no particles entered the Faraday cylinder other than those travelling direct from the source. A large correction is necessary for particles reflected from the metal plates on which the radioactive material was deposited, details of this are given below.

3. *The Magnetic Spectra.*

The beta-ray lines of Thorium (C + D) have been recently remeasured photographically by Black.* The lines which give the strongest photographic density are —

Hρ	Level of Origin.	Intensity.	Energy.
541	L_1 level . .	100	2·52 10^4 volts
658 }	Outer levels .	{ 40	3·69
684 }		{ 25	3·98

He found that there is a complete gap in the line spectrum between Hρ 4040 and Hρ 10080. The curve obtained by plotting the rate of charge of the Faraday cylinder against values of Hρ is given in fig. 1. This demonstrates very clearly the separate existence of continuous and line spectra, for the spectrum curve reaches its maximum above Hρ 4040, where there are no lines. And below the peaks at Hρ 540 and 670 there happens to be no continuous background.

The thorough measurements of Pohlmeyer† showed that some of the beta-ray

* 'Roy. Soc. Proc.,' A, vol. 109, p. 166 (1925).

† *Loc. cit.*

lines of Thorium D produced irregularities in the spectrum curve, but in the portion of the spectrum investigated by him (above Hρ 1000) none of them

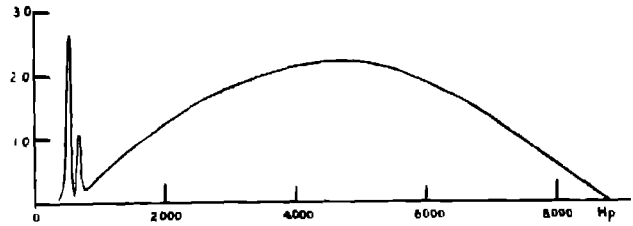

FIG 1 —Thorium (C + D). (Vertical scale represents divisions per minute per milligram.)

were strong enough to give definite peaks. In the present measurements the irregularities were not investigated

The curve for Thorium (B + C + D) is given in fig 2 By subtracting the portion due to Thorium (C + D), as has been done by the broken line, we

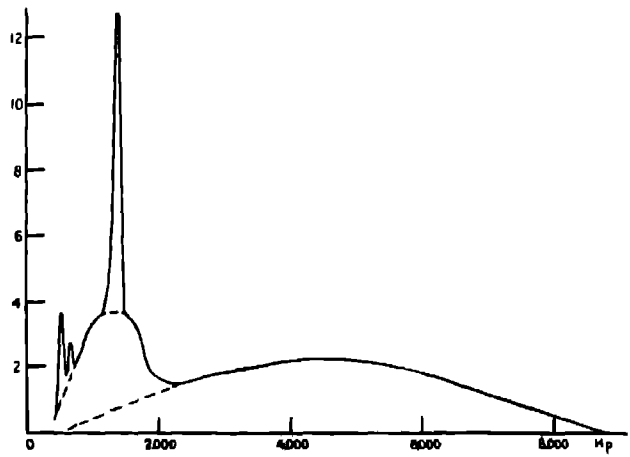

FIG. 2.—Thorium (B+C+D) (Vertical scale represents divisions per minute per milligram.)

obtain the spectrum of Thorium B alone. At first sight this appears to be much smaller than that of (C + D), but this is only a peculiarity of the dispersion. For, as was pointed out in the previous paper, if for a certain value of the magnetic field the Faraday cylinder collects particles over the range of velocities Hρ 500 to 540, then in a field of ten times the intensity particles are collected,

not over the range Hρ 5000 to 5040 but from Hρ 5000 to 5400, that is, over a range ten times as great The experimental curves of figs 1 and 2 do not therefore at all represent the true velocity distribution of the particles as emitted by the source We have to transform the continuous spectrum by dividing the ordinates everywhere by the corresponding field-strength This has been done in fig 5, omitting the peaks. This transformation does not apply to the height with which the peaks stand out above the continuous spectrum. For with the very wide slit used the whole of any beta-ray line will enter the Faraday cylinder at once for some value of the field corresponding to the top of the peak

4 *The Number of Disintegrating Atoms.*

The bodies present in the active deposit of Thorium are shown in fig. 3. Since the period of Th B is much greater than that of the others, they will all be in equilibrium with it three hours after removal from the emanation The number of atoms of Th C and Th D undergoing beta-ray disintegration per second will then be together equal to the number of atoms of B breaking up. The number of atoms of Th C and Th C′ undergoing alpha-ray disintegration will also be together equal to the number of atoms of B. Hence to determine the number of atoms breaking up in a source of Th B with C and D in equilibrium, we have only to count the number of alpha particles emitted To make a direct count of the absolute number of alpha particles emitted within a given solid angle it is necessary to know the efficiency of the counting A simpler indirect method is to compare the number of particles with the number of particles emitted in the same solid angle by a source of Radium (B + C), whose gamma-ray activity is compared with a Radium standard. In this comparison it is unnecessary to know the efficiency of the counting or the value of the solid angle For sources of Thorium (C + D) free from Thorium B this determination has already been made by Shenstone and Schlundt *

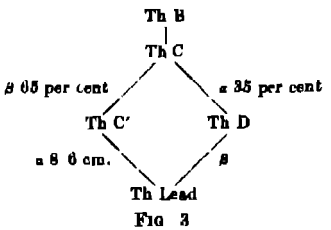

Fig 3

Using the wheel method of counting scintillations, this comparison has been made for sources of Thorium (B + C + D). To ensure that all the

* 'Phil. Mag.,' vol. 43, p. 1038 (1922).

active deposit should be on the front of the source, the metal plate, when exposed to the emanation, was protected by an ebonite cap and backed up by a rubber washer. The way in which the measured gamma-ray effect depends on the thickness of lead surrounding the electroscope is shown in fig. 4.

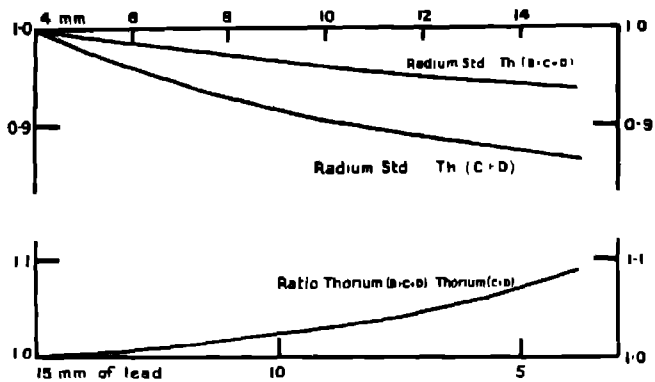

Fig 4.

The curve for Thorium (C + D) given by Shenstone and Schlundt is also shown Since the gamma rays of Thorium B have an absorption coefficient in lead of about 2·0, the gamma-ray effect of a source of (B + C + D) when measured through 15 mm of lead will be due almost entirely to (C + D) alone. Putting them equal at this thickness of lead we obtain the curve in fig 4. The sources used for the beta-ray spectra were measured through 6 mm of lead. At this thickness we see from fig. 4 the ratio is 1·06 Now Shenstone and Schlundt found that the number of alpha particles of range 8·6 cm. emitted by a source of Thorium (C + D) was 0·77 of the number of alpha particles emitted by a source of Radium (B + C) which when measured through 6 mm. of lead had the same gamma-ray effect. It is known that the particles of range 8·6 cm form 65 per cent. of the total from Thorium (C + D), so that the results may be compared.

I have to thank Mr. Wormall, of this laboratory, for his assistance in counting scintillations. When 5,000 particles had been counted, the ratio Thorium to Radium was found to be 1·07 for one observer and 1·06 for the other. From the data given in the preceding paragraph it appears that the value to be expected for (B + C + D) from Shenstone and Schlundt's counting of (C + D) is $\frac{0\cdot77}{0\cdot65\ 1\ 06} = 1\cdot12$. They counted 26,000 particles and claim a probable

error of 2·5 per cent.; so that a value for the ratio of 1·10 is within the probable error of both determinations. The number of disintegrating atoms for equivalent gamma-ray activity is therefore 3 74 10^7 per second per milligram,* taking Geiger's recent value for the number of alpha particles from Radium; Hess and Lawson's value gives 4 09 10^7 as the number for Thorium (B + C + D)

5 *The Number of Beta Particles*

In the diagrams the electron-current has been reduced to a standard sensitivity of 3,000 divisions per volt, and a large correction has been subtracted for particles reflected from the metal plate on which the radioactive material was deposited Schonland has recently measured the amount of reflection of electrons of velocity Hρ 1100, which is where the maximum concentration of particles occurs in fig. 5. He found for aluminium 13 per cent. were reflected, and for nickel 30 per cent Another correction to be applied is 1 per cent to be added for particles which escape from the Faraday cylinder after reflection inside. Corrections of 12 per cent for aluminium and 29 for nickel have therefore been applied.

The method of calculating the solid angle for a line source was given in the previous paper. In the present case it has to be averaged over the surface of the metal plate, the value was found to be 0 048 Owing to the magnetic dispersion the number of beta particles actually entering the Faraday cylinder was a fraction about 1/10,000 of the total number being emitted The electrostatic capacity of the system was redetermined, and it was found that the addition of the compensating chamber had increased the capacity from 87 to 98 cm. A current of one division per minute at standard sensitivity is thus equal to 3,800 electrons per second This means that the total number emitted in all directions which this current represents is $\frac{4\pi \ 3800}{0 \ 048} = 1 \cdot 0$ million electrons.

The method of integrating the spectra to find the total number of particles was described in the previous paper Owing to the much smaller sources available and to their more rapid decay, the accuracy with which the number of particles in the continuous spectra has been determined is less than that obtained for Radium (B + C) using Radon-tubes. The following table gives the approximate number of particles, after making the above corrections for

* For the sake of convenience fig. 1 has been drawn to correspond to the same number of disintegrating atoms as fig. 2, though actually a "milligram" of (C + D) in terms of gamma-ray effect has more disintegrating atoms than (B + C + D) when measured through 6 mm. of lead.

reflection. For Thorium D it must be remembered that the number of disintegrating atoms is only 35 per cent of the number of Thorium B.

—	Divisions per min. per mg	Electrons per sec	Electrons per 100 atoms of Th B
	Thorium B		
Peak at Hρ 1398	0	0 10^6	25
Remainder of Th B Spectrum	45	45 10^6	120
	Thorium D		per 100 atoms of Th D
Peak at Hρ 540	2 7	2 7 10^6	21
Peak at Hρ 670	1 0	1 0 10^6	7 6
	Thorium (C + D)		per 100 atoms of (C + D)
Remainder of spectrum	44	44 10^6	118

It has been pointed out above that the three peaks included in the table are the only beta-ray lines that have been studied The method is not suitable for the investigation of lines which do not stand out as definite peaks

6 *The Internal Conversion Coefficient of the Gamma Rays.*

It is unnecessary to repeat here the argument that the beta-ray lines are due to absorption of the gamma rays not in neighbouring atoms but almost entirely in the atom in which they originate. The origin of a gamma ray is believed to be the transition of the nucleus to a quantised state of lower energy. It is therefore very unlikely that any atom in breaking up should emit more than one gamma-ray quantum of the same energy. The peak of Thorium B at Hρ 1398 is due to the conversion in the K-level of a gamma ray of energy 150,000 volts The peak contains 25 particles per 100 disintegrating atoms, so that if we are right in supposing that no atom can emit more than one quantum of this energy, there cannot be more than 100 gamma rays to produce these 25 beta particles. The chance of a gamma ray being converted in the K-level instead of escaping from the atom must therefore be at least 1 in 4.

The two peaks found for Thorium D are due to the conversion of gamma rays of 40,500 volts Since this is less than the energy of the K-level, absorption in that level is impossible. The peak at Hρ 540, containing 21 electrons per 100 atoms, is due to conversion in the L_1-level, and the other peak, containing 7·6 electrons, to conversion in outer levels Using the same argument as

above, we have at most 100 gamma-ray quanta to produce these 27 electrons, so that the probability of conversion in the atom must be more than 1 in 4. The coefficient for the L-level alone must be more than 1 in 5

These values are even higher than the estimate given previously for Radium B. That calculation was based on Kovarik's experiment, which appeared to show that Radium (B + C) emits two gamma rays per pair of atoms in addition to all the gamma rays which by internal conversion give rise to the beta-ray lines Taking this number it was divided equally between B and C, and the gamma rays of Radium B were then shared out among the various frequencies in the ratio of the observed intensities of the peaks Sixteen gamma-ray quanta per 100 disintegrating atoms would in this way be allotted to the line Hρ 1410, which is the most interesting line to consider, since it has almost the same energy as Hρ 1398 The internal conversion coefficient may well vary with the frequency of the gamma ray, or with the structure of the extra-nuclear levels But since Thorium B is isotopic with Radium B, it would be interesting if the value were different for these two lines of nearly the same energy The number of electrons in the peak at Hρ 1410 was found to be 2 6 per 100 atoms. Thus to give a minimum conversion coefficient of 1 in 4 such as has been found for 1398, we should require the corresponding number of gamma rays to be not more than 10 per 100 atoms. This is quite possible, for we clearly do not know how to share the gamma rays between the lines of Radium B and C It seems clear, however, that the average value of the coefficient is smaller This we should anticipate, since most of the gamma rays are of higher frequency than that giving 1410, and by analogy with external absorption we should expect the absorption to decrease with increasing frequency, the coefficient cannot however decrease so rapidly as λ^3.

The conversion of a soft gamma ray in the L-level is quite analogous to the internal conversion of a quantum of K radiation in the L-level. Values for the coefficient have been found by Auger * and by Bothe.† It has been suggested that the conversion of K radiation is due to a coupling of two electrons, one of which leaves the atom while the other jumps from the L to the K-level. If this is true, then conversion of gamma rays is probably not comparable with that of X-rays, since any coupling between the nucleus and the L-level is likely to be of a different kind

The gamma ray giving the Thorium D peaks has a frequency near that emitted

* 'Comptes Rendus,' vol. 182, pp. 773 and 1215 (1926).

† 'Phys. Z.' vol. 26, p. 410 (1925).

by Radium D. For that gamma ray Gray* deduced an internal conversion coefficient of 0·67. In his calculation he did not, however, take into account the internal conversion of the L radiation in the M ring. This effect is likely to be large, since Auger found a value 0·75 for conversion of the L radiation of Xenon. This would raise the coefficient of the Radium D gamma rays from 0·67 to about 0·9. The size of the Thorium D peaks found here would be consistent with a high value of the coefficient if only about 1 in 3 atoms disintegrating emits a 40,500-gamma ray.

7. *The Continuous Spectra*

The absorption coefficients in aluminium allotted to the beta particles of Thorium C and Thorium D are not very different, 14·4 and 21·6,† while that of Thorium B is 153 0. Since the average velocity of the particles from C and D are nearly the same, we should expect their spectra to be one on top of the other The curve obtained shows no sign of separation into two spectra We expect 35 per cent to belong to C and 65 to D. The total number of particles is sufficient to contain the nuclear electrons of both C and D. We have therefore now six beta-ray bodies known to possess continuous spectra of the appropriate magnitude, Radium B, C and E, Thorium B, C and D. Uranium X_1 has also been shown to possess a continuous spectrum, most intense at 100,000 volts,‡ but the number of beta particles in it is not known There does not seem to be any information about the nuclear electrons of other bodies

If fig. 5 is compared with the curves given previously for Radium B and C, it is seen that a remarkable analogy exists between the two series. The continuous spectra of Radium C and Thorium (C + D) extend over a very wide range of velocities, while those of Radium B and Thorium B are confined to a range of low velocities. Now the important fact emerges that the line spectra of these bodies are confined to the same regions as their continuous spectra. Thus Radium B emits no beta-ray line of velocity greater than Hρ 2480, and Thorium B nothing above Hρ 2095, although the lines of Radium C and Thorium D are spread over a wide range

The continuous spectra and line spectra are roughly co-extensive, and it may be that this points to an important law in beta-ray disintegration ; namely, that no gamma rays of high energy can be emitted by those radioactive bodies

* 'Nature' (Jan. 3, 1925)

† Meyer, 'Jahrb. d. Rad.,' vol. 17, p. 86 (1920); Marsden and Darwin, 'Roy. Soc. Proc.,' vol. 87, p. 17 (1912).

‡ Meitner, 'Z. f. Physik,' vol. 17, p. 54 (1923)

which expel their nuclear electrons with low energies. Another body whose beta particles are known to have low velocities is Radium D. This emits only

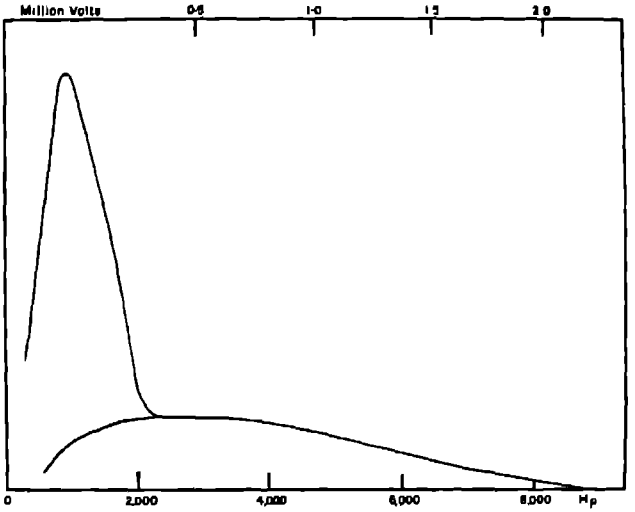

FIG 5.—The vertical scale represents number of particles in arbitrary units.

very soft gamma rays, which may be connected with the fact that its nuclear electrons are slow

The difference between the extent of the line spectra of Radium B and Radium C has been discussed by Ellis and Wooster.* They bring forward an idea due to Mr Skinner, which has also been discussed in more general terms by Meitner, that the limitation of the energies of gamma rays emitted does not at all imply a restriction of the nuclear-level system. The energy of the hardest gamma ray depends only on the level from which the disintegration electron has just been expelled, and the maximum kinetic energy of the nuclear electron itself presumably also depends on the level from which it comes. So that since both are governed by the same factor, it is not surprising that the energies are co-extensive.

8. *The Heating Effect of the Beta Particles*

By integrating the energy in the spectrum we obtain the heating effect due to the kinetic energy carried by the beta particles, as was done for Radium B

* 'Proc. Camb. Phil. Soc.,' vol. 22, p. 849 (1925).

and C. For a source of Thorium (B + C + D) whose gamma-ray activity measured through 6 mm. of lead is the same as that of one gram of Radium, we find the values 4·1 calories per hour due to Thorium (C + D) and 0·65 calories for Thorium B

Summary.

The measurements of the absolute number of beta particles emitted with different velocities in beta-ray spectra have now been extended to the spectra of Thorium B and Thorium (C + D). The separate existence of continuous and line spectra is proved by the presence of the continuous spectrum of Thorium (C + D) in the large gap in the line-spectrum between Hρ 4040 and 10,080 In these spectra, as in the spectra of Radium B, C and E, the total number of particles is found to be consistent with the view that they contain the nuclear electrons, of which there must be one from each atom disintegrating It is suggested that the fact that the energies of the particles in the line spectra of different bodies are roughly co-extensive with the energies of those in the continuous spectra points to a law of beta-ray disintegration, namely, that no gamma rays of high energy can be emitted by those radioactive bodies which expel their nuclear electrons with low energies.

From the measurements of the number of particles in certain beta-ray lines, minimum values have been deduced for the probability that the gamma-ray quantum is concerted into a beta ray instead of escaping from the atom. For the gamma ray of 150,000 volts energy, emitted by Thorium B, it is found that the coefficient of conversion in the K-level must be at least 1 in 4 For the gamma ray of 40,500 volts emitted by Thorium D, the coefficient of conversion in the L-level must be more than 1 in 5.

In conclusion, I wish to express my thanks to Sir Ernest Rutherford for his interest in this work, to Dr. Chadwick for kindly preparing the radioactive sources, and to Dr. Ellis for helpful criticism.

Experiments upon the Reported Transmutation of Mercury into Gold.

By M W. Garrett, B A , Exeter College, Oxford

(Communicated by Prof. F A Lindemann, F R S —Received July 14, 1926)

The possibility of effecting a transmutation of the atom by electronic bombardment, as distinct from the alpha-ray methods so successfully used by Rutherford and others, has attracted attention from time to time in recent years The first to report success in such an experiment was Ramsay, who announced in 1912 the artificial production of helium and neon in X-ray bulbs The controversy aroused by his announcement has not yet subsided, for Riding and Baly have supported quite recently, in this Journal, the genuineness of such a transformation

Miethe,* in 1924, reported the transmutation of mercury into gold, and since the original announcement he has described various experimental arrangements which he claims have proved successful † Two principal methods have been employed by this investigator First, a Jaenicke mercury vapour lamp, operating at atmospheric pressure with a current of 12 5 amperes, a terminal voltage of 170, and a potential gradient of 11 or 12 volts per cm., was run for 20 to 200 hours, and amounts of gold up to 0·1 mg reported, though no direct proportionality existed between the quantity of gold and the number of hours run. Miethe also reported the formation of silver in these experiments, often in larger amounts than the gold, and stated that the yield of noble metals was increased by irregular burning of the arc, with frequent extinction and relighting No gold was obtained from vacuum arcs The second method was a development of the first, in which the effect of irregular burning was artificially enhanced by constant interruption of the arc. The final simplified form of this experiment consisted in the employment of an ordinary rotating mercury interrupter, and with this apparatus Miethe states that he obtained for the first time consistently reproducible results, a direct proportionality existing between the number of ampere hours run and the yield of gold (about 4×10^{-7} gm. per ampere hour.) He also describes a series of experiments in which one and the same quantity of mercury (ca. 1·5 kg) was submitted to a number of successive runs, about a score in all, when no diminution of the

* 'Naturw ,' vol 12, p 597 (1924) ; 'Nature,' vol. 114, p. 197 (1924).

† Stammreich, 'Naturw ,' vol. 12, p 744 (1924) ; Miethe and Stammreich, 'Naturw.,' vol. 13, p. 635 (1925) . 'Z. techn. Phys..' vol. 6, p. 74 (1925) ; 'Z. anorg. Ch.,' vol. 150, p. 350 (1926).

yield was observed. He states that self-inductance was here found to be absolutely without effect, though from certain earlier experiments he had believed that the inclusion of an inductance in the circuit increased the yield. No mention is made of the production of silver in these experiments

Nagaoka,* working quite independently, used an induction coil capable of giving a spark of 120 cm length. With a capacity of 0 002μ F in parallel and a secondary current of 10 ma he sparked for four hours between a tungsten pole and a mercury surface under transformer oil, until the entire mass carbonised. He then tested for gold by methods which, though they could give no quantitative idea of the amount present, seem to have been qualitatively reliable, and he states that all the tests were unmistakably positive In a second, somewhat different, experiment he found mainly silver

It seemed worth while to make some attempt to confirm or refute these experiments, more especially since there appeared, shortly afterwards, an announcement by Smits† that he had succeeded in transmuting lead into thallium and mercury by a somewhat similar method When the work described in this paper was undertaken, only the positive results outlined above were extant. Since then, no further positive results have been reported, whereas negative results have been announced by various experimenters‡ operating under diverse conditions Of these the work of Haber is the most complete, as well as the most recent. In some cases the published papers contain so few details of experimental conditions, duration of the runs, and analytical methods, that it is difficult to draw any conclusions from them A general discussion of the various results will be postponed until after the description of the experimental work carried out by the writer has been completed

Experimental

Distillation of the Mercury

The mercury employed in these experiments was taken from a single stock prepared by two successive distillations and kept in a glass-stoppered bottle

* 'Naturw.,' vol 13, p 692 (1925), and vol. 14, p. 85 (1926); 'Nature,' vol. 116, p. 95 (1925), 'J Physique et Ra.,' vol. 6, p. 209 (1925).

† 'Naturw.,' vol. 13, p. 699 (1925), 'Nature,' vol. 117, p. 13 (1926) (An examination of the results of Smits is now in progress, and it is hoped to be able to report upon it, as well as upon certain related work, in the near future.)

‡ Sheldon and Estey, 'Sci. Amer.,' p. 296 (Nov., 1925), and p. 389 (Dec., 1925); 'Nature,' vol. 116, p. 792 (1925), Tiede, Schleede and Goldschmidt, 'Naturw.,' vol. 13, p. 745 (1925), Piutti and Boggio-Lera, 'Rendic. Accad. Sci. Fis. Mat.' (Naples) (Sept.–Dec., 1925); 'Nature,' vol. 117, p. 604 (1926), Haber, Jaenicke and Matthias, 'Naturw.,' vol. 14, p 405 (1926); 'Z. anorg Ch.,' vol 153, p. 153 (1926).

Two identical stills of Pyrex glass were employed, one for each stage of the distillation. These were of ordinary design, consisting of a wide inverted U-tube and two narrow limbs of barometric height dipping into reservoirs of mercury When once exhausted, baked out and sealed, they were quite continuous in operation, it being necessary only to pour the mercury into one side and draw it off from the other They were electrically heated by means of nichrome coils of high resistance, so that only 50 watts were expended in heating in each still, and in spite of the wide tubes (3 cm) and water cooling, the rate of distillation was only about 100 gm per hour Under these circumstances the temperature of the mercury did not rise much above 150°, and evaporation took place quietly from the surface Since the whole of the input side of the still was heavily lagged with asbestos cord, any particles which might be situated in the free space above the mercury were not subjected to any unnecessarily heavy differential molecular bombardment from below (as in a mercury vapour pump), and there was no tendency for surface impurities to be mechanically carried over with the vapour

These details are mentioned here because of the fierce (and somewhat pointless) battle which has been waged over the question of whether the noble metals are completely removed from mercury by distillation This question is of some interest in itself, but its importance to the transmutation controversy has been greatly over-estimated For Miethe has regularly analysed his mercury after its electrical treatment by the same process which he employed before it, and his blank experiments have been invariably negative The question of whether distillation removes all traces of gold is thus clearly resolved into the question of whether distillation removes electrically treated gold more efficiently than it does ordinary gold. Nobody has yet attacked this problem experimentally , or rather this problem is, experimentally considered, practically identical with the transmutation question proper.

Hulett, Riesenfeld and Haase, and Tiede have all reported* that gold distills over in small quantities with mercury, though all except Tiede agreed that two or three distillations even of a strong amalgam were sufficient to reduce the concentration of gold to the extreme limit detectable. Tiede found that under certain conditions the gold actually concentrated itself in the distillate, a sufficiently improbable result which is in want of confirmation.

Miethe and Stammreich,† as the result of methodical experiments on the

* Hulett, 'Phys. Rev ,' vol. 33, p. 308 (1911); Riesenfeld and Haase, 'Ber. deutsch. Ch. Ges ,' vol 58, p. 2828 (1925); Tiede, 'Phys Z ,' vol 26, p. 845 (1925).

† 'Phys Z ,' vol 26, p 842 (1925); 'Ber deutsch. Ch. Ges.,' vol. 59, p. 359 (1926); 'Z. anorg. Ch ,' vol 149, p. 263 (1925)

distillation of amalgams of various metals, have concluded that with proper precautions these metals pass over into the distillate only by virtue of their own proper vapour pressure (*i.e.*, in very small amounts, so small as to lie beyond the limits of detection in the case of the noble metals). They believe that where gold is not removed from mercury by a single distillation, the cause is to be sought in small particles of it having been carried over mechanically with droplets of mercury which have reached the receiver without passing through the vapour phase at all. This form of mechanical contamination can be eliminated by careful attention to the design of the apparatus and regulation of the conditions of distillation. They quote Michaelis in support of this view, which is shared by the present writer, and is capable of explaining the results of the other experimenters. Hulett distilled at a pressure of over a centimetre with a stream of air bubbling through the mercury, while the work of Riesenfeld and Haase is fragmentary, and is otherwise open to grave objections which have been pointed out by Miethe. Never in the course of the experiments described below has it been found possible to detect gold in mercury which had been distilled, though in the course of the preliminary analytical practice some moderately strong amalgams were distilled.

Analytical Procedure.

Methods of analysis have been described by Haber,* and by Miethe and Stammreich †. The method employed in the present research was essentially that of Miethe. This consists in distilling off the mercury till only about one gram remains, and dissolving up this last drop, under the microscope, in nitric acid of specific gravity 1·20, free from all traces of hydrochloric acid. The gold remains behind as metal, and may be estimated by fusing it in borax and measuring the diameter of the resulting sphere.

This method of analysis was tested on 100 gm. samples of mercury to which known small quantities of gold had been added, and it was found possible to detect 10^{-7} gm., and afterwards, with improved microscopy, 10^{-8} gm. of gold with absolute regularity. It was also repeatedly proved that no gold could be detected in the stock of distilled mercury when analysed by this method. There can be no question that the analysis could have been rendered still more sensitive, but a suitable microscope was not at hand, and it was considered

* Haber, Jaenicke and Matthias, *loc. cit.*, and Haber and Jaenicke, 'Z. anorg. Ch.,' vol. 147, p. 156 (1925).

† 'Z. anorg. Ch.,' vol. 140, p. 368 (1924), and vol. 148, p. 93 (1925).

that quantities of gold less than 10^{-8} gm could have no significance in testing methods said to be capable of producing 10^{-4} gm with moderate energy inputs, particularly since the danger of error through accidental contamination becomes quite large when working with quantities below 10^{-8} gm

All the experiments were so designed as to require minimal quantities of mercury, never more than 100 gm and rarely as much as 50 It is perhaps unnecessary to add that all the vessels employed in the research had been carefully cleaned with boiling aqua regia

Spark Methods

The first experiments were similar to those of Nagaoka, but with slight modifications A transformer giving a peak voltage of 15,000 was employed, with a condenser of 0·006μ F capacity The spark was passed between tungsten wires in a glass vessel containing an emulsion of fine mercury drops in white paraffin oil Miethe, in similar sparking experiments, had always found the gold concentrated entirely in the small droplets of mercury dispersed along the path of the discharge, and the above method, by starting with a fine emulsion, permitted the main mass of inert mercury to be eliminated altogether from the experiment, less than 10 gm being required for each run. Furthermore, in experimenting on the Stark effect in silver arcs Nagaoka had found that the presence of small droplets resulted in a marked local intensification of the potential gradient. It was found necessary to place the two wires constituting the spark gap less than 2 mm apart in order to permit the spark to pass, so that although the actual voltage was much below that employed by Nagaoka, the potential gradient remained substantially the same. The gradient is, in fact, determined by the dielectric strength of the oil, and it should be noted that even this initial gradient becomes much reduced as the experiment proceeds and the oil is carbonised The larger condenser permitted heavier secondary currents (20–30 ma.) to be employed than those used by Nagaoka, and the transformer delivered a much steadier voltage than is obtained from an induction coil.

Considerable trouble was experienced with the bursting of the glass vessel and the splashing of the emulsion, and the final form of apparatus employed was a glass tube about 6 cm. deep by 2 cm. in diameter, with a widely flared top ground flat and held against a sheet of ebonite by rubber bands. The tungsten wires were carried by thick-walled glass capillaries inserted through the ebonite. The sparking vessel was water-cooled It was found possible to run about

half an hour before the oil solidified completely and showed a tendency to arc. The mixture of miscellaneous organic matter, mercury and carbon was then transferred to a Pyrex flask and distilled in an electric furnace, when the carbon remained behind This was oxidised by heating in a stream of oxygen, leaving hardly a trace of residue of any kind The flask was now washed out with hot aqua regia, the solution diluted, and a small drop of mercury added. When this had dissolved, the solution was make alkaline with ammonia, and the mercury reprecipitated by the addition of ammoniacal 6 per cent hydrazine sulphate solution The mercury drop, which would have carried down with it any gold present was filtered off, washed, and dissolved up as usual, under the microscope, in dilute nitric acid This experiment was repeated several times, with uniformly negative results.

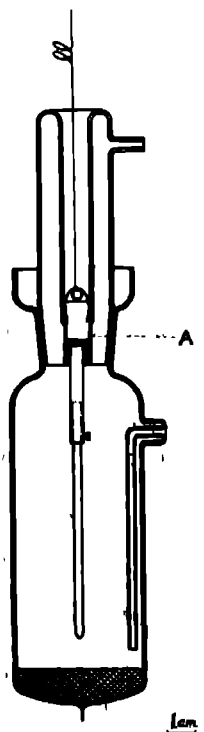

Fig. 1

Distilled water was then substituted for the oil, in the hope that it could be made to run longer without losing its insulating properties Aluminium electrodes were employed, and the emulsion was prepared by passing an arc at 100 volts between an aluminium pole and mercury at the bottom of a beaker of distilled water But the water always became conducting after 20 minutes to half an hour, and the explosive spark at first produced could no longer be maintained One lot of mercury in water emulsion was analysed after about 25 minutes' run, but no gold was found

Longer runs and larger energy inputs were found possible when hydrogen was used as the dielectric. The apparatus used is sketched in fig 1 It was constructed in Pyrex, with a tungsten wire sealed into the bottom to establish contact with the mercury pole The other pole consisted of a 4 mm. iron rod, clamped by means of a set-screw into a steel tube attached to the copper electrode A, The latter was turned down to a thin tube at its upper end, and sealed directly into the central glass tube carried by the ground joint This electrode was kept cool by the boiling of water which filled the central glass tube, and the mercury pole was cooled in a similar manner by a vessel of water in which the outer tube was immersed The apparatus was connected during the experiment to a reservoir of hydrogen, and the ground joint fitted so well

that without any lubrication only a few cubic centimetres of hydrogen per hour escaped through it.

With a spark gap of about 1 cm and a capacity of 0·01μ F, the secondary current of the 15,000-volt transformer was 75 ma., and the current in the spark gap 15–20 amperes. A limit to the useful length of a run was set by the contamination of mercury and glass by fine dust from the iron pole, which burned away at the rate of about half a millimetre an hour, so that the apparatus had to be continually reopened and this pole reset. Two analyses were made on runs with this apparatus, one after five hours and one after twelve. The liquid mercury was mechanically separated from the superincumbent emulsion of finely divided mercury and iron dust, the former was distilled to a residue of 1 gm., and the latter digested with aqua regia until all the mercury had dissolved. The residue from the distillation was dissolved in the solution containing the extract of the emulsion, the mercury precipitated with hydrazine, and the remainder of the analysis proceeded with as usual. The result was negative in both cases.

The conditions in such a spark discharge might be expected to be very favourable to the formation of gold. In the first place, it seems highly probable that doubly charged ions of mercury are present, the significance of this fact will be discussed hereafter. The spectrum of this spark showed a very different intensity distribution from that of the mercury vapour lamp, the three lines 6149, 5679 and 5425 being among the strongest on the plate. The light was nearly white except at the iron pole, where it was coloured quite red by a preponderance of the Hα line.

In the second place, Miethe concluded, from the irregularity of his early results, that the formation of gold depended upon the exact reproduction of certain conditions of potential gradient and current density, which he was unable to define, but which he assumed his arcs passed through at some stage during the changes accompanying extinction and relighting. Now in an oscillatory discharge such as that here employed, the current varies between a maximum value of several hundred amperes and zero, and the voltage between the limits of 15,000 and zero, so that at some time during the cycle the favourable conditions should be reproduced, and the cycle is repeated 100 times per second.

Interrupted Arc Method.

A method was now developed which proved capable of giving more decisive results. Miethe has constantly maintained that the earlier forms of experiment which he employed did not yield consistently reproducible results, and has on

occasion attributed the failure of other experimenters to this fact. But from the first he has considered the interrupted direct-current arc to be quite reliable, and in particular he has found a reasonable proportionality between energy input and yield of gold when using a mercury interrupter of standard design. It was considered desirable, accordingly, to repeat these experiments in some form, but the objections to the ordinary type of interrupter are considerable. It makes use of large electrodes of copper in a case consisting of enamelled iron or some similar material. It is difficult to ensure that these materials are quite free from gold, and since the electric discharge plays continually over their surface and they are gradually worn away, there is great danger of contamination from this source. Large quantities of mercury (1·5 kg.) must be used, and the mercury emerges in a very dirty condition from the run, so that the analytical procedure is also rather unsatisfactory. The "blank" experiments of Miethe (in which the interrupter ran without current and no gold was found) are not convincing as proof that the gold did not arise by contamination from the electrodes, since in this case there is no sparking at the electrode surfaces. It would be interesting to know whether the mercury did not emerge in a cleaner condition from such a "blank" determination, as might have been expected.

To obviate several of these difficulties the construction of an all-glass mercury interrupter, with mercury cups in place of the copper electrodes, was undertaken. Such an interrupter was actually completed, but it was never used, since a much simpler design was evolved which permitted the use of minimal quantities of material and the removal of the foreign electrodes to a point remote from the discharge, while preserving the essential features of the break.

The apparatus consisted of a tube such as that sketched in fig. 2. This was filled with an amount of mercury indicated in the diagram, sealed off in an atmosphere of hydrogen, and fastened to a machine which swung it back and forth in arcs of 50–60° about the point 0, the 100-volt mains being connected to the two ends of the tube. The mercury in the two branches flowed together and then separated twice in every swing, an arc being formed and pulled out to extinction each time. Six or eight interruptions per second were obtained in this way, and the sharpness of the break was attested by the intense condensed spark obtained in the secondary circuit of an induction coil when the break was inserted in the primary circuit. Such tubes were first constructed of Pyrex, with 0·5 mm. tungsten wires sealed into the legs. But the current-carrying capacity of the Pyrex tubes was limited to about 12–15 amperes (at make), and their life to some 60–70 hours. The intense local sparking removed small flakes from the glass surface, which soon became covered with a network of

fine cracks, the mercury was slightly contaminated, and the Pyrex in time blackened. A number of tubes burst after some hours' sparking Nevertheless,

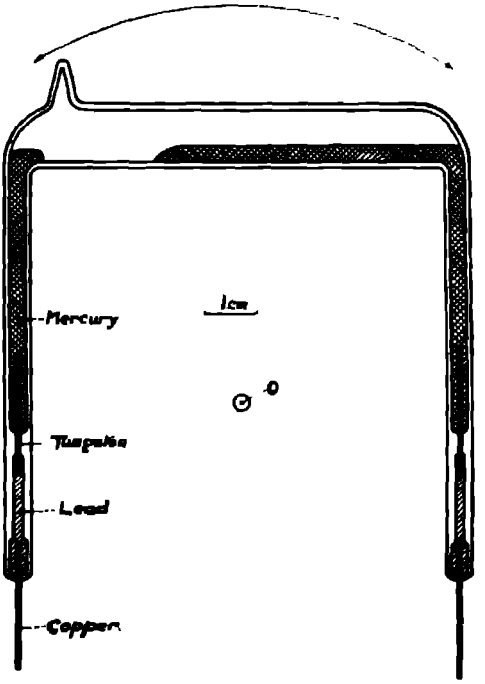

FIG 1

three runs were obtained with Pyrex tubes, the current at make averaging 13 amperes, and the duration of sparking 55 hours. No gold was found in the mercury from these tubes.

A similar tube was now constructed from quartz, as soon as a suitable technique had been developed for making the seals into this material. The 0 5 mm. molybdenum wire to be used was first heated to incandescence *in vacuo* to remove occluded gases, and the quartz was then shrunk upon the molybdenum, also *in vacuo*, and the seal completed by means of pure lead and a short length of copper wire. Such seals were always found to be quite vacuum-tight, but as an additional precaution the hydrogen was introduced, after baking out and filling with mercury, at such a pressure that the constriction would only just collapse on sealing the tube off from the pump. This ensured a pressure greater

than atmospheric at all times on the mercury at the seal, and particularly when the tube was heated by the arc.

It was found possible to operate this tube indefinitely with 30-ampere sparks at 100 volts The mean current was given as 10 amperes by a thermal junction constructed of 22-gauge copper and eureka wires, mounted in a brass case immersed in water, and calibrated on direct current. The tube was run under these conditions for 144 hours It was then operated from a direct-current dynamo, delivering 240 volts in 18 ampere sparks (7 amperes average) for a further 144 hours During the last 24 hours of this run, the primary of an induction coil was included in the circuit, energy being drawn from the secondary in the form of a condensed spark discharge in air At the end of this time the quartz tube remained as clear as at the beginning of the experiment, while the mercury surface was perfectly bright and uncontaminated. The tube was, in fact, indistinguishable in appearance from a fresh one

In the analysis of this run, distillation was avoided, on account of the controversy referred to above Two samples of 15 gm each were drawn from the stock bottle of distilled mercury. To one of these was added 10^{-8} gm of gold Both samples were dissolved in nitric acid, also ready mixed in a stock bottle. The 10^{-8} gm of gold was identified without question by several people when the mercury to which it had been added had dissolved The other sample of mercury left no residue whatever The quartz tube was now opened and found to contain 18·8 gm of mercury, which was dissolved up at once in acid from the same stock bottle as had been used for the blanks. It left behind a residue about 0 03 mm in diameter, consisting of a flattened reticulated skeleton of some dark material, presumably silica Not a trace of the lustre of metallic gold could be discerned The blank tests which were carried out simultaneously with this analysis remove all doubt as to the sensitiveness of the test. 10^{-8} gm. of gold could have been detected with absolute certainty.

It is easy to form a rough idea of the amount of gold which should have been expected in this experiment according to the results obtained by Miethe. If we take the efficiency of the arrangement, expressed in grams of gold per ampere hour, to be the same as that of Miethe's rotating mercury interrupter, we arrive at an estimate of 1 mg. of gold, an amount larger than that which any experimenter has claimed to produce in a single run A more accurate estimate is probably obtained by considering the number of "ampere sparks." That is, if Miethe's view of a "labile state" passed through by the arc once in each cycle is correct, an approximately constant amount of gold should be produced each time an arc of 1 ampere is made and extinguished, and Miethe's

own results indicate that the yield is directly proportional to the current for the same number of interrupted arcs, hence, we arrive at the "ampere spark" as the effective unit of gold-producing electrical energy. Assuming now four interruptions per second (a very conservative figure) in the quartz tube, and taking Miethe's figure of 2,000 per minute for the frequency of interruption in his mercury break, the above estimate is reduced to 0·11 mg., which is still at least 11,000 times the amount of any gold which may actually have been produced.

Discussion

There are various theoretical objections to the work of Miethe and of Nagaoka. Perhaps the most cogent arises from a consideration of the voltages which they employed in their experiments. In order to bring about a transmutation of the atom, it is first necessary that the bombarding particle—in this case an electron—should penetrate the successive electronic orbits, and gain access to the nucleus. The most obvious method of ensuring this is to make use of electrons of sufficient velocity to excite the hardest K radiation of the element in question. The corresponding voltage, in the case of mercury, is about 83,000, and though Nagaoka employed considerably higher terminal voltages than this, it is impossible that any individual electron could have possessed more than a small fraction of the required velocity, for the potential gradient in these experiments was about 15,000 volts per millimetre, so that the electron would have to fall freely through the field for a distance of 5·5 mm. in order to attain the velocity in question. The actual free path must have been of quite a different order of magnitude from this, and it is, of course, well known that the K spectra are not excited under the conditions of Nagaoka's experiment. The highest electronic velocities hitherto applied to the transmutation of mercury were probably those employed by Haber in his experiments with an X-ray bulb whose anticathode consisted of frozen mercury, but here a voltage of 8,000 was not exceeded.

However, the work of Ramsauer* and others on the rare gases indicates that under certain conditions these extreme electronic velocities may not be necessary, for certain atoms show a marked transparency to very low-voltage electrons. Where such a property exists, it is obviously of advantage to use as low a voltage as possible, partly because a slow-moving electron, once safely inside the innermost electronic orbit, might be expected to be more readily attracted into the nucleus than a fast one, but principally because with low voltages it

* 'Ann. d. Physik,' vol. 64, p. 513, and vol. 66, p. 546 (1921).

is possible to use much larger currents, and thus by increasing the number of electrons to ensure a greater chance of scoring a hit upon the nucleus.

Brode* has examined the mean free path in mercury vapour of electrons possessing velocities between 0·4 and 150 volts, and has found between these limits no indication of any special transparency of the mercury atom, neither does extrapolation of his curves suggest the existence of any such property at other voltages Thus it begins to appear doubtful whether any of the electrons in the various transmutation experiments really had access to the mercury nucleus at all. Franck has suggested that doubly charged ions might resemble a rare gas to such an extent as to exhibit transparency to electrons of certain velocities, but an experiment described in this paper, as well as a somewhat similar one performed by Haber, in both of which such doubly charged ions were probably fairly numerous, proved quite as incapable as the rest of yielding gold

We cannot altogether reject the possibility that the electron, once inside the innermost planetary orbit, should be attracted towards the nucleus and might fall into it This might occur with such violence as to produce disruption of the nucleus, or, alternatively, the invading electron might be captured and remain permanently attached to the nucleus, thereby giving rise to the inverse of a beta-ray disintegration, and reducing the atomic number by one unit The latter seems the more likely alternative, though Nagaoka has supported the former. He was led to undertake his experiments by observations on the spectrum of mercury, from which he concluded that the nucleus contained a quasi-elastically bound proton which might be dislodged by bombardment with very swift electrons. But the theory of Nagaoka has been attacked by Runge† and the experimental work by Wood.‡ The theory was based, moreover, on a list of the isotopes of mercury, which has since been revised by Aston.

If a transmutation of the inverse beta-ray type is to occur at all, the most hopeful case would seem to be that of two neighbouring elements in the periodic table exhibiting isobarism. Unfortunately, Aston's table of isotopes does not reveal a single established case of such a relation, though the isotopes of gold, lead and thallium, all of which are involved in the reported transmutations, have not yet been established. Hönigschmid's determination of the atomic weight of Miethe's gold, though a triumph of analytical chemistry, has lost its significance in view of Miethe's recent statement (at a meeting of

* 'Roy. Soc Proc.,' A, vol. 109, p. 397 (1925).
† 'Nature,' vol. 113, p 781 (1924)
‡ 'Nature,' vol. 115, p. 46 (1925).

the German Chemical Society, May 10, 1926) that the gold which he submitted to Hönigschmid for this determination was not actually produced by himself under known conditions, but was obtained from residues found in old mercury lamps

In the present state of our knowledge of atomic physics, it is difficult to form an estimate of the importance of these theoretical considerations In the circumstances, therefore, it is perhaps safest to regard the whole question from the purely experimental point of view When this is done, it is found that the various experimenters have arrived at mutually incompatible conclusions Further, it seems probable that the cause of the contradiction is not to be sought in a difference in the electrical conditions of the experiments Granted that the formation of gold is bound up with some one particular set of conditions (potential gradient, current density, etc), and that these conditions are difficult to reproduce, it may perhaps be argued that no single set of similar experiments leading to negative results is convincing But when the wide diversity of the experimental arrangements which have failed in the hands of several investigators to produce gold is considered, it appears that every positive experiment has been adequately confuted by a negative one

Miethe has always refused to recognise the validity of any negative results obtained by repeating his own earlier experiments, on the ground that only the interrupted-arc methods are capable of giving consistently reproducible results. He is justified in taking this stand, but the interrupter experiments now appear to be at least as conclusively negatived as any of the rest by one of Haber's experiments, in which the fluctuating current passed by a rotating mercury interrupter was made to traverse a mercury vapour lamp, and more particularly by the quartz tube experiment described in this paper, where the electrical conditions were to all intents and purposes identical with those existing in the interrupter experiments of Miethe. For it is hardly conceivable that the actual difference in speed of motion of the mercury in the two cases can appreciably affect the electrical conditions, when it is considered that the maximum velocity of the mercury jet in a rotating break is very small compared with the electronic and even molecular velocities The abrupt and complete extinction of the arc in the tilting quartz tube was shown by the efficiency of the apparatus as an interrupter for an induction coil, by the small ratio of mean to short-circuit current, and by the behaviour of an incandescent lamp connected across the terminals of the tube. Even if one admits a slight difference between the electrical conditions in this experiment and Miethe's, to assume that it could be such as to yield large quantities of gold in the one case and absolutely none in

the other is quite inconsistent with Miethe's own earlier work on continuously burning and interrupted arcs The explanation of the discrepancy between Miethe's results and those described in this paper must be sought elsewhere.

Much the most probable explanation seems to be that Miethe's gold was derived from the electrodes or other materials of the vessels used, though this conclusion is not altogether satisfactory, in view of Miethe's statement that the purity of all the materials he employed was "dauernd kontrolliert" Further details of these controls would seem desirable

Perhaps also it is straining a point to attempt to explain in this way the direct proportionality which he obtained between power input and yield of gold, but it is possible, particularly since discrepancies of the order of 40 per cent were found In this connection it is significant that the method which has given the most consistently reproducible results is one which is so conspicuously untidy that only the most rigid proof will serve to eliminate the suspicion of contamination Apart from the interrupter experiments, it is in general true that the most successful arrangements were the least satisfactory from the point of view of cleanliness

Additional support is lent to this view by a consideration of the status of the silver question Silver was found and reported in many of the earlier experiments, both of Miethe and of Nagaoka, but Miethe makes no mention of it in his later experiments, and has apparently ceased to estimate it. The whole question has been allowed to lapse until Haber in a recent paper called attention to its importance It is almost inconceivable that the silver could be formed by disruption of the mercury atom, and if silver can find its way into the mercury by accidental contamination during the course of the experiments, there is nothing to exclude the possibility of the gold having a similar origin. It would thus seem to be a matter of the utmost importance to determine the silver simultaneously with the gold in every experiment in which gold is believed to be produced, as a direct check upon the thoroughness with which accidental contamination has been eliminated It is unfortunate that Miethe has not continued to carry out this estimation in all his experiments.

Haber has also reached the conclusion that Miethe's gold came from his electrodes, and has given experimental evidence in support of his conclusions, though it must be admitted that this evidence is not altogether consistent with the results of the experiments described in this paper, for, if contamination from the materials of the seals occurs as readily as Haber has found, it is difficult to understand the uniformly negative results of the present investigation. The writer feels that some of the results of Haber stand themselves in

need of further elucidation. In one experiment, in particular, he found an astonishing result. Here 97 per cent. of the entire gold content of several grams of nickel and steel wire, employed in the seals of a hot-filament discharge tube, diffused in some extraordinary way to the surface of the wire, whence it evaporated and found its way quantitatively to the mercury anticathode, from which it was recovered by analysis This surprising observation, if confirmed, would be capable of explaining in a perfectly satisfactory manner most, if not all, of the discordant results obtained by the various experimenters Haber, in a very recent paper (already quoted) has announced his intention of further investigating this phenomenon. In the meantime, an experiment has been carried out by the writer in an attempt to explain it, but without success

Ordinary diffusion seems powerless to account for such a remarkable result, though it might possibly be brought about by some novel form of electrolysis To test this point, a small glass tube was divided into a number of air-tight compartments by shrinking the wall upon pieces of nickel-steel sealing-in wires, which served to establish electrical connection between successive compartments Alternate cells were now filled with pure mercury and a 0·1 per cent gold amalgam, each pure mercury compartment having amalgam on both sides of it, so as to catch gold electrolysing either way A current of 2·5–3 amperes was passed in series through this tube and a similar one containing pure mercury throughout (to provide a blank in case of any positive result) for a number of hours Tubes were analysed after runs of 250, 570 and 820 ampere hours respectively, and again it was proved by direct simultaneous determination that 10^{-8} gm. of gold could have been detected had it been present No gold was found Further results of Haber will be awaited with interest

Summary

The transmutation of mercury into gold, reported by Miethe and Stammreich, and by Nagaoka, has not been confirmed. The methods employed were as follows —

A.—Condensed spark discharges at 15,000 volts were passed—

1. Between tungsten electrodes immersed in an emulsion of mercury droplets in transformer oil.
2. Between aluminium electrodes under the surface of distilled water carrying mercury in suspension
3. Between an iron pole and a mercury surface in an atmosphere of hydrogen.

B.—An interrupted direct-current arc of 30 amperes at 100 volts was run for six days and nights between pure mercury poles in an atmosphere of hydrogen in a quartz tube, followed by a similar arc of 18 amperes at 240 volts for an equal period. Only 18·8 gm. of mercury were used, and the analysis was carried out without distillation, simultaneously with appropriate blank tests, which proved that 10^{-8} gm. of gold, had such a quantity been present, could not have escaped detection. No gold was found.

Special stress is laid upon the last experiment, which duplicates the electrical conditions obtaining in the "most reliable" method of Miethe and Stammreich, while avoiding the attendant danger of contamination from foreign electrodes, and which should, in accordance with the results of these investigators, have yielded gold in quantities at least 10^4 times greater than the amount which could have been detected under the conditions of the experiment.

Since the work of Miethe and Stammreich, in so far as it has dealt with analytical methods and with the distillation of mercury, has been in the main confirmed, the most probable inference is that the gold which they obtained was derived from the materials of their electrodes and their vessels. The same conclusion has been reached by Haber, but it is pointed out that some of the experiments which he has described to prove this point are themselves in need of further explanation.

In conclusion, I wish to thank Prof. F. A. Lindemann for his kind and never-failing interest throughout the work, and for numerous highly valuable suggestions at every stage of its progress. The work described in this paper was carried out at the Clarendon Laboratory, Oxford, under his supervision.

Acknowledgment is also due to the International Education Board, whose generous financial assistance rendered the work possible.

The More Refrangible Band System of Cyanogen as Developed in Active Nitrogen.

By W Jevons, Ph D , A R C Sc , Senior Lecturer in Physics in the Artillery College, Woolwich.

(Communicated by Prof A. Fowler, F R S —Received June 9, 1926)

[Plates 13 and 14]

1 *Introductory.*

In 1911 Lord Rayleigh and Prof A. Fowler* observed that when the vapour of a carbon compound is introduced into the afterglow of active nitrogen, the two CN systems— the so-called " red " and " violet " systems- -are developed, but their appearance in this source is strikingly different from the more familiar appearance of the same bands in the carbon arc in air The " violet " system as ordinarily observed in the arc, comprises the four well-known groups† of bands which degrade towards the further ultra-violet from prominent heads at λλ 4606, 4216, 3883 and 3590 respectively, and four groups of weaker bands, the so-called " tail " bands, degrading towards the red The modifications of the λ 4216 and λ 3883 groups are shown in figs 4 and 5 of Plate 6, in Rayleigh and Fowler's paper. The description of these modifications will be much facilitated by reference to Table 1, which shows the wave-lengths and wave-numbers of the band-heads, and the initial and final vibrational quantum numbers (n', n'') for the bands, as well as other particulars to which frequent reference will be made later. The modifications are conveniently described as two effects .—

First Effect.—In the typical case of the λ 4216 ($n'' - n' = +1$) group in the afterglow, there is a modified development of the lines of the first (0, 1) and the third (2, 3) bands, and a partial suppression of the heads of the second (1, 2) and fourth (3, 4) bands. The lines near the head of the (0, 1) band in the afterglow are apparently identical with lines in the corresponding part of the same band in the arc, but at a short distance, about 9 A U., from the head there is a

* Strutt and Fowler, ' Roy. Soc. Proc.,' A, vol. 86, p. 112 (1912).

† Throughout this paper the word " group " is used in the sense in which it was employed by Rayleigh and Fowler, and by the writer in a recent paper (' Roy. Soc. Proc.,' A, vol. 110, p. 365 (1926)); *i.e.*, to denote a set of neighbouring bands characterised by a common value of $n'' - n'$, designated a " band-sequence " in the recent work of many of the American investigators.

conspicuous gap of about 3 A.U., beyond which the lines recover in intensity and overrun the weakened (1, 2) head. The (2, 3) band, though not nearly so strong as the (0, 1), shows a similar gap and regain of intensity, its lines overrunning the weakened (3, 4) head. A similar effect occurs in the λ 3883 ($n'' - n' = 0$) group.

Second Effect.—While in the arc the bands of each group gradually diminish in intensity from the less to the more refrangible end of the group, *i.e.*, in the direction of increasing vibrational quantum numbers, in the afterglow the more refrangible end of each of the three groups λ 4606, λ 4216, λ 3883 shows a marked increase of intensity, which, according to Rayleigh and Fowler, "may possibly be due to a local intensification of some of the series of structure lines, or to the introduction of entirely new bands. Until still greater resolving power can be employed, it will be difficult to determine the exact nature of the difference, but the development of new bands offers the simplest explanation. In favour of this view is the observation that the structure lines of the afterglow bands do not all occur in the bands of the arc, and also the fact that in some of the photographs the supposed new bands are far stronger than the first heads of the groups. Assuming that new bands are developed, their less refrangible edges would be about 4495 (in the 4606 group), 4153 (in the 4216 group)* and 3850 (in the 3883 group)."

From a study of Rayleigh and Fowler's published photographs of the λ 3883 and λ 4216 groups Birge has given a complete interpretation of the *First Effect*, ascribing it to the low temperature of the active nitrogen. The *Second Effect* finds its interpretation in Mulliken's recent discussions of band intensities. Reference to these interpretations is made later (section 4).

In 1913, the writer, working in Prof. Fowler's Laboratory, photographed the violet system as developed by acetylene in active nitrogen, under higher dispersion than that of the Littrow spectrograph used by Rayleigh and Fowler. An Eagle-mounted Rowland concave grating (10 feet radius of curvature, 14,438 lines per inch) was employed, the first order dispersion being about 5·52 A /mm. The present communication records the result of an examination of the most satisfactory of the first order spectrograms then obtained with an "Imperial Flashlight" plate exposed for about an hour. It includes all four prominent groups of the system, though the λ 4606 ($n'' - n' = +2$) group is only very faintly shown on account of the diminished plate sensitivity in that region; the other three are reproduced in Plates 13 and 14. A second

* In the case of the λ 4216 group the "new" head was recorded in the arc by A. S. King and by Heurlinger; it is the head of the (5, 6) band (see Table I).

order plate of the λ 3883 group was obtained with the same grating, but it is not quite as suitable for reproduction.

The writer's main object has been to discuss in some detail the modification of the λ 3590 ($n'' - n' = -1$) group, which was not included in Rayleigh and Fowler's investigation. Some data obtained for the "tail" bands near λ 3883 are also included (section 6), since these present a general resemblance to bands of the λ 3590 group in the afterglow. Before proceeding to the afterglow observations, however, reference is made in section 2 to the analysis of the available arc data, and to the representation of the system by formulæ. This is followed in section 3 by an application of the combination principle as a check on the formulæ for the λ 3590 group, in section 4 a brief account is given of the grating photographs of the λ 4216 and λ 3883 groups, with reference to the rotational and vibrational distributions of intensity, these sections being preliminary to the discussion of the λ 3590 group in section 5.

2. *The Structure in the Arc.*

As developed in the arc, the band lines of the λ 4216, λ 3883 and λ 3590 groups were measured by Kayser and Runge*. The λ 3883 group was re-measured in greater detail (in R A.) by Jungbluth† and (in I A.) by Uhler and Patterson.‡ Heurlinger§ recorded more precise data (I A.) for the λ 4216 group and also gave empirical formulæ derived from new and correspondingly detailed measurements (I.A.) for the first two bands of each of the groups λ 4606 and λ 3590; so far as the writer is aware, however, the latter measurements have not been published, and only Kayser and Runge's are available for the λ 3590 group, and none at all for the λ 4606 group.

Each band consists of two branches, R[$\equiv m+1 \longrightarrow m$] and P[$\equiv m-1 \longrightarrow m$], the head being formed by the P branch. If each R and P line were single the

* 'Abh. Akad. Wiss. Berlin' (1889), see also H. Kayser, 'Handbuch der Spectroscopie,' vol. 5, p. 229 (1910). (First four orders of a grating giving a fourth order dispersion of about 1·21 A. per mm.)

† Dissertation, Bonn (1904); 'Z. f. Wiss. Phot.,' vol. 2, p. 89 (1904); 'Astrophys. J.,' vol. 20, p. 237 (1904). (Grating dispersion used about 0·80 A. per mm.)

‡ 'Astrophys. J.,' vol. 42, p. 434 (1915). (Grating dispersion used about 0·65 A. per mm.)

§ Dissertation, Lund (1918). (Heurlinger stated that the data he tabulated for the λ 4216 group, and the unpublished data for the λ 4606 and λ 3590 groups were obtained by J. Östner in the third, fourth and fifth orders of a grating giving a fifth order dispersion of about 0·79 A. per mm.)

band-lines of the whole system would be approximately represented by a single set of formulæ of the now well-known types :—

$$\left.\begin{matrix} \mathrm{R}\,(m) \\ \mathrm{P}\,(m) \end{matrix}\right\} = \nu = \nu^{e} + \mathrm{F}'\,(n', m \pm 1) - \mathrm{F}''\,(n'', m) \qquad (1)$$

$$\equiv \nu^{e} + \nu^{n} + \nu^{m}, \qquad (1a)$$

where

$$\nu^{n} = (a'n' - b'n'^{2}) - (a''n'' - b''n''^{2}) \qquad (2)$$

and

$$\nu^{m} = \mathrm{B}' \pm 2\mathrm{B}'m + (\mathrm{B}' - \mathrm{B}'')m^{2} \qquad (3)$$

n' and n'' are the initial and final vibrational quantum numbers for the bands, and a', b' and a'', b'' the initial and final values of the vibrational energy coefficients a, b. B' and B'' are the initial and final values of $\mathrm{B} = \mathrm{B}_0 - \alpha n = h/8\pi^2\mathrm{I}_0 - \alpha n$, where I_0 is the moment of inertia of the vibrationless molecule ($n = 0$) and α is a constant. Thus $\mathrm{B}' = \mathrm{B}_0' - \alpha' n'$, and $\mathrm{B}'' = \mathrm{B}_0'' - \alpha'' n''$ *. m is the final rotational quantum number for each line of a band, in Kratzer's earlier theoretical interpretation† it retained the integral values 1, 2, 3, . . assigned by Heurlinger, but half-integral values, $\frac{1}{2}$, $1\frac{1}{2}$, $2\frac{1}{2}$, . . were subsequently found to be necessary ‡.

Actually each branch is double, the doublet separation $\Delta\nu$ slowly increasing with m from the band-origin ($\nu_0 = \nu^{e} + \nu^{n}$, $\nu^{m} = 0$). For the doublet branches R_1, R_2, P_1, P_2, Kratzer§ has derived four expressions, which, however, need not be invoked for the present purpose (where only low m values will be considered) owing to the fact that the earlier doublets remain unresolved even under the high dispersions which have been employed in obtaining the arc data ||. For the low-m lines —say, the first twenty— of any branch of the system an expression for the doublet centres, *i.e.*, the mean wave-numbers $\frac{1}{2}[\mathrm{R}_1(m) + \mathrm{R}_2(m)]$ and

* The difference between B_0' and B_0'' must be due to the difference between the initial and final electronic configurations. R. S. Mulliken ('Nature,' vol. 114, p. 858 (Dec. 13, 1924), 'Phys. Rev.,' vol. 26, p. 561 (1925)) has pointed out that the common final electronic state for the "red" and "violet" systems is probably the normal state of the CN molecule, and further that it resembles an s state, the initial (excited) state for the "violet" system also resembles an s state, and that for the "red" system an inverted doublet-p state.

† 'Phys. Zeitschr.,' vol. 22, p. 552 (1921).

‡ 'Ann. d. Physik,' vol. 67, p. 127 (1922) (see especially footnote, p. 150), 'Sitzb. Bayer. Akad. München,' p. 107 (1922), and next reference.

§ 'Ann. d. Physik,' vol. 71, p. 72 (1923) (see especially pp. 83–88).

|| For example, in Uhler and Patterson's measures of the R branch of the (0, 0) band λ 3883, the first resolved member is $^{(0,0)}\mathrm{R}\,(31\frac{1}{2})$—their A_1 (60), $\lambda\lambda$ 3864·677, ·063.

$\frac{1}{2}[P_1(m) + P_2(m)]$,† may be used instead of Kratzer's full formulæ for the components, these centres are given by the expression (3) for singlet branches $R(m)$ and $P(m)$.

The missing lines in the four branches are —

$$R_1(-\tfrac{1}{2}),\ \Delta m \equiv \tfrac{1}{2} \to -\tfrac{1}{2}, \qquad P_1(\tfrac{1}{2}),\ \Delta m \equiv -\tfrac{1}{2} \to \tfrac{1}{2},$$
$$R_2(\tfrac{1}{2}),\ \Delta m \equiv 1\tfrac{1}{2} \to \tfrac{1}{2}, \qquad P_2(1\tfrac{1}{2}),\ \Delta m \equiv \tfrac{1}{2} \to 1\tfrac{1}{2},$$

and since the missing $R_2(\frac{1}{2})$ is practically coincident with the observed $R_1(\frac{1}{2})$, $[\Delta m \equiv 1\frac{1}{2} - \to \frac{1}{2}]$, and the missing $P_2(1\frac{1}{2})$ with the observed $P_1(1\frac{1}{2})$, $[\Delta m \equiv \frac{1}{2} - \to 1\frac{1}{2}]$, it appears that each band has only a single null-line very near the band-origin, $\nu' + \nu''$, in the position of the missing $R_1(-\frac{1}{2})$ and $P_1(\frac{1}{2})$, namely, at

$$\nu = \nu' + \nu'' + \tfrac{1}{4}(B' - B'') \qquad (4)$$

For the constants in the above expressions ($1 - 1$) Kratzer has given the following values (cm^{-1}), m taking half-integral values, $\frac{1}{2}$, $1\frac{1}{2}$, $2\frac{1}{2}$, . —

$$a' = 2143{\cdot}88 \qquad a'' = 2055\ 64$$
$$b' = 20{\cdot}25 \qquad b'' = 13\ 75$$
$$2B' = 2(B_0' - \alpha' n') \qquad 2B'' = 2(B_0 - \alpha'' n'')$$
$$= 3\ 918 - 0{\cdot}0443n' \qquad - 3\ 783 - 0\ 0346n''$$

Constant term for the (0, 0) band $= \nu' + B_0' = 25799\ 77$,‡
whence system-origin $= \nu' = 25797{\cdot}81$
and null-line of (0, 0) band $= \nu' + \frac{1}{4}(B_0' - B_0'') = 25797{\cdot}83$

The band-origins are therefore given by (*cf.* 2) —

$\nu' + \nu'' = 25797{\cdot}81 + (2143\ 88n' - 20\ 25n'^2) - (2055\ 64n'' - 13\ 75n''^2)$, (5)

the calculated values are shown in Table I, as also are the values of B', B'' and $B'/(B' - B'')$ for each band.

† m is here used for Kratzer's half-integral m^*, and, for convenience in the application of the combination principle in the next section, the use of Kratzer's whole-number m (for which j is now commonly substituted) has been avoided This avoidance necessitates a re-designation of the lines, instead of retaining Kratzer's numbering of a line by the whole-number j (old m), the half-integral m (old m^*) is employed here, thus, the lines here designated $R_1(m)$, $R_2(m)$, $P_1(m)$, $P_2(m)$ are respectively $R_1(j)$, $R_2(j-1)$, $P_1(j)$, $P_2(j-1)$ in the whole-number designation, in accordance with Kratzer's original $R_1(m)$, $R_2(m-1)$, $P_1(m)$, $P_2(m-1)$.

‡ Kratzer writes "$\nu_0 = 25799\ 77$," but this ν_0 does not appear to be the system-origin ν', ($\nu'' = \nu'' = 0$), but the $\nu' + B_0'$ given above is a probable interpretation R Mecke ('Phys. Zeitschr.,' vol. 26, p. 231 (1025)) renders Kratzer's ν_0 as the null-line of the (0, 0) band, in stating that the null-lines of the system are given by

$$\nu = 25799{\cdot}77 + (2143{\cdot}88n' - 20{\cdot}25n'^2) - (2055{\cdot}64n'' - 13{\cdot}75n''^2).$$

Table I —Constants in Kratzer's Formulæ, and Band-heads.

v'' / $2B'$	v'' 0 / $2B''$ 3 783	1 / 3 7484	2 / 3 7138	3 / 3 6792	4 / 3 6446	5 / 3 6100	6 / 3 5754	7 / 3 5408
0	25797 81	23755 02	21741 53		Band-origin, $\nu'+\nu''$			(i)
	29 0	*23 1*	*19 2*		m_{head} ⌒ B′/(B′ − B″)			(ii)
	25742 93	23712 04	21705 0		ν_{head} (vac) calc			(iii)
3 918	25743 35	23712 28	21704 0		ν_{head} (vac) obs			(iv)
	3883 402	**4216 043**	**4606 15**		λ_{head} (I.A, air) obs			(v)
1	27920 44	25878 55	23864 16	21870 27				(i)
	42 1	*30 9*	*24 2*	*19 9*				(ii)
	27839 66	25820 02	23819 18	21840 6				(iii)
3 8737	27844 01	25822 88	23818 93	21837 5				(iv)
	3590 415	**3871 441**	**4197 163**	**4578 01**				(v)
2		27962 68	25948 29	23961 20	22002 01			(i)
		47 3	*33 1*	*26 5*	*20 7*			(ii)
		27874 08	25886 70	23914 50	21964 2			(iii)
3 8294		27878 99	25886 99	23911 09	21956 8			(iv)
		3585 911	**3861 854**	**4180 984**	**4553 13**			(v)
3		(i)	27990 92	26004 03	24044 64	22112 75		
		(ii)	*53 2*	*35 7*	*26 9*	*21 6*		
		(iii)	27892 35	25938 28	23995 55	22073·7		
3 7851		(iv)	27894 30	25934 74	23986 90	22050 7		
		(v)	**3588 935**	**3854 744**	**4167 770**	**4531 89**		
4		(i)		28006 11	26046 72	24114 83	22210 44	
		(ii)		*60 7*	*38 9*	*28 6*	*22 6*	
		(iii)		27894 4	25975 9	24063 1	22170 0	
J 7408		(iv)				24042 94	22143 3	
		(v)				**4158 057**	**4514 78**	
5		(i) Band origin $\nu'+\nu''$			28008 40	26076 51	24172·12	22295 23
		(ii) m_{head} ⌒ B′/(B′ − B″)			*71 1*	*42 8*	*30 5*	*23 4*
		(iii) ν_{head} (vac) calc					24117 6	22253·2
3 6005		(iv) ν_{head} (vac.) obs					24075 57	22205 2
		(v) λ_{head} (I A, air) obs					**4152 422**	**4502·18**
6		(i)				27907 64	26093 25	24216 36
		(ii)				*86·6*	*47 6*	*32 8*
3 6522								
7		(i)					27973 88	26006 99
		(ii)					*110 7*	*53·8*
J 6070								

Heurlinger had already derived a set of formulæ of the type (*cf.* 3) :—

$$\left.\begin{matrix} R(j) \\ P(j) \end{matrix}\right\} = A \pm 2Bj + Cj^2 \qquad (6)$$

to represent his analysis of the data for the earlier bands of each of the four groups. Heurlinger's values of the constants A, B and C are given in Table II,

Table II —Constants in Heurlinger's Formulæ and Band-Heads

n'	n'' ..		0	1	2	3
0	null line	A	25707 83	23755 44	21730 54	
		2B	3 84	3 83	3·85	
		C	0 068	0 085	0 101	
	$j_{head} \simeq$ B/C		*28 2*	*22 5*	*19 1*	
	ν_{head}	calc	25743 62	23712 31	21702 85	
		obs	25743 35	23712 28	21704 0	
1	null line	A	27021 7	25870 0	23863 0	21873 4
		2B	3 88	3 81	3 80	3 82
		C	0 045	0 004	0 082	0 007
	$j_{head} \simeq$ B/C		*43 1*	*29 8*	*23·2*	*19 7*
	ν_{head}	calc	27837 06	25822 30	23818 98	21835 80
		obs	27844 01	25822 88	23818 93	21837·5
2	null line	A		27062 7	25945 5	23956 6
		2B		3 80	3 88	3 78
		C		0 041	0 056	0 076
	$j_{head} \simeq$ B/C			*46 4*	*34 6*	*24·9*
	ν_{head}	calc		27874 66	25878 30	23909 50
		obs		27878 99	25886 99	23911 09

j taking integral values 1, 2, 3, . for the observed lines (or centres of observed doublets) and 0 for the null-lines

In the present investigation both Heurlinger's and Kratzer's formulæ have been used in calculations of the heads and of low-m lines of the bands The head of a band is located by the line or lines for which m (or j) most closely approximates to the particular value making $d\nu/dm$ (or $d\nu/dj$) zero ; thus in Kratzer's formula (3) m_{head} is the half-integer nearest to $B'/(B' - B'')$ and in Heurlinger's formula (6) j_{head} is the integer nearest to B/C These values, which will be required later (section 5), are shown in Tables I and II respectively, together with the observed* and calculated wave-numbers for the band-heads. Again, it has been necessary to calculate the low-m lines of bands of the λ 3590 group, for which no recent data are available, and Kayser and Runge's data have not been ordered (with values of n', n'' and m) Heurlinger's formulæ may be expected to give satisfactory values since they were empirically derived from

* The observed wave-numbers given in Tables I and II for the band-heads differ from those tabulated in two papers by Kratzer, namely ' Phys. Zeitschr ,' vol. 22, p. 552 (1921) (Table III), and ' Ann. der Phys ,' vol. 67, p. 127 (1922) (Table 5). The observed wave-numbers quoted by Kratzer are obtained from wave-lengths in air measured on the Rowland scale, not, as here, *in vacuo* on the International scale The wave-lengths (I.A.) in Table I are Uhler and Patterson's for the heads of the λ 3590 and λ 3883 groups, Heurlinger's for those of the λ 4216 group, and Kayser and Runge's (converted from R.A.) for those of the λ 4606 group.

new (unpublished) data for these bands. The application of Kratzer's theoretical formula to these bands, however, being in the nature of an extrapolation, cannot be expected to give very close representations. The combination principle has been applied as a check on the formulæ for the λ 3590 group.

3. *The Combination Principle.*

The combination principle, unlike the above formulæ, is independent of any assumption as to the forms of the expressions for the vibrational and rotational energies. The R and P wave-numbers of the (x, y) band are obtained by combining those of three observed bands (w, y), (w, z) and (x, z) as follows:—

Making successive substitutions for n', n'' in (1), we have

$$^{(x\,y)}\mathrm{R}\,(m) = \nu^e + \mathrm{F}'(x, m+1) - \mathrm{F}''(y, m) \qquad (7_1)$$

$$^{(x,z)}\mathrm{R}\,(m) = \nu^e + \mathrm{F}'(x, m+1) - \mathrm{F}''(z, m) \qquad (7_2)$$

$$^{(w,y)}\mathrm{R}\,(m) = \nu^e + \mathrm{F}'(w, m+1) - \mathrm{F}''(y, m) \qquad (7_3)$$

$$^{(w\,z)}\mathrm{R}\,(m) = \nu^e + \mathrm{F}'(w, m+1) - \mathrm{F}''(z, m) \qquad (7_4)$$

By subtraction:—

$$\left.\begin{array}{ll} (7_1) - (7_2) & ^{(x,y)}\mathrm{R}\,(m) \quad ^{(x,z)}\mathrm{R}\,(m) \\ (7_3) - (7_4) & ^{(w\,y)}\mathrm{R}\,(m) \quad ^{(w\,z)}\mathrm{R}\,(m) \\ \text{Similarly} & ^{(x,y)}\mathrm{P}\,(m) - {}^{(x,z)}\mathrm{P}\,(m) \\ \text{and} & ^{(w,y)}\mathrm{P}\,(m) - {}^{(w,z)}\mathrm{P}\,(m) \end{array}\right\} = -\mathrm{F}''(z, m) - \mathrm{F}''(y, m) \qquad \begin{array}{l}(8_1)\\(8_2)\\(8_3)\\(8_4)\end{array}$$

Hence, taking pairs of these expressions, we have

$$(8_1), (8_3) \qquad ^{(x,y)}\mathrm{R}\,(m) = {}^{(x\,z)}\mathrm{R}\,(m) + {}^{(w,y)}\mathrm{R}\,(m) - {}^{(w\,z)}\mathrm{R}\,(m) \qquad (9_{\mathrm{R}1})$$

$$(8_1), (8_4) \qquad = {}^{(x\,z)}\mathrm{R}\,(m) + {}^{(w\,y)}\mathrm{P}\,(m) - {}^{(w\,z)}\mathrm{P}\,(m) \qquad (9_{\mathrm{R}2})$$

$$(8_2), (8_2) \qquad ^{(x\,y)}\mathrm{P}\,(m) = {}^{(x,z)}\mathrm{P}\,(m) + {}^{(w,y)}\mathrm{R}\,(m) - {}^{(w,z)}\mathrm{R}\,(m) \qquad (9_{\mathrm{P}1})$$

$$(8_3), (8_4) \qquad = {}^{(x,z)}\mathrm{P}\,(m) + {}^{(w\,y)}\mathrm{P}\,(m) - {}^{(w,y)}\mathrm{P}\,(m) \qquad (9_{\mathrm{P}2})$$

Thus we may compute lines of the band, (x, y)—	by making either of two different combinations of the available data for lines of the three bands—			giving the following values to—			
	(x, z)	(w, y)	(w, z)	w	x	y	z.
(0, 2), λ4606	(0, 1), λ4216	(1, 2), λ4197	(1, 1), λ3871	1	0	2	1
(1, 3), λ4578	(1, 2), λ4197	(2, 3), λ4181	(2, 2), λ3862	2	1	3	2
(1, 0), λ3590	(1, 1), λ3871	(0 0), λ3883	(0, 1), λ4216	0	1	0	1
(2, 1), λ3586	(2, 2), λ3862	(1, 1), λ3871	(1, 2), λ4197	1	2	1	2
(3, 2), λ3584	(3, 3), λ3855	(2, 2), λ3862	(2, 3), λ4181	2	3	2	3
(2, 0), ?	(2, 1), λ3586	(0, 0), λ3883	(0, 1), λ4216	0	2	0	1

Uhler and Patterson's and Heurlinger's data for the low-m lines (up to $m = 19\frac{1}{2}$) for the earlier bands of the λ 3883 and λ 4216 groups are collected in Table III,* and the above application of the combination principle to these data† is shown in Table IV, where the wave-numbers given by the principle are compared with those given by Heurlinger's and Kratzer's formulæ for the first two bands of the λ 3590 group, the table could, of course, be extended to include combinations for each branch of the first two bands of the λ 4606 group. Wherever there is a marked discrepancy between the two formulæ, it is found that Heurlinger's more closely accords with the combination principle over the range tabulated. Using ordered observational data only, it is not possible at present to extend the combinations (within this range of the low m values) far beyond the branches tabulated, on account of the absence of data for the low-m lines of the P branches of the (2, 2),‡ (3, 3) and (2, 3) bands, the detection of these lines being prevented, evidently, by the superposition of the stronger higher-m lines of the same branches. By combining wave-numbers calculated by formulæ (4) and (6) as well as observed wave-numbers, further branches, *e.g.*, (2, 1) P (m), could be approximately computed.

Heurlinger's formulæ, supplemented by the combination principle, has led to the identification of some of the lines measured by Kayser and Runge; the order of agreement of observed and computed wave-numbers may be seen from Table IV. The list of wave-numbers *in vacuo* from Kayser and Runge's measured wave-lengths§ is given later in Table VI.

* In Table III, the values of ν_{obs} do not include those tabulated by Uhler and Patterson for the (0, 0) band. All values for the λ 3883 group have been computed by those observers' λ_{air} (I.A.) using the vacuum corrections of W. F. Meggers and C. G. Peters ('Bull. Bur. Stand.,' 14, p. 697 (1917)). Heurlinger's values of ν_{obs} have been used without modification, as the use of the newer vacuum corrections did not appear to produce marked differences.

† Though the data obtained by different observers may not generally be combined with safety, it is probable that the aggregate error of combining Uhler and Patterson's and Heurlinger's data will never be serious, for the present purpose at any rate. The former observers estimated that their wave-lengths are correct in absolute value to ±0·005 A. and in relative value to ± 0·002 A., while Heurlinger's estimated errors are from ± 0·002 A. to ±0·004 A.

‡ This limitation will, presumably, soon be removed as R. T. Birge has recently announced that he has obtained new data for the λ 3883 group. ('Nature,' vol. 116, p. 783 (November 28, 1925).)

§ Converted from the Rowland to the International scale by the subtraction of 0·15 A throughout.

Table III.—Low-m lines and heads of bands of λ 3883 and λ 4216 groups.

m	(0, 0) Band, λ 3883.		(1, 1) Band, λ 3871		(2, 2) Band, λ 3862		(0, 1) Band, λ 4216		(1, 2) Band, λ 4197		(2, 3) Band, λ 4181	
	R (m) $\nu_{obs.}$ U.P.	P (m) $\nu_{obs.}$ U.P	R (m) ν_{obs} U P	P (m) ν_{obs} U.P	R (m) ν_{obs} U P	P (m) $\nu_{obs.}$ U P	R (m) ν_{obs} H	P (m) ν_{obs} H	R (m) ν_{obs} H	P (m) ν_{obs} H	R (m) ν_{obs} H	P (m) $\nu_{obs.}$ H
½	25801·82	(25797 83)N	25882·73	(25878 97)N			23759 33	(23755 44)N	(23866 88)	(23863 00)N		
1½	05·80	94 02	86·99	75 33			63 47	51 68	71 14	59 13		
2½	10·02	90 41	90 94	71 78			67 68	48 13	75 19	55 64		
3½	14 23	86·90	95 21	68 14			72 14	44 73	79 46	52 32		
4½	18 76	83 53	99·71	64 90			76 72	41 47	84 00	49 10	23977 31	
5½	(23·34)	80 32	25904 27	61 58			81 47	38 40	88 70	46 04	81 89	
6½	28 06	77 19	08 88	58 50			86·36	35 51	93 50	43 16	86 65	
7½	33·02	74 23	13 55	55 51			91 46	32 78	98 50	40 44	91 58	
8½	37 97	71 34	18 50	52 66	25985 12		96 80	30·15	23903 68	37 86	96 61	
9½	43·13	68 73	23 55	49 97	90 06		23802 22	27 86	09 00	35 52	24002 26	
10½	48 40	66 16	28 82	47 33	95·08		07 89	25 66	14·46	33 26	07 23	
11½	53 77	63 75	34 01	45 02	26000 33		13 63	23 60	20 15	31 20	12 68	
12½	59 29	61 47	39·31	42 59	05 53		(19 60)	21 71	25 92	29 30	18 43	
13½	64 90	59·28	44 99	40 32	10 89		26 00	20 02	31 88	27 58	24·30	
14½	70 59	57 25	50 57	(38·30)	16 38		31 91	18 54	38 04	26 00	30 26	
15½	76 70	55 39	56 40	36 44			38 42	17 14	44 36	24 47	36 39	
16½	82 73	53 48	62 33	34 72	27 57		45 02	15 83	50 96	23 22		
17½	88·91	51·98	68 38	33 02	33 60		51 87	(14·90)	57 57	22 30	49 20	
18½	95 21	50·51	74 49	31 52	39 81		58 75	(14 04)	64 34	21 25	55 93	
19½	25901·64	49 18	80 72	30 10	45 51		65 90	(13 35)	71 29	20 55	62 47	
Head —		43 35		22 88		25886 99		12 28		18 93		23911 09
Column .—	(1)	(2)	(3)	(4)	(5)	(6)	(7)	(8)	(9)	(10)	(11)	(12)

NOTES TO TABLES III AND IV.

U P.—Uhler and Patterson. H.—Heurlinger. Kr.—Kratzer. K.R.—Kayser and Runge. N.—Null-line.

Figures in brackets in Table III are wave-numbers of unrecorded lines, estimated by means of formulæ. In Table IV, the brackets indicate combinations involving an estimated wave-number in Table III for one or more of the lines combined.

Table IV.—Low-m lines and heads of bands of λ 3590 group

	(1, 0) Band, λ 3590										(2, 1) Band, λ 3586							
	R (m)					P (m)					R (m)					P (m)		
m	ν_{comb}		ν_{form}		ν_{obs}	ν_{comb}		ν_{form}		ν_{obs}	ν_{comb}		ν_{form}		ν_{obs}	ν_{form}		ν_{obs}
	9_{R1}	9_{R2}	H.	Kr.	K R	9_{P1}	9_{P2}	H	Kr.	K R.	9_{R1}	9_{R2}	H	Kr	K R	H	Kr	K.R.
½	27925 22	(5 12)	5 22	4 33	5 4†	(27921 46)	(1 36)	1 3	1 45	N			27966 54	6 52		27962 7	2·69	N
1½	29 32	9 33	9 24	8 29	9 1	17 66	7 67	7·47	6·67	7 8			70 46	0 43		58 94	8 94	
2½	33 28	3 22	3 34	2 35		14 12	4 06	3 72	2 98	4 3			74 47	4 42	4 4	55 26	5 26	5 4
3½	37 30	7 38	7 54	6 49	7 3	10 23	0 31	0 07	9 38				78 56	8 49	8 4	51 67	1 69	1 8
4½	41·75	1 77	1 82	0 73	1 6	06 94	6 96	6 50	5 87	6 5			82 74	2 65	2 9	48 16	8 18	8 1
5½	(46·14)	6 19	6 20	5 06	6 2	(03 45)	3 50	3 03	2 45				86 98	6 88	6 8	44 72	4 76	
6½	50·58	0 56	0 66	*9 48	*0 0	00 20	0 18	*9 64	*9 12	*0 2			91 31	1 20	1·3	41 38	1 42	1 6
7½	55 11	5·00	5 22	3 98	5 4	27897 07	6 96	6 35	5 88				95 72	5·59	5 8	38 11	8 15	8 2
8½	59 67	9 69	9 86	8 58	8 9	93 83	3 85	3 14	2·73		27999 94	9 92	*0 22	*0 07	*0 1	34 92	4 97	4 9
9½	64 46	4 42	4 60	3 28	4 5	90 88	0 84	0·03	*9 68		28004 61	4 51	4 80	4 63	5 0	31 82	1 87	2 3?
10½	69·33	9 33	9 42	8 06	9 5	87 84	7 84	7 00	6 71		09 44	9 15	9·46	9 27	9 3	28 80	8 85	9 1
11½	74 15	4 16	4 34	2 93	4 4	85 16	5 17	4 07	3 83		14·19	4 15	4 20	3 99	4 2	25 86	5 91	6 0
12½	79 00	9 07	9 34	7 89	9 4	(82 28)	2 35	1 22	1 05		18·92	8 82	9 03	8 79	8 9	23 00	3 06	3 5
13½	83 89	4 25	4·44	2 95	4 3	79 22	9 58	8 47	8 36		24 00	3 83	3 94	3 67	4 1	20·23	0 28	0 8
14½	89 25	9 28	9·62	8 09	9 6	(76 98)	(7 01)	5 80	5 75	7 3	28 91	(8 68)	8 92	8 64	8 8	17 54	7 58	7·8
15½	94 68	4·65	4 88	3 33	4 8	74 72	4 69	3 23	3 24	4 5	(34 07)	(4 00)	4 00	3 68	4 0	14 92	4 97	5 7?
16½	28000 04	*9 98	*0 26	*8 65	*0 1	72 43	2 37	0 76	0 82	2 4	38 94	9 07	9 15	8 81	9 4	12 40	2 44	2 8
17½	05 42	(4 46)	5 72	4 07	5 6	70 06	(0·10)	*8 35	*8 49	*0·1	44 41	4 32	4 38	4 01	4 4	09 95	9 98	*0 8?
18½	10 95	(0 96)	1·26	*9 58	*1 2	67 98	(7 99)	6 04	6 25	8 1	49 96	*0 58	9 70	9 30	9 8	07 58	7 61	8 2
19½	16 46	(6·55)	9 90	5 18	7·0	65 84	(5 93)	3 83	4 10	6 2	54 94	5 06	5 10	4 67	5 2	05 30	5 32	
Head.—								37 66	9 66	44 7 (K R) 44 01 (U P)						27874 66	4 08	9 8 (K.R.) 8 99 (U P)
Columns of Table III combined.	(3 + 1 − 7)	(3 + 2 − 8)				(4 + 1 − 7)	(4 + 2 − 8)				(5 + 3 − 9)	(5 + 4 − 10)						

A further test of both data and formulæ by the combination principle may be made by considering again the foregoing expressions for $F''(z, m) - F''(y, m)$, from $(8_1) = (8_3)$ and from $(8_2) = (8_4)$ respectively, we have:—

$$\left.\begin{aligned} {}^{(z,v)}R(m) - {}^{(z,v)}P(m) &= {}^{(z,s)}R(m) - {}^{(z,s)}P(m) \\ {}^{(w,v)}R(m) - {}^{(w,v)}P(m) &= {}^{(w,s)}R(m) - {}^{(w,s)}P(m) \end{aligned}\right\}. \qquad (10)$$

That is to say, the R and P branches of all bands having the same *initial* vibrational quantum number are equally divergent. This condition is clearly satisfied by Kratzer's theoretical formula (4), according to which the divergence is

$${}^{(n',n'')}R(m) - {}^{(n',n'')}P(m) = 4B'm = 4(B_0' - \alpha' n')m \qquad (11)$$

On the other hand, it is not satisfied by Heurlinger's empirical formulæ (6) in terms of which the divergence is

$${}^{(n',n'')}R(j+1) - {}^{(n',n'')}P(j) = (2B + C)(2j + 1), \qquad (12)$$

for the values of $(2B + C)$, as may be seen from Table II, do not remain constant for any one value of n'. In Table V this condition is illustrated by the data of Tables III and IV

Table V.—Observed values of $R(m) - P(m)$

	$n' = 0$.		$n' = 1$			$n' = 2$
m	(0, 0) λ 3883 U P	(0, 1) λ 4216 H	(1, 0) λ 3590 K R	(1, 1) λ 3871 U P	(1, 2) λ 4197 H	(2, 1) λ 3586 K R.
½	(3 99)	(3 89)	(4 0)	(3 76)	(3 88)	(3 8)
1½	11 78	11 79	11 3	11 60	12 01	(11 5)
2½	19 61	19 55	(19 0)	19·16	19 55	19 4
3½	27·33	27·41	(27 1)	27·07	27·14	26·6
4½	35 23	35 25	35 1	34 81	34 90	34 8
5½	(43 02)	43 07	(42 7)	42 69	42 66	(42·1)
6½	50 87	50 85	50 7	50 38	50 34	49·7
7½	58 79	58 68		58 04	58 06	57 6
8½	66 63	66 65		65 84	65 82	65·2
9½	74 40	74 36		73 58	73 48	72 7 ?
10½	82 24	82·24		81 49	81 20	80 2
11½	90·02	90 03		88 99	88 95	88·2
12½	97 82	(97 89)		96 72	96 62	95·4
13½	105 62	105 98		104 67	104 30	103 3
14½	113 34	113 37	112 3	(112 27)	112·04	111·0
15½	121·31	121·28	120 3	119 96	119 89	118·3 ?
16½	129·25	129·19	127 7	127·61	127·74	126 6
17½	136 93	(136 97)	135·5	135·36	135 27	134·6 ?
18½	144 70	(144 71)	143 1	142 97	143 09	141·6
19½	152 46	(152·55)	150 8	150·62	150 74	

Notes to Table V.

U.P., H. and K.R. as in Tables III and IV.

Figures in brackets involve an estimated wave-number from Table III or IV for one or both of the lines combined.

4 *Intensity Distribution in the* λ 3883 *and* λ 4216 *Groups in the Afterglow.*

Rotational Distribution – Birge* pointed out that the difference in appearance of a given band of the λ 3883 and λ 4216 groups in the arc and in active nitrogen is due to a difference of intensity distribution with respect to j (or m) in each branch. Whereas in the 4-ampere arc the intensity maximum in each branch of the (0, 1) and (0, 0) bands occurs at $j = 28$† (*i e*, near the head in the case of the P branch), Birge estimated the maximum to be at or near $j = 8$ or 9 in the afterglow. Thus while the arc develops strongly lines having relatively high m values (far exceeding m_{head}), the afterglow only feebly develops these lines and so permits of easy observation of the relatively strong lines of low m values (less than m_{head}) The gap noted by Rayleigh and Fowler (*First Effect* in section 1) marks, in fact, the position of the null-line P ($\frac{1}{2}$), R ($-\frac{1}{2}$) and the weak neighbouring lines P ($1\frac{1}{2}$), R ($\frac{1}{2}$), it becomes inconspicuous in the arc on account of the overlying P lines of high m Further, by an extension of Kemble's relation connecting the absolute temperature of the source with the value of m for the line of maximum intensity in a given branch, Birge showed that the above estimates of this value, m_{max}, in the two sources accorded satisfactorily with the temperatures of the 4-ampere arc and of the afterglow, which latter has been estimated at 100° C or less As a result of Birge's investigation, then, the CN spectrum in the afterglow is shown to be a low-temperature CN spectrum, its essential feature being that low values of m are more favoured than in the high-temperature (arc) spectrum. In the analogous afterglow spectrum of SiN the same modification (*First Effect*) was observed by the writer‡ and, much more completely, by Mulliken,§ whose reproductions of the spectrum show very clearly the null-line gap in many of the bands; in fact, Mulliken obtained some of his null-line data directly from micrometer settings on the gaps. Further, from a rough estimate of m_{max} in the case of SiN, Mulliken deduced a temperature for the afterglow agreeing both with the actual temperature and with Birge's estimate in the case of CN.

Vibrational Distribution.—The intensification of the more refrangible end of each of the groups λ 4216 and λ 3883 (referred to in section 1 as Rayleigh and Fowler's *Second Effect*) finds an interpretation in Mulliken's discussions‖ of the

* 'Astrophys J,' vol. 55, p. 273 (1922); see especially p. 286.

† On Heurlinger's numeration. Heurlinger's R (28) and P (26) are called R ($27\frac{1}{2}$) and P ($28\frac{1}{2}$) respectively in the numeration employed in this paper

‡ 'Roy. Soc. Proc.,' A, vol 89, p. 187 (1913) (see p 189 and Plate 9).

§ 'Phys. Rev.,' vol. 26, p 319 (1925) (see pp. 320 and 325, and Plate 1).

‖ 'Phys. Rev.,' vol. 25, p 292 (1925) (BO), vol. 26, p. 21 (CuI); vol 26, p. 333 (SiN).

intensities of bands with respect to n'. Mulliken has pointed out that, while for thermal equilibrium there should be a steady decrease of intensity with increasing n', the intensity distribution in band spectra developed in active nitrogen differs from this in cases where a chemical reaction is involved, *e.g.*, CN, BO, SiN. In these spectra the intensities of the bands in a given group or, better, the sums of the intensities for all bands with a given n', first increase with n' and then fall off as n' further increases On the other hand, in the spectrum of CuI in the afterglow the summed intensities fall off as n' increases from 0

The present grating observations of the λ 4216 and λ 3883 groups in the afterglow confirm both the above features of the distribution, *i e*, the absence of lines with high m values and the occurrence of bands with high n' values Though the large mass of observational data upon which the conclusions are based cannot be given at this stage, some particulars as to the development of the bands may now be stated

The λ 4216 *Group* ($\Delta n = +1$) --Measurement shows definitely that the afterglow lines are identical with Heurlinger's lines of relatively low m values, especially in the earlier bands, (0, 1), (1, 2) and (2, 3) At the other end of the group, where the lines in both sources are more numerous, comparison becomes more difficult, but many lines have been measured on the high wave-number side of the (2, 3) head, which do *not* appear in Heurlinger's arc list. It would appear, therefore, that there are in the afterglow bands which have still not been traced in the arc Further measurements from spectrograms of still higher dispersion are much to be desired for the identification of lines of the bands of higher n' values

The group as shown in Plate 14, strip 3, is much shorter* in the afterglow than in the arc, thus the lowest wave-length measured in the afterglow is λ 4117·96, while Heurlinger's arc wave-lengths extend to λ 3961·793; the difference could, of course, be somewhat reduced by an increase of the afterglow exposure. The shortening is a direct consequence of the non-development in the afterglow of lines with high m values, which are relatively strong in the arc. Thus the R branch of the (0, 1) band which has been traced only as far as λ 4190·16, R (18½), in the afterglow plate, was measured by Heurlinger in the arc to λλ 4018·489, ·199, R (96½)

* In the case of the BO spectrum in the afterglow a corresponding shortening was observed by the writer ('Roy. Soc. Proc.,' A, vol 91, p 132 (1915)). The advantage (arising from the shortening) of active nitrogen over the arc as a means of producing band-spectra has been emphasised by Mulliken in two of his papers on Isotopes (*loc. cit.*; BO, p. 266; CuI, p. 16, footnote 18).

From the grating observations, of which a brief description follows, it appears that the approximate order of intensity of the bands from strongest to weakest is (4, 5), (5, 6), (2, 3), (0, 1), (3, 4), (1, 2)

The (0, 1) *band* has been identified in the grating photograph from P ($2\frac{1}{2}$) to P ($16\frac{1}{2}$), and thence without resolution to the head λ 4216 04, and from R ($2\frac{1}{2}$) to R ($18\frac{1}{2}$) * The intensity maxima appear to be at about P ($0\frac{1}{2}$ or $10\frac{1}{2}$) and R ($8\frac{1}{2}$ to $10\frac{1}{2}$)

The (1, 2) *band* is the weakest of this group in the afterglow Though it is favourably situated for observation from its head λ 4197 16 to R ($17\frac{1}{2}$), no line of either branch has been detected in the grating plate, only the unresolved head being recorded.

The (2, 3) *band* is developed rather more strongly than the (0, 1) band in the afterglow, and the absence of lines of the (0, 1) and (1, 2) bands in this region favours its observation from its own head λ 4180 98, to that of the (3, 4) band, λ 4167·77 The P lines having low m values are not given in Heurlinger's arc list, but have been identified in the afterglow from P ($2\frac{1}{2}$) to P ($15\frac{1}{2}$) and thence without resolution to the head, the intensity maximum being at about P ($9\frac{1}{2}$). The identification of the R lines in the afterglow is less certain on account of the occurrence of blends, but they have been traced from R ($3\frac{1}{2}$) to at least R ($16\frac{1}{2}$). A few additional lines apparently not belonging to the (2, 3) band have been measured in this region, some of these are definitely absent from Heurlinger's arc list, and others are near the positions of some of the $^{(2,\,3)}$ P lines having high m values,† but appear to be too strong to be identified with the latter, these lines are conspicuous in the null-line region between P ($2\frac{1}{2}$) and R ($3\frac{1}{2}$).

The (3, 4) *band* is very weak, being very little, if any, better developed than the (1, 2) band. By actual measurement only its unresolved head λ 4167 77 has been satisfactorily traced, identification of its weak lines being hampered by the occurrence of lines which do not appear to belong to this or to the overlying (2, 3) band

The (4, 5) *and* (5, 6) *bands* are, as judged by the high intensities of their heads λ 4158 06 and λ 4152 42, the most strongly developed bands of the group.

The λ 3883 *Group* ($\Delta n = 0$).—The λ 3883 group, though the most heavily recorded of all in the afterglow spectrogram, shows a shortening which is even more marked than that of the λ 4216 group, while Uhler and Patterson's arc measurements extend to λ 3590 676, *i.e.*, to the first head of the next ($\Delta n = -1$) arc group, the grating measures in the afterglow extend only to λ 3816·2, beyond which no lines can be detected until λ 3627 4 is reached, there begins the next ($\Delta n = -1$) afterglow group. Generally, a description somewhat similar to that of the previous group applies to the observations of the λ 3883 group

The (0, 0) *band.* The R lines detected range from R ($\frac{1}{2}$) to at least R ($30\frac{1}{2}$), and probably to R ($36\frac{1}{2}$) or even still farther, say, R ($42\frac{1}{2}$). The occurrence of blends accounts for the

* In Heurlinger's original notation the four lines named are respectively $A_1(-2)$ to $A_1(-16)$ and thence to K_1, and $A_1(+3)$ to (A_1+19). The transitions *ass* corresponding to these lines named are $1\frac{1}{2} \to 2\frac{1}{2}$, $15\frac{1}{2} \to 16\frac{1}{2}$, $3\frac{1}{2} \to 2\frac{1}{2}$, $19\frac{1}{2} \to 18\frac{1}{2}$ respectively. Heurlinger's A_2 doublets are absent.

† Heurlinger's C_2 lines: $m > m_{head}$

uncertainty as to the presence or absence of these last lines; the earliest line which is definitely absent is R (46½) In Uhler and Patterson's arc this branch is very long, extending as far as λ 3640 296, R (139½) * This further demonstrates that the shortening of the group must be due to the absence of high-m lines, and not to the absence of high n bands The P branch lines have been identified from P (1½) to P (18½), † and thence without resolution to the very strong head λ 3883·40, the most intense line being probably P (10½). No satisfactory evidence of the development of resolved P lines having m values exceeding m_{head} is afforded by the first order plate, but the second order photograph, though weaker and more coarsely grained, suggests the presence of such lines Contrary to what might appear from casual inspection of the region between the heads of the (0, 0) and (1, 1) bands in the reproduction (Plate 13, strip 2) the lines shown in the two sources are not identical, the prominent arc lines of the P branch have $m > m_{head}$ while the afterglow lines shown have $m < m_{head}$ The apparent contradiction arises from the fact that the resolution is too small to distinguish clearly between the two parts of the P branch, i.e., between the lines with $m > m_{head}$ and those with $m < m_{head}$ ‡ In the null-line gap between P (1½) and R (½) a line was measured (first order) which approximately coincides with P (57½) § This is so near the position of the null-line that on casual inspection of the photograph it might appear that the null-line is actually developed, which of course is not the case. The line may be P (57½), as it is more favourably placed for measurement than the P lines immediately preceding it; or, alternatively, it may belong to another band, e.g., a possible extension of the "tail" band next beyond λ 3883

The (1, 1) *band*, like the second (1, 2) band of the λ 4216 group, is, as Rayleigh and Fowler pointed out, relatively weakened in the afterglow Its P lines have, however, been satisfactorily identified from P (1½) to at least P (11½),|| and less completely (owing to the frequent occurrence of blends) from that point to the head, λ 3871 44, which is strongly developed though it is not easily seen in Plate 13, strip 2, because it has about the same intensity as the neighbouring lines of the preceding band, namely $^{(0,0)}$R (4½) and $^{(0,0)}$R (5½). In the case of the R branch of the (1, 1) band blends are so numerous that only isolated early members have been identified

The (2, 2) *band*.—In the range of low m values Uhler and Patterson identified only the

---

* Uhler and Patterson's designations of these six R lines, in the order named, are A (29), A_1 (59), A_2 (65), A_1 (71), A_1 (75) and A_2 (168).

† Uhler and Patterson's designations of these two P lines are A_1 (27) and A_1 (10) respectively.

‡ The $^{(0,0)}$P (m) lines with $m < m_{head}$ are Uhler and Patterson's A_1 lines as also are $^{(0,0)}$R (m) lines, and those with $m > m_{head}$ are their A_2 lines (doublets). Uhler and Patterson's arc list clearly shows the necessity of high resolution for the separation of neighbouring A_1 and A_2 lines.

§ Uhler and Patterson's A_2 3875·375, ·310

|| These are Uhler and Patterson's B_1 λ 3863·593 and B_1 λ 3868 124 respectively. Though no $^{(1,1)}$P (m) lines with $m > m_{head}$ (i.e., Uhler and Patterson's B_2 doublets) have been definitely detected in the afterglow, it should be mentioned that there are in the region between the (1, 1) and (2, 2) heads two afterglow lines which cannot be identified as either A_1 or B_1 lines, namely λ 3865·05 and λ 3863·14 The latter is very near the position of the (1, 1) null-line, and both are near the positions of B_2 lines. It would appear, however, that they are too strong to be identified with B_2 lines and that they may belong to entirely new bands.

R branch of this band from R ($16\frac{1}{2}$) onwards*, in the absence of ordered data for the P branch either from the arc observations or from the combination principle, the examination of this region in the afterglow is difficult It appears, however, that members of each branch are present in fair intensity, the head λ 3861 85 being, in fact, well developed

The (3, 3) *band*, for which Uhler and Patterson identified the R lines from R ($11\frac{1}{2}$) onwards,† is also present in the afterglow, but to a less extent than the (2, 2) band, its head, λ 3854 74, not being detected in the grating plate

The (4, 4) *band* —The new head observed by Rayleigh and Fowler at λ 3850 is, no doubt, that of the (4, 4) band, which would, in fact, be expected to be strongly developed in view of the high intensity of the (4, 3) band of the former group. The present photograph does not definitely show this head, the position in question being occupied by an unresolved background. The region occupied by the (2, 2) and succeeding bands needs further work, preferably with new plates of still higher dispersion

The order of intensity of the bands is less easily judged in this than in the former group, but would appear to be roughly (2, 2), (0, 0), (3, 3), (1, 1) Thus taking only values of n', it appears from observations of both groups that the band intensities decrease in the approximate order 4, 5, 2, 0, 3, 1 in the afterglow, while in the arc the probable order is 0, 1, 2, 3, 4, 5, that is to say, features of the distribution with respect to n' in the afterglow are, (*a*) association of high values of n' with high band intensities, (*b*) marked weakness of bands with $n' = 1$, and (*c*) a tendency for the intensities to alternate, as well as to show a general increase, as n' increases.

5 *The Afterglow Group near* λ 3590 ($\Delta n = -1$)

It is apparent from the arc and afterglow photographs reproduced in Plates 13, 14, that the change is more marked in the λ 3590 group than in either of the other groups λ 4216 and λ 3883, in which Rayleigh and Fowler discovered the two effects already discussed, indeed, it would hardly appear that the drastic modification of the λ 3590 group is merely a further example of the same two effects. In the first place, the heads λλ 3590 4, 3585 9 and 3583·9 of the (1, 0), (2, 1) and (3, 2) bands respectively, which are prominent in the arc, are not observed at all in the afterglow Secondly, while the arc group as measured by Kayser and Runge extends from λ 3590·33 to λ 3482·26, the afterglow group as now measured extends from λ 3627 42 to λ 3557·05; that is to say, this group, like the λ 4216 and λ 3883 groups, is shorter in the *more* refrangible direction in the afterglow than in the arc, but unlike those groups it extends beyond the *less* refrangible limit of the arc bands On casual inspection of the photographs it would appear that the arc bands (1, 0), (2, 1) and (3, 2), are

* The writer has identified $^{(2,2)}$R ($8\frac{1}{2}$) to $^{(2,2)}$R ($14\frac{1}{2}$) in Uhler and Patterson's list, and included them in Table III $^{(2,2)}$R ($16\frac{1}{2}$) is their C_1 λ 3840·094

† $^{(3,3)}$R ($11\frac{1}{2}$) is Uhler and Patterson's D_1 λ 3836 880.

replaced in the afterglow by an entirely different group of bands. It will now be shown, however, that both of the above features, namely, the absence of heads and the continuation on the less refrangible side of λ 3590, are to some extent explicable if the afterglow group consists of bands having $n'' - n' = -1$ as in the arc group, but with intensity modifications similar to those described in section 4.

The Absence of Heads.—Assuming that the $\Delta n = -1$ bands in the afterglow reach a maximum intensity in each branch at about $m = 9\frac{1}{2} \pm 2$, as in the case of λ 4216 and λ 3883, it can easily be shown that no band of this group is likely to form a head. The values of $m_{\text{head}} \simeq B'/(B' - B'')$, shown in Table I, increase considerably from the less to the more refrangible end of each group of bands, thus, for the λ 3883 ($\Delta n = 0$) group they are 29·0, 30·9, 33·1, 35·7 ... They increase more rapidly from group to group in passing from the less to the more refrangible end of the *system*; being 19·2 ... for the λ 4606 ($\Delta n = 2$) group, 23·1 for the λ 4216 ($\Delta n = 1$) group, 29·0 . for the λ 3883 ($\Delta n = 0$) group and 42·1 for the λ 3590 ($\Delta n = -1$) group. A similar variation is shown in Table II for $\rho_{\text{head}} \simeq B/C$. A band will form a head provided, of course, that one of its branches (the P branch in these CN bands) extends to or beyond m_{head} before the lines fade off to an undetectably low intensity. Thus in the λ 3883 (0, 0) band, the head of which is well-developed, the R lines have been definitely traced to at least R ($30\frac{1}{2}$), and the P lines must also have appreciable intensities for m values exceeding $28\frac{1}{2}$, which is the value of m_{head}, even though the intensity maximum occurs so early in the branch as P ($9\frac{1}{2} \pm 2$). Similarly the P lines of the λ 4216 group are developed to or beyond $m_{\text{head}} = 23\frac{1}{2}$. , although this group is less strongly recorded than the λ 3883 group. The lines of the λ 3590 group are also less heavily recorded than the λ 3883 group, and will probably not be detectable in any branch beyond, say, $m = 30\frac{1}{2}$ to $40\frac{1}{2}$, if it be again assumed that the intensity maximum occurs at about $m_{\text{max}} = 9\frac{1}{2}$. This points to a non-development of the head, since the m_{head} values for all bands of this group exceed $40\frac{1}{2}$. From Tables I and II it would appear that this argument, while satisfactory in the cases of the higher bands of the group, may not indicate an entirely headless structure for the first band (1, 0). But analogy with the other groups would lead us to expect that this band, having $n' = 1$, will be the weakest of the whole group and will not be detected far away from $m_{\text{max.}} = 9\frac{1}{2}$, if at all.

The non-development of high-m lines in the afterglow will also account for the observed shortening of this group, as of the former groups, at the *more* refrangible end.

It may be remarked in passing that, according to the above argument, the $\Delta n = +2$ bands in the λ 4606 afterglow group should have well-developed heads, since m_{head} is not very much greater than m_{max}. This conclusion has, in fact, been verified by observation of the grating spectrogram. Though individual band-lines of this group are only feebly recorded, the *heads* of the higher-n' bands (3, 5), (4, 6), (5, 7) and (6, 8) were actually measured. Those of the low-n' bands (0, 2) and (1, 3) were not detected, and that of (2, 4) was measured with difficulty. This is in general accordance with the observations of the $\Delta n = +1$ and 0 groups in the foregoing section.

The Extension to Wave-Lengths higher than λ 3590.—On the further assumption that, as in λ 4606, λ 4216 and λ 3883 groups, the bands with higher n' values are favoured by the afterglow conditions, it is possible to offer an explanation of the continuation beyond λ 3590. In any one group, as n' increases the intervals between successive bands decrease in arithmetical progression,* *i.e.*, the bands close up in passing from higher to lower wave-lengths, and if enough bands are developed the group will turn back towards the higher wave-length end. According to Kratzer's theoretical analysis of the system, the range of n' within which this return of high-n' bands takes place is smallest for the $\Delta n = -1$ group and increases progressively from group to group in the direction $\Delta n = -1, 0, 1, 2$. This is seen in Table I, which gives a range of values of the band-origins, $\nu' + \nu''$, calculated from Kratzer's formula (5). It would thus appear that the band-lines measured between λ 3590 (or less) and λ 3627 may belong to the high-n' bands which have overrun the (1, 0) band, or indeed that the whole observed afterglow group from λ 3557 to λ 3627 consists of low-m lines of these returning high-n' bands. Mulliken† has expressed the belief that the "tail" bands may be similarly interpreted.

Alternatively, this high wave-length end of the λ 3590 afterglow group may represent an intensification of the structure of the $\Delta n = 0$ group below λ 3627; this, however, seems very improbable, as no lines of that group have been detected between λλ 3816 and 3627. Or again, the afterglow bands may be entirely different ones from those constituting the λ 3590 arc group.

Data for the Lines.—With the object of finding to what extent the arc lines are present in the λ 3590 afterglow group, the grating photograph of the latter has been measured as completely as possible against iron arc wave-

* *Cf.* Deslandres' Second Law for heads.

† The writer is indebted to Dr Mulliken for a privately communicated description of this interpretation.

lengths * The wave-numbers are given in Table VI,† together with those pertaining to the ranges of the λ 3883 and λ 3590 arc groups which occupy this region Many of Kayser and Runge's lines have been allocated, as shown in the table, to the R and P branches of the (1, 0) and (2, 1) bands, the means of their identification being the formulæ and the combination principle as described in sections 2 and 3. Though the arc and afterglow data are not strictly comparable in view of the great difference in the dispersions used in the two cases, certain general results are immediately evident from the table --

1 A great number of lines are common to the two sources, but the distributions of intensities are radically different

2 Certain lines are developed in the afterglow which do not appear in the arc Thus, to take a few examples, allowing a very wide margin of error in the afterglow measures, it is evident that the well-defined lines νν 27609·2, 27613·0, 27616 8, 27624 1 and 27737 4 in the afterglow, less refrangible than λ 3590, are not amongst those listed by Uhler and Patterson. On the more refrangible side of λ 3590, the afterglow line λ 27875·7 is absent from Kayser and Runge's arc list, the position of the last-named line is so favourable for observation in the writer's arc comparison photographs that it is unlikely that the line could escape detection

3. Many of the lines strongly developed in the arc are not detected in the afterglow, even though account must be taken of the much greater probability of blends in the afterglow spectrum than in the higher dispersion arc data. Thus, on the higher wave-length side of λ 3590, there is no trace of the lines νν 27769 03, 27773·92, 27777·25, 27792 25, 27827 32, all of which are given by Uhler and Patterson as intense relatively to neighbouring lines in the arc. On the lower wave-length side of λ 3590, we have important examples in the *heads* of the arc bands (0, 1), (2, 1), (3, 2), no trace of which is detected in the afterglow spectrum. Further, if the writer's identifications of the R and P lines of the (1, 0) and (2, 1) bands are correct, it is evident that the (1, 0) band is *entirely* absent from the afterglow in spite of frequent approximate coincidences of one of its band-lines with an afterglow band-line. Such coincidences are

* To avoid unduly large errors on certain lines which are partly or wholly hidden in the overlap of the CN and Fe spectra, further measures were made at a distance from the latter, using well-defined CN lines (already carefully measured) as standards

† In order to diminish the extent of the table it was thought that the wave-lengths might be omitted, as the arc wave-lengths have been published fully by Uhler and Patterson and by Kayser and Runge The wave-lengths in air may be identified at once by the use of Kayser's "Tabelle der Schwingungszahlen" (Leipzig, 1925), which appeared while the investigation was in progress and has been used in the later stages of the work.

shown in the cases of P ($6\frac{1}{2}$), P ($16\frac{1}{2}$), P ($19\frac{1}{2}$), P ($26\frac{1}{2}$), R ($3\frac{1}{2}$), R ($9\frac{1}{2}$), R ($10\frac{1}{2}$), R ($13\frac{1}{2}$), R ($14\frac{1}{2}$), R ($19\frac{1}{2}$), R ($22\frac{1}{2}$), R ($25\frac{1}{2}$), R ($29\frac{1}{2}$) Since no other lines of this band can be traced in the afterglow spectrum, these apparent coincidences must arise from the occurrence of blends in both spectra and indicate the necessity of still higher resolution. The absence of (1, 0) is in accordance with the previous observations as to the weakness of the bands with $n' = 1$ in the other afterglow groups.

Similar considerations point to the almost entire absence of the (2, 1) band, though the comparisons both of the photographs and of the tabulated data are rather more difficult than for the (1, 0) band It is possible that the R and P lines at or near $m = 9\frac{1}{2}$ are actually present in the afterglow spectrum; these lines, if any, would be expected in the afterglow As no lines of the (3, 2) band have been identified in the arc, nothing can be said of its occurrence in the afterglow, except that its head has not been detected

4 A study of the afterglow spectrogram and of the tabulated data, without regard to the arc, has led to the division of the lines into certain sets or sequences which are suggested by the general run of the intensities and of the first differences of wave-number, though the regularity of both is often vitiated by the occurrence of blends The sets suggested include all but a very few of the observed lines, and are indicated in the table by numbers (I)–(XIV) at the top of each sequence of first differences ($\Delta\nu$) While there is reason for believing that the regularities implied in some of the sequences have a real significance, it is clear that for others no such claim can be made

Taking (I) and (XII) as typical of the more trustworthy sequences, it is seen that each resembles a headless branch of a band in that it is characterised by the usual rise of intensity from each end to a maximum near the middle, and by a steady increase in the first differences from one end to the other, further, the first differences are of the same order of magnitude as those in the known bands of the $\Delta n = +1$, 0 and -1 groups * The same features are shown, though not so clearly, by other sequences, *e.g.*, II, III (apart from its irregular beginning which may be due to blends with lines of II), and IV (again apart from irregularities in the first five lines, which may not actually belong to this set) VI, VII and IX are much less satisfactory, and the rest consist of very few and sometimes doubtful lines †

* See Tables III and IV, and the arc column of Table VI.

† *E g*, Sets V and X each include only three lines, of which one is not completely resolved from a stronger line. VIII also includes only three lines, which, however, might well represent the P branch of the (2, 1) band.

Table VI —The Afterglow Group near λ 3590

Comparison with the λ 3883 arc group between λ 3627·7 and λ3590·6 (Uhler and Patterson), and with the λ 3590 arc group between λ 3590 4 and λ 3556 7 (Kayser and Runge)

Arc.			Afterglow				Arc			Afterglow			
Int.	$\nu_{vac.}$	Line	Int.	ν_{vac}	$\Delta\nu$	Notes	Int	ν_{vac}	Line.	Int	ν_{vac}	$\Delta\nu$	Notes
w	27557 50					a	f	27600 89				3 9	
w	58 66	(1, 1) R			(I)		f	01 38		4	27601 5	—	
wb	60·00		00	27560 0	—	s	w	03 58					
w	62 88				4 6		f	04 43				3 9	
wb	64 34		0	64 6	—		w	05 31		4	05 4	—	
F	66·49				4 4		w	08 68				3 8	
w	68 25									3	09 2	—	
w	68 72		1—	69 0	—		f	09 77				3 8	
w	69 85	(1, 1) R			4 1					2	13 0	—	
w	72·98		1	73 1	—		w	13 52					
w	73 57						f	14 53				3 8	
F	74 44						f	15 14					
F	75 07				4 2					1	16 8	—	
w	76·57						f	17 49					
w	77·16		2	77 3	—		wb	18 17				3 7	
w	79·37						f	19 62					
f	80 22				4 1		w	20 41		1	20 5	—	
w	81·32		2	81 4	—		wb	22 70				3 6	
F	82 66									1—	24 1	—	
F	83 97				4 1		wb	27 19				3 6	
b	85·63		3	85 5	—					0	27 7	—	
w	86·84				4 0		f	29 47				3·6	
w	89 55		3	89 5	—		f	30 27					
w	91·38				4 2		wb	31 57		000	31 3	—	
w	93·71		3	93 7	—		f	34 24				3 5	
f	96 34				3 9		w	35 11		000	34 8	—	
f	96 94						w	35 78					
F	97·52		3	97 6	—		w	36 04					
w	98·11						w	38 93					

w	27639 98				
w	40 35				
w	43·60				
f	44·33				
m	44 57				
w	48·33				
f	48·85				
f	49·30				
wbd	52 81				
w	54·12			(II)	
w	56·73	001	27656 5	—	
w	57·15				
w	58 16			2 9	
		0	59 4	—	
w	59·77				
w	60 82			2 9	
w	61 20				
w	62 32	1	62 3	—	
f	62 96				
wb	64 68			3 3	
wb	65 32				
		2	65 6	—	
w	67 68			3 4	
w	68·00				
w	68·79	2	69 0	—	
m	69 30			3 0	
F	71 88	2	72 0	—	
w	72 87				
m	73 21			2 9	
f	73 84				
w	74·36				
F	74·99	2	74 9	—	
w	76 83			3 1	
w	77 23				
w	77 95	2	78 0	—	
w	78 57				
f	79 77				
f	80 08			3 0	
w	80 79				
w	81 05	3	81 0	—	
f	82 10				
w	82 86			2 9	

w	27683 21			2 9	
F	83 97	2	27683 9	—	
f	84 67			2 9	
m	85 13				
		2	86 8	—	
w	87 10				
w	87 36				
f	88 54			3 0	
f	88 93				
F	89 61	2	89 6	—	
w	91 13				
w	91 45			2 8	
w	92 44	3	92 6	—	
w	92 90				
w	95 03			2 7	
w	95 35	1*b*	95 3	—	
w	96 27	*g*			
f	96 59			2 6	
w	97 95	1–*b*	97 9	—	
w	98 80				
w	99 30			2 4	
f	27700 08				(III)
w	00 48	3	27700 3	—	—
w	02 52				
m	03 06				3 5
F	03 95	2	03 8		—
f	04 24				
w	05 68	1	05 6		
w	06 30				3 9
w	06 82				
		3	07 7		—
m	08 03				
m	09 93				3 7
m	10 48				
F	11 56	2*bd*	11 4		—
F	11 79				
F	12 63				
m } *g*	13 59				3 6
m } *g*	14 22				
		2*bd*	15 0		—
m	17 24				
f	17 80				4 1

Table VI—(continued)

Arc			Afterglow				Arc			Afterglow			
Int.	$\nu_{vac.}$	Line	Int.	ν_{vac}	$\Delta\nu$	Notes	Int	ν_{vac}	Line.	Int	$\nu_{vac.}$	$\Delta\nu$	Notes
							mb	27745 92					
m	27716 49						*m*	46 86				3 7	
fd	10·11		4	27719 1	—		*m*	47 70					
F	19 85						*m*	48 40		2—	27748 5	—	*t*
m	20 75				4 0		*m*	49 28					
w	21 36						*w*	50 73					
f	21 70						*w*	50 99				3 6	
fbd	22 80		2*b*	23 1	—		*m*	51 90					
m	24 30									1	52 1	—	
w	24 93				3 6		*m*	52 74					
f	25·32						*w*	53 68				3 5	
fb	26 87		2*b*	26 7	—		*w*	54 26					
m	27 84						*m*	55 29					
w	28·43				3 5					1—	55 6	—	
f	28·84						*m*	56 17					
Fb	30 14		2	30 2	—		*w*	56 96				3 5	
m	31 27						*w*	57 40					
w	31·93				3·5		*w*	58 64					
f	32·42									0	59 1	—	
fb	33 85		2*bd*	33 7	—		*w*	59 63					
m	34 77						*w*	59 89				3·7	
w	35·43				3 7		*f*	60 45					
f	36·07						*w*	62 06					
f	36·56						*wb*	62 06		00	62 8	—	
			2+	37 4	—		*w*	63 39					
w	38 25						*m*	65 56				3 6	
w	38·95				3 8		*w*	66 29					
			2+	41 2	—		*w*	66 55		000?	66 4	—	
s	41 65						*f*	68·40					
mb	42 34				3 6		s	68 03					
f	43·21						*w*	69 41					
f	43·72						*w*	71·13					
mbd	44 86		2	44 8	—								

w	27771 80			
w	72·30			
i	73 92			
f	74 58			
w	75·72			
f	76 55			
i	77 25			
f	78 63			
m	79 22			
f	79 92			
w	81·85			(IV)
w	82·61			
m	82·96	2	27784 6	
m	84 51			2 9
f	85 31			
w	87 07	3	87 5	
w	87 46			3 5
w	87 85			
w	89 69	2bd	91 0	
wb	90 73			3 2
i	92·25			
m	93 30	2bd	94 2	
				3 3
m	94 98			
w	95 91	1bd	97 5	
w	96·89			3 5
m	97 60			
w	98 68	6	27801 0	
F	99·48			3 6
m	27800 26			
F	00 85	7	04 6	
i	01 51			3 7
f	02 98			
ib	04 56	8	08 3	
f	05 28			3·5
ib	06 01			
m	07 50			
m	08 18			
wb	09 29			
w	10 15			

w	27811 14	8	27811 8		
m	11 70			3 3	
w	12 48	8	15 1		
m	13 13				
ib	15 41			3 4	
w	16 51				
m	16 81				
w	18 10	7	18 5		
i	18 76			3 5	
fb	20 03				
i	21 70	7	22 0		
f	23 41			3 5	
ib	24 61				
w	24 92	7	25 5		
m	25 65			3 5	
F	26 57				
i	27 32				
f	28 09	6	29 0		
f	28 94			3 5	
ib	30 24				
w	31 07				
f	31 85	6	32 5		
ib	32 68			3·4	
F	33 36				
f	34 09				
m	34 86	6	35 9		
ib	35 56			3 5	(V)
f	36 41	1	37 5		
f	37 09				3 2
m	38 03	5	39 4		
m	38 58			3 7	
m	39·57	3	40 7		
f	40 23				3 2
f	40 89				
w	41 27				
w	41 99				

a

Table VI—(continued).

Arc			Afterglow				Arc			Afterglow			
Int.	$\nu_{vac.}$	Line.	Int.	ν_{vac}	$\Delta\nu$	Notes	Int	ν_{vac}	Line.	Int	ν_{vac}	$\Delta\nu$	Notes.
			5	27843 1	— 3 2	} d		27884 5				3 2	
			2	43 9	—					5	27885 2	—	
	27844·7	(1, 0) P (head)			3 4			85 7					
			5	46 5	—	h		86 9				(VII)	
	47 4	(1, 0) P (32½)								2	88 0	— 3 8	
	48·3	(1, 0) P (31½)			3 5			88 2					
	49 4	(1, 0) P (30½)											
			6	50 0	—					2	89 0	—	
	50 6	(1, 0) P (29½)						89 3				3 2	
	51·6	(1, 0) P (28½)			3 4			90 2				3 8	
	52 8	(1, 0) P (27½)								2	91 2	—	
			4	53 4	—			91 6					
	54·3	(1, 0) P (26½)			3 5					2	92 8	3 2 —	
	55·7	(1, 0) P (25½)						93 4					
			4	56 9	—			94 6	(3, 2) P (head)	3	94 4	—	h
	57·2	(1, 0) P (24½)			3 7			—					
	58 7	(1, 0) P (23½)						96 3					
	60·5	(1, 0) P (22½)	4	60·6	—					5d	97 4	3 1	
	62·2	(1, 0) P (21½)			3 3			98 3					
	64·1	(1, 0) P (20½)	2	63 9	— (VI)		1	27900 2	(1, 0) P (6½)				
	66 2	(1, 0) P (19½)	1	66·4	—					6d	27900 5	—	
	68 1	(1, 0) P (18½)	9		3 2			02 1				3 5	
			1	69 6	—			04 0		8d	04 0	—	
	70·1	(1, 0) P (17½)			3 0			05 2				3 5	
	72 4	(1, 0) P (16½)	1	72 6	—			06 5	(1, 0) P (4½)				
n	74 5	(1, 0) P (15½)			3 1			07 2		8d	07 5	—	
			2	75 7	—			08 2	(2, 1) P (18½)			3 4	
n	77·3	(1, 0) P (14½)			3 1			09 4					
			4	78 8	—			10 8	(2, 1) P (17½)	8	10 9	—	
	79·8	(2, 1) P (head)			3 2					2	12 2		
			6	82 0	—	h		13 8	(2, 1) P (16½)			4 0	
	82·3							14 3	(1, 0) P (2½)				

Table VI—(continued).

Arc.			Afterglow				Arc			Afterglow			
Int.	ν_{vac}	Line	Int.	ν_{vac}.	$\Delta\nu$.	Notes	Int	ν_{vac}	Line.	Int.	ν_{vac}	$\Delta\nu$	Notes
i	28005 6	(1, 0) R (17½)			4 1		i	28044 4	(2, 1) R (17½)			4 4	
	07·2							46 1				4 1	
			10	28009·0	—			47 4		7	28047 2	—	} d
	09 3	(2, 1) R (10½)			4 0					2	48 0	—	
i	11 2	(1, 0) R (18½)						49 8	(2, 1) R (18½)			4 8	
	13 1		9	13 0	—			51 1				4 0	
	14 2	(2, 1) R (11½)			4 0		i	52 2	(1, 0) R (25½)	7	52 0	—	
								55 2	(2, 1) R (19½)			4·6	
i	15 6						d	56 9		8	56 6	—	
i	17 0	(1, 0) R (19½)	9	17 0	—			58 5	(1, 0) R (26½)				
	18·9	(2, 1) R (12½)						59 7				4 6	
	20 0				4 2			60 9	(2, 1) R (20½)				
	21 2		8	21 2	—					8	61 2	—	
	22 5	(1, 0) R (20½)						62·1					
i	24·1	(2, 1) R (13½)			4 5			64·2				4 8	
	25 6		7	25 7	—			64 9	(1, 0) R (27½)				
i	26·1	(1, 0) R (21½)										(XIV)	
i	28 8	(2, 1) R (14½)			4 2			66 1	(2, 1) R (21½)	7	66 0	—	
			8	29 9	—			67 1				4 6	
	30·9							68 4				5 6	
	32·2				4 0		i	70 8		5	70 6	—	} d
i	34 0	(1, 0) R (22½)	8	33 9	—		g	—		3	71 6	—	
i		(2, 1) R (15½)					i	72·2	(1, 0) R (28½)			4 5	
					(XIII)				(2, 1) R (22½)				
			4	35 2	—							5 4	
	35·7				4 6					4	75·1	—	
	38 0				4 3			75 4					
			6	38 5	—	} d				2	77 0	—	
	39·4	(2, 1) R (16½)	6	39 5	—			77 5	(1, 0) R (29½)			4 9	
	40 2	(1, 0) R (23½)			4·3		i		(2, 1) R (23½)			5 4	
					4·4			80 1		3	80 0	—	
	42 6		6	42 8	—			81 2					
			5	43 9	—			82 5		0	82 4	—	

28083 5	(2, 1) R (24½)			4 8			28095 1	(2 1) R (26½)			
84 4							97 6				5 3
85 2		3	28084 8	—			98 9				
87 9				4 8		*d*	28100 1		1	28100 1	—
89 0	(2, 1) R (25½)						01 7	(2 1) R (27½)			
		2	89 6	—			02 7				5 1
90 1						*i*	04 4				
91 1							05 6		0	05 2	—
93 3				5 2			08 0	(2, 1) R (28½)			
94 2							09 7				
		2b	94 8	—							

NOTES TO TABLE VI

a.—The arc data from ν 27557 50 to ν 27841 99 are from Uhler and Patterson's λ I A. The letters given by those authors and reproduced here to designate intensities relatively to neighbouring lines, have the following significance —

I = very intense, *s* = intense, *m* = medium, *w* = weak, *f* = faint, F = very faint. The arc data from ν 27844 7 to ν 28109 7 are from Kayser and Runge's λ R.A. reduced to I.A. by the subtraction of 0 15A throughout. Lines marked *s* were noted as "stark" by Kayser and Runge, who gave no other observations of intensities. Lastly, *b* = broad, *n* = nebulous, *d* = probably double (resolution not complete), *g* = dark unresolved background or blurr between lines.

a.—The first differences between wave-numbers marked by a — are placed in separate vertical columns to indicate that they apparently form a number of separate sequences.

c.—These three lines are not clearly resolved. The first of them has the appearance of a band head degraded towards shorter wave-lengths. A dark unresolved background begins at this point and extends to λ 3577 7, ν 37943.

f.—This is one of the "tails," λ 3602 97, given by A. S. King ('Astrophys. J.,' vol. 14, p. 323 (1901)). Uhler and Patterson state that in the arc "it consists of a relatively intense, broad diffuse line with a doublet close to it on the shorter wave-length side and a single medium line close beside it on the longer wave-length side. The lines in this region certainly do not form a series emanating from this so-called tail. This has already been noted by Ritz." In the afterglow there is here one line of what appears to be a fairly regular sequence (III) comprising all the lines detected in the immediate neighbourhood.

h.—The wave-numbers tabulated for the heads are from Kayser and Runge's measures, those from Uhler and Patterson's λ (I A) are $\nu\nu$ 27844 01, 27878 99 and 27894·36. The regions indicated by are occupied by many unresolved P lines of the (1, 0), (2, 1) and (3, 2) bands. In the afterglow there is no trace of the heads of the (1, 0), (2, 1) and (3, 2) bands nor of the neighbouring unresolved P lines, but the structure is comparatively open at each of these three points. The more regular end of a long sequence of lines (IV) occupies the region of the (1, 0) head, a short sequence (VI) that of the (2, 1) head, and a further sequence (VII) that of the (3, 2) head.

The two weak sets I and II at the less refrangible end of the group appear to be the R and P branches of one band, the intervening gap (ν 27634·8 — ν 27656·5) representing the positions of five unobserved lines as well as the null-line of the band. With this interpretation, it is the R branch (II) which converges towards (without reaching) a head, and not the P branch (I), in this respect the band differs from the ordinary bands of the arc groups, but resembles a "tail" band degraded towards the red. For the location of the null-line of this possible band, and for the discussion of the significance, if any, of the other suggested sets a more heavily exposed spectrogram is necessary.

It may be pointed out that while the regularities implied in the table are rather rough and fragmentary and perhaps to some extent fortuitous, they extend to portions of the CN spectrum where no regularities have been previously recorded. This results from the development in the afterglow of only relatively few of the arc band-lines. The writer is of the opinion that although the tabulated afterglow lines overrun λ 3590 into the region occupied by the more refrangible end of the λ 3883 ($n'' - n' - 0$) group in the arc, they all belong, nevertheless, to bands for which $n'' - n' = -1$, the low n' bands (1, 0), (2, 1), and (3, 2) being largely if not completely excluded.

6. *The "Tail" Bands near* λ 3883

Introductory.—It may be recalled that Thiele* regarded a band as beginning with a head and ending with an oppositely degraded head which was appropriately called a "tail"; thus, in passing along a band from head to "tail" the intervals between successive lines first increased from zero up to a flat maximum and then decreased to zero. King† discovered in the carbon arc four groups of faint CN bands the positions of the heads of which bore certain simple numerical relations with those of the bands in the four prominent groups to which we have so far confined our attention, each of the new heads was regarded as the "tail" of one of the prominent bands on its high wave-length side. Thus, taking as examples only two groups, we may write King's wave-length (converted to I.A.) for each "tail" beneath the wave-length (from Table I) for the head with which it was paired by King: thus,

* 'Astrophys. J.,' vol. 6, p. 65 (1897).
† 'Astrophys. J.,' vol. 14, p. 323 (1901).

Heads of group $\Delta n = +2$	—4606·15,	4578·01	4553 13,
	4531 89,	4514 78,	4502 18
"Tails" of King's group IV.	—3984 78,	3944 76,	3910 30 *
Heads of group $\Delta n = +1$	—4216 04,	4197·16,	4180 98,
	4167·77,	4158 06,	4152·42
"Tails" of King's group III	—3658 19,	3628 91,	3602 97

(The first three "tails" of these groups were not detected, they fall within the heavily exposed λ 4216 and λ 3883 groups, respectively) Jungbluth modified King's arrangement, by pairing the head of longest wave-length in a group with the "tail" of shortest wave-length in the associated group, *e g*, the "tails" at λλ 3910·30, 3944 76, 3984 78 with the heads at λλ 4606 15, 4578 01, 4553 13 respectively Uhler and Patterson concluded from their high resolution measurements that some of the "tails" in King's groups I, II and III, which were essential to both King's and Jungbluth's arrangements, bore little or no resemblance to real heads † Mulliken, as has already been remarked, regards the connection between the two sets of bands as quite different from that originally supposed, his view being that a group of "tail" bands is the "returning" high n' portion of the group of prominent bands on the lower wave-length side, thus the "tails" at λλ 3910 30, 3944·76, 3984·78 belong to the high n' extension of the $\Delta n = 0$ group, λλ 3883 40, 3871 44, 3861·85, .

Development in the Afterglow —Rayleigh and Fowler observed that the "tail" bands are developed in the afterglow, and, like the more prominent groups already described, they show very marked changes as compared with their appearance in the arc In particular, the bands of King's group IV, given above, exhibit the *First Effect*, *i e*, the clearness of the null-line gap resulting from the non-development of lines of high m values The gap in each band is beautifully shown in Rayleigh and Fowler's fig 6A

Grating measurements have been made over a short range of the bands of King's group IV in the afterglow, the intensities and wave-numbers are given in Table VII. A very close similarity is shown to exist between the structure of these bands and that of the λ 3590 afterglow group described in section 5. In the first place, no heads are detected,‡ Mulliken's interpretation of the "tail" bands would presumably require this absence of heads in the

* In group IV Rayleigh and Fowler noted an additional band near λ 4030 and another near 3883.

† See, for instance, note *t* to Table VI, where Uhler and Patterson's remark on the "tail" at λ 3603 is quoted

‡ One apparent exception is, however, noted below Table VII.

Table VII "Tail" band lines from λ 3934·5 to λ 3883·7 in the Afterglow.

Int	ν_{vac}	$\Delta\nu$	Notes	Int	ν_{vac}	$\Delta\nu$	Notes
		(I)					
0	25409 3	4 6	a, s	1	25503 7	--	
1	13 0	-		2—	97·8	4 1	
		4 6				--	
2	18 5	—		2	25001 9	4 1	
		1 5				—	
3	23 0	4 4		2	05 0	1 0	
4 -	27 4	--		2	10 0	-	
		4 4				4 1	
4	31 8	—		3	14 0	4 0	
		4 3				—	
3	30·1	—		3	17 8	3 8	
		4 4				—	
2	40 5	--		4	21 8	4 0	
		4 4				—	
1	44 0	--		4	25 7	3 9	
			(II)			—	
36n	49 7	—		4	29 5	3 6	
		3 8				—	
6--	53 5	--		3	33 3	3 8	
		3 0				—	
6 --	57 4	—		3	37 0	3 7	
		3 0				—	
6	61 3	—		3bd	40 7	3 7	
		4 0				—	
6	65 3	—		3	44 5	3 8	
		3 8				-	
6—	69 1	—		3--	48·3	3 8	
		3 8				—	
5	72 9	--		2b	51 8	3 5	
		3 8				—	
4	76 7	--		1b	55 3	3 5	
		3 0				—	
3	80 3	—		1	58 8	3 5	
		3 6				--	
2	83·9	—		00	62 1	3 3	
		3 3				—	
1—	87 2	—		00 ?	65 3	3 2	
		3 4				—	
00 ?	90 6	--				(V)	N
				00	70 4	--	
		(III)	N			3 3	
00	25504 5	—		00	82 7	—	
		3 3				3 5	
0	07·8	—		1	80 2	—	
		3 3				3·4	
1	11·1	—		0	89 0	—	
		2 9				3 3	
2	14 0	—		2bd	02 9	—	
		2 9				3 1	
3	16·9	—		1	96 0	—	
		3 0				3 0	
4—	19 9	—		3	99 0	—	
		3 0				2·7	
4—	22 9	—		1d	25701 7	—	
		2 8				2 6	

Table VII—(continued).

Int	ν_{vac}	$\Delta\nu$.	Notes	Int	ν_{vac}	$\Delta\nu$	Notes
4	25525 7	—		2	25704·3	—	*e*
		2·8					
4	28 5	—		2	05 8		
		2 7					
4	31·2	—		1*d*	08 6		
		2 7					
4	33 9	—		4*bd*	11 0		
		2 6					
4	36 5	—		5	14 7		
		2 6				(VI)	
4	39 1	—	*u*	3*d*	18 8	—	
						3·7	
		(IV)		5	22·5	—	
0 ?	71 9	—				3·7	
		4 3		5*d*	26 2	—	*c*
00 ?	76 2	—				3 7	
		4 3		4	29 9	—	
0	80 5	—				3 8	
		4 7		6	33 7	—	
0	85·2	—				3 7	
		4 3		5	37 4	—	
1	89 5	—				3 8	
		4·2		5—	41 2	—	*h*

NOTES TO TABLE VII.

a.—See Table VI note *a* for *g*, *b*, *n*, *d*.

s.—As in Table VI.

u.—The open structure is interrupted at this point, beyond which there is a grey background of unresolved lines ending in a head at λ 3910 07, ν 25567 8 degraded towards the red, this is one of the "tails" given by King.

N.—From both the grating photograph and Rayleigh and Fowler's reproduction (fig 6A), it is evident that these two gaps represent the null-line regions of two bands consisting of II + III and IV + V respectively.

e.—The appearance of V suggests that it should continue beyond this point, but this is not shown by the tabulated numerical data as the following four lines do not fit in.

c.—Doubtful lines were measured at $\nu\nu$ 25720 2, 25730 8, not satisfactorily resolved from the much more certain lines $\nu\nu$ 25718·8, 25726 2 respectively.

h.—VI evidently continues beyond the strong head λ 3883 40 of the (0, 0) band, and may be followed by other similar sequences of lines which cannot be detected with the resolution employed. See (0, 0) band, p 422.

afterglow spectrum, for high values of n' are accompanied by high values of m_{head} (see Table I). Secondly, it is quite clear from Table VII that the lines fall into a number of sequences (I–VI) closely resembling the more certain of the sequences observed in the λ 3590 group; the smaller degree of overlapping in the "tail" bands favours more complete recognition of the sequences. The distribution of intensities and the progressions of first differences are, as far as can be determined, typical of branches of bands. Sequences II and III appear to be short low-m ranges of the P and R branches of one band,

having its null-line in the intervening gap, and its R branch (III) converging towards, though not reaching, a head; this is, of course, implied in the observed fact that the "tails" in the arc degrade towards the red. Similarly, sequences IV and V are the P and R branches of the next "tail" band, the R branch (V) again proceeding towards the absent head; this is the band near λ 3883 which was noted by Rayleigh and Fowler. For the exact location of the null-lines of these two bands (II + III and IV + V) more heavily exposed plates are necessary; Rayleigh and Fowler's original Littrow spectrograms may suffice.

7. *Summary*

Rayleigh and Fowler described certain modifications in the λ 4216 ($n'' - n' = +1$) and λ 3883 ($n'' - n' = 0$) groups of CN bands developed in the afterglow of active nitrogen as compared with the arc. The modifications of the λ 3590 ($n'' - n' = -1$) group and of some of the "tail" bands are now discussed.

By means of Heurlinger's and Kratzer's formulæ, and the combination principle, data for the (1, 0) and (2, 1) bands of the λ 3590 group are identified in Kayser and Runge's arc list.

The modifications in the λ 4216 and λ 3883 groups and the interpretations of them given by Birge and Mulliken are discussed with the aid of grating measures. The afterglow develops especially lines of low m values and bands of high n' values. As n' increases the intensities of the bands in each group tend to show an alternation as well as a general increase. Bands with $n' = 1$ are the weakest.

The λ 3590 group (like the above) is shortened in the low-λ direction, but (unlike the above) it is prolonged in the high-λ direction in the afterglow as compared with the arc, and also consists of headless bands. It is shown that on the assumption that these bands have $n'' - n' = -1$, the absence of heads follows from the non-development of high-m lines, and the high-λ extension may be due to the enhancement of high-n' bands.

Grating measures of the λ 3590 afterglow group are recorded and compared with the arc data for the same region. Each source develops some lines which the other does not. The (1, 0) and (2, 1) bands are not detected in the afterglow; and the head, at least, of (3, 2) is also absent. The afterglow lines of this group fall into regular sequences (branches), some of which taken in pairs appear to form bands of the PR type, degrading in the opposite direction to the low-n bands. The "tail" bands near λ 3883, for which some grating data are recorded, form similar headless branches in the afterglow.

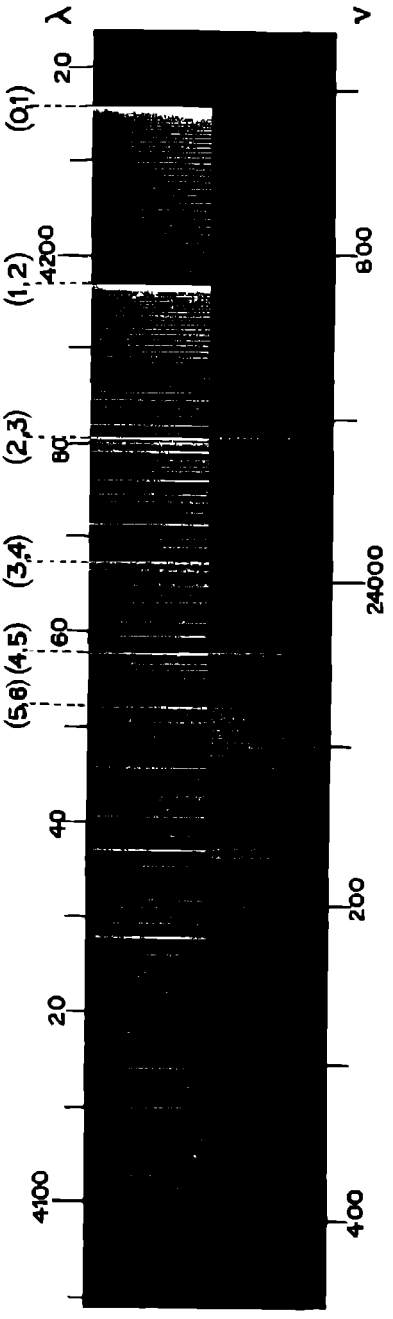

a. b.

3

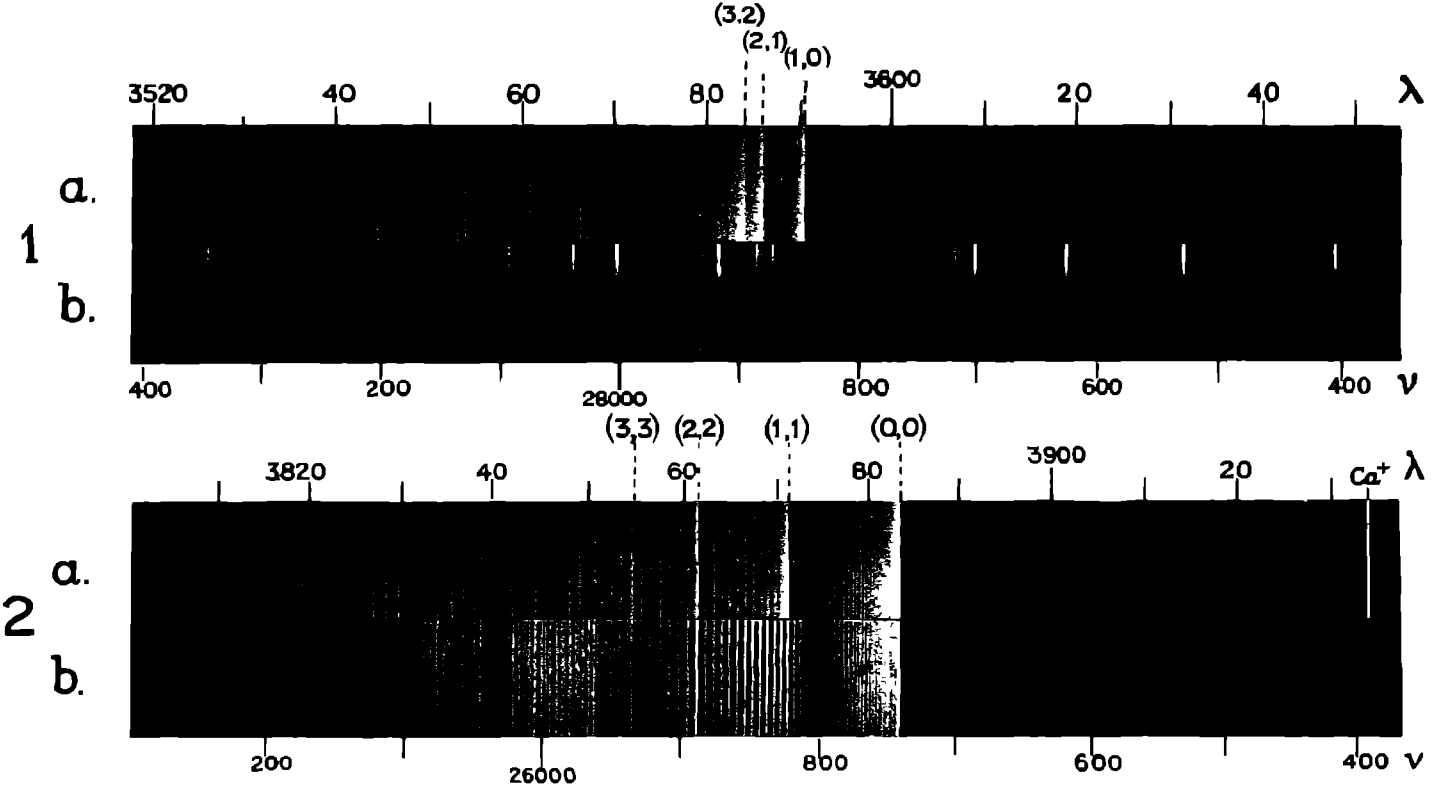

Proc. Roy. Soc. Lond. A, vol. 112, pl. 13

The author has great pleasure in thanking Prof. A Fowler, in whose laboratory the experimental part of the work was carried out, for his unfailing help and interest, and the Government Grants Committee of the Royal Society for the Hilger micrometer used He is deeply indebted also to Prof E N da C Andrade, Dr W E Curtis, and Dr R S Mulliken for very helpful discussions of various points in the investigation

DESCRIPTION OF PLATES 13 and 14

The more refrangible band-system of CN (10 ft concave grating, first order)

(*a*) In the carbon arc in air

(*b*) In the afterglow of active nitrogen with cyanogen

1 The λ 3590 group, $n'' \quad n' = -1$ Fe lines are shown as an impurity in (*a*), and as a comparison spectrum in (*b*)

2. The λ 3883 group, $n'' - n' = 0$

3 The λ 4216 group, $n'' \quad n' = 1$

Crystal Structure and Chemical Constitution of Basic Beryllium Acetate and its Homologues.

By Gilbert T Morgan and W. T. Astbury.

(Communicated by Sir William Bragg, F R S —Received July 21, 1926)

(Plate 15)

The physical and chemical properties of basic beryllium acetate, $OBe_4(CH_3CO_2)_6$, are those of a non-ionised substance having the unitary structure of a typical organic compound, each chemical molecule of which may be regarded as forming one co-ordination complex

The fact that the arrangement of the eleven associating units of which this molecule is composed possesses the geometrical attributes of a tetrahedron has led to a stereochemical conception of the constitution of the compound, which is confirmed by the results of X-ray analysis *

The unique oxygen atom is situated at the centre of the tetrahedron, the four beryllium atoms are arranged on lines joining the centre with the four vertices of this regular solid, whereas the six acetate groups are distributed

* Bragg and Morgan, ' Roy Soc Proc .' A, vol 104, p 437 (1923)

symmetrically about the six sides of the tetrahedron. The precise arrangement of the six pairs of oxygen atoms derived from the six acetate radicals is discussed in detail on p 6 (*loc. cit*)

The three atoms which are attached to the inner carbon atom of the carboxyl group (viz., the outer methyl carbon atom and two similarly situated oxygen atoms) are arranged on a plane passing through the centre of the carbon, but this plane is not necessarily either parallel to the edge of the tetrahedron or perpendicular to it. Nevertheless, the six pairs of oxygen atoms in the acetate groups occupy symmetrical positions in the molecule.

The arrangement of the hydrogen atoms on the methyl carbon atom presents a difficulty There are eighteen of them and they cannot all be symmetrically distributed with respect to either the vertices or the edges of the tetrahedron. But since the crystals of the acetate display cubic symmetry, it must be assumed that, owing to their relatively small importance, the presence of these eighteen hydrogen atoms does not modify appreciably the crystal structure of the compound

When, however, one of the three hydrogen atoms in each methyl group is replaced by a larger methyl radical, as in basic beryllium propionate, $OBe_4(CH_3\,CH_2\,CO_2)_6$, the influence of this substitution on crystal structure becomes at once apparent in the marked change produced in the crystalline form of the beryllium compound. The crystals of basic beryllium propionate belong to the monoclinic system and the crystal unit is made up of two chemical molecules (*loc. cit*).

A similar departure from cubic symmetry was observed (*loc cit.*) in the case of basic beryllium acetate propionate, $OBe_4(CH_3.CO_2)_3\,(CH_3.CH_2\,CO_2)_3$, in which the replacement of hydrogen atoms by methyl groups occurs only in half the acetate radicals present.

This study of the influence of chemical constitution on crystal structure has now been carried farther by an X-ray examination of the following homologues of basic beryllium acetate :—

basic beryllium *iso*butyrate, $OBe_4\left(\begin{matrix}CH_3\\CH_3\end{matrix}\!\!>\!CH\,CO_2\right)_6$,

basic beryllium *n*-butyrate, $OBe_4(CH_3.CH_2\,CH_2\,CO_2)_6$,

basic beryllium pivalate, $OBe_4((CH_3)_3C.CO_2)_6$.

The propionate (already examined), the *iso*butyrate and the pivalate are of special interest in this investigation because they represent the progressive replacement of the hydrogen atoms of the acetate radical by methyl groups.

The following summary includes a brief description of the preparation and properties of these homologous beryllium compounds:—

Basic Beryllium n-*Butyrate*, formerly described as an oil,* was obtained in solid form by dissolving specially purified beryllium hydroxide in the calculated amount of *n*-butyric acid heated to boiling. On cooling, the product separated as an oil and was extracted with cold benzene. The benzene extract was evaporated and the residue crystallised repeatedly from light petroleum boiling below 40° (Found C = 49·76, H = 7·30, Be = 6·42. $C_{24}H_{42}O_{13}Be_4$ requires C = 50·18, H = 7·32, Be = 6·29 per cent.) Basic beryllium *n*-butyrate separated in colourless leaflets melting at 25–27°.

Basic Beryllium iso*Butyrate*, prepared by the foregoing method using *iso*butyric acid, was obtained in needles from light petroleum (b.p. 40–60°). (Found C = 49·56, H = 7·37, Be = 6·42 per cent.).

Large crystals of the *iso*butyrate were isolated by allowing the petroleum solution to evaporate slowly into a confined space. The melting point of this preparation was 88–89°. Lacombe (*loc. cit.*) gave m.p. 76°.

Basic Beryllium Pivalate.—Pivalic or trimethylacetic acid was prepared from pinacolin† and its beryllium derivative was produced by boiling under reflux 6·5 grm. of beryllium hydroxide (BeO = 43 per cent.), 16·6 grm. of pivalic acid and 30 c.c. of petroleum boiling at 80–100°. The filtered solution was concentrated when 15·5 grm. of crude pivalate was obtained (yield 87 per cent.). By crystallisation from petroleum (b.p. 40–60°) needles of beryllium pivalate were isolated. (Found C = 54·44, H = 8·15, Be = 5·56. $C_{30}H_{54}O_{13}Be_4$ requires C = 54·71, H = 8·23, Be = 5·48 per cent.).

On slow evaporation of the petroleum solution large pyramidal crystals of basic beryllium pivalate were obtained melting at 163°.

X-ray Analysis

Basic Beryllium Acetate.—The X-ray analysis of the structure of basic beryllium acetate has been discussed elsewhere (*loc. cit.*), but there are still a few points that may be enumerated here. The abnormal spacings observed ($\{hkl\}$ halved if $(h + k)$, $(k + l)$ or $l + h)$ is odd, and also $\{hko\}$ quartered if $(h + k)$ is odd but halved if even) correspond to either of two cubic space groups, T_h^4 or O_h^7. If the space-group is T_h^4, the crystals belong to the dyakis-dodecahedral class and the molecular symmetry (eight molecules per cell) is that of the tetrahedral-pentagonal-dodecahedron, four triad axes and three

* Lacombe, 'Compt. rend.,' vol. 134, p. 772 (1902).

† Schaubb and Lobl, 'Monatsh.,' vol. 25, p. 1094 (1904).

dyad axes If the space-group is O_h^7, the crystals are holohedral, while the molecules have the symmetry of the regular tetrahedron In both space-groups the molecular arrangement is similar to that of the carbon atoms in diamond, but the molecular symmetry in T_h^4 is lower A Laue photograph, taken with X-rays perpendicular to the octahedron face, discriminates at once between these two groups, for in T_h^4 the diagonal planes of symmetry of the cube are absent, and simple threefold symmetry only is to be expected in the arrangement of the spots Such a Laue photograph is shown in Plate 15 It indicates clearly the lack of diagonal symmetry planes The space-group is therefore T_h^4 This conclusion was confirmed by a photograph perpendicular to the cube face As was to be expected, this photograph showed only symmetry planes parallel to the cube faces Such being the case, the molecular symmetry is only twelve-fold The unique oxygen atom lies at the centre of a regular tetrahedron of beryllium atoms, while the six equivalent acetate groups are associated with the six edges of this tetrahedron Each acetate group is symmetrical about a *dyad* axis, that is, its two oxygen atoms are equivalent and the three-fold symmetry of the (CH_3) group is for some reason non-effective The plane of each acetate group, since full tetrahedral symmetry does not extend beyond the tetrahedron of beryllium atoms, must lie oblique to the tetrahedron edge with which it is associated.

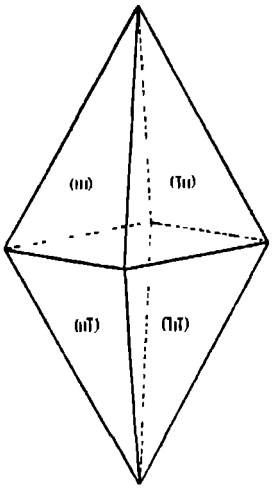

Fig 1.

Basic Beryllium Pivalate.—Crystals of basic beryllium pivalate are soft, colourless bipyramids, frequently of pseudo-orthorhombic habit (fig 1). Their specific gravity by the suspension method was 1 05. As the crystal faces did not reflect light well, their goniometric measurement was carried out entirely by X-ray reflections on the ionisation-spectrometer They proved to be monoclinic with the Bravais-lattice, Γ_m' The bipyramidal habit of the crystals is very marked, and to bring out this characteristic a face-centred cell was chosen. This cell is nearly orthorhombic. its dimensions are

$$a = 19{\cdot}3,\ b = 12\ 4,\ c = 35{\cdot}4,\ \text{A U} \qquad \beta = 91^\circ\ 21'$$

The habit consists therefore of the two forms {111} and {$\bar{1}$11} only.

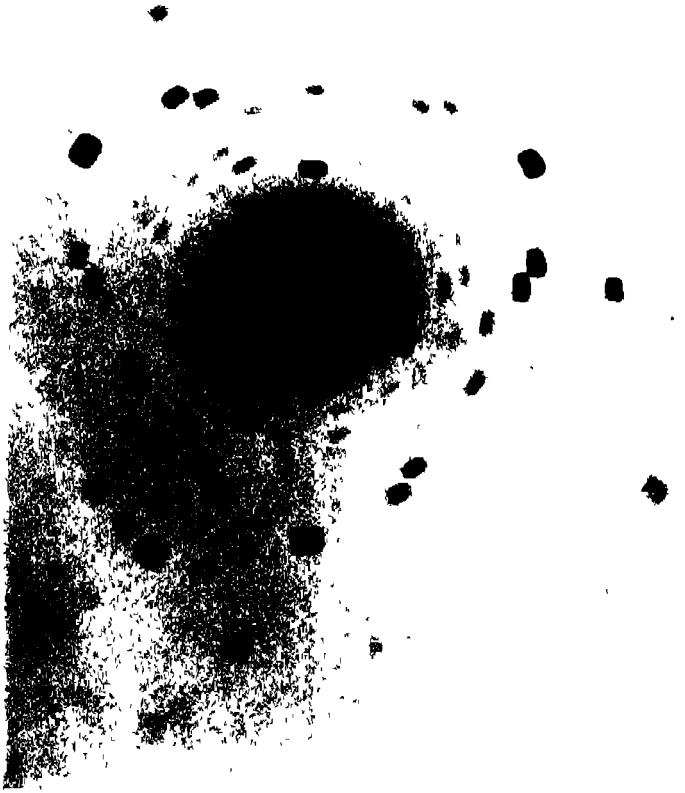

Basic Beryllium Acetate. Laue Photograph

(*Facing p. 444*)

There are eight chemical molecules in the cell and the abnormal spacings observed are. $\{hkl\}$ halved if $(h+k)$, $(k+l)$ or $(l+h)$ is odd, and also $\{hol\}$ quartered if $(h+l)$ is odd but halved if $(h+l)$ is even. These results correspond to two possible monoclinic space-groups, C_s^4 if the crystals are monoclinic domatic, C_{2h}^6 if they are prismatic * The dimensions of the unit cell were confirmed by a series of rotation photographs

The following reflections were observed on the ionisation-spectrometer —

(400) *v s*	(044) *v w*	(804) *m*	(333) *v w*
(800) *w*	(024) *s*	(4016) *v w*	(11$\bar{1}$) *v s*
(1200) *v w*	(048) *v w*	(8012) *v w*	(22$\bar{2}$) *m*
(020) *s*	(026) *m*	(220) *s*	(33$\bar{3}$) *v w*
(040) *v w*	(202) *v s*	(440) *v w*	(113) *s*
(060) *w*	(20$\bar{2}$) *v s*	(240) *v w*	(226) *w*
(004) *s*	(40$\bar{4}$) *v w*	(420) *w*	(115) *m*
(008) *w*	(206) *s*	(111) *v s*	(224) *m*
(022) *m.*	(408) *w*	(222) *m*	(313) *v w*
			(242) *v.w.*

We notice at once a striking similarity between the structure of basic beryllium pivalate and that of the basic acetate. The habits are similar, bipyramids for the pivalate and octahedra for the acetate, and this characteristic springs from the resemblance between the arrangement of molecules in the unit cell. The acetate arrangement corresponds to the well-known "diamond structure" in which each molecule is at the C G of four others, while in the pivalate a closely related molecular distribution prevails. This may be understood from fig 2, which shows diagrammatically the arrangement of molecules in a face-centred cell of C_s^4 This figure is a projection on (001) † The molecules are located at four levels, 0, $c/4$, $c/2$, $3c/4$, marked 0, 1, 2, 3 Molecules 1 and 3 are reflections in the glide-planes (shown dotted) of molecules 0 and 2 This structure has more degrees of freedom than the corresponding cubic arrangement. In the latter, molecules 0 and 2 define *regular* tetrahedra at the C.G.'s of which are located molecules 1 and 3, but in the monoclinic system 0 and 2 define only an oblique bisphenoid and 1 and 3 may move along lines LM away from the central position Such is the arrangement that holds for the molecules of basic

* P Niggli, 'Geom. Kryst des Diskontinuums'; R W. G. Wyckoff, 'Analytical Expression of the Theory of Space-Groups'; W. T Astbury and K Yardley, 'Phil. Trans. Roy. Soc.,' A, vol 224, p 221 (1924)

† See diagrams at end of Astbury and Yardley's paper

beryllium pivalate. As can be seen immediately from the cell dimensions, each molecule is located within (not necessarily at the C G) a quite irregular

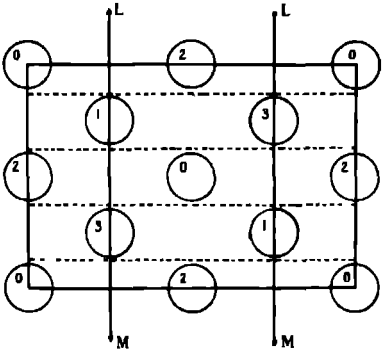

Fig. 2

tetrahedron or bisphenoid, and from this we are forced to the conclusion that any threefold influence, such as predominates in the structure of the basic acetate, either does not exist or is non-effective in the pivalate Strictly speaking, the basic acetate cannot have four trigonal and three dyad axes It is only because the three hydrogen atoms in the (CH_3) group have, for some reason, no appreciable effect on the molecular symmetry that the molecule functions in the crystal as it does And when we pass over to the pivalate, four triad axes are impossible unless the whole of the [C(CH_3)] group is strung out into a line (a dyad axis), which is not at all likely Of course, it is conceivable that the molecular structure of the pivalate is not analogous to that of the acetate, in which case the divergence between the two crystal types is at once explained but it is unnecessary to assume this The substitution of the three methyl groups is quite sufficient to account for the change In the observed molecular distribution we can see a striving after a tetrahedral arrangement, for in the pivalate we have still each molecule surrounded by an irregular tetrahedron of four other molecules, but the methyl groups have here achieved what the hydrogens in the acetate were unable to do The four trigonal axes have been destroyed, and the result is a compromise It is not possible at the present state of our knowledge to deduce anything further from the X-ray results Only one other point needs discussion. As mentioned above, the space-group may either be C_s^4 or C_{2h}^6. If the former, the molecules are crystallographically asymmetric, if the latter, they may be symmetrical about either a dyad

axis or a centre of symmetry With a molecule analogous to that of the basic acetate, both of these possibilities are obviously excluded We must conclude therefore that the crystals are monoclinic domatic, space-group C_s^4, with eight asymmetric molecules in a face-centred cell If they are not of this class, then the molecule cannot be analogous to that of the basic acetate

Basic Beryllium Isobutyrate - This substance forms soft, colourless crystals of the habit shown in fig 3 Their specific gravity by the suspension method was 1·14 The crystal faces do not reflect light well, but a goniometric measurement of the main angles gave -

A– B = 87° 52′ (mean of 11 readings)
A– C′ = 80° 28′ (mean of 4 readings)
B C′ = 70° 30′ (mean of 6 readings)
B *d* = 47° 35′ (mean of 2 readings)
A–*e* = 42° 29′ (one reading only)
A–*f* = 63° 25′ (one reading only)

These measurements correspond to a triclinic pinakoidal unit, and sufficient X-ray observations were taken to confirm this conclusion It did not appear

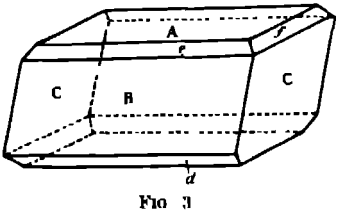

Fig 3

profitable, however, at this stage to pursue the investigations farther Owing to the complexity of the molecules, the unit cell is very large and a reliable determination of its orientation would have involved an unmerited amount of labour Apparently the cell corresponding to fig. 3 contains eight chemical molecules, the edge which is the zone axis of the faces A and B being 9·82 A.U long. It is clear that there has been a complete change of crystal type in passing from the acetate and pivalate to the isobutyrate, and nothing of any value can as yet be deduced about the atomic arrangement within the molecule

Basic Beryllium Normal Butyrate.—This substance can be crystallised only with great difficulty The M P is so low that the crystals at ordinary temperatures quickly pass into a fluid or semi-fluid state which renders them unsuitable for X-ray investigation At the best they could be examined only by the powder

method, and this latter is quite inadequate for the determination of such a complex structure. The crystals are undoubtedly of low symmetry, and in all probability the molecules are crystallographically asymmetric.

The beryl employed in these experiments was obtained by the aid of a grant from the Department of Scientific and Industrial Research, the mineral was worked up into the purified organic compounds with the assistance of Messrs. T. J. Hedley and C. R. Porter.

The X-ray investigation described in this paper was carried out, by aid of a grant from the Department of Scientific and Industrial Research, in the Davy Faraday Laboratory.

The Structure and Isotrimorphism of the Tervalent Metallic Acetylacetones.

By W. T. Astbury, B.A., A.Inst.P.

(Communicated by Sir William Bragg, F.R.S.—Received July 21, 1926.)

Introduction.

A report on the crystallographic characteristics of the acetylacetone derivatives of aluminium, gallium, indium, scandium and iron has been contributed by T. V. Barker to a paper by Morgan and Drew ('Trans. Chem. Soc.,' vol. 119, p. 1059 (1921)). For the sake of convenience his table is reproduced here.

Table 1.

(1) Aluminium, monoclinic, $a : b : c = 1.901 : 1 : 1.111$, $\beta = 98° 54'$.	Isomorphous
(2) Gallium (α-form), monoclinic, $a : b : c = 1.834 : 1 : 1.069$, $\beta = 99° 12'$.	
(3) Gallium (β-form), orthorhombic, $a : b : c = 0.6314 : 1 : 1.253$.	Isomorphous.
(4) Indium (β-form), orthorhombic, $a : b : c = 0.6168 : 1 : 1.291$.	
(5) Indium (γ-form: Jaeger), orthorhombic, $a : b : c = 0.5593 : 1 : ?$	Isomorphous.
(6) Scandium (γ-form: Jaeger), orthorhombic, $a : b : c = 0.5621 : 1 : ?$	
(7) Iron (γ-form: von Lang), orthorhombic, $a : b : c = 0.5689 : 1 : 1.222$	

This table shows how the tervalent acetylacetones present collectively a remarkable case of isotrimorphism With the object of revealing the nature of this isotrimorphism and, if possible, of throwing light on the molecular structure of the acetylacetones, five of the crystals mentioned above and five others have been submitted to an X-ray examination The results may first of all be tabulated after the manner of Barker's.

Table II

	α *Isomorphous Monoclinic Acetylacetones* C_{2h}^5	
(1) Aluminium	$a = 14{\cdot}1$, $b = 7\ 42$, $c = 16\ 5$ A U $\beta = 98°\ 54'$	Four molecules per cell
	Density = 1 27	
(2) Chromium	$a = 14\ 2$, $b = 7\ 62$, $c = 16\ 5$ A U $\beta = 99°\ 8'$	
	Density = 1 34	
(3) Manganese	$a = 14\ 1$, $b = 7\ 68$, $c = 16\ 5$ A U $\beta = 99°\ 24'$	
(4) Cobalt	$a = 14{\cdot}2$, $b = 7\ 50$, $c = 16\ 4$ A U $\beta = 98°\ 38'$	
	Density = 1 43	
(5) Gallium.	$a = 14{\cdot}0$, $b = 7\ 63$, $c = 16\ 3$ A U. $\beta = 99°\ 12'$	
	Density = 1 42	
	β *Isomorphous Orthorhombic Acetylacetones* C_{2v}^7 *or* Q_h^{18}.	
(6) Scandium.	$b = 13{\cdot}52$, $a = 8\ 20$, $c = 16\ 15$ A U	Four molecules per cell
(7) Gallium	$b = 13{\cdot}1$, $a = 8\ 20$, $c = 16\ 3$ A U	
	Density = 1 41	
(8) Indium.	$b = 13\ 4$, $a = 8{\cdot}24$, $c = 16\ 5$ A U	
	Density = 1 51	
	γ *Isomorphous Orthorhombic Acetylacetones* C_{2v}^9 *or* Q_h^{16}.	
(9) Iron	$b = 13\ 68$, $a = 15\ 74$, $c = 33\ 0$ A U	Sixteen molecules per cell.
	Density = 1 33	
(10) Gallium.	$b = 13\ 74$, $a = 15{\cdot}71$, $c = 32\ 76$ A U.	

For comparison purposes, the "b" of the orthorhombic system is placed under the "a" of the monoclinic system The specific gravities mentioned were determined by the suspension method

From these X-ray measurements it is clear that only in the case of the β-form does the unit cell chosen goniometrically correspond to the structural unit cell. To obtain the true cell from the goniometric cell we must, in the case of the α-acetylacetones, double the c-axis, while in the case of the

γ-acetylacetones, we have to double both the *a*-and *c*-axes If we allow for these doublings, we see a striking resemblance between the three structural units The α- and β-cells are practically equivalent in dimensions, both being about one quarter the size of the γ-cell But between the three types there is a closer connection even than that implied by their dimensions, for in "habit" too, they are nearly alike, all three consisting essentially of a pseudo-hexagonal combination, {001}, {100} and {110} for the α-form, {001}, {010} and {110} for the β-form, and {001}, {010} and {210} for the γ-form It should be noticed here that these indices refer to the true cells as determined by X-rays, not to the cells chosen gonimetrically. The true indices will be used throughout the rest of this paper Figs. 1A and 1B are reproduced from Barker and fig 1c from von Lang

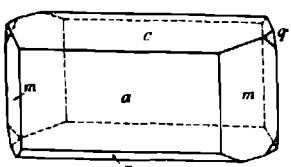

FIG 1A —Aluminium and Gallium Acetylacetones (Monoclinic).

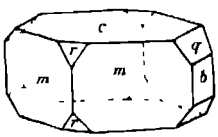

FIG 1B.—Gallium and Indium Acetylacetones (Orthorhombic)

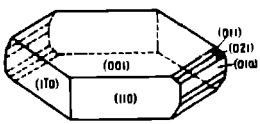

FIG. 1C —Ferric Acetylacetone (Orthorhombic).

Another remarkable point is this, that all three forms of the gallium compound have been observed in one and the same crop of crystals from acetone It is not difficult to obtain a mixture of the α- and β-gallium compounds, but the γ-form had not hitherto been prepared Strange to say, a single crystal, about one millimetre across, was found among a mixture of the α- and β-gallium acetylacetones. In addition to the usual forms {001}, {010} and {210}, this crystal showed four small (101) faces and a single small (011) face. It is on this as yet unique crystal that most of the X-ray investigation of the γ-acetylacetones has been carried out. In a composite crop of crystals the three types are so alike that actual measurement is generally required to discriminate between them, especially between the two orthorhombic forms The specimen of manganese α-acetylacetone grown from benzene showed a tendency to be tabular on the (100) face Perfect {001} cleavage has been observed on the β-form and perfect {010} on the γ-form. The optical properties also of these two forms are different

X-Ray Examination of the Monoclinic Acetylactones (α)

These were examined by the ionisation-spectrometer, rotating crystal and Laue methods The halvings observed are {*hol*} when *l* is odd and {010}. The space-group is therefore the monoclinic prismatic space-group C_{2h}^{5} * The following reflections were observed on the Bragg ionisation-spectrometer with molybdenum anticathode (see Table III). *v s.* = very strong, *s* = strong, *m s* = moderately strong, *m* = moderate, *w m.* = weak to moderate, *w* = weak and *v w.* = very weak.

Table III

Axial Planes	(0010) *v w.*	(024) *v w*	(20$\bar{8}$) *m s*	(60$\bar{6}$) *v w*	*General Planes*
(100) *w m*		(044) *v w*	(40$\bar{2}$) *m*	(90$\bar{6}$) *v.w*	(11$\bar{2}$) *v s*
(200) *v s*	*Prism Planes*	(0312) *v.w*	(10$\bar{2}$) *w m*	(40$\bar{8}$) *v w*	(112) *m*
(300) *s*	{*okl*}	(026) *v w*	(40$\bar{8}$) *w m*	(40$\bar{1}\bar{2}$) *v.w*	(22$\bar{2}$) *w m*
(400) *m s*	(012) *s*		(204) *w*	(20$\bar{1}\bar{0}$) *v w*	(11$\bar{3}$) *w*
(500) *v w*	(021) *s*	*Prism Planes*	(304) *w*		(44$\bar{2}$) *w*
(020) *s*	(022) *m s*	{*hol*}	(20$\bar{2}$) *w.*	*Prism Planes*	(114) *v w.*
(040) *w m*	(014) *m s*	(102) *s*	(30$\bar{6}$) *w.*	{*hko*}	(22$\bar{4}$) *v w*
(060) *v w*	(013) *m s*	(302) *s*	(80$\bar{4}$) *w*	(110) *v s*	(33$\bar{3}$) *v.w*
(002) *v.s*	(011) *w m*	(104) *s*	(306) *v w*	(240) *w*	
(004) *w*	(033) *w m*	(30$\bar{2}$) *s*	(202) *v.w*	(120) *v w*	
(006) *w*	(042) *w m*	(20$\bar{4}$) *s*	(404) *v w*	(220) *v w*	
				(360) *v w*	

The dimensions of the unit cell, which is of the simple monoclinic type, Γ_m, and which contains four molecules of

$$\left[M''' \left\{ \begin{matrix} O\text{--}C(CH_3) \\ \diagdown \\ \diagup \\ O\text{-}C(CH_3) \end{matrix} \right\}_3 \right]^{\cdots},$$

were confirmed by a series of rotation photographs about various crystallographic directions In a subsequent paragraph these photographs will be discussed further

X-Ray Examination of the Orthorhombic Acetylacetones (β)

The β-acetylacetones were examined by the spectrometer method and by Laue, rotation and oscillation photographs With such a large cell and with the necessity of ascertaining the halvings in the three types of prism planes, it was found that successive "layer-lines" ("Schichtlinien") of reflections were too close together to be separated without ambiguity on the spectrometer with

* P Niggli, 'Geom Kryst. des Diskontinuums.' R W. G Wyckoff, 'Analytical Expression of the Theory of Space-Groups' (*a*) W. T. Astbury and K Yardley, 'Phil. Trans Roy Soc.,' A, vol 224, p. 221 (1924).

molybdenum rays A series of 10° oscillation photographs were therefore taken, using copper rays These oscillation photographs were analysed by means of a " rotation-chart " prepared by Mr J D. Bernal, to whom also I am indebted for a number of rotation and oscillation photographs The method of analysis will be described by Bernal in a forthcoming publication. Sufficient photographs were taken to fix the dimensions of the cell without any reasonable doubt It proved to be of the simple orthorhombic type, Γ_0, containing, like the monoclinic crystals, four acetylacetone molecules The halvings observed were $\{hol\}$ when $(h + l)$ is odd and $\{010\}$, giving for the space-group C_{2v}^{7} or Q_h^{13}, according as the crystals are pyramidal or bipyramidal Attention is here directed to the " halving " of the form $\{010\}$, which does not occur in combination with the $\{hol\}$ halvings in the ordinary scheme of orthorhombic spacings Yet there is no doubt that this is a genuine halving, just as those of the $\{hol\}$ forms, since it was examined very carefully both photographically and by the spectrometer No trace of odd-order reflections appeared in either the scandium, gallium or indium crystals It will be seen later that this halving is very simply explained by the structure proposed for the β-acetylacetones The following reflections were observed (Table IV) with gallium β-acetylacetone

Table IV.

Axial Planes	(052) *s*	(402) *s*	(330) *w m*	(152) *m s*	(454) *m*
(200) *m s*	(054) *s*	(103) *m s*	(330) *w m*	(221) *m s*	(411) *m*
(400) *w m*	(064) *s*	(303) *m s*	(210) *v w*	(222) *m s*	(415) *m*
(020) *v s*	(033) *m s*	(208) *m s*	(240) *v w*	(224) *m s*	(424) *m*
(040) *w*	(062) *m s*	(101) *m*	(160) *v w*	(121) *m*	(433) *m*
(060) *w m*	(055) *m*	(206) *m*		(144) *m*	(131) *w m*
(002) *v s*	(048) *m*	(301) *m*	*General Planes*	(151) *m*	(141) *w m*
(004) *w m*	(026) *w m*	(404) *m*	(112) *v s*	(164) *m*	(162) *w m*
(006) *w*	(036) *w m*	(107) *w m*	(114) *v s*	(172) *m*	(171) *w m*
	(061) *w m*		(113) *s*	(174) *m*	(214) *w m*
Prism Planes	(065) *w m*	*Prism Planes*	(116) *s*	(211) *m*	(321) *w m*
{*okl*}	(066) *w m*	{*hko*}	(126) *s*	(215) *m*	(322) *w m*
(014) *s.*	(084) *w m*	(110) *v s*	(127) *s*	(216) *m*	(325) *w m*
(022) *s*	(041) *w.*	(120) *m*	(137) *s*	(217) *m*	(331) *w m*
(023) *s*	(003) *w*	(420) *m*	(154) *s*	(226) *m*	(332) *w m*
(024) *s*	(069) *v w*	(130) *m*	(156) *s*	(311) *m*	(431) *w m*
(032) *s*		(230) *m*	(212) *s*	(313) *m*	(153) *w*
(034) *s*	*Prism Planes*	(150) *m*	(312) *s*	(316) *m*	(163) *w*
(042) *s*	{*hol*}	(170) *m*	(314) *s*	(323) *m*	(414) *w*
(044) *s*	(105) *v s*	(430) *m*	(413) *s*	(324) *m*	(422) *w*
(046) *s*	(202) *s*	(220) *w m*	(136) *m s*	(334) *m*	(185) *v w*
					(213) *v w*

The dimensions of the cell were fixed by the oscillation photographs and a number of rotation photographs The latter will be discussed later, under the heading " Localisation of the Molecules." A Laue photograph of the gallium

compound corresponded to orthorhombic symmetry *It showed no trace of pseudo-hexagonal nature*

X-Ray Examination of the Orthorhombic Acetylacetones (γ)

A number of spectrometer and photographic observations were made on ferric acetylacetone, but most of the results for the γ-form were obtained from the small crystal of gallium γ-acetylacetone mentioned above The unit cell for the γ-acetylacetones is so large (being 15 71 × 13 74 × 32 76 A U for the gallium compound) that spectrometer measurements with a molybdenum anti-cathode are not reliable Moreover, with the small quantity of ferric acetyl-acetone crystals available, the spectrometer gave only one reflection (104), which showed that the goniometric *a*-axis must be doubled, while no reflections showing the true length of the *c*-axis were observed Even a rotation-photo-graph about the *c*-axis failed at first to reveal its great length The existence of very weak intermediate hyperbolæ was first detected on the *c*-axis oscillation photographs Afterwards, a long-exposure rotation photograph was taken about the *c*-axis, and on this photograph the weak intermediate hyperbolæ can just be discerned It should be mentioned here that the indices of the X-ray reflections from the acetylacetones could be ascertained with certainty only by means of a large number of oscillation photographs The cells are too large, and therefore overlapping of spots is too frequent to permit this being done by means of the simple rotation photographs For instance, with the γ-form, as many as 126 planes (*okl*) are theoretically possible in the equatorial zone of a rotation about the *a*-axis, if we use opper rays and a quarter plate at a distance of 4 cms from the crystal Of course, it would be impossible to resolve these planes except by resorting to small oscillations A simple method of crystal-setting for oscillation photographs appears to be worth mentioning here It often happens, as in the case of the single crystal of gallium γ-acetylacetone used in these experiments, that the crystal is too small or too rough to be set by optical means Indeed, for good photographs, showing spots which can be resolved without ambiguity, small crystals are essential If now the points of two needles, supported by adjustable (and, if necessary, detachable) arms from the slit-head, be brought into alignment with the X-ray beam by looking through the slit, the line joining the two needle-points is a base-line from which bearings may be taken This is easily accomplished by means of a tele-microscope of about one centimetre field and containing a cross-wire in the eye-piece The cross-wire is set so as to join the needle-points, and the small face or edge of the

crystal, which requires setting at a known angle to the X-ray beam, is then adjusted to lie in the required direction with respect to the cross-wire. Fig 2 (representing a view looking down the microscope) makes this clear By taking the average of a number of readings, sufficient accuracy is easily attainable.

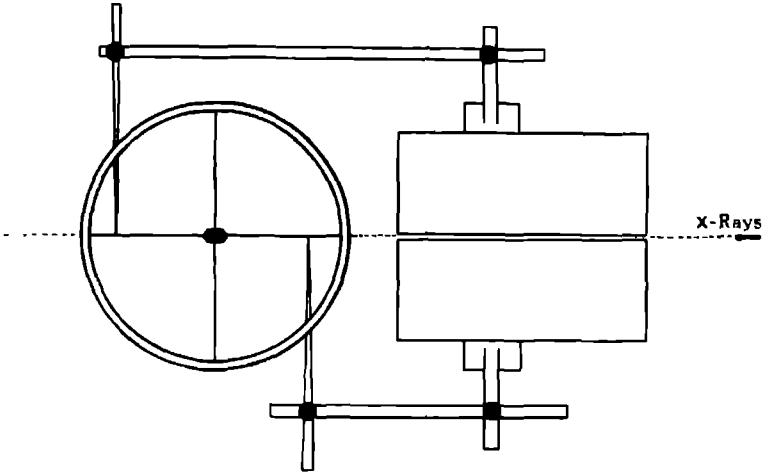

Fig. 2

The following reflections were observed from gallium γ-acetylacetone (Table V). They show the halvings $\{hk0\}$ when h is odd and $\{0kl\}$ when $(k + l)$ is odd, the corresponding space-group being either C_{2v}^{9} or C_{h}^{16}, according as the crystals are pyramidal or bipyramidal There are sixteen chemical molecules per cell, that is, either four times or twice the number of asymmetric molecules required to show the crystal symmetry A Laue photograph of ferric γ-acetylacetone corresponded to orthorhombic symmetry Like that of the β-acetylacetones, this photograph showed no trace of pseudo-hexagonal nature, even though the $(2\bar{1}0)(\bar{2}10)$ is 59° 16′.

Table V.

Axial Planes.	(4014) *m s*	(614) *s*	(2610) *m.s*	(658) *m*	(443) *w*
(200) *m.*	(408) *m.*	(6112) *s*	(278) *m s*	(274) *m.*	(542) *w*
(400) *w.m.*	(504) *m.*	(1210) *s*	(467) *m.s*	(8110) *m.*	(544) *w*
(600) *w.*	(401) *w m.*	(2214) *s*	(469) *m.s.*	(828) *m.*	(546) *w*
(020) *v.s.*	(207) *w*	(324) *s*	(4610) *m.s.*	(128) *w m.*	(642) *w*
(040) *v.w.*	(309) *w*	(428) *s.*	(126) *m.*	(129) *w m.*	(256) *w.*
(004) *v.s.*	(409) *w*	(4212) *s*	(2110) *m*	(413) *w m.*	(2510) *w.*
(008) *m*	(608) *w*	(624) *s*	(2213) *m.*	(4110) *w.m*	(3511) *w*
(0012) *w*		(234) *s*	(315) *m*	(4112) *w m*	(652) *w*
	Prism Planes	(432) *s.*	(316) *m.*	(4113) *w m.*	(656) *w*
Prism Planes	{*hko*}	(435) *s*	(322) *m*	(5113) *w m.*	(264) *w.*
{*okl*}.	(210) *v s*	(4310) *s*	(325) *m*	(137) *w m*	(275) *w*
(024) *v s*	(220) *s*	(632) *s*	(326) *m.*	(1311) *w m.*	(834) *w*
(019) *s*	(420) *s*	(634) *s*	(411) *m*	(438) *w m*	(317) *v w*
(0212) *s.*	(620) *s*	(638) *s*	(4111) *m*	(538) *w m.*	(3110) *v w.*
(044) *s*	(230) *s*	(442) *s*	(422) *m*	(732) *w m*	(513) *v.w*
(068) *s*	(440) *s*	(444) *s*	(424) *m*	(818) *w m.*	(612) *v w*
(0612) *s*	(640) *s*	(448) *s*	(512) *m*	(318) *w.*	(714) *v w.*
(026) *m s*	(650) *s*	(4412) *s*	(5111) *m*	(5110) *w*	(3210) *v w.*
(028) *m.s*	(460) *s*	(258) *s*	(521) *m*	(1211) *w.*	(431) *v w*
(022) *m.*	(410) *m s*	(2512) *s*	(528) *m*	(1212) *w*	(529) *v w*
(048) *m*	(610) *m s*	(354) *s*	(618) *m*	(232) *w*	(3311) *v w*
(0412) *m*	(430) *m s*	(4510) *s*	(621) *m*	(223) *w*	(433) *v w*
(0414) *m*	(630) *m s*	(462) *s*	(622) *m.*	(224) *w*	(4312) *v w*
(0416) *m*	(450) *m s*	(464) *s*	(628) *m*	(423) *w*	(531) *v w*
(0610) *m*	(830) *m*	(466) *s*	(6212) *m*	(429) *w.*	(532) *v w*
(017) *w m*	(240) *w.*	(468) *s*	(139) *m*	(724) *w.*	(635) *v w*
(037) *w m*		(117) *m s*	(232) *m.*	(138) *w*	(737) *v w*
(0410) *w m*	*General Planes*	(127) *m s*	(233) *m*	(1312) *w.*	(242) *v w*
(013) *w*	(118) *v s*	(1214) *m s*	(2310) *m*	(1313) *w*	(244) *v w*
(039) *w*	(214) *v s*	(229) *m s*	(246) *m*	(236) *w*	(641) *v w*
(046) *w*	(218) *v s*	(323) *m s*	(434) *m*	(2313) *w*	(6411) *v w.*
(0214) *v w*	(2112) *v s.*	(414) *m s*	(436) *m*	(331) *w*	(1514) *v w*
	(314) *v s*	(415) *m s*	(445) *m*	(332) *w.*	(254) *v w*
Prism Planes	(226) *v s*	(522) *m s*	(446) *m*	(333) *w*	(457) *v w*
{*hol*}	(2210) *v s*	(614) *m s*	(447) *m*	(336) *w*	(555) *v w*
(108) *v.s*	(238) *v s*	(2316) *m s*	(4410) *m*	(3314) *w*	(556) *v w*
(109) *s*	(2312) *v s*	(2410) *m s*	(452) *m*	(431) *w*	(5510) *v.w*
(304) *s*	(1110) *s*	(2414) *m s*	(454) *m*	(533) *w*	(651) *v w*
(404) *s*	(1111) *s.*	(4314) *m s.*	(458) *m*	(539) *w*	(262) *v w*
(408) *s*	(217) *s*	(456) *m s*	(535) *m*	(631) *w*	(472) *v w*
(4012) *s*	(2111) *s*	(6312) *m s*	(5310) *m*	(6310) *w*	(822) *v w*
(808) *s*	(2113) *s*	(644) *m s*	(548) *m*	(6311) *w*	(832) *v w*
(106) *m.s*	(412) *s.*	(648) *m s*	(633) *m*	(1412) *w*	(834) *v w*
(2012) *m s*	(418) *s*	(654) *m s*	(636) *m*	(1413) *w*	
(4018) *m s*	(4114) *s*	(268) *m s.*	(6410) *m*	(346) *w*	

Localisation of the Molecules.

The great similarity between the respective habits of the three forms of the tervalent acetylacetones has been mentioned above. They have in the main a simple pseudo-hexagonal appearance, due to the predominance of the three forms {001}, {010} or {100}, {110} or {210}. Other forms are either very small or quite absent. The unfailing predominance of the three forms mentioned, considered with regard to the close resemblance between the dimensions of all

three unit cells, points unmistakably to the relative distribution of the molecules in the cells. From these two facts alone there can be little doubt where the molecules lie, but the general appearance of the rotation photographs settles the matter It is clear from the combined evidence that the approximate arrangement of molecules is as in figs. 3A, B and C, for the α-, β- and γ-forms respectively. (The dimensions indicated are those of the gallium compounds)

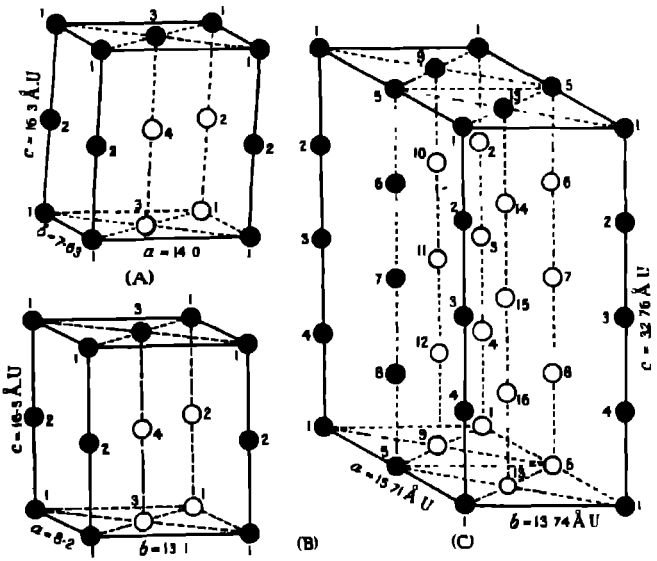

FIG 3.

As a preliminary to this localisation of the molecules by rotation photographs, two photographs were taken, one of naphthalene about the direction [110] as rotation-axis and one of hydrated oxalic acid about the direction [111]. In both these cases the molecules (two per cell) are quite large and their relative positions are fixed by space-group considerations, the second molecule of naphthalene being at the middle of the (001) face and of oxalic acid at the middle of the cell Since, in a rotation photograph about the axis $[uvw]$, the reflection from a plane (hkl) lies on the nth hyperbola when $hu + kv + lw = n$, it is clear that certain reflections will vanish from the odd hyperbolæ of these two rotation photographs simply on account of the ordinary space-group halvings. This circumstance naturally makes the odd hyperbolæ weaker than the even, but the observed weakening is greater than can be ascribed to this cause alone

There is a further general weakening of the odd hyperbolæ with respect to the even on account of the primitive translation parallel to the rotation-axis being approximately halved by the second molecule of the cell This effect is only approximate because of the different orientations of the two molecules, but it often affords a convenient method for making a rapid survey of the relative positions of complex organic molecules in a crystallographic unit The more the molecule which subdivides the primitive-translation parallel to the rotation-axis resembles the two molecules which are connected by the primitive translation, the more complete is the obliteration of certain hyperbolæ From this point of view we can state a simple principle which can be of use for determining the approximate symmetry of an asymmetric organic molecule *When a molecule almost completely subdivides the primitive translation parallel to the rotation-axis, it possesses approximately that element of symmetry which is involved in deriving it from the molecules at the ends of the primitive translation* For instance, in a monoclinic cell, we might find the *c*-axis almost completely halved by a "reflection-molecule" (*i e* the odd hyperbolæ almost completely obliterated), in which case we may conclude that the molecules are approximately symmetrical about the (010) plane.

The acetylacetones afford very good examples of this weakening of certain hyperbolæ by molecules actually or approximately in special positions The following rotation-photographs were taken '—α-*acetylacetones* —1 *a*-axis—normal 2. *b*-axis—normal 3 *c*-axis—marked weakening of odd hyperbolæ 4 [110]—slight weakening of odd hyperbolæ 5. [11½]—odd hyperbolæ very weak; of the even hyperbolæ, the fourth and eighth are rather stronger than the second and sixth. β-*acetylacetones*.—1. *a*-axis—normal 2 *b*-axis—normal. 3 *c*-axis—marked weakening of odd hyperbolæ. 4. [110]—weakening of odd hyperbolæ 5. [011]—normal. 6 [101]—normal. 7. [111]—weakening of odd hyperbolæ γ-*acetylacetones*.—1. *a*-axis—very pronounced weakening of odd hyperbolæ. 2 *b*-axis—normal 3 *c*-axis—odd hyperbolæ almost completely obliterated, second, sixth and tenth hyperbolæ weak, fourth eighth and twelfth hyperbolæ strong 4 [½ 10]—similar features to 3 5. [10½]—fourth and eighth, etc., hyperbolæ strong, others weak except tenth.

It can be readily seen from these results how the general arrangement of molecules in the three types of tervalent metallic acetylacetones must conform approximately to figs 3A, B and C. As mentioned above, these observations are in agreement with the conclusions to be drawn from the habit of the crystals, Similar conclusions may also be drawn, of course, from the lists of reflections

observed on the oscillation photographs. For instance, we notice for the γ-acetylacetones that (*a*) there are 58 *v.s.* and *s.* planes which intersect the *c*-axis; of these 37 have *l* a multiple of 4, 14 have *l* a multiple of 2 but not of 4, while only 7 have *l* odd, and (*b*) not counting the planes (*hko*), which are naturally halved when *h* is odd, there are 51 *v s.* and *s* planes which intersect the *a*-axis, and of these 41 have *h* even and 10 have *h* odd. In other words, the γ-structure behaves approximately as though the cell were one-eighth its actual size

It is an interesting point that the relative intensities of reflection are practically the same for different members of the same group. For instance, a rotation photograph of aluminium α-acetylacetone showed no marked differences from a corresponding photograph of gallium α-acetylacetone The reason for this appears to lie in the fact that the molecular weights of these compounds are so high that the effect of the central metallic atom, even though in the case cited we pass from Al (27) to Ga (70), is a relatively subsidiary one.

Crystal Class

There is considerable difficulty in adducing direct evidence for the respective crystal classes of the acetylacetones Only indirect or negative arguments can be used, but on the whole these support the weightiest consideration, that there is an overwhelming mass of chemical evidence that compounds of the sixfold co-ordination type are based on octahedral symmetry. Those containing three chelate groups, being degenerated to the sixfold symmetry of the quartz class, must also be enantiomorphous.

α-acetylacetones.—The X-ray halvings indicate holohedral symmetry, space-group C_{2h}^{5} This agrees with the etched figures produced by the action of acetone on the (001) face of aluminium α-acetylacetone (fig. 4A). These consist of triangular pyramidal pits with a plane of symmetry parallel to the (010) face. The crystal habit is not in disagreement, and no optical activity has been observed in solutions of single crystals. Neither was any pyro-electric effect observed with sulphur and red lead. We may fairly conclude, then, that the α-acetylacetones are monoclinic prismatic, space-group C_{2h}^{5}.

β-acetylacetones.—The X-ray halvings indicate either rhombic pyramidal symmetry, space-group C_{2v}^{7}, (100) plane of symmetry absent, or rhombic bipyramidal symmetry, space-group Q_h^{13} The habit is non-committal. The etched figures, too, produced by acetone on {001} of indium β-acetylacetone, are indecisive (fig. 4B), being greatly elongated parallel to {010}. It is difficult to say whether the two ends are really alike, though with regard to angles the

figures appeared to correspond to the natural habit, {010} + {110} Neither optical activity nor pyro-electricity was detected If the space-group were

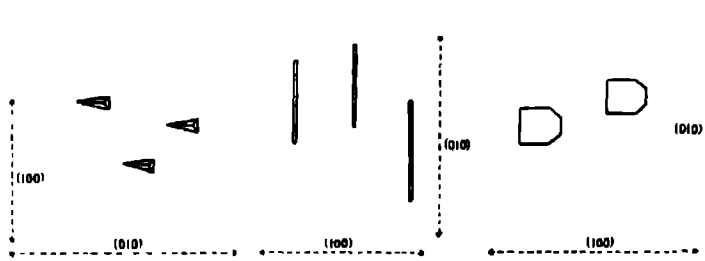

Fig 4A Fig 4B. Fig 4C

Q_h^{16}, the observed positions of the molecules would require them to be symmetrical about (100). In view of the absence of really conclusive evidence that the crystals are bipyramidal, chemistry demands that we should reject this possibility and conclude that the β-acetylacetones are rhombic-pyramidal, space-group C_{2v}^7, (100) plane of symmetry absent

γ-acetylacetones —The X-ray halvings correspond to either rhombic pyramidal symmetry, space-group C_{2v}^9, (010) plane of symmetry absent, or to rhombic bipyramidal symmetry, space-group Q_h^{16}. The habit again is non-committal. On the other hand, etched figures were obtained by the action of acetone on {001} of the crystal of gallium γ-acetylacetone mentioned above. These (fig. 4c) were definitely unsymmetrical about the plane (010) Pyro-electricity was not detected in the few small crystals of ferric γ-acetylacetone available, but we must conclude that, like the β-acetylacetones, the γ-acetylacetones are also rhombic pyramidal, though of space-group C_{2v}^9, with the (010) plane of symmetry absent. If Q_h^{16} were the true space-group, the molecules, in order to lie in the positions observed, would each have to be symmetrical about the plane (010).

The difficulty of determining by ordinary crystallographic methods the true crystal classes of the acetylacetones recalls a similar phenomenon encountered by Jaeger,* also with compounds containing three chelate groups Though many of the crystals described by Jaeger give intensely optically active solutions, yet to ordinary crystallographic tests they appear perfectly holosymmetric. It is possible that both his crystals and those described in this paper would

* F. M. Jaeger, 'Rec. d. Trav. Chim. d. P.B.,' vol 38.

yield evidence of pyro- and piezo-electric properties if they were tested by means of amplifying valves *

Crystal Structure

From the combined crystallographic and X-ray evidence we have concluded above that all three types of tervalent acetylacetones are built up of closely related unit cells with a similar molecular distribution The α-cell is practically a monoclinic distortion of the β-cell, which in turn is about one quarter of the γ-cell The molecules in the α- and β-units lie at or near the centres of the (001) faces and the mid-points of the c-edges, while from this arrangement the γ-form is obtained simply by doubling the *a*- and c-edges. The difference between the three forms thus lies in a difference of molecular orientation Apparently the molecules are effectively asymmetric in all three forms, since none of the sixfold symmetry of the "free" molecule is used in the crystal structure. Hence, referring once more to figs 3A, B and C, we have for the *α-form* (fig. 3A) :—Molecule 2 is obtained from 1 by reflection in the symmetry plane (010) followed by a translation of $c/2$, 3 (or 4) is obtained from 1 by rotation about a dyad axis parallel to *b* followed by a translation of $b/2$, while 4 (or 3) follows from 3 (or 4) as does 2 from 1. For the *β-form* (fig. 3B), we have :—2 is obtained from 1 by reflection in a plane parallel to (001), 4 from 1 by reflection in a plane parallel to (010) followed by a translation of $(a/2 + c/2)$, while 3 follows from 4 as does 2 from 1. (N.B.—Since the observed "halvings" may be considered either as $(h + l)$ odd or $(l + h)$ odd, there are two ways of setting up C_{2v}^7. One of them (symmetry plane parallel to (001) absent) is not possible with the observed distribution of molecules, unless these latter are plano-symmetrical and "associated" in pairs. For the *γ-form* (fig. 3C), we have :—Either 11 or 15 is derived from 1 by reflection in a plane parallel to (100) followed by a translation of $(b/2 + c/2)$, one of the molecules 5, 6, 7 or 8 is derived from 1 by reflection in a plane parallel to (001) followed by a translation of $a/2$, while a similar operation connects 11 or 15 with another molecule inside the cell. There still remain twelve molecules in excess of the four required to produce the class symmetry These twelve must be considered to be associated with the other four so as to complete four sets, each set consisting of four chemical molecules and being related to the other three sets by the symmetry operations outlined above for the γ-form. In other words, the "crystal molecule," instead of corresponding to one chemical molecule (as in the α- and β-acetylacetones and, indeed, in most other cases that have been

* R. Lucas, 'C. R.,' vol. 178, p. 1890 (1924).

investigated), corresponds in the γ-acetylacetones to four "associated" chemical molecules The distribution of molecules and symmetry elements in the space-groups C_{2h}^5, C_{2v}^7 and C_{2v}^9 may be seen at a glance in figs. 14, 22 and 24 of the space-group diagrams mentioned above (Astbury and Yardley)

From these considerations we may now proceed to a more detailed discussion of the three structures This is rather a forbidding task in view of the complexity of the molecules, but it will be seen that a certain amount of information can still be gleaned from a critical examination of the experimental data. For instance, though the centres of the molecules are arranged on a pseudo-hexagonal basis, it is clear from the Laue photographs that the similarity extends no farther and that the structures as a whole are not in the least of a hexagonal or a trigonal nature. This means that the triad axis (and a similar remark applies to the three dyad axes), which one might expect in the "free" molecule, has been rejected in building up the crystal symmetry The molecules are orientated in such a way as to render ineffective the pseudo-hexagonal arrangement of their centres Again, if we look at the respective dimensions of the three cells shown in fig. 3, we see that the molecules are spaced along the *c*-axes all at the same distance, about 8 15 A.U or a little over, a dimension which occurs again in the *a*-axis of the β-form. This, then, is approximately the maximum "diameter" of the molecule · in fact, the general impression we gain from these dimensions is of a molecule which may be rotated about its maximum diameter into various positions and yet always requires a "domain" of space of about the same size and shape when packed in a similar manner with other molecules of its kind. In other words, the structures are built up of rounded molecules, without projecting arms, which might interlace. In support of this inference, we may also cite the very good cleavage which occurs in the β- and γ-forms and the ease with which all three forms may be crumbled.

A molecule which will satisfy these conditions is at once afforded by the ordinary chemical conception of three chelate groups arranged octahedrally around a central atom Such an arrangement would have a maximum diameter of the order observed (8 2 A U), with the same dimension occurring in a direction at right angles to it (*cf* β-form, fig. 3B), and with other equatorial dimensions not very much different, when we allow for the fact that it is only the *linear skeleton* of the molecule which has more or less true octahedral dimensions, and that there are forty-two atoms strung, so to speak, on this framework. This molecule is represented diagrammatically in fig 5 It fits in very well indeed with the results of X-ray and crystallographic observation, and, as we shall see

below, serves to explain and co-ordinate the main features of this remarkable case of isotrimorphism The three forms will be dealt with in turn.

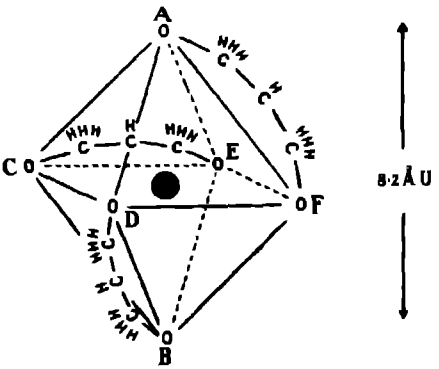

Fig. 5

α-form.—It is not possible to form any precise ideas about this structure. One of the maximum diameters (AB, fig. 5) is apparently directed along the *c*-axis, while the *b*-axis is occupied by one of the smaller dimensions such as CD or DF. It is probable that the molecules 3 and 4 (fig 3A) are not exactly at the centres of the (001) face and cell respectively, but are displaced something less than one-quarter the height of the cell This conclusion is derived from the facts that (*a*) there is no cleavage and (*b*) the rotation photographs about the axes [110] and [11$\frac{1}{2}$] indicate a displacement of between 0 and $c/4$ from the

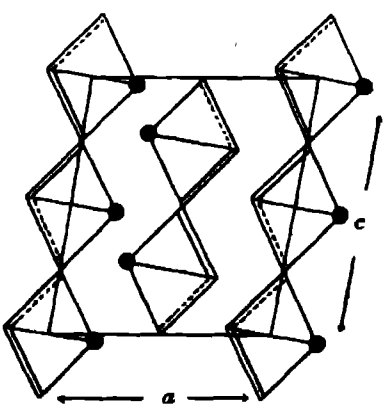

Fig. 6.

symmetrical positions The aspect of the (010) face of such a structure is shown diagrammatically in fig 6 The two molecules in the body of the cell lie in a plane $b/2$ above or below the plane of the other molecules It should be remembered that the molecules in these diagrams are, for convenience, drawn with the full symmetry of the chemical molecule outlined in fig 5. Actually, they must not be quite so symmetrical as that or even quite so symmetrically disposed as the diagrams represent, but the distortions involved are not large

β-*form* —The nature of this structure appears to be quite clear. We have now a maximum diameter lying along both the *a*- and *c*-axes, with the molecules approximately in symmetrical positions Figs 7A and B show the aspect of the (001) face, A representing the upper layer (molecules 1 and 3, fig 3B), and B the lower layer (molecules 2 and 4). Between these two layers we should expect a good cleavage, and, in fact, experiment shows that this good cleavage actually exists But the most remarkable confirmation of this structure arises out of the accidental halving of the form {010}. We can see at once from fig 7 how this halving is brought about We know that the rotation of a molecule about an axis of symmetry followed by a translation along that axis causes an abnormal spacing to be observed by X-rays for the plane perpendicular to the axis In the β-acetylacetones, molecule 3 can be obtained from 1 (and molecule 4 from 2) by a rotation about a dyad-axis parallel to *a*, followed by a translation of $a/2$; but because the molecule consists of three equivalent chelate groups, the same transformation can be achieved by a rotation through 90° about the *b*-axis, followed by a translation of $b/2$ This operation will halve the spacing of (010) Experiment shows that, in addition to the usual halvings of C_{2v}^7, the spacing of the form {010} is completely halved in the β-acetylacetones. It should be noted, too, that the structure proposed agrees with the Laue photograph in that it is not pseudo-hexagonal

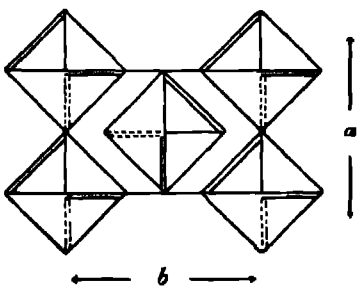

FIG. 7A

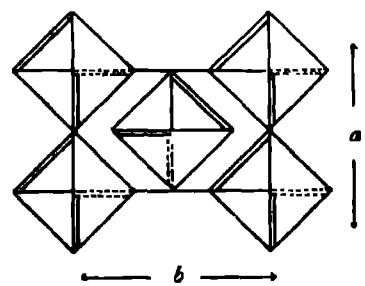

FIG. 7B

γ-form.—The γ-form is closely related to the β-form described above While we have once more a maximum diameter lying along the *c*-axis, the *a*-axis is now occupied by one of the smaller diameters This gives rise to some arrangement such as is shown in fig 8, which represents diagrammatically the aspect of the (001) face In this figure it is assumed that molecules 8 and 15 are obtained from 1 by reflection and molecule 10 by rotation, that is, four levels are shown in the same diagram Of course, as mentioned above, this is only one possible arrangement, but all illustrate the points that now, since the molecules have been rotated through 90° from the β-position, the *a*-dimension is less and a good cleavage on (010) is possible. This cleavage actually exists in the γ-form The (001) cleavage is also still possible, but for some reason it does not occur. Possibly, this absence is connected with the "association" of the molecules In any case, it is not remarkable, since cleavage is in general a relative property, occurring only at the weakest junction. It is not possible to say anything very reliable about the orientations of the remaining twelve molecules of the cell. They are "associated" with the other four so as to form four sets, and their relative positions appear to be quite definite, but of the nature of the fourfold association we can as yet say nothing Possibly, since the (001) cleavage is absent, the sets of four lie each in planes parallel to (010), which is a good cleavage. One experimental observation is worthy of emphasis, and that is that the (001) spacing is not merely halved, as the space-group requires, but actually *quartered*, without any trace of intermediate orders. This suggests that the arrangement shown in fig. 8 is the right one, for inspection of that figure reveals a characteristic similar to the one already observed for the

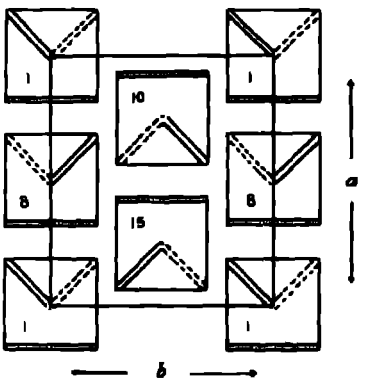

Fig. 8.

β-form. Owing to the peculiar shape of the molecule we see that molecule 10 can be obtained from 1 not only by a rotation about a dyad-axis parallel to *b*, followed by a translation of *b*/2, but also by a rotation about a dyad-axis parallel to *c*, *followed by a translation of* *c*/4.—Such a combination would undoubtedly quarter the (001) spacing, for a similar effect will also be produced by molecule 8, which is the reflection of 1 in a plane parallel to (001). This agreement seems to be more than accidental. It is a direct inference from (1) the observed molecular distribution and (2) the chelate grouping deduced from chemical considerations that a true quartering of the (001) spacing may be expected from certain structural combinations of the molecules, and, as in the β-acetylacetones, experiment shows this abnormal spacing actually to exist. There seems little doubt that the main characteristics of the isotrimorphism of the tervalent metallic acetylacetones are substantially in accordance with the scheme outlined above.

Addendum.

By Gilbert T. Morgan.

In an investigation of the co-ordination compounds of vanadium published thirteen years ago (Morgan and Moss, 'Trans. Chem. Soc.,' vol. 103, p. 81, (1913)), stress was laid on the relationship between the number and spatial distribution of associating units round a central metallic atom and the formation of a stable co-ordination complex.

The case of metallo-β-diketones was examined from this view-point and several new vanadium compounds of this type were then described. This study was extended as occasion offered to acetylacetones of other tervalent metals, and the remarkable stability of scandium acetylacetone at high temperatures was demonstrated by distilling the compound unchanged under reduced pressure ('Trans. Chem. Soc.,' vol. 105, p. 197, (1914)).

More recently gallium acetylacetone has been described (Morgan and Drew, *loc. cit.*) and compared with the acetylacetones of aluminium and indium. Here again the three compounds showed considerable stability, although the tendency to decompose on sublimation increased with the rise in atomic weight of the central metallic atom.

The non-ionised character of the metallo-β-diketones and their solubility in organic media indicate plainly that these substances are not be be regarded simply as metallic salts of organic acids. On the contrary, they are internal metallic complexes of unitary type with the central metallic atom so closely

implicated in the organic radicals of the molecule that the metallic atom no longer has those properties of its ion which are employed for the detection of the ion in qualitative analysis. Moreover, in the case of metals having coloured compounds, the colours of the acetylacetone derivatives are often quite different from those of the ordinary salts of these metals.

In order to account for the exceptional properties of the acetylacetones of the metals other than alkali metals, it was assumed that the univalent acetylacetone radical, $C_5H_7O_2$, was a chelate group functioning in co-ordination complexes as a twofold associating unit (I)

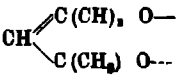

I

This formula was, however, regarded as a dynamic one similar to the Kekulé conception of the benzene ring, so that in the heterocyclic ring completed by implication of the central metallic atom (M) there was an oscillation between the two extreme positions II and III.

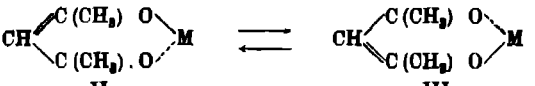

II. III

As a result of this rearrangement the two limbs of the chelate group become identical and the ring system has a plane of symmetry which can be tested for by X-ray analysis

Moreover, the stability of these metallic acetylacetones of tervalent metals has been ascribed to the octahedral distribution of the three chelate groups (six associating units) round the central metallic atom (Morgan and Moss, *loc. cit.*)

These two assumptions in regard to the structure of the acetylacetone radical and to the symmetrical arrangement of three of these chelate groups round a central tervalent metallic atom have now been confirmed by the detailed X-ray analysis described in the present communication.

Summary.

1. Ten tervalent metallic acetylacetones have been examined by X-rays with a view to determining their crystal structures and the nature of the remarkable isotrimorphism which they collectively exhibit. Of the α-(monoclinic) form were examined the acetylacetones of aluminium, chromium, manganese, cobalt

and gallium, of the β-(orthorhombic) form, scandium, gallium and indium, of the γ-(orthorhombic) form, iron and gallium. A single crystal of gallium γ-acetylacetone has been observed for the first time.

2. By means of the spectrometer and photographic methods it has been shown that the α-acetylacetones are monoclinic-prismatic, space-group C_{2h}^5, the β-acetylacetones are rhombic-pyramidal, space-group C_{2v}^7, and the γ-acetylacetones are rhombic-pyramidal, space-group C_{2v}^9. The α-form contains four chemical molecules per unit cell, the β-form four, and the γ-form sixteen. In the γ-form the molecules appear to be associated in four groups of four chemical molecules each.

3. The positions of the molecules in the three forms have been determined by a study of the intensity distribution in a series of rotation photographs about various crystallographic axes.

4. Several of the crystals have been examined for etched figures, pyro-electricity and optical activity.

5. In spite of external appearance, none of the three forms is pseudo-hexagonal.

6. By means of the molecule that has been deduced from chemical considerations, the relation between the three forms and the nature of the isotrimorphism is explained and the main outlines of the three structures sketched.

7. An addendum, from the chemical point of view, has been contributed by Professor G. T. Morgan.

The writer wishes once more to thank Sir William Bragg for his unfailing kindness and encouragement and the Managers of the Davy Faraday Laboratory for affording the facilities for carrying out the work. This was made possible by a grant from the Department of Scientific and Industrial Research. He is indebted also to Prof. G. T. Morgan for supplying the crystals used and for much chemical information, and to Mr J. D. Bernal, of this laboratory, for the use (before publication) of his rotation-chart and the calculations connected with it.

Change of Crystal Structure of Some Salts when Crystallised from Silicic Acid Gel—The Structure of Silicic Acid Gel

By H. A. Fells, B Sc , A I C , and J B Firth, D Sc , F I C

(Communicated by Prof F S Kipping, F R S —Received May 17, 1926)

(Plates 16 and 17)

In a paper, " Liquid Diffusion Applied to Analysis," read before the Royal Society in 1861, Graham describes the diffusion of salts through membranes and gels Crystallisation from gels has, however, only been developed within recent years

The growth of " Rhythmic Bands," so extensively studied by Liesegang,* has been suggested as an explanation of many natural formations in the earth's crust, whilst Hatschek† and others‡ applied the results of Liesegang to explain gel structure Hatschek and Simons§ showed that gold could be obtained in crystal form, when gold chloride is reduced in the presence of silicic acid gel, the gold being deposited either in the gel, at the surface of the gel, or in both positions, according to the osmotic relationship of the solution and the gel

For certain experiments in another research the authors desired to prepare silicic acid gels impregnated with various substances. These substances are introduced in many cases as soluble compounds by dissolving the desired substance in either the sodium silicate solution or the acid, prior to mixing. The added substance decomposes on strongly heating, leaving the desired residue evenly distributed throughout the gel. Under such circumstances, owing to the solubility of the added substance, it was impossible to follow the usual procedure of washing out the sodium chloride before heating Gels were therefore prepared and carefully dried without previous extraction of the sodium salt In carrying out this process the sodium chloride separated out at the surface of the gel, and it was found that the crystal habit was materially changed In order to determine to what extent this phenomenon was characteristic of crystal formation from silicic acid gel, the experiments were

* 'Ann Physik,' vol 10, p. 395 (1906), 'Z. anorg Chem ,' vol. 48, p 364 (1906), 'Z Chem Ind. Koll.,' vol. 12, p. 74 (1913), and vol. 14, p 31 (1914).

† 'Z Chem Ind Koll ,' vol. 10, p. 124 (1912); 'Koll. Z ,' vol. 14, p 115 (1914)

‡ Holmes, 'J Am Chem. Soc.,' vol 40, p 1187 (1918), Bradford, 'Science,' vol 54, p 403 (1921), 'Biochem J.,' vol. 11, p. 14 (1917).

§ 'Zeit Chem Ind. Koll ,' vol 10, p 265 (1912)

extended to other salts, and the results are described in the present communication

Experimental

Specially and freshly prepared sodium silicate was used, free from iron and carbon dioxide The composition of the sodium silicate was approximately one part of Na_2O to two parts SiO_2 Pure acids were used throughout, and the acids used were hydrochloric, hydrobromic, hydriodic, and nitric acids respectively Gels were prepared at 18° C. by mixing equal volumes of 3N acid and sodium silicate solution of density 1·15. A portion of the resulting gel was then transferred to a watch glass and slowly dried *in vacuo*, in a desiccator containing calcium chloride As the gel dried, the surface of the gel became covered with a mass of very fine crystal-like needles, which, as the drying proceeded, increased in size until eventually the product resembled a ball of fluff with a hard silica core

The needles thus obtained were then subjected to microscopic examination and the features observed are herein described

The Chloride and Nitrate of Sodium

The general appearance of the sodium chloride needles is shown in the micro-photograph, fig. 1 Fig 2 shows the ordinary cubic form obtained from a solution of the needles with one or two needles Fig 3 is a micro-photograph of the sodium nitrate needles.

These two salts need not be separately considered since they possess the same general characters Ordinarily sodium chloride crystallises in cubes, though sometimes in the octahedral form, whilst sodium nitrate crystallises in rhombohedra

Habit —The crystals are all fibrous in habit and most of them are blades. The variation in size is considerable, those being formed first having an average width of 0 25 mm , the later ones are much finer, having an average width of 0·01 mm or less Generally the fibres are straight, but they are flexible, since they can be bent in mounting , they are also somewhat elastic In some cases (fig 9*a*) they show abrupt bends, but these are not produced mechanically and show no sign of strain. They seem to be due to changes in the direction of growth owing to changes in the surface of the gel in drying, and the inability of the fibres to adapt themselves to it owing to overcrowding

Optical Properties.—The crystals are all sensibly isotropic and indicate cubic crystals Indications of very faint double refraction are met with in some

cases, giving very low grey colours. The double refraction is so small, however, that it is difficult to determine, sometimes even with a sensitive violet plate.

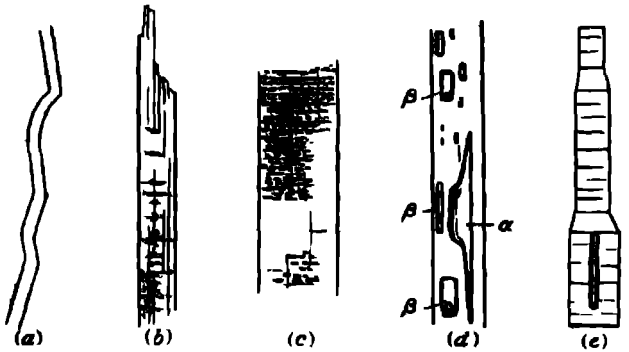

Fig. 9

An X-ray examination of the sodium chloride needles showed an internal structure of the cubic system. The crystals show cleavages both longitudinally and transversely, but the former is more commonly visible This cleavage is parallel to the cube and indicates that the needles are elongated parallel to the cubic axis. (Cleavages are shown in fig. 9*b*) The transverse strias are lines of inclusions, doubtless arranged on the lines of the transverse cleavage These minute inclusions appear to be bubbles (fig. 9*c*).

The longitudinal structure presents no difficulty. They clearly resolve themselves into "negative crystals." The larger are due to coalescence of the smaller; or in some cases at least to the development of a very large negative crystal. The general conditions are shown in the enlarged diagram (fig. 9*d*). The capillary, of which only a portion is shown at "α," runs about half the length of the fibre. It is filled with liquid and contains gas bubbles. Smaller negative crystals are shown at "β," and some of these contain gas bubbles. These smaller negative crystals are the same shape as the fibres. This is, of course, a general and familiar phenomenon in crystals, such as quartz in granites and pegmatites. In the case of the fibres, we have not a true capillary in the sense of a fine tube—there is no tubular growth. The cavities are bounded by crystal faces, and never penetrate to the exterior.

FIG. 1. (× 20 diam.)

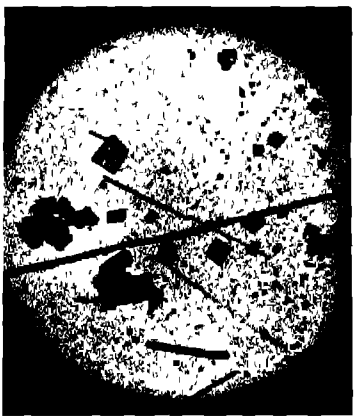

FIG. 2. (× 20 diam.)

FIG. 3. (× 20 diam.)

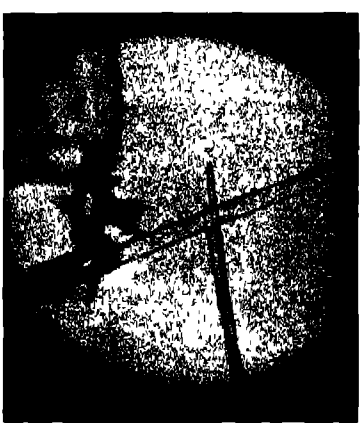

FIG. 4. (× 15 diam.)

(*Facing p. 470*)

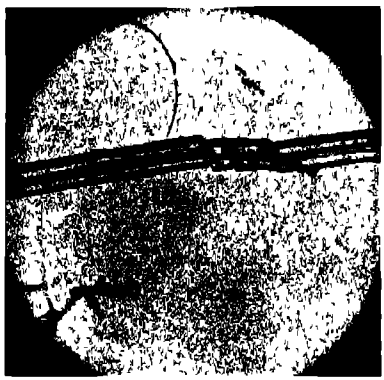

FIG. 5.—(, 18 diam.)

FIG. 6. (20 diam.)

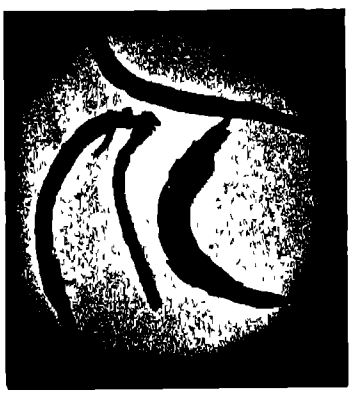

FIG. 7. (20 diam.)

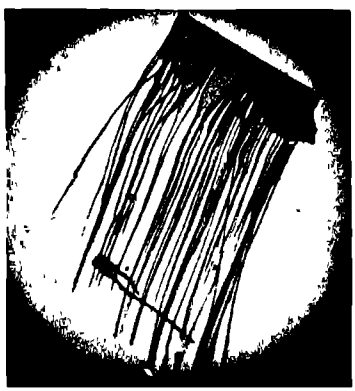

FIG. 8.—(10 diam.)

Sodium Bromide.

The general appearance of the crystals is shown in microphotographs, figs. 4, 5 and 6. Figs. 4 and 5 show clear needles and apparent capillary structure respectively. The forms are exceedingly unstable, a slight alteration of temperature or even application of pressure being sufficient to change the glass-clear crystal into a mass of minutely crystalline material, causing the crystal to lose its transparency. This change is shown in fig. 6.

Habit.—Besides a fibre-like habit resembling the chloride and nitrate just described, the sodium bromide has more commonly a stout prismatic habit, occasionally showing abrupt changes in cross-sectional dimensions (fig. 9*e*).

Optical Properties.—The crystals show a moderate refringence and a weak birefringence. Partial uniaxial interference figures were obtained in some prisms, very oblique to the optic axis. The prisms appeared to be six-sided, and the evidence favours the hexagonal system. Ordinary sodium bromide belongs to the rhombic system. The prisms are elongated parallel to the principal axis and show a perfect basal cleavage, which appears as transverse striations on the faces of the larger prisms. Inclusions are much less common than in the chloride or nitrate, but negative crystals (fig. 9*e*) are present sometimes, giving an appearance of a capillary structure when much elongated.

Sodium Iodide.

Similar in general appearance to the fibres previously described, but changed to an opaque form too rapidly to allow microscopic investigations.

Further Experiments.

(*a*) A purified silicic acid gel containing 7 per cent. water was impregnated with a strong solution of potassium iodide and the resulting gel dried as before. After several days, the gel was covered with fine silky fibres very much distorted (fig. 7), but otherwise very similar to the fibres previously described.

(*b*) 10 c.c. of toluidine was *just* dissolved in concentrated hydrochloric acid and added to 50 c.c. of 3N hydrochloric acid. To the resulting solution, 50 c.c. of the sodium silicate solution was added. The gel obtained was then dried as before. The first crystals to form on the surface were the ordinary plate crystals of toluidine hydrochloride, as the drying continued the plates were lifted from the surface gel, and needle-like formation appeared. Analysis of these needles at various stages of the drying of the gel showed that the needles first formed were mainly toluidine hydrochloride associated with a little

sodium chloride, whilst finally the needles were mainly sodium chloride. This is illustrated by the following results :—

(i) First crop of needles .	85·5 per cent toluidine hydrochloride, 14 5 per cent sodium chloride
(ii) Second crop of needles	74 7 per cent toluidine hydrochloride, 25·3 per cent sodium chloride
(iii) Third crop of needles	32 7 per cent toluidine hydrochloride 67 3 per cent sodium chloride

The formation is shown in microphotograph fig 8 Aniline hydrochloride gave a similar result

(c) A 0 6 N solution of tartaric acid was mixed with an equal volume of a solution of sodium silicate (Δ1 17) and allowed to set The resulting gel was then allowed to stand exposed to the atmosphere at room temperature, after four days small regular prisms of sodium tartrate separated out in the body of the gel No distortion of crystal habit was detected

Discussion

In our opinion the fundamental importance of the results of the experiments herein described does not lie so much with the new features of crystal habit of the various salts described, but with the reason that the salts all tend to change their habit and assume a new one, common to all of them

Generally speaking, no matter what the crystal habit may be under ordinary conditions - cubic in the case of sodium chloride, rhombic in the case of sodium bromide and nitrate, or distorted plates in the cases of aniline and toluidine hydrochloride—all the substances assume a blade-like or fibre-like structure. The photographs and diagrams all show similar features for the various substances, and we are of the opinion that the main features of the changes are due to the same causes—the influence of the gelation of the silicic acid, and the structure of the gel so formed.

The crystallisation of a substance from solution involves the concentration of the molecules about certain points or centres of crystallisation, and in the cases considered in this paper these centres appear to be at the surface of the gel It has been suggested by the authors in a previous paper* that these centres of crystallisation are at the open ends of capillaries or pores of the gel. It was suggested that the solution exudes from the pores of the gel, evaporation of the water takes place immediately, causing the salt to crystallise just at the

* 'J Phys. Chem.,' vol 29, p. 241 (1925).

open end of the pore. As the gel further dried it contracted, with the result that a continuous deposition of salt took place from the pore, leaving a long fibre-like structure protruding from the gel surface This view is further supported by the fact that the later formed "crystals" are much finer or smaller in cross-section than those first formed, the pores themselves being much smaller owing to contraction of the gel.

Arsen* in a contribution on gel structure states that if the conditions favourable to proper crystallisation are departed from, there is a tendency towards irregular arrangements forming the lattice, and irregular-shaped crystals result Often mother liquor is included The inclusion of water in a crystal is some evidence of departure from the regular, close-packed arrangement of atoms, which is characteristic of a normal lattice A crystal containing included liquid may contain a certain proportion of gel structure

Tabor,† in attempting to account for the cross-fibre veins of fibrous minerals, expresses the view that the original fineness of the fibre is dependent on the pore-spacing of the country rock and that crystallisation commences at each pore, the fibres elongating therefrom in the direction from which material is accessible He also states that the growth of the fibres follows the movement of the surface from which they protrude Sudden changes in the direction of the fibres and gradual bending are thus a record of the movement of this surface

It will be observed that the above view is in accordance with our results, the idea of pore structure being responsible for the change of crystal habit is maintained, and, further, the view that bent crystals are due to movement of the surface of crystal growth is also substantiated

Again, Kraus,‡ referring to the Bechhold capillary phenomenon, states that salts concentrate at the surface of porous bodies when evaporation is allowed to take place, and the dissolved substance tends to move towards the end of a capillary which is losing solvent

In our experiments (with the exception of the internal crystallisation of sodium tartrate) crystallisation was associated with loss of solvent No crystallisation took place when the gel was allowed to stand in a moist atmosphere, even though under such conditions the firmness of the gel materially increased—*i e*, the crystallisation was associated with loss of solvent. The loss of solvent took place at definite points on the surface—namely, the open

* 'J. Phys Chem,' vol 30, p. 306 (1926)
† 'Proc Nat Acad Sci,' vol 2, p 659 (1916).
‡ 'Koll. Z.,' vol 28, p 161 (1921).

end of pores—which resulted in a concentration of the salt at these points followed by crystallisation.

In conclusion, the authors are of the opinion that the results recorded in the present contribution lend support (*a*) to the view of capillary structure of silicic acid gel, (*b*) that the change of crystal habit, whereby fibre-like crystals are produced, indicates salt concentration at the pores, the pores become centres of crystal growth, and the growth of the crystal is controlled by the continuous accumulation of salt *at the pore*

The authors are indebted to Sir W Bragg, F.R.S, for making an X-ray examination of the sodium chloride crystals, and to Dr W A Richardson for his assistance in the microscopical examination of the crystals. One of us (H A.F.) is also indebted to the Department of Scientific and Industrial Research for a grant which enabled him to take part in this work

---

Studies upon Catalytic Combustion.—Part III *The Influence of Steam upon the Catalytic Combustion of Carbonic Oxide*

By William A Bone, D Sc, F R S

(Received July 23, 1926)

Introduction

In connection with the researches upon catalytic combustion conducted in my laboratories for some years past, a great deal of attention has been paid to the experimental investigation of the important question of whether or no the presence of moisture has any specific influence upon the catalytic combustion of carbonic oxide The present paper embodies the principal results of our investigations up to date They were begun in 1908 at the University of Leeds, in collaboration with the two Gas Research Fellows—Mr A Forshaw, M Sc, and Dr H Hartley—as well as with Mr A. Appleyard, B.Sc, and have been completed at the Imperial College of Science and Technology, London, with the collaboration of the late W. A Haward, M.Sc, Mr. S Robson, B.Sc, A. Whitaker, B.Sc, and Prof D S Chamberlin, of Lehigh University, U S A, who recently spent a "sabbatical year" working with us

The difficult nature of the experimental work involved operations demanding

the utmost care, great attention to details, and unusual skill on the part of my collaborators The surfaces experimented with were porous porcelain, the oxides of copper and nickel, gold and silver And, in view of the importance of the results in connection with the theoretical aspects of the subject, many independent repetitions of the experiments were made at various times to ensure their complete confirmation In the case of a very porous surface, such as fireclay or porous porcelain, it was ultimately found necessary to extend a given experiment uninterruptedly day and night over three months, in order to ensure complete dryness of the system Indeed, not until the later stages of the research was it possible to view correctly and reconcile all the results

To recount all the details and ramifications of the work would far outrun the limits of a single paper, and therefore no more than a general description of the experimental procedure and results will be attempted, except where details are essential to the understanding of them

It may assist the reader to follow the story if at the outset it is explained that the results of the investigation as a whole have shown that the progressive drying out to completion of a system in which a mixture of carbonic oxide and oxygen is undergoing catalytic combustion at temperatures up to 500° C (and perhaps higher) may have three different consequences, one or more of which may be observed in the case of any given surface, according to circumstances The *immediate* result of such a drying operation is to remove from the surface the film of H_2O molecules which normally lags it to a greater or less extent, according to the physical conditions The removal of this "lagging," which by mechanical obstruction normally hinders the gases reaching the catalysing surface, increases its "effective area" and thereby its apparent catalysing power at a given temperature Such immediate result was most easily seen and demonstrated in the case of a very porous surface like porcelain, or of the oxides of copper and nickel, when the moisture film is very adherent and the removal of it "by drying" comparatively slow Indeed, unless an experiment extends over a long time, it is often the *only* effect of drying observable in such cases, and so is apt to be mistaken for what is the real effect of "dryness" upon the catalytic combustion, which becomes observable only during the last stages of the drying, when the amount of moisture remaining in the system has been reduced almost to vanishing point We ourselves were so misled during the earlier part of the research, when we found that the immediate effect of "drying out" such surfaces was to double their apparent catalysing power; and it was not until its later stages, after we had examined metal surfaces,

that the truth of the matter was revealed It then became clear that the real effect of drying is to stop the catalytic combustion altogether, which was so surprising that it took many repetitions of the experiments to convince us of its reality

The *real* effect of extreme drying upon the catalytic combustion was more easily proved with a metal surface such as gold or silver, where the aforesaid "moisture film" is apparently very much more attenuated and less adherent than in the case of more porous surfaces Indeed, with such metal surfaces, the greater difficulty was to demonstrate the *immediate* rather than the *real* effect of drying, so attenuated normally is the hindering moisture film Such an experiment requires meticulous care and attention to detail, especially in its penultimate stages, but, provided the drying arrangements are satisfactory, and the operation pushed far enough, the final and *real* effect of extreme dryness, which is to stop the catalytic combustion completely, can be demonstrated

The criterion of such being the genuine effect is the fact that, after the reactivity of such a completely dried system at a given temperature has become zero, or nearly so, the re-introduction of a small amount of moisture not only immediately restarts the catalytic combustion, but in course of time completely restores its normal intensity. Moreover, a subsequent second complete drying out of the system will reduce things to a standstill again. We have satisfied ourselves that the alternating operations of rendering such a system unreactive by completely drying it, and restoring its normal activity by reintroducing moisture, can be repeated several times

Besides the aforesaid two effects, in the case of a porous porcelain we have observed another one, namely, that a very prolonged drying apparently brings about a permanent disabling of the surface as a catalyst, presumably because of some structural change having been induced in it. In order to demonstrate such effect, however, the experiment had to be carried on uninterruptedly for three months, so slowly are the final stages of the drying accomplished, but when nothing untoward occurred, the following series of changes in the system were demonstrated, namely: (i) a gradual increase, up to a certain maximum, in the reactivity, due to the dispersal of the aforesaid moisture film from the surface, followed by (ii) a continuous but very gradual decrease in the reactivity, which after some months was reduced to a relatively low value. At first we thought this denoted a suppression of reactivity of the system, by reason of its dryness merely, similar to that which we had observed in experiments with gold and silver surfaces, when restoration had quickly followed the reintroduction of water. But this did not prove to be the case with the porcelain surface,

because, on reintroducing water into the system, not only did no restoration of its reactivity occur but all subsequent attempts to effect it by other special treatments were entirely unavailing. It therefore seemed as though some structural change had occurred in the surface of the catalyst with the drying out of the system which had permanently impaired its activity. This, however, is a point for further investigation, which we propose returning to when circumstances permit.

Experimental.

A.—Experiments showing the Immediate Effect of Drying Out a System upon the Catalytic Combustion.

The immediate effect of drying out a system is, as we have found, to remove from the catalysing surface the film of moisture which normally lags it, more or less according to the hygroscopic conditions. This was discovered at an early stage of the research, when we were experimenting with such highly porous surfaces as fireclay or the granular oxides of copper and nickel, which retain last traces of moisture so tenaciously that it requires a very prolonged and efficient drying operation to render them anything like completely dry. These experiments, most of which were carried out at the University of Leeds during the years 1908–10, will now be briefly described.

The "circulation method" introduced by Bone and Wheeler and described in Part I hereof (*q.v.*) was employed, suitable auxiliary appliances being included in the circuit as and when required (without altering the total volume of gas in the apparatus) for drying out the system. The general arrangement of the apparatus is shown in fig. 1. The surface, S, was contained in the hard-glass reaction tube, AA, which was maintained at a constant temperature in a gas furnace, BB, the gas supply of which was so controlled by a thermostatic arrangement (not shown) that any fluctuation of temperature of S in the reaction tube did not exceed 3° C. on either side of the desired mean. The ends of AA were drawn out and connected by special hard-to-soft fused glass joints, C_1 and C_2, and through the mercury-sealed taps, D_1 and D_2, with the rest of the circuit. This comprised (1) suitable CO_2 absorption vessels, E_1, containing a solution of baryta water, which in the "dry" experiments were replaced by similar vessels, E_2, containing pure concentrated sulphuric acid*,

* The vessels E_1 and E_2, which were similar to those shown at E in the diagram on p. 485 of Part I hereof ('Proceedings,' vol. 109, pp. 459–476), are not reproduced here.

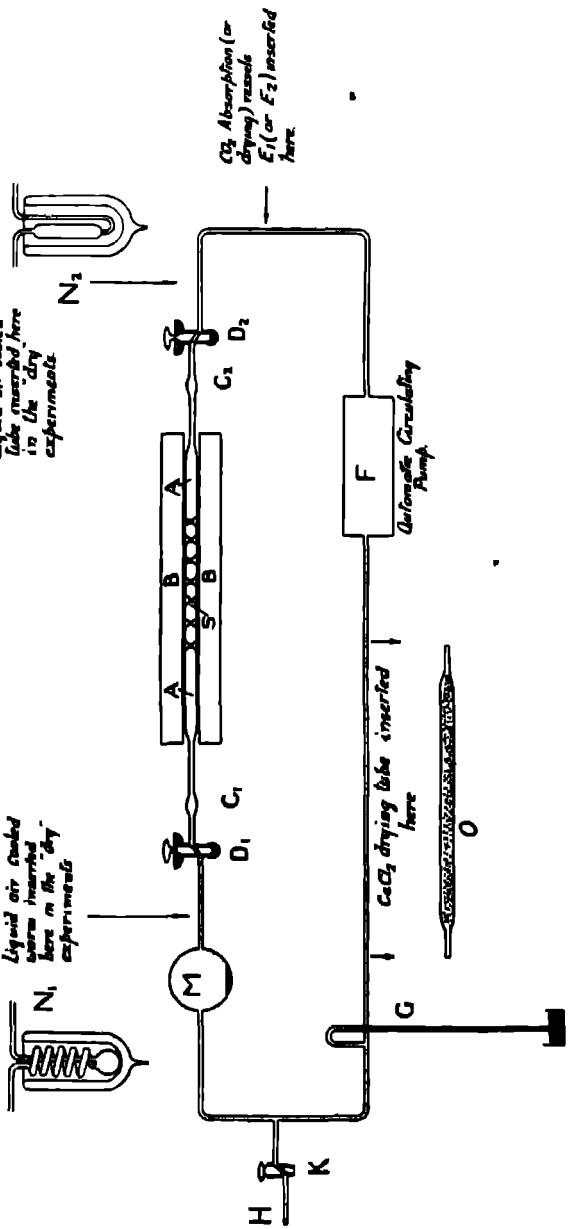
CO2 Absorption (or drying) vessels E1 (or E2) inserted here.
N2
Liquid air cooled tube inserted here in the dry experiments
D2
C2
A
B
S
F
Automatic Circulating Pump
C1
D1
Liquid air cooled tube inserted here in the dry experiments
N1
M
CaCl2 drying tube inserted here
O
G
H
K

FIG. 1.

(II) an automatic Sprengel circulating pump, F, duly protected from extraneous moisture by means of efficient drying trains; (III) a mercury manometer, G, (IV) a side-tube, H, leading (through stop-cock, K) to an outside gas-holder, containing the experimental $2CO + O_2$ mixture, and (V) the spherical capacity vessel, M

For the "dry" experiments small vessels, N_1 and N_2 (inset), immersed in liquid air, were inserted in the circuit near the entrance and exit, respectively, of the reaction vessel, AA, as also was a tube, O, filled with well-ignited calcium chloride, between the pump, F, and the manometer, G. The carbon dioxide formed during the catalytic combustion condensed in N_2. In the "moist" experiments a few cubic centimetres of distilled water were kept in the capacity vessel, M, the temperature of which was kept as nearly constant as possible; in the "dry" experiments this water was replaced by an equal volume of pure concentrated sulphuric acid

The sequence of the experiments was as follows. First of all a series of "moist" experiments were carried out with the particular surface under examination, in which a $2CO + O_2$ mixture, saturated with water vapour at either 0° C. or the room temperature (18° to 20° C.), was circulated over the surface, which was maintained at a suitable constant reaction temperature, the carbon dioxide produced being absorbed by the baryta solution in E_1. The experiments were continued until an absolutely steady rate of combination was established, as shown by the actual constancy of the velocity constant $k_1\left(k_1 = \frac{1}{t}\log\frac{p_0}{pt}\right)$. Preparations were then immediately made for a series of "dry" experiments. All the glass parts of the apparatus were separately dried out in a current of sulphuric-acid-dried hot air, the surface in the reaction vessel being also similarly dried out (at the experimental temperature) for 72 hours continuously. The liquid air-cooled tubes N_1 and N_2 were inserted, E_2 substituted for E_1, and other necessary alterations made in the circuit, after which sulphuric-acid-dried air was circulated through the whole system for about another day. The whole apparatus was then rapidly evacuated through H by means of a Geryk pump; a series of sulphuric-acid-dried $2CO + O_2$ mixture were then successively introduced, and the rate of combination for the "dry" series re-determined, tubes N_1 and N_2 being kept immersed in liquid air throughout each successive experiment. The carbon dioxide formed in the reaction all condensed in N_2, and at the end of each experiment it was got rid of by removing the liquid-air bath, closing tap D_2, and opening a side-tube sealed in the connection near N_2. Finally, after the conclusion

of the "dry" series, the apparatus was restored to its original form, and a second series of "moist" experiments run, so as to show that the original rate of combination for the undried system was restored. Such an alternating series of "moist" and "dry" experiments were sometimes repeated several times, so as to place the results beyond all possible doubt.

The carbon monoxide used throughout the research was prepared by dropping pure strong sulphuric acid into warm formic acid, and bubbling the gas evolved through a strong solution of caustic potash; the oxygen was prepared by heating recrystallised potassium permanganate, and was similarly washed. The experimental mixtures were made in glass gas-holders over *either* (*a*) a mixture of equal volumes of water and glycerine, for the "moist" experiments, *or* (*b*) pure strong sulphuric acid for the "dry" ones. Their compositions were always verified by analyses and adjusted so as to correspond exactly to $2CO + O_2$.

The experimental results for the three surfaces under consideration (fireclay, and the granular oxides of copper and nickel) will now be tabulated, each experiment being numbered and dated in chronological order. In the tables—

T = the reaction temperature in degrees Centigrade.

θ = temperature of the gaseous mixture in the capacity vessel.

p = partial pressure in millimetres of water vapour in the reacting mixture.

P = pressure of the dry $2CO + O_2$ mixture.

t = time in hours from the commencement of each experiment.

k_1 = the velocity constant $= \frac{1}{t} \log P_0/P_t$.

1. *With a Refractory Firebrick Surface* ($T = 500°$ C.).

The results of the following series of ten experiments with a surface composed of small, irregular pieces of a broken "Glenboig" firebrick may be taken as typical of the behaviour of a non-reducible porous refractory surface under the "moist" and "dry" conditions, respectively, already described. The first two experiments (I and II) were made with a "moist" system ($p = 15$ and 16 mm. respectively), and showed a mean velocity constant of $k_1 = 0\ 098$. Then followed a group of "dry" experiments (III to V), in which $k_1 = 0{\cdot}19$. A second group of two "moist" experiments (VI and VII) gave $k_1 = 0{\cdot}10$. A second group of two "dry" experiments (VIII and IX) gave $k_1 = 0{\cdot}175$, and a final "moist" experiment (X) gave as nearly as possible the same k_1

value (0·098) as was observed in the first experiment, showing that the real catalysing power of the surface had remained constant throughout the series. From analyses of the residual mixture at the end of each experiment, it was established that no hydrogen had been liberated (*e.g.*, by possible $CO + OH_2 = CO_2 + H_2$ interaction) during its course, so that it may be taken for granted that only the catalytic combination $2CO + O_2 = 2CO_2$ had occurred.

First Group of "Moist" Experiments ($T = 500°$. $\theta = 18$ *to* $19°$ C.).
Reacting Mixture, saturated with Moisture at 18° C.

$\theta = 18°$	Experiment I 4 5 10	$p = 15$ mm	$\theta = 18.8°$	Experiment II 5 5 10	$p = 16$ mm
t	P	k_1	t	P	k_1
Hrs	mm		Hrs	mm	
0	411·4	—	0	228·3	—
1	328·7	0·097	1	182·6	0·097
2	256·5	0·102	2	145·4	0·098
4	164·3	0·100	4	94·3	0·096

Mean $k_1 = 0·098$

The surface, as well as the whole apparatus, was thereupon subjected to a prolonged drying out, as already described.

First Group of "Dry" Experiments ($T = 500°$).

Experiment III 19 5 10			Experiment IV 23 5 10			Experiment V. 23 5 10.		
t	P	k_1	t	P	k_1	t	P	k_1
Hrs	mm		Hrs	mm.		Hrs	mm	
0	368·5	—	0	407·7	—	0	420·6	—
1	231·3	0·2022	1	250·8	0·1957	1	267·2	0·1970
2	153·6	0·1990	1½	191·8	0·1872	2	172·0	0·1942

Mean $k_1 = 0·190$.

Water was now reintroduced into the capacity vessel, M.

Second Group of "Moist" Experiments ($T = 500°$. $\theta = 20$ *to* $22°$ *C*)

Reacting Mixture saturated with Moisture at 20 to 22° C.

$\theta = 20.5°$	Experiment VI 25.5.10	$p = 19$ mm	$\theta = 22°$	Experiment VII 26.5.10.	$p = 19.6$ mm
t	P	k_1	t	P.	k_1
Hrs	mm		Hrs	mm	
0	401·3	—	0	477 0	—
1	350 0	0 1199	1	377 5	0 1016
3	217 2	0 1090	3	244 9	0 0965

Mean $k_1 = 0$ 102

System again dried out, as described.

Second Group of "Dry" Experiments ($T = 500°$)

Experiment VIII 30.5.10			Experiment IX. 31.5.10		
t	P	k_1	t	P.	k_1.
Hrs	mm		Hrs	mm	
0	300 2	--	0	283·9	—
1	196 7	0 184	1	181 5	0 194
2	130 2	0 171	2	123·6	0 180

Mean $k_1 = 0$ 178

Water was again reintroduced into the capacity vessel, M.

Final "Moist" Experiment, 14/6/10 ($T = 500°$ $\theta = 20$ 7°. $p = 18$ mm)

Time	0	1	3	6	Hrs.
T	442·4	352 8	224 0	116 3	—
k_1	—	0 0983	0 0985	0 0967	—

Summary

Mean k_1 in the 5 "moist" experiments = 0 100
" " " 5 "dry" " = 0·185

Confirmatory Experiments ($T = 500°$ *C.*)

Another series of 13 experiments made independently by Mr. A. Forshaw, with a similar fireclay surface at 500° C., showed a still greater difference between

the apparent catalysing powers under "moist" and "dry" conditions, respectively. Moreover, under "moist" conditions, a perceptible difference in the k_1 values was usually observed according as the reacting $2CO + O_2$ mixture was saturated with water vapour (*a*) at 17° to 21° C. ($p = 14{\cdot}5$ to 18 5 mm) or (*b*) at 0° C. ($p = 4{\cdot}6$ mm), respectively, as the following summarised results indicate.–

	k_1 values obtained for the first hour in					
	"Moist" Experiments				"Dry" Experiments	
	(*a*) $\theta = 17$ to 21° C. $p = 14{\cdot}5$ to 18 5 mm		(*b*) $\theta = 0$° C. $p = 4{\cdot}6$ mm			
I	0 0505	IV	0 0503		VIII	0 156
II	0·0489	V	0·0550		IX	0·186
III	0·0465	VI	0·0524		X	0 192
VII	0·0430				XI	0·180
XIII	0·0515				XII	0 174
Mean =	0·0480	Mean =	0·0525		Mean =	0·178

N.B —The Roman numerals give the order in which the experiments were made.

II. *Experiments with Granular Nickel Oxide* ($T = 210$°).

Similar effects of drying were observed when a $2CO + O_2$ mixture was circulated over a surface of granular nickel oxide at a temperature of 210° C, under which condition no permanent reduction of the surface occurred (*vide* Bone and Andrew, Part II hereof*) In these experiments, which were made by the late Mr. W A. Haward at the Imperial College of Science and Technology, London, during 1918–19, the general arrangements of the apparatus were similar to those previously adopted with the fireclay surface (*q.v.*), except that (i) a mixture of 1 part soda-lime with 3 parts quicklime, made into a paste with water and then dried, was substituted for the barium hydroxide solution as the CO_2 absorbent in the "moist" experiments, and (ii) tubes containing pure redistilled phosphoric anhydride were included in the circuit in the "dry"

* 'Proceedings,' A, vol. 110, pp. 16–34 (1926)

experiments The following summarised statement will sufficiently indicate the general character of the results obtained —

Mean values of k_1 obtained in "Moist" Experiments. $\theta = 17°$ C $p = 14\ 5$ mm		"Dry" Experiments.	
I	0 0068	II	0 0119
VIII	0·0075	III	0 0118
		IV	0 0124
		V	0 0125
		VI	0 0125
		VII	0·0118
Mean =	0 0070	Mean =	0·0120

III *Experiments with Granular Copper Oxide* ($T = 210°$ C)

Similar results to the foregoing were obtained by Dr. Hartley with granular copper oxide at 210° C, though in order to demonstrate most clearly the effect of drying-out surfaces it was found necessary to exclude nitrogen (which is strongly adsorbed by such a surface) from the system, and to dry it out in a current of dry oxygen at the experimental temperature Also, in order best to ensure otherwise perfectly comparable conditions as between the "moist" and "dry" systems, immediately before each actual experiment the surface was heated in the reaction tube for three hours to 480° C. in a stream of dry oxygen, after which the temperature was lowered to 210° for the experiment. In such circumstances the following three typical experiments were made, in the order given —

(1) $T = 210°$ C. working with a "moist" $2CO + O_2$ mixture and system saturated at 20° C $k = 0·0215$.

(2) $T = 210°$ C. working with a $CaCl_2$-dried $2CO + O_2$ mixture after drying out the system as already described. $k = 0·150$.

(3) $T = 210°$ C. with a "moist" $2CO + O_2$ mixture after reintroducing moisture into the capacity vessel, M, of the system. $k = 0\ 0504$.

It is thus seen that, with such porous surfaces as those described, the *immediate* effect of drying out the system was to increase considerably their apparent catalysing powers. this, however, was an *indirect* effect, due to the removal of the moisture film which ordinarily "lags" the surface more or less.

B.—Experiments showing the Ultimate Effects of Drying Out a System upon the Catalytic Combustion with a Metal Surface.

In the experiments now to be described it was proved that with a gold or silver surface the ultimate effect of drying out the system is very greatly to reduce the catalytic combustion or even to stop it altogether. They were all carried out at the Imperial College of Science and Technology, London, in collaboration with the late W. A. Haward, S. Robson and A. Whitaker, during the years 1915–16. Later on, the results with silver were independently confirmed by Prof. D. S. Chamberlin in the year 1922–23.

As the object now aimed at was the complete drying out of the system, the experimental procedure described in the previous section had to be modified, in view of the longer time required, and the necessity of following more closely the effects of the gradual elimination of moisture. The plan adopted in most of the experiments was essentially the following. A mixture of purified carbon monoxide and oxygen in their combining proportions, saturated with moisture at the laboratory temperature, was circulated over the metal surface, which was kept in the reaction tube at a suitable temperature (T = 240° C. for gold and 360° C. for silver) until a perfectly steady rate of combination was established. This having been reached the apparatus (except the reaction tube with the metal surface, which was kept at the reaction temperature and shut off from the air) was taken down, thoroughly cleaned and dried out, and then set up again, but with tubes containing pure redistilled phosphoric anhydride in circuit, care being taken that the total volume accessible to the $2CO + O_2$ mixture remained unaltered. The apparatus, thus reconstructed, is shown in fig. 2, where (using the same lettering as in fig. 1) K_1, K_2, K_3 and K_4 are the P_2O_5 drying tubes, and N_1, N_2, the spiral and tube, respectively, which towards the end of the drying operation were kept immersed in liquid air. To ensure absorption of the reaction product (when the liquid air cooled tube N_2 was not in action), the upper parts of the absorption towers, E_1, E_2, were filled with a specially prepared mixture of soda-lime with three times its weight of quicklime, which was found to absorb carbon dioxide with great rapidity, without showing any sign of absorbing carbon monoxide, and in order to counteract the very small water-vapour tension of the mixture, the lower parts of these towers were filled with quicklime. In this way, the carbon dioxide was rapidly and completely absorbed without any material amount of moisture being acquired by the gaseous mixture during its passage through the said towers.

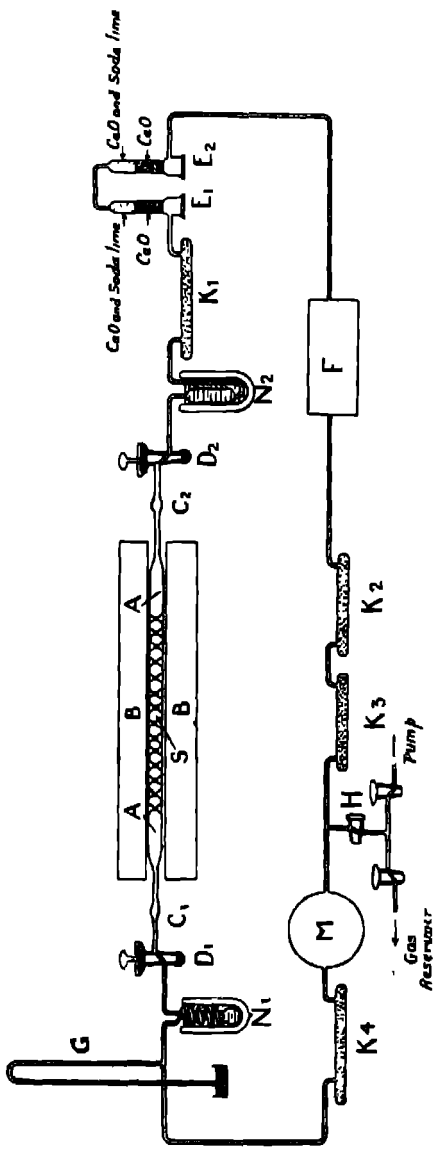
CaO and Soda lime
CaO
CaO and Soda lime
CaO
E2
E1
K1
N2
F
D2
C2
A
B
A
B
S
K2
K3
H
Pump
C1
D1
M
Gas Reservoir
N1
K4
G

FIG. 2.

The apparatus having thus been dried out, and re-set for the series of "dry" experiments, it was thoroughly evacuated, after which an accurately made $2CO + O_2$ mixture was introduced, from a gas holder through an efficient P_2O_5 drying train, and kept continuously circulating round the system, fresh portions of the mixture being added from time to time as required By continuing such procedure over many successive days (or weeks), and periodically observing the rate of combination of the gases as they passed over the heated metal surface, the effects of gradually drying out the system almost to completion could be studied Towards the end of the operation, the further effects of immersing the spiral N_1 and the tube N_2 in liquid air were observed

Finally, having pushed the aforesaid drying operation to its farthest limit possible under the experimental conditions, all the drying arrangements indicated in fig 2 were removed from the circuit (without altering its volume) and water reintroduced into the system at the capacity vessel, M Another similar series of experiments were then made in order to observe the effects of the moisture addition, until another steady state for the "moist" mixture was attained. It will be seen that it always returned, more or less quickly, to the original steady state for the "moist" gases, showing that the metal surface itself had undergone no appreciable alteration from first to last of the long series of operations just described The following are the details of our experiments with gold and silver, respectively —

I. *With a Gold Gauze Surface.*

The gold gauze used was a piece (weighting 31 grms) of that previously employed in Bone and Andrew's experiments (Part I hereof, *loc cit*), it had 22 strands (each 0 15 mm. in diameter) per centimetre, having been woven out of the purest wire obtainable by Messrs Johnson and Matthey, to whom our best thanks are due It was introduced into the reaction tube of the circulation apparatus as a roll about 6 inches long and of such diameter as just fitted that of the tube The temperature chosen for the experiments was 240° C

(1) *Preliminary Experiments with a Moist* $2CO + O_2$ *Mixture.*—The circulation apparatus having been arranged for a "moist" series of experiments, $2CO + O_2$ mixtures, saturated with moisture at the laboratory temperature, were continuously circulated over the surface at 240° C. for three weeks (January 26 to February 14, 1916) until a perfectly steady rate of combination

was attained; the value of "k" thus established is indicated by the following observations extending over the last two days —

t	P	k
Hrs	$2CO+O_2$	
	m m	
0	647·5	—
19	333 0	0 0152
25	265 0	0 0155
43	137 2	0 0157

Therefore, mean "k" value for a moist $2CO + O_2$ mixture = 0 0155

(ii) *Effects of Drying Out the System* —The apparatus was now re-arranged (as already described) for a "dry" series of experiments, which extended altogether over 8 days (February 16 to 23, 1916), the temperature of the gold gauze being kept at 235-240° C. all the time, with the following summarised results :—

Drying Agent in Circuit	Drying Period from beginning	k value for *dry* $2CO+O_2$ mixture at end thereof
	Hrs	
P_2O_5 only	24	0·0148
	42	0 0118
	45½	0·0045
P_2O_5 *plus* liquid air	66	0·0004
	91	0 0004
	114	0·00045

It is thus seen that the effects of the "drying-out" operation were hardly noticeable during the first 24 hours, after 42, however, they were distinctly felt, but it was not until the period 42–45½ hours that anything like the full effects were obtained. From 45 hours onwards the rate of combination of the gases rapidly diminished, until during the period 66 to 114 hours, with liquid air cooling in circuit, it had become almost negligible Indeed, during one particular 25 hours (66 to 91 hours from the beginning) the pressure of the *dry* $2CO + O_2$ mixture fell by 15·8 mm (*i. e.* from 620 8 to 605 mm.) only, as compared with a fall of no less than 182·5 mm. for the *moist* gases during the same period in preliminary "moist" experiments (*q v*). The "dryness" of the system apparently reached a maximum during this period, because subsequently the rate of combination of the gases slightly increased, k rising from 0·0004 (its minimum during the series) to 0·00045 during the next 48 hours.

At no time during the whole period was the combination observed to stop altogether, although at times it was hardly discernible. There can be little doubt but that, had *complete* dryness been attained, the combination would have stopped altogether, as indeed was the case in our subsequent experiments with silver. The attainment of *complete* dryness in such a system is so extraordinarily uncertain and difficult that, however careful may be the conduct of the experiments, it is always largely a matter of chance whether complete success finally results.

(iii) *Effects of reintroducing Moisture into the System.*—At the conclusion of the foregoing series (ii), the drying agents were removed from the circuit, and water reintroduced into the capacity vessel, M, "moist" $2CO + O_2$ mixtures were then kept continuously circulating over the surface during the next 17 days (February 24 to March 11, 1916, inclusive), and observation of the rate of combination made every day or two. The following summarised results, giving the observed k values, show that the effect of reintroducing the moisture was to increase *very gradually* the reactivity of the system, until it was at length completely restored to its former steady condition as observed for the "moist" $2CO + O_2$ mixtures in series (i):—

Observed k_1 Values		
After 22 hours	0·0037	Attention is specially directed to the very gradual increase in these "k" values.
,, 46 ,,	0 0046	
,, 90 ,,	0·0052	
,, 113 ,,	0 0069	
,, 137 ,,	0 0088	
,, 166 ,,	0·0102	
,, 214 ,,	0 0107	
,, 425 ,,	0·0152	

(iv) *Confirmatory Experiments re Effects of Drying.*—Without going into details, it may be said that immediately after the conclusion of the foregoing experiments, the system was once more dried out over a period of 26 days (March 13 to April 7, 1916) in the manner already described. Its reactivity again decreased gradually to a very low value, attaining a minimum ($k = 0·00043$) on the eighth day, as the following observations show —

	k
After 2 days P_2O_5-drying	0 0122
,, 5 ,, ,,	0·0028
,, 8 ,, ,,	0·00043
,, 10 ,, ,,	0·00097

Finally, on again reintroducing moisture into the system (April 11, 1916), the values of "k" gradually rose in 3 days to the "normal" for the "moist" gases, as follows :—

				k
2 hours after reintroducing moisture			..	0 0036
20	,,	,,	..	0 0064
24	,,	,,	.	0 0103
48	,,	,,		0 0143
72	,,	,,		0 0150

It was thus proved (*a*) that the effect of drying out the system was gradually to reduce its reactivity from "normal" almost to zero, and (*b*) that complete restoration of normality gradually resulted from the reintroduction of moisture. Attention is specially directed to the fact that (*b*) was very gradual, because of its important bearing on the theory of catalytic combustion, being very difficult to reconcile with the Langmuir conception of the action being confined to a monomolecular layer of adsorbed gases, but quite explicable on the supposition of its extending also to deeply occluded gases

II *With a Silver Surface*

A long series of experiments were also made with a pure silver-foil surface at a temperature of 360° C, the results of which were extremely interesting, because they brought out very clearly (*a*) the immediate effect of removing the film of moisture which normally "lags" such a surface when "moist" gases are circulated over it, and (*b*) the *ultimate* total paralysis of a completely dried-out system The following summarised results will enable readers to appreciate their significance :—

(1) ***First Group With a "Moist" $2CO + O_2$ Mixture*** ($T = 360°\ C$, $\theta = 15$ to $20°\ C$)—This consisted of five successive experiments in which a mixture of $2CO + O_2$ saturated with moisture at the laboratory temperature (15 to 20° C) was circulated over the surface at 360° C, and the rate of combination determined, as follows :—

Experiment.	k for "Moist" System.
1	0·0682
2 . . .	0·0697
3	0·0703
4	0·0594
5	0·0661

Therefore mean "k" value for "moist" $2CO + O_2$ mixture = *circa* 0·067.

(II) *Second Group. With* $CaCl_2$*-dried System and* $2CO + O_2$ *Mixture* ($T = 360°$ *C.*) —Then followed a group of seven experiments, extending over a week, in which, after removing water as much as possible, tubes packed with well-ignited calcium chloride (instead of P_2O_5-drying tubes) were inserted into the circuit so as to reduce quickly the tension of aqueous vapour in the system down to a comparatively low point. The effect of this was to increase considerably the apparent reactivity of the system, as the following successive daily observations showed —

Experiment.	k for $CaCl_2$-dried System. $T = 360°$ C.
6	0·1590
7	0·1184
8	0·1412
9	0·1469
10	0·1463
11	0·1373
12	0·1483

Therefore mean "k" for $CaCl_2$-dried system = *circa* 0·1400

(III) *Third Group. Showing Effects of Liquid Air Drying* ($T = 360°$ C.) — In order to push the drying still farther, the glass spiral, N_1, and tube, N_2 (fig. 2), were both immersed in liquid air, so that the tension of aqueous vapour of the $CaCl_2$-dried $2CO + O_2$ mixture passing into the reaction tube would be reduced to that corresponding with a temperature of about — 185° C., and those passing out of it would be similarly cooled, a procedure calculated to reduce the amount of water vapour in the reaction zone to a negligible point. The effect of this was immediately seen in a reduction of the "k" values to (in four successive daily experiments) a very low point, as follows .—

Experiment	k for Liquid Air Dried System
13	0·0462
14	0·0458
15	0·0436
16	0·0360

Total Arrestment of the Catalytic Combustion after Continued Liquid Air Drying of the System ($T = 360°$ *C.*).—At this stage the system seemed rapidly to dry out, and with the glass spiral, N_1, and tube, N_2, both kept well immersed in liquid air, *a point was eventually reached when the combination of the liquid air dried* $2CO + O_2$ *mixture completely ceased*, the pressure remaining quite stationary

at 589·7 mm for half an hour. On allowing part of the liquid air surrounding the spiral, N_1, to evaporate, so as to uncover the topmost turn thereof, thus allowing the gases to take up a minute quantity of water vapour, their combination was restored

The foregoing observation was confirmed in three subsequent experiments in which *the catalytic combustion was completely arrested for periods varying between* 30 *and* 60 *minutes* by keeping the spiral, N_1, completely immersed in liquid air for some time previously, whilst a P_2O_5-dried $2CO + O_2$ mixture was kept circulating in the system And in each case, the combination was re-started simply by allowing the level of the liquid air to sink by evaporation below the uppermost turn of the spiral.

(iv) *Fourth Group Showing Effect of reintroducing Water into the System* ($T = 360°C$) —Finally, the drying arrangements were removed from the system, a few cubic centimetres of water reintroduced into the capacity vessel, M, and a moist $2CO + O_2$ mixture circulated over the surface (at 360°) The effect of this procedure was a gradual restoration (in successive days) of the reactivity of the system until reaction constant " k " finally reached a steady value slightly higher than that originally observed for the " moist " system in experiments 1 to 3 (First Group), as follows —

Experiment	k for Moist System
28	0 0164 rising to 0·0393 in
29	0 0399 [2 hours.
30	0 0465
31	0·0530
32	0·0610
33	0·0612
34	0·0870
35	0 0871

Confirmatory Series of Experiments with Silver Foil

As it seemed important to have the foregoing results independently confirmed, Prof D. S. Chamberlin, of Lehigh University, who spent the session 1922 working with me at the Imperial College, kindly undertook to carry out an entirely new series of experiments both with silver and porous porcelain. The procedure was modified from that previously described, in the following particulars, namely :—(1) the experimental $2CO + O_2$ mixtures used had previously been dried for about six months by contact in a large globe (fig. 3) with redistilled

phosphoric anhydride before being introduced into the circulation apparatus; (ii) the drying out of the apparatus was chiefly effected by keeping P_2O_5-dried nitrogen continuously circulating day and night through the system, with P_2O_5 tubes inserted, (iii) at regular intervals of 10 to 14 days, the apparatus being evacuated 20 hours previously, making a determination of the catalysing power of the surface towards the aforesaid P_2O_5-dried $2CO + O_2$ mixture, (iv) the soda-lime tubes previously used for absorbing the CO_2 produced were now omitted, because (v) during each $2CO + O_2$ experiment the spiral, N_1, and tube, N_2, were kept immersed in liquid air, so that the CO_2 produced during the catalytic combustion was completely condensed in N_2. The temperature of the reaction tube containing the silver-foil surface was maintained at 250° C throughout the whole six months' period (commencing September 15, 1922) covered by the series of experiments.

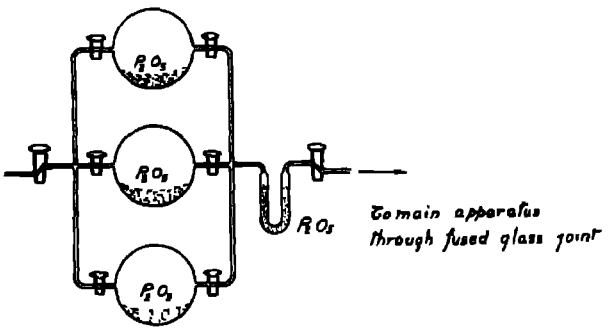

FIG 3

Immediately before commencing the series of experiments, the silver foil used (whose catalysing power towards a moist $2CO + O_2$ mixture at 350° C had been previously ascertained) had been kept *in vacuo* for some days in a desiccator over redistilled P_2O_5, so that its surface had been to some extent dried before being introduced into the reaction tube of the circulation apparatus.

Moreover, after completing the series, the catalysing power of the foil towards a moist $2CO + O_2$ mixture at 350° C was redetermined, whereby it was found to be the same as at the beginning.

Experimental Results.—The experimental results are summarised below: it should be understood that during the intervals between each determination of the "k" value for the six months P_2O_5-dried $2CO + O_2$ mixture, P_2O_5-dried nitrogen was kept continuously circulating through the system, with the

P_2O_5 drying tubes inserted (the silver foil being maintained at 250° all the time), so that the following data show the effects of a five months' progressive drying of the system upon the catalysing power of the metal :—

Determination No	Date.	Observed Velocity Constant K, with Dry $2CO + O_2$ Mixture. T = 250° C.
1 . .	4 10 23	0 1208
2 .	15 10.23	0·1539
3 .	1.11 23	0 0139
4 .	13.11 23	0 0067
5	23 11 23	0 0047
6	6 12 23	0 0050
7	12 2 24	0·0104
8	29.2.24	0·0039

These results, which are plotted on the accompanying curve (fig 4, A) confirm the previous conclusion that, whereas the *immediate* effect of drying is to increase

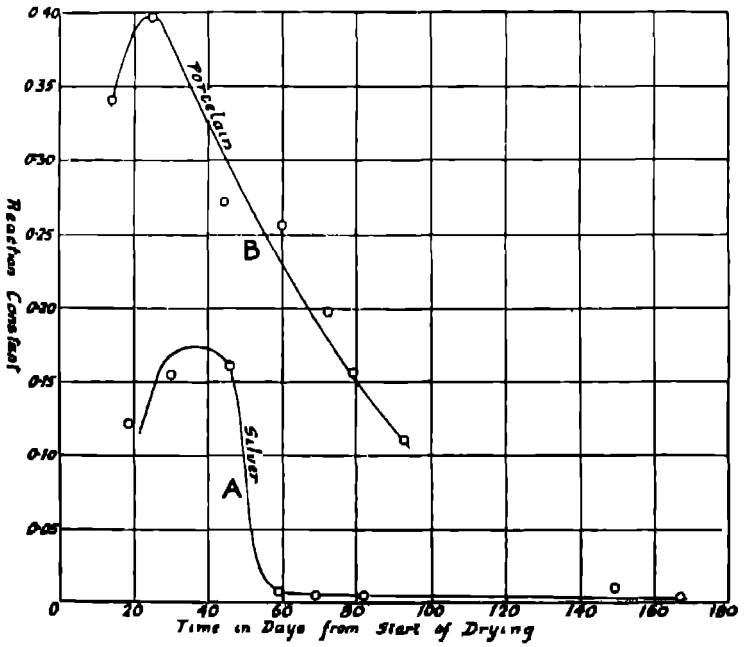

Fig 4.

the apparent catalysing power of the surface, presumably by removing the film of moisture which normally lags it, the real and final effect is well-nigh to suppress it altogether Thus, the surface was actually at its maximum activity about a month after the series of experiments in question had begun ($k = 0$ 1539), when no less than 30 per cent of the $2CO + O_2$ mixture disappeared during the first hour; after this its catalysing power rapidly diminished, until it finally reached a fairly steady minimum ($k = 0$ 0039), when only 1 per cent. of the $2CO + O_2$ mixture combined during the first hour It is, of course, extraordinarily difficult to achieve *complete* dryness in such experiments, but it can hardly be doubted that, had such conditions actually been attained in this case, the catalytic combustion would have ceased altogether. In this connection it is also important again to observe that, on re-introducing moisture into the system, its original reactivity was completely restored, thus proving that the catalysing power of the surface had not been permanently impaired at all by the prolonged drying to which it had been subjected.

C —A Final Series of Experiments with Porous Porcelain at 500° C

Prof Chamberlin also carried out a similar long series of experiments with a surface of porous porcelain, which Mr W C Hancock had kindly prepared for us from pure china clay. The material had been moulded into bars, each of 1 cm.^{2} cross-section, and about 15 cm in length, which were then fired at 1200° for some days, and afterwards kept in a vacuous desiccator until required. Immediately before use the particular bar selected for the experiment was "conditioned" in the following manner, namely :—

(1) First of all, it was completely evacuated in a silica tube for four hours at full red heat.

(2) Next, dry oxygen was admitted to the red-hot surface which, after a suitable interval, was re-exhausted.

(3) Finally, dry air was admitted to the red hot surface, which was subsequently once more exhausted, and then allowed to cool *in vacuo* down to room temperature before being transferred to the reaction tube of the circulation apparatus

Experimental Procedure.—Throughout the whole of the four months' period covered by the experiment, P_2O_5-dried nitrogen was kept circulating through the system, with P_2O_5 drying tubes in circuit, except during the particular days, at considerable intervals apart, when the catalysing power of the surface

(at 500° C) towards a six-months P_2O_5-dried $2CO + O_2$ mixture was being determined The surface itself was kept at 400° during all the long "drying periods"; during the 20 hours preceding each successive determination of its catalysing power towards the said mixture, however, the apparatus was thoroughly exhausted, and the temperature of the reaction tube was raised to 500° C, after which the said mixture was slowly admitted, and the tubes, N_1 and N_2, immersed in baths of liquid air, in which they remained until the determination of the velocity constant "k" was completed Thereupon, the liquid air baths were removed, the apparatus re-exhausted, another charge of P_2O_5-dried nitrogen re-admitted, and the drying-out operation resumed

Experimental Results —The whole "drying-out" operation extended over a period of three months (January 1 to April 4, 1923) continuously day and night, and determinations of "k" value were made at successive intervals as follows —

Determination No	Date	Observed Velocity Constant k_1, with a $2CO + O_2$ Mixture T = 500° C
1	14 1 23	0·3405
2	25.1 23	0·3981
3	13 2 23	0 2711
4	29 2.23	0·2561
5	12.3 23	0·1997
6	19 3 23	0 1559
7	2 4.23	0 1106

These results, which are plotted on the accompanying curve (fig 4, B) showed unmistakably that (i) while the *immediate* effect of the drying was to increase considerably the apparent catalysing power of the surface, which reached a maximum after about a month's drying, (ii) more prolonged drying caused it steadily to diminish, until after three months' drying it had fallen to about 44 per cent of its original value, thus, the respective *relative* values were as follows —

At commencement of the experiment	1·00
After one month drying	1 12
At end of the experiment (3 months)	0·44

So far, then, everything seemed to have happened substantially in accordance with anticipations based on our previous experiments with gold and silver, although the natural expectation that the "drying out" would be a much

slower operation than was the case with the two metal surfaces Accordingly, on April 2, 1923, after the experiments had been in progress for three months, it was decided to try the effect of re-introducing moisture into the system The P_2O_5 drying tubes were therefore removed from the circuit, water was introduced into the capacity vessel, M, and a $2CO + O_2$ mixture, saturated with moisture at room temperature, admitted Contrary to our expectation, however, the catalysing power of the surface was now found to have again diminished as the results of the following two experiments, made with a five days' interval between, showed

Determination No.	Observed "k" Value for "Moist" $2CO + O_2$ Mixture.	Relative Catalysing Power of Surface.
8	0 0784	0·36
9	0 0168	0·08

Such results suggested that the great diminution of the catalysing power of the surface during the aforesaid three months' drying had been due to some permanent structural change, produced in the surface itself by the drying, which the re-introduction of moisture, so far from reversing, actually accentuated, because of its "lagging" effect

To test this view of the matter, calcium chloride drying tubes were subsequently inserted in the circuit, and a week's drying-out of the system (by $CaCl_2$-dried nitrogen circulation) carried out, as anticipated, this had the effect of "unlagging" the surface, and materially increasing its apparent catalysing power, as compared with that observed in No. 9 (*q.v.*).

Determination No.	Observed "k" Values for $CaCl_2$-dried $2CO+O_2$ Mixture	Relative Catalysing Power of Surface.
10 .. .	0 0293	0·12
11 .	0 0281	

Some time after the conclusion of the experiments, thin sections of the catalyst were cut and suitably mounted for microscopic examination, but although careful comparisons were made (using a Zeiss apochromatic oil-immersion N.A. 1·4 objective in conjunction with a Swift oil-immersion achromatic condenser N.A. 1·4, with transmitted ordinary and polarised light) between the original (unused) material and that which had been used in the experiment, no sign of crystallisation in the latter could be detected, nor could the two materials

be differentiated. Therefore, it can be said that any structural change which the surface had undergone, as the result of the prolonged drying operation, was undetectable by microscopic examination referred to

Concluding Remarks.

The experiments described herein have established the following facts with regard to the progressive removal of moisture from a system in which carbonic oxide and oxygen are undergoing catalytic combination in contact with the surfaces referred to, and under the conditions studied, namely —

(1) That the *immediate* effect is always to increase the apparent catalysing power of the surface, presumably by removing from it the film of H_2O molecules which normally lags it, more or less according to the physical condition

(2) That the *ultimate* effect, which, however, is usually observed only after a prolonged drying, is to diminish greatly, or even to stop completely, the catalytic combustion

(3) That in the case of each of the two metal surfaces (gold and silver) examined, the *ultimate* effect of drying was practically to stop the catalytic combustion altogether; but on re-introducing moisture into the system, its reactivity was in time completely restored.

(4) That in the case of the porous porcelain surface, the *ultimate* effect of drying was to diminish greatly its catalysing power, which, however, was not regained on re-introducing moisture into the system.

It seems difficult to reconcile the new facts observed in the case of the two metal surfaces referred to with the Langmuir "adsorption" theory of catalysis, or, indeed, with any modification of it which has yet been suggested. For if, as all such theories suppose, the catalytic combustion of carbonic oxide is conditioned merely by the formation at the surface of a unimolecular layer of the reacting gases definitely orientated, it is not easy to understand why the complete removal of water from the system should stop it altogether. On the contrary, if, as is now shown, the catalytic combustion at such temperatures as have been employed in these experiments is conditioned by the presence of moisture in the system, the fashionable doctrine of its being primarily due to the formation of such specially orientated unimolecular gas layers at the surface seems incapable of explaining the new fact confronting it If, however, the prime function of the surface in such catalytic combustion is to ionise the reacting gases, which in a neutral state are incapable of combining, then the observed influence of

moisture could be explained, because it would prevent "ionised" molecules from reverting to a neutral state, and so aid the combustion And, if such be the case, it is conceivable that at still higher temperatures than those employed in the experiments described herein, the surfaces in question would not require the aid of moisture at all. This is a point which, however, it is desired to reserve for future investigation

In conclusion, the author desires to thank the Government Grants Committee of the Society for grants which have partly defrayed the expenses of the experiments.

Effects of Thermal Treatment on Glass as shown by Precise Viscometry.

By VAUGHAN H. STOTT, M.Sc , D. TURNER, B.Sc. (Tech), and H A SLOMAN, M.A., B.Sc , A I C , National Physical Laboratory, Teddington

(Communicated by Dr W Rosenhain, F.R S —Received June 8, 1926)

[PLATES 18 AND 19]

Viscometers which have previously been described by various authors* for use with molten glass have suffered from a common defect, namely, the impossibility of following any changes which might occur in the viscosity due to prolonged thermal treatment of various kinds This defect can only be overcome by the use of apparatus which is practically insoluble in molten glass, and which permits the glass to be cooled to room temperatures and reheated. In the present state of our knowledge such apparatus must be constructed of a platinum alloy, the high cost of which tends to restrict the weight of the portions of the apparatus in contact with glass In the present apparatus viscosity is measured by a determination of the thickness of the film of glass which adheres to a thin wire of 10 per cent iridio-platinum which is withdrawn at a known velocity from the molten glass contained in a small crucible of the same material. The glass is heated in a vertical cylindrical platinum resistance furnace having two concentric windings of platinum foil 1 inch wide by 0·002 inch thick. The inner tube of the furnace, which is of alundum, has an internal diameter of 1¼ inches, and is 24 inches long. The glass is contained in an iridio-platinum crucible of 1¼ inches diameter at the top, and 2 inches high,

* Washburn and Shelton, 'Bulletin No. 140, Engineering Experiment Station, University of Illinois.' S. English, 'Trans. Soc. Glass Tech.,' vol. 8, p. 205 (1924). Stott, Irvine and Turner, 'Roy. Soc. Proc.,' A, vol 108, p. 154 (1925).

which is supported in the centre of the furnace The furnace stands on three adjustable legs carried by a table, which can be swung to one side of its normal position so as to allow of convenient access to the various parts of the apparatus. Such a furnace is capable of withstanding high temperatures for prolonged periods. During viscosity determinations, the furnace was run continuously at working temperatures when not otherwise mentioned in the text The weighed iridio-platinum wire, which is to be lowered into the glass and thence raised, is tied to platinum wires fixed in slots in the cut-away portion of an alundum tube, as shown in fig 1 The upper end of the alundum tube is fixed to the lower end of a counterpoised steel tube which can be raised or lowered in guides by means of an electric motor. Fig 2 shows the general arrangement with the tube at the bottom of its stroke The useful speeds of the motor can be varied in the ratio of twenty-five to one, and two gears are available in the ratio of four to one, the available linear velocities of the tube varying from 0 01 to 1 cm /sec The steel tube A is actuated by means of a rack and pinion through the agency of a toothed clutch operated by the experimenter The motor carries a flywheel of such inertia that the drop in speed of the motor on letting in the clutch is inappreciable The speed of withdrawal of the wire is measured by an electric chronograph which makes contact with successive teeth of the rack The chronograph is accurate to about 1/100 sec The temperatures are measured with a specially designed disappearing filament pyrometer capable of a precision of one or two degrees between 800° and 1600° The pyrometer is sighted on the glass through a totally reflecting prism B mounted above the steel tube. When the tube rises in the course of an experiment, the prism swings away from it on pivots

The conduct of an experiment is very simple The weighed wire having been placed in position, the lid of the furnace is removed, and the furnace swung against a stop into position below the wire (The lid of the furnace consists of a brick under which is fixed an aluminium plate to prevent any foreign matter dropping into the glass) The wire is then lowered by means of the motor at a suitable velocity The speed at the beginning of the motion is only limited by the thermal endurance of the refractory materials When, however, the end of the wire reaches the glass, it is necessary that the speed should not be greater than that subsequently to be employed for the withdrawal Neglect of this precaution may result in bending the wire, especially at the lower temperatures When the steel tube reaches the bottom of its travel, the driving clutch, which, of course, is travelling backwards, comes out of engagement through ratchet action. Upward motion is also automatically

FIG. 1.

FIG. 2.

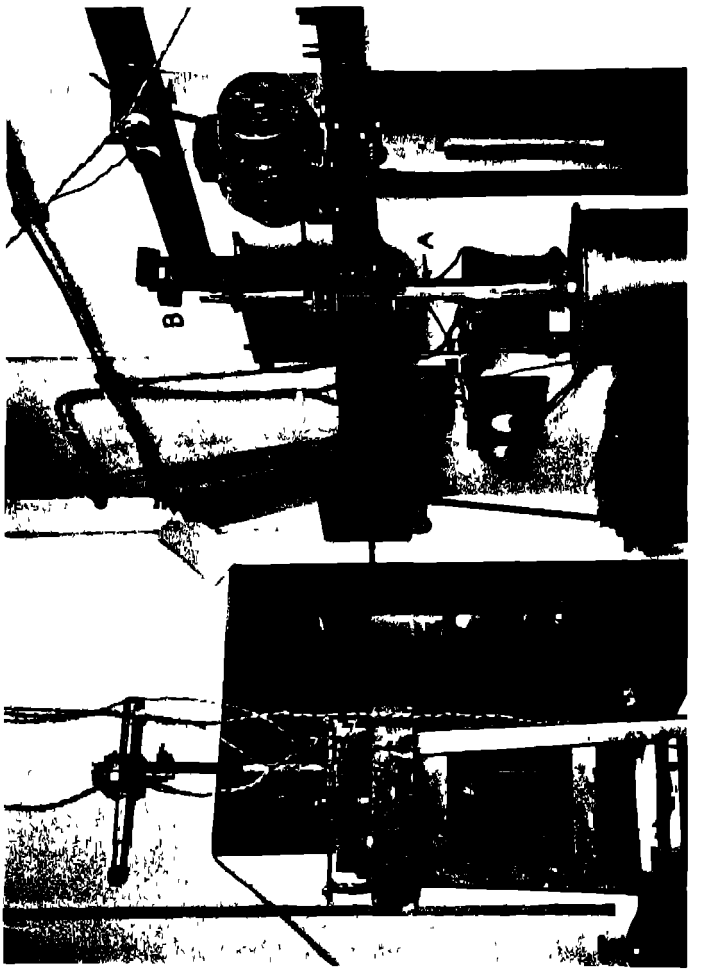

FIG. 2

stopped at the required point by means of a cam which withdraws the clutch and applies a brake The wire having been lowered, a period of ten minutes is allowed to elapse before readings are taken with the pyrometer The alundum tube by this time has practically reached temperature equilibrium

The furnace used in this manner does not behave as a black body, and the true temperature of the glass can only be obtained by comparing, in a separate experiment, the readings of the optical pyrometer with those of a thermocouple directly immersed in the glass, the thermocouple being read immediately after the optical pyrometer readings, so as to correspond in time with an actual viscosity determination The comparison by this method showed a very slow upward creep of the furnace after the first ten minutes, but the difference between the pyrometer and the thermocouple readings was strictly constant In this connection a platinum-rhodioplatinum couple was used, and a slight deposit of platinum sponge was always found afterwards in the glass This would probably be avoided by the substitution of iridio-platinum for rhodioplatinum

To return to the description of the normal experiment, when the temperature has been measured with the optical pyrometer, the wire is withdrawn at a suitable rate, and its weight determined As the wire used has a diameter of only $\frac{1}{4}$ mm., the normal deposit of glass weighs about 10 mgs., and requires weighing very carefully if an ordinary chemical balance be used This was the case in most of the work to be described, although a microbalance accurate to 1/100 mg was used for the last twenty measurements. After weighing, the wire is copper plated in order to differentiate between the bare wire and the parts covered with glass In the absence of some such method it is impossible to see exactly where the glass ends After copper plating, it is found that in general there is a small coppered length of wire at the bottom, which is due to the effect of surface tension causing a longitudinal contraction of the glass film A similar effect occurs at the upper end of the film, and therefore the true effective depth of immersion of the wire is equal to the measured length of glass plus twice the length of the coppered portion at the bottom This deduction has been shown by experiment to be valid Fig 3 shows the appearance of a wire after withdrawal The gathering of the glass into droplets is due to the well-known instability of long cylindrical films, and takes place after the formation of the film

The values of the viscosity at different temperatures are given in terms of the observed quantities t' and v, by the formula, derived in the appendix,

$$\log(k\eta) = \log\left(\frac{t'}{a}\,\gamma\,\frac{+n}{v}\right) + C\left(0{\cdot}8 - \frac{t'}{a}\right),$$

where η is the viscosity of the glass, t' the thickness of the glass deposit, a the radius of the wire, v its velocity of withdrawal, γ the surface tension of the glass, and n is a quantity, small compared with γ, expressing the influence of gravity.

In carrying out the experiments the value of v is selected so that t'/a differs little from 0·8, in order that the last term be small

It has been found experimentally that

$$k = 2 \cdot 8.$$
$$C = 0\ 10$$

The values of γ were obtained from Washburn and Libman's* measurements for a glass having the same percentages of soda and silica as the glass N P L 15, on which the present measurements have been made A linear relation has been assumed for the variation of γ with temperature. (For glasses not within the series investigated by Washburn and Libman, our viscometer could be readily adapted for the measurement of surface tension) The values of n depend upon t'/a, a, and the constant k The variation of n with t'/a, when a is equal to 0 0001695, and k is equal to 2 8, is shown in Table I. For other values of a or k, recourse may be had to the relation

$$n \propto ka^2.$$

Table I

t'/a	n	Diff	t'/a	n	Diff
0·1	0·6	0 7	1·0	9 4	1 3
0 2	1 3	0 7	1 1	10 7	1 4
0 3	2 0	0·8	1 2	12 1	1·5
0 4	2 8	0 9	1 3	13 6	1·5
0·5	3 7	1 0	1 4	15 1	1 6
0 6	4 7	1 1	1 5	16 7	1·6
0 7	5 8	1·1	1 6	18 3	1 7
0 8	6 9	1 2	1·7	20 0	1 8
0 0	8·1	1 3	1·8	21 8	
1 0	9 4				

* Washburn and Libman, 'Bulletin No. 140, Engineering Experiment Station, University of Illinois.'

Owing to the difficulties, discussed later, of assigning an exact value to k, the results of the present measurements have been plotted in terms of $k\eta$ instead of in terms of η, so as to avoid the recalculations which might be necessary if k were subsequently found to be in error. Strictly speaking, n and C also depend on λ, but a large change in k would be required to produce an appreciable change in η due to neglecting to allow for the variation of n and C.

The viscosity measurements which have been made in the manner described have all been carried out on glass of approximately the composition of N.P.L. 15 *. In some cases the glasses were made from batch, and in the last series cullet was used on which viscosity measurements had previously been made by another method. Preliminary measurements with glasses made from batch showed the necessity for taking great care to ensure homogeneity of the glass before making determinations. This is not surprising when it is realised that the average thickness of the glass film is only 0·1 mm. Although from some points of view the extreme sensitivity of the apparatus to slight heterogeneity is disadvantageous, it will be seen later that by this means phenomena have been observed which might readily be overlooked if a more conventional type of apparatus were used.

The measurements on glass E shown in fig. 4 were made mainly to see whether cooling a glass to room temperatures and reheating would modify its viscosity. The glass, initially melted from batch in an iridio-platinum crucible at a temperature of approximately 1450°, was stirred for a short time by hand with a platinum stirrer, and cooled comparatively quickly. An analysis of the glass was made after the viscosity measurements and gave the following composition :—

SiO_2 ..	73·42
Al_2O_3	0·32
Fe_2O_3 . .	0·16
CaO .	6·90
MgO ..	0·28
Na_2O .	18·98
	100·06

The first measurements were made at about 1570° and are shown by crosses. These points are unreliable, as the maximum speed of the motor was too low,

* 'Trans. Soc. Glass Tech.,' vol. 9, p. 220 (1925).

so that the amount of glass adhering to the wire was insufficient for accurate weighing. The speed of the motor has since been increased. Four measure-

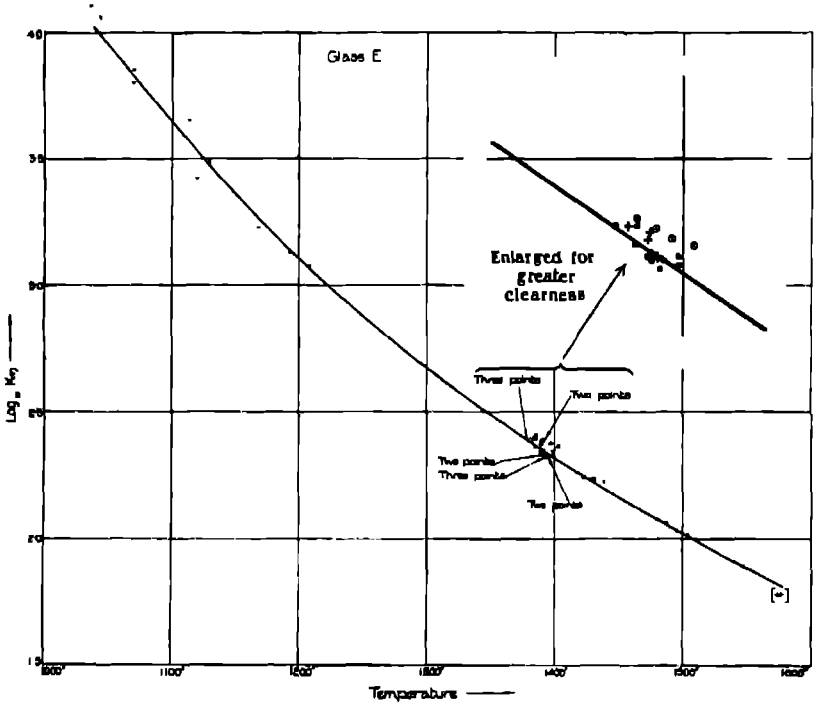

FIG. 4

ments, also shown by crosses, were then made at about 1390°, after which the furnace was switched off.

On reheating, the furnace burnt out at the working temperature before further measurements could be made. The furnace was reconstructed, and the glass again heated to about 1000°, when the furnace had unfortunately to be turned out. The glass was again heated to about 1390° and several measurements made (shown by heavy dots) before switching off the furnace and allowing the glass to cool to room temperatures The last procedure was twice repeated, but on the second occasion the general shape of the log η—temperature curve was obtained before cooling to room temperatures from 1040°. The points (heavy dots) determined by these measurements were irregular in their order

with respect to temperature. On reheating the glass to 1390°, the five points shown by circles were obtained. It will at once be noticed that these points, whilst agreeing excellently amongst each other, are some 10 per cent higher in viscosity than would be anticipated from consideration of the other points. This effect has been found in later work, and appears to be due to shutting off the furnace at a low temperature prior to reheating and making the measurements.

The effect of switching off the furnace at 1040° instead of 1390° would be to cool the glass somewhat more slowly through the temperatures a little below 1040°. In this connection we may note that the devitrification temperature of the glass should be, from the work of Morey and Bowen, about 950° The rise in viscosity, even if due to slow cooling through a critical range, is not necessarily connected with devitrification, as another curious effect exists in the glass at temperatures below about 1200° In the present case this is shown by a loss of precision in the measurements made below 1200°, and it will be seen that this effect has been repeated several times in other experiments, although in certain circumstances the normal precision is obtainable The results of the E series of experiments suggested that the viscosity of the glass between 1200° and 1500° is perfectly definite so long as the glass has first been properly stirred, and so long as it has not been held too long in some temperature range below 1200°.

These considerations further suggested the possibility of calibrating the new method of measurement by means of the glass N P L. 15, of which the viscosity had previously been measured by the falling ball method * Cullet from the falling ball method was available which probably fulfilled the necessary conditions with sufficient accuracy It had been cooled to room temperatures from 1044°, but had been cooled much more quickly than occurs with the present furnace. The "F" series of measurements shown in fig 5 was accordingly carried out on some of this cullet. No preliminary stirring was performed, as the cullet appeared homogeneous As was expected, an extremely concordant series of readings was obtained in an irregular order between about 1200° and 1470°. The readings are shown in the figure as heavy dots close to the lower line. At temperatures near 1160°, however, the points are very scattered, although their geometrical centre lies on a prolongation of the smooth curve passing through points obtained at higher temperatures. This is an important fact in connection with any explanation of the phenomenon, since it eliminates a number of possibilities After obtaining the scattered points below 1200°, the temperature was raised to just about 1200°, and the usual precision of $\pm$ 3 per

* 'Trans. Soc Glass Tech.,' vol. 9, p. 220 (1925).

cent was regained (A variation of 3 per cent in η is roughly equivalent to a temperature variation of 3°) The temperature was subsequently raised to

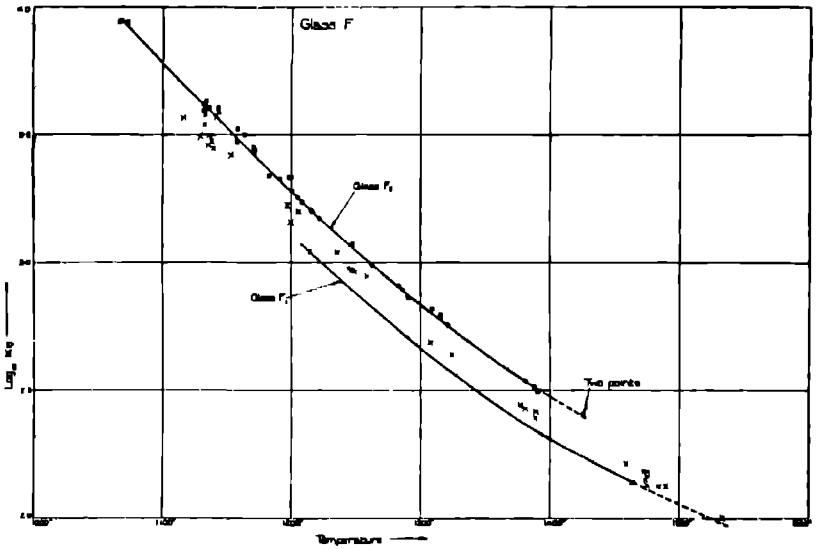

FIG 5

1460°, and a point on the curve obtained. The following day the optical pyrometer was compared with a thermocouple immersed in the glass at 1420°, the day after, this operation was repeated at 1170°, after which the furnace was cooled to room temperatures On reheating the glass to 1380°, the viscosity was found to be some 15 per cent. higher than before This phenomenon had previously been observed in the case of the glass E.

Measurements were then made over a large range of temperature, the results being shown as crosses on the diagram. From 1200° to 1470° the viscosity was consistently 15 per cent. higher than had previously been found. At higher temperatures the increase was only about 5 per cent., although subsequent measurements about 1240° showed the full 15 per cent. rise. The precision of this series of measurements is distinctly lower than the normal Below 1200° erratic results were again obtained, and, as before, varied about a mean point in the anticipated position At the end of this series, a number of measurements were made about 1475°, where a slight discontinuity seemed apparent. (A transformation in silica is known to occur about this temperature.) The

further measurements did not confirm this idea, although they did not definitely disprove it At this stage the temperature was maintained for 24 hours at 1624°, and thereafter a new series of points was obtained, shown in the figure by circles Subsequent analysis showed that the glass lost soda at the high temperature, and the new series showed a marked increase of viscosity (Up to this point the consistency of the various measurements negatives the possibility of appreciable change of composition of the glass with time) The original precision was completely regained in the new series and a curve was obtained substantially parallel to the first curve (The differences in log $k\eta$ are 0 167 at 1200°, 0 170 at 1300°, and 0·164 at 1400°) In this series, however, accurate readings were obtained down to a temperature of 1066°.

At this point the outer winding of the furnace broke, necessitating various repairs. The glass was then reheated to 1440° Measurements at this temperature were vitiated by leakage in the potentiometer owing to damp weather Subsequently, however, a series of measurements was obtained, indicated on the diagram by crossed circles These results are very close to the previous ones, but owing to the repair to the furnace it was not possible to determine whether a slight shift had taken place or not, since the optical pyrometer readings can be influenced by small changes in the temperature gradients The customary variations were observed below 1200° From these results, and those of the "C" series described below, it is concluded that below 1200° a change normally occurs in the glass which had previously been homogeneous at higher temperatures, but that in some circumstances this change may not occur, the glass being then metastable, and yielding a definite viscosity-temperature curve continuous with that obtained at higher temperatures. The nature of the change below 1200° is not known, but it is interesting to note that if the furnace, at a temperature above 1200°, is turned down in the evening, irregular results are found the next morning at a temperature below 1200°. (Measurements at a new temperature cannot be made sooner than this, owing to the necessity for reaching temperature equilibrium in the furnace) Further, maintaining the glass for a week at about 1130°, making frequent measurements, failed to reveal any tendency towards a new equilibrium on the one hand, or towards greater irregularity on the other The analyses of the glass F before and after heating to 1624° are given below :—

	F_1	F_2
SiO_2	72 22	74·20
Al_2O_3	0·71	0 82
Fe_2O_3	0·11	0 22
CaO	6 94	7·00
MgO	0·53	0 25
Na_2O	19·49 (By diff.)	17·40
	100 00	99·89

The "C" experiments, to which reference has been made, were done, before the others, on a glass of the following composition —

SiO_2	72·80
$Al_2O_3 + Fe_2O_3$	0·84
CaO	7·13
MgO	0 22
Na_2O	18·96
	99·95

The glass was melted from batch at about 1450°, but was not stirred It was cooled to room temperature comparatively quickly before viscosity measurements were made The depths of immersion used in the calculations were not corrected for the longitudinal contraction of the glass at the upper end of the deposit. The contraction may also have been somewhat variable owing to a slight difference in technique as compared with the later work Neglect of this correction tends to raise slightly the apparent viscosity at the higher temperatures Fig 6 shows the results obtained, the first series of measurements being indicated by crosses Since the glass was not stirred, it was probably not quite homogeneous, and therefore the measurements were less concordant than in later work. In spite of this, the scattering of the points below 1200° is very noticeable After these measurements, the temperature of the glass was raised to about 1450° in the hope of producing complete homogeneity The points shown as circles were then obtained, and it is interesting to note that the usual effect below 1200° was not apparent, the glass being presumably in a metastable state. This series was terminated by cooling the glass to room temperature from 1339°, after which the points indicated by

heavy dots were obtained. The experiments were ended at a temperature of 1088°, as traces of platinum sponge due to the thermocouple were observed in the glass.

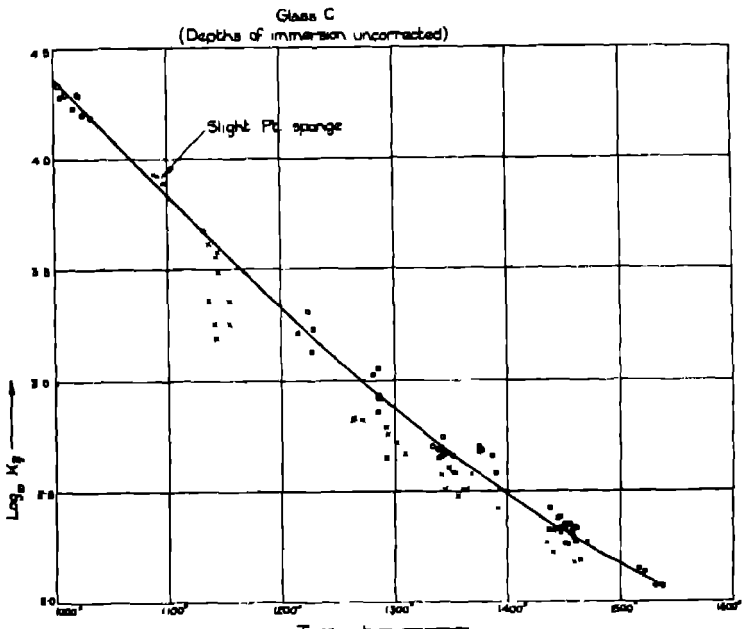

Fig 6.

From the foregoing it will be seen that the present apparatus shows a considerable advance over previous viscometers for molten glass, both from the point of view of precision (± 3 per cent of the viscosity) and also because of the possibility of prolonged experiments on the same specimen of glass, which, if required, may be cooled to room temperatures and reheated an indefinite number of times In the case of the particular glass experimented upon, it has been shown that, once homogeneity has been attained at a high temperature, its viscosity at temperatures above 1200° is repeatable to ±3 per cent This holds so long as the composition of the glass has not been changed by volatilisation, and this is inappreciable except at extremely high temperatures. The viscosity at temperatures above 1200° is unaffected by cooling the glass to room temperature and reheating, provided that the glass be not held too long within a certain critical temperature range which is below 1200°.

At temperatures below 1200° it appears that the glass is capable of existing in at least two states, resulting in considerable variations of viscosity. The mean viscosity in this case is that which would be anticipated from an extrapolation of the curve from temperatures above 1200°. In certain circumstances it is possible to obtain the glass at temperatures below 1200° in a metastable state similar to its state at high temperatures In this case the viscosity-temperature curve is continuous, and of the same precision throughout

These observations may have an important bearing on certain phenomena which are well known to the glass maker. Numerous observations have been made which show that many properties of glass, including brittleness, and more particularly the complex factors which govern its mechanical behaviour during working, are influenced by variations in the conditions of founding which are without effect on the final chemical composition Such variations may be, for example, changes in the moisture content of the batch, differences of heat treatment, or variations in the proportion of cullet, *i e*, previously melted glass, added to the batch * Since it has been shown that a glass, homogeneous at high temperatures, may exist in more than one state when cooled below a certain temperature, it is no longer surprising that the working properties should be influenced by variations in the melting procedure The variations of viscosity, which may be present in glass below a certain temperature, indicate some degree of heterogeneity which may be a cause both of unsatisfactory working properties when hot and of brittleness when cold

Appendix.

Theory of the New Viscometer.

Experiment shows that the thickness of the deposit on the wire very quickly approaches a limiting value on withdrawal at a uniform velocity.

Let t' = mean thickness of deposit.
a = radius of the wire.
η = viscosity of glass.
ρ = density of glass.
γ = surface tension of glass.
g = acceleration due to gravity.
v = velocity of wire.
l = depth of immersion of wire.

* W. E S. Turner, 'Glass Research Association Bulletin,' No. 12 (Feb., 1025) F. Eckert, 'Trans Soc. Glass Tech.,' vol. 10, p 09 (1926).

Then, since t'/a is dimensionless, we must have

$$\frac{t'}{a} = f\left(\frac{l}{a}, \frac{\eta v}{\gamma}, \frac{\eta v}{g\rho a^2}, \frac{av\rho}{\eta}\right),$$

the function on the right including all possible independent dimensionless combinations of the variables presumed to be involved in determining the course of the phenomenon.

It is also known from experiment that the value of t'/a is independent of l/a unless the latter be very small As regards the second term, experiment shows that, between certain limits of t'/a,

$$\frac{t'}{a} = \frac{x\eta v}{\gamma},$$

where, as is shown later, x has a value varying slightly with t'/a

An approximation to the effect of the third term can be calculated by regarding it as a correction to be applied to allow for the effect of gravity In the present experiments the value of this correction has only rarely exceeded 10 per cent, in the case of the "C" series In later experiments it has always been well below 10 per cent, since t'/a has not been allowed to differ greatly from the value 0·8, which has been adopted as the most convenient The fourth term obviously expresses a pure inertia effect It is not possible to calculate the whole work done in accelerating the various portions of the liquid disturbed, but we can calculate the work done in accelerating the liquid which adheres to the wire, and this work must be an appreciable fraction of the whole work in question

Let M = total mass of glass lifted Then the work done in changing its velocity from 0 to v_0, is $\frac{1}{2}Mv_0$

The work done against gravity is $\frac{1}{2}Ml_0g$ where l_0 is the length of immersion

The greatest value of v_0^2 in our experiments is 0·64, whereas l_0g has the

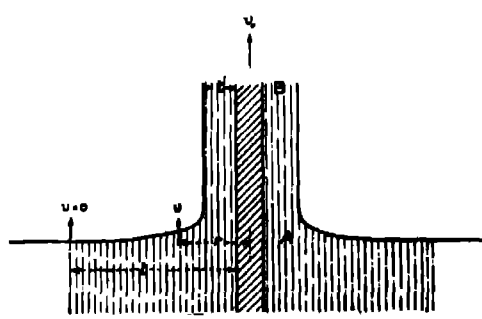

FIG. 7.

value 2943. The ratio of these figures is sufficient to show that the fourth term is small compared with the third, and may therefore be neglected.

Let us now calculate the effect of gravity. We shall suppose that a wire of radius a is pulled out of a liquid of zero surface tension. (See fig. 7)

Following the method of the Research Staff of the General Electric Company,* we write

$$\frac{d}{dr}\left(\eta r \frac{dv}{dr}\right) = \rho g r,$$

therefore

$$\eta \int^{\eta} d\left(r\frac{dv}{dr}\right) = \int^{l+a} \rho g r\, dr,$$

therefore

$$-\eta r \frac{dv}{dr} = \frac{\rho g}{2}\left[(l+a)^2 - r^2\right],$$

therefore

$$\int_{v}^{v_0} dv = -\frac{\rho g}{2\eta}\int_{r}^{a}\left[\frac{(l+a)^2}{r} - r\right] dr,$$

therefore

$$v_0 - v = \frac{-\rho g}{2\eta}\left[(l+a)^2 \log\frac{a}{r} - \frac{a^2 - r^2}{2}\right],$$

or

$$v = v_0 - \frac{\rho g}{2\eta}\left[\frac{a^2 - r^2}{2} + (l+a)^2 \log\frac{r}{a}\right] \tag{1}$$

Now when $r = a + l$, $\quad v = 0$,

whence

$$v_0 = \frac{\rho g}{2\eta}\left[(l+a)^2 \log\left(1 + \frac{l}{a}\right) - \frac{l^2 + 2al}{2}\right] \tag{2}$$

If we now take $l = 3a$ as a particular case, we have from (1)

$$v = v_0 - \frac{\rho g}{2\eta}\left[16a^2 \log\frac{r}{a} - \frac{r^2 - a^2}{2}\right],$$

and since the upward flow of glass at A must be equal to that at B,

$$v_0\pi\left(2al' + l'^2\right) = \int_{a}^{4+a} v\,(2\pi r)\, dr,$$

therefore

$$v_0'(2al' + l'^2) = 2\int_{a}^{4a}\left[v_0 r - \frac{\rho g}{2\eta}\left(16a^2 r \log\frac{r}{a} - \frac{r^3}{2} + \frac{a^2 r}{2}\right)\right] dr$$

$$= 2\left[\frac{v_0 r^2}{2} - \frac{\rho g}{2\eta}\left(16a^2\left\{\frac{r^2}{2}\log r - \frac{r^2}{4} - \frac{r^2}{2}\log a\right\} - \frac{r^4}{8} + \frac{a^2 r^2}{4}\right)\right]_{a}^{4a}$$

$$= 15 v_0 a^2 - \frac{\rho g a^4}{\eta}(89{\cdot}3),$$

* "A Problem in Viscosity," 'Phil. Mag.,' vol 44, p. 1002 (1922).

therefore

$$v_0 t'^2 + 2v_0 a t' + \left(\frac{89\ 3\rho g a^4}{\eta} - 15 v_0 a^2\right) = 0,$$

whence

$$t' = -a + \sqrt{16a^2 - \frac{89\ 3\rho g a^4}{v_0 \eta}}$$

Now the value of $\rho g / v_0 \eta$ must satisfy equation (2). Whence

$$\rho g / v_0 \eta = 2/[16a^2 \log 4 - \tfrac{1}{2}(15a^2)]$$
$$= 1/7\ 338\ a^2,$$

therefore

$$t' = -a + \sqrt{16a^2 - \frac{89\ 3}{7\ 338} a^2}$$
$$= 0 \cdot 96a$$

Returning to equation (2) and substituting therein $t = 3a$, we obtain

$$v_0 = \frac{\rho g a^2}{2\eta} (14 \cdot 68) \qquad (3)$$

We are now in a position to find what value g would have to take in order that for the value of v_0 which gives $t' = 0\ 96a$ when surface tension is alone operating, t' for the purely gravitational case would have the same value, namely, $0\ 96a$

For the surface tension case we have sufficiently nearly

$$t'/a = 2 \cdot 8 \eta v_0 / \gamma$$

(The derivation of this relation from experiment appears later.)
Therefore

$$0\ 96 = 2\ 8 \eta v_0 / \gamma,$$

therefore

$$\eta v_0 = 0 \cdot 342 8 \gamma.$$

Now from (3) we have

$$g' = \frac{2\eta v_0}{14 \cdot 68 \rho a^2} = \frac{0\ 6856 \gamma}{14\ 68 \rho a^2}$$

(where g' is the sought fictitious value of g)
Whence, finally, since $g = 981$,

$$\frac{g}{g'} = \frac{8 \cdot 91}{\gamma}.$$

These calculations have been repeated for various values of t as shown in the table below.—

Table II

t/a	t'/a	g/g'
0	0	0
1	0 33	2 25/γ
3	0 96	8 91/γ
6	1 84	22 53/γ

From these results Table I, in the text, was derived by interpolation, the quantity n being defined by the relation

$$n = \gamma g/g'$$

It will be seen that the implicit assumption has been made that if g' be a suppositious value of g which, in the absence of surface tension, would give a value of t' equal to that given by a surface tension γ in the absence of gravity, then the effect of γ and g acting simultaneously is equivalent to a surface tension γ' acting alone, where

$$\gamma' = \gamma + \gamma g/g'$$

In this way we are now able to write our fundamental equation

$$t'/a = f\left(\frac{\eta v}{\gamma'}\right).$$

This equation may be written

$$t'/a = x\eta v/\gamma',$$

where x is a function of t'/a.

By suitably choosing the values of v in the various experiments we can arrange for t'/a, and therefore x, to be constant (The value 0·8 has been selected as the best value to take for t'/a.)

Writing k for the constant value of x, we have, finally,

$$t'/a = 0{\cdot}8 = k\eta v/\gamma'. \qquad (4)$$

As it is not practicable to withdraw the wire at the precise value of v required to make t'/a equal to 0·8, the variation of x with t'/a was determined by experiment, keeping the temperature approximately constant, and correcting the results to the mean temperature of 1390°. Fig. 8 shows log $x\eta$ (η being constant) plotted against t'/a in the case of glass E. A straight line represents the relationship obtained with sufficient accuracy. From the slope of this line (denoted on page 4 by "C"), experimental results can be corrected to the standard value of $t'/a = 0{\cdot}8$, thus permitting the use of equation (4). The

assumption is here made that the correction is independent of viscosity As this assumption is not likely to be strictly correct, the experiments should be conducted so that the correction is small.

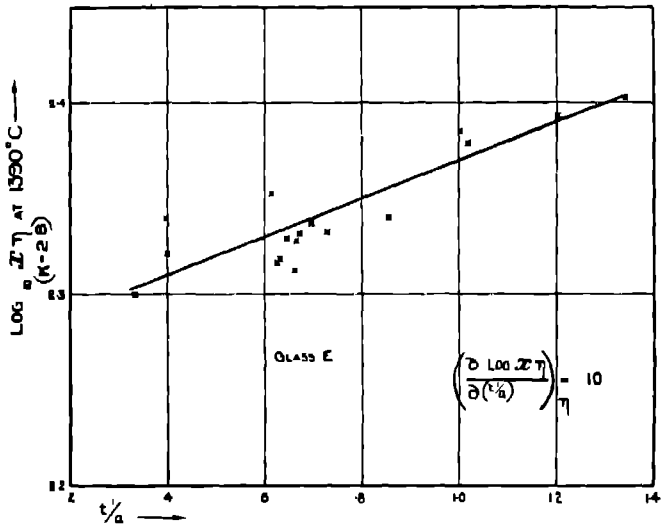

FIG. 8.

The concordance of the results obtained in the "E" and "F" series of measurements shows that errors due to inaccuracy of this correction are small compared with errors due to other causes It will be seen later that this correction probably represents chiefly an effect due to the influence of the rate of shear on the apparent value of η, a phenomenon which could not be taken into account in the dimensional analysis. If this be really the case, "χ" has a constant value in the case of an ideal liquid, and the empirical correction which we are considering must be regarded as applying only to the particular glass on which it was determined

Let us now turn our attention to the experimental determination of the constant k This determination depends upon the measurements, to which reference has already been made, on the glass N.P.L. 15.

It has previously been suggested* that the variation of the calibration factor with η of the falling platinum ball apparatus used for the measurements in question is due to a variation with rate of shear of the apparent viscosity

* Stott, Irvine and Turner, 'Roy. Soc. Proc.,' A, vol. 108, p. 154 (1925).

of the syrup used for calibration. Careful consideration of our own and Washburn's measurements lends colour to this hypothesis, and our own measurements have now been corrected in the following manner —

For the large ball the average velocity of fall determining the calibration factor may be taken as 4 cms /sec Now the calibration factor is obtained from the ratio of viscosity determined by the falling of the large ball to that determined by the falling of a very small ball If the calibration be performed at such a viscosity that the ratios of the velocities of the large and small balls are in the ratio of their radii, the motion will be similar in the two cases, and the true calibration factor will be obtained

The ratio of the radii being 1/0 1189 the velocity of the small balls must be

$$v = 4\ (0\ 1189)$$

We have also, for the particular small balls used,

$$v = 4/\eta$$

Whence

$$4\ (0\ 1189) = 4/\eta,$$

therefore

$$\eta = 8{\cdot}41$$

and

$$\log \eta = 0\ 934$$

The true calibration factor should therefore be obtained when $\log \eta = 0{\cdot}934$ The curve* showing the values of the calibration factor plotted against $\log \eta$ does not extend far enough, but by extrapolation the value of the calibration factor is found to be 22 0. Fig 9 shows the original $\log \eta$ — temperature curve A, of glass N P L 15, together with the revised curve, B, calculated from a constant calibration factor of 22·0. (As a result of minor corrections, the experimental points shown lie somewhat nearer to the curve than in the previous publication, but the line itself is unchanged) Comparison of the $\log \eta$ — temperature curve, B, of the glass N P L 15, with the measurements made on glass F_1 (taken from the centre of the pot on which the measurements were made on glass N.P.L. 15) showed at once a considerable variation with viscosity of the factor k, which was much greater than the corresponding apparent variation of the calibration factor of the platinum ball apparatus when using syrup.

Since dimensional analysis fails to account for such a variation of k, it is reasonable to enquire whether the viscosity of glass is really independent of the rate of shear, as was necessarily assumed for the purpose of analysis. Should

* *Loc. cit.*

this not be the case, it is interesting to note that the variation of x with velocity would be due to this phenomenon rather than to the normal hydrodynamical

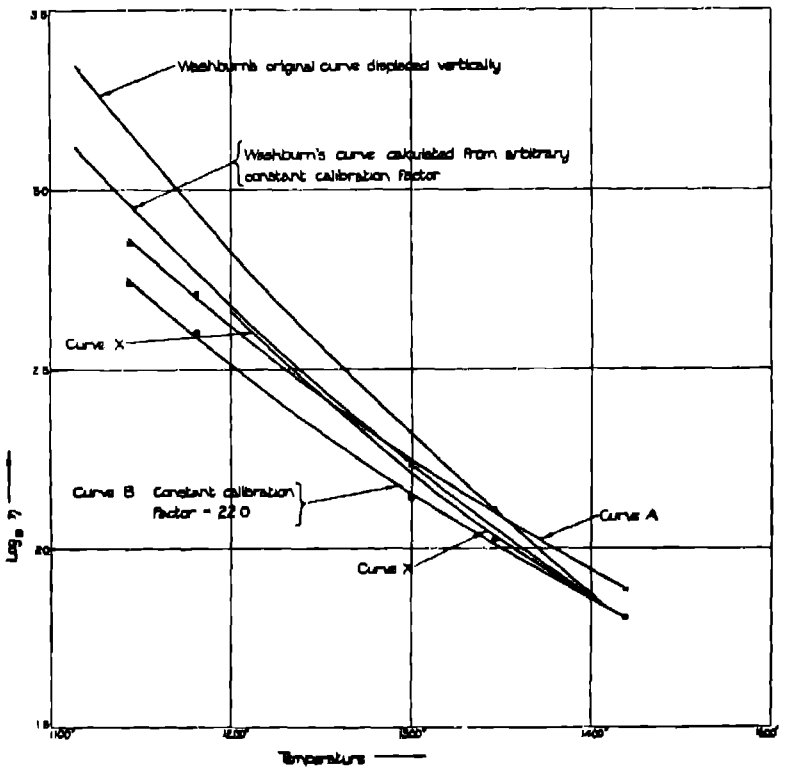

FIG. 9

behaviour of a perfect fluid defined by ρ, η, and γ only. This is shown by the following calculation :—

From fig 8 when

$$\left.\begin{aligned}(t'/a)_1 &= 0{\cdot}40\\ \log_{10} x_1\eta &= 2{\cdot}310\end{aligned}\right\}.$$

When

$$\left.\begin{aligned}(t'/a)_2 &= 1{\cdot}20\\ \log_{10} x_2\eta &= 2{\cdot}390\end{aligned}\right\}.$$

Now

$$v_1 = \left(\frac{t'}{a}\right)_1 \frac{\gamma + n_1}{x_1 \eta} = \frac{(0{\cdot}40)\ (152{\cdot}5 + 2{\cdot}8)}{10^{2\ 310}}$$

and

$$v_2 = \left(\frac{t'}{a}\right)_2 \frac{\gamma + n_2}{x_1 \eta} = \frac{(1{\cdot}20)\ (152\ 5 + 12\ 1)}{10^{2\ 390}},$$

therefore

$$v_2/v_1 = 2\ 645.$$

Hence, when v varies in the ratio $2{\cdot}645$. 1, $\log x$ varies by $0{\cdot}080$, or x varies by 20 per cent

Further, $\log 2\ 645 = 0\ 422$, and $\log \eta$ for N P L 15 (fig 9, curve B) varies by this amount from 1400° to 1202° Over the same temperature range $\log k$ varies from 0 454 to $0{\cdot}545$, that is, k varies by 23 per cent The concordance of measurements made over a considerable range of values of v at various temperatures shows that the variation of x with v does not depend very greatly on temperature The approximate equality of the figures calculated above may therefore be regarded as evidence that the change of x with v is mainly due to the influence of rate of shear.

We are now in some difficulty with regard to the value of k. If we reject the idea that the viscosity of glass is influenced by the rate of shear, we can only ascribe the variation of k to experimental error If, as is more reasonable, we accept the idea, k should be determined at a viscosity such that the effect of rate of shear is the same in the two types of viscometer The value of k thus determined would be the true value applicable to a perfect liquid. Unfortunately we are unable to make such a determination. Actually we have adopted for k a value of $2{\cdot}8$ This is derived from observations made above 1400°, where the effect on the apparent viscosity of different rates of shear would presumably be less than at lower temperatures By the use of this value for k approximate values of η may be calculated which may not be quite comparable with values derived from another apparatus owing to differences between the functional relationships of the mean rates of shear to the viscosities measured. In the case of the wire viscometer the mean rate of shear is inversely proportional to η. In the case of our older method, and that of Washburn, the rate of shear is independent of η, and is roughly constant. Owing to these difficulties, we have plotted our results in terms of $k\eta$ rather than in terms of η. It may also be noted that the value of the gravity correction n depends on k A change in the calculated value of η of 1 per cent. may occur for this reason, if we vary k by the amount found in the calibration

over the whole range of our experiments. A further small source of error is involved in the assumption of linearity for the variation of the surface tension of the glass with temperature. Judging from an exact curve given by Washburn for a somewhat different glass, the error due to this cause may amount to $\pm$ 2 or 3 per cent

Turning again to fig 9, an interesting comparison can be made between the slopes of the log η—temperature curves of the glass N.P.L. 15 obtained in various ways Curve A represents the results of the platinum ball determinations as calculated in the original manner Curve B represents the same results

Table III

Expt	t'/a	v	γ	n	$\gamma + n$.	Log $x\eta$	$\left(8 - \frac{0\ 10}{a}\right)$	Log $k\eta$	Temp.	Date
1F	0 7123	0 533	152 4	5·9	158 3	2 325	0 009	2 334	1391 5	7 12.25
2	0 6180	0 4995	151 9	4·9	156 8	2 288	0 018	2 306	1400 4	8 12 25
3	0 6616	0 5025	152 3	5 4	157 7	2 317	0 014	2 331	1393 0	
4	0 6663	0 508	152 2	5 4	157 6	2 315	0 013	2 328	1394 1	
5	0 0115	0 05455	164 9	4 8	169 7	3·279	0 019	3 298	1172 6	9 12 25
6	0 0085	0 06105	165 4	7 0	172 4	3 358	—0 001	3 357	1164 0	
7	0 6389	0·04825	165 8	5 1	170 9	3 355	0 016	3 371	1156 2	
8	0 7144	0 0634	166 5	6 0	172 5	3 280	0·009	3 298	1144 6	
9	0 5095	0 595	148 1	3 8	151 9	2 114	0 029	2 143	1465·5	10 12 25
10	0 5365	0 640	148 2	4·1	152 3	2 106	0 026	2 132	1463 0	
11	0 5911	0 6375	149 0	4 6	153 6	2 154	0·021	2 175	1450 4	
12	0 5586	0·205	157 7	4·3	162 0	2 645	0 024	2·669	1299 3	11 12.25
13	0·8046	0 262	158 1	7 0	165 1	2 705	—0 000	2 705	1290 8	
14	0 8127	0 262	158 1	7 1	165 2	2·710	—0 001	2 709	1290 6	
15	0·6205	0 0615	165 6	4 9	170 5	3 236	0 018	3 218	1161 5	14 12 25
16	0 9432	0 07455	166 0	8 7	174 7	3 345	—0 014	3 331	1153 9	
18	1 0584	0 0663	165 5	10 1	175 6	3 446	—0 026	3 420	1161 6	15.12.25
19	1 0006	0 0553	166 2	9 4	175 6	3 502	—0 020	3·482	1150 7	
20	0 7139	0 0553	166 4	6 0	172 4	3 347	0 009	3 356	1147 3	
21	0 6879	0 0579	166 5	5·7	172 2	3 311	0 011	3·322	1144 6	
22	0 7026	0 1242	161·8	5·8	167 6	2 976	0·010	2·986	1220·6	16 12.25
23	0 8133	0 1233	162·5	7 1	169 6	3 049	—0 001	3 048	1215·3	
24	0 6891	0 10905	162 5	5 7	168 2	3 026	0 011	3·037	1214 2	
25	0 7831	0·1124	162 8	6·7	169 5	3 072	0 002	3 074	1208·2	
26	0 5932	0 674	148 4	4·6	153 0	2 129	0 021	2 150	1460·5	17 12 25
33	0 8400	0 496	153 0	7 1	160 1	2 433	—0 004	2 429	1381 0	4 1 26
34	0 7628	0 497	152 5	6 2	158 7	2 387	0 004	2 391	1388 7	5.1 26
35	0·8118	0·495	152 5	6 8	159 3	2 417	—0 001	2 416	1389 4	
36	0·9649	0 495	153 2	7 4	160 6	2 448	—0·006	2·442	1377·1	
37	0 6554	0 250	156·2	5·1	161·3	2 626	0 014	2 640	1324 5	6 1.26
38	0 8365	0 279	157 1	7 1	164 2	2 692	—0·004	2 688	1307·9	
39	0 5554	0·547	148 5	4·1	152·6	2·190	0 024	2 214	1459·4	7 1.26
40	0·7898	0 906	147 6	6·5	154 1	2 128	0 001	2 129	1475·2	
41	0 7965	0 919	147 0	6·6	153·6	2 124	0 000	2·124	1484·1	8 1.26
42	0 5776	0 696	144 2	4·3	148 5	1·981	0·022	2·003	1533 3	
43	0 7715	0·1356	160 5	6·3	166·8	2 968	0·003	2·971	1248 4	11 1 26
44	0 7475	0·134	160 6	6·1	166·7	2·968	0 005	2·973	1247·2	
45	0·9211	0 1373	161 3	8·1	169 4	3 055	—0 012	3·042	1236 0	
46	0 8001	0 0851	163 0	6 7	169·7	3·203	—0 000	3 203	1206 3	12.1.26
47	0 8365	0 0977	163 4	7 1	170·5	3·164	—0 004	3·160	1199 7	

Table III—(continued).

Expt	t'/a	v	γ	n	$\gamma + n$	Log x_η	$\left(\frac{0\ 10}{8} - \frac{t'}{a}\right)$	Log k_η	Temp	Date
48F	1 2410	0 117	163·5	12 2	175 7	3 270	—0 044	3 226	1197 1	
49	0 9180	0 0498	167 0	8 0	175 0	3 509	—0 012	3 497	1156 3	13 1 26
50	0 8858	0 0413	168 1	7·6	175 7	3 576	—0 009	3 567	1116 1	
51	0·6290	0 0401	166 8	4 8	171 6	3 439	0 017	3 447	1139·7	14 1 26
52	0 7268	0 0428	166 9	5 0	172 8	3 468	0 007	3 475	1138 1	
53	0 8610	0 0476	167·4	7 4	174 8	3·500	—0 006	3 494	1129 3	
54	1 2643	0 0499	167·2	12 6	179 8	3 659	—0·046	3 613	1132 7	15 1.26
55	0 7357	0 0449	167 0	6 0	173 0	3·453	0 006	3 459	1135 5	
56	1·0704	0 0470	167·2	9 9	177 1	3 606	—0 027	3 579	1133 2	
57	0 9781	0 04435	166 7	8 8	175 5	3 588	—0 018	3 570	1141 6	16.1 26
58	0·7413	0 0486	166 0	6 0	172 0	3 417	0·006	3 423	1153 0	18.1.26
59	1 0648	0 0457	166·6	9 8	176 4	3·614	—0 026	3 588	1143 6	
60	0 8263	0 1540	160·0	6 9	166 9	2 962	—0 003	2 949	1259 6	19.1 26
61	0 7754	0 1396	160 6	6 4	167 0	2 967	0 002	2 969	1246 2	
62	0 7407	0 1355	160 5	6 0	166 5	2 959	0 006	2 965	1249 7	
63	0 7876	0 1387	160 8	6 5	167 3	2 978	0 001	2 979	1241 8	
64	0 7318	0·751	147 5	5 9	153·4	2 175	0 007	2 182	1475 6	20.1 26
65	0 6713	0 748	147 6	5 3	152 9	2 137	0 013	2 150	1474·1	
66	0 7127	0 7375	147 7	5·7	153 4	2 171	0 009	2 180	1473 0	
67	0 6869	0 743	147·6	5·4	153 0	2 151	0 011	2·162	1475 7	
68	0 6822	0·7975	146 7	5 4	152 1	2 114	0 012	2·126	1489 7	21 1 26
70	1 2111	0 2552	158 1	11 8	169 9	2 906	—0 041	2·865	1290 7	25 1 26
71	1 0031	0 2031	158 4	9 1	167 5	2 918	—0 020	2 898	1286 2	
72	0 8873	0·1784	158 6	7 6	166 2	2 917	—0 009	2·908	1283 5	
73	0 8487	0 4305	152 4	7 2	159 6	2 498	—0 005	2 493	1390·5	26 1 26
74	0 7670	0 375	152 6	6 3	158 9	2 512	0 003	2 515	1387 9	
75	0·7302	0·343	153 0	5 9	158 9	2 529	0·007	2 536	1381 2	
76	0 7457	0 1281	159 8	6 1	165 9	2 985	0 005	2 990	1262 7	27 1 26
77	0 9531	0 1310	160 6	8 4	169 0	3 090	—0 015	3 075	1247 7	
78	0 8817	0 1247	160 6	7·6	168 2	3 075	—0 008	3 067	1246 4	
79	0 6072	0 0606	163 3	5·2	168 5	3 268	0 013	3 281	1200 8	28 1 26
80	0·7368	0 0597	163 8	6 0	169 8	3 321	0 006	3 327	1191·2	
81	0·9380	0 04075	167 2	8 3	175·5	3·006	—0 014	3·592	1131 6	29 1.26
82	0·6605	0·01368	170 6	5 2	175 8	3 929	0 014	3 943	1072 7	1 2 26
83	0·7217	0 01461	170 9	5 8	176 7	3 941	0 008	3·949	1067 4	
84	0 7363	0 01493	171 0	5 8	176 8	3 935	0 007	3·942	1066 2	2 2.26
88	0 7307	0·2102	156 4	5 9	162 3	2 781	0 007	2·788	1321·3	11 2 26
89	0 7642	0 2015	156·7	6 3	163 0	2 791	0 004	2·795	1316 0	
90	0 8471	0 208	157 0	7 2	164 2	2 825	—0 005	2·820	1309·7	
91	0 9431	0 07205	163 3	8 3	171·6	3 351	—0 014	3·337	1200 6	12 2 26
92	0 7775	0 0615	163·4	6 4	169·8	3 332	0·002	3·334	1198 4	
93	0 5860	0 0685	162 0	4·4	166·4	3 153	0 021	3·174	1221·8	13 2.26
94	0 6131	0·0683	162·4	4 7	167·1	3 176	0 019	3 195	1216 8	
95	0 7268	0 0709	162 4	5·9	168 3	3 202	0·007	3·209	1216 5	15 2 26
96	0 6862	0 0686	162 8	5 4	168 2	3 226	0 011	3 237	1208 5	
97	0 9098	0 0841	163·0	7·9	170 9	3 267	—0 011	3 256	1205·3	
98	0·8063	0 06285	164 3	6 7	171·0	3 341	—0·001	3 340	1182 5	16.2.26
99	0 8594	0 0530	165 0	7 3	172 3	3 446	—0 006	3·440	1171 9	
100	0·9201	0 0544	165 0	8 0	173 0	3·466	—0 012	4 454	1170 9	
101	1·0035	0 0527	165 4	9 1	174 5	3 521	—0 020	3 501	1164 1	18 2.26
102	0·9477	0 0478	165 7	8 4	174 1	3 538	—0 015	3·523	1158·7	
103	0 8425	0 04855	165 8	7 1	172·9	3 477	—0 004	3 473	1158 1	
104	1 1636	0 0471	167 0	11·0	178·0	3 639	—0·035	3·604	1136 8	19.2.26
105	0·6011	0 03143	167·2	4·6	171·8	3·517	0·020	3·537	1132·7	
106	0 9405	0 03953	166 6	8 3	174·9	3·619	—0·014	3·605	1143·5	22.2 26
107	0·7670	0 03116	167 1	6·3	173 4	3·680	0·003	3·683	1134·3	
108	0 7832	0 485	150·4	6 5	156 9	2·404	0 002	2 406	1425·6	23.2.26
109	0 7859	0·486	150·4	6 5	156·9	2 404	0 001	2·405	1426·1	

calculated with a constant calibration factor of 22·0 For similar reasons to those given with regard to our own experiments, it would appear that a constant calibration factor should be used for Washburn's experiments Two curves are therefore shown representing the results of the alternative calculations applied to Washburn's results Finally, the curve X represents the measurements on glass F_1 (the same as N P.L. 15) calculated on the basis of $k = 2\ 8$ All the curves except A and B have been displaced vertically by arbitrary amounts so as to show more conveniently the differences of slope It will be quite clear, from a consideration of fig. 9 and the preceding discussion, that no method has yet been devised of determining the viscous properties of glass at high temperatures in a manner which is entirely independent of the type of apparatus used, and perhaps also of the properties of other liquids employed for calibration. Accordingly, for the possible convenience of other workers, Table III (pp. 519–520) contains the essential figures from which the results of the F series of measurements have been calculated

Remarks relating to Table III

For Expts. 1F to 26F inclusive ... $a^2 = 0{\cdot}0001695$
For Expts. 33F to the end $a^2 = 0{\cdot}0001629$ } $\rho = 2{\cdot}50$.

After Expt 26F a check against a thermocouple was performed at a temperature of 1460°; on the following day a further check was carried out at 1170°, at which temperature the furnace was switched off.

On reheating to a temperature of about 1390°, a few experiments were vitiated by the usual presence of platinum sponge in the glass due to the thermocouple This sponge was all removed in the glass adhering to the wires in Expts. 27F to 32F.

After Expt. 68F the furnace was taken to 1624° and held there for 24 hours before reducing the temperature to 1290° for Expt 69F.

After Expt. 84F the outer winding of the furnace failed On completion of the repairs, the glass was reheated to 1440°, but Expts 85F to 87F at this temperature were vitiated by leakage in the potentiometer owing to damp weather

Amplitude of Sound Waves in Pipes.

By E G. Richardson, B A , M Sc , Ph D, (University College, London).

(Communicated by Prof. A W Porter, F R S —Received April 15, 1926)

Introduction.

There has always existed considerable doubt as to the magnitude of the periodic pressure changes, and the concomitant velocity and temperature changes which the air in a sounding organ pipe undergoes The difficulty of following these rapid changes has prevented the success of many attempts, and results obtained by a few successful experimenters have not been in agreement Kundt,* and, later, Dvorak,† using a manometer provided with a valve, which opened and shut with the frequency of the air oscillations in the pipe, measured the cumulative pressure of the condensations. Töpler and Boltzmann‡ used an optical method That part of a stopped pipe close to the node was fitted with glass windows and placed between the plates of a Jamin interferometer, so that part of the light which produced the interference bands in the instrument passed through and part outside the pipe The interference bands appeared to be broadened when the pipe was sounded, from the extent of the broadening, the change of density or of pressure at the node due to the vibration was calculated Raps§ obtained actual photographs of the oscillating bands, which the optical fatigue of the eye made to appear widened in the earlier experiments A summary of their results is given in Table I

Table I

Wind pressure (inches of water)	2 35	3 1	3 9	4 7	8 6	9 4	14 0
Pressure change at node (atmospheres)	0·0066	0 0117	0 0143	0 0193	0 021	0 027	0 035

(Pipe 46 × 3 5 × 5 5 cm Mouth . 2 5 × 3·5 cm

Of course, the oscillatory change of pressure will depend on the form of the pipe and the pressure at which it is blown, but with the average stopped

* 'Ann. d Physik,' vol. 128, p 337 (1866).
† 'Ann d Physik,' vol. 150, p. 410 (1873)
‡ 'Ann d. Physik,' vol 141, p. 321 (1870)
§ 'Ann d. Physik,' vol. 50, p. 193 (1891)

diapason, blown at a few inches of water, the discrepancy between the results by different methods is still too great. Against the valve-manometer the criticism may be levelled that the motion of the air in the pipe is seriously affected by the motion of the valve pallet, which will cause additional variations of pressure in the pipe. Kundt's values are the highest (his maximum recorded amplitude was 1/16 atmosphere); Töpler and Boltzmann recorded 1/60, Raps 1/22. Interference methods have the advantage of leaving the air entirely undisturbed, but are troublesome both in their adaptation to existing pipes and in their interpretation, while slight vibration of the walls under the action of the sound waves or the blast produces shifts of the bands of the same order as those sought for in the air motion.

The recent development of the hot-wire anemometer suggested the adaptation of this instrument to measuring the average *velocity* at different points in the organ pipe, as the displacement amplitude can be calculated from this. At the outset the object was to evolve a method by which, with a single apparatus, velocity distribution in the usual form of pipe at any blowing-pressure could be found, the instrument being of such form as not to affect appreciably the movement of the air, either by causing a leak of pressure or by obstructing the flow. By using a calibrated hot-wire, each velocity is read as the resistance in a Post Office box required to reduce a galvanometer deflection to zero, and a complete velocity distribution curve for the pipe, blown at a constant pressure, can be obtained in less than an hour.

Measurements with Hot-Wire Grids

The idea of this method came after reading a paper by Richards.* This author placed the grid of a Tucker-Paris hot-wire microphone on one prong of a vibrating tuning-fork, and measured the steady drop of resistance produced when the microphone was rocked through various amplitudes. By comparing this with the resistance drop produced when the grid was used as an anemometer in a steady wind, he found that the effect of the oscillating draught was the same as that of a steady wind, whose velocity was equal to the *maximum* velocity in the period of oscillation. When the air surrounding the wire is executing S.H.M. with an instantaneous displacement given by $y = a \sin 2\pi nt$, a being the amplitude of the vibration, the maximum velocity $= 2\pi na$. Measurement of the steady resistance drop of a hot-wire placed at any point in a pipe, containing particles of air executing S.H.M., will therefore enable

* 'Phil. Mag.,' vol. 45, p. 925 (1923).

us to determine the amplitude of the vibration at this point, if the hot-wire is calibrated in a steady draught.

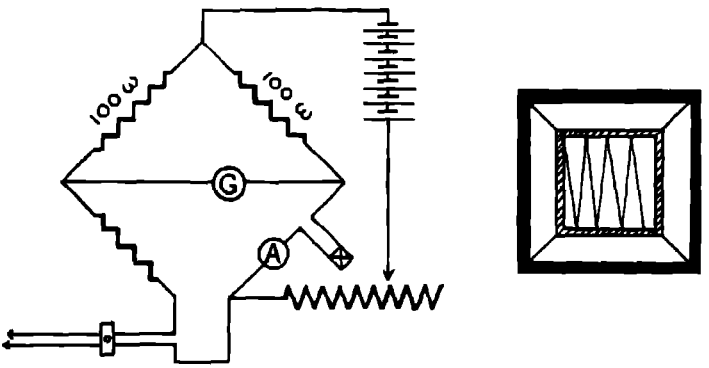

Fig 1

The grid used consisted of 0 001-inch platinum wire wound criss-cross fashion on a thin square mica frame, supported by thin copper wires attached to an ebonite frame (2¼ inches square) made to fit a wooden diapason of the same section (fig. 1) Both frames were designed to obstruct the movement of the air as little as possible, but, as will be shown later, this was not entirely avoided The grid, together with an ammeter, formed one arm of a Post Office box, in which ratio coils of 100 ohms were employed The balancing arm of the box was extended by a sliding resistance of 1 ohm, consisting of a meter wire, enabling adjustments to be made to 0 01 ohm (fig. 1). It was necessary that the slider should always make contact during the balancing, for, if this failed, the increased current through the hot-wire was sufficient to burn it out. The current through the grid kept it just at red heat in the absence of air movements, by balancing the altered resistance in the air current on the Post Office Box, the grid was employed at constant heating current. The grid was first calibrated in the steady draught produced in a horizontal wooden tube, by running water in and out of a reservoir to which it was connected. From the rate of rise or fall of water measured on a glass gauge the velocity of the steady draught was obtained. On the first grid used, the wire lay alternately on each face of the mica frame. Calibration curves of this grid for negative and positive velocities (sucked and blown air) showed asymmetry about an axis corresponding to $V = 0$; that is to say, the greatest resistance was found when V had a small value in one direction, and fell off on both

positive and negative sides of this value. This occurred whether the grid wires were horizontal or vertical. A corresponding asymmetry was observed by Tucker and Paris* when they calibrated their hot-wire microphone, and is probably due to interference of the convection currents from individual wires, the resistance having its greatest value when the individual wires are experiencing the greatest "assistance" from the rest. In an endeavour to make a grid whose resistance should be independent of the direction of the draught, the wire was wound so that the exposed portions lay all on the same face of the mica frame, and therefore all in one plane When this was placed with the strands horizontal in the tube, the convection interference was a maximum when no draught was present, and its resistance fell symmetrically in nearly parabolic form, when an increasing wind from either direction played on the grid At about 4 cm per second a point of inflexion occurs (fig. 2) The first part of this curve corresponds to that obtained by Tucker and Paris

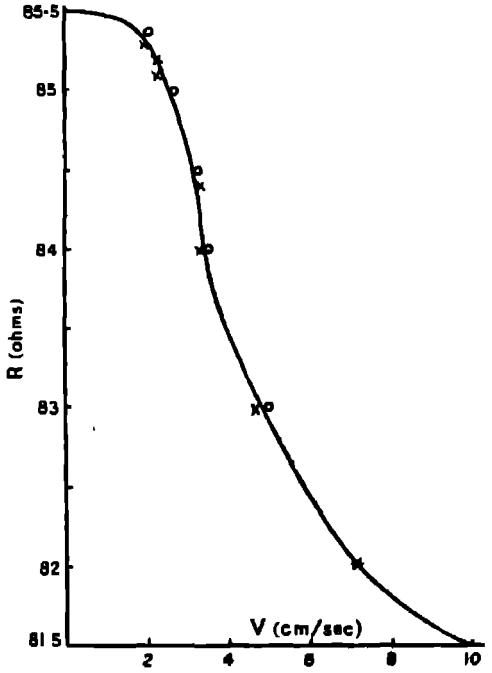

Fig. 2.

* 'Phil. Trans.,' A, vol. 221, p. 389 (1921).

As soon as the investigation in the organ pipe was commenced, it was found that the resistance-drops near the mouth of the pipe were much beyond those which could be obtained with the tube and water tank. Accordingly, a 50-cm. wind channel was erected in the Carey Foster Laboratory, capable of producing velocities up to 500 cm per second with its $\frac{1}{2}$ h p fan In the experimental portion of the channel there was a "static hole" so that the pressure difference between the outside atmosphere and that caused by suction over the hole could be read on a Chattock tilting manometer The static hole was first standardised by comparing readings taken on it with those from a Pitot pair placed in the centre of the channel, the calibration of the grid was then completed in the channel The complete curve is shown in fig 3, when V exceeds 40, the relation between V and dR becomes linear King,* who worked with a single hot-wire in these high velocity winds, found a linear relation to hold. The actual calibration curve therefore incorporates the low-speed relation of Tucker and Paris with King's law at high speeds.

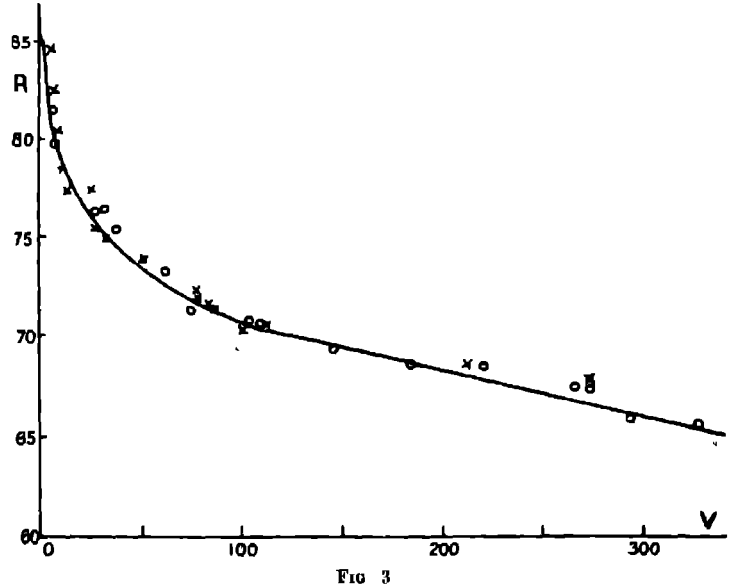

Fig 3

Before using the calibrated grid in the organ pipe, one more experiment was necessary The relation found by Richards that the steady drop in a

* 'Phil. Trans,' A, vol. 214, p 373 (1914).

S H alternating draught was proportional to the maximum velocity in the S H.M. required extending to the linear part of the R V curve, as his results cover the curvilinear part only That the relation holds over the entire portion of the curve required in these experiments (up to V = 100) was verified by oscillating the grid in a direction at right angles to the plane of the frame on the piston of a reciprocating engine, at large amplitudes and frequencies Values of the maximum velocities calculated from the formula $V = 2\pi na$ appear as crosses on the steady draught curve of fig 3 As the motion in the organ pipe is not always even approximately simple harmonic, but is represented by a Fourier series of decreasing amplitude and increasing frequency, it may be inquired what is the equilibrium velocity which the grid registers under such conditions A few results were obtained when the grid was rocked by means of a double cam at a large amplitude of frequency n, superposed on an oscillation of frequency $2n$ and smaller amplitude, imitating an open pipe with fundamental and first harmonic The resistance attained by the grid represented that due to the fundamental, slightly reduced by the presence of the overtone, but no simple relation could be found, consequently the calculations of amplitude made are confined to the pure tone of the stopped wooden diapason

The grid was now ready for use in the stopped organ pipe, which was of square section 5 cm. wide and 75 cm. from upper lip to stop, the mouth being 6 by 2·25 cm. high; the material, pine (A section across the mouth of the pipe is shown in fig 7) The grid was supported by two thin connecting wires at opposite corners, let into the pipe to the requisite distance The pipe was supported horizontally (though it was found that it made very little difference if it was vertical), the heating current adjusted to give a resistance corresponding to V = 0 on the calibration curve, the pipe blown at constant pressure (assured by an adjustable valve between the wind chamber and the mouth), and, after a few seconds, the new resistance found on the Post Office box. From this resistance the corresponding V, and from the known frequency the amplitude of the vibration was calculated A series of readings, taken when the pipe was sounding its fundamental, is shown in Table II

The slight drop in amplitude round about $x = 50$ seems to indicate a trace of the second harmonic, though this could not be detected by ear Fig. 4 shows the variation of amplitude along the pipe at various blowing pressures, in the form of $V : x$ curves. At 5 inches pressure both fundamental and second harmonic were sounding well; at 10 inches only the latter could be heard, so that this curve represents the "overblown" state.

Table II.—Blowing Pressure 1·8 inches* Water. Frequency 105

Distance x Centimetres from Stop	Zero Resistance	Blown Resistance	V.	a in Millimetres.
3	85 58	85 58	0	0
6	85 5	85 49	0 02	0 0003
9	85 48	85 45	0 1	0·0015
12	85 5	85 4	1 8	0 0273
15	85 5	85 17	2 28	0 0346
18	85 5	85 1	2 35	0 0356
21	85 5	84 95	2 55	0 0386
24	85 5	84 8	2·75	0 0416
27	85 5	84 72	2 85	0 0431
30	85 5	84·98	2·55	0 0386
33	85 5	84 7	2 9	0 043
36	85 5	84 5	3	0 0455
39	85 5	84 38	3 1	0 047
42	85 5	84 4	3 05	0 0465
45	85 5	84 05	3 25	0 049
48	85·5	84·77	2 8	0 0425
51	85 5	84 46	3	0 0455
54	85 5	84 5	3	0 0455
57	85 5	84 9	2 6	0 0395
60	85 5	82 8	4 8	0 072
63	85 5	80 95	10	0 116
66	85 5	70	16	0 242
69	85·5	73	68	1 03
72	85 5	72 55	76	1·15

* In common with current musical practice, these pressures are given in inches

Fig 4 makes it obvious that the simple sine relation for the change of velocity or displacement amplitude along the pipe is far from being satisfied at the mouth and for a considerable distance along the pipe. While the formula $y = a_0 \sin 2\pi nt \sin (2\pi x/4L)$, where L represents the total distance from node to antinode, fits the experimental results for a fraction of the length of the pipe, varying from $\frac{1}{2}$ to 1/10, as the pressure measured from the node is increased, beyond this point (marked with an arrow in fig. 4), the motion suffers a rapid magnification as the mouth is approached, due to the circulation of the vortices at the mouth It appears that the circulating air in these vortices contributes nothing to the pressure variations in the pipe itself. If Γ represents the average strength of the vortices, which observation shows are formed by the air, issuing from the slit of the mouthpiece, with the same frequency as that of the pipe to which they are "coupled," we can represent the consequent motion in the pipe under the form:

$$y = a_0 \sin 2\pi nt \sin (2\pi x/4L) + \Gamma e^{-kx}.$$

k is a function of the blowing pressure and the shape of the mouth In a well-voiced pipe the stream of air is carefully directed on to the upper lip;

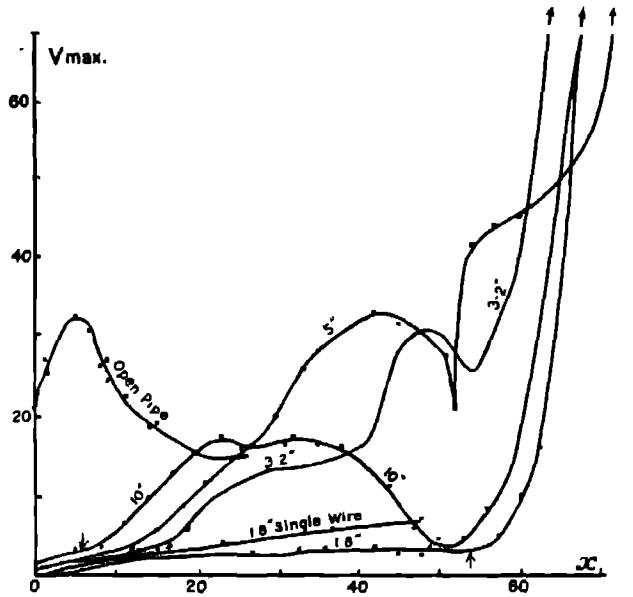

Fig 4

any misdirection of the stream into the interior of the pipe will increase the circulation at the expense of the intensity of the sound produced by the pipe.

In order to find to what extent the air near the mouth was in rotation, a single hot-wire, stretched between two brass rods, mounted on a micrometer screw, was made to traverse the width of the pipe, the wire being kept parallel to the mouth, first on a level with the upper lip and at another level an inch above this Readings of the steady resistance drop were taken every few millimetres of each traverse After calibration of the hot-wire in a steady draught, the velocity distribution across the mouth, shown in fig. 5, was obtained. Herein we see that about 60 cm./sec. of the integrated velocity given by the grid is due to actual oscillatory motion of the air (that is, if the motion is truly two-dimensional, i.e. no rotation in planes parallel to the slit). Traversing the pipe at a point higher up, *e.g.*, at 15 cm. from the upper lip, variations of a few per cent. only in the resistance were found, while beyond the region of circulation a constant resistance drop across the section was

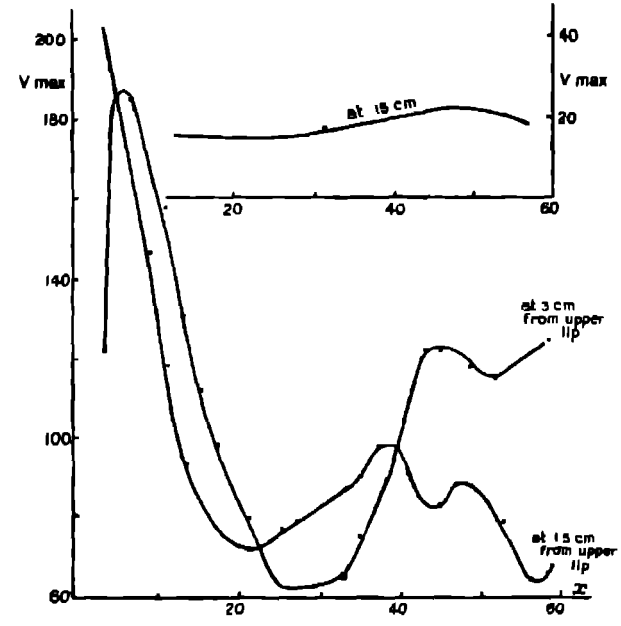

Fig. 5

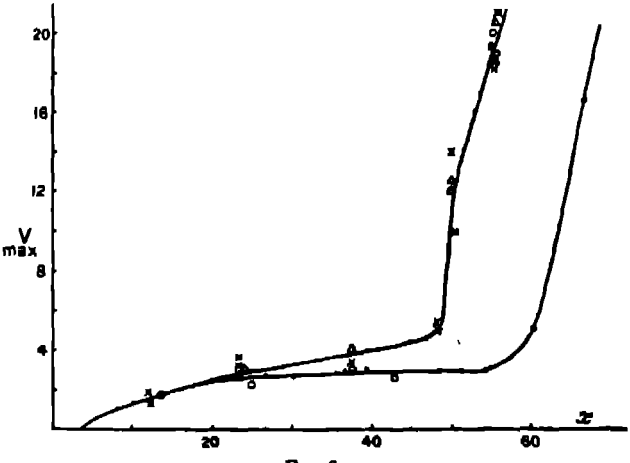

Fig. 6.

Grid, ·001 in. × Str. wire, ·001 in. ○ Str. wire, ·002 in. △ Str. wire, ·001 cm.

found. Even after subtraction of the circulation, the whole of the remaining amplitude near the mouth would not contribute to the pressure changes in the pipe, because the cross-section enlarges rapidly at the mouth

Possible Errors in the Use of the Grid.

It has been shown that a grid may be used to measure the maximum velocity, and, therefore, the amplitude of an oscillating draught. The question arises whether it accurately measures the "stationary vibration" in an organ pipe of the type used here. The possible sources of error presented themselves as follows.—

(1) Vibration of the wire composing the grid
(2) Obstruction of the motion of the air in the pipe by the grid frame, in spite of its tenuity.
(3) Effect of the thickness of the wire composing the grid
(4) Effect of the temperature changes in the pipe which accompany the pressure changes

The possible motions of the wire itself under the action of the pipe group themselves under two heads. Resonance with the pipe tone, and Æolian tones. Owing to the fineness and short length of the wire, the pitch of its fundamental was usually very high, beyond the range of the lower partials of the pipe. Any sympathetic response by the wire of a particular grid to the note in the pipe would have manifested itself by abnormally large resistance drops, compared with another grid in which the tension happened to be different. The Æolian tones of a wire are produced only at definite and steady values of the wind velocity,* and have also the natural frequencies of the wire. In an alternating draught of the organ pipe they would not be maintained. In the steady draught of the wind channel they would, if produced, show an abnormal resistance drop.

To test the second point, *i.e.* whether the frame obstructed the motion, single platinum wires were stretched straight across the pipe at a number of points, so that their leads projected a millimetre or two merely into the pipe, and the holes made for the leads well sealed up with wax. These straight hot-wires were calibrated *in situ*; the stop was replaced by a wide connection to the aspirator, converting the pipe into a miniature wind channel. The results are shown in fig. 4, and also, by crosses, in fig. 6, and indicate that

* V would have to exceed 5,000 in the case of the 0·001-inch wire before an Æolian tone could be produced (*cf.* 'Proc. Phys. Soc.,' vol. 36, p. 165 (1924)).

the original grid does give rather low results, compared with the straight wire, though the former seems to preserve the correct proportion down the pipe.

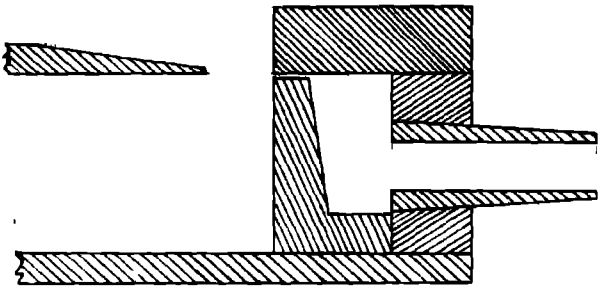

Fig 7

In measuring small oscillations where the amplitude is comparable with the thickness of the wire, an error may arise in the sense that a thick wire may not measure the whole amplitude given by $V = 2\pi na$. Accordingly, beside the 0·001-inch straight-wire grids, others of wires 0 002 inch and 0 001 cm. were tested A comparison of the readings of these different wires in the non-turbulent region of the pipe, blown at 1 8 inch pressure, appears on fig 6. The two thinner wires give practically identical values at the same place in the pipe, while the 0 002-inch wire registers a somewhat lower value. A 0 001 inch wire seems therefore sufficiently fine for our purpose, and can stand a reasonable strain It must be remembered that an organ pipe is a rather unstable source of sound The mere removal and replacement of the wooden stop is sufficient to produce changes in the amplitude, especially at the point ($x = 54$ cm) where the second harmonic has a node. This accounts for some of the variation noticed between different grids, or between the readings of the same grid on different occasions.

With the pressure variations in the pipe, there is a simultaneous change in the temperature of the air, deducible from the adiabatic rule, which will affect the resistance of the grid, apart from the cooling due to the air currents which one claims to measure. The temperature change in the node of a stopped pipe was measured by Neuscheler* using a 0·001-inch Wollaston wire at 150° C., the oscillatory change in resistance being observed The maximum estimated temperature change was 0·13° C., corresponding to a pressure variation in the node of 0·0155 atmosphere, the pipe being blown at

* 'Ann. d. Physik,' vol. 35, p. 131 (1912).

5 inches water. Pressure and temperature (T) are connected by the relation $\delta T = \frac{\gamma - 1}{\gamma} \frac{T}{p} \delta p$ Taking the temperature coefficient of resistance of platinum as 40×10^{-4}, this would produce a resistance change of 4×10^{-4} ohm, which can be ignored in comparison with the cooling effect observed in the method of this paper It is doubtful whether the indications of a resistance thermometer can be relied on in such small but rapid fluctuations, in spite of the careful technique developed by Neuscheler In a recent paper, Friese and Waetzmann* claim that such a " thermometer registers a fraction (depending on the fineness of the wire) only of the temperature changes in an oscillation of 100 periods per second "

Calculation of Pressure from Displacement Amplitude

Following Topler and Boltzmann, we can, if we wish, calculate from the amplitude a_0 at the mouth the total pressure change at the node during the period, using the elementary theory The instantaneous displacement at x being given by $\xi = a_0 \sin 2\pi nt \sin (2\pi x/4L)$ the density $= 1 - \frac{d\xi}{dx} = 1 - \frac{2\pi n a_0}{c} \sin 2\pi nt \cos \frac{2\pi x}{4L}$, where the normal density is 1. Using the adiabatic relation between density and pressure, and taking the normal pressure = 1 atmosphere, we find the total pressure change at $x =$ twice the pressure amplitude. $\frac{4\pi\gamma n a_0}{c} \cos \frac{2\pi x}{4L}$ (γ = ratio of specific heats). In fig. 6, if there were no circulation, and the graph had continued in sine form to the mouth, V_{max} at the antinode would have been 6 cm /sec., and therefore the pressure change at the node $= \frac{4\pi\gamma n a_0}{c} = \frac{2\gamma}{c} V_{max} = 0\ 000085\ V_{max}$ $= 0{\cdot}0003$ atmosphere, considerably lower than in the organ pipe of Raps.

Open Pipe.

In an open pipe, a considerable proportion of the resistance drop is due to the through current of air. Results for the upper half of the same pipe, with the stop removed, appear in fig 4 After subtraction of the 15 cm./sec. of draught at the central node, the remainder indicates increase in sine form to the open end.

A simple open tube without mouthpiece in which the sound is maintained by the heat of the grid itself, on the principle discovered by Rijke,† forms an

* 'Ann. d Physik,' vol. 76, p 39 (1925)

† 'Ann. d. Physik,' vol 107, p. 339 (1859).

interesting subject for investigation. An iron wire grid, passing 3 amps., placed in the lower half of a brass tube, round which cold water circulated, caused it to sound its fundamental when the grid became red-hot When a small hole was opened at the central node, the leak of pressure stopped the sound. Simultaneously, a fall of a few per cent. in the resistance of the grid was noticed, representing the magnitude of the effect of the oscillation which had been imposed on the upward draught. This Rijke tube is more readily examined through the oscillatory change of resistance, and so will be dealt with in a later paper.

Sound Waves in Narrow Tubes

The propagation of sound waves in narrow tubes in which viscosity may be expected to play a part has been dealt with by Helmholtz, Kirchhoff, and the late Lord Rayleigh * Measurements of the velocity of sound under such circumstances (by German and American scientists), and of decay of amplitude along the tube (by Simmons and Johansen†), have been almost entirely confined to comparatively wide sections, in which the layer affected by viscosity can only be a small fraction of the diameter. By using a tube 0·17 cm. in diameter, and "aural frequencies," the writer hoped to have the main body of air in the tube moving under viscous retardation Simmons and Johansen produced slow harmonic motions of the air at one end of a rubber tube (either 4 75 or 9·53 mm diameter) by means of a large piston operating into a reservoir Different lengths of the rubber tube were taken and the transmitted pressure measured by a diaphragm gauge which rocked a mirror. To produce the waves, in the work about to be described the oscillating engine previously described was used to produce displacement waves The piston was made to oscillate the air in a little cylinder, having a brass tube leading out, to which the rubber tube could be adapted. At the other end of the rubber tube, 1·7 mm. diameter, a similar adapter of the same diameter led to a box, 20 cm long, open at the other end, made to hold the platinum grid, which was placed about 4 cm. from the point where the narrow tube debouched on the wide box With various lengths of the tube from the shortest possible up to 1 m., the amplitude transmitted to different distances from the source was found by the usual method of measuring V_{max}. No evidence of resonance *in the box* at these frequencies was obtained Four frequencies and four initial amplitudes were used, and the 16 curves so obtained are shown in fig. 8.

* 'Phil. Mag.,' vol. 1, p. 301 (1901).

† 'Phil. Mag.,' vol. 50, p. 553 (1925).

A theory accounting for the observed decay as the waves traverse the tube, together with the resonant lengths, may be developed by assuming the walls

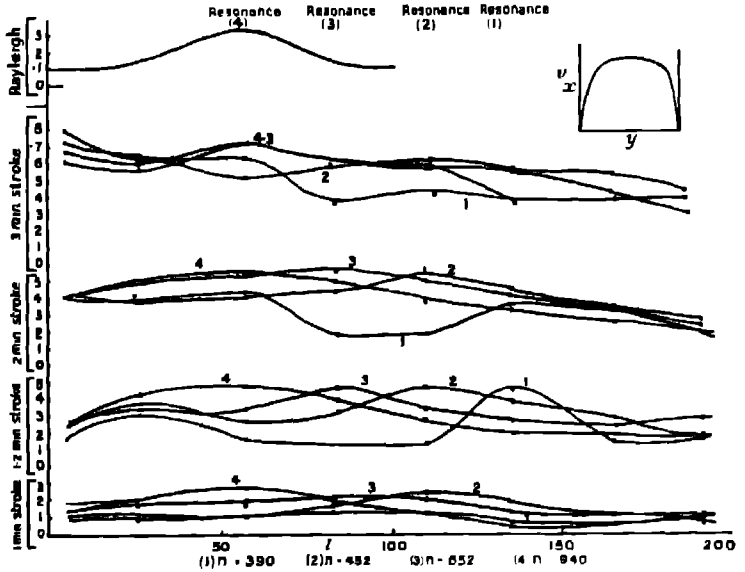

Fig. 8.

of the tube to exert a dragging effect on the air in their immediate neighbourhood. Starting with the Eulerian equations of motion:

$$\rho \frac{\delta u}{\delta t} = -\frac{\delta p}{\delta x} + \mu \Delta u, \text{ etc.}, \tag{1}$$

with the equation of continuity:

$$\frac{\delta u}{\delta x} + \frac{\delta v}{\delta y} + \frac{\delta w}{\delta z} = 0, \tag{2}$$

Prandtl assumes that in a medium of small viscosity like air, the operation of the viscous forces is restricted to a thin layer adjacent to the boundary. In this "boundary layer," the tangential velocity u falls very rapidly from the mean velocity in the body of the fluid to 0 at the boundary, in a fraction of a millimetre; the motion in this layer is approximately stream-line even when it is turbulent outside. These assumptions have the experimental support of Stanton and Marshall,* one of whose curves is shown in fig. 8, exhibiting the

* 'Roy. Soc. Proc.,' A, vol. 97, p. 413 (1920).

velocity gradient across the channel in which air is flowing. A new co-ordinate is taken across the tube $\eta = y/\epsilon$, where ϵ is a small quantity, so that $\eta = 0$ at the boundary and infinity at the outer edge of the layer. For simplicity he treats the motion as two-dimensional in planes at right angles to the wall, and the assumption of stream-line motion in the boundary layer allows him to neglect v or v_η in comparison with u. The friction being entirely in this thin layer requires a new and larger co-efficient than that given by Poiseuille's law; it is found that, with the above change of co-ordinates, it is necessary that $\mu = \mu_1 \epsilon^2$. Prandtl's equations finally become

$$\rho\left[\frac{\delta u}{\delta t} + v_\eta \frac{\delta v_\eta}{\delta x} + v_\eta \frac{\delta u}{\delta \eta}\right] = -\frac{\delta p}{\delta x} + \mu_1 \frac{\delta^2 u}{\delta \eta^2} \qquad 0 = -\frac{\delta p}{\delta \eta}, \tag{3}$$

or, with the further approximation,

$$\frac{\delta u}{\delta x} + \frac{\delta v_\eta}{\delta \eta} = 0, \quad \frac{\delta v_\eta}{\delta \eta} = 0 \text{ and } v_\eta = 0,$$

$$\frac{\delta u}{\delta t} = -\frac{1}{\rho}\frac{\delta p}{\delta x} + \nu_1 \frac{\delta^2 u}{\delta \eta^2}, \tag{4}$$

which is the equation we can apply to the propagation of waves in pipes. Putting $u_1 = Ce^{i(kx + nt)}$ and $u_0 = Ce^{int}$ the applied alternating velocity produced by the piston at $x = 0$. Outside the boundary layer $-\frac{1}{\rho}\frac{\delta p}{\delta x} = \frac{\delta u_1}{\delta t}$ approximately, where $u =$ the mean velocity along the tube at this point.

Prandtl has considered the stationary state, where $\frac{\delta u}{\delta t} = 0$. Equation (3) is then unchanged on multiplication by $\sqrt{\frac{\nu_1 l}{u}}$, if l represents the length of boundary against which the fluid rubs. In the case of our S.H.M., this quantity is represented by a, and u by $2\pi n a$. Then the factor $\sqrt{\frac{\nu_1 l}{u}} = k\sqrt{\frac{\nu_1}{n}}$ represents the order of the dragging effect on the fluid, *i.e.* the thickness of the boundary layer is proportional to $\sqrt{\frac{\nu_1}{n}}$.

Inside the boundary layer, let us put

$$u' = f(\eta)\, e^{i(kx + nt)},$$

with $f(0) = -C$ to satisfy the boundary condition.

Then putting $u = u_1 + u'$ in (3), we obtain

$$inf(\eta) = \nu \frac{\delta^2 f}{\delta \eta^2},$$

whence

$$f(y) = -Ce^{\pm(1+i)\eta\sqrt{\frac{n}{2\nu_1}}}$$

$$u = C/_4 n\,[1 - e^{-(1+i)\sqrt{\frac{n}{2\nu_1}}\,\eta}]\,e^{int}$$

The second term in the bracket represents the extent to which the motion is dissipated by friction during propagation, and shows that, as might have been guessed, it is the thickness of the boundary layer which determines the rate of decay

Equating the tangential force on unit length of the tube $-\mu^1\frac{\delta u}{\delta\eta}2\pi na$ to the difference of the forces on a corresponding section of air ; $\pi a^2\left[\rho_0\frac{\delta u}{\delta t}+\frac{\delta\bar{p}}{\delta x}\right]$ and using the sound-wave relation .

$$\frac{\delta}{\delta t}\left(-\frac{1}{\rho_0}\frac{\delta\bar{p}}{\delta x}\right) = -\frac{1}{\rho_0}\frac{\delta}{\delta x}\left(\frac{\delta\bar{p}}{\delta t}\right) = C^2\frac{\delta}{\delta x}\left(\frac{\delta u}{\delta x}\right)$$

we get

$$\frac{\delta^2 u}{\delta t^2} = \left[1 - \frac{1-i}{a}\sqrt{\frac{2\nu_1}{n}}\right]C^2\frac{\delta^2 u}{\delta x^2} \qquad (5)$$

This corresponds to the formula obtained by Rayleigh and others, save that their ν is replaced by ν_1, the value of which will be determined by the experimental results. Incidentally (5) shows that the velocity of sound in the tube is $\left(1-\sqrt{\frac{2\nu}{n}}\cdot\frac{1}{2a}\right)c$, as against c in free air. (5A)

For convenience, we now modify our expression for u and put

$$u = Ce^{i(nt + (\phi + i\psi)x},$$

and in accordance with (5) we must have

$$\phi = \frac{n}{c}\frac{\sqrt{\frac{2\nu_1}{n}}}{2a} \text{ and } \psi = \frac{n}{c}\left[1 + \frac{\sqrt{\frac{2\nu}{n}}}{2a}\right].$$

In our tube we have both incident and reflected waves, and a particular solution to satisfy these conditions is

$$x = M\left[e^{-\phi x}\sin(nt - \psi x) + e^{-\phi(2l-x)}\sin(nt - \psi\overline{2l-x})\right]$$
$$+ N\left[e^{-\phi x}\cos(nt - \psi x) + e^{-\phi(2l-x)}\cos(nt - \psi\overline{2l-x})\right]$$
$$= V_s\sin(nt - \psi l + \omega), \text{ say.}$$

Substituting the initial condition, $u = V_0\sin nt$ at $x = 0$, we find

$$V_0\cos\theta = 2Me^{-\phi l}$$
$$V_0\sin\theta = 2Ne^{-\phi l},$$

Substituting these values for M and N, we get at $x = l$ the value of the maximum velocity at this point,

$$V_l = \frac{V_0 \; 2e^{-\phi l}}{\sqrt{(1 + 2e^{-2\phi l}\cos 2\psi l + e^{-4\phi l})}}. \qquad (6)$$

Resonance will occur at a value, L, of the length of the tube, given by $\cos 2\psi L = -1$, and the amplitude in such cases will be $2e^{-\phi L}$ approx. As ψ involves ν_1 in a term forming a small fraction of the whole, we should not expect its value to affect the *positions* of resonance to a great extent. In fig. 8 we find the experimental resonance positions corresponding with those plotted from the Rayleigh formula, with $\nu = 0{\cdot}15$. For the same initial amplitude, the amplitudes at resonance average half the Rayleigh values. Simmons and Johansen found in one case resonance at the same length as the Rayleigh theory but with amplitude 0·425 of the theoretical. The logarithm of this amplitude ratio will give us the approximate ratio of $\sqrt{\nu}$ to $\sqrt{\nu_1}$. In the present case a value of 1·3 instead of 0·15 is indicated. The value of this coefficient will be a function of the roughness and elasticity of the material of the tube, as both these factors affect the thickness of the boundary layer and reduce the maximum amplitude attainable on resonance. The above treatment is an attempt to account for this. Several experimenters on the velocity of sound in narrow tubes agree that the formula of Helmholtz $v' = v\left(1 - \frac{\mu}{2a\sqrt{n}}\right)$ (*cf.* equation 5*a*) can be made to fit experimental results *if a larger coefficient is put instead of the viscosity* μ.

Absorption Coefficients of Materials

We can investigate the change of amplitude, by means of a grid, at a point in a cylindrical resonator when different materials are placed at the stopped end, and, from the change of amplitude, we can gain information of the absorbing qualities of the material of the stop to the waves which are incident upon it from the source of sound at the open end of the resonator. Although observations of absorbing power are more accurately determined by experiments with a large partition between two chambers, when time and expense have not to be considered, yet Taylor* by a small-scale method† has obtained results in good agreement with these. His plan was to send waves down a long resonator, which by reflection at the stopped end formed nodes and loops in the tube.

* 'Phys. Rev.,' vol. 2, p. 270 (1913).

† First suggested by Tuma.

The relative intensities in these nodes and loops was reduced by placing absorbent material against the stop, these intensities were measured by a long search-tube connected to a Rayleigh disc resonator pushed down the pipe until the maxima and minima were discovered. This gives a measure of the relative amplitudes in the incident and reflected waves. In the present research, the grid (either in the reticolate or, better, the straight-wire form) is placed at any convenient point in the pipe, consisting of a wooden box of about the same size as the organ pipe to which it resounded. Values of V_{max} were found, first (V_1), when a thick varnished wooden stop 12 cm. deep was fixed in the end, and again (V_2) when the face of the stop was covered with material.

It was essential that the stop tightly fitted the pipe under all circumstances, and the stop was adjusted so as to bring the surface of the material to the same point in the tube. From the ratio V_1/V_2 we can calculate the ratio of the incident and reflected amplitudes, assuming the thick stop to be a perfect reflector.

Taking the equation for an incident progressive wave as

$$y = a \sin \omega (t + x/c),$$

where x represents distance from the stop, the equation of the reflected wave will be

$$y = -b \sin \omega (t - x/c).$$

Here a and b are the amplitudes of the incident and reflected waves, respectively.

Case 1.—Perfect reflector, $a = b$. Resultant amplitude at x,

$$y_1 = 2a \cos \omega t \sin (2\pi x/\lambda).$$

Maximum value of velocity in S.H.M.,

$$V_1 = -2a\omega \sin 2\pi x/\lambda.$$

Case 2.—$b < a$. Resultant amplitude at x,

$$y_2 = (a - b) \sin \omega t \cos 2\pi x/\lambda + (a + b) \cos \omega t \sin 2\pi x/\lambda.$$

Maximum velocity,

$$V_2 = \omega \left[-\frac{(a-b)^2}{\sqrt{2a^2 + 2b^2}} \cos 2\pi \frac{x}{\lambda} - \frac{(a+b)^2}{\sqrt{2a^2 + 2b^2}} \sin 2\pi \frac{x}{\lambda} \right].$$

$$\therefore \frac{V_1}{V_2} = \frac{2\sqrt{2}\sqrt{1 + b^2/a^2}}{(1 - b/a)^2 \cot 2\pi x/l + (1 + b/a)^2}. \quad \text{Put } b/a = \theta, \text{ which we want to find.}$$

$$\frac{V_1}{V_2} = \frac{2\sqrt{2}\sqrt{1 + \theta^2}}{(1 - \theta)^2 \cot 2\pi x/l + (1 + \theta)^2}.$$

(The "absorption coefficient" $\alpha = 1 - \theta$.)

This equation may be solved by putting an approximate value (1·5) for $\sqrt{1+\theta^2}$, or by plotting V_2/V_1 from trial values of θ. This has been done

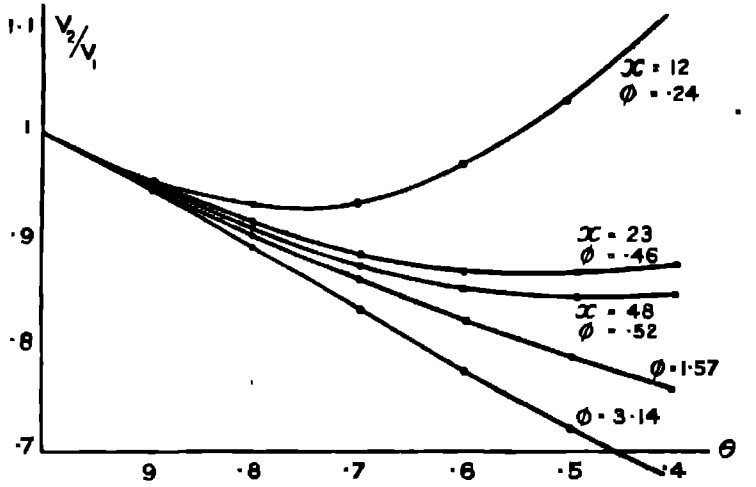

FIG 9

in fig 9 for a number of values of $2\pi x/\lambda$,* from which we see that judgment is needed to get sensitivity, in selecting the distance x at which the measurements are to be made. Results are shown in Table IV, making use of this graph and values for similar materials from Taylor's and other researches. By obviating the employment of Taylor's long search-tube, with its consequent

Table IV.

Material	Grid at $x = 12$ $n = 104$		Grid at $x = 23$ $n = 104$		Grid at $x = 12$ $n = 315$.		Average results of other workers
	V_2/V_1	α	V_2/V_1	α	V_2/V_1	α	α
½-inch hair felt	0 95	0 58	0·88	0 545	0·87	0·58	0 55
¼-inch hair felt	0 955	0·21	0 96	0·16	0·96	0 2	—
½-inch asbestos	0 965	0·16	0 97	0 12	—	—	0 26 (¼-inch)
2-inch cork	0 955	0 2	0 93	0·3	0·94	0 23	0 32
½-inch cabot quilt	1 03	0·75	0 865	0 7	0 85	0·72	0 6
½-inch carpet	—	—	0·935	0·34	—	—	0·25 to 0 50

* Denoted by ϕ in the figure.

interference with the motion and the uncertainty of what is happening in the search-tube itself, it is hoped that the present method is an improvement.

Summary and Conclusions.

The steady drop of resistance of a hot-wire grid is suitable for the study of the amplitude of vibration in organ pipes, without cutting into or specially adapting the pipe, and in the form of a single wire offers the minimum disturbance to the motion. The method is also adapted to measurements of the decay of sound in narrow tubes and of absorption coefficients of materials.

An instrument is much needed in applied sound at present that will give absolute measurements *in free air* of sounds of any frequency. If the above method were employed to measure amplitudes in the open air, it would only be of use for very loud sounds All local air currents would have to be obviated, as any attempt to cover the grid would introduce resonance effects Supposing that all air movements other than those due to the passage of the sound were eliminated, the greatest V_{max} which could be read with accuracy is 2 cm./sec., corresponding to amplitudes of the order 10^{-3} cm. at a frequency of 100, whereas the ear can detect amplitudes of 10^{-6} cm at this frequency. When pressure amplitude is required, a manometric capsule with a mirror recorder instead of a flame can be used, but, being less sensitive, is of no use in the open air.

My thanks are due to Prof A. W Porter, D.Sc., F R S, for giving every encouragement to this work, and to Mr. R C. Richards, B A, M Sc., for giving me a more complete account of his work than appears in the paper cited.

The Solubility and Rate of Solution of Oxygen in Silver.

By E. W. R Steacie, M.Sc., Ph.D., and F. M. G. Johnson, M.Sc., Ph.D., McGill University, Montreal.

(Communicated by Prof. A. S Eve, F R.S.—Received May 25, 1926.)

Introduction

A large number of investigations have been made on the solubility of gases in metals, and on the rate of diffusion of gases through metals. Hydrogen-platinum and hydrogen-palladium are, however, the only systems which have been thoroughly investigated. The behaviour of these systems is such that they can by no means be regarded as typical. The system oxygen-silver was chosen as a more typical one which was suitable for purposes of investigation. The rate of diffusion of oxygen through silver has been measured by Johnson and Larose *. This paper deals with the solubility and rate of solution of oxygen in silver.

Historical

It has been known for a long time that molten silver will absorb oxygen from the air and will "spit" on solidification. Sieverts and Hagenacker† found an absorption of 20 volumes of gas per volume of silver at the melting point. The solubility decreases as the temperature increases beyond the melting point. The absorption is proportional to the square root of the pressure. Dumas‡ showed that a portion of the oxygen is retained by silver on solidification. He obtained 57 c.c. of oxygen from 1 kilogram of silver. Brauner§ found that 0·04 volumes of gas were retained on solidification. Richards and Wells|| found 0·6–1·8 volumes. Graham¶ found that silver takes up oxygen at a red heat. He obtained an absorption of 0·7 volumes. Neumann** found a somewhat larger absorption, while Berthelot†† obtained a smaller value. More recently Sieverts‡‡ obtained an absorption of 0·3 volumes of gas per volume.

* 'J. Am. Chem. Soc.,' vol. 46, p. 1377 (1924), and unpublished results.
† 'Zeit. f. Physik. Chem.,' vol. 68, p. 115 (1910).
‡ 'Comptes Rendus,' vol. 86, p. 68 (1878).
§ 'Bull. Acad. Belg.,' vol. 18, p. 81 (1889).
|| 'Zeit. Anorg. Chem.,' vol. 47, p. 79 (1906).
¶ 'Roy. Soc. Proc.,' vol. 15, p. 502 (1866).
** 'Monats. f. Chemie,' vol. 13, p. 40 (1892).
†† 'Ann. Chim. Phys.,' vol. 22, p. 289 (1901).
‡‡ 'Zeit. physik. Chem.,' vol. 60, p. 129 (1908).

of silver His results, however, do not check closely and he does not place much confidence in them himself

All that can be concluded, therefore, from previous work is that solid silver absorbs a small amount of oxygen.

Description of Apparatus.

In principle the apparatus was extremely simple. A definite volume of gas was introduced into a bulb of known volume, which contained silver foil, and was connected to a manometer. At any temperature the pressure of the gas in the bulb could be calculated from the gas laws If any absorption took place, the observed pressure would be less than that calculated, and the difference between the two pressures would be a measure of the absorption

The apparatus is shown in fig. 1 Three bulbs, A, B, D, were contained in

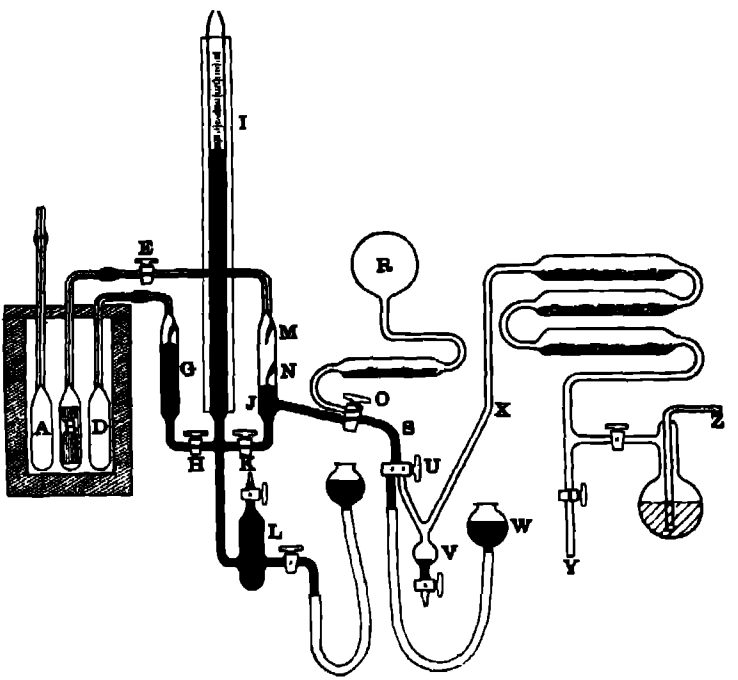

FIG. 1.—Absorption Apparatus.

an electric furnace F. The bulb A was filled with air and led to a thermal regulator. D was part of a constant-volume gas thermometer. The third

bulb B contained silver foil The bulbs and connecting tubes were made of either Pyrex glass or of quartz, and were connected to the remainder of the apparatus by means of de Khotinsky cement

The bulb containing the silver was connected, through the tap E, with a manometer IJ. A glass pointer M was sealed into the top of the tube J. By means of the taps H and K either the silver bulb or the gas thermometer could be connected to the manometer The volumes of the tube J from the pointer M to the tap E, of the capillary tube from the tap to the furnace, and of the bulb containing the silver were all known

The tube J was connected to one arm of a two-way tap O. The other arm of the tap led through a phosphorus pentoxide tube to the gas reservoir R The tube S led to another two-way tap U One arm of U led to a mercury container W, and the other led through three phosphorus pentoxide tubes to the gas supply Z and the pumping system Y. The bulb V was inserted to catch any mercury which might inadvertently be let through the tap U

In carrying out an experiment, the bulb containing the silver was connected to the pumping system by means of the taps E, O, U and Y, and the whole system was evacuated The taps E and O were then closed. The tap U was turned so as to connect S with the mercury reservoir W, and mercury was allowed to rise and fill the tube S S was then connected to the gas reservoir R by means of the tap O, the mercury reservoir was lowered, and gas was drawn into S. O was then turned to connect S to the manometer tube J, and the mercury reservoir was raised, forcing the gas into J. The mercury was allowed to run up the tube after the gas till it took up the position shown in the figure. O was then closed and K opened, connecting J to the manometer. The mercury was brought to the lower pointer N and the pressure was read. Then, knowing the volume of the tube and the room temperature, the volume of the gas under standard conditions could be calculated.

The tap E was then opened and the gas was admitted to the bulb. The mercury level was brought up to M and the pressure read, after equilibrium had been reached. The absorption was then calculated from the difference between the calculated and the observed pressure.

Measurement of Temperature.—The temperatures were measured by means of the ordinary type of constant-volume gas thermometer DGHI The bulb D was filled with nitrogen By means of the taps H and K, the same manometer was used for the absorption apparatus and the gas thermometer. The thermometer was checked at 0° C., 100° C., and at the boiling point of sulphur 444·7° C. The maximum divergence was 0·2° C. In calibrating at

the boiling point of sulphur, the procedure recommended by Meissner* was followed.

Electric Furnace.—A 15-inch length of 2½-inch iron pipe was covered with asbestos paper and then wound with 18-gauge nichrome wire, the turns being about ¼-inch apart. This was covered with another layer of asbestos paper and packed in an iron container with loose asbestos. The tubes were placed in position in the furnace and the top was covered with a layer of "asbestos cement." The high heat conductivity of the iron ensured an even temperature throughout. The furnace would maintain a temperature of 1000° C. with a power consumption of 600 watts.

Temperature Regulation.—The temperature was controlled by the usual type of thermal regulator, using air as the expanding medium. The circuit was arranged so that only about 10 per cent. of the current going to the furnace was cut out by the regulator. The temperature could be kept constant to within 1–2° C.

Pumping System.—At the conclusion of an experiment the tap K was shut and E opened. The two-way tap O was turned so as to connect the tubes J and S, and the tap U so as to connect S to the mercury reservoir W. The reservoir was lowered and the mercury in J and S was allowed to run out. O, U and Y were then turned to connect the bulb containing the silver to the pumping system.

The pumping system consisted of a two-stage mercury vapour condensation pump, backed up by a Hyvac pump. A McLeod gauge was used to indicate the pressure. If it was desired to collect the gas pumped out, a Toepler pump was used as a fore-pump instead of the Hyvac. The gas from the Toepler pump was collected in the usual manner, transferred to an apparatus of known volume, the pressure measured, and the volume of the gas calculated.

Silver.—Four samples of silver foil were used which were, approximately, 0·10, 0·15, 0·30 and 0·15 mm. thick, respectively. The first two samples were of commercially pure silver. Analysis showed them to contain 0·02 per cent. copper, 0·001 per cent. iron, and 0·005 per cent. lead. The presence of tin, bismuth and antimony could not be detected in a 5-gram sample. For the third and fourth samples the same metal was purified by one of the methods of Stas†. The metal was dissolved in nitric acid and the solution diluted with water and allowed to settle. Silver chloride was precipitated from the filtered solution by the addition of hydrochloric acid. The silver chloride was boiled with

* 'Ann. Phys.,' vol. 39, p. 1230 (1912).

† 'Mem. l'Acad. Belg.,' vol. 33, p. 1 (1865).

hydrochloric acid and washed with water until free from acid. It was then reduced to the metal by boiling it with invert sugar and sodium hydroxide. The precipitate was thoroughly washed with hot distilled water and fused to a button in a crucible under borax. The button was cleaned by scrubbing it with sand and was rolled out into a sheet. The purified silver gave, on analysis, 0·004 per cent copper, 0·001 per cent lead, and a trace of iron

Gases.—The nitrogen used was the ordinary commercial variety, supplied in cylinders It was bubbled twice through alkaline pyrogallate to free it from oxygen, dried by bubbling through concentrated sulphuric acid, and stored in the gas reservoir over phosphorus pentoxide.

The oxygen was also the commercial variety It was dried in the same way with sulphuric acid and phosphorus pentoxide.

Experimental Procedure.

Prior to making an experiment, the furnace was raised to a temperature of about 550° C in the case of the Pyrex glass apparatus, or 750° C. with quartz, and the bulb was evacuated continuously for 6 to 8 hours. The silver was allowed to stand *in vacuo* over night, and the next morning the bulb was again pumped out for about an hour.

The tap next to the bulb was then closed, and gas from the reservoir was admitted to the tube and measured as previously described. The gas was then let into the bulb, and after equilibrium had been reached the temperature and pressure were read. A series of observations was made without changing the gas At high temperatures equilibrium was quickly reached, at temperatures around 200° C., however, several days were required for equilibrium.

At the conclusion of the experiment the bulb was again evacuated continuously for several hours, and the gas pumped out was collected and measured, and the volume compared with the volume originally admitted to the bulb. If any discrepancy between the two volumes existed, the results were discarded.

This long-continued pumping out is absolutely essential in order to obtain consistent results The last traces of the gas are only very slowly removed from the silver. This point has, however, been overlooked by the majority of investigators.

Preliminary Results

Some preliminary results were obtained with a simplified form of apparatus. They did not agree very well and several sources of error had to be eliminated.

(1) Originally a quartz, nitrogen filled, mercury thermometer was used. If, however, the temperature of the furnace was not even throughout, this would

only indicate the temperature of one particular place What is really needed for purposes of calculation is the mean temperature of the bulb containing the silver. The mercury thermometer was accordingly replaced by a gas thermometer The bulb of this was made the same size and shape as the bulb containing the silver and was placed next to it In this way the gas thermometer automatically compensated for any irregularity in the temperature of the bulb containing the silver.

(2) During preliminary experiments the tap between the silver bulb and the short arm of the manometer was left open. It was found that there was a slow steady drop in pressure amounting to about 1 mm. per day The only possible cause of this appeared to be oxidation of the mercury. This idea was supported by the fact that there was a small reddish-brown deposit on the walls of the capillary tube just outside the furnace

A blank experiment was tried with an empty bulb at 500° C., and it was found that about 0·1 c c of gas disappeared in 10 days, but no oxidation was detectable if the bulb was kept at room temperature The drop in pressure is apparently due to the oxidation of mercury vapour in the bulb The oxide then distils out and condenses in the colder part of the apparatus, more mercury vapour diffuses in and the process goes on continuously. By keeping the tap between the bulb and the mercury surface closed between readings, the difficulty was overcome and no further drop in pressure was noticed.

(3) A further difficulty was met with in connection with the use of tap grease on the tap mentioned above Blank experiments showed a slow but appreciable absorption of oxygen by the ordinary type of grease, consisting of rubber, paraffin, and vaseline A mixture of paraffin and vaseline did not absorb oxygen and gave satisfactory results.

Sample Calculation

In order to illustrate how the calculations were carried out, the complete data of one experiment are given below

Table I

Volume of gas (N T P) 2 985 c.c.
K 0 8307
Volume of gas pumped out 2 981 c c.

Room temp	Press. obs	T° C	T° K	Press. calc	Press diff	C.c. abs	Vols. abs.
24 0° C.	76 56	473	746	81·74	5·18	0·188	0·097

The volume of gas admitted to the bulb was 2·985 c.c. under standard conditions, or 3·247 c.c. at room temperature. The total volume of the bulb and dead space was 5 222 c c Hence the pressure exerted by the above amount of gas at room temperature would be $\frac{3\cdot247 \times 76}{5\cdot222} = 47\cdot25$ cms.

Here we have a volume of gas which is all at the same pressure, but the different parts of which are at different temperatures Now from the gas laws,

$$\Sigma \frac{PV}{T} = \Sigma \frac{P_1 V_1}{T_1} = K,$$

or

$$P\left(\frac{\text{Vol. of bulb}}{\text{Temp. of bulb}} + \frac{\text{Vol of dead space}}{\text{Temp. of dead space}}\right) = K$$

This equation will hold for any mass of gas in the apparatus Inserting the actual values in this case, we have, at 24° C,

$$47\ 25\left(\frac{3\cdot668}{297} + \frac{1\ 554}{297}\right) = K,$$

whence K = 0·8307.

According to the table, when the room temperature was 24° C and the temperature of the furnace was 473° C, the observed pressure was 76 56 cms. If there were no absorption the pressure would be given by

$$P\left(\frac{3\cdot668}{746} + \frac{1\cdot554}{297}\right) = 0\cdot8307,$$

hence P = 81·74 cms. This is 5·18 cms. higher than the observed pressure. Hence an amount of gas has been absorbed which would be sufficient to exert a pressure of 5·18 cms. in the apparatus when the temperature of the bulb is 473° C and the temperature of the dead space is 24° C Bringing this to N.T.P., we have,

(1) For the gas in the bulb (at 746° abs.)—

$$\frac{5\cdot18 \times 3\cdot668 \times 273}{76 \times 746} = 0\cdot091 \text{ c c.}$$

(2) For the gas in the dead space (at 297° abs.)

$$\frac{5\cdot18 \times 1\ 554 \times 273}{76 \times 297} = 0\cdot097 \text{ c.c.}$$

Total volume of gas absorbed = 0·188 c.c.

The weight of silver in the bulb was 20·315 grams. Taking the density of

silver to be 10·5, this is equivalent to 1·93 c c of silver Hence the number of c.c of gas absorbed by 1 c c of silver under the conditions of the experiment is 0·097. That is, 0 097 volumes of gas at N T.P are absorbed by one volume of silver at 746° abs and a pressure of 76·56 cms. of mercury

Experimental Results.

No apparent change took place in the silver used in the experiments except the development of a somewhat crystalline appearance on the surface due to evaporation The Pyrex bulbs turned a dark brown colour, apparently due to the presence of colloidal silver in the glass The quartz bulbs developed a milky appearance.

Owing to the large number of observations which were made, only the smoothed curve values are given in the following tables of solubilities The results for one series of observations on the rate of solution are given in full The maximum divergence of any observation from the smoothed curve was about 5 per cent

The results are discussed in the next section

(A) *Solubility of Nitrogen* —No measurable absorption of nitrogen by silver was found between 200° and 800° C If any absorption takes place, it is certainly less than 0·002 volumes of gas per volume of silver This is to be expected, as it has been found by a large number of observers that nitrogen is not absorbed by metals except in cases where a well-defined nitride is formed

(B) *Solubility of Oxygen* —

Table II.

Pressure (cm.)	T_1 = 200° C		T_2 = 300° C		T_3 = 400° C		T_4 = 500° C		T_5 = 600° C		T_6 = 700° C		T_7 = 800° C	
	vols	$\sqrt{P}/Q$	vols	$\sqrt{P}/Q$	vols	$\sqrt{P}/Q$	vols	$\sqrt{P}/Q$	vols	$\sqrt{P}/Q$	vols.	$\sqrt{P}/Q$	vols.	$\sqrt{P}/Q$
5	0·030	74 5	0 021	106 5	0 020	112·0	0 022	102 0	0 033	68 0	0 048	46 7	0 068	25 5
10	0·050	63 4	0·032	90 8	0·031	102 3	0 034	93 2	0 047	67 5	0 068	46 6	0·124	25 6
20	0 071	63·3	0 045	91·0	0 044	102·3	0 048	93 4	0 066	67·9	0 096	46·7	0·175	25 6
40	0 100	63 5	0 070	90 5	0 061	103 9	0 067	94 5	0·093	68 1	0 134	46 3	0 247	25·7
80	0 142	63 2	0·097	91 7	0 087	103 0	0 095	94 3	0 132	67·9	0 193	46 5	0·354	25 3

(C) *Rate of Solution of Oxygen.*—

Table III

Initial Pressure	33 64	7 55	13·94	31 34	39 55	55 18	57 52
Temperature	280° C	310° C	310° C	310° C	310° C	310° C	310° C
Time mins.	Volumes Absorbed.						
½	0 008	0 0020	0 003	0 004	0 007	0·014	0 015
1	0 011	0 0038	0 006	0 013	0 017	0 024	0 025
2	0 017	0 0055	0 009	0 018	0 026	0 035	0 035
3	0 020	0·0065	0·011	0 024	0 032	0 039	0 041
4	0 021	0 0075	0 013	0·028	0 038	0 045	0 046
5	0 027	0 0080	0·014	0 031	0 042	0 047	0 051
6	0·031	0 0088	0 016	0 034	0 045	0 051	0 056
8	0 034	0 0100	0 018	0 037	0 051	0 058	0 063
10	0·040	0 0110	0·020	0·041	0 055	0 064	0 067
12	0·042	0 0120	0 022	0 0425	0 059	0 069	0 073
15	0 045	0 0135	0 024	0 0465	0 062	0 072	0 078
18	0 050	0 0145	0 026	0·050	0 065	0 075	0·080
21	0 053	0 0155	0 027	0 052	0 067	0·076	0·082
25	0 057	0 0170	0 0285	0 0535	0·071	0·078	0 084
Final	0 068	0 0225	0 034	0 058	0 075	0 081	0·087
K (mean)	0 025	0 0195	0 028	0 042	0 047	0 057	0·058
C	0 10	0·10	0 10	0 10	0 10	0 10	0 10
$\sqrt{P}/K$	232	140	133	133	134	130	131

Discussion of Results.

The values obtained for the solubility of oxygen in silver are given in Table II for various temperatures and pressures. From the constancy of $\sqrt{P}$ / Q (where P is the pressure and Q the absorption), it is apparent that the solubility is proportional to the square root of the pressure. There is, however, a deviation from this relationship at the lowest pressures, the amount absorbed being too small. This deviation is not noticeable at the higher temperatures The absorption has been found to be proportional to the square root of the pressure in several other cases, for example, the absorption of hydrogen by tantalum,* copper,† iron,‡ and nickel,§ and for the absorption of sulphur dioxide by copper.‖

The variation of solubility with temperature is shown in fig. 2. The solubility

* Sieverts and Bergner, 'Ber.,' vol 44, p. 2394 (1911).
† Sieverts and Krumbhaar, 'Ber ,' vol. 43, p. 893 (1910).
‡ Sieverts and Krumbhaar, 'Ber.,' vol. 43, p. 893 (1910).
§ Sieverts and Hagenacker, 'Z. physik. Chem.,' vol. 68, p. 115 (1910).
‖ Pease, 'J. Am. Chem. Soc.,' vol. 45, p. 2296 (1923).

is a minimum in the neighbourhood of 400° C. On account of the extreme slowness of the process of diffusion at low temperatures, it was not practicable

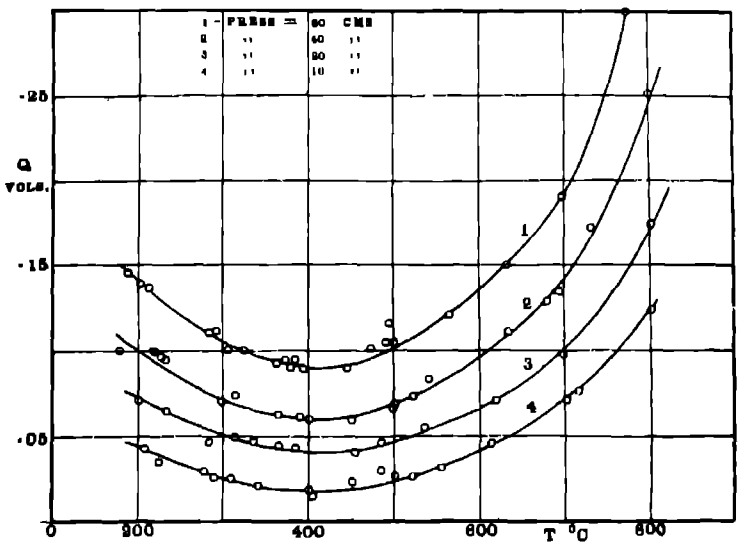

FIG. 2.—Curves showing the Variation of Solubility with Temperature.

to make any measurements below 200° C., but from the form of the curve it appears probable that the solubility is considerably greater at room temperature than it is at 200° C

Above 400° C. the equation

$$1/Q = K\,(930 - t),$$

where Q is the absorption and t is the temperature in degrees Centigrade, fitted the experimental results quite accurately. The melting point of silver is 960° C., but this is lowered by the dissolved oxygen. Hence, it may be said that above 400° C. the reciprocal of the solubility is approximately proportional to the distance below the melting point. Molten silver dissolves about 20 volumes of oxygen at the melting point It seems probable that there is no very abrupt change in solubility on melting, but that the solubility curve is merely very steep in the neighbourhood of the melting point.

As previously mentioned, four samples of silver of various thicknesses were used. No difference in solubility was detected due to the difference in thickness

or surface, hence adsorption is apparently negligible at the temperatures employed.

As the solubility was the same for the highly purified and the commercially pure silver, small traces of impurities such as copper and iron have no measurable effect

Rate of Solution.—Some of the experimental results for the rate of solution of oxygen in silver are given in Table III. All these experiments were made with a piece of silver foil 0 15 mm. thick. Some sample absorption-time curves are given in fig. 3.

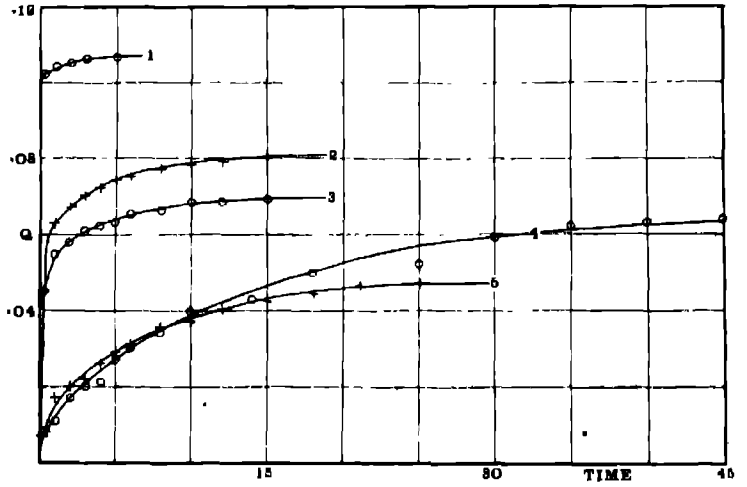

Fig 3.—Absorption-Time Curves.

No 1.—600° C, 31 38 cm No 2.—508° C., 65 85 cm. No 3.—560° C., 31·24 cm. No. 4.—280° C., 33 64 cm. No. 5.—400° C., 32·18 cm.

In order to derive an equation for the rate of solution, consider a block of silver placed in an atmosphere of oxygen. Assume that the surface layer of the silver is immediately saturated with the gas in the dissociated condition. The process of solution will consist of diffusion of the gas from this saturated layer into the body of the metal. As the gas diffuses inwards from the surface layer, more gas will dissolve in it so as to keep it saturated. Let S be the saturation concentration, and X be the average concentration of gas in the body of the silver. Then, according to Fick's Diffusion Law, the rate of diffusion

inwards will be proportional to the concentration gradient, that is to S − X Hence

$$\frac{dx}{dt} = K(S - X).$$

Integrating and evaluating the constant of integration by putting X = 0 when $t = 0$, we obtain

$$K = \frac{1}{t} \log \frac{S}{S - X}.$$

As may be seen from figs 4, 5 and 6, log S/S − X plotted against t gives a

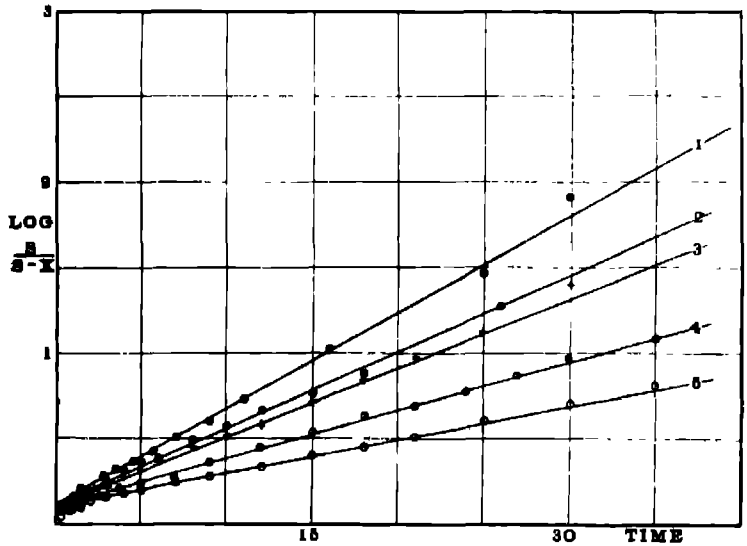

Fig 4.—Variation of Solution Velocity with Pressure at 310° C.

No 1.—57·52 cm No 2.—39 55 cm No 3.—31 34 cm. No. 4.—13 94 cm. No 5.—7 55 cm

straight line. The first two or three points, however, generally lie below the line, and the line does not pass through the origin, as the foregoing equation would require Apparently the first part of the gas is absorbed much faster than the equation would indicate. The process evidently consists of two stages. If we neglect the first two or three points on the curve, and take into account the fact that the line does not pass through the origin, we obtain a corrected equation of the form

$$K = \frac{1}{t}\left(\log \frac{S}{S - X} - C\right),$$

where K is a constant depending on the temperature and pressure and C varies with the temperature but is independent of the pressure. This equation has been found to give good agreement with the experimental results.

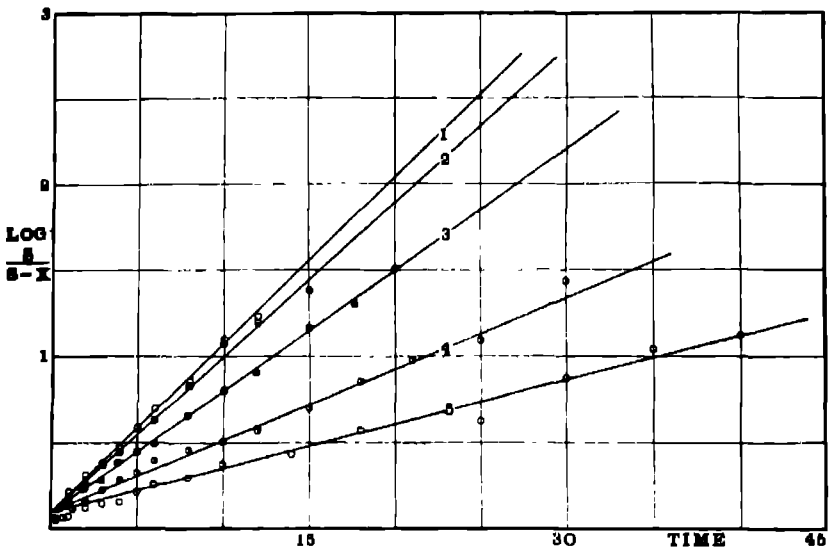

FIG 5.—Variation of Solution Velocity with Temperature at a Pressure of 30 cm. (Part I).
No. 1 —390° C. No 2.—375° C. No 3.—337° C No. 4 —310° C No. 5 —280° C

In fig 4 log $S/S - X$ is plotted against time for various pressures at 310° C. All the lines cut the axis at the same point, showing that C in the solution velocity equation does not change with pressure K, that is, the slope of the line, is proportional to the square root of the pressure, as may be seen from Table III. This is to be expected, diffusion is the predominating factor in the process of solution, and Johnson and Larose* have shown that the rate of diffusion of oxygen through silver is proportional to the square root of the pressure

The effect of temperature on the velocity of solution is shown in figs. 5 and 6. At temperatures below 400° C. (that is, below the position of the minimum in the solubility-temperature curve), the value of C in the equation remains constant at 0·10, while K increases as the temperature is raised. Between 400° and 440° C, C increases rapidly while K decreases. Above this temperature C

* 'J.A.C.S.,' vol. 46, p. 1377 (1924).

continues to increase as the temperature is raised, and K increases slowly and regularly. The peculiar behaviour of the solution velocity in the neighbourhood of 400° C. makes it impossible to obtain any simple expression for the effect of

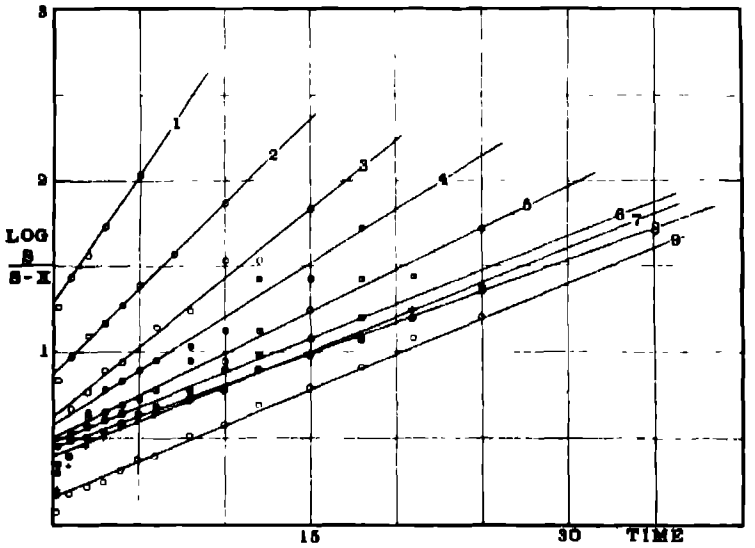

Fig. 6.—Variation of Solution Velocity with Temperature at a Pressure of 30 cm (Part II).

No 1 —690° C No 2 —605° C No. 3 —560° C No 4 —508° C No. 5 —465° C.
No 6 —450° C No 7 —430° C No 8 —440° C. No 9 —400° C

temperature The temperature coefficient is low, however, as would be expected in a process in which diffusion is the controlling factor

General Discussion.

As pointed out by Donnan and Shaw,* the variation of the solubility with the square root of the pressure shows definitely that a dissociation of the oxygen takes place on solution. The actual condition of the oxygen after the dissociation has taken place cannot be definitely established. The two most likely possibilities are the solution of the oxygen in the atomic state, or as Ag_2O. At the temperatures investigated Ag_2O would be in existence at oxygen pressures far below its dissociation pressure. It is possible, however, that Ag_2O would be stable, even under these conditions, when in dilute solution.

* 'J. Soc. Chem. Ind.,' vol. 29, p. 987 (1910).

The explanation of the minimum in the solubility-temperature curve is difficult. The fact that a sudden change occurs in the rate of solution at this temperature seems to point to a transition of the silver from one allotropic form to another. It is interesting to note in this connection that Holt* was obliged to assume two forms of the metal in order to explain his results on the rate of solution of hydrogen in palladium.

There is also the possibility of a change in the manner of combination of the oxygen. From the shape of the solubility-temperature curve, the heat of solution is obviously positive at the lower temperatures, zero at about 400° C., and negative at higher temperatures. The heat of formation of Ag_2O, calculated from the measurements of Lewis,† is positive, while the heat of dissociation of oxygen is negative. It is therefore possible that at low temperatures the majority of the dissolved oxygen exists as Ag_2O, while at temperatures above 400° C. it is mostly atomic oxygen.

Solution and Diffusion.—The phenomena of absorption of gases by metals and diffusion of gases through metals must be fundamentally connected. It is virtually impossible to conceive of a mechanism for diffusion other than that of solution on the high-pressure side of the metal and subsequent giving up of the gas on the low-pressure side which is supersaturated. Apparently, then, solution must precede diffusion. This conclusion is substantiated by the fact that there is no known case of a gas diffusing through a metal in which it is not appreciably soluble.

In the case of oxygen and silver, the solubility and the rate of diffusion are both proportional to the square root of the pressure. Hence, both phenomena point to a dissociation of the gas.

If we assume that diffusion is due to solution, we can calculate the actual distribution of oxygen in a silver plate through which the gas is diffusing into a vacuum. Consider a plate of silver of unit cross-section and thickness T, through which oxygen is diffusing from one side on which the pressure is P to the other side which is kept at zero pressure. Let the concentration of gas dissolved in the metal be C_b at the high-pressure side, and C_x at any distance x in from this side. The number of c.c. of oxygen diffusing through per second, Q, is given by

$$Q = \frac{k\sqrt{P}}{T} \qquad (1)$$

* 'Roy. Soc. Proc.,' A, vol. 90, p. 226 (1914).
† 'Z. physik. Chem.,' vol. 55, p. 465 (1906).

The amount of oxygen dissolved in the surface layer, C_0, will be given by

$$C_0 = k_1 \sqrt{P},$$

since the solubility is proportional to the square root of the pressure. Substituting for P in equation (1), we obtain

$$Q = \frac{KC_0}{T}. \qquad (2)$$

This amount of gas must cross any plane in the metal per second.

The amount of gas diffusing towards the low-pressure side at x is given by an expression similar to (2),

$$Q_x = \frac{KC_x}{T - x}$$

But the total amount of gas crossing any plane in the metal per second is the same, hence $Q_x = Q$, so that

$$\frac{KC_0}{T} = \frac{KC_x}{T - x},$$

whence

$$C_x = \frac{(T - x)}{T} C_0$$

This gives the concentration of oxygen at any point in the plate.

We can also calculate the average velocity of the oxygen atoms through the plate. If S be the quantity of oxygen dissolved in a plate of thickness T and unit cross-section, and if Q be the rate of diffusion through the plate, then the average velocity of the gas through the plate will be QT/S. For a plate 1 mm. thick at 500° C., with a pressure of 76 cms., we have $S = 0{\cdot}0104$, $T = 0{\cdot}1$, $Q = 2{\cdot}2 \times 10^{-7}$ c.c. per second. Hence

$$\text{Velocity} = \frac{2{\cdot}2 \times 10^{-7} \times 0{\cdot}1}{0{\cdot}0104} \text{ cms. per sec}$$

$$= 2\ 2 \times 10^{-6} \text{ cms per sec}$$

This is extremely small compared with the probable mean displacement of an oxygen molecule in oxygen.

Since the solubility is a minimum at 400° C., and there is also a sudden change in the rate of solution at this temperature, it is probable that the rate of diffusion would also undergo an abrupt change below this temperature. Unfortunately, no measurements of the rate of diffusion below 400° C. have yet been made. The authors hope to investigate in the future the rate of diffusion of oxygen

through silver at low temperatures, and also the rate of diffusion, rate of solution, and solubility for hydrogen and silver

Summary

The solubility of oxygen in silver has been measured over a wide range of temperature and pressure. The solubility is proportional to the square root of the pressure. The solubility-temperature curve has a minimum at 400° C. Above this temperature the solubility is expressed by $1/Q = K(930 - t)$, where Q is the solubility and t is the temperature in ° C.

The rate of solution of oxygen in silver has also been measured. The equation $K = 1/t\ (\log (S/S - X) - C)$ has been found to express the experimental results, where S is the saturation concentration, X is the amount dissolved at time t, and K and C are constants The rate of solution is proportional to the square root of the pressure. The variation with temperature is complicated and suggests a transition of the silver, or a change in the manner of combination of the oxygen in the vicinity of 400° C

By comparison with diffusion measurements, the concentration gradient of the oxygen in a silver plate through which the gas is diffusing has been calculated

Nitrogen has been shown to be insoluble in silver

Acknowledgment is made of the receipt by one of us of a Studentship from the National Research Council of Canada, during the tenure of which part of this work was performed.

The Flexure of Thick Circular Plates *

By C A Clemmow, B A , B Sc , Research Department, Woolwich

(Communicated by Prof A E H Love, F R S —Received December 2, 1925)

Introduction

(1) *The Genesis and Objects of the Investigation*

The investigation undertaken in this paper arose out of a suggestion that the deflexion of a circular steel plate, firmly held at the edge, might be used as a measure of high explosive pressures The plate would be securely screwed into, and form the base of, a cylindrical closed vessel of the usual type, and the measurement made would be that of the normal central deflexion of its external flat surface

These deflexions, which are, of course, necessarily small, can be suitably magnified by optical means, and thus a pressure-time curve of the explosion would be obtained in the usual way.

Originally, it was taken for granted that the bending of the plate would depend on the pressure in the manner indicated in the standard text-books on elasticity and engineering (*vide* Love, 'Elasticity,' chap XXII), so that the usually accepted formulæ for a *clamped* plate would apply to the case under consideration.

This being so, it would be possible to obtain some idea of the orders of magnitude of the deflexions to be obtained with a thick plate when subjected to high pressures, of the order of several tons per square inch, a point of great importance when considering methods of measuring such deflexions.

It was felt, however, that further investigation was needed for two reasons, firstly, because the plates to be used would be very thick, the ratio of thickness to diameter being one-fifth or more, and, secondly, because of the doubt as to what boundary conditions would apply at the circular edge, as these plates would have to be turned out of solid metal

As regards the thickness of the plate, this has been tacitly assumed in the past to be of slight importance, at any rate within limits, so that, in the classical treatment of the problem, the assumption is made that the forces applied to the edge of the plate, considered as a cylindrical surface, can be expressed adequately by a line distribution of force and a line distribution of flexural couple, both

* The writer is indebted to the Director of Artillery, War Office, for permission to publish the paper.

being reckoned per unit length of the edge line, which is the curve in which the middle plane of the plate cuts the edge surface (*vide* Love, 'Elasticity,' 2nd edn, p 453)

Such an assumption is valid only when the plate is thin, for then "the actual distribution of the tractions applied to the edge, regarded as a cylindrical surface, is of no practical importance" (Love, *loc cit*, p 438). The question of the boundary conditions at the edge is also of fundamental importance It is impossible, with thick plates, to fix the edge by "clamping," and so, for experimental purposes, the plates were turned out of a block of metal, leaving them with a heavy flange, this method being necessary to permit of calibration.

The boundary conditions in such a case cannot be specified beforehand, and the problem has thus to be approached indirectly by postulating various boundary conditions at the circular edge and investigating their consequences analytically

Experimental work carried out on thick plates of the type described has given remarkable results, the deflexions obtained greatly exceeding the expected values Practical considerations have thus shown the necessity for a re-examination of the subject from a theoretical standpoint, and they constitute the apology for the present paper So far as is possible the results have been expressed arithmetically to render them of practical use, and the investigations have been confined to the case of circular plates as the type obviously meant for use in experiment.

It may be noticed that the ordinarily accepted formulæ fail also for very thin plates, *i.e.* plates for which the thickness-diameter ratio is of the order of $\frac{1}{100}$ or less Experimentally it has been found that the deflexions obtained are markedly less than those indicated by the usual theory. An investigation is in progress to try to account for the discrepancies observed, but the matter will not be dealt with in this paper.*

(2) *The Statement of the Problem*

The plate is taken to be a right circular cylinder in elastic equilibrium under tractions applied to its flat ends, being held so that there is no displacement at

* The case of thin plates is peculiar in that deflexions greater than the thickness can be obtained without the plate suffering overstrain, and so the theory that treats the displacements as infinitesimal, compared with the plate dimensions, must obviously be wrong. For a very thin plate the flexural rigidity can almost be neglected entirely, and the plate treated as a membrane reacting by tension alone In intermediate cases, both flexural rigidity and tension have to be taken into account, and the problem becomes complicated. These matters have been discussed in a paper by J. Prescott ("Elastic Plate under Normal Pressure," 'Phil. Mag,' (ser. 6), vol. 43, pp. 97–125 (1922)).

any point of its cylindrical edge, body forces being neglected. The problem is to determine completely the stress-strain system throughout the plate in cases where the tractions on the plane ends are such as can be applied experimentally. We thus confine ourselves to cases where the plate is subjected to uniform pressures over one of the flat surfaces or to loads concentrated over small areas at the centre, or acting solely at the centre of the plate So far as is known, this problem, in its complete generality, has not yet been solved, and apparently cannot be solved by the methods of this paper, and so, analytical solutions have been obtained partially fulfilling the conditions at the edge, and possibly adapted to various practical methods of fixing the edge.

In particular, an attempt is made to obtain solutions which give results in accord with experiment, so that the paper is limited to certain specific problems of practical interest, and no attempt is made at a general discussion *

(3) *Methods of Solution Employed*

The problem is one of symmetric strain in a right circular cylinder, and solutions of the fundamental equations of elastic equilibrium applicable to this case are well known (*vide* Love, 'Elasticity,' 2nd edn, p. 263)

Corresponding to any such solution, expressions for the displacements and stresses can be found, and these have to be manipulated to satisfy certain boundary conditions both at the curved edge surface and over the plane ends, and then the stress-strain distribution inside the plate can be calculated

The boundary conditions over the plane ends of the plate are known at once, and the method adopted is to fit the solutions to satisfy these conditions, and then to examine what particular edge conditions can be satisfied

We take Oz to be the axis of the plate, and then, from symmetry, everything is expressed in cylindrical co-ordinates, r, z

The solutions referred to are of three types :—

(i) Rational integral functions of r and z

(ii) Solutions which are exponential in z, and contain Bessel functions of r

(iii) Compound solutions of (i) and (ii).

It will be seen in the sequel that the last type is the most useful. The satisfaction of the boundary conditions over the flat surfaces of the plate, viz, $z = \pm h$, where $2h$ is the thickness, is straightforward in the case of type (i), and is effected in the cases of types (ii) and (iii) by the use of certain Fourier-

* Such a discussion of exact solutions for a general distribution of load is to be found in a paper by J. Dougall ('Trans R.S.E.,' vol. 41, (1904)) He does not discuss the edge conditions.

Bessel expansions It will be shown that solutions (i) and (ii) are of limited application when we try to satisfy the boundary conditions at the circular edge, and it is with the mixed solution (iii) that we shall be chiefly concerned. Nevertheless, it is thought to be of importance to indicate the limitations of the simpler solutions

(4) *The Three Types of Solution.*

In cases of symmetrical strain such as we are considering, the stress components and the displacements can all be expressed in terms of a single function χ as follows —

$$\left.\begin{aligned} \widehat{rr} &= \frac{\partial}{\partial z}\left\{\sigma\nabla^2\chi - \frac{\partial^2\chi}{\partial r^2}\right\}, & \widehat{zz} &= \frac{\partial}{\partial z}\left\{(2-\sigma)\nabla^2\chi - \frac{\partial^2\chi}{\partial z^2}\right\} \\ \widehat{\theta\theta} &= \frac{\partial}{\partial z}\left\{\sigma\nabla^2\chi - \frac{1}{r}\frac{\partial\chi}{\partial r}\right\} & \widehat{rz} &= -\sigma\frac{\partial}{\partial r}(\nabla^2\chi) + \frac{\partial}{\partial r}\left(\frac{\partial^2\chi}{\partial r^2} + \frac{1}{r}\frac{\partial\chi}{\partial r}\right) \end{aligned}\right\} \quad (1)$$

$$\left.\begin{aligned} \overline{U} &= -\frac{1+\sigma}{E}\frac{\partial^2\chi}{\partial r\partial z} \\ w &= \frac{1+\sigma}{E}\left\{(1-2\sigma)\nabla^2\chi + \frac{\partial^2\chi}{\partial r^2} + \frac{1}{r}\frac{\partial\chi}{\partial r}\right\} \end{aligned}\right\}, \quad (2)$$

the usual notation being employed (*vide* Love, 'Elasticity,' 2nd edn, pp. 260–263).

The function χ itself satisfies the equation

$$\nabla^4\chi = 0, \quad (3)$$

and we have also

$$\nabla^4 w = 0, \quad (4)$$

whilst the stress equations of equilibrium are

$$\left.\begin{aligned} \frac{\partial\widehat{rr}}{\partial r} + \frac{\partial\widehat{rz}}{\partial z} + \frac{\widehat{rr} - \widehat{\theta\theta}}{r} &= 0 \\ \frac{\partial\widehat{rz}}{\partial r} + \frac{\partial\widehat{zz}}{\partial z} + \frac{rz}{r} &= 0 \end{aligned}\right\}, \quad (5)$$

Solutions of equations (3) and (4) of the three types referred to above are well known.* and corresponding to any such solution, the complete stress-displacement system can be calculated by equations (1) and (2).

* *Cf* Love, 'Elasticity,' 2nd edn, p 263, where references are given.

The solution of type (i) is constituted by the equations

$$\left.\begin{aligned} w &= \sum_{n=0}^{n=N} (\alpha_n + \beta_n z)\, V_n \\ \frac{1+\sigma}{E}\chi &= \sum_{n=2}^{n=N+2} (A_n + B_n z)\, V_n \end{aligned}\right\}, \tag{6}$$

where V_n is the solid zonal harmonic of degree n

The connection between the sets of constants α, β, A, B are obtained from the second of equations (2), and we find the following —

$$\left.\begin{aligned} &\alpha_0 = -2\ 1A_2 && \beta_1 = -3\ 2B_3 \\ &\alpha_1 = 2(1-2\sigma)\,2B_2 - 3\ 2A_3 - 2B_2 && \beta_2 = -4\ 3B_4 \\ &\alpha_2 = 2(1-2\sigma)\,3B_3 - 4\ 3\,.\,A_4 && \\ &\alpha_n = 2(1-2\sigma)(n+1)B_{n+1} && \beta_n = -(n+2)(n+1)B_{n+2} \\ &\qquad -(n+2)(n+1)A_{n+2} && \end{aligned}\right\}, \tag{7}$$

notice being taken of the fact that, since $V_1 = zV_0$, the term $\beta_0 z V_0$ can be taken up with $\alpha_1 V_1$, so that we drop β_0 and write $\beta_2 z V_0$ as $\beta_2 V_1$.

For the solution of type (ii) we may write

$$\left.\begin{aligned} w &= \Sigma\{(\alpha + \beta z)\cosh kz + (\gamma + \delta z)\sinh kz\}\, J_0(kr) \\ \frac{1+\sigma}{E}\chi &= \Sigma\{(A + Bz)\cosh kz + (C + Dz)\sinh kz\}\, J_0(kr) \end{aligned}\right\}, \tag{8}$$

where the summation includes any finite or an infinite number of terms The relationships between the constants, found as before, are

$$\left.\begin{aligned} &\alpha = 2(1-2\sigma)Dk - Ak^2 && \gamma = 2(1-2\sigma)Bk - Ck^2 \\ &\beta = -Bk^2 && \delta = -Dk^2 \end{aligned}\right\} \tag{9}$$

To get the solutions of type (iii) we merely combine the above solutions, the part of the solution corresponding to type (ii) being necessarily an infinite series, to permit of satisfying the boundary conditions over $z = \pm h$ by the use of Fourier-Bessel analysis.

The solutions corresponding to (8) with k imaginary, leading to circular functions of kz and to the Bessel functions with imaginary argument, viz., $I_0(kr)$, can be shown to be ineffective for the problems we have in view, and there is also a solution of the type

$$w = \Sigma(\alpha' \cosh kz + \beta' \sinh kz)\, rJ_0'(kr),$$

which contains insufficient constants to permit of the stress boundary conditions over $z = \pm h$ being satisfied

The Rational Integral Solution and its Application to the Plate Problem.

(5) *A Specific Problem*

We consider the case of a plate bounded by the surface $r = a$ and the planes $z = \pm h$, subjected to a uniform pressure p over $z = +h$, zero pressure over $z = -h$, and no shear stress over $z = \pm h$, and determine a solution of type (1) which fits these boundary conditions, and then discuss the conditions at $r = a$. The boundary conditions at $z = \pm h$ are $\widehat{rz} = 0$ for $z = \pm h$, $\widehat{zz} = 0$ for $z = -h$, $\widehat{zz} = -p$ for $z = +h$, in each case for all values of r

These conditions, in combination with the second of equations (5), lead to the equations

$$\left.\begin{aligned} \widehat{rz} &= r(h^2 - z^2) f_1(z) \\ \widehat{zz} &= (h + z) f_2(z) \end{aligned}\right\}, \tag{10}$$

where f_1, f_2 are rational integral functions

We take the expressions for w and χ given in equations (6), and the following properties of V_n are used —

$$\left.\begin{aligned} V_n &= z^n - \tfrac{1}{2}\frac{n!}{2!\,(n-2)!} r^2 z^{n-2} + \frac{1}{2}\frac{3}{4}\frac{n!}{4!\,(n-4)!} r^4 z^{n-4} - \ldots \\ \frac{\partial V_n}{\partial z} &= n V_{n-1} \\ r\frac{\partial V_n}{\partial r} &= n(V_n - z V_{n-1}) = -\tfrac{1}{2}\frac{(n-1)!}{(n-2)!} r^2 z^{n-2} + \frac{1}{2}\frac{3}{4}\frac{(n-1)!}{3!\,(n-4)!} r^4 z^{n-4} - \ldots \end{aligned}\right\} \tag{11}$$

The equations (1) then give

$$\begin{aligned} \frac{1+\sigma}{E}\cdot\frac{\widehat{rz}}{r} = &-2\sigma[3.2B_3(-\tfrac{1}{2}) + 4.3B_4(-z) + 5.4B_5(-\tfrac{3}{2}z^2 + \tfrac{3}{8}r^2) + \ldots] \\ &- [4.3.2(A_4 + B_4 z)(-\tfrac{1}{2}) + 5.4.3(A_5 + B_5 z)(-z) \\ &+ 6.5.4(A_6 + B_6 z)(-\tfrac{3}{2}z^2 + \tfrac{3}{8}r^2) + \ldots], \end{aligned} \tag{12}$$

which, by (10), must be a function of z only, and it is easily seen that the terms written down in (12) are all that can occur.

The expression for $\widehat{zz}$ thus becomes

$$\frac{1+\sigma}{E}\,\widehat{zz} = (1-2\sigma)[2B_2+3.2B_3z+4\ 3B_4(z^2-\tfrac{1}{2}r^2)+5\ 4B_5(z^3-\tfrac{1}{2}r^2z)]$$
$$-3.2.1(A_3+B_3z)-4\ 3\ 2(A_4+B_4z)z$$
$$-5\ 4\ 3(A_5+B_5z)(z^2-\tfrac{1}{2}r^2)-6.5.4\ A_6(z^3-\tfrac{3}{2}r^2z) \quad (13)$$

In (12) the terms in r^2z and r^2 must vanish and the remaining terms must be equivalent to a constant multiplier of h^2-z^2, in (13) the terms in r^2z and r^2 must likewise vanish, and $\widehat{zz}$ become equal to $-p$ and zero for $z=\pm h$ respectively

The constants A, B are thus determined as follows —

$$\left.\begin{aligned} (1-2\sigma)B_2-3A_3 &= -\frac{p(1+\sigma)}{4E}, & A_4=B_5=B_6&=0\\ \sigma B_3+2A_4 &= \frac{p(1+\sigma)}{16Eh}, & A_6&=\frac{p(1+\sigma)\sigma}{480Eh^3}\\ B_5 &= -\frac{p(1+\sigma)}{160Eh^3} \end{aligned}\right\}, \quad (14)$$

leaving three arbitrary

The expressions for w and $\overline{U}$ may now be worked out, using equations (2) and (7), and it is found that, by writing the three arbitrary constants in the forms $\alpha=-2A_2$, $\beta=6A_4-3(1-2\sigma)B_3$, $\gamma=3A_3+B_2$, we have finally,

$$w=\left\{\alpha+\beta r^2-\frac{3p(1-\sigma^2)}{128Eh^3}r^4\right\}-\left\{\frac{2\sigma}{1-\sigma}\gamma+\frac{p(1+\sigma)(1-2\sigma)}{2E(1-\sigma)}\right\}z$$
$$+\left\{\frac{2\sigma}{1-\sigma}\beta-\frac{3p(1+\sigma)}{8Eh(1-\sigma)}-\frac{3p\sigma(1+\sigma)}{16Eh^3}r^2\right\}z^2+\frac{p(1+\sigma)^2}{16Eh^3}z^4 \quad (15)$$

$$\overline{U}=\gamma r+\left[\left\{\frac{3p(1+\sigma)}{4Eh}-2\beta\right\}r+\frac{3p(1-\sigma^2)}{32Eh^3}r^3\right]z-\frac{p(1+\sigma)(2-\sigma)}{8Eh^3}rz^2. \quad (16)$$

These expressions constitute the most general values of the displacements, corresponding to the solution of type (i), which are in accordance with the assigned boundary conditions over $z=\pm h$.

(6) *The Known Results for the Clamped and Supported Plates.*

In equations (15) and (16) there are three constants at our choice, and they can only be determined by assigning conditions to be satisfied at the edge

$r = a$. The classical procedure (*vide* Love, 'Elasticity,' chap. XXII) is to consider only the middle surface of the plate, *i. e.* the plane $z = 0$

We denote by w_0 the value of w for $z = 0$, and then, taking as the conditions for a clamped plate, $w_0 = 0$, $dw_0/dr = 0$ for $r = a$, we get from (15)

$$w_0 = -\frac{p(a^2 - r^2)^2}{64D}, \qquad (17)^*$$

where $D = \frac{2}{3}\frac{Eh^3}{1-\sigma^2}$ is known as the "flexural rigidity" of the plate

This result might well apply when the plate is sufficiently thin, and, in fact, is found experimentally to hold in such cases, although it is difficult to determine for what range of values of h/a the equation (17) is valid.

For a thick plate it would appear that the conditions of clamping are not sufficiently represented by making w_0 and dw_0/dr vanish for $r = a$

Further, it should be noticed that the result (17) does not depend in any way on γ, so that the middle plane may either be stretched or unstretched.

Assuming $\gamma = 0$, so that the middle plate is bent without extension, we find easily from (15) and (16)

$$w = w_0 + \frac{pz}{D}\left[\frac{1}{24}\frac{1+\sigma}{1-\sigma}z^3 + \frac{1}{16}\frac{\sigma}{1-\sigma}za^2 - \frac{1}{8}\frac{\sigma}{1-\sigma}zr^2 - \frac{1}{4}\frac{zh^2}{(1-\sigma)^2} - \frac{1}{3}\frac{1-2\sigma}{(1-\sigma)^2}h^3\right],$$

a result given by Love (*loc. cit.*, p. 463)

For the supported plate we assume at $r = a$, $w_0 = 0$ and

$$\int_{-h}^{h} \widehat{rr}\,.\,dz = \int_{-h}^{h} \widehat{rr}\; r dz = 0,$$

i. e. that the integrated radial pull over $r = a$, $h > z > -h$ does not give rise to forces or couples, and the usual result is obtained.

Incidentally we find $\gamma = \frac{1}{E}(\sigma p/E)$, so that the middle plane is stretched.

(7) *Some Further Results.*

The solution of the problem of the uniformly loaded plate comprised in (15) and (16) can be made to satisfy certain other edge conditions.

Thus, suppose $\bar{U} = 0$ for $r = a$, $z = \pm h$, then β and γ are determined, γ being zero, making $w_0 = 0$ for $r = a$, gives α and the result is

$$w_0 = -\frac{pa^4}{64D}\left(1 - \frac{r^2}{a^2}\right)\left(1 - \frac{r^2}{a^2} + \frac{8}{3}\frac{4+\sigma}{1-\sigma}\frac{h^2}{a^2}\right). \qquad (18)$$

* This is generally known to engineers as the Grashof formula, and is quoted as such in works on Strength of Materials, although it was originally worked out by Poisson.

Another case is $\bar{U} = \partial\bar{U}/\partial z = w = 0$ for $r = a$, $z = 0$, which gives $\gamma = 0$ and determines α and β. We find for w_0,

$$w_0 = -\frac{pa^4}{64D}\left(1 - \frac{r^2}{a^2}\right)\left(1 - \frac{r^2}{a^2} + \frac{10}{1-\sigma}\frac{h^2}{a^2}\right) \tag{19}$$

These boundary conditions may not be practicable, but we quote these results for comparison with others to be obtained later.

In each case the normal deflexion of the middle plane is much greater than that given by (17) if h/a be at all large, i.e. for a thick plate

(8) *Remarks on the Solution of Art. 5*

It is to be observed that, with the solution given by equations (15) and (16), we cannot make either w or $\bar{U}$ vanish at every point of $r = a$

By choice of α, β, γ all but the last term in w (equation (15)) can be made zero, and similarly for $\bar{U}$, so that the limitations of the solution in finite terms are manifest and the problem of a thick plate must be investigated by a fresh type of analysis

The solutions given above are thus necessarily approximate, even for thin plates, but it will be shown in the sequel that the results obtained by more elaborate analysis can be expressed in a form similar, for example, to that of (17), with a correction term which is of small consequence when h/a is small.

(9) *The Stresses in a Thin Plate*

Some remarks on the stresses in a clamped or supported *thin* plate may be interposed here before we pass on to the next type of solution. The following results are easily obtained.—

$$\left.\begin{aligned}
\widehat{rr} &= \frac{2E\gamma - \sigma p}{2(1-\sigma)} + \left[\frac{3p}{4h(1-\sigma)} - \frac{2E\beta}{1-\sigma} + \frac{3(3+\sigma)p}{32h^3}r^2\right]z - \frac{(2+\sigma)p}{8h^3}z^3 \\
\widehat{zz} &= -\frac{p}{2} - \frac{3pz}{4h} + \frac{pz^3}{4h^3} \\
\widehat{rz} &= \frac{3pr(h^2 - z^2)}{8h^3} \\
\widehat{\theta\theta} &= \frac{2E\gamma - \sigma p}{2(1-\sigma)} + \left[\frac{3p}{4h(1-\sigma)} - \frac{2E\beta}{1-\sigma} + \frac{3(1+3\sigma)p}{32h^3}r^2\right]z - \frac{(2+\sigma)p}{8h^3}z^3
\end{aligned}\right\} \tag{20}$$

The stress $\widehat{zz}$ is of the order of p only, and the greatest value of $\widehat{rz}$ is of the order of pa/h (viz. at $r = a$, $z = 0$), but $\widehat{rr}$ and $\widehat{\theta\theta}$ will, at the edges $r = a$, $z = \pm h$, contain terms of the order pa^2/h^2.

For a *clamped* plate, $\beta = pa^2/32D$ and γ, although undetermined, is of the

order of p only, so that the greatest stress is the radial pull at the edges, which is numerically equal to $\frac{1}{16}(pa^2/h^2)$, the value of $\widehat{rr}$ at $r = a$, $z = +h$ being actually the greater, the difference being of the order of p.

The value of $\widehat{\theta\theta}$ at the edges is $3\sigma pa^2/16h^2$.

For a supported plate, we find

$$\widehat{rr} = \left[\frac{3(2+\sigma)p}{40h} - \frac{3(3+\sigma)}{32h^3}p(a^2-r^2)\right]z - \frac{(2+\sigma)pz^3}{8h^3},$$

so that $\widehat{rr}$, for $r = a$, is only of the order of p, and the maximum stress is at the centre of the plate, or rather of its upper and lower surfaces, and is, numerically

$$\frac{3(3+\sigma)pa^2}{32h^2}$$

These results will be compared with those to be obtained later for the case of a plate, definitely thick.

The Solution of the Problem by Infinite Series involving Bessel Functions.

(10) *Discussion of the Methods.*

The solution given by equations (8) can obviously be made to satisfy conditions at $r = a$ more general than those considered in the last section. Thus w can be made to vanish at all points of $r = a$ by choosing k so that $J_0(ka) = 0$, and, therefore, there are possible applications to the thick plate problem We have next to consider the method of satisfying the stress boundary conditions over $z = \pm h$, which involve $\widehat{zz}$ and $\widehat{rz}$ (art 5)

Equations (1) show that, χ being of the form given in equation (8), $\widehat{zz}$ and $\widehat{rz}$ are respectively expressions of the types $\Sigma P(z)\,J_0(k_r)$ and $\Sigma Q(z)\,J_0'(k_r)$, so that, when z is constant, $\widehat{zz}$ takes the form $\Sigma P J_0(k_r)$ and $\widehat{rz}$ the form $\Sigma Q J_1(k_r)$, P and Q being independent of r.

Now it is known that if $f(r)$ is any function which could represent a displacement or a stress in the range 0 to a, then the constants P_n can be so chosen as to satisfy an equation of the form

$$f(r) = \sum_1^\infty P_n J_0(k_n r), \tag{21}$$

where $J_0(k_n a) = 0$, $(n = 1, 2, 3, \ldots)$

If $J_0(k_n a) = 0$ we have also

$$J_1(k_n a) + k_n a J_1'(k_n a) = 0, \tag{22}$$

and this result can be used to determine the constants Q_n in an equation of the form

$$F(r) = \sum_1^\infty Q_n J_1(k_n r). \tag{23}$$

In fact we have (*vide* Gray and Mathews, 'Bessel Functions,' chap VI)

$$\left.\begin{aligned} P_n &= \frac{2}{a^2 J_1^{\,2}(k_n a)} \int_0^a J_0(k_n r) f(r)\, r dr \\ Q_n &= \frac{2}{a^2 J_1^{\,2}(k_n a)} \int_0^a J_1(k_n r) F(r)\, r dr \end{aligned}\right\}. \tag{24}$$

It follows that, if we take an infinite number of terms in the expressions for w and χ, the boundary conditions over $z = \pm h$ can be satisfied provided that the integrals in (24) can be determined for the particular forms of $f(r)$ and $F(r)$ which may arise

To this end, a number of results in Fourier-Bessel analysis are required, which we proceed to detail.

(11) *Collation of Necessary Results in Fourier-Bessel Analysis.*

(*a*) *Results involving the Roots of* $J_0(k_n a) = 0$.—We have the following results, m being a positive integer and $J_0(ka) = 0$ —

$$\left.\begin{aligned} I_m &= \int_0^a J_0(kr)\, r^{2m+1}\, dr \\ &= \frac{a^{2m+2} J_1(ka)}{ka}\left[1 - \frac{4m^2}{(ka)^2} + \frac{4m^2(m-1)^2}{(ka)^4} \right. \\ &\qquad \left. + (-1)^m \frac{4^m \cdot m^2 (m-1)^2 \quad 2^2 \quad 1^2}{(ka)^{2m}}\right] \\ I_m' &= \int_0^a J_1(kr)\, r^{2m}\, dr \\ &= \frac{2ma^{2m+1} J_1(ka)}{k^2 a^2}\left[1 - \frac{4(m-1)^2}{(ka)^2} + \frac{4^2 (m-1)^2 (m-2)^2}{(ka)^4} \cdots \right. \\ &\qquad \left. \cdots + (-1)^{m-1} \frac{4^{m-1}(m-1)^2 \quad 2^2 \quad 1^2}{(ka)^{2m-2}}\right] \end{aligned}\right\}. \tag{25}$$

Now, assuming the equation $r^{2m} - a^{2m} = \sum_1^\infty P_n J_0(k_n r)$, where $J_0(k_n a) = 0$, which is legitimate since both sides vanish for $r = a$, we have, from (24),

$$P_n \frac{a^2}{2} J_1^{\,2}(k_n a) = I_m - \frac{a^{2m+2}}{k_n a} J_1(k_n a),$$

which determines P_n, so that

$$\tfrac{1}{4}\left\{\left(\frac{r}{a}\right)^{2m}-1\right\}=-4m^2\sum_1^\infty\frac{J_0(k_nr)}{k_n^3a^3J_1(k_na)}+4m^2(m-1)^2\sum_1^\infty\frac{J_0(k_nr)}{k_n^5a^5J_1(k_na)}\ \ldots.$$

This equation must be identically true for all values of m, and putting $m=1, 2, 3, \ldots$, and sorting out the various series, we find the following.—

$$\sum_1^\infty\frac{J_0(k_nr)}{k_n^3a^3J_1(k_na)}=\frac{1}{8}\left(1-\frac{r^2}{a^2}\right) \tag{26}$$

$$\sum_1^\infty\frac{J_0(k_nr)}{k_n^5a^5J_1(k_na)}=\frac{1}{128}\left(1-\frac{r^2}{a^2}\right)\left(3-\frac{r^2}{a^2}\right) \tag{27}$$

$$\sum_1^\infty\frac{J_0(k_nr)}{k_n^7a^7J_1(k_na)}=\frac{1}{4608}\left(1-\frac{r^2}{a^2}\right)\left(19-8\frac{r^2}{a^2}+\frac{r^4}{a^4}\right) \tag{28}$$

etc., etc.

Putting $r=0$ in the above, we have

$$\sum_1^\infty\frac{1}{k_n^3a^3J_1(k_na)}=\frac{1}{8},\quad\sum_1^\infty\frac{1}{k_n^5a^5J_1(k_na)}=\frac{3}{128};$$

$$\sum_1^\infty\frac{1}{k_n^7a^7J_1(k_na)}=\frac{19}{4608} \tag{29}$$

Using the equation $r^{2m-1}=\sum_1^\infty Q_nJ_1(k_nr)$, or, alternatively, differentiating the above results term-by-term (which can easily be justified), we find.—

$$\sum_1^\infty\frac{J_1(k_nr)}{k_n^3a^3J_1(k_na)}=\frac{1}{4}\frac{r}{a} \tag{30}$$

$$\sum_1^\infty\frac{J_1(k_nr)}{k_n^4a^4J_1(k_na)}=\frac{1}{16}\frac{r}{a}-\frac{1}{32}\frac{r^3}{a^3} \tag{31}$$

$$\sum_1^\infty\frac{J_1(k_nr)}{k_n^6a^6J_1(k_na)}=\frac{3}{256}\frac{r}{a}-\frac{1}{128}\frac{r^3}{a^3}+\frac{1}{768}\frac{r^5}{a^5} \tag{32}$$

etc, etc,

and, with $r=a$,

$$\sum_1^\infty\frac{1}{k_n^3a^3}=\frac{1}{4},\quad\sum_1^\infty\frac{1}{k_n^4a^4}=\frac{1}{32},\quad\sum_1^\infty\frac{1}{k_n^6a^6}=\frac{1}{192} \tag{33}$$

(*b*) *Results involving the Roots of* $J_1(k_na)=0$ (*excluding the Zero Root*).— To discuss the plate problem when the radial displacement $\bar{U}$ is assumed to vanish at all points of $r=a$ $(h>z>-h)$, it is necessary to use results similar to the above, but involving the roots of $J_1(k_na)=0$.

These are obtained by assumptions of the type $\sum_1^\infty P_nJ_1(k_nr)=r(r^{2m}-a^{2m})$, since $J_1(k_nr)$ vanishes for $r=0$ and $r=a$.

The results required are as follows: —

$$\sum_1^\infty \frac{J_0(k_n r)}{k_n^2 a^2 J_0(k_n a)} = -\frac{1}{8} + \frac{1}{4}\frac{r^2}{a^2} \tag{34}$$

$$\sum_1^\infty \frac{J_0(k_n r)}{k_n^4 a^4 J_0(k_n a)} = -\frac{1}{96} + \frac{1}{32}\frac{r^2}{a^2} - \frac{1}{64}\frac{r^4}{a^4} \tag{35}$$

$$\sum_1^\infty \frac{J_0(k_n r)}{k_n^6 a^6 J_0(k_n a)} = -\frac{7}{9216} + \frac{1}{384}\frac{r^2}{a^2} - \frac{1}{512}\frac{r^4}{a^4} + \frac{1}{2304}\frac{r^6}{a^6} \tag{36}$$

$$\sum_1^\infty \frac{J_1(k_n r)}{k_n^3 a^3 J_0(k_n a)} = -\frac{1}{16}\frac{r}{a} + \frac{1}{16}\frac{r^3}{a^3} \tag{37}$$

$$\sum_1^\infty \frac{J_1(k_n r)}{k_n^5 a^5 J_0(k_n a)} = -\frac{1}{192}\frac{r}{a} + \frac{1}{128}\frac{r^3}{a^3} - \frac{1}{384}\frac{r^5}{a^5} \tag{38}$$

$$\sum_1^\infty \frac{J_1(k_n r)}{k_n^7 a^7 J_0(k_n a)} = -\frac{7}{18432}\frac{r}{a} + \frac{1}{1536}\frac{r^3}{a^3} - \frac{1}{3072}\frac{r^5}{a^5} + \frac{1}{18432}\frac{r^7}{a^7}. \tag{39}$$

Putting $r = 0$ and $r = a$ in equations (34) to (36) we have

$$\left.\begin{aligned} \sum_1^\infty \frac{1}{k_n^2 a^2 J_0(k_n a)} &= -\frac{1}{8} & \sum_1^\infty \frac{1}{k_n^2 a^2} &= \frac{1}{8} \\ \sum_1^\infty \frac{1}{k_n^4 a^4 J_0(k_n a)} &= -\frac{1}{96} & \sum_1^\infty \frac{1}{k_n^4 a^4} &= \frac{1}{192} \\ \sum_1^\infty \frac{1}{k_n^6 a^6 J_0(k_n a)} &= -\frac{7}{9216} & \sum_1^\infty \frac{1}{k_n^6 a^6} &= \frac{1}{3072} \end{aligned}\right\}. \tag{40}$$

(*c*) *Results involving Logarithmic Functions with* $J_0(k_n a) = 0$ —To discuss the case of the bending of a plate when the load is concentrated at the centre, some further results are required.

Consideration of the integral $V_m = \int_0^a J_0(kr)\, r^{2m+1} \log \frac{r}{a}\, dr$ (m a positive integer) on the lines of (*a*) above gives the following .—

$$\sum_1^\infty \frac{J_0(k_n r)}{k_n^2 a^2 J_1^2(k_n a)} = \frac{1}{2}\log\frac{a}{r} \tag{41}$$

$$\sum_1^\infty \frac{J_0(k_n r)}{k_n^4 a^4 J_1^2(k_n a)} = \frac{1}{8}\left(1 - \frac{r^2}{a^2}\right) - \frac{1}{8}\frac{r^2}{a^2}\log\frac{a}{r} \tag{42}$$

etc , etc.

Multiplying by r and then integrating term-by-term, we find

$$\sum_1^\infty \frac{J_1(k_n r)}{k_n^3 a^3 J_1^2(k_n a)} = \frac{1}{8}\frac{r}{a}\left(1 + 2\log\frac{a}{r}\right) \tag{43}$$

$$\sum_1^\infty \frac{J_1(k_n r)}{k_n^5 a^5 J_1^2(k_n a)} = \frac{1}{16}\frac{r}{a}\left(1 - \frac{5}{8}\frac{r^2}{a^2} - \frac{1}{2}\frac{r^2}{a^2}\log\frac{a}{r}\right), \tag{44}$$

this process being legitimate because of the uniform convergence of (41) and (42) in the range 0 to a.

Putting $r = 0$ in (42) gives $\sum_1^\infty \frac{1}{k_n^4 a^4 J_1^2(k_n a)} = \frac{1}{8}$, whilst $r = a$ in (43) and (44), leads to the results (29).

(12) *The Elastic Problem—Reasons for the Choice of Solution of Type* (iii).

From art. (10) it is apparent that, with the solution of type (ii), the boundary conditions over $z = \pm h$ lead to equations of the type $\sum_1^\infty P_n J_0(k_n r) =$ a constant or zero, in the case of a uniformly loaded plate.

If $\sum_1^\infty P_n J_0(k_n r) = A$ say, (24) gives $P_n = \frac{2A}{k_n a J_1(k_n a)}$, but this is equivalent to assuming that $\sum_1^\infty \frac{J_0(k_n r)}{k_n a J_1(k_n a)} = \frac{1}{4}$, a result which is untrue for $r = a$, although it can be shown to hold for $0 \leqq r < a$. It will be necessary, therefore, to use a solution which does not depend on this result for the satisfying of the boundary conditions at $z = \pm h$.

Furthermore, the assumption

$$w = \sum_1^\infty \{(\alpha_n + \beta_n z)\cosh k_n z + (\gamma_n + \delta_n z)\sinh k_n z\} J_0(k_n r)$$

with $J_0(k_n a) = 0$, gives $w = 0$ for every point of the edge surface, but permits of no other edge condition being satisfied, because the series constants α_n, β_n, γ_n, δ_n are completely determined by the stress conditions over $z = \pm h$.

It may be noticed, as a matter of interest, that if this solution be worked out, we arrive at the following result for the deflexion of the middle surface of a *thin* plate (using methods of approximation to be explained later),

$$w_0 = -\frac{pa^4}{64D}\left(1 - \frac{r^2}{a^2}\right)\left(3 - \frac{r^2}{a^2}\right). \tag{45}$$

A result, in partial agreement with this, can be obtained from (15). By choice of α, β, γ, w can be made to vanish at $r = a$, except for the final term, $\frac{p(1+\sigma)^2}{16Eh^2} z^4$, so that w at the edge will vanish for $z = 0$, and attain its greatest numerical value at $z = \pm h$, viz., $\frac{p(1+\sigma)^2 h}{16E}$.

The ratio of this quantity to the central deflexion is $\frac{8(1+\sigma)^2}{1-\sigma^2}\frac{h^4}{a^4}$, so that,

for thin plates, the condition $w = 0$ at all points of $r = a$ is approximately secured. Determining α, β, γ as indicated, we find

$$w_0 = -\frac{pa^4}{64D}\left(1 - \frac{r^2}{a^2}\right)\left[3 - \frac{r^2}{a^2} + \frac{8}{\sigma(1-\sigma)}\frac{h^2}{a^2}\right], \tag{46}$$

which is nearly the same as (45) if h/a be small

It should be noticed that the central deflexion with the sole edge condition $w = 0$ is three times the value for a clamped plate.

(13) *The Solution of Type* (III)—*Expressions for the Displacements and Stresses*

We take as the solution

$$\left.\begin{aligned} w &= \alpha_0' + (\alpha_1' + \beta_1' z)\,V_1 + (\alpha_2' + \beta_2' z)\,V_2 + \ldots \\ &\quad \ldots + \sum_1^\infty \{(\alpha_n + \beta_n z)\cosh k_n z + (\gamma_n + \delta_n z)\sinh k_n z\}\,J_0(k_n r) \\ \frac{1+\sigma}{E}\chi &= (A_2' + B_2' z)\,V_2 + (A_3' + B_3' z)\,V_3 + \\ &\quad \ldots + \sum_1^\infty \{(A_n + B_n z)\cosh k_n z + (C_n + D_n z)\sinh k_n z\}\,J_0(k_n r) \end{aligned}\right\}, \tag{47}$$

where the number of terms in the finite part of w is, at present, undetermined.

The connections between the sets of constants α', β' and A', B' are given by (7), and those between α, β and A, B by (9).

We require for our immediate purpose the values of $\overline{U}$, $\widehat{rz}$ and $\widehat{zz}$, which are determined from the function χ by equations (1) and (2).

We find, using the results of (11),

$$\left.\begin{aligned} r(\overline{U}) &= -2(B_2' + 3A_3' + 3B_3' z)(V_2 - zV_1) \\ &\qquad - 3(B_3' + 4A_4' + 4B_4' z)(V_3 - zV_2) \ldots \\ &\quad + \sum_1^\infty \left[\left(A_n + B_n z + \frac{D_n}{k_n}\right)\sinh k_n z \right. \\ &\qquad \left. + \left(C_n + D_n z + \frac{B_n}{k_n}\right)\cosh k_n z\right] k_n^2 r J_1(k_n r) \end{aligned}\right\}, \tag{48}$$

$$\left.\begin{aligned} \frac{1+\sigma}{E}\,\widehat{zz} &= 2(2-\sigma)[2\,.\,1B_2' + 3\,.\,2B_3'\,.\,V_1 + 4\,.\,3\,.\,B_4' V_2 + \ldots] \\ &\quad -[6B_2' + 3\cdot 2(A_3' + B_3' z) + 3\,.\,2\,(3B_3' + 4A_4' + 4B_4' z)V_1 \\ &\qquad + 4\,.\,3\,(3B_4' + 5A_5' + 5B_5' z)V_2 + \ldots] \\ &\quad - \sum_1^\infty \left[\left\{A_n + B_n z - (1-2\sigma)\frac{D_n}{k_n}\right\}\sinh k_n z \right. \\ &\qquad \left. + \left\{C_n + D_n z - (1-2\sigma)\frac{B_n}{k_n}\right\}\cosh k_n z\right] k_n^2 J_0(k_n r) \end{aligned}\right\} \tag{49}$$

$$\left.\begin{aligned}\frac{1+\sigma}{E}\widehat{rr}, \widehat{rz} = &-2\sigma[3.2B_3'(V_2 - zV_1) + 4.3B_4'(V_3 - zV_2) \\ &\qquad + 5.4B_5'(V_4 - zV_3) + \ldots] \\ &-[4.3.2(A_4' + B_4'z)(V_2 - zV_1) \\ &\qquad + 5.4.3(A_5' + B_5'z)(V_3 - zV_2) + \ldots] \\ &+\sum_1^\infty \left[\left(A_n + B_n z + 2\sigma\frac{D_n}{k_n}\right)\cosh k_n z \right. \\ &\qquad \left. + \left(C_n + D_n z + 2\sigma\frac{B_n}{k_n}\right)\sinh k_n z\right] k_n^3 r J_1(k_n r)\end{aligned}\right\}. \quad (50)$$

(14) *The Problems to be Discussed—the Forms of the Solutions*

It is clear from the above that *both* displacements w and $\bar{U}$ cannot be made to vanish at all points of $r = a$, so that the general problem of art. 2 cannot be solved by this type of analysis.

It is possible to make one displacement zero for $r = a$, $h > z > -h$, and then to choose the constants to make the other vanish for $r = a$ and particular values of z, such conditions constituting approximations to the general case of the fixed edge.

We shall, therefore, discuss the problem of the plate under uniform pressure p over $z = +h$ with the following boundary conditions :—

(*a*) $w = 0$ for $r = a$, $h > z > -h$; $\bar{U} = 0$ for $r = a$, $z = \pm h$,

(*b*) $\bar{U} = 0$ for $r = a$, $h > z > -h$, $w = 0$ for $r = a$, $z = 0$,

and shall refer to them subsequently as problems A and B respectively.

We have first to determine the number of terms required in the finite parts of the solutions in each case, the constants in the infinite series parts being, of course, determined by the stress boundary conditions over $z = \pm h$.

From equations (7) it is seen that the A′, B′ constants are given in terms of the α', β' constants, with the exception of B_2', which is left undetermined.

The constants to be obtained from the edge boundary conditions can, therefore, be regarded as the α', β' constants, plus B_2'. We shall call these the accented constants.

Suppose now that the finite part of w contained terms up to, and including, V_m. Then the total number of accented constants is $2m + 2$.

In virtue of equations (11) the finite parts of $\bar{U}$ and $\widehat{rz}$ can be expressed as series of odd powers of r, and the finite part of $\widehat{zz}$ as a series of even powers (including a term independent of r), the coefficients involving z.

To satisfy the boundary conditions of problem A we must have $J_0(k_n a) = 0$, and, as the finite part of w must also vanish for $r = a$ and all values of z, we have $m + 2$ relations between the accented constants, since the highest power of z occurring is z^{m+1}.

The $\widehat{zz}$ conditions at $z = \pm h$ give two relations between the constants, and the $\overline{U}$ conditions two more, making $m + 6$ in all

In the case of problem B, the vanishing of $\overline{U}$ at $r = a$ requires $J_1(k_n a) = 0$, and the vanishing of the finite part for $r = a$. The highest power of z occurring therein is easily seen to be z^m, so we have $m + 1$ equations between the accented constants The finite part of $\widehat{rz}$ must vanish for $r = a$, $z = \pm h$, and this gives two relations between the constants, and, in applying the results of (34) and (35) to satisfy the zz conditions at $z = \pm h$, we obtain two more Finally, the condition $w = 0$ at $r = a$, $z = 0$ provides a further equation, so that, as before, we have altogether $m + 6$ relations between the accented constants

To solve each problem, then, we must take $m = 4$.

It is clear that, by taking more terms, *i.e* increasing m, w could be made to satisfy further conditions at $r = a$ in problem B, but the solutions become very lengthy, and, in any case, the main object in solving this particular problem is to indicate the effect, on the flexure of the plate, of assuming zero radial displacement

Making w vanish at $r = a$, $z = 0$ will lead to a comparatively simple solution.*

(15) *Problem A—Calculation of the Constants and the Stress-Displacement System.*

By the argument of the preceding article it is seen that the finite part of w can be written (the V functions being obtained from (11))

$$w = \alpha_0' + (\alpha_1' + \beta_1' z)\, z + (\alpha_2' + \beta_2' z)(z^2 - \tfrac{1}{2} r^2) + (\alpha_3' + \beta_3' z)(z^3 - \tfrac{3}{2} r^2 z) + (\alpha_4' + \beta_4' z)(z^4 - 3r^2 z^2 + \tfrac{3}{8} r^4).$$

This must vanish for $r = a$ and all values of z, giving six equations between nine unknowns. Equations (7) determine all the A′, B′ constants in terms of these, except B_1', so that there are four undetermined constants, which we choose to be α_2', α_3', α_4', and B_2'.

Omitting the algebra, the finite part of w becomes

$$w = (a^2 - r^2)[\tfrac{1}{2}\alpha_2' + \alpha_3' z + \tfrac{3}{2}\alpha_4' z^2 - \tfrac{3}{8}\alpha_4'(a^2 + r^2)]. \qquad (51)$$

* In this connection, remarks in art. 25 should be noticed.

We now calculate $\overline{U}$, $\widehat{zz}$ and $\widehat{rz}$, as given in art 13, and the results are as follows, the constants A_n, B_n, C_n, D_n being replaced in terms of α_n, β_n, γ_n, δ_n as shown in equations (9) :—

$$\left.\begin{aligned}\overline{U} = {} & [2(1-2\sigma)B_2' - \tfrac{1}{2}\alpha_3' a^2 + (1-2\sigma)\alpha_2' z - 3(1-\sigma)\alpha_4' a^2 z \\ & + (1-2\sigma)(\alpha_3' z^2 + \alpha_4' z^3)]r + \tfrac{1}{2}\sigma(\alpha_3' + 3\alpha_4' z)r^3 \\ & - \sum_1^\infty \Big[\Big\{\alpha_n + \beta_n z + (3-4\sigma)\frac{\delta_n}{k_n}\Big\}\sinh k_n z \\ & + \Big\{\gamma_n + \delta_n z + (3-4\sigma)\frac{\beta_n}{k_n}\Big\}\cosh k_n z\Big] J_1(k_n r)\end{aligned}\right\} \quad (52)$$

$$\left.\begin{aligned}\frac{1+\sigma}{E}\cdot\widehat{zz} = {} & [4\sigma B_2' + \alpha_3' a^2 + 2\sigma\alpha_2' z + 2\sigma\alpha_3' z^2 + 3(1-\sigma)\alpha_4' a^2 z \\ & + 2\sigma\alpha_4' z^3] - (1+\sigma)(\alpha_3' + 3\alpha_4' z)r^2 \\ & + \sum_1^\infty \Big[\Big\{\alpha_n + \beta_n z + (1-2\sigma)\frac{\delta_n}{k_n}\Big\}\sinh k_n z \\ & + \Big\{\gamma_n + \delta_n z + (1-2\sigma)\frac{\beta_n}{k_n}\Big\}\cosh k_n z\Big] k_n J_0(k_n r)\end{aligned}\right\} \quad (53)$$

$$\left.\begin{aligned}\frac{1+\sigma}{E}\widehat{rz} = {} & [-\sigma\alpha_2' - \tfrac{3}{2}(1-\sigma)\alpha_4' a^2 - 2\sigma\alpha_3' z - 3\sigma\alpha_4' z^2]r \\ & + \tfrac{3}{8}(1+\sigma)\alpha_4' r^3 \\ & - \sum_1^\infty \Big[\Big\{\alpha_n + \beta_n z + 2(1-\sigma)\frac{\delta_n}{k_n}\Big\}\cosh k_n z \\ & + \Big\{\gamma_n + \delta_n z + 2(1-\sigma)\frac{\beta_n}{k_n}\Big\}\sinh k_n z\Big] k_n J_1(k_n r).\end{aligned}\right\} \quad (54)$$

We now apply the stress boundary conditions, viz., $\widehat{rz} = 0$ for $z = \pm h$, $\widehat{zz} = 0$ for $z = -h$, $\widehat{zz} = -p$ for $z = +h$, in each case for all values of r.

Putting $r = a$, $z = \pm h$ in (53), the $\widehat{zz}$ conditions give

$$-\frac{1+\sigma}{2E}p = 4\sigma B_2' - \sigma(a^2 - 2h^2)\alpha_3', \quad (55)$$

$$-\frac{1+\sigma}{2E}\frac{p}{h} = 2\sigma\alpha_2' - 2\sigma(3a^2 - h^2)\alpha_4'. \quad (56)$$

Denote by P_n, P_n' the coefficients of $J_0(k_n r)$ in $\widehat{zz}$ with $z = \pm h$, and similarly by Q_n, Q_n', R_n, R_n' the coefficients of $J_1(k_n r)$ in $\widehat{rz}$ and $\overline{U}$ respectively. Then $R_n \pm R_n'$ can be expressed in terms of $P_n \pm P_n'$, $Q_n \pm Q_n'$, and

these latter are obtained from the boundary conditions, by application of the equations (26) (30) and (31), in such forms, as, for example,

$$P_n + P_n' = -\frac{16(1+\sigma)\alpha_3' a^2}{k_n^3 a^3 J_1(k_n a)}.$$

The conditions $\bar{U} = 0$ at $r = a$, $z = \pm h$ then give, after considerable reduction,

$$B_2' = \left[-\frac{1-3\sigma}{8(1-2\sigma)} - \tfrac{1}{2}\frac{h^2}{a^2} + \frac{8(1-\sigma^2)}{1-2\sigma} S_1 - \frac{16\sigma(1-\sigma)}{1-2\sigma} S_2\right]\alpha_3' a^2 \quad (57)$$

$$\alpha_2'\left[16\sigma(1-\sigma)T_2 + (1-2\sigma)\frac{h^2}{a^2}\right] = \alpha_4' a^2\left[48(1-\sigma^2)(T_1 - 2T_3) + 48\sigma(1-\sigma)\left(1-\frac{h^2}{a^2}\right)T_2 + \frac{3(3-7\sigma)}{4}\frac{h^2}{a^2} - (1-2\sigma)\frac{h^4}{a^4}\right], \quad (58)$$

where

$$\left.\begin{aligned} S_1 &= \sum_1^\infty \frac{\sinh 2k_n h}{\sinh 2k_n h + 2k_n h}\frac{1}{k_n^4 a^4}, & S_2 &= \sum_1^\infty \frac{k_n h \cosh^2 k_n h}{\sinh 2k_n h + 2k_n h}\frac{1}{k_n^4 a^4}, \\ T_1 &= \sum_1^\infty \frac{k_n^2 h^2 \sinh 2k_n h}{\sinh 2k_n h - 2k_n h}\frac{1}{k_n^6 a^6}, & T_2 &= \sum_1^\infty \frac{k_n h \sinh^2 k_n h}{\sinh 2k_n h - 2k_n h}\frac{1}{k_n^4 a^4}, \\ & & T_3 &= \sum_1^\infty \frac{k_n h \sinh^2 k_n h}{\sinh 2k_n h - 2k_n h}\frac{1}{k_n^6 a^6} \end{aligned}\right\}. \quad (59)$$

Equations (55) to (58) determine α_2', α_3', α_4' and B_2', and then $P_n \pm P_n'$, $Q_n \pm Q_n'$ are known, so that α_n, β_n, γ_n, δ_n can be found, and the solution is complete.

(16) *The Normal Deflexion of the Central Plane and the Limiting Case of a Thin Plate.*

Equations (47) and (51) give, with $z = 0$,

$$w = (a^2 - r^2)\left[\tfrac{1}{2}\alpha_2' - \tfrac{1}{8}\alpha_4'(a^2 + r^2)\right] + \sum_1^\infty \alpha_n J_0(k_n r),$$

and α_n is known in terms of $P_n - P_n'$ and $Q_n + Q_n'$.

The expression for w ultimately reduces to

$$-w = -\alpha_2'\left[\tfrac{1}{2}(a^2 - r^2) + \frac{8\sigma a^4}{h^4}\{V_r + (1-2\sigma)W_r\}\right] + \alpha_4'\left[\tfrac{1}{8}(a^4 - r^4) + \frac{24\sigma a^4(a^2 - h^2)}{h^4}\{V_r + (1-2\sigma)W_r\} + \frac{48(1+\sigma)a^4}{h^4}\{W_r + (1-2\sigma)X_r\}\right], \quad (60)$$

where

$$\left.\begin{aligned} V_r &= \sum_1^\infty \frac{k_n^3 h^3 \cosh k_n h}{\sinh 2k_n h - 2k_n h} \cdot \frac{J_0(k_n r)}{k_n^5 a^5 J_1(k_n a)}, \\ W_r &= \sum_1^\infty \frac{k_n^2 h^2 \sinh k_n h}{\sinh 2k_n h - 2k_n h} \cdot \frac{J_0(k_n r)}{k_n^5 a^5 J_1(k_n a)} \\ X_r &= \sum_1^\infty \frac{k_n h \cosh k_n h - \sinh k_n h}{\sinh 2k_n h - 2k_n h} \cdot \frac{J_0(k_n r)}{k_n^5 a^5 J_1(k_n a)} \end{aligned}\right\}. \quad (61)$$

The forms of the infinite series in (59) and (61) are chosen so that the limiting values, when $h/a \to 0$, of the multipliers of the Bessel function terms are pure numbers, and thus the limits of the above series can be found from the results of art 11. The formula (60) cannot be simplified, but we can obtain the formula for the deflexion at the centre of the plate ($r = 0$, $z = 0$) in a shape permitting of exact or approximate calculation for any specified value of h/a, and we can also show that (60) becomes the same as (17) in the limit when $h/a \to 0$. To obtain these results it is necessary to determine the constants α_2', α_4' from (56) and (58) in appropriate forms, and to do this we anticipate some results to be obtained later (see art 17).

Thus we write

$$T_1 - 2T_3 = \frac{h^2}{a^2} T_4 = \frac{h^2}{a^2}\left(\frac{1}{64} + \frac{h^2}{a^2} T_4'\right) \quad \text{and} \quad T_2 = \frac{3}{128} + \frac{h^2}{a^2} T_2'. \quad (62)$$

Also, to the order of h^2/a^2, we have

$$V_r = \tfrac{1}{4}\Sigma_5 + \frac{9}{40}\frac{h^2}{a^2}\Sigma_3; \quad W_r = \tfrac{1}{4}\Sigma_5 - \frac{1}{40}\frac{h^2}{a^2}\Sigma_3; \quad X_r = \tfrac{1}{4}\Sigma_5 - \frac{1}{40}\frac{h^2}{a^2}\Sigma_3, \quad (63)$$

where

$$\Sigma_3 = \sum_1^\infty \frac{J_0(k_n r)}{k_n^3 a^3 J_1(k_n a)} = \frac{1}{8}\left(1 - \frac{r^2}{a^2}\right);$$

$$\Sigma_5 = \sum_1^\infty \frac{J_0(k_n r)}{k_n^5 a^5 J_1(k_n a)} = \frac{1}{128}\left(1 - \frac{r^2}{a^2}\right)\left(3 - \frac{r^2}{a^2}\right),$$

by (26) and (27).

The above are approximate only, but with $r = 0$, for exact calculation, we write

$$V_0 = \frac{9}{512} + \frac{h^2}{a^2} V_0'; \quad W_0 = \frac{9}{512} + \frac{h^2}{a^2} W_0'; \quad X_0 = \frac{3}{512} - \frac{h^2}{a^2} X_0', \quad (64)$$

and then, putting $r = 0$ in (60), calculating α_2' and α_4' using the equations (62), and replacing V_0, W_0, X_0 by the expressions in (64), we obtain, finally,

$$-w_0 = \frac{pa^4}{64D}\left[3 - \frac{1+\frac{h^2}{a^2}\left\{\frac{128}{3}T_2' + \frac{16}{3(1-\sigma)}\right\}}{16\sigma(1-\sigma)T_2' - 24(1-\sigma^2)T_4'}\{-1 + 32\sigma V_0' - 32(2\sigma^2+2\sigma+3)W_0' - 96(1+\sigma)(1-2\sigma)X_0'\} + \frac{16}{3\sigma(1-\sigma)}\{1+16\sigma V_0' + 16\sigma(1-2\sigma)W_0'\}\frac{h^2}{a^2}\right], \quad (65)$$

this expression permitting of direct comparison with the usual formula for thin plates. If, further, we replace T_2' and T_4' in (62) by their limiting values, viz $\frac{1}{40}$ and $\frac{1}{120}$ respectively, and use the results of (63), the expression for w in (60) can be reduced in the limit to $-w = \frac{p(a^2-r^2)^2}{64D}$.

(17) *The Numerical Calculation of the Infinite Series involved.*

We propose now to indicate methods of calculation which will give numerical results for thick plates and approximations for plates whose thickness, though small, cannot be neglected.

The numerical values, for specific values of h/a, of the various series can be obtained by direct calculation without undue labour in most cases correct to six or seven decimal places.

In some cases, however, the procedure involves finding a remainder after the calculation of the first few terms, the expressions involving h being replaced by simpler expressions, use being made of the facts that the differences of successive roots of $J_0(x) = 0$ tend to π in the limit, and that when x is moderately large, $J_1(x) = \pm\sqrt{\frac{2}{\pi x}}$ approximately.

For $h/a = \frac{1}{5}$ it is usually sufficient to calculate about ten terms and then to find a remainder; for $h/a = \frac{1}{2}$ fewer terms would be required.

These methods become impossibly laborious for smaller values of h/a, say of the order of 1/10, but suitable approximations can be obtained in such cases by expanding the terms in the series involving h in powers of $k_n h$ and applying the results of art. 11.

Thus, for example, we have

$$\sum_1^\infty \frac{k_n^2 h^2 \sinh 2k_n h}{\sinh 2k_n h - 2k_n h} \frac{1}{k_n^6 a^6} = \frac{3}{2} \sum_1^\infty \left[1 + \frac{7}{15} k_n^2 h^2 + \frac{11}{525} k_n^4 h^4 + \ldots \right] \frac{1}{k_n^6 a^6}$$

$$= \frac{1}{128} + \frac{7}{320} \frac{h^2}{a^2} + \frac{11}{1400} \frac{h^4}{a^4} + \ldots,$$

by equations (33), and it is found that the expression written down is a very close approximation even for values of h/a as large as $\frac{1}{2}$.

The above procedure is not, perhaps, sufficiently rigorous as it stands, but the values of the series can be shown to lie between limits which are pretty close if h/a is not too large

Table I on p. 581 gives results for the series which occur in the discussion of problem A , some of the approximations are not valid for other than small values of h/a, so that the results must be used with discretion

(18) *Numerical Values of the Central Normal Deflexion for a Thick Plate.*

Equation (65) gives the required expression for w at $r = 0$, $z = 0$.

From the results of the last article it is seen that V_0', W_0', X_0' can all be expressed approximately in terms of h/a correct to the order of h^2/a^2, but, unfortunately, T_2' and T_4' cannot, so that only their limiting values are known. Thus a simple expression for w_0 correct to the order of h^2/a^2 cannot be found, but exact results for $h/a = \frac{1}{4}$ and $h/a = \frac{1}{2}$ can be given, and these are important as showing the great divergence between the laws governing the bending of a thick plate and that of a thin clamped plate.

Taking $\sigma = \frac{1}{3}$, equation (65) gives the results,

$$\left.\begin{aligned} &\text{for } h/a = \tfrac{1}{4}, \quad -w_0 = \frac{pa^4}{64D} \times 1{\cdot}3612 \\ &\text{for } h/a = \tfrac{1}{2}, \quad -w_0 = \frac{pa^4}{64D} \times 2\ 2262 \end{aligned}\right\}, \tag{66}$$

whilst with $\sigma = \frac{1}{3}$, the results are

$$\left.\begin{aligned} &\text{for } h/a = \tfrac{1}{4} \quad -w_0 = \frac{pa^4}{64D} \times 1{\cdot}4918 \\ &\text{for } h/a = \tfrac{1}{2} \quad -w_0 = \frac{pa^4}{64D} \times 2{\cdot}9312 \end{aligned}\right\}. \tag{67}$$

The above are outside values of σ, but it is important to notice the marked effect on the deflexion formulæ of variations in σ.

Table I

Series.	Approximation	Correct value $h/a = \frac{1}{2}$.	Approximate value $h/a = \frac{1}{2}$	Correct value $h/a = \frac{1}{4}$	Approximate value $h/a = \frac{1}{4}$.
$S_1 = \sum_1^\infty \frac{\sinh 2k_m h}{\sinh 2k_m h + 2k_m h} \frac{1}{k_m^4 a^4}$	$\frac{1}{64} + \frac{1}{24}\frac{h^2}{a^2}$	0 017714	0 018229	—	—
$S_2 = \sum_1^\infty \frac{k_m h \cosh^2 k_m h}{\sinh 2k_m h + 2k_m h} \frac{1}{k_m^4 a^4}$	$\frac{1}{128} + \frac{1}{24}\frac{h^2}{a^2}$	0 0102985	0 0104167	—	—
$T_1 = \sum_1^\infty \frac{k_m^2 h^2 \sinh 2k_m h}{\sinh 2k_m h - 2k_m h} \frac{1}{k_m^4 a^4}$	$\frac{1}{128} + \frac{7}{320}\frac{h^2}{a^2} + \frac{11}{1400}\frac{h^4}{a^4}$	0 0092062	0 00921038	0 0137394	0 01377232
$T_2 = \sum_1^\infty \frac{k_m h \sinh^2 k_m h}{\sinh 2k_m h - 2k_m h} \frac{1}{k_m^4 a^4}$	$\frac{3}{128} + \frac{1}{40}\frac{h^2}{a^2}$	0 02491075	0 25000	0 02898015	0 0296875
$T_3 = \sum_1^\infty \frac{k_m h \sinh^2 k_m h}{\sinh 2k_m h - 2k_m h} \frac{1}{k_m^6 a^4}$	$\frac{1}{256} + \frac{1}{320}\frac{h^2}{a^2} - \frac{1}{4200}\frac{h^4}{a^4}$	0 00410059	0 00410063	0 00467058	0 0046726
$V_0 = \sum_1^\infty \frac{k_m^2 h^2 \cosh k_m h}{\sinh 2k_m h - 2k_m h} \frac{1}{k_m^2 a^2 J_1(k_m a)}$	$\frac{9}{512} + \frac{9}{320}\frac{h^2}{a^2} - \frac{157}{11200}\frac{h^4}{a^4}$	0 0192812	0 0192812	0 02373002	0 0237333
$W_0 = \sum_1^\infty \frac{k_m^2 h^2 \sinh k_m h}{\sinh 2k_m h - 2k_m h} \frac{1}{k_m^2 a^2 J_1(k_m a)}$	$\frac{9}{512} - \frac{1}{320}\frac{h^2}{a^2} - \frac{17}{11200}\frac{h^4}{a^4}$	0 0173769	0 0173769	0 01670219	0 0167020
$X_0 = \sum_1^\infty \frac{k_m h \cosh k_m h - \sinh k_m h}{\sinh 2k_m h - 2k_m h} \frac{1}{k_m^3 a^3 J_1(k_m a)}$	$\frac{3}{512} - \frac{1}{320}\frac{h^2}{a^2} + \frac{19}{33600}\frac{h^4}{a^4}$	0 0056656	0 0056663	0 00511368	0 00511347

The blanks in the above table must be taken to imply that the approximations are not sufficiently close to be usable

(19) *The Deflexions at the Centres of the Upper and Lower Surfaces of a Thick Plate.*

In experimenting with plates the deflexion can be measured only at the flat surface other than that to which pressure is applied, and so it is important to calculate the value of w at the point $r = 0$, $z = -h$.

It is shown below, however, for a plate in which $h/a = \frac{1}{4}$ or less, that there is little variation between the values of w at the points $r = 0$, $z = 0$, $z = \pm h$. Denoting by w_{+h}, w_{-h} the normal displacements at $r = 0$, $z = \pm h$, we have, naturally, $w_{+h} > w_0 > w_{-h}$.

From (47) and (51) we find $w_{+h} - w_{-h} = 2a^2\alpha_3' h + \sum_1^\infty (\beta_n h \cosh k_n h + \gamma_n \sinh k_n h)$, and β_n, γ_n are known in terms of $P_n + P_n'$ and $Q_n - Q_n'$, whilst α_3' is found from (55) and (57). Replacing the various series that occur by their values as given by (29), or by their approximate values determined as in art. 17, as the case may be, we find the approximate result

$$w_{+h} - w_{-h} = \frac{256\,(1-2\sigma)}{9\left\{1 - 3\sigma - \frac{3}{2}(1-\sigma)^2\,\frac{h^2}{a^2}\right\}}\,\frac{h^6}{a^6}\cdot\frac{pa^4}{64D}. \qquad (68)$$

This shows that the difference between the displacements is of a high order in h/a, and, although only approximate, should give results of the correct order of magnitude.

With $h/a = \frac{1}{4}$ and $\sigma = \frac{1}{4}$ we find $w_{+h} - w_{-h} = \frac{2}{117}\cdot\frac{pa^4}{64D}$, and since the central displacement in this case is $w_0 = \frac{pa^4}{64D} \times 1{\cdot}3612$, the difference between w_{+h} and w_{-h} is only about $1\frac{1}{2}$ per cent of w_0, and so can be neglected for experimental purposes.

(20) *Stress Calculations for the Thick Plate.*

The expressions for $\widehat{zz}$ and $\widehat{rz}$ are given by (53) and (54), and those for the remaining stresses are as follows :—

$$\left.\begin{aligned}\frac{1+\sigma}{E}\widehat{\theta\theta} = {} & 2B_2' - \tfrac{1}{2}\alpha_3' a^2 + \tfrac{1}{2}\sigma\alpha_3' r^2 + (\alpha_2' - 3\alpha_4' a^2 + \tfrac{9}{2}\sigma\alpha_4' r^2)z + \alpha_3' z^2 + \alpha_4' z^3 \\ & - \sum_1^\infty \Big[\Big\{\alpha_n + \beta_n z + (3-2\sigma)\frac{\delta_n}{k_n}\Big\}\sinh k_n z \\ & \qquad + \Big\{\gamma_n + \delta_n z + (3-2\sigma)\frac{\beta_n}{k_n}\Big\}\cosh k_n z\Big] k_n J_0(k_n r) \\ & + \sum_1^\infty \Big[\Big\{\alpha_n + \beta_n z + (3-4\sigma)\frac{\delta_n}{k_n}\Big\}\sinh k_n z \\ & \qquad + \Big\{\gamma_n + \delta_n z + (3-4\sigma)\frac{\beta_n}{k_n}\Big\}\cosh k_n z\Big]\frac{J_1(k_n r)}{r}.\end{aligned}\right\} \qquad (69)$$

$$\left.\begin{aligned}\frac{1+\sigma}{E}\widehat{\theta\theta} = 2B_2' - \tfrac{1}{2}\alpha_2' a^2 - \tfrac{1}{2}\sigma\alpha_3' r^2 + (\alpha_2' - 3\alpha_4' a^2 - \tfrac{1}{2}\sigma\alpha_4' r^2)z + \alpha_3' z^2 + \alpha_4' z^3 \\ - 2\sigma \sum_1^{\infty} (\delta_n \sinh k_n z + \beta_n \cosh k_n z)\, J_0(k_n r) \\ - \sum_1^{\infty} \Big[\Big\{ \alpha_n + \beta_n z + (3-4\sigma)\frac{\delta_n}{k_n} \Big\} \sinh k_n z \\ + \Big\{ \gamma_n + \delta_n z + (3-4\sigma)\frac{\beta_n}{k_n} \Big\} \cosh k_n z \Big] \frac{J_1(k_n r)}{r}.\end{aligned}\right\} \quad (70)$$

With these equations the stresses may be calculated at various points inside and on the boundary of the plate, results of simple form being obtained by using the approximate methods outlined in art 17. Whilst not strictly accurate, they cannot be more than one or two per cent in error provided that h/a does not exceed $\frac{1}{4}$, and they suffice to indicate the distribution of stress throughout the plate Certain of the results require careful examination as they present striking differences from the corresponding stress values deduced from the rational integral solution (see art. 9).

Thus, putting $r = a$ in (69) and (70), and using (52) with $\bar{U} = 0$ for $r = a$, $z = \pm h$, we find

$$\begin{aligned}\frac{1+\sigma}{(1-\sigma)E}(\widehat{rr})_{\substack{r=a \\ z=\pm h}} &= \frac{1+\sigma}{E}(\widehat{rr} + \widehat{\theta\theta})_{\substack{r=a \\ z=\pm h}} \\ &= 4B_2' - (a^2 - 2h^2)\alpha_3' \pm 2h\{\alpha_2' - (3a^2 - h^2)\alpha_4'\} \\ &= -\frac{1+\sigma}{E\sigma}p \text{ or } 0,\end{aligned}$$

by equations (55) and (56).

The stresses $\widehat{rr}$ and $\widehat{\theta\theta}$ are thus of the order of p only at the edge for any value of h/a, whilst with the rational integral solution they can be shown to be of order pa^2/h^2, whichever of the various sets of boundary conditions in arts. 6 and 7 be assumed, in particular the set $\bar{U} = 0$ for $r = a$, $z = \pm h$, $w = 0$ for $r = a$, $z = 0$.

This latter set would appear, at first sight, to tend to the edge conditions of problem A, when $h/a \longrightarrow 0$, but, as the value of $\partial w/\partial z$, which is zero in the latter case, is of order $(p/E)a^2/h^2$ in the former, the two sets of boundary conditions are not effectively the same even for a thin plate

The point has been raised* that the discrepancy may occur because certain of the series have a discontinuity at $r = a$, $z = \pm h$, due to non-uniform

* By one of the referees.

convergence in the range 0 to a. If the terms in $\widehat{rr}$ and $\widehat{\theta\theta}$, with $z = \pm h$, involving $J_0(k_n r)$ are written out in full, we find series of the types

$$\sum_1^\infty f(k_n h) \frac{J_0(k_n r)}{k_n^3 a^3 J_1(k_n a)}, \qquad \sum_1^\infty F(k_n h) \frac{J_0(k_n r)}{k_n^5 a^5 J_1(k_n a)},$$

the functions f and F being of the same general form as already met with in equations (59) and (61), and such series are absolutely and uniformly convergent in the range 0 to a.

An examination of the conditions near the edge, say at $r = a - \epsilon$, shows that the terms in $\widehat{rr}$ and $\widehat{\theta\theta}$ involving $J_0(k_n r)$ contribute an expression which vanishes with ϵ, but becomes large, and of order pa^2/h^2 or higher if ϵ be taken of the order of h/a, so that there is a very rapid variation of stress near the edge if the plate is thin, but no actual discontinuity.

The boundary conditions of problem A do not therefore approximate to any of those previously considered, nor can they be considered as the equivalent of those of problem B when the plate is thin.

The collected results for the stresses are given in tabular form below, those which are valid for any value of h/a being starred, and the remainder must be regarded as accurate only to the order of the lowest power of a/h occurring.

Thus, for example, at $r = 0$, $z = +h$, $\widehat{rr} = -\frac{3p}{32}(1+\sigma)\frac{a^2}{h^2} - \frac{\sigma p}{1-\sigma}$ plus additional terms of the order of ph^2/a^2 which, however, the approximate methods employed do not enable us to obtain.

For thick plates the position and magnitude of the greatest stress will depend on the values of σ and h/a; thus for $\sigma = \frac{1}{4}$ and $h/a = \frac{1}{4}$ it would appear that the numerically greatest stress is $(\widehat{rr})_{\substack{r=a \\ z=+h}} = -3p$, whilst for $\sigma = \frac{1}{4}$ it is $(\widehat{rr})_{\substack{r=0 \\ z=+h}} = -\frac{5p}{2}$

In the case of definitely thick plates the variation of stress near the edge complicates the question too much for a definite answer to be given.

Table II.

Stress	$r=0, z=0$	$r=0, z=+h$	$r=0, z=-h$	$r=a, z=0$	$r=a, z=+h$	$r=a, z=-h$
$\widehat{rr}/p$	$-\frac{\sigma}{2(1-\sigma)}$	$-\frac{3}{32}\frac{(1+\sigma)a^2}{h^2}-\frac{\sigma}{1-\sigma}$	$\frac{3}{32}(1+\sigma)\frac{a^2}{h^2}$	$\frac{1-2\sigma-2\sigma^2}{4\sigma(1-\sigma)}$	$-\frac{1-\sigma^2}{\sigma}$	0*
$\widehat{\theta\theta}/p$	$-\frac{\sigma}{2(1-\sigma)}$	$-\frac{3}{32}(1+\sigma)\frac{a^2}{h^2}-\frac{\sigma}{1-\sigma}$	$\frac{3}{32}(1+\sigma)\frac{a^2}{h^2}$	$\frac{1-2\sigma-2\sigma^2}{4(1-\sigma)^2}$	-1*	0*
$\widehat{zz}/p$	$-\frac{1}{2}$	-1*	0*	$\frac{1-2\sigma-2\sigma^2}{4(1-\sigma)^2}$	-1*	0*
$\widehat{rz}/p$	0*	0*	0*	$3a/h$	0*	0*

(21) *Problem B—Calculation of the Stress-Displacement System.*

By the argument of art 14 it is seen that the A′, B′ constants which occur are A_2', A_3' . A_6', B_2', B_3' .. B_6', and since the polynomials in $\overline{U}$ and $\widehat{rz}$, equations (48) and (50), must vanish for $r=a$ and all values of z, by reason of $J_1(k_n a)=0$, we have seven linear equations between these ten constants.

The stress boundary conditions satisfied by $\widehat{rz}$ and $\widehat{zz}$ at $z=\pm h$ give, by use of (34) and (37), two further equations between the A′, B′ constants, and also determine $P_n \pm P_n'$, $Q_n \pm Q_n'$ in terms of the A′, B′ constants (actually only B_5' is involved) and functions of $k_n a$

We have, thus, nine equations which determine all the constants, except A_2', as follows .—

$$\left.\begin{aligned} A_2' &= \frac{(1+\sigma)p}{24(1-\sigma)E}, \qquad A_4' = -\frac{(1+\sigma)pa^2}{64Eh^2(1-\sigma)}\left(1-2\frac{h^2}{a^2}\right), \\ A_6' &= -\frac{(1+\sigma)p}{240Eh^2(1-\sigma)}, \\ B_2' &= -\frac{(1+\sigma)p}{8E(1-\sigma)}, \qquad B_3' = \frac{(1+\sigma)pa^2}{64Eh^2(1-\sigma)}\left(1-4\frac{h^2}{a^2}\right), \\ B_5' &= \frac{(1+\sigma)p}{160Eh^2(1-\sigma)}, \\ A_5' &= B_4' = B_6' = 0 \end{aligned}\right\} \quad (71)$$

The α', β' constants are known in terms of the A', B' constants by equations (7), and so we find the following expression for w,

$$\left.\begin{aligned} w = \Big[&- 2A_2' - \frac{3(1+\sigma)(3-2\sigma)pa^2}{64(1-\sigma)Eh^3}\left\{1 - \frac{8(1-\sigma)}{3-2\sigma}\frac{h^2}{a^2}\right\} r^2 \\ &\qquad + \frac{3(1+\sigma)(3-2\sigma)p}{128(1-\sigma)Eh^3} r^4\Big] \\ &- \frac{(1+\sigma)(1-2\sigma)p}{2(1-\sigma)E} z + \Big[\frac{3(1+\sigma)pa^2}{16Eh^3}\left\{1 - \frac{2(1-2\sigma)}{1-\sigma}\frac{h^2}{a^2}\right\} \\ &\qquad - \frac{3(1+\sigma)p}{8Eh^3} r^2\Big] z^2 \\ &+ \frac{(1+\sigma)(1-2\sigma)p}{16(1-\sigma)Eh^3} z^4 + \sum_1^\infty \{(\alpha_n + \beta_n z)\cosh k_n z \\ &\qquad + (\gamma_n + \delta_n z)\sinh k_n z\} J_0(k_n r) \end{aligned}\right\} \quad (72)$$

A_2' is determined by the condition $w = 0$ for $r = a$, $z = 0$, so that it can be found when $\sum_1^\infty \alpha_n J_0(k_n a)$ is known, and α_n depends on $P_n - P_n'$, $Q_n + Q_n'$, which involve B_2', and this constant is given above

Thus all the constants are determined and the problem may be regarded as solved.

(22) *The Bending of the Middle Surface, and the Central Normal Deflexion.*

Since $w = 0$ for $r = a$, $z = 0$, (72) gives with $z = 0$,

$$\left.\begin{aligned} w = &\frac{3(1+\sigma)(3-2\sigma)pa^2}{64(1-\sigma)Eh^3}\left\{1 - \frac{8(1-\sigma)}{3-2\sigma}\frac{h^2}{a^2}\right\}(a^2 - r^2) \\ &- \frac{3(1+\sigma)(3-2\sigma)p}{128(1-\sigma)Eh^3}(a^4 - r^4) + \sum_1^\infty \alpha_n \{J_0(k_n r) - J_0(k_n a)\} \end{aligned}\right\}, \quad (73)$$

We find

$$\sum_1^\infty \alpha_n J_0(k_n r) = \frac{3(1+\sigma)(2-\sigma)pa^4}{(1-\sigma)Eh^3}[L_r + (1-2\sigma)M_r], \quad (74)$$

where

$$\left.\begin{aligned} L_r &= \sum_1^\infty \frac{k_n^2 h^2 \sinh k_n h}{\sinh 2k_n h - 2k_n h}\frac{J_0(k_n r)}{k_n^4 a^4 J_0(k_n a)} \\ M_r &= \sum_1^\infty \frac{k_n h \cosh k_n h - \sinh k_n h}{\sinh 2k_n h - 2k_n h}\frac{J_0(k_n r)}{k_n^4 a^4 J_0(k_n a)} \end{aligned}\right\}. \quad (75)$$

The coefficients involving h in L_r and M_r are the same as those of the series W_r and X_r of equations (61), and so we can write as in (63)

$$\left.\begin{aligned} L_r &= \tfrac{1}{2}\sum_1^\infty \frac{J_0(k_n r)}{k_n{}^4 a^4 J_0(k_n a)} - \frac{1}{40}\frac{h^2}{a^2}\sum_1^\infty \frac{J_0(k_n r)}{k_n{}^2 a^2 J_0(k_n a)} \\ M_r &= \tfrac{1}{2}\sum_1^\infty \frac{J_0(k_n r)}{k_n{}^4 a^4 J_0(k_n a)} - \frac{1}{40}\frac{h^2}{a^2}\sum_1^\infty \frac{J_0(k_n r)}{k_n{}^2 a^2 J_0(k_n a)} \end{aligned}\right\}, \tag{76}$$

correct to the order of h^2/a^2.

Thus, by (35), we have

$$\left.\begin{aligned} L_r &= -\frac{1}{256}\left(2 - 6\frac{r^2}{a^2} + 3\frac{r^4}{a^4}\right) + \frac{h^2}{a^2}L_r' \\ M_r &= -\frac{1}{768}\left(2 - 6\frac{r^2}{a^2} + 3\frac{r^4}{a^4}\right) + \frac{h^2}{a^2}M_r' \end{aligned}\right\}, \tag{77}$$

where L_r', M_r' are assumed to be defined by these equations, whilst, for small values of h/a, we have by (76) and (34),

$$L_r' = M_r' = \frac{1}{320}\left(1 - 2\frac{r^2}{a^2}\right).$$

Putting $r = a$ in (77) we have

$$\left.\begin{aligned} L_a &= \frac{1}{256} + \frac{h^2}{a^2}L_a' \\ M_a &= \frac{1}{768} + \frac{h^2}{a^2}M_a' \end{aligned}\right\}, \tag{78}$$

so that $\sum_1^\infty \alpha_n J_0(k_n a)$ can be found.

Using (74), (77) and (78), the expression for w in (73) reduces to

$$-w = \frac{pa^4}{64D}\left[\left(1 - \frac{r^2}{a^2}\right)^2 + \frac{h^2}{a^2}\left\{\frac{16}{1-\sigma}\left(1 - \frac{r^2}{a^2}\right)\right.\right.$$
$$\left.\left. - \frac{128(2-\sigma)}{(1-\sigma)^2}(L_r' - L_a' + (1-2\sigma)(M_a' - M_a'))\right\}\right]. \tag{79}$$

In the limiting case when $h/a \longrightarrow 0$ we get back to the usual result.

To find the central normal deflexion we put $r = 0$ in (79) so that the values of L_a', M_0', L_a', M_a' are required.

Using the approximate methods of art. 17 and the equations (40), we have

$$\left.\begin{aligned} L_0 &= -\frac{1}{128} + \frac{1}{320}\frac{h^2}{a^2}, & M_0 &= -\frac{1}{384} + \frac{1}{320}\frac{h^2}{a^2} \\ L_a &= \frac{1}{256} - \frac{1}{320}\frac{h^2}{a^2}, & M_a &= \frac{1}{768} - \frac{1}{320}\frac{h^2}{a^2} \end{aligned}\right\}. \tag{80}$$

The results in (80) are reasonably accurate for values of h/a up to $\frac{1}{4}$.

Thus, for $h/a = \frac{1}{4}$, (80) gives $L_0 = -0\ 0076172$, the correct value being $-0{\cdot}00760533$, and for $h/a = \frac{1}{8}$, the respective values are $-0{\cdot}00703125$ and $-0{\cdot}00684539$, similar results holding for the other series, so that the approximations (80) may be taken as valid for any value of h/a likely to occur in practice. Hence, to this degree of approximation, $L_0' = M_0' = \frac{1}{320} = -L_a' = -M_a'$ and we have from (79)

$$-w_0 = \frac{pa^4}{64D}\left[1 + \frac{8(8+\sigma)}{5(1-\sigma)}\frac{h^2}{a^2}\right]. \tag{81}$$

With $h/a = \frac{1}{4}$ and $\sigma = \frac{1}{4}$, this formula gives 2·1 times the deflexion given by the thin plate formula, and with $\sigma = \frac{1}{3}$, the ratio is 2·25

For direct comparison with experimental results, the deflexion at $r = 0$, $z = -h$ is required (see art. 19).

This can be calculated from the foregoing analysis, and the final result is

$$w = \frac{3pa^4(1+\sigma)}{128Eh^3}\left[1 - 128\,(2-\sigma)\,(X_0 - X_a)\right], \tag{82}$$

where

$$X_r = \sum_1^\infty \frac{\sinh 2k_n h - 2k_n h \cosh {}^3k_n h}{\sinh 2k_n h - 2k_n h}\,\frac{J_0(k_n r)}{k_n{}^4 a^4 J_0(k_n a)}.$$

We find the approximations, using the results (40),

$$\left.\begin{aligned} X_0 &= \frac{1}{192} + \frac{1}{40}\frac{h^2}{a^2} \\ Xa &= -\frac{1}{384} - \frac{1}{40}\frac{h^2}{a^2} \end{aligned}\right\}. \tag{83}$$

For $h/a = \frac{1}{4}$, the approximate and correct values of X_0 are 0 00677083 and 0 0066559, and for X_a they are $-0{\cdot}004167$ and $-0{\cdot}00399661$, the latter not being in particularly good agreement.

The approximation to (82) is, therefore,

$$-w = \frac{pa^4}{64D}\left[1 + \frac{32}{5}\,\frac{2-\sigma}{1-\sigma}\,\frac{h^2}{a^2}\right]. \tag{84}$$

This equation gives, as we shall see, results in fair agreement with experiment. It should be noticed that the difference between the deflexion at $r = 0$, $z = 0$ and at $r = 0$, $z = -h$ are here greater than in the case of problem A.

(23) *Stress Calculations for the Thick Plate*

The stresses at various points in the plate are determined as in art. 20, and, as before, certain of the results are exact, especially for the value $z = 0$.

This arises from the fact that β_n and γ_n are found to vanish in this solution, and so the expressions for the stresses involve only the finite terms when $z = 0$.

The result $\widehat{rz} = \dfrac{3pa}{8h^3}(h^2 - z^2)$ should be noticed in comparison with that given in equation (20), viz., $\widehat{rz} = \dfrac{3pr}{8h^3}(h^2 - z^2)$

There is some little difficulty in determining approximate values for $\widehat{rr}$ and $\widehat{\theta\theta}$ when $z = \pm h$. Thus, for $r = 0$, $z = \pm h$ we find in the expressions for these stresses, besides terms in p and pa^2/h^2, a term of the type $\dfrac{pa^4}{h^4}(S - 2S')$, where

$$S = \sum_1^\infty \frac{k_n^2 h^2 \sinh 2k_n h}{\sinh 2k_n h - 2k_n h} \frac{1}{k_n^4 a^4 J_0(k_n a)} = -\frac{1}{64} - \frac{7}{80}\frac{h^2}{a^2}$$

$$S' = \sum_1^\infty \frac{k_n h \sinh^2 k_n h}{\sinh 2k_n h - 2k_n h} \frac{1}{k_n^4 a^4 J_0(k_n a)} = -\frac{1}{128} - \frac{1}{80}\frac{h^2}{a^2}$$

Approximately, $S - 2S' = -\dfrac{1}{16}\dfrac{h^2}{a^2}$, correct to the order of h^2/a^2, and we should have terms in p if the approximation could be carried as far as h^4/a^4.

The correct value of $S - 2S'$ for $h/a = \frac{1}{4}$ is $-0{\cdot}0040342$ as against the approximate value $-0{\cdot}00390625$, the values being sufficiently close to permit of the omission of the extra terms in p.

For $r = a$, $z = \pm h$ we have similar terms $\dfrac{pa^4}{h^4}(T - 2T')$, where

$$T = \sum_1^\infty \frac{k_n^2 h^2 \sinh 2k_n h}{\sinh 2k_n h - 2k_n h} \frac{1}{k_n^4 a^4} = \frac{1}{128} + \frac{7}{80}\frac{h^2}{a^2},$$

$$T' = \sum_1^\infty \frac{k_n h \sinh^2 k_n h}{\sinh 2k_n h - 2k_n h} \frac{1}{k_n^4 a^4} = \frac{1}{256} + \frac{1}{80}\frac{h^2}{a^2}.$$

Here the approximation $T - 2T' = \dfrac{1}{16}\dfrac{h^2}{a^2}$ is not very good, since for $h/a = \frac{1}{4}$ the correct value is $0{\cdot}00477417$.

We cannot, therefore, neglect the extra term, and we write $T - 2T' = \dfrac{1}{16}\dfrac{h^2}{a^2} + k\dfrac{h^4}{a^4}$, where k is an undetermined quantity which varies with h/a, and so we have a term pk in the expressions for the stresses.

For $h/a = \frac{1}{4}$ we find $k = 0{\cdot}222$.

The values of the stresses at various points are given below, it being understood that the remarks of art. 20 have equal force in this case.

Correct results are starred as before.

Table III.

Stresses.	$r=0, z=0$.	$r=0, z=+h$.	$r=0, z=-h$.	$r=a, z=0$	$r=a, z=+h$.	$r=a, z=-h$
$\widehat{rr}/p$	$\frac{\sigma}{2(1-\sigma)}$	$-\frac{\sigma}{1-\sigma}-\frac{3a^2}{32h^2}$	$\frac{3a^2}{32h^2}$	$-\frac{\sigma}{2(1-\sigma)}$	$-\frac{\sigma}{1-\sigma}+\frac{3(1+\sigma)h}{2(1-\sigma)}+\frac{3(2-\sigma)a^2}{32(1-\sigma)h^2}$	$-\frac{3(1+\sigma)h}{2(1-\sigma)}-\frac{3(2-\sigma)a^2}{32(1-\sigma)h^2}$
$\widehat{\theta\theta}/p$	$\frac{\sigma}{2(1-\sigma)}$	$-\frac{\sigma}{1-\sigma}-\frac{3a^2}{32h^2}$	$\frac{3a^2}{32h^2}$	$-\frac{\sigma}{2(1-\sigma)}$	$-\frac{\sigma}{1-\sigma}+\frac{3(1+\sigma)h}{2(1-\sigma)}-\frac{3\sigma a^2}{32(1-\sigma)h^2}$	$-\frac{3(1+\sigma)h}{2(1-\sigma)}+\frac{3\sigma a^2}{32(1-\sigma)h^2}$
$\widehat{zz}/p$	-1	-1	0	-1	-1	0
$\widehat{rz}/p$	$\frac{3\pi a}{8h}$	0	0	$\frac{3\pi a}{8h}$	0	0

For $h/a = \frac{1}{4}$, we have $k = 0\ 222$, so that, with $\sigma = \frac{1}{4}$, the numerically greatest stress is $(\widehat{rr})_{\substack{r=a \\ z=-h}} = -\frac{7+5k}{2}p = -4{\cdot}05\ p$, which is somewhat greater than in the previous case (see Table II).

The values of $\widehat{rr}$ and $\widehat{\theta\theta}$ at $r = a$, $z = \pm h$ are of the order of pa^2/h^2 in contrast to the results of problem A, and this is considered, as before (art 20), to be due to the fact that $\partial w/\partial z$ is of the order of pa^2/Eh^2 at the edge in this case, so that the conditions of problems A and B do not become equivalent when $h/a \longrightarrow 0$.

(24) *Some Problems of Non-Uniform Loading.*

We propose now to consider briefly some cases of non-uniform loading, the object being rather to indicate methods than to work out particular problems in detail The loading is considered to be symmetrical, so that we have $\widehat{zz} = f(r)$ over $z = +h$, where $f(r)$ is a specified function, and this condition is to be satisfied as in art 10 Assuming, for example, the edge boundary conditions of problem A, we have $J_0(k_n a) = 0$, and the integral $\int_0^a f(r)\, J_0(k_n r) r\, dr$ is to be found.

This integral can be obtained for many values of $f(r)$, but here we confine the discussion to the case where the plate is loaded only over a small concentric circular area, or, in particular, where the load is wholly concentrated at the centre.

Suppose, then, that there is uniform pressure p' over the area of the circle $r = b$ $(b < a)$ and zero pressure over the remainder of the plane $z = +h$. Then we have

$$\int_0^a f(r)\, J_0(k_n r) r\, dr = -p' \int_0^b J_0(k_n r) r\, dr = -\frac{p'b}{k_n} J_1(k_n b) \qquad (85)$$

If the total load is equivalent to a uniform pressure p over the whole plate, we have $p'b^2 = pa^2$, and we can pass to the limiting case of central loading by making $b \to 0$ and keeping $p'b^2$ finite.

The type of solution given in art. 15 will serve, and we have from (53), writing $\widehat{zz} = f(r)$ for $z = +h$,

$$\sum_1^\infty \frac{P_n + P_n'}{2} J_0(k_n r) = \frac{1+\sigma}{2E} f(r) - (4\sigma B_3' + \alpha_3' a^2 + 2\sigma\alpha_3' h^2) + (1+\sigma)\alpha_3' r^2,$$

$$\sum_1^\infty \frac{P_n - P_n'}{2} J_0(k_n r) = \frac{1+\sigma}{2E} f(r) + 2\sigma\alpha_2' h + 3(1-\sigma)\alpha_4' a^2 h - 2\sigma\alpha_4' h^3 + 3(1+\sigma)\alpha_4' h r^2,$$

where $f(r) = -p'$ for $0 \leq r \leq b$, and vanishes for $b \leq r \leq a$.

Since $J_0(k_n a) = 0$ and $f(a) = 0$, we arrive at equations (55) and (56) with the omission of the terms in p, and, multiplying throughout by $J_0(k_n r)r$, integrating from 0 to a and using the result of (85), we get expressions for $P_n \pm P_n'$. The results are, as before (art 15), with added terms of the type $\frac{p}{k_n b} \frac{J_1(k_n b)}{J_1^2(k_n a)}$; the remainder of the analysis of art. 15 is unchanged

The equations corresponding to (57) and (58) are the same with added terms, so that the constants of the solution can be determined.

The results for a thick plate can be worked out if required, but are, necessarily, rather complicated.

To proceed to the case of central loading we make $b \to 0$, so that $\frac{J_1(k_n b)}{k_n b} \to \frac{1}{2}$.

The equation giving the normal deflexion of the middle surface is then the same as (60) with the following added term :—

$$\frac{1+\sigma}{E}\frac{pa^4}{h^3}\left[2(1-\sigma)\sum_1^\infty \frac{k_n{}^3h^3\cosh k_n h}{\sinh 2k_n h - 2k_n h}\frac{J_0(k_n r)}{k_n{}^4a^4 J_1{}^2(k_n a)} + \frac{h^2}{a^2}\sum_1^\infty \frac{k_n{}^2h^2\sinh k_n h}{\sinh 2k_n h - 2k_n h}\frac{J_0(k_n r)}{k_n{}^2a^2 J_1{}^2(k_n a)}\right].$$

Approximate results for the new series introduced can be obtained as in art. 17, using the results of art 11 (c), and the normal deflexion can be calculated as before for a specified value of h/a

There is one point to be made clear concerning the value of the deflexion at $r = 0$, $z = 0$ We have, by (41),

$$\sum_1^\infty \frac{J_0(k_n r)}{k_n{}^2a^2 J_1{}^2(k_n a)} = \frac{1}{2}\log\frac{a}{r},$$

which becomes infinite for $r = 0$, and so the expression

$$\frac{h^2}{a^2}\sum_1^\infty \frac{k_n{}^2h^2\sinh k_n h}{\sinh 2k_n h - 2k_n h}\frac{1}{k_n{}^2a^2 J_1{}^2(k_n a)}$$

must be examined more closely, because the deflexion at $r = 0$, $z = 0$ is finite.

We have

$$\frac{\theta^2\sinh\theta}{\sinh 2\theta - 2\theta} = \frac{1}{2}\cdot\frac{1 + \frac{\theta^2}{6} + \ldots + \frac{\theta^{2r}}{(2r+1)!} + \ldots}{1 + \frac{\theta^2}{5} + \ldots + \frac{6\cdot 2^{2r}}{(2r+3)!}\theta^{2r} + \ldots} = \frac{1}{2}f(\theta), \text{ say,}$$

and $f(\theta) < 1$, for $\theta > 0$.

Clearly

$$f(\theta) < \frac{1 + \frac{\theta^2}{6} + \ldots}{\frac{\theta^2}{5} + \ldots} = \frac{5}{\theta^2}\phi(\theta), \text{ say,}$$

where

$$\phi(\theta) = \frac{1 + \frac{\theta^2}{6} + \ldots + \frac{\theta^{2r}}{(2r+1)!} + \ldots}{1 + \frac{2}{21}\theta^2 + \ldots + \frac{30 \cdot 2^{2r+2}}{(2r+5)!}\theta^{2r} + \ldots}.$$

The ratios of corresponding coefficients in the numerator and denominator of $\phi(\theta)$ decrease steadily from 1 to zero, so that $\phi(\theta) < \frac{1}{4}$.

Thus

$$f(\theta) < \frac{35}{4\theta^2} \text{ and } S = \sum_1^\infty \frac{k_n^2 h^2 \sinh k_n h}{\sinh 2k_n h - 2k_n h} \frac{1}{k_n^2 a^2 J_1^2(k_n a)}$$

$$= \tfrac{5}{4} \sum_1^\infty f(k_n h) \frac{1}{k_n^2 a^2 J_1^2(k_n a)},$$

i.e.,

$$S < \frac{105}{16} \sum_1^\infty \frac{1}{k_n^2 h^2} \frac{1}{k_n^2 a^2 J_1^2(k_n a)} = \frac{105 a^2}{16 h^2} \sum_1^\infty \frac{1}{k_n^4 a^4 J_1^2(k_n a)},$$

so that $\frac{h^2}{a^2} S < \frac{105}{128}$ (art. 11 (*c*)), and the deflexion at $r = 0$, $z = 0$ is finite.

To proceed to the limiting case of a thin plate, we follow out the method of art. 16, replacing the various infinite series that occur by their equivalents as given by equations (26), (41) and (42), and the result given by Love ('Elasticity,' p. 468) is obtained.

The problem can also be discussed using the boundary conditions of problem B, and detailed results obtained in both cases for the case of central loading, but enough has been said to indicate the possibilities of the methods of this paper.

Some General Considerations.

(25) *The Question of Uniqueness of Solution.*

The question arises as to whether the solutions, given in this paper, of the problem of the thick circular plate, with assigned stress boundary conditions over the plane faces and displacement boundary conditions at the cylindrical edge, are true solutions in the sense that they are the only solutions.

If either the surface tractions or the surface displacements are given completely, it is known that the solution of the problem of elastic equilibrium

is unique, so that the stress displacement system throughout the body is determinable without ambiguity (*vide* Love, 'Elasticity,' p. 167).

The argument can easily be turned to suit the case where the tractions are given over part of the bounding surface and the displacements over the remainder, so that, in the case of the circular plate, with symmetrical loading, if $\widehat{zz}$ and $\widehat{rz}$ are given over $z = \pm h$ and $\bar{U}$, w over $r = a$, the problem would have a unique solution.

In the cases worked out in this paper the stresses are so given over $z = \pm h$, but one only of the displacements $\bar{U}$, w has been completely specified over $r = a$, for all values of z, the remaining displacement being given for particular values of z only. Thus, in the sense of the above remarks, the solution, certainly, is not unique

It has been shown, however, that a complete solution as such is not possible by the methods employed, and, therefore, it becomes necessary to consider the limitations of the partial solutions obtained

It is clear from the argument in art. 14 that solutions could be obtained to satisfy more general boundary conditions at $r = a$, although they would be very complicated.

Thus, in the case of problem A, we could by choice of m (art 14) make $\bar{U}$ vanish at s positions, say, on the cylindrical edge by choosing $m = 2 + s$.

If, for example, we make $\bar{U} = 0$ for $r = a$, $z = \pm h$ and also for $r = a$, $z = 0$, so that $m = 5$, the solution gives the same equations for α_2' and α_4' as before, so that the law of bending of the middle surface, which depends only on these constants (equation (60)), is unchanged.

In the solution as given, $\bar{U}$ does not vanish at $r = a$, $z = 0$, and it is interesting to note that the vanishing, or otherwise, of $\bar{U}$ at this position has no effect on the bending of the middle surface.

Similarly, in the case of problem B, we may take $w = 0$ for $r = a$, $z = \pm h$, instead of merely $w = 0$ for $r = a$, $z = 0$, as worked out.

The more general solution is very lengthy, but, on working it through, and approximating as usual to the infinite series which occur, we find that the normal deflexion of the centre of the plate is the same as before to the order of h^2/a^2.

It is found that the analytical difficulties of the problem are greatly increased as the number of terms in the finite part of the solution becomes greater, and it seems advisable to content ourselves with the simplest possible solutions which apparently give a unique value for the bending of the middle surface,

and so, in a sense, may be regarded as the appropriate solutions consistent with the given boundary conditions.

(26) *Experimental Determination of the Elastic Contents*

A point of some importance, upon which, it is hoped, the present investigation may serve to throw some light, is the fact that different values of the fundamental elastic constants, Young's modulus and Poisson's ratio, are obtained when various tests are applied to specimens of metal

Thus the tensile test and the bender test give slightly different values of Young's modulus, and it is clear that tests on the bending of plates will give values differing from those obtained by the other tests mentioned, if the accepted formula for *thin* plates is used.

Filon, in a memoir "On the Equilibrium of Circular Cylinders under Certain Practical Systems of Load" ('Phil. Trans.,' A, vol 198 (1902)) has shown that the values of the elastic constants determined by a tensile test depend on the dimensions of the test piece, and it is clear that similar considerations apply to the bending of plates, as the effective thickness (h/a) of the plate must be taken into account

Most experimental work in the past* has been done with plates for which the Grashof formula, so called (p. 566, equation (17)), applies fairly well, as the thickness-diameter ratio was of the order $\frac{1}{5}\frac{1}{0}$ to $\frac{1}{10}\frac{1}{0}$, so that the effect of the dimensions of the plate was not important, but more recent work, as mentioned below, has shown that this formula fails for thick plates

(27) *Experimental Results for Thick Plates*

Experiments on an extensive scale have recently been made, using plates of varying thickness-diameter ratio up to a value exceeding $\frac{1}{4}$, these plates being manufactured by turning out a block of metal in order, as was thought at the time, to secure effective clamping.

The results, however, showed central normal deflexions for thick plates greatly exceeding those calculated for a clamped plate by the usual formula, the discrepancies increasing with the thickness

They have been compared with the values calculated from the various formulæ arrived at in this paper

* Experimental researches which have been consulted are the following.—
Crawford, 'Proc R.S.E.,' vol. 32, p. 348 (1911–12).
Steinthal, 'Engineering,' vol. 91, p. 677.
Enslin, 'Dingler's Polytechnischer Journal,' vol. 318 (1903).

It is curious that the best agreement with experiment is given by the formula for w at $r = 0$, $z = -h$, using the boundary conditions $\bar{U} = w = \dfrac{\partial \bar{U}}{\partial z} = 0$ for $r = a$, $z = 0$, for which (19) gives the deflexion at $r = 0$, $z = 0$.

It is not considered, however, that the simple solution, with these assumptions, can be applied to the case of a thick plate, since the boundary conditions refer only to the middle surface, and the agreement with experiment must be regarded as accidental

Of the solutions which are taken specifically to apply to the case of a thick plate with a fixed cylindrical edge, the better agreement is found with those values calculated from the formula (84), which was obtained on the assumption $\bar{U} = 0$ for $r = a$, $h > z > -h$

The results tabulated below were obtained using plates 3 inches in diameter, and they are compared with the calculated deflexion in inches given by the thin plate formula (17), the appropriate formula for $r = 0$, $z = -h$ corresponding to (19), and the formula (84)

The value of σ used in calculating these results was 0 266, but this figure is not very reliable, and it is probable that the value should be somewhat greater, if so, the figures in columns 4, 5 and 6 would be increased

The agreement between columns 3 and 5 is far from perfect, but it must

Table IV.

1	2	3	4	5	6*	7	8	9
Thickness in inches	h/a.	Deflexion for $p = 1000$ lb per sq in	Deflexion from (17).	Deflexion from (84).	Deflexion from (19′)	Col 3 / Col. 4	Col 3 / Col 5	Col 3 / Col. 6
0·1	1/30	0·03100	0 029800	0 030300	0 030426	1 040	1 023	1 018
0 2	1/15	0 00443	0·003728	0 003980	0 004040	1 188	1·112	1 096
0 3	1/10	0 001575	0 001105	0 001272	0 001313	1·425	1·238	1 200
0 4	2/15	0 000740	0 000466	0 000591	0 000621	1·588	1 252	1 192
0 5	1/6	0 000427	0 000239	0 000340	0 000363	1 787	1 256	1·176
0 6	1/5	0 000287	0·000138	0 000221	0·000240	2 080	1 298	1·196
0 7	7/30	0 000203	0 0000870	0 000159	0·000172	2 333	1·280	1·180
0·8	4/15	0 000150	0 0000582	0·000121	0 000134	2·578	1·242	1·120

* (19′) is used to refer to the formula for w at $r = 0$, $z = -h$, corresponding to (19).

be realised that there is no guarantee that the boundary conditions postulated have been secured; the more or less steady values in column 8, for the thicker plates, would appear to show that the theory is on the right lines

It could hardly be expected that an admittedly tentative set of boundary conditions would be realised in practice, and it is possible that there exists unavoidable boundary strain which cannot be taken account of in the theoretical treatment of the problem.

(28) *Summary and Conclusions*

The investigation in this paper is that of the flexure of a thick circular plate, held so that there is no displacement at the cylindrical edge, subjected to a uniform pressure over one of the flat surfaces

Three types of solution have been considered --

(i) The solution in finite terms,

(ii) The solution in infinite series involving hyperbolic functions of z and Bessel functions of r;

(iii) The solution afforded by a combination of (i) and (ii).

It has been shown that no one of these solutions can solve the problem in its complete generality, and each has been examined in turn to discover what problems can be discussed by its aid.

The solution (i) leads easily to the usually accepted results for thin plates, but is incapable of dealing with the case where the thickness of the plate cannot be neglected.

Solution (ii) is of restricted application, as boundary conditions at the edge referring to one displacement only can be satisfied.

Solution (iii), in various forms, permits of the discussion of a variety of problems, the method being to satisfy the stress boundary conditions over $z = \pm h$, and then to consider different boundary conditions at $r = a$, such conditions being expressed in terms of w and $\overline{U}$

It is possible to satisfy *one* condition only at $r = a$, for all values of z, such as $w = 0$ or $\overline{U} = 0$, and these have been considered in turn, the remaining displacement being made to vanish for specified values of z only, thus leading to partial solutions of the problem.

It is found that, for a thick plate, the condition $\overline{U} = 0$ for $r = a$, $h > z > -h$ leads to greater bending for a given pressure than the condition $w = 0$, which,

in its turn, gives more than that according to the usual formula for thin plates.

In each case, the usual result for a thin *clamped* plate is obtained in the limit when h/a tends to zero.

Methods have also been indicated for the discussion of the problem for the case of non-uniform loading, particularly when the load is concentrated entirely at the centre The theoretical results for thick plates are expressed in the form of infinite series, which have been reduced to simple terms by the methods described in the paper, so that concise approximate expressions for stresses and displacements are obtained which are valid in most cases even for comparatively thick plates (*e g.*, $h/a = \frac{1}{2}$).

The distribution of stress throughout the plate in the cases considered is indicated by tables giving the values of the stresses at various particular points, and attempts are made to determine the greatest stress in terms of the applied pressure and the ratio h/a

The maximum stresses vary in position and magnitude according to the values of σ and h/a, and are best determined at *ınıtio* in any particular case. It is hoped later to obtain, experimentally, some criterion for elastic failure in the case of the bending of thick plates, and then, perhaps, to make further applications of the results of this paper

In conclusion I wish to make my grateful acknowledgments to the following gentlemen :—Prof A E. H Love, F.R.S , who read the paper in its first form and made valuable suggestions for alteration and improvement ; my friend and colleague Captain W. E. Grimshaw, O B E., who also read the paper and with whom I have discussed various points ; my colleague Mr. G. M. Russell, who undertook the experimental part of the research* ; and Mr. N. M H. Lightfoot, now assistant lecturer in the University of Sheffield, who carried out a good deal of the numerical work involved.

* The work was carried out in the Ballistic Branch of the Research Department, Woolwich

On the Total Photo-Electric Emission of Electrons from Metals as a Function of Temperature of the Exciting Radiation.

By S. C. Roy, M.Sc., Physics Research Department, King's College, London

(Communicated by Prof O W Richardson, F R S —Received July 29, 1926)

1. *Introduction.*

In the year 1913 K T. Compton and O. W Richardson ('Phil. Mag.,' vol. 26, p. 549 (1913)) published a paper containing an important investigation on the action of homogeneous mono-chromatic radiation on a number of metals The essential characteristics of the photo-electric activity of various metals are set out in their experimental curves obtained by plotting photo-electric yield of electrons against exciting frequency These curves contain double maxima in the case of extremely electro-positive elements like Na, and one maximum for a less electro-positive metal Al, while the curves for Pt exhibit no maximum in the range of frequencies covered by their experiments Later investigations by Souder ('Phys. Rev.,' vol. 8, p 327 (1916)) and O. W. Richardson and A F. A. Young ('Roy. Soc Proc.,' A, vol. 107, p 377 (1925)) have confirmed these general characteristics of photo-electric activity-frequency curves A photo-electric maximum for the "selective" effect was observed by Pohl and Pringsheim ('Verh. d. Deutsch. Physik. Ges,' vol 11, p. 1039 (1910)) as early as 1910 in the case of some electro-positive elements. The general shape of the humps in their curves appears to be a function of the angle of incidence of the exciting radiation, nevertheless, the position of the maximum is quite independent and definite. Lately, R. Dopel ('Zeits. für Phys.,' vol. 33, p. 237 (1925)) has shown that a less electro-positive metal like Sr also shows the photo-electric maximum It is therefore probable that all metals would exhibit such maximum photo-electric effect if it were possible to extend the range of exciting frequencies far into the ultra-violet. The presence of double maxima in the curves for Na and K probably points to the existence of two photo-electric thresholds in these elements, as suggested by O. W. Richardson ('Proc. Phys. Soc. London,' vol. 36, p. 388 (1924)), and may lead to interesting developments in future.

In the following Table I are collected the observed values of the long wave-length limit λ_0 and the wave-length λ_m of the maximum photo-electric effect. A comparison of the figures in columns 1 and 3 shows that the frequencies

ν_0 and ν_m can be correlated within the range of accuracy and consistency attainable in photo-electric measurements by a simple relation,

$$\nu_m = \tfrac{3}{2}\nu_0 \qquad (1)$$

Table I.

Metals	$\lambda_m\mu\mu$ (obs)	$\lambda_0\mu\mu$ (obs)	$\frac{3}{2}\lambda_0\mu\mu$
Cs	550*	>750‡	>500
Rb	480*	—	—
K	440*	700§	465
Na	360†	577†	385
Ca	360*	400‖ (?)	267
Ba	280*	—	—
Mg	250*	390†	260
Al	247·5†	360†	240

* Pohl and Pringsheim, 'Verh d D Phys Ges,' vol 12, p 349 (1910); vol. 12, p. 682 (1910); vol 13, p 474 (1911), vol 14, p 46 (1912), etc
† K. T. Compton and O. W Richardson, *loc cit.*
‡ Cornelius, 'Phys. Rev,' vol 30, p 3 (1910)
§ A. F A Young, 'Roy. Soc Proc,' A, vol 104, p 611 (1923).
‖ Richard Hamer, Optical Soc of America, 'J & Rev. Sc. Inst,' vol. 9, p. 251 (1924)

This significant result leads at once to the formulation of a functional relation between photo-electric activity and exciting frequency Thus if F_ν represents the number of electrons emitted by the absorption of unit quantity of radiant-energy of frequency ν, then the relationship (I) is satisfied if F_ν be of the form

$$F_\nu = \text{const } \frac{\nu - \nu_0}{\nu^3}. \qquad (2)$$

These two important relations were given by O. W. Richardson ('Phys Rev.,' vol 34, p. 119 (1912); 'Phil. Mag.,' vol. 23, p. 615 (1912); vol. 24, p. 570 (1912)) on the basis of some thermodynamic and statistical reasoning. As a matter of fact, these two relations represent all the important aspects of the photo-electric operation of monochromatic light on metals. A. Becker ('Ann der. Phys.,' vol. 60, p. 30 (1919)) attempted to represent the photo-electric activity of platinum by an empirical relation of the form

$$F_\nu = \text{const.} \left(1 - \frac{\nu_0}{\nu}\right)^2. \qquad (3)$$

No importance can probably be attached to this empirical relation inasmuch as it is based on data of photo-electric activity of a single element over a limited range of frequencies, and also particularly because it fails to represent a very important feature of the photo-electric activity-frequency curve, namely, the

existence of a frequency of maximum effect related to the threshold frequency in some such simple manner as is expressed in relation (I).

It should, however, be pointed out that the theoretical curve of photo-electric activity according to the expression (2) differs somewhat in shape from the experimental one, but there are a number of causes which might furnish a natural explanation of this discrepancy. This is, however, of secondary importance for a study of the broad features of the photo-electric activity of metals.

The total photo-electric yield of electrons resulting from the action of a "black-body" spectrum is obtained by multiplying the function F_ν by the intensity K_ν and integrating it over all frequencies greater than the threshold. One thus obtains

$$N_{phot} = \int_{\nu_0}^{\infty} F_\nu . K_\nu \, d\nu$$

$$= \text{const.}\, T^3 . \varepsilon^{-h\nu_0/kT}. \qquad (4)$$

It is clear that a law of total photo-electric emission in the form (4) is a consequence of the presence of a maximum photo-electric effect at a frequency $\nu_m = \frac{3}{2}\nu_0$.

William Wilson ('Roy. Soc. Proc.,' A, vol. 93, p. 359 (1917)) was the first to make measurements on the total photo-electric emission, using Na. He was able to represent his results by a law of the form,

$$N_{phot} = \text{const.}\, T^a . \varepsilon^{-b/T}, \qquad (5)$$

where a lies between 1 and 2. A. Becker ('Ann. der Physik,' vol. 78, p 83 (1925)) has recently studied the photo-electric excitation of Al by the complete radiation from a tungsten source at temperatures of 2100–3200 abs. He concludes that a is greater than 2 and probably lies between 3 and 4. Owing to the predominating influence of the exponential term in (5), it is scarcely possible to decide experimentally between values of a such as 1, 2, or even 3. So far as the writer is aware, these are the only two experiments on record * O. W. Richardson ('Emission of Electricity from Hot Bodies,' pp. 97–100 (1916), and 'Phil Mag.,' vol. 31, p. 149 (1916)), on some computations based on experimental data on the action of monochromatic light on Pt, pointed out that the value of the total photo-electric current from Pt by "black-body" radiation

* Langmuir ('Journ. Am Chem. Soc.,' vol. 42, p. 2190 (1920)) mentions in a footnote (p. 2204) that some careful experiments (unpublished) made by him on the total photo-electric emission from tungsten had shown that the magnitude of the photo-electric currents was of the order of one-millionth of the corresponding thermionic currents.

at 2000°A should be about 10^7 times less than the thermionic current from Pt at the same temperature

The idea that the thermionic emission from hot bodies may really be due to the photo-electric activity of the radiation of the hot body itself owes its origin to O W Richardson (*loc. cit*) and W. Wilson ('Ann. der Physik,' vol. 42, p. 1154 (1913)) So far as variation with temperature is concerned, Wilson's experiment substantiated this view. Further, A Becker (*loc. cit*) brought forward another fact to strengthen the basis of the radiation theory of thermionic emission—namely, that the distribution of velocities amongst photo-electrons is the same as is found in the thermionically emitted electrons But although no systematic attempt has been made to study quantitatively the magnitude of the total photo-electric emission, it is generally known that the amount of thermionic emission of electrons is vastly in excess of the total photo-electric emission. This fact has been made the basis of some comments against the radiation theory of thermionic emission It is obvious that the origin of such adverse criticism lies in the fact that one is apt to overlook the distinction between thermionic and photo-electric phenomena when laying too much emphasis on the resemblance between them That both kinds of processes are promoted by radiation of course constitutes a resemblance, but the distinction lies in the fact that one is due to the action of radiation on a system in temperature equilibrium, while the other is due to the action of high-temperature radiation on a cold system. In the thermionic phenomenon the exciting radiation is isotropic, and has the same intensity throughout the body of the emitting system, while in the photo-electric experiments the intensity of the exciting radiation is greatest at the surface of incidence, and falls off exponentially with the depth of penetration.

Recently the writer ('Phil. Mag.,' vol. 50, p 250 (1925), 'Roy Soc Proc.,' A, vol 110, p. 543 (1926); 'Z. für. Physik,' vol 34, p. 499 (1925)) made some attempts to renew an interest in the radiation theory of thermionic emission and chemical reactivity The phenomena which may be supposed to be due to the action of radiation on a system in temperature equilibrium are (I) the thermionic emission of electrons from solids, (II) the thermal ionisation of gases, (III) the unimolecular decomposition of chemical molecules by heat; while those promoted by the action of high-temperature radiation on a cold system are (I) the photo-electric emission of electrons from solids, (II) the photo-electric ionisation of gases, and (III) the photo-chemical decomposition of chemical molecules. It occurred to the writer that if one could explain the quantitative discrepancy between thermionic and total photo-electric currents,

one would strengthen the basis of the radiation hypothesis of chemical reactivity in general But before one can do so, one must have at one's disposal some quantitative data on total photo-electric emission It was with this object in view that the present experiments were undertaken by the writer

2 *Experimental Arrangements.*

The apparatus (as shown to scale in plan in fig 1) is made of transparent quartz-glass, and was originally designed by Prof O. W Richardson for the

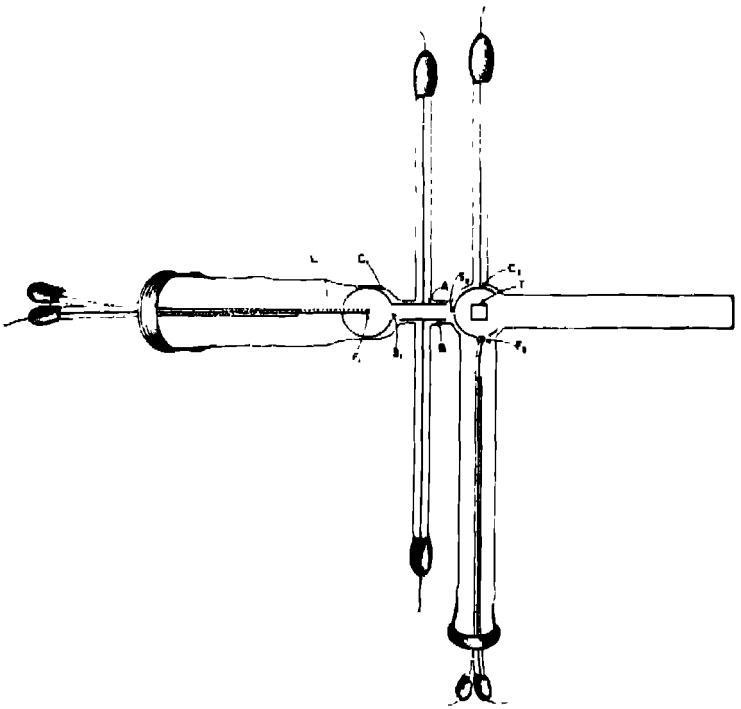

FIG. 1

study of soft X-rays It was found, however, that the same quartz-tube could be adapted with certain modifications in arrangements to the study of total photo-electric emission of electrons from metals by the action of radiation from an approximate "black-body" source

The source of radiation is an electrically heated tungsten wire of radius 0·005 cm., and of length about 10 cm., wound into a spiral of 11 or 12 turns.

This spiral, F_1, is kept centrally suspended inside a closed copper cylinder, C_1, of height 2·3 cm. and of diameter 2 2 cm., by means of two stout leads, L, of constantan wire. The use of a fairly large length of tungsten ensures precision in the measurements of temperatures and reduces to a minimum any correction due to end-losses The copper cylinder, C_1, is put to earth and the filament is maintained at a positive potential of about 10 volts in order to prevent emission of electrons The radiation from the filament streams out of the copper cylinder through a rectangular slit, S_1, 2 cm × 5 mm. in dimension Any positive ions or electrons diffusing with the stream of radiation are trapped by a pair of metal condenser plates, A and B, which are held tight against the flat walls of the apparatus These plates are, respectively, 2·2 × 1·8 and 2 × 1 8 sq. cm in size, and about 0·52 cm apart. A potential difference of about 50 volts or even less between the plates suffices to extract all the ions or electrons from the beam of radiation when the pressure inside the apparatus is less than 10^{-6} mm.

The radiation enters through a second slit, S_2, of dimensions 2 cm × 2·3 mm., into the copper half-cylinder, C_2, and impinges upon the photo-electric targets enclosed by C_2 The electrons liberated from the target by the incident radiation are drawn to C_2, which is maintained at a positive potential of about 20 volts. This potential is sufficient to saturate the photo-electric currents, which range from 10^{-11} to 10^{-14} amp in the present experiments These currents are measured by a suitable electrometer of sensibility 30 4 cm. deflection on the scale per volt, and of capacity 96 cm

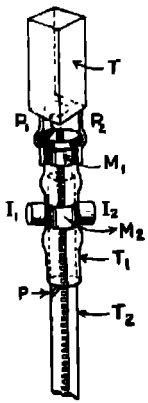

Fig. 2.

In order to ensure that the current so measured is really due to photo-electric action, and also to enable a comparison of the photo-electric properties of various metals to be made under the same experimental conditions, the experiment is so arranged that four different metal targets can be studied at the same time. For this purpose four metal targets (2 cm × 1 cm.) are mounted in a nickel framework, T (fig. 2), which is held by means of two metal spikes, P_1 and P_2, to a metal collar, M_1, fixed tightly round a short glass tube, T_1, carrying two iron arms, I_1 and I_2, by means of a second metal collar, M_2. The glass tube, T_1, has four grooves cut in its bottom at equal angular distances of 90°, and can rest vertically through any of these grooves on a pin, P, attached to a glass tube, T_2. The electrical connection to the target-holder, T, is made by means of a spiral of

thin copper wire passing through T_2. The target-holder, T, can thus be lifted and turned from outside by means of a small electro-magnet so as to present any of the metal targets to the action of the impinging radiation.

The evacuation of the apparatus is done by means of Volmer's condensatio pump system backed by a Fleuss oil pump. The apparatus is connected to the pump system through two double-walled glass condensers in series, one of them containing coconut charcoal. Both of these glass condensers are kept immersed in liquid air after complete evacuation by the pumps. The joints and seals are all made with hard sealing wax of very low vapour pressure. The central parts of the quartz apparatus can be heated to red heat to get rid of occluded gases. The metal cylinder, C_1, is degassed by electron-bombardment from the filament, F_1, and the half-cylinder, C_2, and the metal targets can be cleaned up by bombardment of electrons from an auxiliary filament, F_2. In this way it is always possible to maintain a pressure lower than 10^{-6} mm inside the apparatus when the temperature of the filament, F_2, does not exceed 3,000°A.

3. *Electrical Connections*

The electrical connections are shown diagrammatically in fig. 3. The resistance of the tungsten spiral, F_1, is measured by a simple Wheatstone bridge

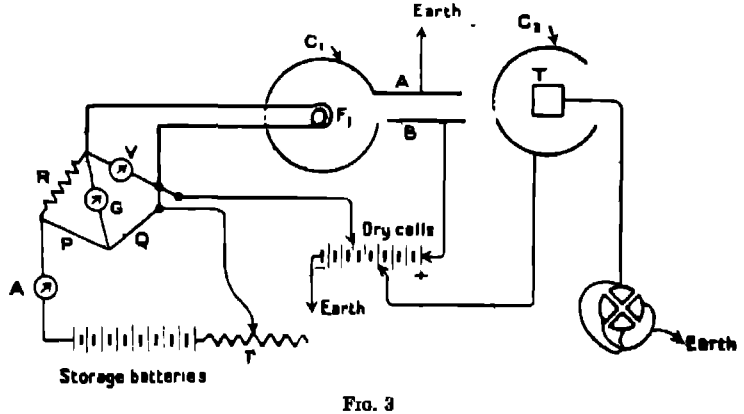

FIG. 3

arrangement, of which F_1 constitutes one arm and P, Q and R are the other arms. R is made of very thick manganine wire, so as to be capable of carrying a large current without heating, and has a resistance of 5·44 ohms., which is comparable with that of the spiral at high temperatures. The resistance of the arm P is 2,000 ohms and that of Q is variable. The P–Q circuit has a resistance large

compared to that of the R-F_1 circuit, so that a very negligible fraction of the current passes through P–Q The heating current of the filament is supplied by a set of storage batteries of about 52 volts through an adjustable rheostat, r. G is the bridge-galvanometer The ammeter, A, measures the heating current of the filament, and the voltmeter, V, records the voltage drop across it The positive potentials on the filament, F_1, the metal plate, B, and the copper cylinder, C_2, are taken from a set of dry cells of about 50 volts, whose negative terminal is put to earth The cylinder, C_1, with the condenser metal plate, A, is also earthed. The target-holder is connected to the electrometer by means of a wire running through an earthed metal tube

4. *Measurements of Temperature*

The temperature of the filament is estimated by three independent methods: (I) by direct measurement of its resistance, (II) by the wattage input given by the voltage drop and heating current in the filament, and also (III) by measurement of saturated thermionic current. Owing to the fairly large length of the tungsten wire used for the filament, any correction due to end-losses is very small, and it is thought unnecessary to introduce it, particularly in view of the fact that radiation from all parts of the filament is operative in producing the observed photo-electric current so that an estimate of the average temperature of the source is more desirable than that of its central part alone In practice it is found troublesome to employ the three methods of measurement in each individual experiment Occasional comparison of the estimation of temperature by the different methods shows fairly satisfactory agreement. The methods (I) and (II) can be equally relied upon. The estimations of temperature given in the following pages are all made from direct measurements of resistances of the filament, and the scale of temperature adopted is that of Worthing and Forsythe *

5. *Experimental Results*

Measurements on total photo-electric emission of electrons from eleven elements—Al, Fe, Mo, C, Zn, Pt, Ag, Au, Ta, W and Ni—are given, and the constants of the equation

$$I_{phot} = A_{phot}\ T^2\ \varepsilon^{-b/T} \left[b = \frac{h\nu_0}{k} \right]$$

are determined from these data by plotting graphs of $(\log_{10} I - 2\log_{10} T)$ against T^{-1} (figs. 4, 5 and 6).

* Report on 'The Properties of Tungsten and the Characteristics of Tungsten Lamps.' See also Worthing, 'Phys. Rev.,' vol. 19, p. 436 (1922).

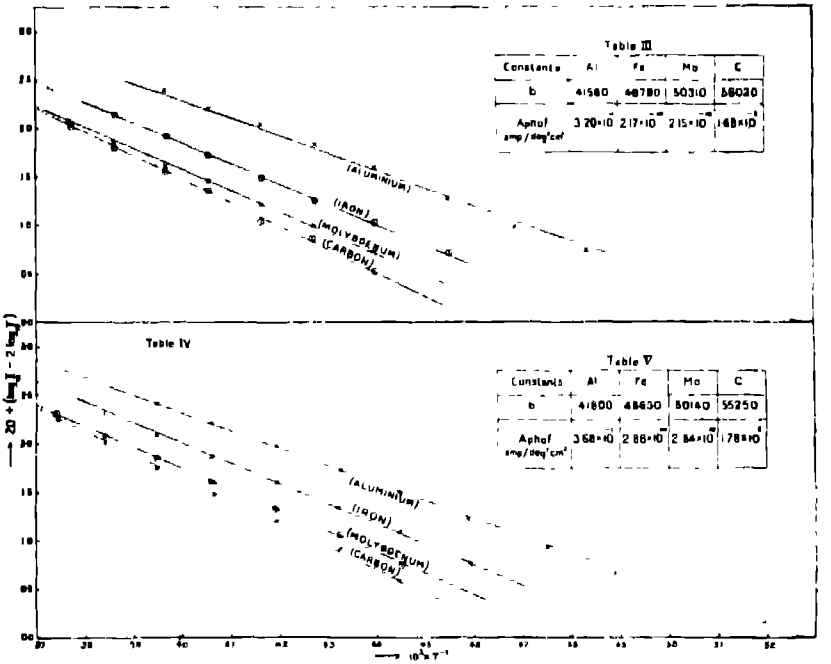
Table III
Constants | Al | Fe | Mo | C
b | 41580 | 48780 | 50310 | 58020
Aphof | 3·20×10 | 2·17×10 | 2·15×10 | 1·68×10
(ALUMINIUM)
(IRON)
(MOLYBDENUM)
(CARBON)
Table IV
Table V
Constants | Al | Fe | Mo | C
b | 41800 | 48630 | 50140 | 55250
Aphof | 3·68×10 | 2·88×10 | 2·84×10 | 1·78×10
(ALUMINIUM)
(IRON)
(MOLYBDENUM)
(CARBON)

FIG. 4

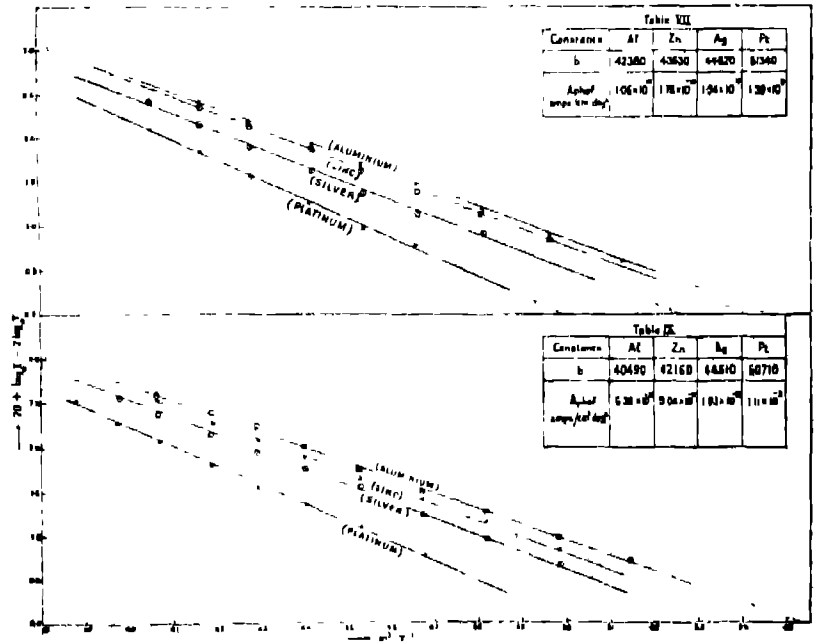
Table VII
Constants | Al | Zn | Ag | Pt
b | 42380 | 43630 | 44820 | 51340
(ALUMINIUM)
(ZINC)
(SILVER)
(PLATINUM)
Table IX
Constants | Al | Zn | Ag | Pt
b | 40490 | 42150 | 44810 | 50710
(ALUMINIUM)
(ZINC)
(SILVER)
(PLATINUM)

FIG. 5

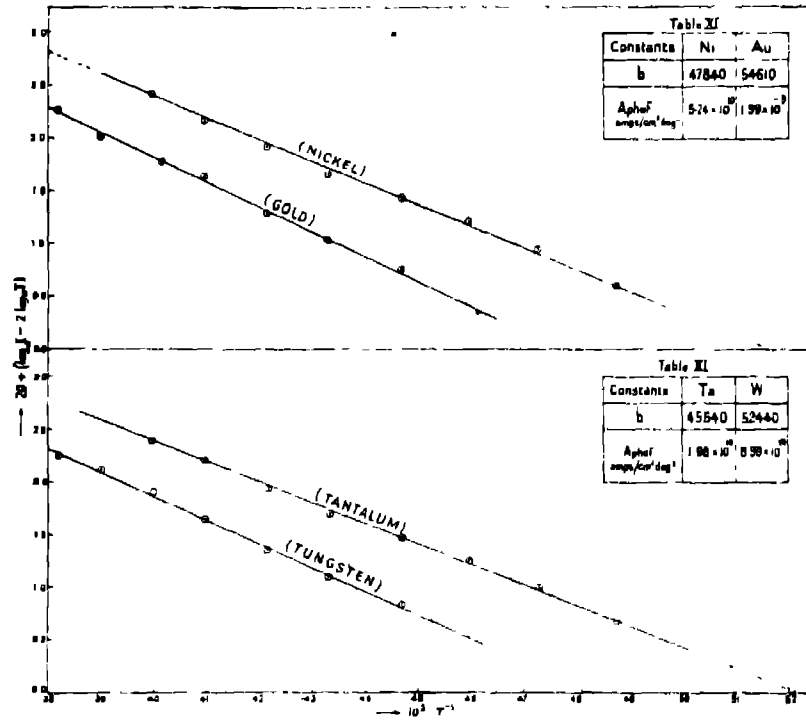

FIG 6

The specimens were supplied by Johnson, Mathey and Co They were not subjected to any special heat-treatment in these experiments, but were cleaned with sand-paper before inserting the target-holder into the apparatus. The pumps were started just after its insertion, and a vacuum of the order 10^{-6} mm. could be attained in about two hours' time

The range of temperatures covered by the present experiments extends from 1900°A to 2700°A. The pressure inside the apparatus was always about 10^{-7} mm. when the photo-electric currents were measured At higher temperatures evaporation of tungsten from the radiating source interferes with the maintenance of satisfactory working conditions inside the apparatus, and it is found difficult to maintain a vacuum at a pressure lower than 10^{-6} mm.

Table II

T°A	$I_{phot} \times 10^{10}$ amps per sq cm			
	Al	Fe	Mo	C
2072	2 240	—	—	—
2139	4 340	—	—	—
2194	9 241	3 151	—	—
2272	20 02	5 672	2 801	1 761
2339	40 40	9 590	5 463	5 042
2402	68 71	17 53	10 11	10 92
2465	127 4	31 80	17 07	14·62
2528	169 2	53·90	24 56	24 16
2587	—	93 11	43 76	41·90
2650	—	-	82·60	72·11

Table III

$10^4 \times T^{-1}$	$20 + (\log_{10} I_{phot} - 2 \log_{10} T)$			
	Al	Fe	Mo	C
0 4826	0·7174	—	—	—
0 4688	0 9795	—	—	—
0 4557	1 2833	0 7160	—	—
0·4401	1 5888	1 0412	0 7348	0·5331
0·4276	1 8684	1 2538	0 9994	0 9646
0 4164	2 0761	1 4827	1 2437	1·2772
0 4057	2 2216	1 7196	1·4488	1 3814
0·3972	2 4220	1 9258	1 5845	1 5773
0 3865	—	2 1433	1 8155	1·7956
0 3774	—	—	2 0706	2 0116

Table IV *

T°A	$I_{phot} \times 10^{10}$ amp per sq cm			
	Al	Fe	Mo	C
2040	1 792	—	—	—
2106	4 048	—	—	—
2181	7 508	2 800	—	—
2248	14 90	6 278	2·804	2 024
2317	29 16	11 87	6 034	4·550
2396	55·12	23·34	11 87	9 094
2461	103 7	42 42	23 34	18 42
2531	175 0	77 78	43 74	30·30
2602	—	127 3	77 78	71·82
2676	—	—	155 6	140·0

* Tables IV and VIII contain a second set of observations made on these specimens after fresh scraping with a sharp knife

Table V.

$10^4\ T^{-1}$	$20 + (\log_{10} I_{phot} - 2\log_{10} T)$			
	Al	Fe	Mo	C
0 4898	0 6318		—	—
0 4749	0 9151	—	—	—
0 4585	1 2016	0·7698	—	—
0 4448	1 4694	1 0941	0·7440	0·6024
0 4316	1 7350	1·3447	1 0508	0 9282
0 4198	1 9822	1 6080	1 3153	1·1996
0 4063	2 2334	1 8454	1·5840	1·4831
0 3951	2 4362	2 0840	1 8341	1 7588
0 3843	—	2 2740	2 0600	2 0254
0 3737	—	—	2 3370	2 2911

Table VI.

T°A	$I_{phot} \times 10^{13}$ amp per sq cm.			
	Al	Zn	Ag	Pt
1050	1 405	—	—	—
2014	3·222	2 678	—	—
2080	6 500	5 859	3 485	—
2145	12 56	10 97	0·162	2 726
2210	23 40	19 50	10·97	4 556
2278	43 87	37 94	21·94	9·523
2337	82 62	73 91	45·29	19·50
2402	155 6	134 4	87·74	41·29
2463	—	—	158 8	82 62
2526	—	—	—	128 4
2584	—	—	—	219 4

Table VII

$10^4\ T^{-1}$	$20 + (\log_{10} I_{phot} - 2\log_{10} T)$			
	Al	Zn	Ag	Pt
0 5128	0 5947	—	—	—
0 4965	0 9001	0 8206	—	—
0·4808	1 1469	1·1309	0 0063	—
0·4662	1 4854	1 3774	1 1268	0·7995
0·4525	1 6805	1 6015	1·3516	0 9599
0·4421	1 9270	1 8839	1·6260	1·2636
0·4279	2 1705	2 1311	1·9184	1·5749
0·4170	2·4319	2·3861	2 1820	1·8782
0·4060	—	—	2·4176	2·1559
0·3959	—	—	—	2·3850
0·3870	—	—	—	2·5171

Table VIII

T°A	$I_{phot} \times 10^{13}$ amp per sq cm			
	Al.	Zn	Ag	Pt
1045	1 045	—	—	—
2008	3 816	2 079	1 819	—
2076	7 889	5 754	3 813	—
2140	14 47	11 00	7·672	2 590
2209	27 54	21 04	16 91	6·158
2271	51 05	41 29	28 95	11 61
2330	93·56	66 85	47 25	19·83
2394	140 4	107 9	77 98	36·04
2460	234 0	200 5	140 4	70·20
2517	—	—	234 0	117·0
2578	—	—	—	216 0

Table IX.

$10^3 \times T^{-1}$	$20 + (\log_{10} I_{phot} - 2 \log_{10} T)$			
	Al	Zn	Ag	Pt
0 5142	0 7110	—	—	—
0 4981	0 9759	0·8224	0 6542	—
0 4817	1·2626	1 1256	0·9471	—
0·4673	1 4996	1·4145	1 2239	0 7523
0·4529	1 7516	1 6530	1 5401	1 1012
0·4403	1 9956	1 9034	1 7492	1·3522
0 4292	2 2365	2 0905	1 9398	1·5560
0·4191	2 3880	2 2748	2 1336	1 9091
0 4065	2 5873	2 5204	2·3655	2 0645
0 3973	—	—	2 5673	2 2664
0 3879	—	—	—	2 5119

Table X.

T°A	$I_{phot} \times 10^{13}$ amp /cm ^{2}			
	Ta	W	Ni.	Au
2051	1 072	—	1 713	—
2116	4 555	—	3 087	—
2175	8 090	—	7·798	—
2240	15 60	3·474	13·50	2 864
2310	26 00	6·619	24·21	5 846
2371	47·40	13 00	46·80	10·97
2441	93 58	26 00	90·56	27 05
2502	147 8	50·14	164 8	36 65
2562	—	85·09	—	70·20
2623	—	122·1	—	127 4

Table XI.

10^3 T^{-1}	$20 + (\log_{10} I_{phot} - 2 \log_{10} T)$			
	Ta	W	Ni	Au
0·4876	0·6708	—	0·6095	—
0·4726	1·007	—	0·9492	—
0·4597	1·2784	—	1·2172	—
0·4464	1·4929	0·8407	1·4301	0·7572
0·4329	1·6880	1·0928	1·6570	1·0360
0·4217	1·9257	1·3640	1·9203	1·2902
0·4096	2·1962	1·6400	2·1847	1·6571
0·3998	2·3729	1·9036	2·4206	1·7542
0·3909	—	2·1128	—	2·0293
0·3821	—	2·2490	—	2·2883

That the variation of total photo-electric currents from all these metals with temperature of the source are satisfactorily represented by Richardson's law of thermionic emission is shown by the linear plots of $(\log_{10} I_{phot} - 2 \log_{10} T)$ against T^{-1} in figs. 4, 5 and 6.

7. *Intensity of the Incident Radiation at the Surface of the Targets.*

In order to be able to compare the observed photo-electric currents with any theoretical calculations, one has to know what proportion of the radiation emitted by the tungsten-source reaches the photo-electric target. An estimation of this necessarily involves considerable uncertainty, owing to the geometrical arrangements of the apparatus and the unknown correction for cooling at the ends of the filament.

If E_ν be the emissivity of tungsten for radiation of frequency ν, and K_ν be the specific intensity of "black-body" radiation of the same temperature as that of the tungsten-source, its specific intensity of emission is $E_\nu . K_\nu$, and the amount of radiation falling per second on unit area of the target is equal to $f . E_\nu . K_\nu$, where f is a fraction determined by the distance between the source and the target, and other geometrical arrangements of the equipment.

The distance between the source and the target in the present experiments is 6·5 cm. The slit S_2 is about 5 mm. in front of the target, and has a width 0·23 mm. For practical purposes, therefore, the portion of the target receiving radiation can be regarded as a part of a cylinder coaxial with a thin cylindrical source of light, and an approximate calculation can be made by taking the effective emitting surface of the helical source of radiation as equal to half the total surface of the tungsten-wire wound into the spiral.

The calculation of f is made as follows :—

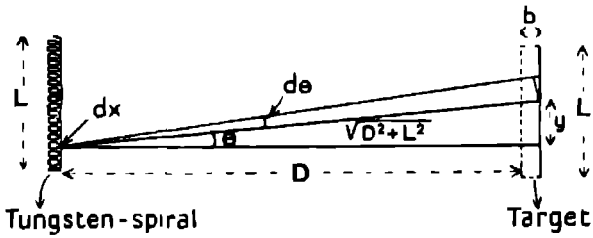

FIG. 7.

L = height of the target and also of the tungsten-spiral D = distance between the target and the source. b = breadth of the target receiving light.

The solid angle subtended at a point dx in the filament by a surface-element $b \cdot dy$ of the target (fig. 7) is equal to

$$\frac{b\ dy \cos\theta}{(D^2+y^2)} = \frac{b \cdot D\ dy}{(D^2+y^2)^{3/2}}. \tag{1}$$

Let Q be the quantity of light emitted per second by unit length of the helical source of light. The amount received per second by the target of area $b \times L$ is therefore given by

$$Q \int_0^{L} dx \times \frac{b\ D}{4\pi} \cdot \int_0^{L} \frac{dy}{(D^2+y^2)^{3/2}}$$
$$= \frac{Q\ L}{4\pi} \cdot \frac{b \cdot L}{D \cdot (D^2+L^2)^{1/2}} \tag{2}$$

Now $Q \times L$ represents the total quantity of radiation emitted outwards by the source per second, and is equal to

$$\frac{2\pi r\ l}{2} \times 4\pi E_\nu \cdot K_\nu$$
$$= 4\pi^2 \cdot r \cdot l \cdot E_\nu \cdot K_\nu \tag{3}$$

where r and l are the radius and length of the tungsten-wire wound into the spiral and K_ν is the specific intensity of unpolarised "black-body" radiation of frequency ν.

Thus the quantity of radiant energy falling per second on a square centimetre of the target is equal to

$$\frac{\pi\ r\ l \cdot E_\nu \cdot K_\nu}{D \cdot (D^2+L^2)^{\frac{1}{2}}} = f\ E_\nu \cdot K_\nu. \tag{4}$$

In the present experiments $r = 0{\cdot}005$ cm., $l = 8{\cdot}5$ cm., $D = 6{\cdot}5$ cm., $L = 2{\cdot}0$ cm.

Therefore $$f = 3\ 02 \times 10^{-3}. \qquad (5)$$

8. *Rôle of Radiation in Thermionic and Photo-Electric Phenomena*

As a preliminary to the following discussion, it is necessary to state briefly the recent developments in the ideas of radiation-structure, a comprehensive account of which has been given by E. C. Stoner ('Proc. Camb. Phil. Soc.,' vol. 22, part 4, p. 577 (1925)). It is well known that the whole range of phenomena typified by the photo-electric action necessitates the adoption of some form of light-quantum hypothesis. The question whether radiation spreads in waves with power to collapse at a point or travels linearly as discrete entities of energy is, perhaps, still an open one.

But if energy and momentum are to be conserved in the individual processes of emission, absorption and scattering, there seems no escape from the conclusion that radiation is propagated in linearly directed quanta. The writer believes that the recent experiments on the "Compton effect" and on the associated idea of mono-electronic scattering in relation to "fish tracks"* due to recoil electrons have sufficiently strengthened the position of the corpuscular theory of radiation to warrant a speculation on the "size" of a light-quant. Such speculations have already enabled Ornstein and Burger ('Z. f. Physik,' vol. 20, pp. 345, 351, and vol. 21, p. 358 (1924), and other papers) to give a coherent account of various physical facts hitherto unexplained on the quantum theory. There is, however, some vagueness in the definition of the terms "cross-section" and "volume" of a light-quant. As pointed out by Stoner, the same difficulty arises in defining exactly the size of an electron. Several writers agree that a light-quant has its energy concentrated in a "sphere" of volume $q\lambda^3$, where λ is the wave-length. The value of q crudely estimated by different writers† does not agree, but is found to be of the order of a tenth. It is assumed in this paper that a light-quant is linearly directed and spatially localised, and that its sphere of action has a radius equal to λ.

In order to appreciate fully the distinction between the operation of radiation

* C. T. R. Wilson, 'Roy. Soc. Proc.,' A, vol. 104, p. 1 (1923); Skobelzyn, 'Z. f. Physik,' vol. 28, p. 278 (1924); Compton, 'Phys. Rev.,' vol. 23, p. 439 (1924); W. Bothe, 'Z. f. Physik,' vol. 16, p. 319 (1923); *ibid.*, vol. 26, p. 59 (1926).

† Ornstein and Burger (*loc. cit.*), "volume" of a light-quant $= \frac{1}{6\pi^3}.\lambda^3$. Erich Marx, ('Z. f. Physik,' vol. 27, p. 248 (1924)), "cross-section" $= \frac{3}{4\pi}\lambda^2$.

on a system in temperature-equilibrium and that of high-temperature radiation on a cold system, it is necessary to direct attention to the essentially different conditions under which the molecules or atoms execute their functions as converters of radiation. The conception of matter and radiation being at one and the same temperature means that, as a result of absorption or emission, a certain fixed and stationary distribution of energies is maintained amongst the various frequencies. If by any process a set of frequencies is removed, the system has to make good the loss by a corresponding reverse process For the maintenance of the stationary and isotropic character of the radiation, the molecules or atoms are, therefore, constrained to work in two reverse processes

In the action of high-temperature radiation on a cold system, the atoms or molecules accommodate and utilise radiant energy for any purpose by means of unidirectional processes. The absence of any constraint on their functioning as converters of radiation leaves them free to run the different unidirectional processes of conversion at rates compatible with their mechanical power under their working condition The intensity of radiation is highest just at the surface of incidence, and falls off rapidly with the depth of penetration, the energy being absorbed in the processes (i) of photo-electric ejection of electrons, (ii) of excitation of atoms to states of higher energy, (iii) of thermal degradation, and also (iv) of scattering or dispersion

Superficially it appears anomalous that the atomic converters should work faster under some constraint than when they are free A little consideration, however, shows that molecules or atoms in the first case cannot afford to be slower in one direction than in the other; so that, when matter and radiation are at one and the same temperature, the rivalling process compels the atomic machines to display a high mechanical power of conversion of radiation But they can afford to be lazy when they have no rivalling process with which to compete.

9. *Radiation Theory of Thermionic Emission*

In a previous paper (*loc. cit.*) an attempt was made by the writer to explain thermionic emission of electrons from hot bodies on the basis of the radiation theory. This phenomenon is the simplest of a class of thermal reactions which go by the name "evaporation." Some points of interest in connection with the present discussion were not made clear in the former paper. In view of the fact that this phenomenon is fully illustrative of the principles involved in the study of the action of radiation on matter in temperature equilibrium, a fresh discussion on the subject is given below.

Consider a piece of metal immersed in a bath of "black-body" radiation

with which it is in equilibrium at a temperature T°A. If the absorption of a light-quant $h\nu$ by the metal results in the evaporation of an electron with velocity v, it is believed that the condensation of a v-electron is invariably attended by the emission of a light-quant $h\nu$. The stationary state of the radiation in the "Hahlraum" is maintained by the working of the two reverse processes according to the unit mechanism

$$h\nu \rightleftarrows \tfrac{1}{2}mv^2 + \phi, \tag{1}$$

where ϕ represents the energy necessary to release an electron from its bondage and is equal to $h\nu_0$

The number of "light-quants" with frequencies between ν and $\nu + d\nu$ passing through unit area in time dt in a cone of solid angle $d\Omega$ in the direction θ is given by the expression*

$$2\ \frac{K\nu\, d\nu}{h\nu} \cos\theta \,.\, d\Omega\ \ dt, \tag{2}$$

where $K\nu$ is the specific intensity of radiation of frequency ν Similarly, the stream of electrons moving with velocity v through unit area in time dt in a cone $d\Omega$ in direction θ is given by the expression

$$n_v\ v \,.\, \cos\theta \,.\, d\Omega\ \ dt, \tag{3}$$

where n_v is the density of v-electrons in the Hahlraum

Let there be N atomic centres of condensations or evaporation of electrons per unit area of the metal surface. The "cross-section" of a light-quant for collision is $\pi\lambda^2$, but each quant-atom encounter is not inelastic. If $C(\nu)$ be the chance that an atom-quant encounter results in the ejection of an electron, then we can take the "effective area" for an inelastic quant-atom collision to be α_ν equal to $\pi\lambda^2 \,.\, C(\nu)$. Thus the number† of condensations of light-quants per unit area of the metal surface in time dt is

$$4\pi \,.\, \alpha_\nu \,.\, N \,.\, \frac{K\nu \,.\, d\nu}{h\nu} \,.\, dt \tag{4}$$

α_ν has the dimension of an area and may be defined as the atomic co-efficient of absorption of radiation. Also if β_v be the "effective area" presented by an atom to the capture of a v-electron, the number of condensations of such electrons per unit area in time dt is

$$4\pi \,.\, \beta_v \,.\, N \,.\, n_v \,.\, v \,.\, dt. \tag{5}$$

* The radiation is unpolarised and isotropic. So the factor 2.

† Those moving towards the surface at any instant only count in the collisions.

In the stationary state of temperature radiation the expressions (4) and (5) must be equal. Hence one obtains

$$n_\nu \cdot v = \frac{\alpha_\nu}{\beta_\nu} \frac{K\, d\nu}{h\nu}. \tag{6}$$

The corpuscular theory of radiation regards the events of emission and absorption by atoms as independent phenomena, all involving the same energy $h\nu$, but it has no measure of the frequency of occurrence of such events. The presence of thermo-dynamic equilibrium between matter and radiation in the present problem, however, enables one to correlate the probabilities of photo-electric ejection and the associated reverse process of photo-electric capture of electrons by the method of calculation introduced by Einstein in his well-known deduction of Planck's law of radiation, wherein he confines his attention only to the processes of excitation of atoms to states of higher energy and of reversion of excited atoms to the normal state. The relation* between α_ν and β_ν obtained by the use of Einstein's line of reasoning is as follows:

$$\frac{\alpha_\nu}{\beta_\nu} = \frac{2m\nu^2}{\sigma h^2 \nu^2} \cdot (h\nu - h\nu_0), \tag{7}$$

where σ is a statistical weight factor determined by the relative *a priori* probabilities of an atom in the normal and ionised states.

The relation (7) embodies the nature of interdependence of the probabilities of the two competing processes. On combining relations (7), (6) and (3), one obtains after integration the following expression for the rate of thermionic emission per second per unit area:

$$N_{therm} = \frac{2\pi m k^2}{\sigma h^3}\, T^2\, \epsilon^{-h\nu_0/kT}. \tag{8}$$

Also from (7) it follows that

$$C(\nu) = \frac{2}{\pi\sigma} \cdot \frac{m}{h} \cdot \beta_\nu \cdot (\nu - \nu_0),$$

i.e. apart from the indirect dependence on ν through β_ν, the chance that a quant-atom encounter shall result in the ejection of a v-electron is proportional to $(\nu - \nu_0)$. This conclusion will be found of interest in connection with the study of the action of high-temperature radiation on a cold system.

10. *Photo-Electric Emission.*

The absorption of radiation can be brought about by various conceivable atomic processes. But attention will be confined here only to the process of photo-electric absorption.

* S. C. Roy, 'Roy. Soc. Proc.,' A, vol. 110, relation (12), p. 549 (1926).

In the present problem there is no rivalling process with which to relate the process of absorption The conditions of the problem are such as to demand a fuller knowledge of the mechanism of photo-electric absorption of radiation than one possesses at present All one knows is that the catastrophic event of the absorption of a light-quant $h\nu$ by the atomic machine results in the expulsion of an electron with velocity v given by Einstein's equation,

$$\tfrac{1}{2}mv^2 = h\nu - h\nu_0,$$

when ν is greater than ν_0. How frequently the atoms allow such catastrophic events to take place one does not know. The problem, however, entails in it the idea of "continuity of happening" of quantum events in so far as such events are taking place smoothly in one direction, and one naturally enquires if one can call in the aid of the classical theory to formulate a scheme of the mechanical power with which the atomic systems work out such catastrophic events A way of possible approach to the missing statistics of quantum events of photo-electric absorption is indicated in the following pages The attempt, however, is only a tentative one, and the assumptions and arguments adopted are mainly of a provisional character

It is supposed that a light-quant offers a target of area $\pi\lambda^2$ in its encounter with an atom, and that the time* for which the quant-atom encounter lasts is equal to T/8, where T is the period of the radiation and is equal to $1/\nu$

The effective time τ for an inelastic collision is, however, equal to only a fraction of the whole time of encounter A certain inference as to this "effective time" τ is made from a well-known result† of the classical electro-magnetic theory, namely, if an electron moving with a constant velocity v (*i.e.* without radiation), at an instant t, has its velocity changed by Δv in time Δt, and then again moves with the constant velocity $v + \Delta v$ (*i.e.* without radiation), then if v be small compared to the velocity of light,

$$\frac{\text{(Energy radiated)}}{\text{(Work done on the electron)} - \text{(Energy radiated)}} = \frac{a}{2c}\,\frac{1}{\tau}, \qquad (1)$$

* In making this assumption the writer has kept in mind the following picture of a light wave acting on an electron inside an atom. It is imagined that the atom offers an opportunity to the periodic electric force to break loose the electron only during the interval in which the force is in the increasing phase. This interval comprises all values between zero and T/4. Hence in a large number of wave-atom encounters the average time of encounter is equal to T/8.

† See O W. Richardson's 'Electron Theory of Matter,' p. 261, equation (16), 1916 edition.

where a is the radius of the electron and the reciprocal of the time τ is equal to $\frac{1}{v} \cdot \frac{\Delta v}{\Delta t}$.

In analogy with this classical result, one infers that in the converse process of the photo-electric absorption of a light-quant $h\nu$, the "effective time" τ is given by the relation

$$\frac{h\nu \text{ (absorbed)}}{h\nu \text{ (absorbed)} - h\nu_0 \text{ (work done by the electron)}} = \frac{a}{2c} \cdot \frac{1}{\tau}, \tag{2}$$

i e

$$\tau = \frac{a}{2c} \cdot \frac{\nu - \nu_0}{\nu}. \tag{3}$$

Thus the chance that a quant-atom encounter shall be inelastic is given by

$$C(\nu) = \tau \Big/ \frac{T}{8} = 8\nu \cdot \tau = \frac{4a}{c}(\nu - \nu_0), \tag{4}$$

and so the "effective area" for an inelastic quant-atom collision is,

$$\alpha_\nu = C(\nu) \times \pi\lambda^2$$

$$= \frac{8\pi}{3} \cdot \frac{e^2}{mc} \cdot \frac{\nu - \nu_0}{\nu^2}, \tag{5}$$

where the electronic radius is taken equal to $\frac{2}{3}\frac{e^2}{mc^2}$

The relation (5) is in accord with the various outstanding facts pertaining to the operation of monochromatic radiation on metals discussed in the introductory chapter

Consider first the photo-electric absorption of isotropic radiation in a thin metal slab of thickness dx and of area 1 sq cm. If K_ν be the intensity of radiation at the surface of incidence, the amount of energy absorbed by dx per sec. is given by,

$-dK_\nu = h\nu \times$ total number of inelastic atom-quant collisions per sec. in dx,

$= h\nu \times$ "effective collision-area" $\times$ stream of light-quants $\times$ number of atoms in the slab dx,

$$= h\nu \times \pi\lambda^2 \quad C(\nu) \times \frac{K_\nu}{h\nu} \times \frac{D}{M} \cdot dx, \tag{6}$$

where D is the density of the metal and M is the atomic mass of the element. The relation (6) can be re-written in the form

$$\frac{dK_\nu}{K_\nu} = -\pi\lambda^2 \cdot C(\nu) \frac{D}{M} \cdot dx, \tag{7}$$

so that,

$$[K_\nu]_x = [K_\nu]_0 \cdot \epsilon^{-\alpha_\nu \rho x}, \tag{8}$$

where μ_ν is the exponential co-efficient* of photo-electric absorption of radiation of frequency ν and is given by

$$\mu_\nu = \frac{8\pi}{3} \cdot \frac{e^2}{mc} \cdot \frac{\nu - \nu_0}{\nu^2} \cdot \frac{D}{M}. \tag{9}$$

Putting

$$\left.\begin{aligned} e &= 4{\cdot}774 \times 10^{-10} \text{ E S U} \\ m &= 8{\cdot}495 \times 10^{-28} \text{ grams.} \\ c &= 3 \times 10^{10} \text{ cms /sec} \end{aligned}\right\}$$

$$\mu_\nu = 7{\cdot}08 \times 10^{-2} \quad \frac{\nu - \nu_0}{\nu^2} \quad \frac{D}{M} \text{ cm}^{-1} \tag{10}$$

For silver

$$\frac{D}{M} = 5{\cdot}87 \times 10^{22}$$

and

$$[\mu_\nu]_{Ag} = 4{\cdot}16 \times 10^{21} \quad \frac{(\nu - \nu_0)}{\nu^2}. \tag{11}$$

The exponential co-efficient of extinction of light in silver has been determined very carefully by Hagen and Rubens and also by Minor over a considerable range of frequencies in the ultra-violet. The extinction of light is brought about by various atomic processes. The photo-electric absorption, however, sets in only when the frequency exceeds the threshold value. The co-efficient of photo-electric absorption starts by being zero at ν_0, and increases rapidly to higher values according to the relation (11) If, therefore, one plots $\Sigma\mu_\lambda$† against λ, one would expect to find a break in the curve at a particular wave-length shorter than λ_0, when the photo-electric absorption becomes a predominating process. How far this expectation is fulfilled will be evident from the graph (fig. 8) obtained by plotting the experimental data of Minor, and Hagen and Rubens.

* Elements with n electrons in the optical level may be expected to have a co-efficient n times this. But the absorption-data available at present do not enable a decision to be obtained on this point.

† The summation sign signifies that the processes of absorption are more than one.

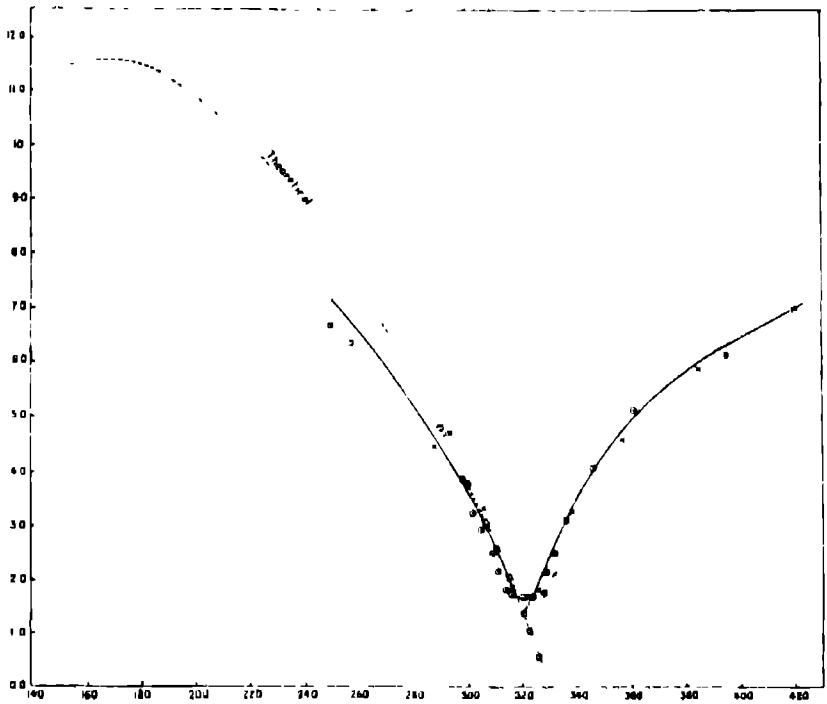

FIG 8.

The theoretical curve, according to expression (11), is also given side by side with the experimental one The expression (11) agrees quantitatively as well as qualitatively with experiment as far as observations go Theory predicts a maximum co-efficient of photo-electric absorption at a wave-length $\lambda_0/2$. How far this is true must be left for future experiments to decide.

The long wave-length limit λ_0 for silver obtained from the $\lambda - \Sigma\mu_\lambda$ curve is 330 $\mu\mu$. This is in good agreement with the value 339 $\mu\mu$ directly determined by Richard Hamer, and also with the value 321·3 $\mu\mu$ given by the present experiment on total photo-electric emission from silver. This method* should form a very satisfactory way of computing short wave-length limits. Unfortunately, the experimental data on other metals available at present are not

* J. J. Weigle (' Phys. Rev.,' vol. 25, p. 893 (1925)) and Richard Hamer (*ibid.*, p. 894) have independantly pointed out this possibility. It should, however, be noted that the break does not occur at the wave-length λ_0 but at a slightly shorter wave-length.

Table XII. Silver.

Minor		Hagen and Rubens.	
$\lambda_{\mu\mu}$	$10^{-5} \times \varkappa_{\mu\lambda}$ cm $^{-1}$ *	$\lambda_{\mu\mu}$.	$10^{-5} \times \varkappa_{\mu\lambda}$ cm $^{-1}$ *
250	6 637	251	5·007
257 3	6 305	288	4 408
274 0	5·865	305	3·256
293	4 161	310	2·514
298 1	3·837	316	1 799
303	3·195	321	1 644
306	2 876	326	1 736
309	2·441	332	2·083
311	2 101	338	3 187
314	1 762	357	4 506
316	1 711	385	5·811
320	1 650	420	6 913
324	1 629	—	—
328	1 724	—	
329	2 131	—	—
332	2 461	—	—
336	3 068	—	—
346	3 996	—	—
361 1	5·048	—	—
395	6 0771	—	—

* Taken from Landolt and Börnstein's Tables of k in the equation

$$\frac{I_x}{I_0} = e^{-\frac{4\pi k}{\lambda} x}, \text{ so that } \varkappa_{\mu\lambda} = \frac{4\pi k}{\lambda}.$$

sufficiently close near the break to ascertain with any degree of precision the values of λ_0, but the experimental measures of the optical absorption on the short wave side of the threshold are in good agreement with the theoretical formula for all metals for which I have been able to find optical data.

Calculation of the photo-electric yield of electrons involves in it not only the problem of absorption of radiation, but also that of absorption of electrons by metals. In the absence of any knowledge of the law of absorption of electrons it is not possible to estimate what fraction of the electrons liberated inside a metal is able to escape out of its surface. In making some measurements on the photo-electric absorption of ultra-violet light by a thin film of gold, Rubens and Ladenburg ('Verh. der. Deutsch. Phys. Ges. Jahrg.,' vol. 9, p. 749 (1907)) observed that while the intensity of radiation on the incident side was about 1,000 times that on the emergent side, the emission of electrons on the front side was about 100 times greater than on the back side. From these data Partzsch and Hallwachs ('Ann. der. Physik,' vol. 41, p. 269 (1913)) have calculated the exponential co-efficients of absorption of radiation and electrons. The values are $\Sigma\overline{\mu}_\nu = 1{\cdot}03 \times 10^6$ cm.$^{-1}$ and $\Sigma\overline{\eta}_\nu = 5{\cdot}96 \times 10^5$ cm.$^{-1}$, where

$\Sigma\bar{\eta}_\nu$ refers to the average value of the electron absorption co-efficient. It is known that $\Sigma\mu_\nu$ is a function of frequency, and presumably $\Sigma\eta_\nu$ also varies with the velocity of electrons, and hence is indirectly a function of frequency. Assuming exponential laws of absorptions, one obtains the following expression for the photo-electric yield of electrons promoted by the action of unit quantity of radiation falling per second per unit area of a metal.

$$F_\nu = N \cdot \frac{8\pi e^2}{3mc} \cdot \frac{\nu - \nu_0}{\nu^3} \cdot \frac{1}{h\nu} \left[1 + \epsilon^{-(\Sigma\mu_\nu + \Sigma\eta_\nu)d} + \epsilon^{-2(\Sigma\mu_\nu + \Sigma\eta_\nu)d} + \ \right]$$

$$= N \cdot \frac{8\pi e^2}{3mch} \cdot \frac{\nu - \nu_0}{\nu^3} \cdot \left[1 - \epsilon^{-(\Sigma\mu_\nu + \Sigma\eta_\nu)d}\right]^{-1}, \qquad (12)$$

where N = number of atoms per unit area

and d = distance between successive atomic layers.

The experimental data on various metals for $\Sigma\mu_\nu$—given by Minor, Drude, Hagen and Rubens, and others—show that its value is greater than 10^5 cm.$^{-1}$ for all frequencies. The maximum amount of photo-electric emission of electrons results from the action of radiation of frequencies near about $\frac{3}{2}\nu_0$. For frequencies in this range, the theoretical expression (11) gives for $\Sigma\mu_\nu$ a value about 10^6 cm.$^{-1}$ for different metals in agreement with Partzsch and Hallwach's computed value for gold. A rigid evaluation of the factor

$$\left[1 - \epsilon^{-(\Sigma\mu_\nu + \Sigma\eta_\nu)d}\right]^{-1}$$

in expression (12) is impossible without a knowledge of the functional relation between $\Sigma\eta_\nu$ and frequency. One can, however, see the order of magnitude of this factor by taking $(\Sigma\mu_\nu + \Sigma\bar{\eta}_\nu)$, equal to $1{\cdot}6 \times 10^6$ cm.$^{-1}$, and $d = 4 \times 10^{-8}$ cm. as an illustration. To a first approximation, the factor is equal to

$$\frac{1}{(\Sigma\bar{\mu} + \Sigma\bar{\eta})\,d} = 15\,6 \qquad (13)$$

Multiplying (12) by the electronic charge and using the values of the constants,

$$F_\nu = 7\ 19 \times 10^{13} \cdot N \cdot \frac{\nu - \nu_0}{\nu^3} \text{coulombs/calorie per sec. per sq. cm.} \qquad (14)$$

except for a factor of the order 15, which probably varies with frequency. It is not known whether $\Sigma\eta_\nu$ increases or decreases with frequency. To simplify the complexity of the problem, let us suppose that $\Sigma\eta_\nu$ increases with frequency in such a manner as to keep $(\Sigma\mu_\nu + \Sigma\eta_\nu)$ practically a constant. If this be so, then from (12),

$$\frac{dF_\nu}{d\nu} = -\frac{3}{\nu^3} + \frac{3\nu_0}{\nu^4}. \qquad (15)$$

For F_ν to be maximum, one obtains the condition

$$\nu_m = \tfrac{1}{2}\nu_0 \tag{16}$$

Experiments on photo-electric emission from several metals have confirmed this relation of O. W Richardson It would be an additional support to the theory if extinction co-efficients show a maximum at a frequency equal to $2\nu_0$ It ought to be possible to verify this point by measurements on metals whose long wave-length limits lie in the visible spectrum

One important conclusion emerging out of the discussion given in the foregoing pages is that the density of the incident stream of light-quants decreases very rapidly with the depth of penetration As regards order of magnitude, it is sufficient, therefore, to estimate the number of electrons emitted from the first layer of atoms, for the bulk of the emitted electrons originates certainly from quant-atom collisions in the first few layers Hence the order of magnitude of the total photo-electric emission per second per unit area is given by

$$N_{phot} = N \int_{\nu_0}^{\infty} \frac{f\ E_\nu\ K_\nu\ d\nu}{h\nu}\ \pi\lambda^2\ C(\nu), \tag{17}$$

where

$$K_\nu = \frac{h\nu^3}{c^2}\ \varepsilon^{-h\nu/kT}$$

E_ν is a function of the frequency, but E O Hulbert's ('Astrophy Journ,' vol 45, p. 149 (1917)) experiments show that its variation with frequency towards the ultra-violet is limited to a very small range The order of photo-electric emission of electrons cannot, therefore, be appreciably affected by its variation To all intents and purposes one can take E_ν as constant in the present calculation. Thus, substituting for C (ν) and K, in (12), and performing the integration, one obtains

$$N_{phot} = f.\bar{E}.N.\frac{8\pi\varepsilon^2k^2}{3mc^3h^3}.\ T^2\ \varepsilon^{-h\nu_0/kT} \tag{18}$$

For a perfect 'black-body' radiator $\bar{E} = 1$

11. *Comparison of Thermionic and Total Photo-Electric Currents.*

The thermionic current from a square centimetre of a hot body at $T^{\circ}A$ is given by

$$I_{therm} = A_{therm}.T^2.\varepsilon^{-h\ \nu_{therm}/kT}, \tag{1}$$

where

$$A_{therm} = \frac{2\pi mk^2}{\sigma h^3}. \tag{2}$$

The total photo-electric current from unit area excited by radiation from a source at T°A is given as regards order of magnitude, by

$$I_{phot.} = A_{phot}\ T^2\ \varepsilon^{-h\nu_{phot}/kT}, \tag{3}$$

where

$$A_{phot} = f\,\bar{E}.N.\frac{8\pi e^2k^2}{3mc^2h^2}. \tag{4}$$

Taking $m = 8\ 995 \times 10^{-28}$ grams, $e = 4{\cdot}774 \times 10^{-10}$ E S U, $k = 1\ 37 \times 10^{-16}$ ergs/deg, $h = 6{\cdot}55 \times 10^{-27}$ ergs/sec, $c = 3 \times 10^{10}$ cm/sec, $\sigma = 1$, $\bar{E} = 0\ 5$ (for tungsten),

$$A_{therm.} = 1\ 81 \times 10^{11}\ \text{E.S.U./cm}^2\text{deg.}^2 = 60\ 2\ \text{amp/cm}^2\ \text{deg}^2 \tag{5}$$

$$A_{phot} = 8{\cdot}22 \times 10^{-12} f.N.\ \text{E S U /cm.}^2\text{deg.}^2$$

$$= 2\ 74 \times 10^{-21} f.N\ \text{amp./cm}^2\text{deg.}^2 \tag{6}$$

The above calculation of A_{phot} takes no account of the electrons emitted from the inside atomic layers. The actual theoretical value of A_{phot} is therefore greater than (6) by a factor of the order 10 as seen from the considerations given in the previous chapter. But until one knows more about electron absorption in metals, one has to remain satisfied only with the calculation of the order of magnitude of the total photo-electric emission.

Putting

$$N = 1/d^2$$

and

$$f = 3\ 02 \times 10^{-3}$$

$$A_{phot} = 8{\cdot}32 \times 10^{-24}\ 1/d^2\ \text{amp/cm}^2\text{deg.}^2, \tag{7}$$

where d is the lattice-constant of the metal.

The following table gives a comparison between the calculated and the experimental values of A_{phot}.

Table XIII

Elements	$10^{10} \times A_{phot}$ (observed)	$10^8 \times d$ cm	$10^{10} \times A_{phot}$ (calculated)	$\frac{A_{phot}\ (calculated)}{A_{phot}\ (observed)}$
Al	0 82	4 040*	50 8	61·9
Zn	1 34	—	—	—
Fe	2 52	2 855*	104 2	41·2
Ni	5 24	3 499*	69 3	13 2
Ag	1 94	4 079*	51 1	26·3
Au	19 9	4 065*	51 3	2 6
Ta	1·98	—	—	—
Pt	12 5	3 912*	55 8	4 4
Mo	2·45	3 142*	85 7	35 0
W	8·99	3 155*	85 2	9·5
C	17·3	—	—	—

* W. P. Davey, 'Phys Rev.,' vol. 25, pp 753–61 (1925)

* The order of the numbers in the last column is generally that of the voltaic series, and the reduction of the observed values of $A_{phot.}$ from the theoretical is of the character to be expected if surface films are present

Also according to theory,

$$\frac{I_{phot.}}{I_{therm}} = \frac{A_{phot.}}{A_{therm}} \cdot \varepsilon^{-h(\nu_{phot.} - \nu_{therm})/kT} = 1\ 38 \times 10^{-25} \cdot N\ \varepsilon^{-h(\nu_{phot.} - \nu_{therm})/kT}. \quad (8)$$

A comparison of (8) with the experimental data given below shows that the theory is not wide off the mark

Table XIV

T°A.	Tantalum			Molybdenum			Tungsten		
	$I_{phot.} \times 10^{12*}$	$I_{therm} \times 10^{11}$†	$\frac{I_{phot.}}{I_{therm}} \times 10^{12}$	$I_{phot.} \times 10^{12*}$	$I_{therm} \times 10^{11}$†	$\frac{I_{phot.}}{I_{therm}} \times 10^{12}$	$I_{phot.} \times 10^{12*}$	$I_{therm} \times 10^{11}$†	$\frac{I_{phot.}}{I_{therm}} \times 10^{12}$
2300	2 72	5 28	5·15	5 28	1 15	4 59	6 29	3 71	1 69
2400	6·65	13·4	4 97	14 1	3 09	4 56	16 7	10 5	1 59
2500	1 52	31 4	4·84	35 1	7 76	4·52	45 3	27 4	1 66

* Taken from the graphs

† Data given by S Dushman and J W Ewald, 'General Electric Review,' p 156 (March, 1923).

It will be seen from this table that the experimental ratio $\frac{I_{phot.}}{I_{therm}}$ is practically constant and independent of temperature, which indicates that the exponential factor in the expression (8) is unimportant Hence $\nu_{phot.}$ and ν_{therm} are either identical for Ta, Mo and W, or differ from each other by an insignificant amount.

The data in the following table suggests that this is true generally.

$$\phi = \frac{kb}{e} = 0{\cdot}862 \times 10^{-4}\ b \text{ volts},$$

$$\lambda_0 = \frac{12{\cdot}36}{\phi} \times 10^{-5} \text{ cm.}$$

Elements.	Atomic Volume	Thermionic †			Total Photo-electric.*			Direct.
		b_{therm}	ϕ_{therm}	λ_{therm} Å.U	b_{phot}	ϕ_{phot}	λ_{phot} Å.U.	λ_0 Å U
Cs	70 6	16,000 (1)	1·38	9954	—	—	—	7500 (10)
K	45 5	18,670 (3)	1 61	7680	—	—	—	7000 (3)
Na	23 7	24,240 (4)	2·09	6149	—	—	—	5770–5830 (11)
								6235 (12)
								6800 (13)
								5980–6330 (14)
Ca	25 8	26,000 (1)	2 24	5517	—	—	—	4000 (2)
Al	10 4	—	—	—	41,430	3 57	3480	3595 (2)
								3600 (11)
								3342 (15)
Zn	9 22	—	—	—	42,890	3 68	3358	3425 (2)
								3570 (11)
								3010–3060 (16)
								3130–3340 (15)
Fe	7·12	—	—	—	48,700	4 2	2944	2870 (2)
								2800–3130 (15)
Ni	6 67	—	—	—	47,840	4 12	2996	3050 (2)
Ag	10 28	—	—	—	44,620	3 85	3213	3390 (2)
								3350 (17)
Au	10 2	—	—	—	54,610	4 71	2625	—
Th	21 1	34,000 (1)	2 94	4201	—	—	—	3465 (2)
Mo	10 7	50,000 (1)	4·31	2867	50,230	4·33	2854	—
Ta	10 93	47,800 (1)	4 12	2997	45,540	3 93	3148	—
		44,500 (5)	3 84	3221				
Pt	9·12	49,660 (5)	4·28	2906	51,020	4·4	2809	2780 (2)
		49,550 (6)	4 27	2914				2800 (11)
								2840 (17)

* Mean of the different determinations is given.

† Computed from thermionic emission data by using the equation $I_{therm} = 60{\cdot}2\ T^2\ e^{-b_{therm}/T}$ amp/cm².

Elements	Atomic Volume.	Thermionic.†			Total Photo electric *			Direct
		$b_{therm.}$	ϕ_{therm}	λ_{therm} Å U	b_{phot}	ϕ_{phot}	λ_{phot} Å U	λ_0 Å U
W	9 63	52,600 (1) 52,300 (7)	4 53 4 51	2728 2738	52,440	4 52	2734	2615 (2) 2650 (18)
C	3·41 (Diamond)	52,430 (8)	4 52	2735				
	5 3 (Graphite)	52,410–57,600 (9)	4 51–4 97	275–250	55,640	4 82	2585	2615 (2) 2550–2600 (16)

(1) Directly taken from a table given by S Dushman, 'Trans. Am Electrochem Soc.,' vol 44, p 111 (1923).
(2) Richard Hamer, 'Jour. Am Optical Soc.,' vol. 9, pp 251–57 (Sept., 1924)
(3) O. W. Richardson and A. F A. Young, *loc. cit.*
(4) O. W. Richardson, 'Phil Trans.,' A, vol. 201, p 497 (1903).
(5) R. Suhrmann, 'Zeits f Physik,' vol. 13, pp. 17–34 (1923).
(6) Schlichter, 'Ann. der Physik,' vol. 47, p. 573 (1915)
(7) C. Davisson and L. H. Germer, 'Phys Rev.,' vol. 20, p 300 (1922)
(8) Langmuir, 'Phys. Rev.,' vol. 11, p. 450 (1913)
(9) Pring and Parker, 'Phil Mag.,' vol. 23, p 102 (1912)
(10) D. W. Cornelius, 'Phys. Rev.,' vol. 1, p 16 (1913).
(11) O. W. Richardson and K. T. Compton, *loc. cit.*
(12) Souder, *loc. cit.*
(13) R. A. Millikan, 'Phys. Rev.,' vol. 7, p 30 (1916).
(14) F. K. Richtmeyer, 'Phys. Rev.,' vol 30, p. 385 (1910)
(15) A. E. Hennings and W. H. Kadesh, 'Phys. Rev.,' vol. 8, p. 209 (1916)
(16) A. Ll. Hughes, 'Photo-Electricity'
(17) O Stuhlmann, 'Phys. Rev.,' vol. 15, p. 550 (1920).
(18) T. H. Harrison, 'Proc. Phys. Soc.,' London, vol. 38, p. 214 (1926) (value for large emission).

10. *Summary.*

(1) This paper contains an account of the measurements of total photo-electric currents from eleven metals excited by complete radiation from a tungsten source at temperatures between 1900–2700° abs. These currents are found to vary with the temperature of the radiating source according to Richardson's law of thermionic emission

(2) Considerations are brought forward to show that the interaction between matter and radiation in the state of thermal equilibrium can proceed much faster than the action of high-temperature radiation on a cold system, and a tentative attempt is made to work out this idea in a quantitative form

(3) An expression is given for the exponential co-efficient of photo-electric absorption in the form

$$\mu_\nu = \frac{8\pi}{3} \frac{e^2}{mc^2} \frac{\nu - \nu_0}{\nu^2} \frac{D}{M}$$

(where D and M are the density and atomic mass of an element), which is in quantitative as well as in qualitative agreement with Minor, Hagen and Rubens, and other observers' optical absorption data on the short-wave side of the threshold.

(4) The photo-electric yield of electrons promoted by the action of unit quantity of radiation of frequency ν falling per second per unit area of a metal is shown to be given by

$$F_\nu = N \frac{8\pi}{3} \cdot \frac{e^2}{mch} \cdot \frac{\nu - \nu_0}{\nu^3} \cdot \left[1 - \varepsilon^{-(\Sigma\mu_\nu + \Sigma\eta_\nu)}\right]^{-1},$$

where $\Sigma\mu_\nu$ and $\Sigma\eta_\nu$ are respectively the co-efficients of absorption of radiation and electrons, d is the distance between successive atomic layers, and N is the number of atoms per unit area.

(5) An approximate calculation of the total photo-electric current leads to the expression,

$$I_{phot} = f \bar{E} N \cdot \frac{8\pi e^3 k^2}{3mc^3 h^3} \cdot T^2 \cdot \varepsilon^{-h\nu_0/kT},$$

which is in fair agreement with observed values, f being a constant of the apparatus equal to $3\ 07 \times 10^{-3}$ and $\bar{E}$ being the average emissivity of tungsten.

In conclusion, the writer wishes to express his deep sense of gratitude to Prof. O. W. Richardson for his continued interest and guidance during the progress of this work, and to Mr R. H. Fowler for looking into the manuscript and advancing helpful criticisms

The writer is also indebted to the Government of Assam, India, for a research grant, which enabled him to carry this work to its present condition

---

The Crystal Structure of Meteoric Iron as determined by X-Ray Analysis.

By J Young, B.Sc , F R A S , Lecturer in Physics, University of Birmingham

(Communicated by Prof S W. J Smith, F R S —Received July 23, 1926.)

[Plate 20]

1. *Introduction*

The well-known " Widmanstatten " figures, obtained by etching the polished surface of meteoric iron, suggest the occurrence of two types of crystal structure in alloys of the nickel-iron series

Those figures, easily obtained when the meteorite contains more than 7 per cent. and less than about 14 per cent. of nickel, owe their existence to the presence of two constituents One of these, " taenite," contains a higher percentage of nickel than the other, " kamacite," and is much less easily attacked by etching reagents.

In typical cases the taenite occurs in thin lamellæ, separating much thicker lamellæ of kamacite, arranged octahedrally with respect to one another.

It was suggested to me by Prof. S. W. J. Smith, who placed suitable meteorites at my disposal, that it would be of interest to examine the structure of kamacite and taenite by X-ray methods.

In the materials supplied, the crystal grains were large enough to permit good X-ray reflexions to be obtained from prepared surfaces of single crystals, and it was found to be possible to examine not only the space lattices of kamacite and taenite but also the way in which the two kinds of lattice are orientated with respect to one another at their common boundary.

It is now known that segregation of the type to which the Widmanstätten structure is due is not confined to meteorites, but occurs frequently in artificial alloys of various kinds. Consequently the results of a study of the kind here proposed are of general interest and are the more important in that the structure of artificial alloys is usually so fine grained that it would be difficult, if not impossible, to apply to them the X-ray methods which the large-scale structure of meteoric iron permits

The crystal structure of artificial nickel-iron alloys has been studied by McKeehan,* who has found that in general the crystals are of two types, whose occurrence depends upon the composition of the alloy. When less than 25 per cent. of nickel is present, the structure is body-centred cubic with a parameter which increases from 2·87 A U for pure iron to about 2·89 A U in the alloy richest in nickel, when more than 25 per cent. of nickel is present, the structure is face-centred cubic with a parameter which diminishes from about 3 60 A U in the alloy richest in iron to 3·51 A U. in pure nickel.

McKeehan found that when the percentage of nickel lies between 25 and 30, either or both of these structures can occur in the same alloy. Although his observations seem to show that the body-centred cubic lattice is unobservable in alloys containing more than 30 per cent. of nickel, they are insufficient to fix the percentage of nickel at which, in its turn, the face-centred lattice disappears It can, however, be inferred from the measurements described in the present paper that in meteoric nickel-iron, at any rate, the face-centred lattice persists until the percentage of nickel falls below 7.

2. *The X-Ray Reflexions from the Octahedral Planes of Meteoric Iron*

The first experiments were made to find out the particular crystal planes which the kamacite and taenite present to one another along their common plane surface boundary The Carlton meteorite was selected for this investigation on account of the very regular development of the Widmanstätten structure in it and the consequent ease with which a small area of taenite may be exposed by grinding parallel to an octahedral plane of the structure. As the taenite plates are only about 10 μ thick, it was found a somewhat difficult matter to obtain an area large enough to give a strong X-ray reflexion, but after a number of trials an irregular area of about 5 sq. mm. was exposed, embedded in and surrounded by the kamacite to which it was expected it would be related crystallographically. This face was polished and then lightly etched in dilute nitric acid Plate 20 (*a*) is a low-power photograph of the face. Taenite appears

* 'Phys. Rev.,' vol. 21, p 402 (1923).

as jet black areas and kamacite is shown in half tone. The X-ray reflexions from the surface were examined photographically, using a Shearer tube with interchangeable anticathodes as a source of X-rays, and a Muller X-ray spectrograph made by Hilger. The preliminary experiments were carried out with molybdenum as anticathode, but more accurate results were obtained with a copper anticathode, when it became apparent that the first-order reflexion angles would not be too great with this element. In computing the results the following wave-lengths were adopted —

Copper . .	K_{α_1}	$1\ 537 \times 10^{-8}$ cm.
	K_{α_2}	$1\ 543 \times 10^{-8}$ cm.
	K_β	$1{\cdot}389 \times 10^{-8}$ cm.
Molybdenum . .	K_{α_1}	$0{\cdot}708 \times 10^{-8}$ cm.
	K_{α_2}	$0{\cdot}712 \times 10^{-8}$ cm.

The reflecting angles found for this prepared face of the meteorite are given in Table I, together with the nature of the radiation, the spacing of the crystal planes, the probable source of the reflexions, and the probable parameters of the lattices Results from the same plate are bracketed together. During the exposures the crystal was slightly rocked about an axis parallel to the spectrometer slit.

Table I.

	Radiation	Reflexion Angle	Spacing	Crystal Plane	Parameter	Source.
		° ′	Å U		Å.U	
1.	K_{α_1} Mo	10 4 5	2·022	110	2 860	Kamacite
2	K_{α_1} Mo	0 54	2 060	111	3 570	Taenite
3	K_{α_2} Mo	10 3 5	2·029	110	2·870	Kamacite
4	K_{α_2} Mo	10 7 5	2 027	110	2 867	Kamacite
5.	K_{α_2} Mo	9 57	2 05	111	3 55	Taenite
6	K_{α_1} Cu	21 45	2 075	111	3 595	Taenite
7.	K_{α_1} Cu	22 15	2 030	110	2 873	Kamacite
8	K_{α_2} Cu	22 19	2·022	110	2·865	Kamacite
9	K_{α_2} Cu	21 51	2·066	111	3 579	Taenite
10.	K_{α_2} Cu	21 54	2 062	111	3·573	Taenite

An examination of the above table shows that there are two different spacings parallel to an octahedral plane of the meteorite. These spacings are very nearly equal, and in the photographs give rise to doublets, the components of which are of approximately equal intensity, but are found at different levels on the plate. These levels were found to correspond to the different levels of

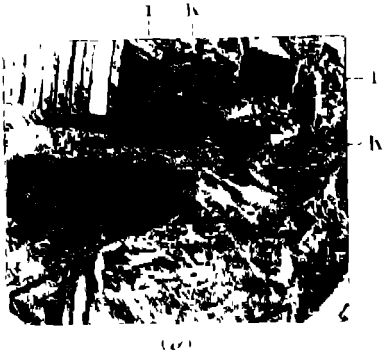

(*a*)

(*b*)

(*a*) Octahedral section of Carlton meteorite, showing taenite (TT) and kamacite (KK)
(*b*) "Prismatic" section of Cañon Diablo meteorite, showing true thickness of crystals of kamacite

(*Facing p. 612*)

the kamacitic and taenitic regions of the specimen, and a careful comparison indicated that in kamacite the spacing is about 2·027 A.U., while in taenite it is about 2·063 A.U. In order to confirm this result the kamacitic region of the specimen was covered with a sheet of lead foil in which a small aperture had been cut. The position of the sheet was adjusted until only taenite could be seen on looking through the aperture, and an X-ray photograph was then taken. This photograph (result 10), indicated a strong reflexion at 21° 54′, and except for some faint lines due to the lead, which were easily identified, there was no other line on the plate. It was therefore clear that the 2·063 A.U. spacing belonged to taenite.

There can hardly be any doubt that kamacite, like iron, is a body-centred cubic crystal. The lattice-constant, calculated on this assumption, agrees with that of iron, while photographs of kamacite taken for other purposes have yielded reflexions from the (211), (100) and (111) planes of such a lattice. The face-centred nature of taenite was shown by taking a powder photograph of a part of the specimen relatively rich in taenite. This showed strong (111), (100), (110) and (311) lines from a face-centred lattice. The kamacitic lines were weak and could only just be identified.

It is therefore clear that, as implied in Table I, the kamacite and taenite grow with respect to one another in such a way that a (110) plane of the kamacite is parallel to a (111) plane of the taenite. The next matter suggesting itself for investigation was to find whether the same relation existed between the small crystals of kamacite and taenite present in the relatively fine-grained regions known as "plessite," which are frequent in the Carlton meteorite. An octahedral area of plessite was therefore X-rayed in the manner described above. The results of the two photographs are given in Table II, an examination of which reveals the same kind of relation in the plessite. A comparison photograph in which the kamacitic-taenitic specimen was mounted on the crystal holder below the plessitic specimen established the complete identity of the lines from the plessite with those from kamacite and taenite separately. The plessitic lines, however, were more diffuse than those obtained from kamacite and taenite separately, and on this account the K_α doublet was not resolved in the photographs giving Table II.

Table II

Radiation	Reflecting Angle	Spacing	Crystal Plane	Parameter	Source
	′ ″	A U		A U	
K_α Mo	10 2	2 033	110	2 874	Kamacite
K_α Mo	9 52	2 009	111	3 480	Taenite
K_α Cu	21 48	2 073	111	3 590	Taenite
K_α Cu	22 14 5	2 033	110	2 872	Kamacite
K_β Cu	19 38 5	2 065	111	3 580	Taenite
K_β Cu	20 4 5	2 024	110	2 862	Kamacite

3. *The Determination of the Orientation of the Kamacite Crystal with respect to the Widmanstätten Structure*

The Widmanstatten structure of the meteorite is determined by the plate-like crystals of kamacite, of which there are four families, corresponding to the planes of a regular octahedron. As shown in § 2, the crystals of kamacite grow with a rhombic dodecahedral plane parallel to the plane of the plate, that is, to a Widmanstatten plane, but as this does not wholly determine the orientation of the kamacite crystal, it is both interesting and important to examine whether this orientation can be fixed more precisely.

As the thickness of the kamacitic plates in the Carlton meteorite (containing about 13 per cent of nickel) is small, necessitating long exposures when sections are examined, another meteorite, the Cañon Diablo (containing about 7 per cent of nickel) was selected for this test on account of the relatively large crystals of kamacite which it contains. The Widmanstätten planes are not so well defined by individual crystals in this meteorite, but by considering the setting of numerous crystals, a fairly good estimate of the position of these planes can be made. X-ray examination of these planes showed that in this meteorite also the Widmanstätten plane is a rhombic dodecahedral plane of the kamacite.

The specimen was then cut perpendicularly to a Widmanstätten plane in such a way that the section exposed was parallel to one of the sides of the equilateral triangles formed by the intersections of the remaining Widmanstatten planes with the above-mentioned Widmanstätten plane.

For convenience, such a plane of section will be referred to as a "prismatic plane" and the sections of the kamacitic plates which it exposes will be described as prismatic areas. The importance of a prismatic plane lies in the fact that although it is not necessarily a rational plane of the kamacite, yet it belongs to a zone which contains several rational planes of both kamacite

and taenite The determination of the angles which the kamacitic planes (100), (110) and (211) of this zone make with the associated prismatic plane would serve to fix the position of the kamacite crystal with respect to the Widmanstatten structure

When the meteorite was cut in the way just described, the section exhibited, after etching, the structure shown in Plate 20 (*b*) The prismatic areas A, B, C, and D of this section belong to a set of parallel kamacitic plates and show the true thicknesses of these plates These areas were examined separately by X-rays from a molybdenum target, the specimen being mounted on the crystal table so that the planes of the kamacite plates were horizontal By using cams varying from 4° to 0 5", the setting of the plane of section at which reflexion occurred in each case could be fixed within a degree

The results are given in Table III, which shows the crystal setting (ι ϵ, angle between X-ray beam and plane of section), the reflecting angle (ι ϵ, the angle between the diffracted beam and the diffracting planes), the plane causing reflexion, and the angle which the reflecting plane makes with the plane of section

Table III.

Area	Crystal Setting	Reflecting Angle	Reflecting Plane	(Crystal Setting) — (Reflecting Angle)
	°	° ′		° ′
A	14·5	17 40	(112)	− 3 10
B	15 5	10 5	(110)	+ 5 25
C	14	17 40	(112)	− 3 40
D	14	17 40	(112)	− 3 40

The inclination of each reflecting plane to the plane of section is indicated by an arrow in Plate 20 (*b*)

The actual plane of section was found by measurement to be about 1·5° from parallelism with a truly prismatic plane as defined above, and, in consequence, the angles in the last column of Table III require correction, by the addition of this amount, to give the inclination of the reflecting planes to a truly prismatic plane of section.

The results suggest two possible arrangements of the kamacite crystal in the meteorite. These are shown diagrammatically in fig. 1, in which the traces of prismatic planes on a Widmanstatten plane are shown as the equilateral triangles, $a\,b\,c$ and $a'\,b'\,c'$, and the traces of the (211) and (110) planes of the kamacite belonging to the same zone are shown as broken lines. The

angles which these latter planes make with the former planes are also indicated in the figure

An X-ray examination of each of the four crystals on another prismatic plane confirmed the existence of the above types of growth in the meteorite, the crystals A and D belonging to type (*a*) and B and C to type (*b*) (see fig 1).

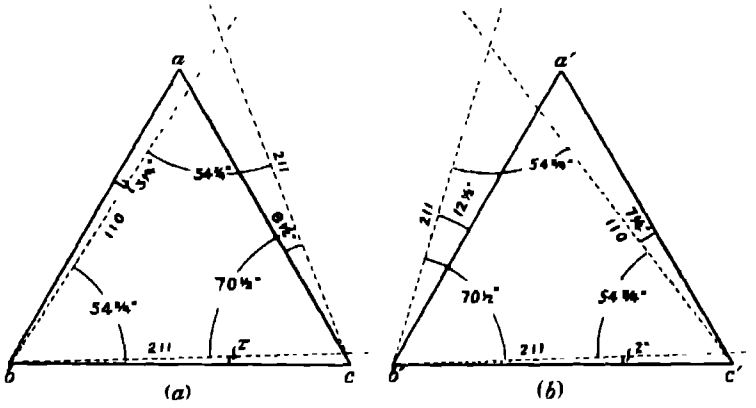

FIG. 1.

4. *Discussion of Results.*

Adopting the values 2 870 A U. and 3·590 A.U. for the respective parameters of the lattices of kamacite and taenite, it is easy to calculate the number of atoms per square A U on the most important planes of the lattices These are given in Table IV.

Table IV.

Plane.	Atoms/10^{-16} cm ^{2}	
	(Kamacite)	(Taenite)
100	0 1214	0 1552
110	0 1718	0 1097
211	0 0992	
111	0 0702	0 1780
310	0 0768	
311		0 0936
312	0 0650	

It will be seen that the two connected planes, (110) of kamacite and (111) of taenite, contain very nearly the same number of atoms per unit area, the number being greater in taenite by about 4 per cent

Even without knowing the crystallographic nature of the solid solution from which the kamacite and taenite crystallise out (though this is almost certain to be, like "γ" iron, face-centred cubic), it may be anticipated that these crystals will orient themselves to that solution in such a way as to make the rearrangement of the atoms a minimum, and, therefore, that the spacings of the atoms in the kamacite and taenite in any particular direction will be those which most resemble each other. When it is remembered that the spacings of the connected planes of kamacite and taenite only differ by 2 per cent. and the concentrations in these planes by 4 per cent, it is immediately obvious that the above condition has been partly satisfied

Fig. 2 shows the atoms on a (111) plane of taenite, together with those on a (110) plane of kamacite on the same scale

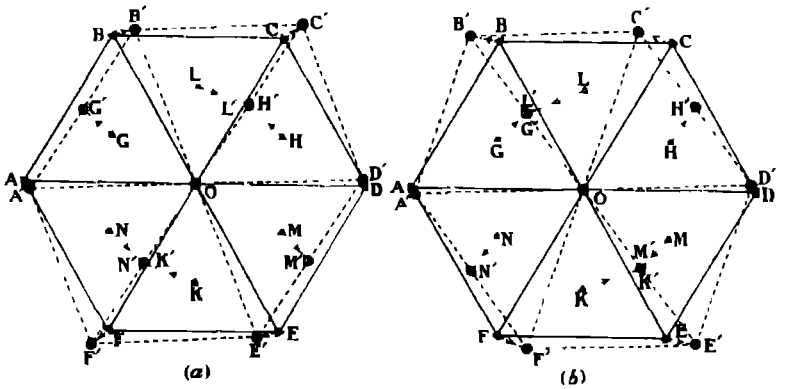

Fig 2

In 2*a* the lattices have been superposed so that the traces of the (211) planes of kamacite which are perpendicular to the plane of the diagram make angles of 2° and 8 5°, respectively, with two of the sides of the equilateral triangles formed by joining the taenite atoms. in 2*b* the superposition is such that the corresponding angles are 2° and 12·5° These are the orientations of the kamacite crystal which were actually found to exist in the Cañon Diablo meteorite (see fig 1)

Consider now the arrangement of atoms in fig. 2. In taenite the atoms

are at the apices of equilateral triangles of side 2·54 A U ; in kamacite the atoms are at the apices of isosceles triangles of base 2 87 Å.U. and side 2·485 Å.U. The approximate equality of the equal sides of the isosceles triangles with those of the equilateral triangles is very striking, and no doubt the approximate coincidence of A O D with A′ O′ D′ is partly due to this equality. Two other considerations should also be noted, viz .—

(1) In fig 2*a*, the trace A E of a (110) plane of taenite, at right angles to the plane of the figure, is inclined at only 3·25° to the trace A′ E′ of a (100) plane of kamacite , in fig 2*b*, the trace A C of a (110) plane of taenite at right angles to the plane of the figure is inclined at 7 25° to the trace A′ C′ of a (100) plane of kamacite As the spacings of these planes differ by about 11 per cent and their atomic concentrations by about 10 per cent , some physical connection between these planes seems not unlikely

(2) In both diagrams of fig 2, the trace F B of a (110) plane of taenite at right angles to the plane of the figure is inclined at only 2 degrees to the trace B′ N′ of a (111) plane of kamacite, and the atomic concentrations and spacings of the (110) planes of taenite are approximately one and a half times those for (111) planes of kamacite

Here also there seems to be some evidence for physical connection between planes which are very nearly parallel in the two types of lattice

5 *The Origin of the Widmanstätten Structure.*

It is of interest, in conclusion, to attempt to find reasons why the relationship between the kamacite and taenite lattices should be that which the experiments have disclosed

For this purpose it is necessary to adopt some view as to the sequence of the transformations from which the Widmanstätten structure results

This sequence has been the subject of many investigations,* which it is outside the purpose of the present communication to discuss According to a view commonly held, the structure is a consequence of recrystallisation, beginning much below the solidification temperature of the meteorite, of which the first stage is the formation of kamacite and the second that of taenite. Prior to this recrystallisation, the material is a homogeneous alloy of iron and nickel with a face-centred lattice of which the parameter is about 3·60 Å U ,† and thus not very different from that of taenite

To a first approximation, therefore, we may take the taenite lattice of

* *Cf.*, *e.g* , S. W J. Smith, 'Phil. Trans.,' A, vol 208, p. 21 (1908)

† *Cf.*, *e g* , Westgren, 'Journ. Iron and Steel Inst.' (1921, 1922, and 1924).

fig 2 as representing that of the "solid solution" from which the kamacite segregates.

In an attempt to form a body-centred lattice, the atoms G and L, fig 2*b*, of the solid solution in octahedral planes respectively above and below the plane of the figure may be imagined to move in their own planes parallel to A C so as to occupy positions respectively above and below the middle point of O B This cannot take place without an outward movement of B, because G and L would then be at distances from O and B less than the minimum distance permitted in the body-centred lattice But such an outward displacement is resisted by the surrounding atoms, with the result that the displacement of B takes the form of a slip B B′, the atoms G and L reaching G′ and L′ In a similar way, C slips to C′, E to E′, F to F′, etc

It is then possible to picture how, by shearing in rows approximately parallel to A D, the atoms in an octahedral plane of the solid solution can arrange themselves in positions conforming with the lattice of kamacite

It is interesting to note, in this connection, that rows of atoms such as A′ O D′ are parallel to a (211) plane of the kamacite, which we have found to be a cleavage plane of this type of crystal. This was proved by X-raying a cleavage plane of the Coahuila meteorite, of which the main constituent is kamacite

With respect to the movement of the atoms in the planes adjacent to those of fig 2, it is to be noted that those of atoms N, K, L, H, *etc*, of fig 2*a* are all very nearly in (100) planes of the kamacite. To a slightly less extent, the same is true of the corresponding atoms of fig. 2*b*

Cleavage along a (100) plane is well known to occur in "α iron," of which the space lattice is practically the same as that of kamacite.

Since a cleavage plane is probably one of considerable stability, the formation of a (100) plane from a plane of the solid solution, having approximately the required number of atoms per unit area, by rearrangement of atoms already in this plane, would not be surprising

Careful examination of the Widmanstatten structure has led others* to suppose that it begins with the formation, along the octahedral planes of the original solution, of very thin lamellæ of kamacite which, as the structure develops, increase in thickness by parallel growths outwards from the initial surfaces

It seems now to be possible to suggest more explicitly why growth should occur in this manner

* *Cf.*, *e.g.*, S. W. J. Smith, *loc. cit.*, p. 102.

On account of the marked resemblance of the (111) plane of the solid solution and the (110) plane of kamacite, it is possible to form from the solid solution, by simply shearing rows of atoms and rearranging the atoms in adjacent planes, as already described, a crystal of kamacite which is only a few planes in thickness but of considerable area This crystal can spread indefinitely in its own plane without causing very much disturbance of the atoms, but is prevented from growing rapidly at right angles to the plane because the atomic movements required are much greater and do not take place in the same direction

Thus, while shearing of rows of atoms in an octahedral plane of the solid solution is relatively easy, the atomic movements involved in forming a (100) plane of kamacite from a (110) plane of the solid solution are more complicated Briefly, there is a "ready-made" plane of kamacite in the solid solution, and for this reason growth is rapid parallel to this plane but slow at right angles to it The parallel growth of the kamacite in Widmanstätten planes is probably emphasised still further by the fact that these planes are not only the planes of kamacite and of the solid solution in which the atomic densities are most nearly equal, but are also the planes of maximum atomic density

If, as is commonly assumed, the temperature at which kamacite begins to separate from the solid solution depends upon the percentage of nickel which the latter contains, decreasing as that percentage increases, it can be inferred that the composition of the kamacite must differ from that of the solution from which it separates The nickel content of the kamacite must, in fact, be less than that of the solid solution with which, at a given temperature, it is in equilibrium Unfortunately, it does not seem very likely at present that this inference can be tested satisfactorily by X-ray methods, but it has two important consequences. The first is that the composition of the kamacitic layers must change continuously as they increase in width The second is that, during the growth towards one another, as the temperature falls, of two adjacent kamacite plates, the nickel content of the narrowing layer of solid solution, which lies between them, must steadily increase. It is probably not yet possible to decide whether the final composition and structure of this latter taenitic layer is always the same Attempts to settle this question by other methods are in progress in this laboratory Meanwhile, by the kindness of my colleague, Mr A A Dee, who has made a detailed photo-micrographic investigation of the Carlton meteorite, I have been able to examine photographs, at high magnifications, of transverse sections of taenite similar to that upon which my X-ray measurements were made. From these it is obvious that the

taenitic bands are not homogeneous, although their surface layers are relatively uniform and are probably those to which my measurements refer

Prof Smith has suggested to me that, if the duplex structure of the taenite band is due to the fact that it contains a eutectoid of kamacite and a nickel-rich alloy, it is possible that when the eutectoid strength of the solid solution is reached, at the surface of a growing kamacite crystal, the eutectoid kamacite which segregates from the surface layer of this solution may attach itself to the already existing kamacite band, leaving behind a thin band of the nickel-rich face-centred alloy which will separate it from the interior of the solid solution in which the conditions of recrystallisation will be different, as Mr Dee's observations show

My warmest thanks are due to Prof Smith not only for suggesting meteorites as a suitable subject for X-ray study and for placing at my disposal the necessary apparatus, but also for the great interest he has taken in the work and the many helpful suggestions he has made I am also indebted to Mr Dee for much information about the metallography of meteorites and of the nickel-iron alloys My best thanks are also due to Mr. G O Harrison of the Physics Workshop for his invaluable help with much of the high-vacuum technique, and for making many of the accessories required in the research

On the Excitation of Polarised Light by Electron Impact.

By H. W B. Skinner, Ph D , M A , Exhibition of 1851, Senior Student.

(Communicated by Sir Ernest Rutherford, Pres R S -- Received July 1, 1926)

(Plate 21)

§ 1 *Introduction*

In the course of some experiments* on polarisation effects shown by mercury lines, emitted from a low-pressure electron-maintained arc, it was found that the yellow mercury lines λ 5770, 5791 are weakly polarised even in the absence of a magnetic field, the direction of the maximum electric vector being parallel to the direction of the discharge From the general characteristics of the effect, it appeared likely that the polarisation is due to the partly directed character of the electron tracks in the arc , and, in this way, one was led to the view that an electron is capable of exciting an atom to the emission of polarised light The present paper describes an attempt to investigate this point more thoroughly.

While the work was in progress, two papers have appeared in which a search for signs of polarisation in the light excited by electron impact has been made The first is by Kossel and Gerthsen† who examined the case of the D lines of Sodium with a negative result This was confirmed by Ellett, Foote and Mohler,‡ who also investigated the case of the mercury line λ 2537 with a positive result, which will be described subsequently These experiments, however, only dealt with a few individual spectral lines. In the present work data have been obtained for all the more prominent lines of the mercury spectrum §

§ 2 *The Source of Light*

It is clear that the chief necessity for the experiments is an electron tube which is capable of producing an intense, perfectly directed stream of electrons.

After some trials, a tube was designed which has proved to work well The design is shown in fig 1 (approximately a quarter of actual size) and fig 2 (half of actual size).

It is an electron tube which runs on mercury vapour at a pressure of one-

* An account of these is in the press.

† 'Ann. d. Physik,' vol. 77, p 273 (1925).

‡ 'Phys Rev ,' vol. 27, p. 31 (1926).

§ Preliminary results were published in 'Nature,' vol. 117, p. 418 (1926).

thousandth of a mm. or less. The tube was exhausted continuously by means of a diffusion pump, and the pressure may be controlled by altering the temperature of the mercury bead M

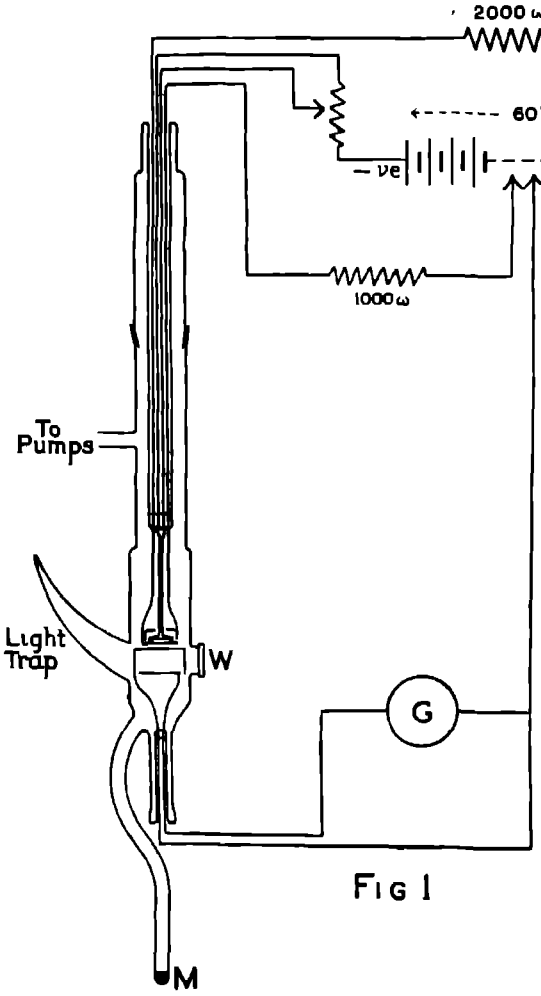

Fig 1

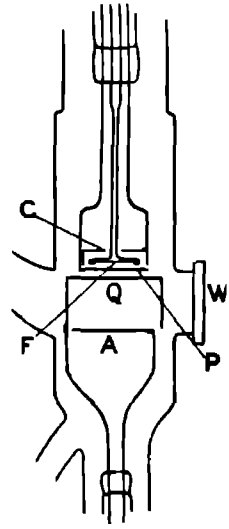

Fig. 2

F is the filament, a narrow platinum strip coated with a mixture of Ba, Sr and Ca oxides. The potential drop across it when heated is about 2 volts C is a cup maintained at a suitable positive potential with respect to F and

acts as a focussing cylinder P is a metal plate with a slit 2 mm. wide, and Q a second plate with a slit 1½ mm. wide Finally there is a third plate A as anode The space between Q and A is surrounded by a metal cylinder joined to Q Two holes are cut in it for observation and its function is electrostatic shielding

The filament, together with the plates C and P, can be removed by means of a ground-glass joint The window W (of fluorite) had to be fixed on with wax, since it must pass the ultra-violet In spite of this the spectrum emitted is one of pure mercury, and the amount of impurity present was certainly less than 10^{-4} mm.

The plate P serves as a grid Normally an accelerating field of 60 volts is applied between F and P, and a retarding field between P and Q. The object of this double potential is to obtain an intense stream of slow electrons Sufficient visible light is emitted for visual observations when the speed of the electrons corresponds to 20 volts A is connected to Q through the galvanometer G which measures the current in the electron jet This at 20 volts is of the order of 1/10th m a

When the tube is working, a well-defined stream of electrons is obtained in the region between Q and A This is made visible by the light emitted from the mercury atoms along its track The light appears as a narrow bluish streak, which hardly spreads out at all in passing from Q to A, and little light comes from points outside the streak. The application of a magnetic field showed that the velocities of the electrons were very uniform, the bright streak was bent into a circle without being noticeably diffused

A photograph showing (slightly enlarged) the appearance of the stream (*a*) without a magnetic field, and (*b*) in a magnetic field of 5 gauss is given in fig 3 (see Plate 21).

§ 3 *Magnetic and Optical Apparatus.*

The tube is placed so that the electron stream runs vertically The light emitted from points immediately under the slit Q is observed in a direction perpendicular to the stream A pair of Helmholtz coils 60 cm in diameter is provided, with axis in the magnetic meridian for balancing out the earth's field. With the aid of a horizontal and a vertical magnetometer this could be accomplished with great accuracy. The main part of the metal portions of the apparatus are of molybdenum, so as to be non-magnetic and not to absorb mercury The electrode seals through the glass are, however, of nickel-iron alloy, welded to molybdenum, close to the seal, and were found to have a negligible magnetic effect in the region used for observation.

There remains the difficulty of heating the filament without providing a greater magnetic field than can be helped This is accomplished by bending the filament leads as shown in fig 2 With a heating current of 4 amps the field in the observation space 15 mm away from the filament is less than 1/50th gauss, and this accuracy of balancing was considered sufficient

A second pair of Helmholtz coils was provided in order to impose a magnetic field These can be placed in any position, but the standard position is with the axis in the direction of observation

For visual observation, an Ilford filter has been used to isolate the yellow mercury lines A Babinet compensator and analysing Nicol prism have been used for detecting polarised light, and measurement is performed by means of the interposition of glass plates at an angle.

Spectroscopic work has also been carried out, using a large Hilger quartz spectrograph (E_1) The high dispersion is necessary in order to separate the lines while using a broad slit. This is required in order that faint fringes may be visible on the spectrum plate

The method adopted for the photographic work is to focus the electron stream on to the Babinet compensator by means of a fluorite lens. The Babinet fringes and electron stream are then focussed with a quartz lens on to the slit of the spectrograph

When the Babinet is employed, we have no direct means of determining the plane of polarisation (*e g*, whether horizontal or vertical). This can, however, be determined by omitting the Babinet and using a Wollaston double-image prism of calcite The method then is simply to place the prism at a distance immediately in front of the tube and to focus the two images of the electron stream with quartz lenses on to the slit of the spectroscope, which is aligned accurately with the direction of the stream. In this way we get two spectra, one corresponding to vibrations parallel to the electron stream and the other to vibrations perpendicular to it It is true that the reflexion losses for these two beams during their passage through the spectrograph may differ slightly, but to the present degree of accuracy this correction proves to be negligible. Thus the relative densities of the two images give the direction and percentage of the polarised light; but the determination of the percentages involves a considerable amount of photometric work and has not yet been accomplished.

To find out whether the upper or lower image of the double-image prism corresponds to light polarised with the electric vector parallel or perpendicular to the stream, a source of light reflected from a glass plate was examined

through the prism The stronger image then corresponds to light polarised with the electric vector parallel to the glass plate.

§ 4. *Results*

In this way it has been found that, in the absence of a magnetic field, most of the mercury lines are polarised, if the speed of the electron is sufficiently near to that corresponding to the excitation voltage. In most cases, the light is polarised with the direction of the maximum electric vector parallel to the electron stream, but in a few instances the perpendicular direction is found

The direction of the plane of polarisation rotates when the tube is turned through an angle about the direction of observation, and, since the direction of the stream is the only factor which can determine the plane of polarisation, there can be no doubt that the effect is caused by the uni-directional character of the electron stream Further, the fact that the light is concentrated in the electron stream instead of spreading out throughout the tube shows (since the mean free path of the mercury atoms is about 3 cm) that the light observed is emitted immediately after an electron impact, and thus the light observed is that directly excited by the impact We are, therefore, dealing with the direct excitation of polarised light by electron impact

Fig 4 is an example of a plate taken with the double-image prism, showing the polarisation of some of the lines by intensity differences between the upper and lower spectra The upper spectrum corresponds to light polarised parallel to the stream Fig 5 shows the lines λ 4347 and 4358 photographed, using a Babinet compensator Here oblique bands show the polarisation of λ 4347 clearly (see Plate 21)

The lines which we have investigated most completely are the lines λ 5770 ($2^1P_1 - 3^1D_2$) and 5791 ($2^1P_1 - 3^1D_2$). These have been produced with a mercury pressure of one-thousandth mm. in the tube Both are polarised with the maximum electric vector parallel to the electron stream. The polarisation measurements have been carried out visually on the two lines together, using a filter for analysis of the light.

The lines passed by this filter are the yellow lines λ 5770 and 5791, a faint and inseparable companion to λ 5791, and three very faint red lines. The red lines certainly, and probably the faint companion also, will have no appreciable influence on the results. The line 5770 is rather fainter than 5791. An exact test of the equality of the degree of polarisation for these two lines has not been performed, but no difference can be noticed by mere inspection, and as we shall

sec later, the percentages of polarisation cannot differ by more than about 5 per cent

The curve of fig 6 shows the variation with the voltage (*i e*, with the energy of the exciting electrons) of the degree of polarisation of the two yellow lines

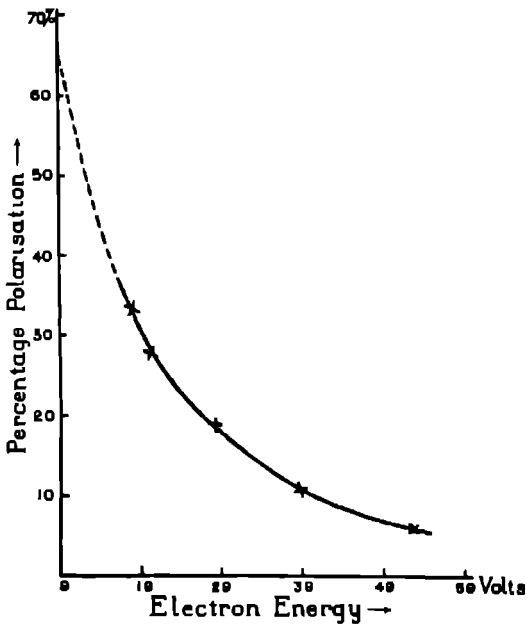

Fig 6

together (for which the excitation voltage is 9 volts) The percentage polarisation is approximately an exponential function of the energy of the electron after impact.

We now come to the effects produced by the application of a magnetic field. These measurements again apply to the case of the two yellow lines together, a filter being used

In the first place we consider the effect of a magnetic field parallel to the electron stream. Fields of strength up to 40 gauss in this direction have been tried and have proved to be without influence on the polarisation.

A field applied at right-angles to the stream has a depolarising action which is at a maximum when the direction of the field coincides with the direction of observation This, then, is the most interesting case. The depolarisation is

then accompanied by a rotation of the plane of polarisation about the axis of the field. The rotation produced by a field of 2 gauss is quite appreciable, but in the strongest fields possible (namely, 12 gauss) there is always some polarisation left. A limit is set to the strength of field which can be used, for, of course, the electron stream is bent into a circle, and if the curvature is too great, observations are not possible In determining the rotation this curvature of the stream was allowed for.

Curves of the rotation and depolarisation due to a magnetic field are given in fig 7. For a reason which will appear subsequently, we have here plotted against H, tan 2δ, where δ is the rotation, and $\sqrt{\Pi_0^2/\Pi^2 - 1}$, where Π is the observed percentage polarisation* and Π_0 is the percentage polarisation in a zero

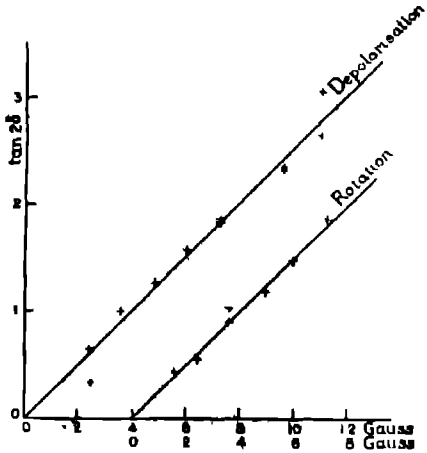

Fig. 7.

field. In both cases the method adopted is such as to exaggerate greatly small errors in the measurements, which can hardly be made more accurately than to within 2° in the case of rotation and to within 1 per cent. in the case of polarisation. The points in both curves corresponding to the stronger fields are particularly liable to error, owing to the considerable depolarisation.

The case of λ 2537 ($1^1S_0 - 2^3P_1$) has also received a good deal of attention.

If the rest of the mercury spectrum is being emitted, the light from this line

* $\Pi = 100\,\frac{I_\parallel - I_\perp}{I_\parallel + I_\perp}$ where $I_\parallel, I_\perp$ are the intensities of the light polarised parallel and perpendicular to a given direction.

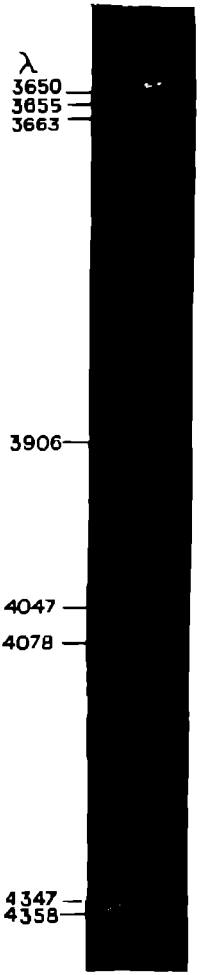

Fig. 4

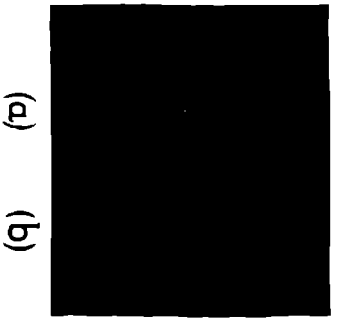

Fig. 3

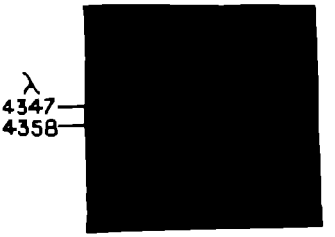

Fig. 5

which is observed will not be wholly that due to direct excitation of the 2^3P_1 state by electron impact. We must work therefore at such a voltage that the other mercury lines are not emitted. One must also work at a much lower pressure than is necessary in the case of the other lines on account of the fact that λ 2537 is absorbed by the normal mercury atom. In a recent paper* Ellett, Foote and Mohler have described the results of this experiment. Working at a pressure of mercury corresponding to a temperature of $-18°$ C. and with an electron speed of 6–7 volts, they found λ 2537 to be 30 per cent. polarised in a plane perpendicular to the electron stream.

This result is, as was pointed out by Ellett, Foote and Mohler, and as will be seen subsequently, difficult to interpret theoretically, and therefore it seemed worth while to obtain confirmatory evidence. With a mercury temperature of $-12°$ and an electron speed of 8 volts, a considerable polarisation perpendicular to the stream was observed. The same result was also obtained using a small spectrograph to analyse the light, thus removing any slight doubt that the effect might be one belonging to "false" light. Ellett, Foote and Mohler arranged their experimental conditions very carefully in such a way that it seems impossible that the light observed should have any other origin than direct electron impact.

They further showed that the effects of a magnetic field on the polarisation of λ 2537 are similar in nature to those we have found for λ 5770, 5791. We have, in fact, also confirmed their conclusion that the polarisation in a plane perpendicular to direction of the electron stream is practically removed by a magnetic field of 3 gauss in the direction of observation.† This is of importance in that it shows that the polarisation effect observed on λ 2537 is of a similar nature to those found for the remaining lines.

We have finally to give a list of the mercury lines which have been observed. Exact polarisation measurements have not yet been made in most cases.

Table I shows the observed polarisation of the mercury lines examined when produced with a pressure of 1/1000th mm. of mercury in the tube. The residual magnetic field was not greater than 1/50th gauss. The electron voltage to which the observations correspond is 20 volts, while the excitation potentials of the lines are between 8 and 9 volts.

The signs $\parallel$ and $\perp$ imply polarisation with the maximum electric vector parallel or perpendicular to the electron stream. The symbols *s*, *m* and *w*

* *Loc. cit.*

† It is probable that the main effect of this field is a rotation of the plane of polarisation through nearly 45°.

Table I

Δj	Series	Wave-Length	Polarisation observed at 20 volts	Polarisation calculated at Excitation Voltage
				Per cent
+1	$2^1P_1 - 3^1D_2$*	5791	$m \parallel$	60 ∥
	($2^1P_1 - 3^3D_1$)			
+1	$2^1P_1 - 4^1D_2$	4347	$m \parallel$	60 ∥
+1	$2^1P_1 - 5^1D_2$	3906	$m \parallel$	60 ∥
+1	$2^1P_1 - 3^3D_2$	5770	$m \parallel$	60 ∥
+1	$2^3P_0 - 3^3D_1$	2987	$w \parallel$	100 ∥
+1	$2^3P_1 - 3^1D_2$	3132	$m \parallel$	60
	($2^3P_1 - 3^3D_1$)			
+1	$2^3P_1 - 4^1D_2$	2655	$m \parallel$	60 ∥
+1	$2^3P_1 - 3^3D_2$	3126	$m \parallel$	60 ∥
+1	$2^3P_1 - 4^3D_2$	2652	$m \parallel$	60 ∥
+1	$2^3P_2 - 3^3D_3$	3650	$w \parallel$	50 ∥
+1	$2^3P_2 - 4^3D_3$	3021	$w \parallel$	50 ∥
0	$2^3P_2 - 3^3D_2$	3663	$s \perp$	100 ⊥
	($2^3P_2 - 3^3D_1$)			
0	$2^3P_2 - 4^3D_2$	3027	$s \perp$	100 ⊥
0	$2^3P_2 - 3^3D_2$	3655	$s \perp$	100 ⊥
0	$2^3P_2 - 4^3D_2$	3023	$s \perp$	100 ⊥
−1	$2^1P_1 - 2^1S_0$	4108	0	0
−1	$2^3P_1 - 4^1S_0$	4077	0	0
+1	$2^3P_2 - 2^3S_1$	4047	0	100 ∥
0	$2^3P_1 - 2^3S_1$	4358	$w \perp$	100
−1	$2^3P_2 - 3^3S_1$	5461	0	14
+1	$1^1S_0 - 2^3P_1$	2537	30 per cent ⊥†	100 ∥

give a scale of polarisation based on visual estimates, in which, very roughly speaking,

$$s = 40 \text{ per cent.}, \quad m = 30 \text{ per cent}, \quad \text{and} \quad w = 20 \text{ per cent}$$

But these values, except for the value of m, may need considerable correction when photometric measurements have been made

* We are using the series notation of Russell and Saunders ('Astrophys. Journ.,' vol. 61, p. 38 (1925)), in which terms with increasing azimuthal quantum number are represented by the symbols S, P, D. We write for a term e.g., $^{s'}$P, where s is the total quantum number, r is the multiplicity of the term and j is the inner quantum number. For convenience an integral scale for r is taken, and in the cases where j is half-integral, we substitute for it the value $(j - \frac{1}{2})$.

† At 7 volts (observation of Ellett, Foote and Mohler)

The lines whose series are given in brackets are considerably weaker and inseparable companions to the lines above them

The calculated values of the fifth column will receive explanation later and are connected with the values (column 1) of the change of the quantum number j (which represents the angular momentum of the atom) calculated for an absorption switch

§ 5 *Discussion of Results*

It can scarcely be doubted that the polarisation effects in question have their origin in the fact that the electron stream is unidirectional We must therefore assume that in the case of many spectral lines, at any rate, the impact of an electron on an atom has the result of exciting the atom to produce plane-polarised light The effect is analogous in some respects to the known result that the X-rays emitted from an ordinary target are polarised But the analogy seems rather superficial because it has been shown* that this polarisation is only found in the case of the continuous X-ray spectrum and not for the lines

Assuming that an atom is in a position to emit plane-polarised light, one would expect that the effects of an external field on it will be independent of the mechanism by which it has reached this excited state This fact suggests an obvious analogy between the results we have described and the results found in experiments of the type initiated by Wood and Ellett† These experiments deal with observations of the polarisation of resonance radiation and the effects of a magnetic field on it In their case, the excitation of the atoms is by the absorption of radiation, and in our case by electron impact, but the effects of an external field on the polarisation may be expected to be the same

This actually proves to be the case The most completely studied case of resonance is that of the Mercury Line λ 2537, for which observations have been made most completely by Hanle‡ and von Keussler,§ who have found the depolarisation and rotation effects exactly as we have described them

The theory of the effect which Hanle has given is the following.—Suppose there is a linear vibrator in the atom which is emitting the light as on the classical theory. If a magnetic field is applied in a direction at right angles to the direction of vibration, a Larmor precession will be superposed on the motion. Since, further, we must assume that the vibration is damped, the motion will be of the type shown in fig 8 It can be seen from this that the plane of polarisa-

* Bassler, 'Ann. d Physik,' vol. 28, p 808 (1909).
† 'Phys. Rev.,' vol. 24, p 243 (1924)
‡ 'Z f. Physik,' vol 37, p 93 (1925).
§ 'Phys Zeit.,' vol 27, p. 331 (1926).

tion of the total light emitted can be considered as rotated to a direction indicated by the arrow and the total light partially depolarised. If a Babinet

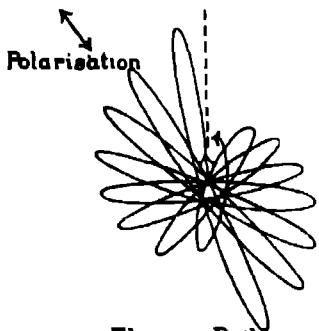

Fig 8

compensator is used for detection, it is easy to calculate that the apparent rotation will be given by the relation

$$\tan 2\delta = \frac{\omega}{2\pi\beta},$$

where ω is the magnetic rotation frequency corresponding to the field strength H, and β is the damping constant of the oscillation, defined by the statement that the amplitude of the vibration is given by

$$a = a_0 e^{-\beta t}.$$

The apparent depolarisation is also given by the formula

$$\left(\frac{\omega}{2\pi\beta}\right)^2 = \frac{\Pi_0^2}{\Pi^2} - 1,$$

where Π_0 is the percentage polarisation in a zero field and Π the percentage in the field H.

In the case of the singlet 2^1P_1—3^1D_2 combination, λ 5791, there is no ambiguity as to what we shall take for ω The Zeeman splitting is normal and so we naturally take the Larmor frequency. In the case of the line λ 5770 (2^1P_1—3^3D_2), the Zeeman effect is anomalous, since the $^3D_2$ term has a Landé splitting factor (g) of 7/6, that for the $^1P_1$ term being of course 1. But since the value 7/6 is not very different from 1, it would seem that in this case also we shall not be much in error if we again take the Larmor frequency for ω.

We are now in a position to interpret the curves of the rotation and

depolarisation which have been given in fig 7 The curves should, according to the theory, be straight lines, which within the limits of error they are The slope of these lines gives in each case the value of $\omega/2\pi\beta$ for a field of 1 gauss The values obtained also agree well. From them one can calculate β, but it is of more significance to calculate $\tau = 1/\beta$ τ, on the classical theory, is the time taken for the vibrations to die down to 1/eth of their initial value It corresponds on the quantum theory to the mean life of the atom in the excited state.

We obtain, in fact, the following values for the mean life of the mercury atom in the 3^1D_2 and 3^3D_2 states before the switch to the 2^1P_1 state

From rotation $= 2\ 85 \pm 0\ 15\ 10^{-8}$ sec

From depolarisation $= 2{\cdot}88 \pm 0\ 15\ 10^{-8}$ sec

We may therefore take $2\ 9\ 10^{-8}$ sec as the value of τ for these states.

The value found by von Keussler for the 2^3P_1 state of mercury is $1{\cdot}12\ 10^{-7}$ sec,* and that of the mean of the 2^2P_1 and 2^2P_2 states of sodium is considerably less. These results are in general agreement with the results of Wien on the mean time of life of an atom in the excited state

We may here also note that if the τ for the 3^1D_2 and 3^3D_2 states are not the same, we should not expect the curves of fig 7 to be straight lines The fact that they are approximately so shows that the τ's must be nearly, at any rate, the same as has already been mentioned.

The τ's for the other lines have not so far been determined, but the method described evidently admits of a wide application

These effects of a magnetic field on the polarisation have been interpreted on Hanle's classical theory We are here dealing with such weak magnetic fields that the atoms are not space-quantised For if they were, it has been pointed out by Hanle that the rotation effect could not exist For this is essentially an interference effect between the light of different frequencies emitted by an atom in a magnetic field, and he concludes that in the case of these weak fields all the Zeeman components of a line must be emitted by the same atom We have here, then, a case to which the rigid quantum theory seems quite inapplicable

This remark is of some importance when we attempt to frame a quantum theory of the mechanism by which an electron can excite an atom to emit polarised light. For it shows that we cannot hope to do so while the atom remains in a degenerate state On this ground the theory of Ellett, Foote and Mohler would seem to be open to criticism They predict theoretically that

* Their value is further confirmed as regards order of magnitude by the experiments of Ellett, Foote and Mohler which have been mentioned

polarisation should only occur for the transitions in which j, the quantum number representing the angular momentum of the atom, changes by one unit, and this proves to be by no means the case

The simplest method of treatment would seem to be to suppose a magnetic field parallel to the electron beam, of sufficient strength to ensure orientation of the atoms, but not strong enough to split the lines appreciably We have seen that experimentally such a field produces no effect on the polarisation, and Heisenberg* has shown, in the case of resonance radiation, from arguments based on a generalised correspondence principle, that this may be expected

We now come to the fundamental basis of the theory To simplify matters we shall at first suppose that the impacting electron has just that velocity necessary for excitation of the line in question and no more This means that after the collision the electron is reduced to rest One may reasonably assume that the angular momentum which is given by the electron to the atom must be in a direction at right angles to the initial direction of motion of the electron †

Since the angular momentum transferred during the collision is at right angles to the direction of the electron stream, it is at right angles to the magnetic field which we are supposing to be applied in the direction of the stream

We represent by j the quantum number expressing the total angular momentum of the atom, and by m its component in the direction of the magnetic field H It follows that in the transitions induced by the impact of an electron moving in the direction of H that the change in m, namely,

$$\Delta m = 0 \qquad (1)$$

This equation therefore expresses the condition that in the excitation of light by electron impact the angular momentum communicated must be at right angles to the direction of motion of the impacting electron previous to collision

Now the magnetic field has the property of splitting the levels of the atom. The way in which the splitting takes place is well known from the analysis of the Zeeman effect Actually, the normal unexcited state of the mercury atom, the 1^1S_0 state, is not split, the magnetic quantum number of this state being given by $m = 0$ In general the states will, however, be split, and m will have for them, in the case of the mercury atom, the values $0, \pm 1, \pm 2 \ldots \pm (j - \frac{1}{2})$

We may represent these states diagrammatically, for the sake of simplicity

* 'Z. f. Physik,' vol. 31, p. 617 (1925).

† This point also forms the basis of the theory of Ellett, Foote and Mohler.

only three terms being taken - the 1^1S_0 term, the 2^1P_1 term and the 3^1D_2 term (fig 9).

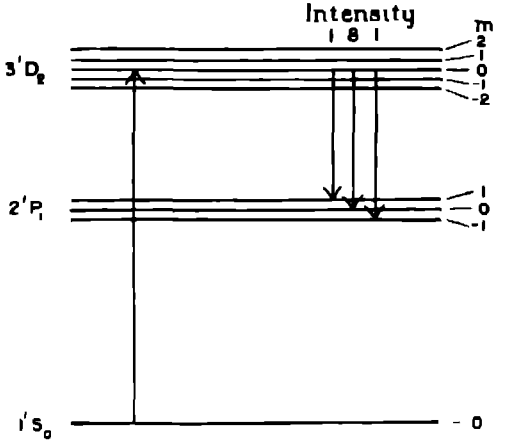

Fig 9

Now the atom is initially in the 1^1S_0 state and has $m = 0$. Using equation (1) we see that by the impact of an electron it must be transferred (for example) into the 3^1D_2 term ($m = 0$). This is represented by the upward arrow.

The atom is now free to emit light, and, according to the rules of the Zeeman effect, it is known that the following transitions can occur, for instance to the 2^1P_1 state

(*a*) $m = 0$ corresponding to light polarised parallel to H ($\parallel$)

(*b*) $m = \pm 1$ corresponding to light polarised perpendicular to H ($\perp$).

Since there are no atoms in the $^1D_2$ state corresponding to $m = \pm 1$, ± 2, the lines which will be emitted are represented by the downward arrows.

The intensities of these Zeeman components are calculable on the basis of the "Summation rules" of Ornstein, Burger and Dorgelo. A useful account is given by Kronig* of the application to the case of the Zeeman components.

We have in our case only three Zeeman components emitted, one polarised $\parallel$ and the other two polarised $\perp$. The net polarisation of the emitted light is thus calculable. In the case of all transitions involving $\Delta j = \pm 1$ (as in the example given) the intensity of the component polarised $\parallel$ is greater than the sum of the intensities of the components polarised $\perp$. The net polarisation is thus

* 'Z. f. Physik,' vol. 31, p. 885 (1925).

a || polarisation, the value of which varies with the precise j and k values involved in the transition.

However, in the case of the transitions $\Delta j = 0$, the state of affairs is quite different. The essential distinction is that the analysis of the Zeeman effect has shown that the transitions

$$\Delta j = 0 \qquad \Delta m = 0$$

do not occur, and this also follows from the theory of Kronig.

If the atom is excited by electron impact, it will, as before, be in an $m = 0$ state. In the emission of a line corresponding to $\Delta j = 0$, therefore, only the transitions

$$\Delta m = \pm 1$$

can take place, and the light will be polarised perpendicular to the direction of motion of the electron.

These considerations are based on the assumption that the electron has just enough energy to excite the atom, and no more. However, observations at such velocities are not possible on account of the faintness of the light, and hence the experimental results apply to electrons of higher speed. If the electron has a finite velocity after the impact, it is clear that it will be possible for it to transfer angular momentum in a direction parallel to that of its initial motion to the atom.

Unfortunately, it is not possible to calculate precisely the ratio of the amount of angular momentum perpendicular to the initial direction of motion of the electron transferred in a number of collisions to the amount transferred in the perpendicular direction. The reason for this is, that in the general case under consideration, the relations of energy and momentum do not suffice. We require a more detailed knowledge of the forces acting on the electron during impact, and this at present is lacking.

However, it would seem reasonable to suppose that the probability of a collision in which angular momentum in a direction parallel to the initial direction of motion of the electron is transferred will increase with the emerging velocity of the electron. The magnitude of the polarisation effects will, therefore, be expected to decrease with the increasing initial velocity of the electron. In the case of λ 5770, 5791 a steady decrease with increasing velocity was observed (see fig. 5).

In the case of λ 5770, 5791 we have already sufficient material for a rough numerical test between theory and experiments. The polarisation of these lines is parallel to the stream. We require the degree of polarisation when the

electron speed corresponds to the excitation voltage of the line, and this can only be obtained by extrapolation of the results obtained with greater electron speeds In fact, an extrapolation back to 9 volts by means of an exponential formula (see fig 5) gives a value of about 65 per cent of polarisation This corresponds very nearly to the calculated value of 60 per cent

In the cases of the other lines, we have at the present moment to fall back on a qualitative test The values of the polarisation calculated for electrons of speed corresponding to the excitation potential have been inserted in Table I and may be compared with the experimental results for an electron speed of 20 volts

It is seen that, in spite of some exceptional cases to be mentioned later, there is a general agreement both as regards the direction of the plane of polarisation and the relative magnitudes of the polarisation

We may here also notice that the case of the D lines of sodium also agrees with the theory This case has been investigated by Kossel and Gerthsen,* who found no polarisation effect, and their result was confirmed by Ellett, Foote and Mohler * The normal 1^2S_1 state of sodium splits in a magnetic field into two states with $m = \pm\frac{1}{2}$ and one sees at once that on this account the effects will be smaller than in the case of mercury with its unsplit normal state Actually, calculation shows 0 per cent and 60 per cent with a mean (bearing in mind the relative intensities of the D lines) of 20 per cent , and remembering the rapid decrease of the percentage polarisation with increasing speed of electrons, an effect of this magnitude might well escape detection

It will be seen therefore, that the theory goes a considerable way towards explaining the facts But returning now to the mercury lines it appears from Table I that there are four lines for which the observed polarisation seems definitely not to agree with the calculated. These are --

Table II

λ	Series
2537	$1^1S_0 - 2^3P_1$
4047	$2^3P_0 - 2^3S_1$
4358	$2^3P_1 - 2^3S_1$
2967	$2^3P_0 - 3^3D_1$

Of these the most flagrant case is λ 2537, which shows a ⊥ polarisation of 30 per cent. at 7 volts in place of the theoretical value of 100 per cent ∥ at

* *Loc. cit*

the excitation voltage. In the other cases the plane of polarisation is correctly given, but the observed magnitude is smaller than expected.

It will be noticed that all these lines involve impact switches from the normal 1^1S_0 state of mercury for which $\Delta j = 1$, while for the lines for which the theory seems to hold, in the impact transition, $\Delta j = 0$, 2 or 3 *

Let us take the case of λ 2537 as the clearest example for which the theory fails The observed ⊥ polarisation, if our picture is correct at all, shows that the probability of the excitation of the states 2^3P_1 ($m = \pm 1$) must be greater than the probability of the excitation of the state 2^3P_1 ($m = 0$)

It is not definitely proved yet whether or not this ⊥ polarisation occurs when the speed of the electrons corresponds exactly to the excitation voltage All that is proved is that there is a ⊥ polarisation at an electron speed of 7 volts This fact may provide a loophole for the applicability of the theory, for, as we saw, if the electron goes away from the excited atom with a finite velocity, the impact switches $\Delta m = \pm 1$ are possible, and we have no means of determining the relative probabilities of these switches and of the impact switch $\Delta m = 0$.

But although further work on this point is needed, it would seem fair to state that the experiments make it appear unlikely that, for an electron speed of 4 9 volts (the excitation potential), the line λ 2537 will be found polarised 100 per cent ‖ If this is not the case, there would be a definite disagreement with the theory suggested above. We may perhaps put forward some tentative speculations on this point

The difficulty might be avoided by making the assumption that the impacting electron may possess angular momentum of spin This is the model proposed by Uhlenbeck and Goudsmid† which has proved successful in resolving many of the difficulties connected with the multiplicity of spectra and the Zeeman effect. On this hypothesis, when an electron in an atom is orientated by the magnetic field within the atom, it adds a half of a quantum of angular momentum in the direction of the field, or in the opposite direction. We may perhaps extend this case by supposing that a free electron when orientated by an external field has half a quantum of angular momentum in the direction of the field or in the opposite direction

In the present problem, if we suppose, as before, that there is a magnetic field, in the direction of the electron stream, it is clear that, with the hypothesis of the spinning electron, we have the possibility that an electron (by changing

* Except in the case of the mean line λ 5461 ($2^3P_2 - 2^3S_1$), for which the calculated polarisation is too small for any decision to be possible.

† 'Nature,' vol. 117, p. 264 (1926).

its direction of orientation) may on impact transfer to the atom *one* quantum of angular momentum in the direction of the field. (We call this process "Process B.")

Now it is just in the case of the lines which involve impact switches $\Delta j = \pm 1$ (i.e. the atom, on impact, gains or loses one quantum of angular momentum) that the simple theory suggested above appears to break down, and this fact is suggestive.

Of course, we still have the possibility of the transfer of any number of quanta of angular momentum in a direction *perpendicular* to the field, as described previously ("Process A"). We may suppose, therefore, that a line like λ 2537 which involves an impact switch $\Delta j = \pm 1$ may be excited either by Process A or by Process B, and the degree of polarisation to be expected will be indeterminate.

In the case of the lines involving impact switches $\Delta j = 2, 3$, we have seen that, experimentally, the part played in excitation by Process B, if any, must be small. Since, by Process B, exactly one quantum of angular momentum must be transferred, it is evident that Process A must be concerned in every excitation of this type. If both processes were concerned in an excitation, the angular momentum transferred by process A would not be quantised.* If, therefore, we were to make the hypothesis that the angular momenta transferred by Process A and Process B are quantised individually, the simple theory involving Process A only, which was described above, might be retained for these lines.

Experiments on the excitation of polarised light by electron impact are still in progress, and it is hoped that before long it will be possible to subject these speculations to a more rigid test.

Summary

1. An electron tube producing an intense unidirectional stream of electrons of slow speed is used for the excitation of the mercury spectrum, and polarisation measurements are made on the light emitted from the tube in a direction at right angles to the direction of the stream. It is found that with an electron speed corresponding to 20 volts many of the mercury lines are partially plane-polarised, most with direction of the maximum electric vector parallel to the stream, but some in the perpendicular direction. The experiments of

* For example, in the case of an impact transition in which $\Delta j = 2$, if one quantum of angular momentum parallel to the field is transferred by Process B, it would be necessary for $\sqrt{3}$ quanta perpendicular to the field to be transferred by Process A.

Ellett, Foote and Mohler, who found that λ 2537 was polarised in the latter direction, are confirmed. In the cases of λ 5770, 5791 the polarisation parallel to the stream decreases rapidly as the speed of the electrons increases.

2 The application of a magnetic field in the direction of the stream has no influence on the polarisation, but a weak field of the order of 2 gauss causes two effects to appear which increase with the field strength, namely, (*a*) a depolarisation and (*b*) a rotation of the plane of polarisation. These are investigated in the case of the lines λ 5770, 5791.

3 The magnetic effects are interpreted satisfactorily on a theory of Hanle put forward in connection with work on resonance radiation Each effect (*a*) and (*b*) leads to determination of τ, the mean life of the atom in the excited state, and these values are concordant

4 The polarisation effects are due to the direct excitation of polarised light by electron impact An attempt is made to picture this process. The theory is based on the fact that, in excitation, an electron may, if its speed corresponds nearly to the excitation voltage, be expected to transfer angular momentum to the atom in a direction perpendicular to the initial direction of motion of the electron The facts in the case of most of the lines agree well with the theoretical expectation, but in a few cases the theory seems to be inadequate.

In conclusion, the author wishes to express his thanks to Prof Sir Ernest Rutherford, O M, P R.S, for his constant interest and helpful criticism, and to Mr R. H. Fowler, F.R S, for valuable discussion

On the Theory of Quantum Mechanics.

By P A M. Dirac, St John's College, Cambridge

(Communicated by R H Fowler, F R S —Received August 26, 1926)

§ 1. *Introduction and Summary.*

The new mechanics of the atom introduced by Heisenberg* may be based on the assumption that the variables that describe a dynamical system do not obey the commutative law of multiplication, but satisfy instead certain quantum conditions One can build up a theory without knowing anything about the dynamical variables except the algebraic laws that they are subject to, and can show that they may be represented by matrices whenever a set of uniformising variables for the dynamical system exists † It may be shown, however (see § 3), that there is no set of uniformising variables for a system containing more than one electron, so that the theory cannot progress very far on these lines.

A new development of the theory has recently been given by Schrödinger.‡ Starting from the idea that an atomic system cannot be represented by a trajectory, *i.e.*, by a point moving through the co-ordinate space, but must be represented by a wave in this space, Schrodinger obtains from a variation principle a differential equation which the wave function ψ must satisfy This differential equation turns out to be very closely connected with the Hamiltonian equation which specifies the system, namely, if

$$\mathrm{H}(q_r, p_r) - \mathrm{W} = 0$$

is the Hamiltonian equation of the system, where the q_r, p_r are canonical variables, then the wave equation for ψ is

$$\left\{\mathrm{H}\left(q_r, \frac{\hbar}{i}\frac{\partial}{\partial q_r}\right) - \mathrm{W}\right\}\psi = 0, \tag{1}$$

where $\hbar$ is $(2\pi)^{-1}$ times the usual Planck's constant. Each momentum p_r in H is replaced by the operator $\frac{\hbar}{i}\partial/\partial q_r$, and is supposed to operate on all that exists on its right-hand side in the term in which it occurs. Schrodinger takes the values of the parameter W for which there exists a ψ satisfying (1) that is

* See various papers by Born, Heisenberg and Jordan, 'Zeits f. Phys ,' vol. 33 onwards.

† 'Roy Soc. Proc ,' A, vol. 110, p 561 (1926).

‡ See various papers in the 'Ann d. Phys ,' beginning with vol. 79, p 361 (1926).

continuous, single-valued and bounded throughout the whole of q-space to be the energy levels of the system, and shows that when the general solution of (1) is known, matrices to represent the p_r and q_r may easily be obtained, satisfying all the conditions that they have to satisfy according to Heisenberg's matrix mechanics, and consistent with the energy levels previously found. The mathematical equivalence of the theories is thus established.

In the present paper, Schrodinger's theory is considered in § 2 from a slightly more general point of view, in which the time t and its conjugate momentum $-W$ are treated from the beginning on the same footing as the other variables. A more general method, requiring only elementary symbolic algebra, of obtaining matrix representations of the dynamical variables is given.

In § 3 the problem is considered of a system containing several similar particles, such as an atom with several electrons. If the positions of two of the electrons are interchanged, the new state of the atom is physically indistinguishable from the original one. In such a case one would expect only symmetrical functions of the co-ordinates of all the electrons to be capable of being represented by matrices. It is found that this allows one to obtain two solutions of the problem satisfying all the necessary conditions, and the theory is incapable of deciding which is the correct one. One of the solutions leads to Pauli's principle that not more than one electron can be in any given orbit, and the other, when applied to the analogous problem of the ideal gas, leads to the Einstein-Bose statistical mechanics.

The effect of an arbitrarily varying perturbation on an atomic system is worked out in § 5 with the help of a new assumption. The theory is applied to the absorption and stimulated emission of radiation by an atom. A generalisation of the description of the phenomena by Einstein's B coefficients is obtained, in which the phases play their proper parts. This method cannot be applied to spontaneous emission.

§ 2. *General Theory*

According to the new point of view introduced by Schrodinger, we no longer leave unspecified the nature of the dynamical variables that describe an atomic system, but count the q's and t as ordinary mathematical variables (this being permissible since they commute with one another) and take the p's and W to be the differential operators

$$p_r = -ih\frac{\partial}{\partial q_r}, \qquad -W = -ih\frac{\partial}{\partial t}. \tag{2}$$

Whenever a p_r or W occurs in a term of an equation, it must be considered as meaning the corresponding differential operator operating on all that occurs on its

right-hand side in the term in question Thus, by carrying out the operations, one can reduce any function of the p's, q's, W and t to a function of the q's and t only.

The relations (2) require two obvious modifications to be made in the algebra governing the dynamical variables Firstly, only rational integral functions of the p's and W have a meaning and, secondly, *one can multiply up an equation by a factor (integral in the p's and* W) *on the left-hand side, but one cannot, in general, multiply up by factor on the right-hand side* Thus, if one is given the equation $a = b$, one can infer from it that $Xa = Xb$, where X is arbitrary, but one cannot in general infer that $aX = bX$.

There are, however, certain equations $a = b$ for which it is true that $aX = bX$ for any X, and these equations we call identities The quantum conditions

$$q_r p_s - p_s q_r = ih\delta_{rs}, \qquad p_r p_s - p_s p_r = 0$$

with the similar relations involving $-W$ and t, are identities, as it can easily be verified (and has been verified by Schrodinger) that the relations

$$(q_r p_s - p_s q_r)X = ih\delta_{rs}X,$$

etc, hold for any X These relations form the main justification for the assumptions (2).

If $a = b$ is an identity, we can deduce, since $aX = bX$ and $Xa = Xb$, that

$$aX - Xa = bX - Xb,$$

or

$$[a, X] = [b, X]$$

Thus we can equate the Poisson bracket of either side of an identity with an arbitrary quantity, and so our quantum identity is the analogue of an identity on the classical theory. We assume the general equation $xy - yx = ih[x, y]$ and the equations of motion of a dynamical system to be identities

A dynamical system is specified by a Hamiltonian equation between the variables

$$H(q_r, p_r, t) - W = 0, \tag{3}$$

or more generally

$$F(q_r, p_r, t, W) = 0 \tag{4}$$

and the equations of motion are

$$dx/ds = [x, F],$$

where x is any function of the dynamical variables, and s is a variable which depends on the form in which (4) is written, and, in particular, is just t if (4) is written in the form (3) On the new theory we consider the equation

$$F\psi = 0, \tag{5}$$

which, if we take ψ to be a function of the q's and t only, is an ordinary differential equation for ψ. From the general solution of this differential equation the matrices that form the solution of the mechanical problem may be very easily obtained.

Since (5) is linear in ψ, its general solution is of the form

$$\psi = \Sigma c_n \psi_n, \tag{6}$$

where the c_n's are arbitrary constants and the ψ_n's are a set of independent solutions, which may be called eigenfunctions. Only solutions that are continuous, single-valued and bounded throughout the whole domain of the q's and t are recognised by the theory. Instead of a discreet set of eigenfunctions ψ_n there may be a continuous set $\psi(\alpha)$, depending on a parameter α, and satisfying the differential equation for all values of α in a certain range, in which case the sum in (6) must be replaced by an integral $\int c_\alpha \psi(\alpha)\, d\alpha$,* or both a discreet set and a continuous set may occur together. For definiteness, however, we shall write down explicitly only the discreet sum in the following work.

We shall now show that any constant of integration of the dynamical system (either a first integral or a second integral) can be represented by a matrix whose elements are constants, there being one row and column of the matrix corresponding to each eigenfunction ψ_n. Let a be a constant of integration of the system, *i.e.*, a function of the dynamical variables such that $[a, \mathrm{F}] = 0$ identically. We have the relation

$$\mathrm{F}a = a\mathrm{F},$$

which, being an identity, we can multiply by ψ_n on the right-hand side. We thus obtain

$$\mathrm{F}a\psi_n = a\mathrm{F}\psi_n = 0,$$

since $\mathrm{F}\psi_n = 0$ (although not identically). Hence $a\psi_n$ is a solution of the differential equation (5), so that it can be expanded in the form (6), *i.e.*,

$$a\psi_n = \Sigma_m \psi_m a_{mn},$$

where the a_{mn}'s are constants. We take the quantities a_{mn} to be the elements of the matrix that represents a. The matrix rule of multiplication evidently holds, since, if b is another constant of integration of the system, we have

$$ab\psi_n = a\Sigma_m \psi_m b_{mn} = \Sigma_{mk} \psi_k a_{km} b_{mn},$$

* The general solution may contain quantities, such as ψ_α and $\partial\psi_\alpha/\partial\alpha$, which satisfy the differential equation (5), but which cannot strictly be put in the form $\int c_\alpha \psi_\alpha d\alpha$, although they may be regarded as the limits of series of quantities which are of this form.

and also

$$ab\psi_n = \Sigma_k \psi_k (ab)_{kn},$$

so that

$$(ab)_{kn} = \Sigma_m a_{km} b_{mn}$$

As an example of a constant of integration of the dynamical system, we may take the value $x(t_0)$ that an arbitrary function x of the p's, q's, W and t has at a specified time $t = t_0$. The matrix that represents $x(t_0)$ will consist of elements each of which is a function of t_0. Writing t for t_0, we see that an arbitrary function of the dynamical variables, $x(t)$, or simply x, can be represented by a matrix whose elements are functions of t only.

The matrix representation we have obtained is not unique, since any set of independent eigenfunctions ψ_n will do. To obtain the matrices of Heisenberg's original quantum mechanics, we must choose the ψ_n's in a particular way. We can always, by a linear transformation, obtain a set of ψ_n's which makes the matrix representing any given constant of integration of the dynamical system a diagonal matrix. Suppose now that the Hamiltonian F does not contain the time explicitly, so that W is a constant of the system, and is the energy, and we choose the ψ_n's so as to make the matrix representing W a diagonal matrix, i.e., so as to make

$$W\psi_n = W_n\psi_n, \tag{7}$$

where W_n is a numerical constant. Let x be any function of the dynamical variables *that does not involve the time explicitly*, and put

$$x\psi_n = \Sigma_m x_{mn}\psi_m,$$

where the x_{mn}'s are functions of the time only. We shall now show that the x_{mn}'s are of the form

$$x_{mn} = a_{mn}e^{2\pi i(W_m - W_n)t/h}, \tag{8}$$

where the a_{mn}'s are constants, as on Heisenberg's theory. We have

$$\begin{aligned} Wx\psi_n &= \Sigma_m W x_{mn}\psi_m \\ &= \Sigma_m (Wx_{mn} - x_{mn}W)\psi_m + \Sigma_m x_{mn}W\psi_m \\ &= \Sigma_m ihx_{mn}\psi_m + \Sigma_m x_{mn}W_m\psi_m \end{aligned} \tag{9}$$

Also, since x does not contain t explicitly,

$$\begin{aligned} Wx\psi_n &= xW\psi_n = xW_n\psi_n = W_n x\psi_n \\ &= W_n\Sigma_m x_{mn}\psi_m. \end{aligned} \tag{10}$$

Equating the coefficients of ψ_m in (9) and (10), we obtain

$$ihx_{mn} = x_{mn}(W_n - W_m),$$

which shows that x_{mn} is of the form (8).

We have thus shown that with the ψ_n's chosen in this way the matrices satisfy all the conditions of Heisenberg's matrix mechanics, except the condition that the matrices that represent real quantities are Hermitic (*i.e.*, have their mn and nm elements conjugate imaginaries). There does not seem to be any simple general proof that this is the case, as the proof would have to make use of the fact that the ψ_n's are bounded. It is easy to prove the particular case that the matrix representing W is Hermitic, *i.e.*, that the W_n's are real, since from (7) ψ_n must be of the form

$$\psi_n = u_n e^{-iW_n t/h},$$

where u_n is independent of t, and if W_n contains an imaginary part, ψ_n would not remain bounded as t becomes infinite. In general, the matrices representing real quantities could be Hermitic only if the arbitrary numerical constants by which the ψ_n's may be multiplied are chosen in a particular way.

We may regard an eigenfunction ψ_n as being associated with definite numerical values for some of the constants of integration of the system. Thus, if we find constants of integration $a, b, \ldots$ such that

$$a\psi_n = a_n\psi_n, \qquad b\psi_n = b_n\psi_n, \ldots \tag{11}$$

where $a_n, b_n, \ldots$ are numerical constants, we can say that ψ_n represents a state of the system in which $a, b, \ldots$ have the numerical values $a_n, b_n, \ldots$. (Note that $a, b, \ldots$ must commute for (11) to be possible.) In this way we can have eigenfunctions representing stationary states of an atomic system with definite values for the energy, angular momentum, and other constants of integration.

It should be noticed that the choice of the time t as the variable that occurs in the elements of the matrices representing variable quantities is quite arbitrary, and any function of t and the q's that increases steadily would do. To determine accurately the radiation emitted by the system in the direction of the x-axis, one would have to use $(t - x/c)$ instead of t.* It is probable that the representation of a constant of integration of the system by a matrix of constant elements is more fundamental than the representation of a variable quantity by a matrix whose elements are functions of some variable such as t or $(t - x/c)$. It would appear to be possible to build up an electromagnetic theory in which the potentials of the field at a specified point x_0, y_0, z_0, t_0 in space-time are represented by matrices of constant elements that are functions of x_0, y_0, z_0, t_0.

§ 3. *Systems containing Several Similar Particles.*

In Heisenberg's matrix mechanics it is assumed that the elements of the matrices that represent the dynamical variables determine the frequencies and

* 'Roy. Soc. Proc.,' A, vol. 111, p. 405 (1926).

intensities of the components of radiation emitted The theory thus enables one to calculate just those quantities that are of physical importance, and gives no information about quantities such as orbital frequencies that one can never hope to measure experimentally We should expect this very satisfactory characteristic to persist in all future developments of the theory

Consider now a system that contains two or more similar particles, say, for definiteness, an atom with two electrons Denote by (mn) that state of the atom in which one electron is in an orbit labelled m, and the other in the orbit n The question arises whether the two states (mn) and (nm), which are physically indistinguishable as they differ only by the interchange of the two electrons, are to be counted as two different states or as only one state, i e , do they give rise to two rows and columns in the matrices or to only one ? If the first alternative is right, then the theory would enable one to calculate the intensities due to the two transitions $(mn) \to (m'n')$ and $(nn) \to (n'm')$ separately, as the amplitude corresponding to either would be given by a definite element in the matrix representing the total polarisation. The two transitions are, however, physically indistinguishable, and only the sum of the intensities for the two together could be determined experimentally. Hence, in order to keep the essential characteristic of the theory that it shall enable one to calculate only observable quantities, one must adopt the second alternative that (mn) and (nm) count as only one state

This alternative, though, also leads to difficulties. The symmetry between the two electrons requires that the amplitude associated with the transition $(mn) \to (m'n')$ of x_1, a co-ordinate of one of the electrons, shall equal the amplitude associated with the transition $(nm) \to (n'm')$ of x_2, the corresponding co-ordinate of the other electron, i e ,

$$x_1(mn\ ,\ m'n') = x_2(nm\ ,\ n'm'). \tag{12}$$

If we now count (mn) and (nm) as both defining the same row and column of the matrices, and similarly for $(m'n')$ and $(n'm')$, equation (12) shows that each element of the matrix x_1 equals the corresponding element of the matrix x_2, so that we should have the matrix equation

$$x_1 = x_2.$$

This relation is obviously impossible, as, amongst other things, it is inconsistent with the quantum conditions. We must infer that unsymmetrical functions of the co-ordinates (and momenta) of the two electrons cannot be represented by matrices. Symmetrical functions, such as the total polarisation of the atom, can be considered to be represented by matrices without inconsistency,

and these matrices are by themselves sufficient to determine all the physical properties of the system.

One consequence of these considerations is that the theory of uniformising variables introduced by the author can no longer apply. This is because, corresponding to any transition $(mn) \to (m'n')$, there would be a term $e^{i(\omega t)}$ in the Fourier expansions, and we should require there to be a unique state, $(m''n'')$, say, such that the same term $e^{i(\omega t)}$ corresponds to the transition $(m'n') \to (m''n'')$, and $e^{2i(\omega t)}$ corresponds to $(mn) \to (m''n'')$. If the m's and n's are quantum numbers, and we take the case of one quantum number per electron for definiteness we should have to have

$$m'' - m' = m' - m, \qquad n'' - n' = n' - n$$

Since, however, the state $(m'n')$ may equally well be called the state $(n'm')$, we may equally well take

$$m'' - n' = n' - m, \qquad n'' - m' = m' - n,$$

which would give a different state $(m''n'')$. There is thus no unique state $(m''n'')$ that the theory of uniformising variables demands.

If we neglect the interaction between the two electrons, then we can obtain the eigenfunctions for the whole atom simply by multiplying the eigenfunctions for one electron when it exists alone in the atom by the eigenfunctions for the other electron alone, and taking the same time variable for each.* Thus if $\psi_n(x, y, z, t)$ is the eigenfunction for a single electron in the orbit n, then the eigenfunction for the whole atom in the state (mn) is

$$\psi_m(x_1, y_1, z_1, t)\, \psi_n(x_2, y_2, z_2, t) = \psi_m(1)\, \psi_n(2),$$

say, where x_1, y_1, z_1 and x_2, y_2, z_2 are the co-ordinates of the two electrons, and $\psi(r)$ means $\psi(x_r, y_r, z_r, t)$. The eigenfunction $\psi_m(2)\, \psi_n(1)$, however, also corresponds to the same state of the atom if we count the (mn) and (nm) states as identical. But two independent eigenfunctions must give rise to two rows and columns in the matrices. If we are to have only one row and column in the matrices corresponding to both (mn) and (nm), we must find a set of eigenfunctions ψ_{mn} of the form

$$\psi_{mn} = a_{mn}\psi_m(1)\, \psi_n(2) + b_{mn}\psi_m(2)\, \psi_n(1),$$

where the a_{mn}'s and b_{mn}'s are constants, which set must contain only one ψ_{mn} corresponding to both (mn) and (nm), and must be sufficient to enable one to

* The same time variable t must be taken in each owing to the fact that we write the Hamiltonian equation for the whole system. $H(1) + H(2) - W = 0$, where $H(1)$ and $H(2)$ are the Hamiltonians for the two electrons separately, so that there is a common time t conjugate to minus the total energy W.

obtain the matrix representing any symmetrical function A of the two electrons. This means the ψ_{mn}'s must be chosen such that A times any chosen ψ_{mn} can be expanded in terms of the chosen ψ_{mn}'s in the form

$$A\psi_{mn} = \Sigma_{m'n'} \psi_{m'n'} A_{m'n',\, mn}, \tag{13}$$

where the $A_{m'n',\, mn}$'s are constants or functions of the time only

There are two ways of choosing the set of ψ_{mn}'s to satisfy the conditions We may either take $a_{mn} = b_{mn}$, which makes each ψ_{mn} a symmetrical function of the two electrons, so that the left-hand side of (13) is symmetrical and only symmetrical eigenfunctions will be required for its expansion, or we may take $a_{mn} = -b_{mn}$, which makes ψ_{mn} antisymmetrical, so that the left-hand side of (13) is antisymmetrical and only antisymmetrical eigenfunctions will be required for its expansion Thus the symmetrical eigenfunctions alone or the antisymmetrical eigenfunctions alone give a complete solution of the problem The theory at present is incapable of deciding which solution is the correct one We are able to get complete solutions of the problem which make use of less than the total number of possible eigenfunctions at the expense of being able to represent only symmetrical functions of the two electrons by matrices

These results may evidently be extended to any number of electrons. For r non-interacting electrons with co-ordinates $x_1, y_1, z_1 \quad , x_r, y_r, z_r$, the symmetrical eigenfunctions are

$$\Sigma_{\alpha_1 \ldots \alpha_r} \psi_{n_1}(\alpha_1)\, \psi_{n_2}(\alpha_2) \ldots \psi_{n_r}(\alpha_r), \tag{14}$$

where $\alpha_1, \alpha_2 \quad \alpha_r$ are any permutation of the integers $1, 2 \ldots r$, while the antisymmetrical ones may be written in the determinantal form

$$\begin{vmatrix} \psi_{n_1}(1), & \psi_{n_1}(2) & \psi_{n_1}(r) \\ \psi_{n_2}(1), & \psi_{n_2}(2) & \psi_{n_2}(r) \\ \cdot & \cdot & \cdot \\ \psi_{n_r}(1), & \psi_{n_r}(2) & \psi_{n_r}(r) \end{vmatrix}. \tag{15}$$

If there is interaction between the electrons, there will still be symmetrical and antisymmetrical eigenfunctions, although they can no longer be put in these simple forms In any case the symmetrical ones alone or the antisymmetrical ones alone give a complete solution of the problem

An antisymmetrical eigenfunction vanishes identically when two of the electrons are in the same orbit This means that in the solution of the problem with antisymmetrical eigenfunctions there can be no stationary states with

two or more electrons in the same orbit, which is just Pauli's exclusion principle.* The solution with symmetrical eigenfunctions, on the other hand, allows any number of electrons to be in the same orbit, so that this solution cannot be the correct one for the problem of electrons in an atom †

§ 4. *Theory of the Ideal Gas*

The results of the preceding section apply to any system containing several similar particles, in particular to an assembly of gas molecules. There will be two solutions of the problem, in one of which the eigenfunctions are symmetrical functions of the co-ordinates of all the molecules, and in the other antisymmetrical.

The wave equation for a single molecule of rest-mass m moving in free space is

$$\{p_x^2 + p_y^2 + p_z^2 - W^2/c^2 + m^2c^2\}\psi = 0$$

$$\left\{\frac{\partial^2}{\partial x^2} + \frac{\partial^2}{\partial y^2} + \frac{\partial^2}{\partial z^2} - \frac{1}{c^2}\frac{\partial^2}{\partial t^2} - \frac{m^2c^2}{h^2}\right\}\psi = 0,$$

and its solution is of the form

$$\psi_{\alpha_1,\alpha_2,\alpha_3} = \exp.\, i\,(\alpha_1 x + \alpha_2 y + \alpha_3 z - Et)/h, \tag{16}$$

where α_1, α_2, α_3 and E are constants satisfying

$$\alpha_1^2 + \alpha_2^2 + \alpha_3^2 - E^2/c^2 + m^2c^2 = 0.$$

The eigenfunction (16) represents an atom having the momentum components α_1, α_2, α_3 and the energy E.

We must now obtain some restriction on the possible eigenfunctions due to the presence of boundary walls It is usually assumed that the eigenfunction, or wave function associated with a molecule, vanishes at the boundary, but we should expect to be able to deduce this, if it is true, from the general theory. We assume, as a natural generalisation of the methods of the preceding section, that there must be only just sufficient eigenfunctions for one to be able to represent by a matrix any function of the co-ordinates that has a physical meaning Suppose for definiteness that each molecule is confined between two boundaries at $x = 0$ and $x = 2\pi$ Then only those functions of x that are defined only for $0 < x < 2\pi$ have a physical meaning and must be capable of being represented by matrices. (This will require fewer eigenfunctions than if every

* Pauli, 'Zeits f. Phys.,' vol 31, p. 765 (1925).

† Prof Born has informed me that Heisenberg has independently obtained results equivalent to these. (Added in proof)—see Heisenberg, 'Zeit. fur Phys.,' vol. 38, p. 411 (1926).

function of x had to be capable of being represented by a matrix.) These functions $f(x)$ can always be expanded as Fourier series of the form

$$f(x) = \Sigma_n a_n e^{inx}, \tag{17}$$

where the a_n's are constants and the n's integers. If we choose from the eigenfunctions (16) those for which α_1/h is an integer, then $f(x)$ times any chosen eigenfunction can be expanded as a series in the chosen eigenfunctions whose coefficients are functions of t only, and hence $f(x)$ can be represented by a matrix. Thus these chosen eigenfunctions are sufficient, and are easily seen to be only just sufficient, for the matrix representation of any function of x of the form (17). Instead of choosing those eigenfunctions with integral values for α_1/h, we could equally well take those with α_1/h equal to half an odd integer, or more generally with $\alpha_1/h = n + \epsilon$, where n is an integer and ϵ is any real number. The theory is incapable of deciding which are the correct ones. For statistical problems, though, they all lead to the same results.

When y and z are also bounded by $0 < y < 2\pi$, $0 < z < 2\pi$, we find for the number of waves associated with molecules whose energies lie between E and $E + dE$ the value

$$\frac{4\pi}{c^3h^3}(E^2 - m^2c^4)^{\frac{1}{2}} E\, dE.$$

This value is in agreement with the ordinary assumption that the wave function vanishes at the boundary. It reduces, when one neglects relativity mechanics, to the familiar expression

$$\frac{2\pi}{h^3}(2m)^{\frac{3}{2}} E_1^{\frac{1}{2}} dE_1, \tag{18}$$

where $E_1 = E - mc^2$ is the kinetic energy. For an arbitrary volume of gas V the expression must be multiplied by $V/(2\pi)^3$.

To pass to the eigenfunctions for the assembly of molecules, between which there is assumed to be no interaction, we multiply the eigenfunctions for the separate molecules, and then take either the symmetrical eigenfunctions, of the form (14), or the antisymmetrical ones, of the form (15). We must now make the new assumption that all stationary states of the assembly (each represented by one eigenfunction) have the same *a priori* probability. If now we adopt the solution of the problem that involves symmetrical eigenfunctions, we should find that all values for the number of molecules associated with any wave have the same *a priori* probability, which gives just the Einstein-Bose statistical mechanics.* On the other hand, we should obtain a different

* Bose, 'Zeits. f. Phys.,' vol. 26, p. 178 (1924); Einstein, 'Sitzungsb. d. Preuss. Ac.,' p. 261 (1924) and p. 3 (1925).

statistical mechanics if we adopted the solution with antisymmetrical eigenfunctions, as we should then have either 0 or 1 molecule associated with each wave. The solution with symmetrical eigenfunctions must be the correct one when applied to light quanta, since it is known that the Einstein-Bose statistical mechanics leads to Planck's law of black-body radiation. The solution with antisymmetrical eigenfunctions, though, is probably the correct one for gas molecules, since it is known to be the correct one for electrons in an atom, and one would expect molecules to resemble electrons more closely than light-quanta.

We shall now work out, according to well-known principles, the equation of state of the gas on the assumption that the solution with antisymmetrical eigenfunctions is the correct one, so that not more than one molecule can be associated with each wave. Divide the waves into a number of sets such that the waves in each set are associated with molecules of about the same energy. Let A_s be the number of waves in the sth set, and let E_s be the kinetic energy of a molecule associated with one of them. Then the probability of a distribution (or the number of antisymmetrical eigenfunctions corresponding to distributions) in which N_s molecules are associated with waves in the sth set is

$$W = \Pi_s \frac{A_s!}{N_s!\,(A_s - N_s)!},$$

giving for the entropy

$$S = k \log W = k\Sigma_s \{A_s(\log A_s - 1) - N_s(\log N_s - 1) - (A_s - N_s)[\log(A_s - N_s) - 1]\}$$

This is to be a maximum, so that

$$0 = \delta S = k\Sigma_s \{-\log N_s + \log(A_s - N_s)\}\,\delta N_s$$
$$= k\Sigma_s \log(A_s/N_s - 1)\,.\,\delta N_s,$$

for all variations δN_s that leave the total number of molecules $N = \Sigma_s N_s$ and the total energy $E = \Sigma_s E_s N_s$ unaltered, so that

$$\Sigma_s \delta N_s = 0, \qquad \Sigma_s E_s \delta N_s = 0.$$

We thus obtain

$$\log(A_s/N_s - 1) = \alpha + \beta E_s,$$

where α and β are constants, which gives

$$N_s = \frac{A_s}{e^{\alpha + \beta E_s} + 1} \tag{19}$$

By making a variation in the total energy E and putting $\delta E/\delta S = T$, the temperature, we readily find that $\beta = 1/kT$, so that (19) becomes

$$N_s = \frac{A_s}{e^{\alpha + E_s/kT} + 1}$$

This formula gives the distribution in energy of the molecules On the Einstein-Bose theory the corresponding formula is

$$N_s = \frac{A_s}{e^{\alpha + E_s/kT} - 1}$$

If the sth set of waves consists of those associated with molecules whose energies lie between E_s and $E_s + dE_s$, we have from (18) [where E_s now means the E_1 of equation (18)],

$$A_s = 2\pi V (2m)^{\frac{3}{2}} E_s^{\frac{1}{2}} dE_s/(2\pi h)^3$$

where V is the volume of the gas This gives

$$N = \Sigma N_s = \frac{2\pi V (2m)^{\frac{3}{2}}}{(2\pi h)^3} \int_0^\infty \frac{E_s^{\frac{1}{2}} dE_s}{e^{\alpha + E_s/kT} + 1}$$

and

$$E = \Sigma E_s N_s = \frac{2\pi V (2m)^{\frac{3}{2}}}{(2\pi h)^3} \int_0^\infty \frac{E_s^{\frac{3}{2}} dE_s}{e^{\alpha + E_s/kT} + 1}$$

By eliminating α from these two equations and using the formula $PV = \frac{2}{3}E$, where P is the pressure, which holds for any statistical mechanics, the equation of state may be obtained

The saturation phenomenon of the Einstein-Bose theory does not occur in the present theory. The specific heat can easily be shown to tend steadily to zero as $T \to 0$, instead of first increasing until the saturation point is reached and then decreasing, as in the Einstein-Bose theory

§ 5. *Theory of Arbitrary Perturbations.*

In this section we shall consider the problem of an atomic system subjected to a perturbation from outside (*e.g.*, an incident electromagnetic field) which can vary with the time in an arbitrary manner. Let the wave equation for the undisturbed system be

$$(H - W)\psi = 0, \tag{20}$$

where H is a function of the p's and q's only Its general solution is of the form

$$\psi = \Sigma_n c_n \psi_n, \tag{21}$$

where the c_n's are constants. We shall suppose the ψ_n's to be chosen so that one is associated with each stationary state of the atom, and to be multiplied

by the proper constants to make the matrices that represent real quantities Hermitic

Now suppose a perturbation to be applied, beginning at the time $t = 0$ The wave equation for the disturbed system will be of the form

$$(H - W + A)\,\psi = 0, \tag{22}$$

where A is a function of the p's, q's and t, and is real. It will be shown that we can obtain a solution of this equation of the form

$$\psi = \Sigma_n a_n \psi_n, \tag{23}$$

where the a_n's are functions of t only, which may have the arbitrary values c_n at the time $t = 0$ We shall consider the general solution (21) of equation (20) to represent an assembly of the undisturbed atoms in which $|c_n|^2$ is the number of atoms in the nth state, and shall assume that (23) represents in the same way an assembly of the disturbed atoms, $|a_n(t)|^2$ being the number in the nth state at any time t We take $|a_n|^2$ instead of any other function of a_n because, as will be shown later, this makes the total number of atoms remain constant

The condition that ψ defined by equation (23) shall satisfy equation (22) is

$$\begin{aligned} 0 &= \Sigma_n (H - W + A)\, a_n \psi_n \\ &= \Sigma_n a_n (H - W + A)\, \psi_n - ih\Sigma_n a_n \psi_n, \end{aligned} \tag{24}$$

since H and A commute with a_n,† while $Wa_n - a_nW = iha_n$ identically. Suppose $A\psi_n$ to be expanded in the form

$$A\psi_n = \Sigma_m A_{mn} \psi_m,$$

where the coefficients A_{mn} are functions of t only, and satisfy $A_{mn}^* = A_{nm}$, where the * denotes the conjugate imaginary. Equation (24) now becomes, since $(H - W)\,\psi_n = 0$,

$$\Sigma_{mn} a_n A_{mn} \psi_m - ih\Sigma_m a_m \psi_m = 0.$$

Taking out the coefficient of ψ_m, we find

$$iha_m = \Sigma_n a_n A_{mn}, \tag{25}$$

which is a simple differential equation showing how the a_m's vary with the time.

Taking conjugate imaginaries, we find

$$-iha_m^* = \Sigma_n a_n^* A_{mn}^* = \Sigma_n a_n^* A_{nm}$$

Hence, if $N_m = a_m a_m^*$ is the number of atoms in the mth state, we have

$$\begin{aligned} ihN_m &= ih\,(a_m a_m^* + a_m^* a_m) \\ &= \Sigma_n\,(a_n A_{mn} a_m^* - a_n^* A_{nm} a_m) \end{aligned}$$

† The statement a commutes with b means $ab = ba$ identically.

This gives

$$i\hbar\Sigma_m N_m = \Sigma_{nm}(a_m^* A_{mn} a_n - a_n^* A_{nm} a_m) = 0,$$

as required.

If the perturbation consists of incident electromagnetic radiation moving in the direction of the x-axis and plane polarised with its electric vector in the direction of the y-axis, the perturbing term A in the Hamiltonian is, with neglect of relativity mechanics, $\kappa/c \quad \eta,$† where η is the total polarisation in the direction of the y-axis and O, κ, O, O are the components of the potential of the incident radiation We can expand $\eta\psi_n$ and $\eta\psi_n$ in the form

$$\eta\psi_n = \Sigma_m \eta_{lmn} e^{i(W_m - W_n)t/\hbar}\psi_m,$$
$$\eta\psi_n = \Sigma_m \eta_{mn} e^{i(W_m - W_n)t/\hbar}\psi_m$$

where the η_{lmn}'s and η_{mn}'s are constants and $\eta_{mn} = \iota(W_m - W_n)/h \quad \eta_{lmn}$ Our previous A_{mn} is now $\kappa/c \quad \eta_{lmn} e^{i(W_m - W_n)t/\hbar}$, and equation (25) becomes

$$i\hbar\dot{a}_m = \Sigma_n \iota_n \kappa \eta_{mn} e^{i(W_m - W_n)t/\hbar} \tag{26}$$

We can integrate this equation to the first order in κ by replacing the a_n's on the right-hand side by their values c_n at the time $t = 0$ This gives

$$a_m = c_m + 1/i\hbar c \cdot \Sigma_n c_n \eta_{mn} \int_0^t \kappa(s)\, e^{i(W_m - W_n)s/\hbar}\, ds. \tag{27}$$

To obtain a second approximation, we write for the a_n's on the right-hand side of (26) their values given by (27) We thus find for the value of a_m at the time T,

$$a_m = c_m + 1/i\hbar c \quad \Sigma_n c_n \eta_{mn} \int_0^T \kappa(t)\, e^{i(W_m - W_n)t/\hbar}\, dt$$
$$- 1/\hbar^2 c^2 \quad \Sigma_{nk} c_k \eta_{nk} \eta_{mn} \int_0^T \kappa(t)\, e^{i(W_m - W_n)t/\hbar}\, dt \int_0^t \kappa(s)\, e^{i(W_n - W_k)s/\hbar}\, ds \tag{28}$$
$$= c_m + c_m' + c_m'',$$

say, where c_m' and c_m'' denote the first- and second-order terms respectively

This gives for the number of atoms in the state m at the time T

$$N_m = a_m a_m^* = c_m c_m^* + c_m' c_m^* + c_m c_m'^* + c_m' c_m'^* + c_m'' c_m^* + c_m c_m''^*$$

If we wish to obtain effects that are independent of the initial phases of the atoms, we must substitute $c_m \exp. \iota\gamma_m$ for c_m and average over all values of γ_m

† We have neglected a term involving κ^2 This approximation is legitimate, even though we later evaluate the number of transitions that occur in a time T to the order κ^2, provided T is large compared with the periods of the atom.

from 0 to 2π. This makes the first-order terms in N_m, namely, $c_m' c_m^*$ and $c_m c_m'^*$, vanish, while the second-order terms give

$$1/\hbar^2 c^2 \cdot \Sigma_n c_n c_n^* \eta_{mn} \eta_{mn}^* \int_0^T \kappa(t)\, e^{i(W_m - W_n)t/\hbar}\, dt \int_0^T \kappa(t)\, e^{-i(W_m - W_n)t/\hbar}\, dt$$

$$-1/\hbar^2 c^2 \Sigma_n c_m c_m^* \eta_{mn} \eta_{mn} \int_0^T \kappa(t)\, e^{i(W_m - W_n)t/\hbar}\, dt \int_0^T \kappa(s)\, e^{i(W_m - W_n)s/\hbar}\, ds$$

$$-1/\hbar^2 c^2 \cdot \Sigma_n c_m c_m^* \eta_{mn}^* \eta_{mn}^* \int_0^T \kappa(t)\, e^{-i(W_m - W_n)t/\hbar}\, dt \int_0^T \kappa(s)\, e^{i(W_m - W_n)s/\hbar}\, ds,$$

which reduces to

$$1/\hbar^2 c^2 \cdot \Sigma_n \{ |c_n|^2 - |c_m|^2 \} |\eta_{mn}|^2 \left| \int_0^T \kappa(t)\, e^{i(W_m - W_n)t/\hbar}\, dt \right|^2 \qquad (29)$$

This gives ΔN_m, the increase in the number of atoms in the state m from the time $t = 0$ to the time $t = T$. The term in the summation that has the suffix n may be regarded as due to transitions between the state m and the state n.

If we resolve the radiation from the time $t = 0$ to the time $t = T$ into its harmonic components, we find for the intensity of frequency ν per unit frequency range the value

$$I_\nu = 2\pi\nu^2 c^{-1} \left| \int_0^T \kappa(t)\, e^{2\pi i \nu t}\, dt \right|^2.$$

Hence the term in expression (29) for ΔN_m due to transitions between state m and state n may be written

$$1/2\pi\hbar^2\nu^2 c \{ |c_n|^2 - |c_m|^2 \} |\eta_{mn}|^2 I_\nu,$$

where

$$2\pi\nu = (W_m - W_n)/\hbar,$$

or

$$2\pi/\hbar^2 c \cdot \{ |c_n|^2 - |c_m|^2 \} |\eta_{mn}|^2 I_\nu.$$

If one averages over all directions and states of polarisation of the incident radiation, this becomes

$$2\pi/3\hbar^2 c \cdot \{ |c_n|^2 - |c_m|^2 \} |P_{mn}|^2 I_\nu,$$

where

$$|P_{mn}|^2 = |\xi_{mn}|^2 + |\eta_{mn}|^2 + |\zeta_{mn}|^2,$$

ξ, η and ζ being the three components of total polarisation. Thus one can say that the radiation has caused $2\pi/3\hbar^2 c \cdot |c_n|^2 |P_{mn}|^2 I_\nu$ transitions from state n to state m, and $2\pi/3\hbar^2 c \cdot |c_m|^2 |P_{mn}|^2 I_\nu$ transitions from state m to state n, the probability coefficient for either process being

$$B_{n \to m} = B_{m \to n} = 2\pi/3\hbar^2 c \cdot |P_{mn}|^2,$$

in agreement with the ordinary Einstein theory.

The present theory thus accounts for the absorption and stimulated emission of radiation, and shows that the elements of the matrices representing the total polarisation determine the transition probabilities One cannot take spontaneous emission into account without a more elaborate theory involving the positions of the various atoms and the interference of their individual emissions, as the effects will depend upon whether the atoms are distributed at random, or arranged in a crystal lattice, or all confined in a volume small compared with a wave-length The last alternative mentioned, which is of no practical interest, appears to be the simplest theoretically.

It should be observed that we get the simple Einstein results only because we have averaged over all initial phases of the atoms The following argument shows, however, that the initial phases are of real physical importance, and that in consequence the Einstein coefficients are inadequate to describe the phenomena except in special cases If initially all the atoms are in the normal state, then it is easily seen that the expression (29) for ΔN_m holds without the averaging process, so that in this case the Einstein coefficients are adequate If we now consider the case when some of the atoms are initially in an excited state, we may suppose that they were brought into this state by radiation incident on the atoms before the time $t = 0$. The effect of the subsequent incident radiation must then depend on its phase relationships with the earlier incident radiation, since a correct way of treating the problem would be to resolve both incident radiations into a single Fourier integral If we do not wish the earlier radiation to appear explicitly in the calculation, we must suppose that it impresses certain phases on the atoms it excites, and that these phases are important for determining the effect of the subsequent radiation. It would thus not be permissible to average over these phases, but one would have to work directly from equation (28).

The Structure of γ-Brass.

By A. J. Bradley, M.Sc., Ph.D., and J. Thewlis, B.Sc., the Physical Laboratories, the University of Manchester.

(Communicated by Prof. W. L. Bragg, F.R.S.—Received August 31, 1926.)

(1) *Introduction.*

Westgren and Phragmén* have recently described the results of investigations on the structures of Cu–Zn, Ag–Zn and Au–Zn alloys. As a result of X-ray analysis by the powder method, five different types of structure were found in the case of the Cu–Zn alloys. Structures were successfully assigned to four of these phases, but in the case of the γ-phase a complete elucidation was not attempted. The structure is cubic, and contains 52 atoms to the unit cube. The following table is taken from Westgren and Phragmén's paper:—

Table I.—Lattice Dimensions and Number of Atoms per Elementary Cube in the γ-Phases.

Alloy.	Percentage Zn.	Av. Atomic Wt.	Density.	d_{100} in Å.	Number of Atoms per Elementary Cube.
Cu–Zn	61·7	64·67	8·04	8·850	52·22
Cu–Zn	64·7	64·72	7·99	8·860	52·05
Cu–Zn	67·7	64·78	7·92	8·870	52·02
Ag–Zn	50·3	81·29	8·66	9·327	52·37
Au–Zn	36·9	113·07	12·25	9·288	52·27
Au–Zn	41·1	107·71	11·76	9·223	51·96

Further information was obtained from examination of single crystals of a γ Cu–Zn alloy. Laue photograms and rotation photograms were both used for this purpose. By way of conjecture, Westgren and Phragmén suggested the formulæ Cu_4Zn_9, Ag_4Zn_9, and Au_4Zn_9, as these correspond to compositions coinciding with one of the homogeneous γ-phase ranges. We have found that these formulæ are incorrect, the true formulæ being Cu_5Zn_8, Ag_5Zn_8, and Au_5Zn_8.

It is at first sight surprising to find such a large number of atoms in the unit,

* "X-Ray Analysis of Copper–Zinc, Silver–Zinc and Gold–Zinc Alloys," by Arne Westgren and Gösta Phragmén, 'Phil. Mag.,' vol. 50, p. 311 (1925).

but this is by no means an isolated instance The γ'-phase of the Cu–Al alloys,* and even two distinct modifications of the element manganese,†‡ present the same phenomenon. It is a remarkable fact that α-manganese,§ γ Cu Zn, γ Ag–Zn, γ Au–Zn, and γ' Cu–Al all have a unit cell of about the same dimensions, and containing about the same number of atoms Moreover, the intensities of the reflexions from many planes of these structures are found to be extraordinarily alike, whatever substance is examined In particular, the two strongest lines on a powder photograph invariably occur at the same part of the film, so that for all these substances two interplanar spacings are particularly pronounced. It is significant that these are the spacings of the (110) and (211) planes of a body-centred cubic lattice whose lattice constant is about $a = 2{\cdot}95$Å

There is clearly a fundamental relationship between the structures of the above substances and the simple body-centred cubic structure The present paper gives the results of an attempt to determine the relationship in the case of the Cu-Zn alloys

(2) *Possible Space-Groups for γ-Brass.*

The only reflexions found for Cu–Zn and Au–Zn are those from planes (*hkl*), for which $(h + k + l)$ is even. In the case of the Ag–Zn alloy there are lines which are exceptions to this rule, but these extra lines are all very weak, and are probably either β-lines or are due to impurities There are no extra lines on the rotation photogram of γ-brass, taken from a single crystal This may be taken as conclusive evidence that the structure is built up from the space-lattice Γ''. According to Westgren and Phragmén, there are 52 atoms per unit cell, so that the structure contains 26 inter-penetrating body-centred cubic lattices, each of dimensions 8 85 Å

From a Laue photograph Westgren and Phragmén deduce that the symmetry of γ-brass is either T_d, O, or O_h The only abnormal spacings are (*hkl*), where $(h + k + l)$ is odd, which are halved Three space-groups satisfy these conditions, namely, T_d^3, O^5, and O_h^9. These are therefore the only possible space-groups

The above are the only conclusions for which there is direct experimental evidence

* Jette, Phragmén and Westgren, 'Journ. Inst Met.,' vol. 31, p 193 (1924).

† Westgren and Phragmén, 'Z f Physik,' vol 33, p 777 (1925)

‡ A J. Bradley, 'Phil. Mag.,' vol 50, p 1018 (1925)

§ In order to avoid further confusion the authors have decided to adopt the nomenclature devised by Westgren and Phragmén for the modifications of manganese.

(3) *Approximate Positions of the Atoms.*

To test directly every possible arrangement of atoms which would satisfy the above space-group conditions would be almost impossible We have selected the most probable types of structure, and tested such arrangements of atoms by comparing the intensities calculated for these arrangements with the intensities of the lines as observed by Westgren and Phragmén. In order to determine which arrangements were feasible, use was made of the following criteria —

(1) A clue to the approximate positions of the atoms is obtained by considering the positions and intensities of the strongest lines

(2) The distance of closest approach of the atoms is not likely to be very different from that in other crystals of a similar type containing the same atoms

With one exception, the strongest lines on the film of γ-brass are identical in position and intensity with the lines on the β-brass film

The lattice of β-brass is body-centred cubic, the lattice constant d_{100} is 2 945 Å, the unit cell contains two atoms The lattice constant of γ-brass (61 7 per cent. Zn) d_{100} is 8·85 Å, and each unit cell contains 52 atoms The side of the unit cube of γ-brass is therefore exactly three times that of β-brass, and its volume is 27 times as great. It follows that if γ-brass had 54 atoms to the unit cell, they might be arranged in exactly the same way as the atoms of β-brass, namely, on a body-centred lattice.

In such a case, γ-brass would only give rise to those lines which appear on the film of β-brass. The existence of extra lines on the film of γ-brass can be accounted for if we suppose two of the 54 atoms to be removed without greatly displacing the remaining 52 atoms

These considerations show that a possible structure for γ-brass consists of a body-centred cubic arrangement with 1 atom in 27 removed, the remaining atoms being slightly displaced, but necessarily in such a manner that the cubic symmetry is preserved.

Fig. 1 shows a unit cell containing the whole 54 atoms in the correct positions for a body-centred cubic structure. With the exception of one atom at the centre, all the atoms lie on the surfaces of three concentric cubes which are shown in the figure The diagram illustrates the special case where every atom is situated at exactly the same position as in a body-centred lattice, but since the unit cell contains so many atoms, they need not all be structurally equivalent. Cubic symmetry will be preserved and the space-group requirements fulfilled

if the atoms are divided into four or five groups of equivalent positions. The most general case, which corresponds to the space-group T_d^3, is shown in the

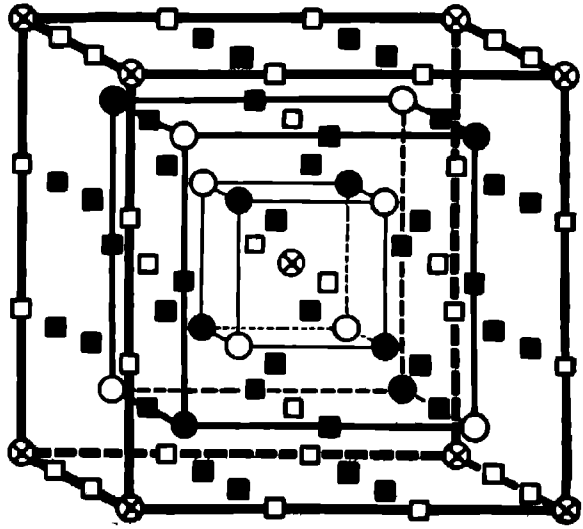

FIG. 1.—The Derivation of the Structure of γ-Brass from a Simple Cube-Centred Arrangement of Atoms.

figure. Structurally equivalent atoms are denoted by the same symbols. The 54 atoms are divided between five groups of equivalent positions in the following manner —

Table II.

Type of Atom	Symbol of Type	No. of Atoms per Unit Cell
"X"	⊗	2
"A"	●	8
"B"	○	8
"C"	□	12
"D"	■	24
		Total No. 54

There are more than 54 atoms shown in the figure, as the atoms on the outer faces of the cube are shared with the neighbouring cubes. The eight atoms at

the cube corners are each shared between eight cubes. The atoms on the cube edges are each shared between four cubes. All the other atoms on the outer faces are shared between two cubes.

The atoms may be displaced in different ways while still conforming to the space-group T_d^3, but atoms belonging to the same set must be displaced in the same manner. Fig. 1 will also represent the case of the space-group O_h^9, the additional condition being imposed that the "A" and "B" atoms must be equivalent. Consideration shows that it is not necessary to discuss the case of O^5, since any displacements from the arrangement of fig. 1 which are consistent with the symmetry elements of O^5 also satisfy the requirements of O_h^9.

A possible structure of γ-brass must have two atoms per unit cell less than the arrangement of fig. 1. It is clear that the only two atoms which could be removed, if our general scheme of arrangement is correct, are the "X" atoms, because there are more than two atoms of each other type in the unit cube.

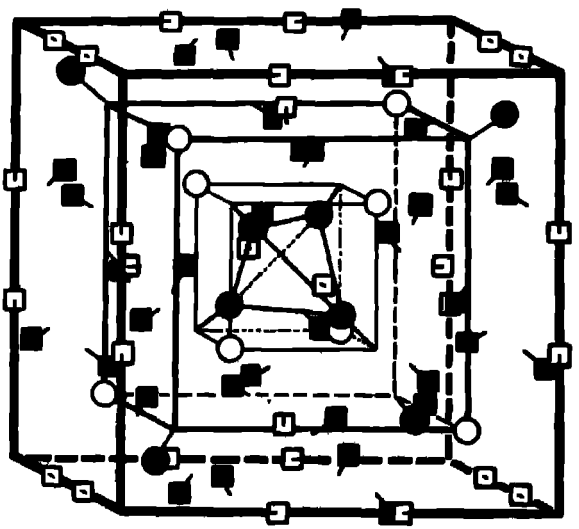

Fig. 2.—Structure of γ-Brass.

Fig. 2 represents a unit cell from which the "X" atoms have been removed. The remaining atoms are slightly displaced from the positions of fig. 1, the displacement being shown by the short lines. The extents of the displacements actually shown in the figure are those assigned to γ-brass by the present

analysis. The displacements have carried some of the D atoms, which were formerly on the boundary faces of the unit cell, entirely into neighbouring cells. These atoms have been inserted in fig. 2, in order to facilitate comparison with fig 1

(4) *Choice of Space-Groups*

The arrangement of fig 2 would correspond to the space-group O_h^9 only if "A" and "B" atoms were made equivalent As actually drawn it corresponds to the space-group T_d^3. We need not consider space-group O^7, as this requires the atoms to be placed in exactly the same positions as O_h^9, if the structure is to be at all similar to the body-centred cube.

To decide between T_d^3 and O_h^9 requires a determination of the parameters of the atoms, which can be made from considerations of intensities and interatomic distances.

The co-ordinates of the atoms are as follows.

"*A*" *Atoms.*

$(a\ a\ a)$, $(a\ -a\ -a)$, $(-a\ a\ -a)$, $(-a\ -a\ a)$,
$(\frac{1}{4}+a\ \frac{1}{4}+a\ \frac{1}{4}+a)$, $(\frac{1}{4}+a\ \frac{1}{4}-a\ \frac{1}{4}-a)$, $(\frac{1}{4}-a\ \frac{1}{4}+a\ \frac{1}{4}-a)$,
$(\frac{1}{4}-a\ \frac{1}{4}-a\ \frac{1}{4}+a)$

"*B*" *Atoms*

$(-b\ -b\ -b)$, $(-b\ b\ b)$, $(b\ -b\ b)$, $(b\ b\ -b)$,
$(\frac{1}{2}-b\ \frac{1}{2}-b\ \frac{1}{2}-b)$, $(\frac{1}{2}-b\ \frac{1}{2}+b\ \frac{1}{2}+b)$ $(\frac{1}{2}+b\ \frac{1}{2}-b\ \frac{1}{2}+b)$,
$(\frac{1}{2}+b\ \frac{1}{2}+b\ \frac{1}{2}-b)$

"C_4" *Atoms.*

$(c\ 0\ 0)$, $(-c\ 0\ 0)$, $(0\ c\ 0)$, $(0\ -c\ 0)$, $(0\ 0\ c)$, $(0\ 0\ -c)$,
$(\frac{1}{2}+c\ \frac{1}{2}\ \frac{1}{2})$, $(\frac{1}{2}-c\ \frac{1}{2}\ \frac{1}{2})$, $(\frac{1}{2}\ \frac{1}{2}+c\ \frac{1}{2})$, $(\frac{1}{2}\ \frac{1}{2}-c\ \frac{1}{2})$, $(\frac{1}{2}\ \frac{1}{2}\ \frac{1}{2}+c)$, $(\frac{1}{2}\ \frac{1}{2}\ \frac{1}{2}-c)$

"*D*" *Atoms.*

$(d\ d\ e)$, $(d\ -d\ -e)$, $(-d\ d\ -e)$, $(-d\ -d\ e)$,
$(\frac{1}{4}+d\ \frac{1}{4}+d\ \frac{1}{4}+d)$, $(\frac{1}{4}+d\ \frac{1}{4}-d\ \frac{1}{4}-e)$, $(\frac{1}{4}-d\ \frac{1}{4}+d\ \frac{1}{4}-e)$,
$(\frac{1}{4}-d\ \frac{1}{4}-d\ \frac{1}{4}+e)$,
$(d\ e\ d)$, $(d\ -e\ -d)$, $(-d\ e\ -d)$, $(-d\ -e\ d)$,
$(\frac{1}{4}+d\ \frac{1}{4}+e\ \frac{1}{4}+d)$, $(\frac{1}{4}+d\ \frac{1}{4}-e\ \frac{1}{4}-d)$, $(\frac{1}{4}-d\ \frac{1}{4}+e\ \frac{1}{4}-d)$,
$(\frac{1}{4}-d\ \frac{1}{4}-e\ \frac{1}{4}+d)$,
$(e\ d\ d)$, $(e\ -d\ -d)$, $(-e\ d\ -d)$, $(-e\ -d\ d)$,
$(\frac{1}{4}+e\ \frac{1}{4}+d\ \frac{1}{4}+d)$, $(\frac{1}{4}+e\ \frac{1}{4}-d\ \frac{1}{4}-d)$, $(\frac{1}{4}-e\ \frac{1}{4}+d\ \frac{1}{4}-d)$,
$(\frac{1}{4}-e\ \frac{1}{4}-d\ \frac{1}{4}+d)$.

For space-groups O^3 and O_h^9 $a=b$ and $e=0$.

At this stage no discrimination will be made between Cu and Zn atoms. The atomic numbers are so nearly equal that Cu and Zn may be considered to scatter X-rays by the same amount No appreciable error will be introduced into the calculations by this assumption. The structure-amplitude of any plane (hkl) is given by the following equation :—

$$S = 8\cos 2\pi ha \,.\, \cos 2\pi ka \,.\, \cos 2\pi la + 8\cos 2\pi hb \quad \cos 2\pi kb \,.\, \cos 2\pi lb \,.$$
$$+ 4(\cos 2\pi hc + \cos 2\pi kc + \cos 2\pi lc) + 8(\cos 2\pi hd \,.\, \cos 2\pi kd \,.$$
$$\cos 2\pi le + \cos 2\pi hd \,.\, \cos 2\pi ke \,.\, \cos 2\pi ld$$
$$+ \cos 2\pi he \,.\, \cos 2\pi kd \quad \cos 2\pi ld)$$
$$+ i\{-8\sin 2\pi ha \,.\, \sin 2\pi ka \,.\, \sin 2\pi la + 8\sin 2\pi hb \quad \sin 2\pi kb \,.$$
$$\sin 2\pi lb - 8(\sin 2\pi hd \quad \sin 2\pi kd \quad \sin 2\pi le + \sin 2\pi hd \,.$$
$$\sin 2\pi ke \,.\, \sin 2\pi ld + \sin 2\pi he \,.\, \sin 2\pi kd \,.\, \sin 2\pi ld)\} *$$

In the arrangement shown in fig. 1, $a = \frac{1}{8}$, $b = \frac{1}{8}$, $c = \frac{1}{8}$, $d = \frac{1}{8}$, $e = 0$ If the atoms of γ-brass were situated in these positions, the "X" atoms being absent, the interatomic distances would be 2·55 A. This is the same value as the distance of closest approach of the centres of copper atoms in the lattice of pure copper The zinc atom in metallic zinc has two interatomic distances, namely, 2·66 A and 2·91 A, whilst in β-brass the interatomic distance is again 2·55 A. One may anticipate that in γ-brass the interatomic distances will again be of the same order of magnitude

Displacements of the atoms consistent with the symmetry requirements of O_h^9 and T_d^3 may now be tried in order to explain the observed intensities of reflexion. The parameter values were tested by the use of the structure-amplitude formula, comparing the values of S so obtained with the observed intensities. In such a comparison allowance must be made for two other factors which affect the observed intensities. These are the frequency factor N, giving the total number of planes corresponding to the form $\{hkl\}$, and a factor expressing the general falling off in intensity as the angle of reflexion increases. This is due to a number of superimposed effects, and to allow for each separately would bring in many unproved assumptions. The net effect may to some extent be compensated for by the insertion of a factor $\mathrm{cosec}^2\,\theta$ in the intensity formula. We then obtain the expression $NS^2/\sin^2\theta$ for comparison with the observed intensities. The use of this purely empirical formula is only justified by its value in affording a rough comparison between reflexions at not too widely differing angles of reflexion. In the present case of a cubic crystal it may be expressed as $NS^2/(h^2 + k^2 + l^2)$.

* In order to cut down the arithmetic, the above expression for S was divided by a factor 4 in all calculations.

Table III.

hkl	Obs. Intensity	$NS^2/(h^2+k^2+l^2)$		
		Holohedral	Hemihedral	
		$a' = b' = 32°$ * $c' = 120°$ $d' = 120°$ $e' = 0$	$a' = 37°$ $c' = 120°$, $d' = 120°$	$b' = 60°$ $c' = 16°$ $d' = 110°$
110	abs	0 0	0 8	1 4
200	abs.	0 4	0·8	0 1
211	abs	0 5	1 5	0 0
220	abs	2 4	0 4	0 9
310	abs	1 3	0 0	0 7
222	weak	3 2	0 9	2 9
321	weak	3 2	6 1	0 0
400	abs	1 0	2 0	0 0
330 }	strong	102 5	68 2	55 1
411 }		2 4	11 4	36 2
420	abs	0 5	0 7	0 4
332	mod	0 5	4 0	9 2
422	weak	0 0	5 5	6 1
521	abs	0 0	2 8	0 0
440	abs	8·2	0 9	0 1
433 }	abs	1 5	0 6	1 3
530 }		3 2	0 0	1 8
620	abs	0 4	0 5	0·7
622	abs	1 0	1 2	0 9
444	mod.	4 2	2 3	9 2
640	abs	1 6	1·4	2 5
642	very weak	0 7	1 4	3·3
730	abs	11 0	1 3	1 6
800	abs	1 3	0 3	1 2
653	very weak	2 6	0 1	1·4

* For convenience in calculation the parameters are expressed here in degrees, so that a' is equal to $360a$.

Table III compares the calculated and observed intensity values for a number of planes selected from the powder photograph data. In the case of the holohedral structure the symmetry requirements, combined with the criterion that the interatomic distance must not depart too widely from 2·55 A, limit the displacement of the "A" and "B" atoms to a small amount, and hardly permit the "C" and "D" atoms to be displaced at all. On the other hand, the lower symmetry requirements of T_d^3 allow much larger displacements. In Column III are given values calculated for the holohedral structure with those parameter values which give the best correspondence between the observed intensities and the calculated values. This is so unsatisfactory as to make it clear that considerable readjustments are required in the parameter values. So long as the structure remains holohedral, no appreciable change can be brought about without bringing some pairs of atoms much closer together

than 2·55 A. It may be concluded that no arrangement based upon space-group O_h^9 can satisfy all the requirements, and that it remains to consider arrangements based on T_d^3.

The values shown in Column IV of Table III were obtained by giving the d' and e' parameters the greater displacement which is permitted by T_d^3. The much closer correspondence indicates a closer approximation to the correct structure. These parameter values are actually the maximum displacements allowed by considerations of interatomic distance. The other parameter values were unchanged. A much better agreement was obtained by putting $d' = 110°$, as in the last column of Table III.

Table IV

hkl	Obs Int.	$NS^2/(h^2+k^2+l^2)$ $c'=120°$	$c'=125°$	$c'=129°$	hkl	Obs Int.	$NS^2/(h^2+k^2+l^2)$ $c'=120°$	$c'=125°$	$c'=129°$
110	abs	0·46	0·22	0·10	002	abs	0·10	0·03	0·00
200	abs	0·10	0·03	0·00	202	abs	0·20	0·07	0·02
220	abs.	0·30	0·07	0·02	222	st	1·30	1·87	2·37
310	abs	0·24	0·15	0·06	312	w	0·08	0·62	0·62
400	abs	0·02	0·00	0·01	402	v w	0·08	0·10	0·11
420	w	0·15	0·20	0·22	422	m	2·01	1·96	1·83
330	abs	0·60	0·32	0·19	512	w	0·02	0·05	0·19
440	m.	0·82	0·56	0·34	622	abs	0·30	0·24	0·24
730	m	0·54	0·33	0·26					
800	m	0·79	0·52	0·36	103	abs	0·12	0·06	0·04
750	w	0·04	0·04	0·06	213	w	0·08	0·62	0·62
					433	v w	0·43	0·24	0·12
					503		0·30	0·16	0·10
101	abs	0·46	0·22	0·10	703	w	0·27	0·17	0·13
301	abs	0·12	0·08	0·04	653	m	0·22	0·21	0·21
321	w.	0·68	0·62	0·62					
521	w	0·02	0·05	0·19					
831	w.	0·23	0·22	0·22					

Further information with regard to parameter values was obtained by the use of the rotation crystal data. Table IV shows that the best agreement is obtained by increasing the value of c'.

Table V.—Powder Photogram of γ-Brass from Westgren and Phragmén's Observations.

hkl	$h^2+k^2+l^2$	Square of structure-amplitude $= S^2$	N	$NS^2/(h^2+k^2+l^2)$.	Observed Intensity
110	2	0 1	12	0 3	abs
200	4	0 0	6	0·0	abs
211	6	0 1	24	0 6	abs.
220	8	0 0	12	0 1	abs
310	10	0 1	24	0 2	abs
222	12	7 2	8	4 8	weak
321	14	1 1	48	3 7	weak
400	16	0 0	6	0 0	abs
330	18	78 3	12	32·5	strong
411		31 7	24	42 1	
420	20	0 5	24	0 7	v weak*
332	22	8 4	24	9 2	mod
422	24	5 5	24	5 5	weak
510	26	3 3	24	3 0	weak
431		0 5	48	0 0	
521	30	0 7	48	1 2	abs
440	32	2 2	12	0·8	abs.
433	34	0 5	24	0 4	abs
530		0 8	24	0 6	
600	36	24 0	6	4 1	strong
442		8 4	24	5·6	
611	38	3 4	24	2 1	weak
532		1 5	48	1 9	
620	40	0 1	24	0 0	abs
541	42	0 1	48	0 1	abs.
622	44	1 3	24	0 7	abs.
631	46	8 0	48	8·3	weak
444	48	63 6	8	10 8	mod
710	50	0 4	24	0·2	weak
543		3 0	48	2·0	
550		27·7	12	6 7	
640	52	2 3	24	1 1	abs.
633	54	27 2	24	12 0	strong
721		23 0	48	20 4	
552		6 0	24	3 1	
642	56	3 4	48	3 0	v weak
730	58	1 8	24	0 8	abs
732	62	6 3	48	4 9	weak
651		3 8	48	3 0	
800	64	6 0	6	0 5	abs
811	66	0·7	24	0 2	strong
741		22 9	48	16 7	
554		2 3	24	0 8	
820	68	8 9	24	3 1	weak
644		5 1	24	1·8	
653	70	1·9	48	1 3	v weak
822	72	10 2	24	3 4	strong
660		31 1	12	5 3	
831		2 0	48	1 9	
750	74	0 7	24	0 2	weak
743		2·1	48	1·4	
662	76	15 7	24	5 0	weak
752	78	6·1	48	3 8	v. weak

* This line corresponds to the K_β line of (332)

Table VI.—Photogram of a γ-Brass Crystal rotating about (001), from Westgren and Phragmén's Observations.

hkl	N	$NS^2/(h^2+k^2+l^2)$	Obs Int	hkl	N	$NS^2/(h^2+k^2+l^2)$	Obs Int.
110	4	0 10	abs.	002	4	0 00	abs
200	4	0 00	abs.	112	4	0 10	abs
220	4	0 02	abs	202	4	0 03	abs.
310	8	0 08	abs	222	4	2 37	st
400	4	0 01	abs	312	8	0 62	w
330	4	17 2	st	402	4	0 11	v w *
420	8	0 22	w	332	4	1 52	m
510	8	1 01	m	422	8	1 83	m.
440	4	0 28	v w	512	8	0 19	w
530	8	0 19	abs	442	4	0·93	m
600	4	2 04	st	532	8	0 31	v w
620	8	0 01	abs	602	4	0·01	abs
710	8	0 06	st	622	8	0 24	abs
550	4	2 22		712	8	3 45	st
640	8	0 34	mod	552	4	0·50	
730	8	0 26	mod.	642	8	0 48	w
800	4	0 36	mod	732	8	0 82	m
820	8	1 07	st	802	4	0 54	m
660	4	1 87	st	822	8	1 12	st
750	8	0 08	s	002	4	0 79	st
				732	8	0 61	st
101	4	0 10	abs				
211	8	0 19	abs	103	4	0 04	abs.
301	4	0 04	abs	213	8	0·02	w
321	8	0 62	w	303	4	17 2	st
411	8	13 0	st.	323	8	3 04	st
501	4	0 50	w.	413	8	0 16	abs
431	8	0 16		433	8	0 12	v w
521	8	0 19	w.	503	4	0 10	
611	8	0·71	m	523	8	0 31	v w.
541	8	0 01	abs	613	8	1 30	st
631	8	1 30	m	543	8	0·48	w
701	4	0 09	abs	633	8	4 08	st.
721	8	3 45	st.	703	4	0·13	w.
651	8	0·50	w	723	8	0·82	m
811	8	0 08	st.	653	8	0 21	m
741	8	2 75		813	8	0 22	
831	8	0 22	w	743	8	0 23	m

* Coincides with (332) K_β

The best value is about $c' = 129°$. No further change is indicated in the values of the other parameters.

The parameter values, now expressed again as fractions of the side of the unit cell, which give the best agreement between the observed and calculated intensity values, are $a = 0{\cdot}10_8$, $b = 0{\cdot}16_7$, $c = 0{\cdot}35_8$, $d = 0{\cdot}30_8$, $e = 0{\cdot}04_8$.

Tables V and VI give complete lists of observed and calculated intensities from the powder photogram and the rotation photogram. With regard to the powder photogram, it may be noted that lines 36 and 72 are marked "strong"

by Westgren and Phragmén, while lines 46 and 50 are marked "weak," but on the reproductions of their photographs all four lines appear to have about the same intensity as line 48, which is marked "moderate" With these exceptions, the agreement between observed and calculated values is sufficiently good to afford strong confirmation of the correctness of the parameter values and entirely confirms the original supposition that γ-brass has very nearly a body-centred cubic structure

(6) *Identification of the Atoms*

The scattering powers of copper and zinc are so nearly equal that there was some difficulty in distinguishing the respective copper and zinc atoms, and an indirect method had to be employed for this purpose.

The powder photograms of γ-Cu–Zn, γ-Ag Zn, and γ Au-Zn are so similar that there can be no doubt that they have the same type of structure. Table VII gives a list of the lines which have slightly different intensities for the three series of alloys. Lines 48, 50 and 72 need not be considered, as the remarks made above are applicable again here In all other cases the differences in

Table VII.

hkl	$h^2 + k^2 + l^2$	Observed Intensities			Positions of Atoms which would account for Intensity Changes			
		Cu–Zn	Ag–Zn	Au–Zn	A	B.	C	D
211	6	abs	v w	w	Zn	Cu Ag Au	Cu Ag Au	—
222	12	w.	w	abs	Zn	Cu Ag Au	Cu Ag Au	Zn
321	14	w	abs	abs	—	Cu Ag Au	—	Zn
420	20	v w.	abs	?	Zn	Cu Ag Au	—	Zn
332	22	m.	w.	w	Zn	—	—	Zn
422	24	w	w	m	Cu Ag Au	Cu Ag Au	Cu Ag Au	Zn
431	26	w	v w	v w	Zn	Cu Ag Au	Cu Ag Au	Zn
510								
440	32	abs	w	v w	Cu Ag Au	Cu Ag Au	Cu Ag Au	Zn
530	34	abs	abs	v.w.	Zn	—	—	Cu Ag Au
433								
541	42	abs.	v w	?	Zn	Cu Ag Au	Cu Ag Au	—
444	48	m	m	st				
550								
710	50	w	w.	m				
543								
642	56	v w	abs.	?	Zn	—	—	Zn
644	68	w	w	st.				
820								
662	70	v w	abs	abs	Zn	—	—	Zn
822	72	st.	st	m.				
660								

intensity are either due to slight differences in parameter values or to the replacement of the copper atoms by the more efficient scatterers, silver and gold. The table shows what distribution of atoms would produce the observed intensity changes. Evidently "A" and "D" atoms are zinc and "B" and "C" atoms are either copper, silver or gold. There is no indication of any change in the values of the parameters.

(7) *Discussion of the Structure*

The complete arrangement of atoms in the structure found for γ-brass is shown in fig. 2. The open squares and circles represent copper atoms, the solid ones represent zinc atoms. The arrangement corresponds to the space-group T_d^3, the atoms being situated in the following positions —

Zn *Atoms.*

(0·10 0·10 0·10) (0·10 0·90 0 90) (0 90 0·10 0 90) (0 90 0·90 0·10)
(0·60 0·60 0·60) (0·60 0·40 0·40) (0·40 0·60 0·40) (0·40 0·40 0 60)
(0 31 0 31 0 05) (0·31 0 69 0 95) (0 69 0·31 0·95) (0·69 0·69 0·05)
(0·81 0·81 0 55) (0·81 0·19 0 45) (0·19 0·81 0·45) (0·19 0·19 0·55)
(0·31 0·05 0·31) (0 31 0·95 0 69) (0·69 0 95 0·31) (0·69 0·05 0·69)
(0 81 0 55 0·81) (0 81 0·45 0·19) (0·19 0·45 0·81) (0·19 0·55 0 19)
(0·05 0·31 0·31) (0 95 0·69 0·31) (0·95 0 31 0·69) (0·05 0 69 0·69)
(0·55 0·81 0 81) (0·45 0·19 0·81) (0·45 0·81 0·19) (0 55 0·19 0·19)

Cu *Atoms.*

(0·83 0 83 0·83) (0 83 0·17 0·17) (0·17 0·83 0·17) (0·17 0·17 0·83)
(0·33 0·33 0·33) (0·33 0 67 0·67) (0·67 0·33 0·67) (0·67 0 67 0·33)
(0·36 0 0) (0·64 0 0) (0 0·36 0) (0 0·64 0) (0 0 0 36) (0 0 0·64)
(0·86 0 0) (0·14 0 0) (0 0·86 0) (0 0·14 0) (0 0 0·86) (0 0 0·14)

There are 32 zinc atoms and 20 copper atoms in the unit cell. The corresponding formula is Cu_5Zn_8. A confirmation of this formula is given by metallographic data. Several properties of γ-brass alloys exhibit a maximum at compositions corresponding to just over 60 per cent. zinc. For this reason metallographers ascribed the formula Cu_2Zn_3 to the alloy. In view of the X-ray data this formula must now be considered untenable. However, Cu_5Zn_8 contains 62·5 per cent. Zn, and this accounts equally well for the observed maximum.

Table VIII gives a list of the interatomic distances found in Cu_5Zn_8. This completely confirms the hypothesis put forward in section 3, that these distances

would prove to be very nearly the same as the interatomic distances in Cu, Zn and CuZn.

Table VIII.

Metal or Alloy	Cu Cu		Cu–Zn		Zn Zn	
	Neighbouring Atoms	Dist. in Å	Neighbouring Atoms	Dist. in Å	Neighbouring Atoms	Dist. in Å
In Cu_5Zn_8	C–C	2·5	B–A	2·55	A–A	2·55*
	B–C	2·7	B–D (1)	2·55*	A–D	2·6
			B–D (2)	2·55	D–D	2·7
			C–A	2·6		
			C–D (1)	2·6		
			C–D (2)	2·75		
			C–D (3)	2·94		
In metallic Cu		2·55				
In CuZn				2·55		
In metallic Zn						2·65
						2·9

The two distances marked with a * were assumed as guides for selecting parameter values for purposes of calculation. The agreement of the intensity values shows the validity of this choice. With regard to the remaining distances, no assumption whatever was made. They are deduced directly from the parameter values which were found to give the best agreement for the intensities. The accuracy is about 0·1 Å. The mean value, not including the value 2·95 Å, which probably does not represent any real point of contact between two atoms, is 2·6 Å. This is just a little greater than in CuZn, which would be expected from the fact that there are fewer atoms per unit volume in Cu_5Zn_8.

The copper and zinc atoms are distributed symmetrically throughout the unit so that each atom has the greatest possible number of neighbours of the opposite sort. These neighbours are distributed as follows:—

Copper Atoms.

"C" atoms have 10 zinc and 3 copper atoms as neighbours.

"B" atoms have 9 zinc and 3 copper atoms as neighbours.

Zinc Atoms.

"A" atoms have 6 zinc and 6 copper atoms as neighbours.

"D" atoms have 5 zinc and 6 copper atoms as neighbours.

Summary

(1) The structure of γ-brass has been deduced from the data of Westgren and Phragmén, who had already shown that it was cubic, the lattice dimensions of the unit cell being about 8·9 A

(2) γ-brass has the forumla Cu_5Zn_8, each unit cell containing 20 copper atoms and 32 zinc atoms.

(3) The space-group is T_d^3. There are four sets of equivalent positions containing, respectively, 8, 8, 12 and 24 atoms.

(4) The arrangement of atoms is almost body-centred, but in each unit cell there are two atoms less than would be required for such a simple arrangement.

(5) The different sets of atoms are displaced by definite amounts from the body-centred positions These displacements have been measured.

(6) The interatomic distances are about 2·6 A, which is about the same value as in the elements Cu and Zn.

(7) γ-Ag–Zn and γ–Au–Zn are similarly constituted, the formulæ being Ag_5Zn_8 and Au_5Zn_8, respectively

The authors desire to express their thanks to Prof. W L Bragg, F.R.S, for his kind interest and valuable suggestions during the progress of the work, and to Mr A P. M Fleming, C.B.E, M Sc. (Tech.), Director of Research of Metropolitan-Vickers Electrical Co, Ltd., for permission to publish the results

INDEX TO VOL. CXII. (A)

END OF THE ONE HUNDRED AND TWELFTH VOLUME (SERIES A).

Date of issue.	Date of issue.	Date of issue.